



Lille University

Doctoral School of Health and Biology

**Regulation of cellular Mn homeostasis:  
Unexpected functions of TMEM165, SERCA and SPCA1**

**Marine Houdou**

**Doctoral Thesis**

to obtain the degree of PhD

Discipline: Cellular and molecular aspects of biology

Specialty: Biochemistry and molecular biology

PhD defense December, 10<sup>th</sup> 2020

**Examination board**

|                       |   |
|-----------------------|---|
| <b>President</b>      | Dr. Dominique Legrand, CNRS, University of Lille  |
| <b>Reporters</b>      | Pr. Peter Vangheluwe, Katholieke Universiteit Leuven<br>Pr. Vivek Malhotra, Catalan Institution for Research and Advanced Studies |
| <b>Examiners</b>      | Pr. Vladimir Lupashin, University of Arkansas for Medical Sciences<br>Pr. Muriel Bardor, University of Rouen                      |
| <b>PhD Supervisor</b> | Dr. François Foulquier, CNRS, University of Lille   |





Collège Doctoral  
Lille Nord de France

Université de Lille

Ecole Doctorale Biologie Santé de Lille

## **Régulation de l'homéostasie cellulaire du Mn : Rôles insoupçonnés de TMEM165, SERCA et SPCA1**

**Marine Houdou**

**Thèse de Doctorat**

pour l'obtention du grade de Docteur

Discipline: Aspects cellulaires et moléculaires de la biologie

Spécialité : Biochimie et biologie moléculaire

Soutenance le 10 Décembre 2020

### **Commission d'examen**

|                           |   |
|---------------------------|---|
| <b>Président</b>          | Dr. Dominique Legrand, CNRS, Université de Lille  |
| <b>Rapporteurs</b>        | Pr. Peter Vangheluwe, Katholieke Universiteit Leuven<br>Pr. Vivek Malhotra, Catalan Institution for Research and Advanced Studies |
| <b>Examineurs</b>         | Pr. Vladimir Lupashin, University of Arkansas for Medical Sciences<br>Pr. Muriel Bardor, Université de Rouen                      |
| <b>Directeur de thèse</b> | Dr. François Foulquier, CNRS, Université of Lille   |





*A Mamie Josette,  
A mes parents et mes deux sœurs,  
A mes beaux-parents,*



« Il n'y a qu'une façon d'échouer, c'est d'abandonner avant d'avoir réussi. »

G. Clémenceau

« Si la matière grise était plus rose, le monde aurait moins les idées noires. »

P. Dac





## Acknowledgements

To **each member of my examination board**, I would like to thank all of you for having accepted to evaluate my PhD. It is a great honor for me to have such expert scientists as jury members. I hope to have a fruitful scientific discussion with all of you, mixing all our domains of expertise.

- ✧ To Pr. **Peter Vangheluwe**, our meeting a year ago has changed my future. In addition to have kindly accepted to evaluate my thesis, you offered me a Post-Doc position in your lab. I will never forget the support you gave me during the writing of the GlyPICAN proposal. Thank you.
- ✧ To Pr. **Vivek Malhotra**, I am very grateful to you that you have kindly accepted to evaluate my thesis.
- ✧ To Pr. **Vladimir Lupashin**, it is a great honor to have you in my jury members. Given that I used “your” cells for my whole PhD, I am more than honored that you kindly accepted to examine my thesis.
- ✧ Au Pr. **Muriel Bardor**, je tiens à vous remercier chaleureusement d’avoir accepté d’examiner mes travaux. Depuis le premier CSI jusqu’à ma soutenance de thèse, vous avez suivi de près mes avancées, critiqué mes travaux et m’avez donné de précieux conseils. Merci.

Au Dr **Dominique Legrand**, le plus fin blagueur de tous les temps. Dominique, je te remercie tout particulièrement d’avoir accepté de présider le jury de ma thèse. Je n’oublierai jamais le soutien que tu as apporté à ma candidature lors des résultats du grand jury, il y a trois ans. L’accès à la thèse s’est fait pour moi ce jour-là. Je te remercie pour ta bonne humeur constante et tes blagues « à papa » qui nous font toujours rire. Merci pour ton regard critique sur mes travaux, pour tes conseils apportés tout au long de ma thèse et la veille scientifique que tu as fait pour nous avec la rédaction de cette incroyable revue dans BBA. Je te remercie également pour tes conseils avisés en matière de poids et de fonte !

Au Dr **François Foulquier**, mon directeur de thèse. François, il y a quatre ans maintenant, tu as su me tendre la main alors que je nageais en plein doutes. Je te remercie pour ton écoute, ta sympathie, ton empathie, ta patience, ta présence, ta passion et l’énergie que tu mets dans tout ce que tu entreprends. Je te suis extrêmement reconnaissante pour ta confiance, pour tous les stagiaires que tu m’as laissé guider, pour tous les congrès auxquels tu m’as emmenée, pour tous les projets auxquels tu m’as fait participer et pour la liberté que tu m’as laissée dans la réalisation de cette thèse. Je te remercie grandement pour tous tes précieux conseils, qu’ils soient scientifiques, professionnels, humains ou encore sportifs ! Merci pour ton esprit critique, ta franchise et ton investissement à mon égard.

Tu es quelqu'un d'entier, d'humble et de profondément humain. Tes nombreux « Tu peux y aller comme ça, ça passe... MAIS moi je ferai l'inverse » m'ont grandement aidée à mieux penser et organiser mes idées. Merci de m'avoir si bien accueillie dans ton équipe, le « 020 ».

Au Dr **Sandrine Duvet**, ma « saloperie » gourmande préférée. Derrière ses petits yeux noirs et son nez bouché, se cache une personne unique en son genre, le cœur sur la main et toujours le mot pour rire. Je te souhaite de garder ce dynamisme et cette franchise qui te caractérisent tellement. D'un point de vue plus scientifique, je te remercie pour ton écoute et tes précieux conseils en spectrométrie de masse. Je tenais également à te remercier de m'avoir initiée à l'enseignement, que ce soit en TP, TD ou projet. D'un point de vue plus culinaire, je te remercie de m'avoir fait découvrir les fameuses guimauves de « chez Raoul » dont je raffole, promis je passerai encore commande à Noël !

Au Dr **Geoffroy de Bettignies**, le levuriste hors-pair du 020. Merci Geoffroy pour tes nombreux conseils lors de mes essais en levure et de façon générale lors de chaque présentation et réunion. Tu as toujours eu un esprit critique sur mes travaux, à la fois sur l'aspect fondamental et sur l'aspect technique et je t'en remercie.

Au Pr **Willy Morelle**, le massiste de l'équipe. Merci Willy d'avoir su répondre à mes questions lors de mes essais en spectrométrie de masse.

Au Dr **Marie-Ange Krzewinski-Recchi**, experte en biologie moléculaire. Mon attrait pour les protéines a toujours dissimulé ma phobie des acides nucléiques et tu le savais. Merci d'avoir toujours répondu à mes questions de biologie moléculaire quand j'en ai eu besoin. Aussi, j'emporte avec moi la figurine du lapin crétin qui m'a toujours porté bonheur partout où je l'ai emmenée.

Au Dr **André Klein**, le cycliste du CHU-020. Par temps de pluie, de vent, de grêle ou de grand soleil, je t'ai toujours vu venir en vélo au C9 pour tes réunions avec François et Elodie. Tu es une force tranquille de la nature. Je te remercie d'avoir toujours suivi mes travaux et maintenant, je te souhaite une joyeuse retraite !

A **Dorothee Vicogne**, la reine de la culture cellulaire. Merci Dorothee de m'avoir initiée à la culture cellulaire et de m'avoir inculqué la rigueur scientifique dans la réalisation des expériences. Je suis très contente d'avoir pu contribuer à ton papier et qu'ensemble on ait enfin résolu le mystère du « shift de LAMP2 qui remonte ». A **Céline Schulz**, mon équivalent « free-hug ». Je me souviendrai toujours de notre première rencontre à Paris, lors du concours CNRS. Tu m'avais l'air super sympa et ce n'était pas qu'une apparence. Être associée à trois équipes fait de toi une petite pile électrique, toujours à courir entre le SN3 pour la microscopie confocale, le second pour la radioactivité, le premier étage avec l'équipe de Tony et le rez-de-chaussée avec François et Anne. Le fait est que tu es là pour tout le

monde, sur tous les fronts. Tu as toujours su prendre le temps de m'expliquer les choses à chaque fois que j'ai pu te demander de l'aide et je t'en remercie. Tes doux jurons me manqueront... A vous deux les filles, vous avoir au laboratoire est une chance inestimable, et travailler avec vous était un vrai plaisir.

To my dearest **Kateryna**, working with you was a real pleasure. You were all the time cheering me up and helping me at any time for anything. You have been a great support for me during this thesis. I would also thank your husband Artem, for his "new eye" and all the good advice he brought to our project. I know you will continue our amazing project with Zoé and Aurore and I am confident: you will succeed and maybe find the first "SIME" pathway, who knows? Дякую за все, Катерина!

A **Zoé**, le bébé M1 devenu thésarde. Merci Zoé pour ton infinie reconnaissance. Notre rencontre si particulière a fait naître en toi une âme de chercheuse et je suis ravie que tu aies choisi l'équipe de François pour te réaliser. Ton arrivée dans l'équipe pour ton stage de M1 a été une véritable bouffée d'oxygène pour moi. Je suis très contente d'avoir pu t'encadrer et t'accompagner au cours de ton M1 et de ton M2. Tu as une âme de bosseuse, je te souhaite de faire une très belle thèse. Dans trois ans, ce sera à mon tour d'être assise dans le public ! A **Aurore**, globe trotteuse aux quatre coins de la France. Je te remercie Aurore pour ton dynamisme et ta joie de vivre. Travailler avec toi était un plaisir, un plaisir scientifique, gustatif (je me souviens bien de l'aligot !) et sportif ! A vous deux, Aurore et Zoé, l'alpha et l'oméga enfin le zêta. Un binôme très complémentaire et pétillant. Toujours plein de bonne volonté et d'entrain, vous avez clairement re-dynamiser l'équipe. Je suis ravie d'avoir travaillé avec vous. Vous avez mis des paillettes dans ma thèse les filles ! Merci pour tous nos moments de complicités en dehors du labo et merci pour votre soutien indéfectible pendant le confinement.

Aux anciens membres de l'équipe, **Jean-Claude**, je garderai un souvenir festif de nos rencontres : des premiers moments de convivialité aux repas de Noël en passant par votre pot de retraite. Merci d'avoir toujours suivi mes travaux pendant mes années au C9. **Eudoxie**, je me souviens bien de nos longues discussions le soir, sur le parking du C9. Je te remercie de m'avoir initiée à la levure et de ton dynamisme quotidien dans l'équipe. **Sven**, je te suis très reconnaissante pour tout le temps que tu as passé à m'expliquer la science. Depuis mes premiers pas au C9 en 2014 jusqu'à la soutenance de ta thèse en Décembre 2017 tu n'as cessé d'être bienveillant à mon égard. Tu as su me transmettre la passion de TMEM165. J'ai beaucoup appris de toi. **Dounia**, (alias Chewbacca pour les intimes de la préparation du mariage), je te remercie de m'avoir initiée à la spectrométrie de masse. Il y a encore du boulot pour que j'arrive à lire à travers les pics d'un spectre mais les bases me sont venues de toi et je t'en suis très reconnaissante.

Et parce qu'on ne dit « jamais deux sans trois », je remercie également mes **co-thésardes** et désormais **Drs** : Dr **Elodie** et Dr **Anne-Sophie**. Au-delà de vous remercier pour votre aide scientifique à la

réalisation de cette thèse, je vous remercie surtout de m'avoir supportée pendant trois ans ! Vous avez chacune un caractère différent et des qualités humaines différentes. Elodie, c'est l'électron libre et mystérieux du 020 et Anne-Sophie, c'est la miss pipelette du 020. Je vous souhaite à toutes les deux de vous épanouir professionnellement et surtout personnellement.

Dans l'ensemble, je remercie du fond du cœur toute l'équipe du « **020** ». Chacun d'entre vous a contribué de près ou de loin à ma réussite et sans vous, la thèse aurait été bien morose. Une thèse c'est un étudiant, un projet, un directeur mais aussi et surtout, une équipe, des collègues, des joies partagées et des frustrations aussi, des coups de gueule, des fous rires, des Noël's américains, des pots de retraite, des pots d'anniversaire, des pots pour les papiers, des pots de thèse (oui, ça fait beaucoup de pots... !), de l'entre-aide et de la bienveillance. Je vous suis très reconnaissante pour l'enrichissement que vous m'avez transmis. Aussi, j'adresse mes remerciements à **tous les membres du C9** et de l'**UGSF**. Chacun d'entre vous a contribué à cette thèse, par un sourire, un conseil, une réservation de billets pour un congrès, un soutien moral, une écoute. Je remercie particulièrement les **Prs Christophe d'Hulst** et **Yann Guérardel** d'avoir permis la réalisation de cette thèse dans leur unité. Mais aussi, le **Pr Philippe Delannoy** que je remercie grandement pour son soutien et ses bons conseils lors de la présentation de ma candidature à l'école doctorale. Merci Philippe de votre écoute et de votre soutien également tout au long de ma thèse. **Patricia**, je te remercie pour la confiance que tu m'as accordée en me laissant intervenir sur le projet d'Alex. Tu es quelqu'un d'entier avec j'aime beaucoup discuter sciences et cactus. D'ailleurs, toujours pas de fleurs... **Cécile** ma PRAG préférée. J'ai adoré faire des enseignements avec toi. Tu es une personne hors-norme, ultra-dynamique et toujours à l'écoute de tes étudiants. Ton soutien *via* Skype et Whats'App pendant le confinement m'a fait beaucoup de bien et je t'en remercie. Sans oublier les membres de la startup **eZyvec** : Sylvain, Carine, Vianney et Kévin. Merci d'avoir généré des mutations à foison de notre protéine préférée !

Je tiens également à remercier le Dr **Anne Garat** et **Valérie Decool**, d'avoir pris en main les analyses d'ICP-MS pour les nombreux échantillons que vous avez gentiment passés. Aussi, je remercie **Christian Slomiany** et **Elodie Richard**, de m'avoir formée à la microscopie confocale. Plus particulièrement, merci Christian d'avoir évalué mes travaux de thèse au cours de mon premier CSI.

Mes remerciements s'adressent aussi à l'équipe du **Pr Gert Matthijs** avec qui j'ai passé de très bons moments lors de congrès scientifiques en Belgique et en France. **Eline**, it was nice to have you in Lille for a couple of weeks. Enjoy your time in Spain and do not hesitate to come and see me in... Leuven!

Ingénieure de formation, je tiens également à remercier l'ensemble de mes professeurs de l'**ENSTBB** pour la formation qu'ils m'ont transmise. Enfin, j'adresse un remerciement particulier à Mme **Nathalie**

**Berton-Quiniou**, ma professeure de SVT en terminale qui m'a donné goût à la biologie et qui a scellé mon destin en me faisant prendre la voie de la classe préparatoire.

Plus personnellement, mes remerciements et pensées vont à ma famille : mes parents, mes sœurs et mes beaux-parents. Ces dernières années n'ont pas été faciles pour vous, à toujours m'entendre parler de cellules et de « trucs de Golgi ». Merci pour le soutien moral indéfectible que chacun d'entre vous m'a apporté tout au long de ces trois dernières années. **Maman** et **papa**, les deux seules personnes à qui tout le mérite de cette thèse revient. Vous avez su me donner une éducation pleine de valeurs et de bon sens. Vous avez su me porter vers le haut dans toutes les circonstances. Si j'en suis là aujourd'hui, c'est grâce à vous. **Jean-Marie**, j'ai appris à te connaître au cours des dix dernières années. Tu es une personne formidable, bienveillante qui a toujours su être à mon écoute. Merci ! **Nathalie**, je n'ai pas eu la chance de te connaître plus longtemps et je le regrette. Je garde de toi une force et une énergie incroyables. **Elodie**, ma grande-sœur, malgré nos différends, tu restes et resteras un modèle pour moi. **Coraline**, ma petite sœur, merci d'être toujours là pour moi et de me soutenir. J'espère que tu viendras me voir de temps en temps en Belgique, promis on ira visiter le musée Magritte ! Mamie **Josette**, la raison de cette vocation et de cet investissement dans la recherche en santé humaine. Ton départ fut un réel électrochoc dans ma vie. Depuis, je garde à l'esprit qu'il faut toujours se battre et persévérer quoique l'on fasse mais aussi, qu'il faut savoir profiter de ses proches parce que malheureusement, la vie est trop courte. J'espère que de là-haut, tu es fière de moi. Enfin, **Catherine**, la marraine que je n'ai jamais eue et **Josiane** qui me rappelle tant le souvenir de ce qu'est une grand-mère. Je tiens à vous remercier de votre soutien durant toutes ces années. Ca y est, j'ai (enfin) fini les études, ce diplôme sera le dernier !

A mes trois frenglaises préférées : **Carole**, **Marie** et **Flore**. Outre-Manche, ce n'est pas toujours facile de garder le contact quand chacune construit sa vie et son avenir, avec des rythmes de vie différents. Pour autant, je sais que je peux compter sur vous les filles. Vous représentez pour moi une véritable source de bonne humeur. J'ai hâte que l'on puisse se retrouver, à Amsterdam, Slough, Londres, Oxford, Bordeaux, Lille ou pourquoi pas Leuven ?



## Foreword

This work has been supervised by **Dr François Foulquier** in the Structural and Functional Unit of Glycobiology (UGSF) belonging to the Mixt Research Unit (UMR) 8576, currently headed by Pr. Yann Guérardel.

The financial support for this thesis was provided by an allocation from the “Ministère de l’Enseignement Supérieur et de la Recherche”. The work resulting from this thesis was published in international journals and exposed during scientific meetings as oral communications and posters.





# Publications

## 1. Review

- **Congenital Disorders of Glycosylation (CDG): from 1980 to 2020, 40 years to understand.**

Houdou, M. and Foulquier, F. *Médecine/sciences.* (2020)

## 2. Scientific articles

- **Investigating the functional link between TMEM165 and SPCA1.**

Lebredonchel, E.\*, Houdou, M.\*, Hoffmann, H.H., Krzewinski-Recchi, M.-A., Vicogne, D., Rice, C., Klein, A. and Foulquier, F. *Biochem. J.* (2019)

- **Dissection of TMEM165 function in Golgi glycosylation and its Mn<sup>2+</sup>-sensitivity.**

Lebredonchel, E., Houdou, M., Potelle, S., de Bettignies, G., Schulz, C., Krzewinski-Recchi, M.-A., Lupashin, V., Legrand, D., Klein, A. and Foulquier, F. *Biochimie* (2019)

- **Fetal Bovine Serum impacts the observed N-glycosylation defects in TMEM165 KO HEK cells.**

Vicogne, D., Houdou, M., Garat, A., Morelle, W. and Foulquier, F. *JIMD.* (2019)

- **Involvement of thapsigargin and cyclopiazonic acid sensitive pumps in the rescue of TMEM165-associated glycosylation defects by Mn<sup>2+</sup>.**

Houdou, M., Lebredonchel, E., Garat, A., Duvet, S., Legrand, D., Decool, V., Klein, A., Ouzzine, M., Gasnier, B., Potelle, S.\* and Foulquier, F.\*. *Faseb Journal* (2018)

- **Protein N-glycosylation alteration and glycolysis inhibition both contribute to the antiproliferative action of 2-deoxyglucose in breast cancer cells.**

Berthe, A., Zaffino, M., Muller, C., Foulquier, F., Houdou, M., Schulz, C., Bost, F., De Fay, E., Mazerbourg, S., and Flamnet, S. *Breast Cancer Res. Treat.* (2018)

- **Investigating the function of Gdt1p in yeast Golgi glycosylation.**

Dulary, E.\*, Yu, S.-Y.\*, Houdou, M.\*, de Bettignies, G., Decool, V., Potelle, S., Duvet, S., Krzewinski-Recchi, M.-A., Garat, A., Matthijs, G., Guerardel, Y. and Foulquier, F. *Biochim. Biophys. Acta.* (2017)

- **Manganese-induced turnover of TMEM165.**

Potelle, S., Dulary, E., Climer, L., Duvet, S., Morelle, W., Vicogne, D., Lebredonchel, E., Houdou, M., Spriet, C., Krzewinski-Recchi, M.-A., Peanne, R., Klein, A., de Bettignies, G., Morsomme, P., Matthijs, G., Marquardt, T., Lupashin, V. and Foulquier, F. *Biochem. J.* (2017)

## Oral communications

### 1. Talks

- **Glycans & Proteoglycans: The Sweet and Smart Molecules of the 21<sup>st</sup> Century.**  
Nancy, October 18-19<sup>th</sup>, 2017. *“Mn<sup>2+</sup> and D-Galactose: the miracle molecules to rescue the glycosylation defects in TMEM165-CDG.”*
- Seminar at UGSF, November 10<sup>th</sup>, 2017. *“When Mn<sup>2+</sup> meets glycosylation”*.
- **3<sup>èmes</sup> Journées scientifiques du GDR Gagosciences.**  
UGSF, Lille, September 24-25<sup>th</sup>, 2018. *“TMEM165; a new key player in Golgi glycosylation and cellular Mn<sup>2+</sup> homeostasis.”*
- **Gordon Research Seminar.**  
Lucca Barga, Italy, March 9-10<sup>th</sup>, 2019. *“TMEM165; a new key player in Golgi glycosylation and cellular Mn<sup>2+</sup> homeostasis.”*
- **Flash Talk at “Journée André Verbert”, PhD symposium.**  
Lille, September 10<sup>th</sup>, 2019. *“TMEM165; a new key player in Golgi glycosylation and cellular Mn<sup>2+</sup> homeostasis.”*

### 2. Posters

- **3<sup>èmes</sup> Journées scientifiques du GDR Gagosciences.** UGSF, Lille, September 24-25<sup>th</sup>, 2018.
- **29<sup>th</sup> Joint Glycobiology Meeting.** Ghent, October 21-23<sup>rd</sup>, 2018.  
*“TMEM165; a new key player in Golgi glycosylation and cellular Mn<sup>2+</sup> homeostasis.”* **Houdou, M.**, Lebretonchel, E., Kondratska, K., Potelle, S., Mouajjah, D., Morelle, W., Klein, A. and Foulquier, F.
- **Gordon Research Conferences Glycobiology.** Lucca Barga, Italy, March 10-15<sup>th</sup>, 2019.
- **30<sup>th</sup> Joint Glycobiology Meeting.** Lille, October, 2019.  
*“Interplay between TMEM165, SPCA1 and SERCA2 to sustain Golgi glycosylation”.* **Houdou, M.**, Lebretonchel, E., Vicogne, D., Kondratska, K., Garat, A., Hoffmann, H.H., Klein, A., Lupashin, V., Rice, C.M. and Foulquier, F.

## Distinctions

- André Verbert-Bernard Fournet Prize from the French Group of Glycosciences (June, 30<sup>th</sup> 2020).
- Outstanding “Flash Talk Communication” at André Verbert’s Day, PhD symposium in Lille (September, 10<sup>th</sup> 2019).
- Outstanding Poster presentation Award at Gordon Research Conferences Glycobiology in Lucca Barga, Italy (March, 10-15<sup>th</sup> 2019) and at 29<sup>th</sup> Joint Glycobiology Meeting in Ghent, Belgium (October 21-23<sup>rd</sup>, 2018).

## Table of contents

|   |    |
|---|----|
| <b>General introduction</b> .....   | 1  |
| 1. Generalities about the secretory pathway .....   | 3  |
| 1.1. The ER as a hub for (secretory) protein synthesis .....  | 4  |
| 1.2. The Golgi apparatus: between protein PTMs and trafficking .....  | 4  |
| 1.3. How to traffic through the Golgi apparatus? .....  | 5  |
| 2. Golgi ion homeostasis .....  | 8  |
| 2.1. pH .....   | 8  |
| 2.2. $\text{Ca}^{2+}$ , $\text{Mn}^{2+}$ and additional cations .....   | 8  |
| 3. Disrupted Golgi homeostasis and CDGs .....   | 10 |
| 3.1. Glycosylation and CDGs .....   | 10 |
| 3.2. Membrane trafficking in CDGs .....   | 11 |
| 3.3. Golgi pH regulation in CDGs .....  | 11 |
| 3.4. Golgi $\text{Mn}^{2+}$ homeostasis in CDGs .....   | 12 |
| <br>  |    |
| <b>Chapter 1: ER and Golgi glycosylation pathways in yeast and human</b> .....  | 13 |
| 1. General introduction about the glycosylation process* .....  | 15 |
| 1.1. The glycosylation reaction .....   | 15 |
| 1.2. Diversity of the glycosylation pathways in yeast <i>Saccharomyces cerevisiae</i> and human .....                           | 24 |
| 2. N-linked glycosylation .....   | 32 |
| 2.1. Initiation in the ER: from the synthesis to the transfer of the lipid-linked oligosaccharide (LLO) precursor .....         | 33 |
| 2.2. Early trimming during the ER quality control for N-glycoproteins .....   | 40 |
| 2.3. Maturing in the Golgi apparatus: between polymannans and complex N-glycans .....   | 42 |
| 2.4. Cytosolic, proteasomal and lysosomal degradation of human N-glycans .....  | 47 |
| 3. On the ion side of the N-linked glycosylation pathway .....  | 50 |
| <br>  |    |
| <b>Chapter 2: <math>\text{Ca}^{2+}/\text{Mn}^{2+}</math> homeostasis within the secretory pathway: yeast versus human</b> ..... | 53 |
| 1. General introduction about $\text{Ca}^{2+}$ and $\text{Mn}^{2+}$ in yeast and human .....                                    | 55 |
| 1.1. $\text{Ca}^{2+}$ and $\text{Mn}^{2+}$ main storage organs/organelles .....   | 55 |
| 1.2. $\text{Ca}^{2+}$ and $\text{Mn}^{2+}$ regulation at the body level .....   | 58 |

|      |  |     |
|------|--|-----|
| 1.3. | Ca <sup>2+</sup> and Mn <sup>2+</sup> in cellular processes.....                                     | 61  |
| 1.4. | Ca <sup>2+</sup> and Mn <sup>2+</sup> in human diseases.....   | 63  |
| 2.   | Interplay between Ca <sup>2+</sup> and Mn <sup>2+</sup> import/export within the secretory pathway.. | 66  |
| 2.1. | Role of Ca <sup>2+</sup> /Mn <sup>2+</sup> P-type ATPases.....                                       | 67  |
| 2.2. | Role of (un)specific transporters.....   | 80  |
| 2.3. | Role of (un)specific channels.....   | 98  |
| 2.4. | Overview of Mn <sup>2+</sup> and Ca <sup>2+</sup> key transporters within the secretory pathway..... | 111 |
| 3.   | Intracellular Ca <sup>2+</sup> and Mn <sup>2+</sup> regulation.....                                  | 114 |
| 3.1. | Calcium binding proteins.....  | 114 |
| 3.2. | Regulation of intracellular Ca <sup>2+</sup> /Mn <sup>2+</sup> -ATPases.....                         | 114 |
| 3.3. | Regulation of intracellular Ca <sup>2+</sup> /Mn <sup>2+</sup> transporters and some channels.....   | 123 |

**Chapter 3: TMEM165 and Gdt1p: between glycosylation and Ca<sup>2+</sup>/Mn<sup>2+</sup>/H<sup>+</sup> homeostasis: what would be their biological function(s)? .....131**

|      |  |     |
|------|--|-----|
| 1.   | TMEM165 at the genomic level.....  | 133 |
| 1.1. | <i>TMEM165</i> gene.....   | 133 |
| 1.2. | <i>TMEM165</i> splicing leading to TMEM165 isoforms.....                                 | 133 |
| 1.3. | <i>TMEM165</i> patients' mutations.....  | 134 |
| 2.   | TMEM165 and Gdt1p at the protein level.....  | 135 |
| 2.1. | TMEM165 and Gdt1p topologies.....  | 135 |
| 2.2. | The Uncharacterized Protein Family 0016 (UPF0016).....                                   | 137 |
| 2.3. | TMEM165 and Gdt1p subcellular localization(s).....                                       | 144 |
| 2.4. | TMEM165 and Gdt1p stabilities.....   | 144 |
| 3.   | Insights into TMEM165 and Gdt1p biological functions.....                                | 146 |
| 3.1. | TMEM165/Gdt1p involvements in pH and Mn <sup>2+</sup> /Ca <sup>2+</sup> homeostasis..... | 146 |
| 3.2. | TMEM165 and Gdt1p involvements in glycosylation.....                                     | 154 |

**Results .....163**

|    |   |     |
|----|---|-----|
| 1. | Part I: Insights into the Mn <sup>2+</sup> -induced Golgi glycosylation rescues in TMEM165 KO HEK cells.....  | 165 |
|    | Paper 1: Involvement of thapsigargin and cyclopiazonic acid sensitive pumps in the rescue of TMEM165-associated glycosylation defects by Mn <sup>2+</sup> ..... | 167 |
|    | Paper 2: FBS impacts the observed N-glycosylation defects in TMEM165 KO HEK cells.....  | 188 |

|   |            |
|---|------------|
| <b>General discussion and perspectives on Part I .....</b>  | <b>201</b> |
| 2. Part II: Investigating the functional link between TMEM165/Gdt1p and SPCA1/Pmr1p .....               | 219        |
| Paper 3: Investigating the function of Gdt1p in yeast glycosylation .....                               | 219        |
| Paper 4: Investigating the functional link between TMEM165 and SPCA1 .....                              | 219        |
| <b>General discussion and perspectives on Part II.....</b>  | <b>259</b> |
| <br>  |            |
| <b>General conclusion .....</b>   | <b>267</b> |
| 1. Role of TMEM165/Gdt1p in Golgi glycosylation .....   | 269        |
| 1.1. TMEM165 in Golgi glycosylation.....  | 269        |
| 1.2. Gdt1p in Golgi glycosylation.....  | 273        |
| 1.3. Differences between TMEM165 and Gdt1p in Golgi glycosylation .....                                 | 274        |
| 2. TMEM165/Gdt1p as Golgi Mn <sup>2+</sup> sensitive proteins .....                                     | 275        |
| 3. TMEM165 and Golgi ion homeostasis: Mn <sup>2+</sup> , Ca <sup>2+</sup> and... H <sup>+</sup> ! ..... | 277        |
| 4. TMEM165 and SPCA1 in human related diseases.....   | 280        |
| 4.1. TMEM165 and SPCA1 deficiencies .....   | 280        |
| 4.2. TMEM165 and SPCA1 overexpression in cancers .....  | 281        |
| <br>  |            |
| <b>References.....</b>  | <b>283</b> |
| <br>  |            |
| <b>Appendix.....</b>  | <b>311</b> |



## Table of figures and tables

### 1. Figures

|   |    |
|---|----|
| <b>Figure 1:</b> Simplified representation of the secretory pathway in yeast <i>Saccharomyces cerevisiae</i> and in mammalian cells.....  | 5  |
| <b>Figure 2:</b> Schematic representation of two models for membrane trafficking through the Golgi apparatus: cisternal maturation model and vesicular transport model. Inspired from [7]. .....            | 7  |
| <b>Figure 3:</b> Simplified overview of Golgi ion homeostasis regulation. ....  | 9  |
| <b>Figure 4 :</b> Key players required during a glycosylation reaction in the lumen of the Golgi apparatus in yeast (A.) and human (B.). ....   | 16 |
| <b>Figure 5:</b> Formal nomenclature for the glycosyltransferases (GTs) applied to one of them. ....  | 18 |
| <b>Figure 6:</b> Topologies of human ER and Golgi glycosyltransferases. . ....  | 19 |
| <b>Figure 7:</b> Simplified overview of the biosynthesis pathways yielding the production of the nine NM/DP-sugars involved in human N-linked glycosylation process.. ....                                  | 22 |
| <b>Figure 8:</b> Schematic representation of the initiation sites (core glycan structure, upper panel) and maturation of human glycan structures associated with the different glycosylation pathways. .... | 27 |
| <b>Figure 9:</b> Schematic representation of the initiation sites and maturation of yeast glycan structures associated with the different glycosylation pathways. ....                                      | 30 |
| <b>Figure 10:</b> Main N-glycan structures found on yeast <i>Saccharomyces cerevisiae</i> and human N-glycoproteins. ....   | 31 |
| <b>Figure 11:</b> Dolichol cycle initiating the N-linked glycosylation process in human and yeast <i>Saccharomyces cerevisiae</i> . ....  | 34 |
| <b>Figure 12:</b> Subunit organization of human and yeast <i>Saccharomyces cerevisiae</i> oligosaccharyltransferase (OST) complex.....  | 35 |
| <b>Figure 13:</b> ER quality control for N-glycoproteins in yeast <i>Saccharomyces cerevisiae</i> and human cells. . .  | 41 |
| <b>Figure 14:</b> Processing and maturation of yeast <i>Saccharomyces cerevisiae</i> N-glycans in the Golgi apparatus. ....   | 43 |
| <b>Figure 15:</b> Processing and maturation of a human biantennary complex N-glycan in the Golgi apparatus. ....  | 45 |
| <b>Figure 16:</b> Initiation of the different branches found in human complex N-glycans following the action of GnTs. ....  | 46 |
| <b>Figure 17:</b> Human N-glycoproteins and free oligosaccharides (FOS) catabolism. ....  | 49 |
| <b>Figure 18:</b> Overview of the N-linked glycosylation pathway in human and yeast <i>Saccharomyces cerevisiae</i> . ....  | 51 |

|   |     |
|---|-----|
| <b>Figure 19:</b> Main Ca and Mn storage organs and organelles in human and yeast. ....   | 56  |
| <b>Figure 20:</b> Simplified representation of calcium (Ca) regulation in human. ....   | 59  |
| <b>Figure 21:</b> Simplified representation of manganese (Mn) metabolism in human. ....   | 60  |
| <b>Figure 22:</b> Post-Albers cycle generalized for P-type ATPases. ....  | 69  |
| <b>Figure 23:</b> Interconnection between SLC30A10, SLC39A14 and SLC39A8 functions in regulating Mn homeostasis in enterocytes and hepatocytes.. ....                               | 92  |
| <b>Figure 24:</b> Schematic diagram illustrating the three states of an ion channel (here, a voltage-gated ion channel). ....   | 99  |
| <b>Figure 25 :</b> The CRAC channel STIM1/Orai1: structure and simplified mechanism of activation....   | 101 |
| <b>Figure 26:</b> Schematic representation of the mammalian VGCC. ....  | 106 |
| <b>Figure 27:</b> Subcellular localization of the main actors involved in Mn <sup>2+</sup> homeostasis in yeast <i>Saccharomyces cerevisiae</i> and humans. ....                    | 112 |
| <b>Figure 28:</b> Subcellular localization of the main actors involved in Ca <sup>2+</sup> homeostasis in yeast <i>Saccharomyces cerevisiae</i> and humans. ....                    | 113 |
| <b>Figure 29:</b> Simplified representation of PMCA autoinhibited and activated states mediated by CaM-binding domain and elevation of cytosolic Ca <sup>2+</sup> levels. ....      | 115 |
| <b>Figure 30:</b> Schematic representation of SPCA2-Orai1 interaction. ....   | 120 |
| <b>Figure 31:</b> Schematic representation of SPCA1 interaction with ADF/Cofilin 1 for subsequent Cab45-dependent sorting at the TGN. ....  | 121 |
| <b>Figure 32:</b> Schematic representation of Smf1p regulation and relocalization mediated by changes in Mn levels (inspired by Culotta et al. [336]). ....                         | 124 |
| <b>Figure 33:</b> Simplified overview of Smf1p and Smf2p localization and redistribution upon surrounding changes in Mn levels. ....  | 125 |
| <b>Figure 34:</b> Simplified illustration of the Ca <sup>2+</sup> - CaM/Calcineurin/Crz1p pathway involving Pmc1p, Pmr1p, Rch1p and Vcx1p. ....                                     | 127 |
| <b>Figure 35:</b> <i>TMEM165</i> genomic localization and organization leading to WT-TMEM165 transcript...  | 133 |
| <b>Figure 36:</b> <i>TMEM165</i> alternative splicing variants generating the short-form (SF) and long-form (LF) isoforms of TMEM165. ....  | 134 |
| <b>Figure 37:</b> TMEM165 predicted topology highlighting its conserved domains. ....   | 136 |
| <b>Figure 38:</b> Protein sequence alignment of TMEM165 and Gdt1p, adapted from [66]. ....  | 137 |
| <b>Figure 39:</b> Common predicted topology of the Metoza and Fungi eukaryotic UPF0016 subfamilies X and XI. ....   | 138 |
| <b>Figure 40:</b> Subcellular localization and putative function of PAM71 and CMT1 in the regulation of Mn <sup>2+</sup> /Ca <sup>2+</sup> homeostasis within the chloroplast. .... | 141 |



|   |     |
|---|-----|
| <b>Figure 41:</b> Subcellular localization(s) and function of SynPAM71 in the regulation of Mn <sup>2+</sup> homeostasis. ....  | 143 |
| <b>Figure 42:</b> Site-directed mutagenesis of TMEM165.....   | 145 |
| <b>Figure 43:</b> Site-directed mutagenesis of Gdt1p. ....  | 148 |
| <b>Figure 44:</b> Putative involvement of TMEM165 as a Ca <sup>2+</sup> , Mn <sup>2+</sup> and H <sup>+</sup> transporter supporting lactose biosynthesis during milk production in mammary glands in lactation (inspired from Snyder <i>et al.</i> ). .. | 151 |
| <b>Figure 45:</b> Putative role of TMEM165 in Golgi Mn <sup>2+</sup> homeostasis in physiological conditions and in case of Mn <sup>2+</sup> excess. ....   | 152 |
| <b>Figure 46:</b> Comparison between TMEM165 and Gdt1p function in Golgi glycosylation and Mn <sup>2+</sup> homeostasis. ....   | 159 |
| <b>Figure 47:</b> Impact of <i>SLC11A2</i> and <i>SLC39A14</i> silencing by siRNA on the rescue of LAMP2 glycosylation defect induced by MnCl <sub>2</sub> supplementation. ....  | 182 |
| <b>Figure 48:</b> Effect of <i>ATP2A2</i> silencing by siRNA on the rescue of LAMP2 glycosylation defect induced by MnCl <sub>2</sub> supplementation.....  | 183 |
| <b>Figure 49:</b> Potential involvement of SERCA2 pumps in cytosolic Mn <sup>2+</sup> pumping to sustain the Golgi glycosylation process in TMEM165 KO cells.....   | 184 |
| <b>Figure 50:</b> LAMP2 glycosylation defect observed in TMEM165 KO cells is no more detectable. ....   | 185 |
| <b>Figure 51:</b> Changes in cell culture conditions impact Golgi glycosylation defects associated with TMEM165 deficiency. ....  | 186 |
| <b>Figure 52:</b> Suppression of LAMP2 glycosylation defect in TMEM165 KO cells induced by change in FBS used for cell culture.....   | 187 |
| <b>Figure 53:</b> Involvement of thapsigargin- and cylopiazonic acid-sensitive pumps in Gal-induced rescue of LAMP2 glycosylation.. ....  | 204 |
| <b>Figure 54:</b> Gal pre-treatment influences Mn <sup>2+</sup> quenching observed in both control and TMEM165 KO HEK cells.....  | 205 |
| <b>Figure 55:</b> Impact of Gal and MnCl <sub>2</sub> supplementations on UDP-sugar pools in control versus TMEM165 KO HEK cells.....   | 206 |
| <b>Figure 56:</b> Indirect evidence for O-linked mucin type defects in TMEM165 KO HEK cells. ....   | 208 |
| <b>Figure 57:</b> Influence of MnCl <sub>2</sub> and/or Gal supplementations on VVL-FITC staining in TMEM165 KO HEK cells.....  | 209 |
| <b>Figure 58 :</b> Gal supplementation efficiency depends on external Mn availability. ....   | 213 |
| <b>Figure 59:</b> Gal supplementation fails to rescue TGN46 electrophoretic gel mobility in TMEM165 KO HEK cells.....   | 214 |
| <b>Figure 60:</b> Schematic representation of LAMP2 highlighting its different glycosylation sites. ....  | 215 |

|  |     |
|--|-----|
| <b>Figure 61:</b> Insights into the nature of TGN46 glycosylation sites.....   | 216 |
| <b>Figure 62:</b> Pmr1p defective mutants and associated ion pumping capacity used in the study.....   | 222 |
| <b>Figure 63:</b> Current model proposed for Gdt1p and Pmr1p function in Golgi glycosylation.....  | 234 |
| <b>Figure 64:</b> TMEM165 protein expression in SPCA1 KO HeLa and HAP1 cells..   | 237 |
| <b>Figure 65:</b> SPCA1 defective mutants and associated ion pumping capacity used in the study. ....  | 238 |
| <b>Figure 66:</b> In SPCA1 KO cells, TMEM165 expression depends on the FBS used for cell culture....   | 253 |
| <b>Figure 67:</b> Model of Mn <sup>2+</sup> -induced TMEM165 lysosomal degradation due to a lack of SPCA1. ....                                    | 254 |
| <b>Figure 68:</b> How to rescue TMEM165 abundance and Golgi subcellular localization in SPCA1 KO cells?<br>.....                                   | 255 |
| <b>Figure 69:</b> TMEM165 and GPP130 stabilities towards cytosolic or intraluminal Mn <sup>2+</sup> excess..                                       | 256 |
| <b>Figure 70:</b> Involvement of thapsigargin sensitive pumps in regulating Golgi glycosylation in SPCA1 KO<br>HeLa and Hap1 cells.....            | 262 |
| <b>Figure 71:</b> Thapsigargin induces Golgi glycosylation defect only in SPCA1 deficient Hap1 cells lacking<br>functional SPCA1 and TMEM165. .... | 263 |
| <b>Figure 72:</b> SPCA1 Mn <sup>2+</sup> pumping activity is not required to sustain glycosylation in TMEM165 KO<br>HEK cells.....                 | 264 |
| <b>Figure 73:</b> Putative models for the Mn <sup>2+</sup> -induced degradation of TMEM165.....  | 276 |
| <b>Figure 74:</b> Putative model for the Mn <sup>2+</sup> -induced degradation of Gdt1p in yeast <i>Saccharomyces cerevisiae</i> .<br>.....        | 277 |
| <b>Figure 75:</b> Importance of Golgi ion homeostasis to sustain glycosylation reactions..   | 279 |

## 2. Tables

|  |     |
|--|-----|
| <b>Table 1:</b> List of human activated sugars used by GTs as substrate donors. ....   | 17  |
| <b>Table 2:</b> Main characteristics of the three classes of human glycosyltransferases (GTs). ....  | 20  |
| <b>Table 3:</b> List of human NSTs belonging to the SLC35 family. ....   | 23  |
| <b>Table 4:</b> List of yeast <i>Saccharomyces cerevisiae</i> NSTs. ....   | 24  |
| <b>Table 5:</b> Diversity of human glycosylation pathways and associated characteristics towards their first glycosidic bonds. ....  | 28  |
| <b>Table 6:</b> Diversity of yeast glycosylation pathways and associated characteristics towards their first glycosidic bonds. ....  | 29  |
| <b>Table 7:</b> Oligosaccharyltransferase subunits and associated functions in human and yeast <i>Saccharomyces cerevisiae</i> . ....  | 36  |
| <b>Table 8:</b> List of human CDGs associated with genes encoding enzymes involved in (oligo)saccharide precursors synthesis and transfer onto protein during the N-linked glycosylation process. .... | 38  |
| <b>Table 9:</b> List of human CDGs associated with genes encoding GTs and GHs directly involved in ER trimming of N-glycans. ....  | 42  |
| <b>Table 10:</b> List of human CDGs associated with genes encoding GTs directly involved in Golgi maturation during the N-linked glycosylation process. ....   | 47  |
| <b>Table 11:</b> List of all P-type ATPases found in human and in yeast <i>Saccharomyces cerevisiae</i> . ....   | 68  |
| <b>Table 12:</b> List of human diseases related to $\text{Ca}^{2+}/\text{Mn}^{2+}$ -ATPases (P2A and P2B) and P5B-ATPases deficiencies. ....   | 80  |
| <b>Table 13:</b> Yeast and human $\text{Ca}^{2+}/\text{Mn}^{2+}$ transporters acting in $\text{Ca}^{2+}/\text{Mn}^{2+}$ homeostasis within the secretory pathway. ....                                 | 81  |
| <b>Table 14:</b> SLC30A10, SLC39A14 and SLC39A8: from systemic to intracellular regulation of Mn homeostasis. ....   | 89  |
| <b>Table 15:</b> List of human diseases related to $\text{Ca}^{2+}/\text{Mn}^{2+}$ transporters deficiencies. ....   | 98  |
| <b>Table 16:</b> Yeast and human $\text{Ca}^{2+}$ channels acting in $\text{Ca}^{2+}/\text{Mn}^{2+}$ homeostasis within the secretory pathway. ....  | 100 |
| <b>Table 17:</b> Classification of the mammalian VGCC. ....  | 107 |
| <b>Table 18:</b> List of human $\text{Ca}^{2+}$ channelopathies. ....  | 110 |
| <b>Table 19:</b> List of the main small transmembrane proteins (STMP) regulating SERCA pumps activity by direct binding. ....  | 118 |
| <b>Table 20:</b> List of reported TMEM165 patients' mutation causing a TMEM165-CDG. ....   | 135 |
| <b>Table 21:</b> List of studied UPF0016 orthologs presented in this manuscript. ....  | 140 |

|   |     |
|---|-----|
| <b>Table 22:</b> Current state-of-the-art about glycosylation defects associated with TMEM165 deficiency and effects of MnCl <sub>2</sub> and/or Gal supplementation as glycosylation suppressors. .... | 211 |
| <b>Table 23:</b> Summary about Gdt1p/TMEM165 and Pmr1p/SPCA1 involvement in Golgi glycosylation. ....   | 221 |
| <b>Table 24:</b> List of putative and known Mn <sup>2+</sup> -dependent GTs.....  | 271 |

---

## **General introduction**

---



Resulting from many years of evolution, eukaryotic cells have acquired a complex network of endomembranes forming distinct intracellular compartments; each specialized in given cellular functions. The segregation of these functions into different organelles allows cells to rapidly achieve many tasks at the same time, with a high efficiency and specificity. In mammalian cells as well as in yeast *Saccharomyces cerevisiae*, the rough endoplasmic reticulum (ER) and the Golgi apparatus are two central organelles belonging to the secretory pathway and particularly involved in proteins fate from their synthesis and post-translational modification(s) (PTMs) to their trafficking and targeting to their final destination. However, to ensure the proper realization of some specific reactions, each organelle requires a unique lumenal environment in terms of proteins, lipids, enzymes and ions that are crucial to maintain specific functions. In particular, Golgi pH and ion homeostasis are critical to preserve Golgi functions in glycosylation. Glycosylation is defined as one of the most PTMs of proteins and lipids. Well conserved between yeast *Saccharomyces cerevisiae* and human, glycosylation reactions are tightly regulated and dramatically illustrated by Congenital Disorders of Glycosylation (CDGs), a set of rare human genetic disorders related to impaired glycosylation capacities. Hereafter, some generalities about (i) the secretory pathway, (ii) the Golgi ion homeostasis maintenance and (iii) CDGs, will be provided to introduce the concepts that will be further detailed in the next chapters. In addition, from here and extended to the whole manuscript, as often as possible, a comparison between yeast *Saccharomyces cerevisiae* and mammalian (human) cells will be done. Actually, I decided to write this manuscript in a mirror fashion since my PhD dealt with both organisms.

## **1. Generalities about the secretory pathway**

In all eukaryotic cells, the secretory pathway refers to the ER, the Golgi apparatus and all the vesicles traveling in between them up to the plasma membrane. The secretory pathway is so-called since it is the primary route of secreted proteins from their synthesis in the ER to their secretion out of the cell, passing through the Golgi apparatus for potential PTMs or proteolytic cleavages. However, other proteins than secreted ones can also be processed through the secretory pathway such as soluble, membrane-bound proteins (bound to either the ER, Golgi, lysosome or plasma membrane) or resident proteins of the secretory pathways itself. In addition, apart from proteins, lipids can be synthesized and also processed in the ER and the Golgi apparatus, such as glycolipids for instance. Secretory organelles are delimited by a phospholipid bilayer, so that their own lumens never mix with the cytosol. All intracellular lumens share a common oxidative environment allowing specific lumenal biochemical reactions to occur. As an example, the oxidative environment of the ER enables protein conformational changes through disulfide bonds formation in order to achieve their final conformation.

### **1.1. The ER as a hub for (secretory) protein synthesis**

The ER is a multifunctional organelle, including secretory proteins and lipids synthesis, drug metabolism,  $\text{Ca}^{2+}$  storage and many others [1]. These various functions require the ER to be a large organelle, widely distributed into the cytosol. Its architecture is complex with both tubular and lamellar membrane structures but offers a huge functional area. Although its membrane is continuous with the outer nuclear envelope, it is not likely that proteins begin their synthesis in the nucleus. Indeed, right after DNA transcription into mRNAs in the nucleus, mRNAs are released into the cytosol where ribosomes bind them to initiate their translation into proteins. The specific translation of secretory proteins involves the recruitment of the cytosolic ribosome/mRNA/nascent polypeptide complex to the ER membrane *via* a signal sequence within the amino-terminus of the protein that is recognized and bound by the signal recognition particle (SRP). The binding of SRP then triggers the targeting of the ribosome complex to the ER membrane where SRP docks on its receptor allowing the further translation of the nascent protein through the translocon channel directly into the ER lumen. During protein synthesis, co-translational modifications may occur on the nascent polypeptide such as N-linked glycosylation (see Chapter 1). Secretory proteins then acquire their proper folding thanks to the activity of specific ER chaperones and once properly folded, they accumulate at specific ER exit sites (ERES). Also named transitional ER, ERES are discrete membrane domains where coat protein complex II (COPII)-coated vesicles form, allowing the subsequent transport of newly synthesized secretory cargo from the ER to the Golgi apparatus [2].

### **1.2. The Golgi apparatus: between protein PTMs and trafficking**

Discovered in the 1870's by Camillo Golgi, the Golgi apparatus is a central hub for membrane trafficking within the secretory pathway. In mammalian cells, the Golgi apparatus shares a ribbon-like structure made of several (3 to up to 20) stacked and polarized cisternae in a *cis-/medial-/trans-* fashion, and is found localized next to the microtubules organizing center. The Golgi apparatus received a constant flux of membranes from the ER, the endosomes and the plasma membrane, making it the most dynamic intracellular compartment with a structure in constant remodeling. This Golgi plasticity results from very complex and highly regulated interactions with the cytoskeleton. Conversely, in yeast *Saccharomyces cerevisiae*, the spatial organization of the Golgi apparatus completely differs. It is not likely organized in stacks but rather displays a scattered shape with individual cisternae throughout the cytosol (Figure 1).



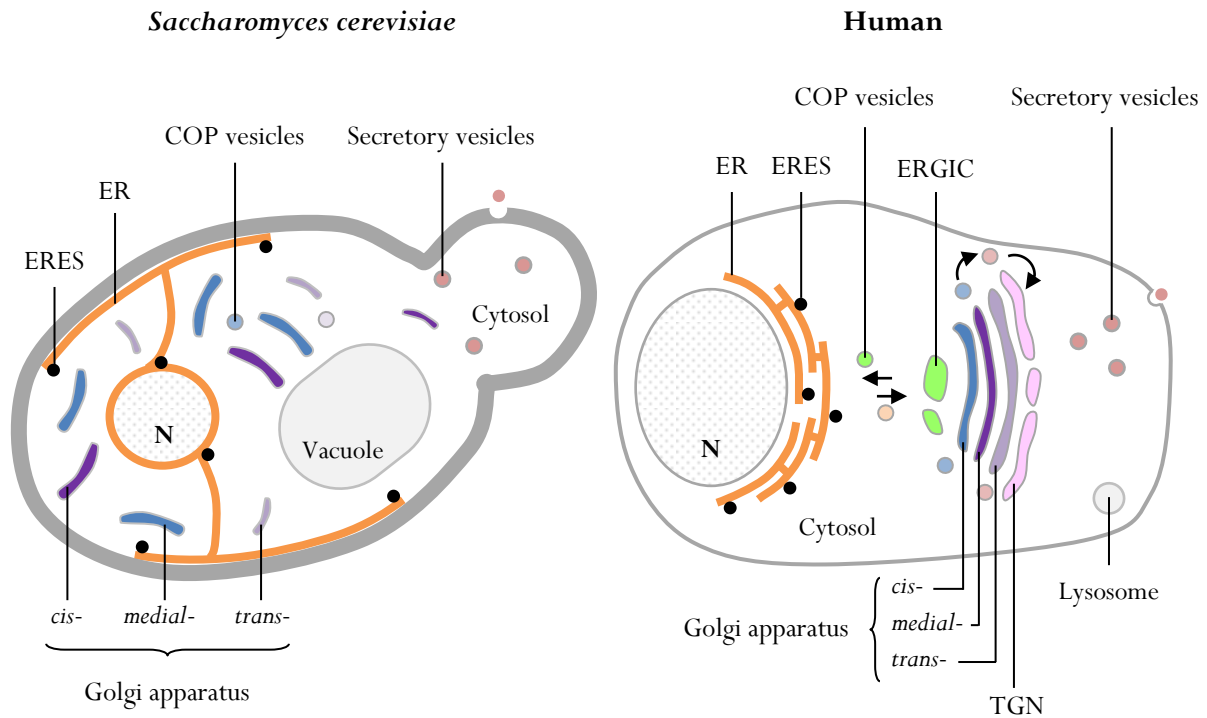


**Figure 1: Simplified representation of the secretory pathway in yeast *Saccharomyces cerevisiae* and in mammalian cells.** Inspired from [3]. The scheme points the main differences in the spatial organization of the ER and the Golgi apparatus between the two organisms. COP: coat proteins, ER: endoplasmic reticulum, ERES: ER exist site, ERGIC: ER-Golgi intermediate compartment and TGN: *trans*-Golgi network.

Another architectural difference relies in the absence of the ER-Golgi intermediate compartment (ERGIC) between the ER and the *cis*-Golgi in yeast meaning that anterograde trafficking from the ER starts directly to the *cis*-Golgi. Therefore, although Golgi functions have been roughly conserved during evolution, the structural differences of the Golgi apparatus between yeast *Saccharomyces cerevisiae* and mammals raise the question of its proper structure/function. Actually, molecular evolutionary researches assumed that ancestral unicellular eukaryotes possessed a stacked Golgi apparatus. Then, why *Saccharomyces cerevisiae* lost this stacking organization and what is the selective advantage conferred by the dispersed cisternae are opened and elusive questions [4,5]. In all eukaryotic cells, the Golgi apparatus is considered as the central hub for proteins PTMs including glycosylation, phosphorylation, methylation, sulfation, acetylation, palmitoylation and proteolytic processings [6]. In addition to protein modifications, the Golgi apparatus is responsible for sorting, targeting and packing of secretory cargo for subsequent secretion. However, before being secreted, proteins have to travel from the ER to the Golgi apparatus and then reach cell surface *via* secretory vesicles.

### 1.3. How to traffic through the Golgi apparatus?

Trafficking through the Golgi cisternae has been deeply studied in yeasts (*Saccharomyces cerevisiae* but also other species) and mammalian cells, and revealed similar and conserved mechanisms. However, depending of the Golgi dynamics, two models (amongst additional newer) have been proposed to

explain protein transport and sorting through the Golgi apparatus: the cisternal maturation model and the vesicular transport model [7] (Figure 2). Briefly, in the cisternal maturation model each Golgi cisterna is considered as a transient compartment maturing from *cis*- to *medial*- and *medial*- to *trans*-. In this model, secretory cargo remains in the cisternae during the maturation from *cis*- to *trans*- while Golgi resident proteins are sent backwards to their proper location thanks to a retrograde trafficking mediated by COPI-coated vesicles. A *trans*-cisterna then breaks down into transport carrier at the TGN to ensure protein secretion/targeting to its final destination. In this model, the cisterna is viewed as a secretory cargo carrier while COPI-coated vesicles are assumed to be enriched in Golgi resident proteins. In contrast, the vesicular transport model rather defines each Golgi cisterna as a long-living compartment in which secretory cargo are transported from a cisterna to the other *via* a COPI-mediated anterograde trafficking. In this case, resident Golgi proteins remain in their own cisterna and only secretory cargo moves forward from *cis*- to *trans*-Golgi. Comparing these two models, cisternal maturation is widely accepted over vesicular transport. However, additional models have emerged such as the partitioning model highlighting other possible ways of transport from the ER and within the Golgi apparatus. For instance, in addition to vesicles, tunnels between adjacent cisternae could also ensure large secretory cargo, especially those that do not enter into COP vesicles, to pass from one cisterna to another. In mammals, members of the TANGO1 family have been identified to initiate a tunnel between the ER and the ERGIC rather than COPII-coated vesicles [8].

Overall, a common and critical point is the proper distribution and localization of Golgi resident proteins to ensure Golgi functions by preserving the different ion, protein and lipid homeostasis of each Golgi cisterna. In case of mis-localization and/or improper distribution of the Golgi machinery, homeostasis is disrupted resulting in severe diseases [9–11]. Therefore, a balance between anterograde and retrograde trafficking has to be tightly regulated [12]. Actually, vesicle formation, tethering and fusion events within the Golgi cisternae are well orchestrated and involved several molecular players amongst Rab proteins, Soluble N-ethylmaleimide-sensitive-factor Attachment protein Receptors (SNAREs) and tethering complexes. Within the Golgi cisternae, retrograde trafficking particularly involved a multi-proteins complex named conserved oligomeric Golgi (COG) that have been extensively studied by Pr Lupashin's group [12–14]. This is particularly of interest in the manuscript since COG defects have been associated to Congenital Disorders of Glycosylation (CDG), human diseases related to impaired Golgi glycosylation reactions (see below) [15,16].

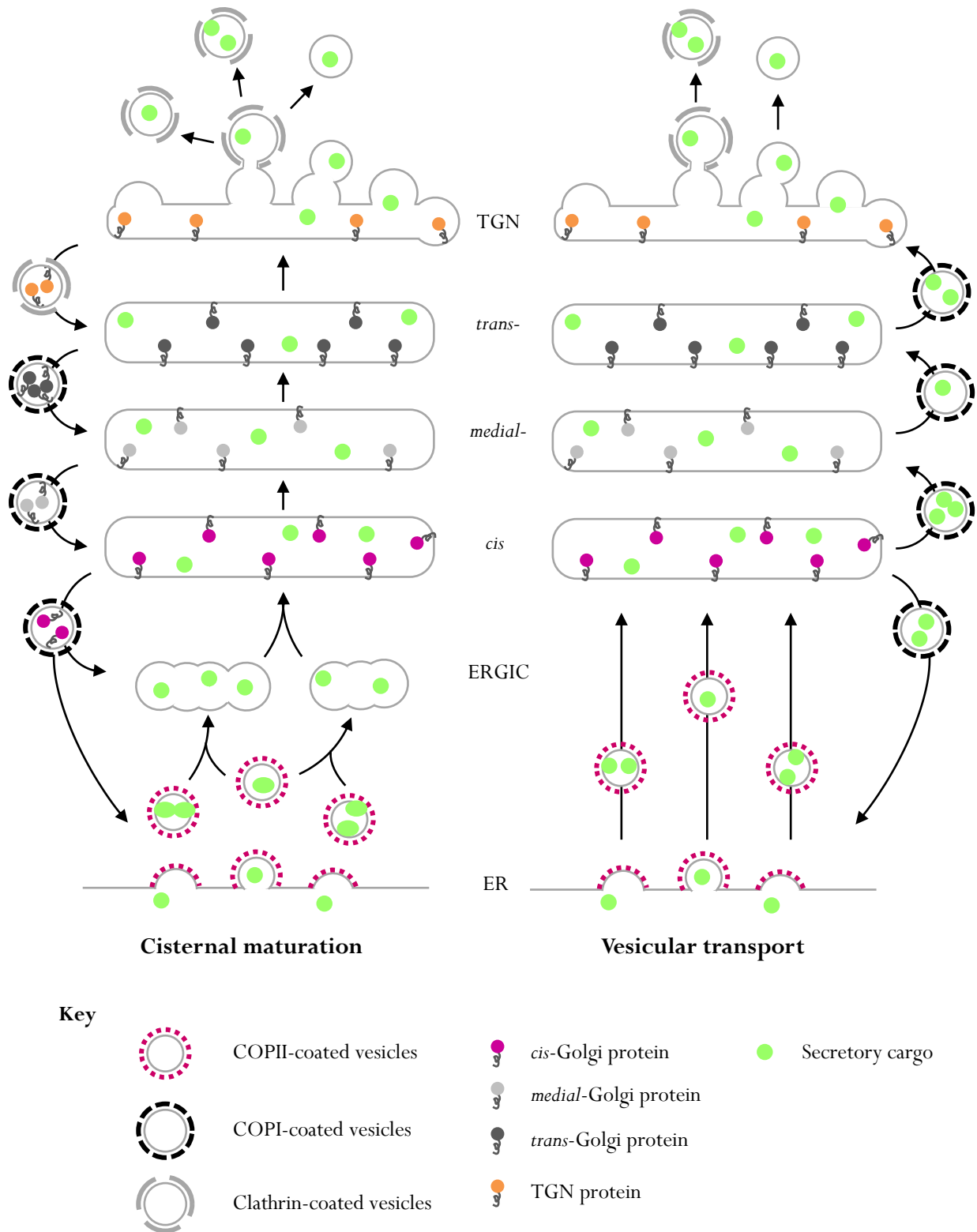


**Figure 2: Schematic representation of two models for membrane trafficking through the Golgi apparatus: cisternal maturation model and vesicular transport model. Inspired from [7].** COP: coat protein, ER: endoplasmic reticulum, ERGIC: ER-Golgi intermediate compartment and TGN: *trans*-Golgi network.

In my PhD, I focused on the maintenance of the Golgi ion homeostasis to ensure one of the main protein PTM: glycosylation. Then, I will briefly introduce (i) the key players involved in Golgi ion homeostasis maintenance and (ii) expose why this homeostasis is so important for Golgi glycosylation reactions through the pathological condition of CDGs. This part will mainly describe mammalian cell systems.

## 2. Golgi ion homeostasis

### 2.1. pH

In mammals, a decreasing resting pH gradient can be observed from the *cis*-Golgi (pH 6.7) to *medial*- (pH 6.5) and the *trans*-Golgi (pH 6.3) to reach pH 6 in the TGN [11,17–19]. How this pH gradient is established along the Golgi apparatus is unclear but might involve specific proton ( $H^+$ ) pumps, transporters or leak channels. Actually, three main transport systems have been identified: the vacuolar (V)-ATPase, the  $Cl^-/K^+$  counter ion transporter and some proton leak channels. These three ion transport systems are thought to have distinct functions in the regulation of the Golgi pH. While V-ATPases are responsible for active  $H^+$  pumping into the Golgi lumen [20], proton leak channels are assumed to send  $H^+$  back to the cytosol not to overacidify the lumen. However, as a direct consequence of the  $H^+$  pumping activity of V-ATPases, the potential of Golgi membrane increases, altering V-ATPases function up to their inhibition. Therefore,  $H^+$  import into the Golgi lumen needs to be counteracted by anion entry or cation efflux. It is likely that chloride ions ( $Cl^-$ ) are required to prevent the increase of membrane potential [17]. In this line, Maeda *et al.* identified a Golgi  $Cl^-$  channel named Golgi pH regulator (GPHR) as a key player to sustain a constant membrane potential upon  $H^+$  pumping from the V-ATPase [21]. Other studies also pinpointed the role of passive potassium ( $K^+$ ) efflux instead of  $Cl^-$  influx to counterbalanced  $H^+$  entry, that could be mediated by sodium ( $Na^+$ ) and  $K^+$  conductive channels or the  $Na^+/K^+$ -ATPase [11]. With regards to proton leak channels, despite their crucial importance in the regulation of Golgi pH, their identification remains elusive. So far, although further investigations need to be done, NHE7 and NHE8, two Golgi  $Na^+/H^+$  exchangers belonging to the family of sodium/hydrogen exchangers (NHE) are potential candidates [22–24].

It is to note that this section is not exhaustive and only highlights the main key players acting in concert to sustain Golgi pH. Many others can be found in literature [11,17,19,25] and will not be further discussed here and even not represented in Figure 3.

### 2.2. $Ca^{2+}$ , $Mn^{2+}$ and additional cations

Despite  $H^+$ , additional cations including calcium ( $Ca^{2+}$ ), manganese ( $Mn^{2+}$ ), magnesium ( $Mg^{2+}$ ), zinc ( $Zn^{2+}$ ) and copper ( $Cu^{2+}$ ) are found highly concentrated in the Golgi lumen [18,26]. While  $Ca^{2+}$  ions are required for trafficking, secretory cargoes concentration and secretion,  $Mn^{2+}$  ions are essential to sustain

glycosylation reactions since they act as cofactors of many glycosylation enzymes named glycosyltransferases. The regulation of such  $\text{Ca}^{2+}$  and  $\text{Mn}^{2+}$  homeostasis within the secretory pathway, including the Golgi apparatus, will be extensively reviewed in Chapter 2. Briefly, Golgi  $\text{Ca}^{2+}/\text{Mn}^{2+}$  import/export is regulated through the activity of many Golgi-localized pumps such as the Secretory Pathway  $\text{Ca}^{2+}/\text{Mn}^{2+}$ -ATPases 1/2 (SPCA1/2), transporters as the transmembrane protein 165 (TMEM165) and channels like the  $\text{Ca}^{2+}$ -release channel ryanodine receptor (RyR) in addition to  $\text{Ca}^{2+}$  retention by  $\text{Ca}^{2+}$ -binding proteins [26–30]. With regards to  $\text{Mg}^{2+}$ ,  $\text{Zn}^{2+}$  and  $\text{Cu}^{2+}$ : (i)  $\text{Mg}^{2+}$  is thought to be imported along the secretory pathway *via* the activity of Magnesium Transporter 1 (MagT1) likely expressed at the plasma membrane [31,32] and Membrane Magnesium Transporters 1 and 2 (MMgT1/2) expressed in post-Golgi vesicles [33], (ii)  $\text{Zn}^{2+}$  import into the Golgi lumen is mediated by members of the Zinc Transporter (ZnT) family also known as solute carrier (SLC) 30 while SLC39 family of Zinc-regulated, Iron-regulated transporter like family Protein (ZIP) send  $\text{Zn}^{2+}$  back to the cytosol [34–36], finally (iii)  $\text{Cu}^{2+}$  transport into the Golgi lumen is exclusively mediated by two P-type ATPases ATP7A and B [37].

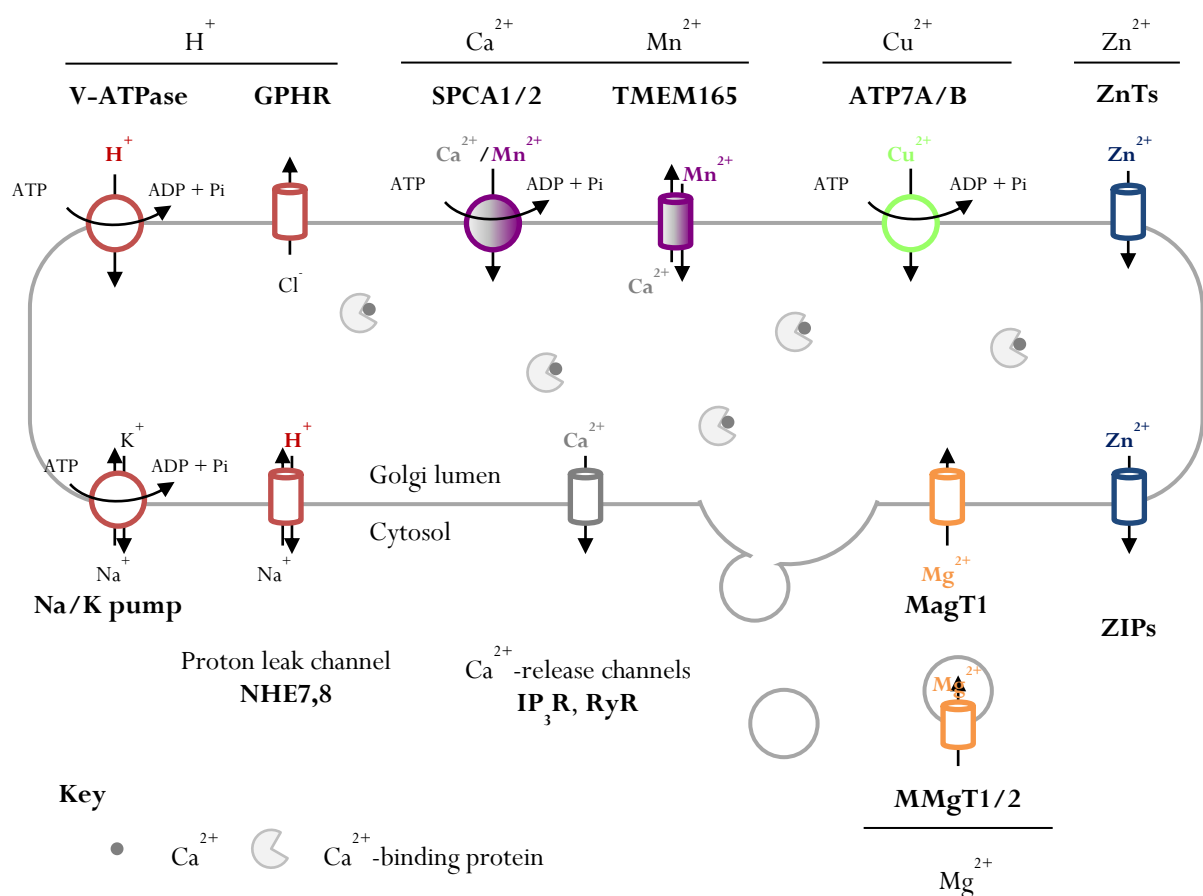


**Figure 3: Simplified overview of Golgi ion homeostasis regulation.** This scheme replaces the main key players acting in the regulation of the Golgi ion homeostasis. For simplicity reasons, the Golgi apparatus is represented as a single cisterna. However, it is to note that the subcellular localization of each pump, transporter or channel may differ from one cisterna to the other. Abbreviations are identical to the one used in the text.

A simplified overview of the Golgi cation homeostasis is depicted in Figure 3, with the same caution that Figure 3 only highlights key players and is not exhaustive. Additional information about Golgi ion homeostasis can be found in the last review of our team [38]. Given that the Golgi apparatus houses various enzymatic reactions, one can imagine that any pH modification or unbalanced ion homeostasis would affect enzymatic activities. In addition, as mentioned earlier, enzymes' mis-localization may also result in improper enzymatic activities since each Golgi cisterna has its own ion environment. As an example, consequences of such disrupted Golgi pH, ion homeostasis or impaired intravesicular trafficking result in strong alterations during the Golgi glycosylation process, a hallmark of type II CDGs. In the last part of this general introduction, I will briefly introduce what are CDGs and type II CDGs resulting from impaired Golgi homeostasis in terms of pH, structure (intravesicular trafficking) and  $Mn^{2+}$  homeostasis.

### **3. Disrupted Golgi homeostasis and CDGs**

#### **3.1. Glycosylation and CDGs**

Glycosylation is a highly conserved cellular process and by far the major PTM of proteins and lipids. For Golgi glycosylation to occur, (secretory) proteins must correctly travel from the ER to the different cisternae of the Golgi apparatus where distinct sugar residues (also called monosaccharides) are sequentially added (one by one) onto the protein to yield various and complex glycan structures. Glycosylation corresponds to a series of enzymatic reactions requiring donor substrates (nucleotide sugars) and acceptor substrates (the protein to be glycosylated) to be fully efficient. In this way, the correct subcellular localization of each glycosylation enzymes as well as the trafficking of the glycosylated protein and the targeting of nucleotide sugar transporters to the correct Golgi cisternae are crucial to ensure each glycosylation reaction. Therefore, the intravesicular trafficking within the Golgi apparatus and the correct delivery of the glycosylation machinery to each Golgi compartment is essential for the Golgi glycosylation process to be fully achieved. Moreover, as already mentioned, in addition to gather the entire glycosylation machinery close enough in the same cisterna; the luminal environment of each Golgi compartment is also essential. Together, proteins involved in vesicular trafficking and in the regulation of Golgi ion homeostasis sustain trafficking of the glycosylation machinery and proper ion environment that subsequently enable efficient glycosylation reactions. However, in some instances, pathogenic mutations in genes encoding such proteins can result in strong Golgi glycosylation deficiencies characterizing a type II Congenital Disorders of Glycosylation (CDG). These specific subtypes of CDGs have been particularly well investigated over the last decade and the three following sections will retrace the main outcomes for some of them. Here again, a brief description will be given

since I will join to this manuscript a complete review on the topic that I have written in French six months ago (Appendix I). In addition, the last review of Peter Linders also provides an excellent overview of the current knowledge about CDGs and membrane trafficking associated with a beautiful iconography: [39].

### **3.2. Membrane trafficking in CDGs**

In this first section, I decided to highlight one the main CDGs related to impaired intravesicular trafficking: the COG-CDGs. As briefly mentioned earlier, according to the cisternal maturation model for Golgi trafficking (Figure 2), a retrograde COPI-mediated intravesicular trafficking occurs within the Golgi compartment. The major function of these vesicles is to transport and recycle enzymes in specific Golgi cisternae. Over the past decade, substantial work on the proteins of the Conserved Oligomeric Golgi or COG complex pinpointed its crucial role in retrograde Golgi trafficking as a multi-protein tethering complex enabling the anchoring of COPI-coated vesicles to the Golgi membrane [40,41]. Basically, the COG complex is made of eight unique subunits (COG1 to COG8) distributed in two distinct lobes. Deeply investigated by Pr Lupashin's lab, each COG subunit directly interact with various proteins involved in intravesicular trafficking such as SNAREs, Rab GTPases and vesicle coating proteins [12,41–45]. Since pathogenic mutations affecting seven out of the eight genes encoding a COG subunit lead to a type II CDG [46–53], the critical importance of the COG complex in Golgi glycosylation was deeper investigated. Individual COG deletions cause huge morphological changes of the Golgi apparatus (fragmentation and dilatation of the cisternae) that in turn affects the glycosylation and also the endolysosomal system with an accumulation of enlarged acidic compartments named enlarged endolysosomal structures (EELs) [54]. For many years, COG deficiency were associated to the destabilization of certain proteins (so-called COG sensitive proteins) which were assumed not to be functional due to a mis-localization [13,16,55,56]. Amongst them, many glycosyltransferases were found destabilized. Recently the last studies from Pr Lupashin's group unravel part of the function of the COG complex in Golgi glycosylation. More than an abnormal subcellular localization, many glycosyltransferases were found addressed to the EELs for subsequent degradation making the COG complex a key component in glycosyltransferases intravesicular trafficking during Golgi glycosylation reactions [54].

### **3.3. Golgi pH regulation in CDGs**

Within the Golgi cisternae, a decreasing pH gradient is mainly established through the activity of the V-ATPase (Figure 3), a multi-subunit complex whose isoforms are expressed all along the secretory pathway. Given that (i) glycosylation enzymes required an optimal pH to be fully active and (ii)

intravesicular trafficking of these glycosylation enzymes also depends on the pH in each Golgi compartment, Golgi pH dysregulations are expected to alter either activities or subcellular localization of these enzymes, which in turn lead to Golgi glycosylation defects [11,19,25,57,58]. Indeed, pathogenic mutations in the genes encoding different subunits of V-ATPase cause types II CDG [9]. Discovered in 2008 by Kornak et al., *ATP6VOA2*, a gene encoding the  $\alpha_2$  subunit of the  $V_0$  domain of V-ATPase, was the first case of CDG reported as *cutis laxa* type 2 [59,60]. Mutations in *ATP6VOA2* affect the functionality of V-ATPase in Golgi acidification resulting in glycosylation abnormalities. However, why an alkalinization of the Golgi compartment impairs the Golgi glycosylation capacities is unclear. One can suppose that either an increased pH in the Golgi directly affects the enzymatic activity of the glycosyltransferases or, it might rather alter their transport up to the correct Golgi cisternae. Recently, additional mutations in genes encoding other subunits of the V-ATPase (*ATP6V1A* and *ATP6V1E1*) or accessory proteins of the V-type ATPase involved in its assembly (*ATP6AP1* and *ATP6AP2*) have also been identified as type II CDG [61–63], enlarging the number of type II CDG resulting from an impaired Golgi homeostasis/intravesicular trafficking.

### 3.4. Golgi $Mn^{2+}$ homeostasis in CDGs

As an optimal pH is required for an enzyme to be fully active, co-factors are also critical to trigger/ensure an enzymatic reaction. While many Golgi glycosylation enzymes were known to be  $Mn^{2+}$ -dependent [38] (see Table 24), no evidences about Golgi  $Mn^{2+}$  homeostasis and the glycosylation process were provided before our pioneer study on TMEM165-CDG [64–66]. In 2012, our lab identified that pathogenic mutations in *TMEM165* resulted in a type II CDG so-called TMEM165-CDG. Couple of years later, we demonstrated that the strong Golgi glycosylation defects associated with TMEM165 deficiency were due to a disrupted Golgi  $Mn^{2+}$  homeostasis. Our statements were even reinforced by the similarity of the results we obtained in yeast *Saccharomyces cerevisiae* lacking *TMEM165* ortholog, Gdt1p. In addition, and very interestingly, we also demonstrated that Golgi glycosylation defects due to TMEM165 deficiency could be suppressed by  $Mn^{2+}$  supplementation in the cell culture medium of TMEM165 deficient cell line. This observation defined the starting point of my PhD. To date, another single case of CDG resulting from intracellular  $Mn^{2+}$  deficiency has been reported in 2015 by Park et al. named SLC39A8-CDG [67]. SLC39A8, also known as ZIP8, has been described as a plasma membrane  $Mn^{2+}/Zn^{2+}$  importer. Similarly to TMEM165 deficiency, a lack of SLC39A8 drastically alters Golgi glycosylation reactions and  $Mn^{2+}$  supplementation also suppresses glycosylation defects [68].



---

**Chapter 1:**  
**ER and Golgi glycosylation pathways**  
**in yeast and human**

---



Glycosylation is a highly conserved cellular process found in every kingdoms of life and defined by far as the most complex and studied class of post-translational modifications (PTMs). Several glycosylation pathways can be found in a given organism, increasing the number, the diversity and the subsequent functions of these glycan structures. In mammals, three different types of glycosylation have been identified: (i) N-linked glycosylation, (ii) multiple O-linked glycosylations and (iii) C-mannosylation. In contrast, in the yeast *Saccharomyces cerevisiae*, no C-mannosylated proteins have been found. In this chapter, a main focus will be addressed on the N-linked glycosylation process in both yeast and human. When applicable, a parallel will be done between yeast and human to pinpoint both commonalities and differences. As the ultimate goal of this chapter, a “Glyco-ion map” will be drawn to highlight the relevance of the requirement of cation ions during this cellular process which represents one critical way of regulation. The following chapter (Chapter 2) will be entirely dedicated to the maintenance and regulation of two specific cation homeostasis within the secretory pathway ( $\text{Ca}^{2+}$  and  $\text{Mn}^{2+}$ ), including the ER and the Golgi apparatus where most of the glycosylation reactions take place.

## 1. General introduction about the glycosylation process\*

### 1.1. The glycosylation reaction

As a whole cellular process, glycosylation of proteins and lipids is a complex and non-template-driven process implying hundreds of enzymes, transporters, chaperones and lectins culminating in the sequential addition, elimination and/or modification of monosaccharides onto proteins, lipids, other monosaccharides or small molecules. More strictly, glycosylation refers to an enzymatic reaction involving a set of different key players amongst (i) glyco-enzymes: glycosyltransferases (GT) and glycosylhydrolases (GH), (ii) donor substrates such as nucleotide sugars mono/diphosphate (NM/DP-sugars), (iii) nucleotide sugars transporters (NST) and, (iv) acceptor substrates, most of the time proteins, lipids or other monosaccharides, all of them localized in close proximity to ensure the reaction. The ER and the Golgi apparatus are the two main organelles ensuring such glycosylation function in both yeast and human. These two subcellular compartments share a specific ion environment in terms of pH and divalent cation ions that are especially required for GT activity while binding covalently a monosaccharide to an acceptor molecule (Figure 4). As depicted in Figure 4, four cations transporters have been mentioned: SPCA1 and TMEM165 in human cells and Pmr1p and Gdt1p, their yeast orthologs. They are particularly involved in  $\text{Ca}^{2+}$ ,  $\text{Mn}^{2+}$  and even  $\text{H}^+$  Golgi homeostasis and will be further detailed in additional parts of this manuscript (Chapter 3 especially).

---

\* This part is a barely modified translation of a review that I have written in French for *médecine/sciences*.

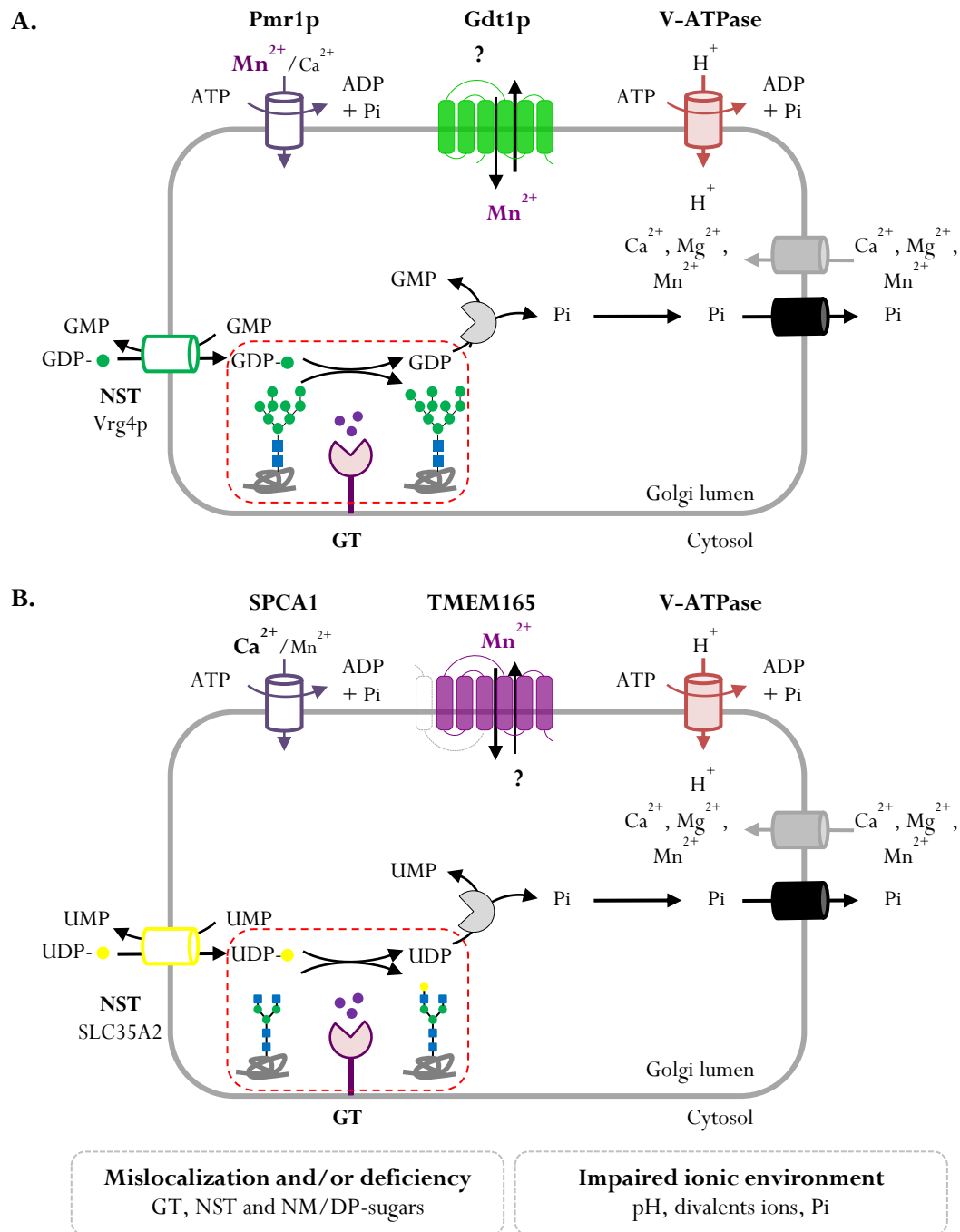


**Figure 4: Key players required during a glycosylation reaction in the lumen of the Golgi apparatus in yeast (A.) and human (B.).** The glycosylation reaction involves primary actors: an enzyme called glycosyltransferase (GT), here it is a mannosyltransferase (A.) and a galactosyltransferase (B.); a donor substrate, GDP-mannose (A.) or UDP-galactose (B.), a nucleotide sugar transporter (NST), Vrg4p (A.) or SLC35A2 (B.) and an acceptor molecule, N-glycoprotein (red dotted frames in A. and B.). These diagrams also depict secondary players involved in such glycosylation reaction. In particular, different known and unknown transporters of cations (Mn<sup>2+</sup>, Mg<sup>2+</sup>, Ca<sup>2+</sup>), protons (H<sup>+</sup>) and inorganic phosphate (Pi). **Bottom.** The gray dotted boxes highlight the main causes leading to the deregulation of the glycosylation process, leading to human congenital disorders of glycosylation. The question mark represents an ion that still needs to be identified. Purple dots above the GT symbolize Mn<sup>2+</sup> ions. Gdt1p: Gcr1 [glycolysis regulation] dependent translation factor 1, Pmr1p: plasma membrane related protein 1, SPCA1: Secretory Pathway Ca<sup>2+</sup> / Mn<sup>2+</sup> ATPase 1, SLC35A2: Solute Carrier Transporter 35A2, TMEM165: transmembrane protein 165 and Vrg4p: vanadate resistance glycosylation protein 4.

Here, as general introduction on glycosylation, I will briefly expose the main characteristics of human GT, GH and NST and then offer a panorama on the diversity of the glycosylation pathways in both yeast and human.

### 1.1.1. Human ER and Golgi glycosyltransferases (GTs)

According the Carbohydrate-Active enzyme database (CAZy, <http://www.cazy.org>) [69], human GTs are gathered in 48 distinct families. Each of these families comprises at least 1 to 35 members, yielding the total number of human GTs over than 200. In 2015, Hansen *et al.* identified 214 GTs in the human genome of which, 167 were predicted to be involved in one of the numerous glycosylation pathways [70]. To date, mutations in 58 different genes encoding human GTs have been reported to be pathogenic and responsible for a Congenital Disorder of Glycosylation (CDG) [70,71]. GTs are the key enzymes at the heart of all glycosylation reactions. Most of the time, they catalyze the group-transfer of a monosaccharide from an activated sugar donor substrate (i.e. NM/DP-sugar) to an acceptor molecule (Figure 4). NM/DP-sugar-dependent GTs are often referred to Leloir enzymes in the memory of Luis Frederico Leloir, the biochemist who discovered the first nucleotide sugar and was awarded the Nobel Prize in Chemistry in 1970. The most common nucleotide sugar donors in human (and yeast) are listed in Table 1.

**Table 1: List of human activated sugars used by GTs as substrate donors.** This table also defines the abbreviations that will be used in this manuscript to refer to monosaccharide and activated nucleotide sugars. In the last column, the three bolded NM/DP-sugars are the only ones found in yeast *Saccharomyces cerevisiae*.

| Monosaccharide ('sugar')       | Nucleotide mono/diphosphate (NM/DP) | Activated form (NM/DP-sugar) |
|--------------------------------|-------------------------------------|------------------------------|
| Glucose (Glc)                  |                                     | UDP-Glc                      |
| Galactose (Gal)                |                                     | <b>UDP-Gal</b>               |
| N-acetylglucosamine (GlcNAc)   | Uridine diphosphate (UDP)           | <b>UDP-GlcNAc</b>            |
| N-acetylgalactosamine (GalNAc) |                                     | UDP-GalNAc                   |
| Glucuronic acid (GlcA)         |                                     | UDP-GlcA                     |
| Xylose (Xyl)                   |                                     | UDP-Xyl                      |
| Mannose (Man)                  | Guanosine diphosphate (GDP)         | <b>GDP-Man</b>               |
| Fucose (Fuc)                   |                                     | GDP-Fuc                      |
| Sialic acid (Sia)              | Cytidine monophosphate (CMP)        | CMP-Sia                      |

However, in some instances, the donor substrate differs from a NM/DP-sugar and the monosaccharide is linked to a lipid moiety such as dolichol-phosphate (Dol-P) or dolichol-pyrophosphate (Dol-P-P), rather than a nucleotide. In eukaryotes, this is the case for Dol-P-Man, Dol-P-Glc and Dol-P-P-GlcNAc<sub>2</sub>Man<sub>9</sub>Glc<sub>3</sub> that are used by specific GT-C enzymes in the ER (see below) and involved in N-

glycosylation, glypiation (transfer of a glycosylphosphatidylinositol (GPI)-anchors onto a protein), O-mannosylation and C-mannosylation of proteins. In addition to their specificity towards the donor, GTs are also specific to the acceptor substrates and to the linkage of the glycosidic bond they catalyze ( $\alpha$ - or  $\beta$ - anomerism). Hence, based on the strict donor, acceptor and linkage specificity shared by most of the GTs, glyco biologists often refer to the “one glycosidic-linkage, one enzyme” as the central dogma of glyco biology. However, few exceptions to this rule exist. For instance, (i) several GTs can use the same acceptor to make the same glycosidic bonds or (ii) a single GT can catalyze more than one reaction using either the same donor substrate linked in both  $\alpha$ - or  $\beta$ - anomerism or, different donor substrates bound with the same linkage anomerism. In addition, some GTs share specific structural features like (i) two catalytic domains or, (ii) two functional sites including a lectin domain that recognizes and strongly binds to the acceptor and a catalytic domain that ensures the glycosidic bond. Nonetheless, these exceptions remain exceptions. Due to the huge number of reactions that can be catalyzed by GTs, a formal nomenclature has been established referring to both donor and acceptor substrates, linkage, activity and isomer number within a given GT family (Figure 5).

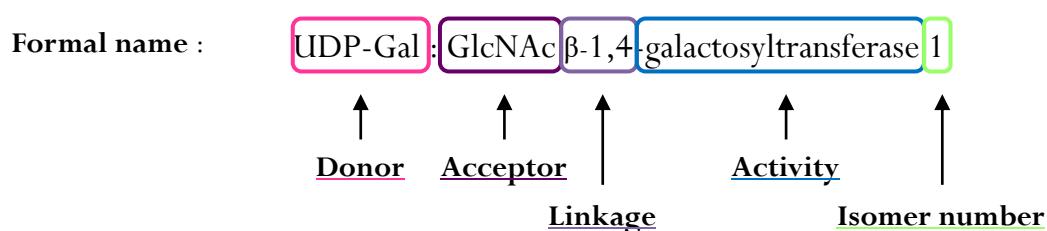


**Figure 5: Formal nomenclature for glycosyltransferases (GTs) applied to one of them.**

However, this nomenclature is poorly used and referenced since GTs are preferentially nicknamed with shorter and/or trivial names. For instance, the UDP-Gal:GlcNAc- $\beta$ -1,4-galactosyltransferase 1 is often shortened as  $\beta$ -1,4-galactosyltransferase 1 or commonly named B4GALT1 referring to the gene encoding the protein. Hence, according to author’s preferences, a given GT may share different names. This lack of systemic nomenclature may put off people to further study these enzymes, which are at the basis of glycosciences.

At the structural level, human GTs can be classified in three main classes according to their folds: GT-A, GT-B and GT-C [72–76]. Both GT-A and -B share a topology that derives from a specific structural motif named Rossmann fold (alternative  $\beta$ -sheets and  $\alpha$ -helices,  $\beta/\alpha/\beta$ ) which is commonly found in nucleotide binding proteins. Thus, GT-A and GT-B use NM/DP-sugar as donors. In addition to this Rossmann fold, GT-A possess a highly conserved DXD motif (or Asp-X-Asp, aspartic acid-any amino acid-aspartic acid) in their active site allowing the coordination of a divalent metal ion required for the stabilization of the NM/DP-sugar. Therefore, most of the GT-A are considered as metal-ion-dependent

enzymes requiring either  $Mn^{2+}$ ,  $Mg^{2+}$ ,  $Zn^{2+}$  or  $Co^{2+}$  as cofactor to fulfill their proper function. With regards to GT-B, two Rossmann-like motifs face each other, forming a cleft hosting their catalytic site (black arrow, Figure 6B.).

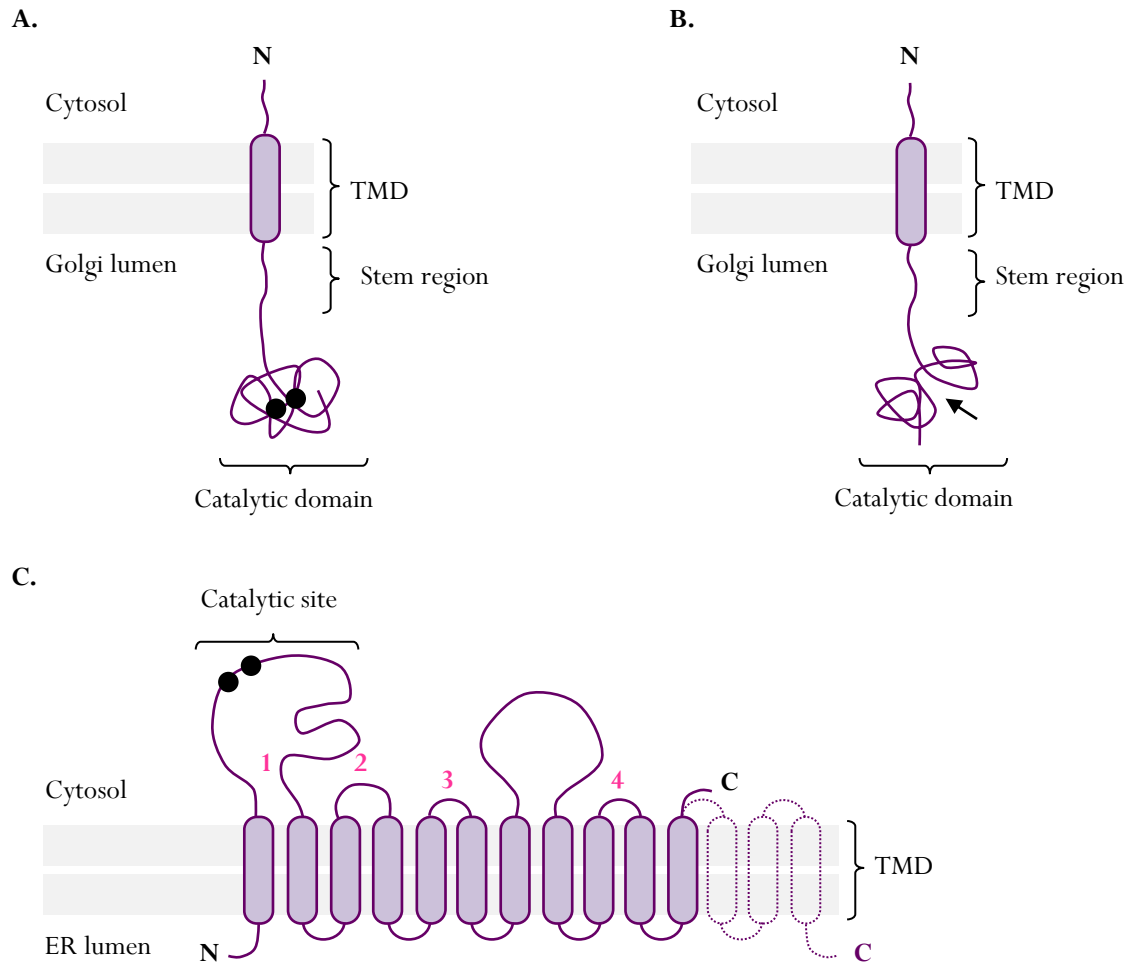


**Figure 6: Topologies of human ER and Golgi glycosyltransferases.** **A.** and **B.** Golgi-localized GT-A (**A.**) and GT-B (**B.**) display a short cytosolic amino-terminus, a single TMD, a luminal stem domain and a luminal catalytic domain containing (**A.**) or not (**B.**) a DXD motif (black circles). The black arrow indicates the catalytic site, in the cleft between the two Rossmann-like domains. **C.** All ER-localized GT-C enzymes exhibit a core membrane domain comprises 11 TMD and four conserved cytosolic loops (pink numbers). Of them, the first cytosolic loop contains a D(X)D motif (black circles), supposed to be part of the catalytic site. Additional TMD can be found at the carboxy-terminus of GT-C (dashed TMD) yielding the total number of TMD up to 14.

GT-B are generally metal-ion-independent enzymes since no DXD motif has been found in their structure. Beyond their own structural features, human GT-A and GT-B of the Golgi apparatus are all type II transmembrane proteins exhibiting (i) a short cytosolic amino-terminus, (ii) a single TMD that retains them in the Golgi apparatus, (iii) a luminal stem region and (iv) a luminal catalytic domain (Figure 6A. and B.) [77,78]. More recently, GT-C have been identified as a new structural family of GTs [72,75,76]. GT-C enzymes are hydrophobic transmembrane proteins that recognize lipid phosphate-linked sugar as donor substrate. As already mentioned, in eukaryotes such GTs act in the ER

and catalyze the transfer of mannose from Dol-P-Man, glucose from Dol-P-Glc and oligosaccharidic precursor  $\text{Glc}_3\text{Man}_9\text{GlcNAc}_2$  from Dol-P-P-GlcNAc<sub>2</sub>Man<sub>9</sub>Glc<sub>3</sub>. Hence, most of the GT-C are mannosyltransferases or glucosyltransferases. Structurally, all eukaryotic GT-C characterized so far possess a DXD or even DD motif in which aspartic acid may be replaced by glutamic acid (E). This motif belongs to the first cytosolic loop and is supposed to be part of the catalytic domain of the enzyme since it is crucial for their enzymatic activity [76,79]. Moreover, additional charged amino acids residues (arginine (R) and lysine (K)) are also found conserved in the first three and fifth predicted cytosolic loops, suggesting their involvement in substrates recognition and/or catalysis [76]. A simplified topology of GT-C enzymes is depicted in Figure 6C., inspired by [76]. A last fundamental point about GTs lies in their ability to catalyze the group-transfer of mono/oligosaccharides with either inverting or retaining the anomeric configuration of the product [73]. Hence, GTs can be classified as either inverting or retaining enzymes, depending on the outcome of the reaction. However, these two different catalytic mechanisms are not correlated to the fold-type (-A, -B or -C) of the GT since both GT-A and GT-B can be inverting or retaining enzymes [73]. All in all, as a summary of this section, Table 2 summarizes the main characteristics of human GTs according to their catalytic mechanisms, structural features, metal-ion dependency, donor substrates and the glycosylation pathways in which they are involved.

**Table 2: Main characteristics of the three classes of human glycosyltransferases (GTs).** This table summarizes some generalities about the three main classes of GTs described in the text.

| GT fold | Mechanism | Structural features   | Donor substrates                   | Glycosylation pathways                        |
|---------|-----------|---|------------------------------------|---|
| GT-A    | Inverting | 2 abutting Rossmann-like domains  | NM/DP-sugars                       | All<br>(Golgi apparatus)                      |
|         | Retaining | DXD motif<br>Metal-ion-dependent<br>Type II transmembrane protein             |                                    |   |
| GT-B    | Inverting | 2 Rossmann-like domains facing each other                                     |                                    |   |
|         | Retaining | Metal-ion-independent<br>Type II transmembrane protein                        |                                    |   |
| GT-C    | Inverting | DXD or DD motif<br>Metal-ion-dependent<br>11 TMD<br>Conserved cytosolic loops | Lipid-linked mono/oligosaccharides | N-linked, glypiation, O-/C-mannosylation (ER) |

### 1.1.2. Human glycosylhydrolases (GHs)

In contrast to GTs that contributes to the synthesis of glycan structures by adding monosaccharides, glycosidases, also known as glycosylhydrolases (GHs), remove monosaccharides to a given glycan structure. According to the CAZy database, human GHs are classified into 29 families and almost a hundreds of them have been identified [69]. Basically, GHs catalyze the hydrolysis of glycosidic bonds



between two monosaccharides or a monosaccharide and a non-carbohydrate moiety. Hence, GTs act in glycosylation while GHs ensure deglycosylation reactions. These deglycosylation steps mainly occur (i) during the folding of N-linked glycoproteins in the ER, (ii) for cytosolic and lysosomal degradation of misfolded and/or misglycosylated proteins and (iii) for lysosomal degradation of mature glycoproteins. These three different pathways will be better described in the corresponding sections 2.2.1, 2.4.1. and 2.4.2.. Most of the GHs do not share a strict specificity for their donor substrates or the linkage they cleave but all of them can act in either a retaining or an inverting mode, like GTs. In addition, some GHs preferentially cleave their substrates at their free ends (more often the non-reducing ends) while other can act in the middle of an oligosaccharidic structure. These two kinds of GHs are commonly and respectively named exoglycosidases and endoglycosidases.

### 1.1.3. Cytosolic (and nucleic) biosynthesis of human NM/DP-sugars

As described earlier, NM/DP-sugars are donor substrates for many GTs. Basically, the incorporation of monosaccharides into glycan structures first requires their activation by specific ATP-dependent kinases. Then, these “sugar phosphates” are further converted to NM/DP-sugars *via* UTP-, GTP- or CTP-dependent reactions releasing free pyrophosphates as byproducts. As depicted in Figure 7, most of the NM/DP-sugars reported in Table 1 are synthesized in the cytosol, except for the last step of CMP-Sia synthesis which is achieved in the nucleus. Before activation, the bulk of monosaccharides (*i.e.* Glc, Gal, Man, Fuc, GlcNAc, GalNAc, Sia, Xyl, GlcA) can be (i) directly imported from the diet involving plasma membrane transporters such as GLUT ones belonging to the SLC2A family of hexose transporters [80,81], (ii) synthesized *de novo* from glucose or (iii) salvaged/recycled from glycans degradation into the lysosomes [82,83]. Whatever the cellular route yielding NM/DP-sugars, their bioavailability is essential to further support all the reactions gathered under the biosynthetic umbrella of glycosylation. This has been dramatically evidenced forty years ago with the identification of the two first cases of human Congenital Disorders of Glycosylation by Prof. Jack Jaeken due to a defect in *PMM2*, the gene encoding the phosphomannomutase 2, an enzyme responsible for the conversion of mannose-6-phosphate (Man-6-P) to Man-1-P during GDP-Man synthesis [84–87]. In Figure 7, a simplified overview of the biosynthetic pathways of NM/DP-sugars is shown with examples of monosaccharide and NM/DP-sugars interconversion. All genes written in pink have been further identified in CDGs.

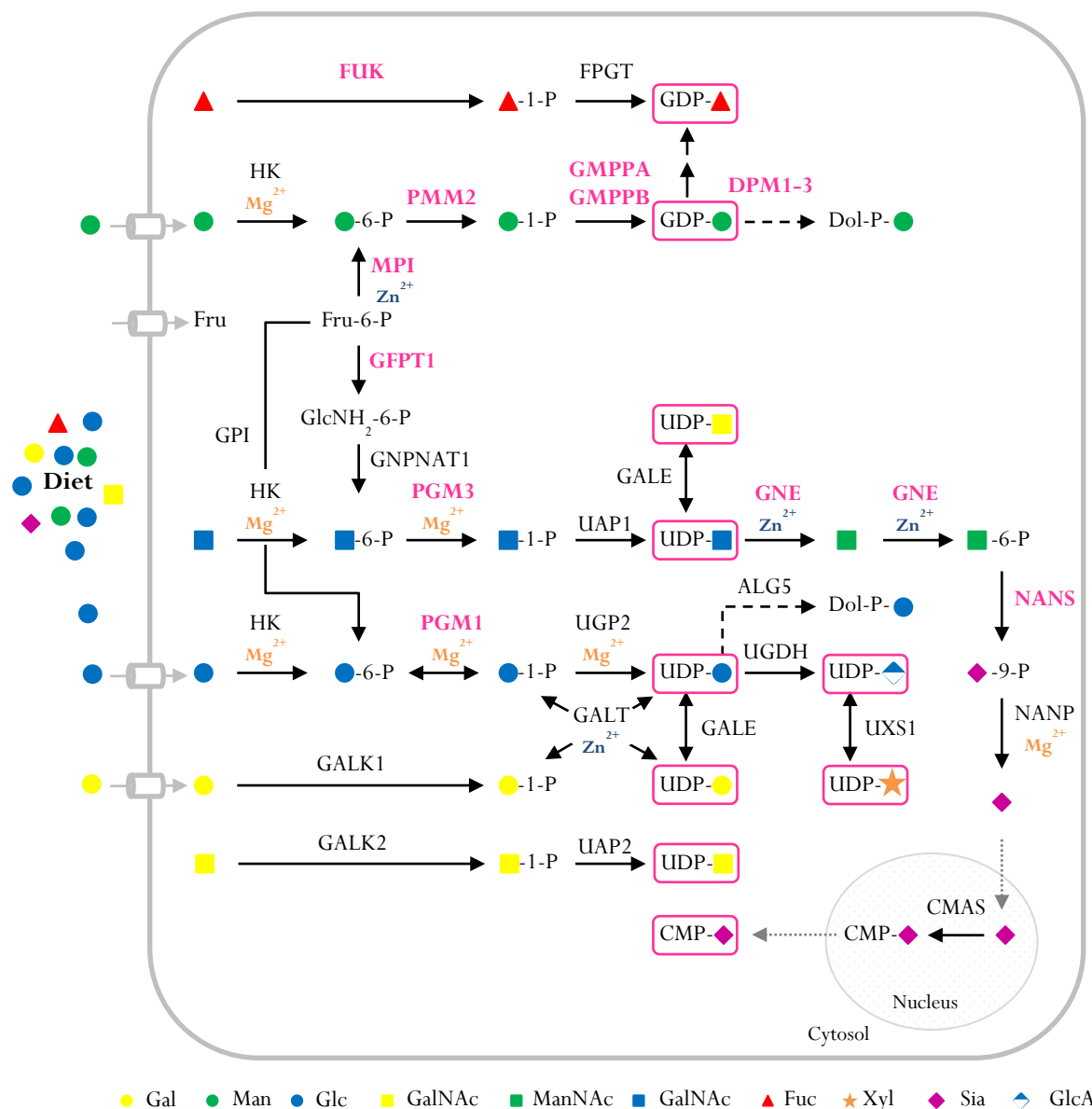


**Figure 7: Simplified overview of the biosynthesis pathways yielding the production of the nine NM/DP-sugars involved in human N-linked glycosylation process.** Monosaccharides can come from the diet and cross the plasma membrane thanks to members of the hexose transporter family named GLUTX and encoded by *SLC24X*. Then, a set of cytosolic enzymatic reactions (except for the last step of the CMP-Sia synthesis that occurs in the nucleus) leads to the production of the nine NM/DP-sugars used during human N-linked glycosylation (pink frames). The name of each gene encoding enzymes responsible for a reaction is mentioned above the corresponding arrow. Some enzymes need specific divalent ions as cofactors that are mentioned in orange or blue, under the name of the corresponding gene. Genes written in pink have been identified in CDG. The abbreviations used for the key have been defined in Table 1. ALG5: asparagine-linked glycosylation protein 5, CMAS: CMP-sialic acid synthetase, DPM1-3: dolichol-phosphate mannosyltransferase subunit 1 to 3, FPGT: fucose-1-phosphate guanylyltransferase, Fru: fructose, FUK: L-fucose kinase, GALE: UDP-galactose 4' epimerase, GALK: galactokinase, GALT: galactose-1-phosphate uridylyltransferase, GFPT1: glutamine fructose-6-phosphate aminotransferase 1,  $\text{GlcNH}_2$ : glucosamine, GMPPA/B: mannose-1-phosphate guanylyltransferase  $\alpha/\beta$ , GNE: bifunctional UDP-GlcNAc 2' epimerase/ManNAc kinase, GNPAT1: glucosamine-6-phosphate N-acetyltransferase, GPI: glucose-6-phosphate isomerase, HK: hexokinase, MPI: mannose-6-phosphate isomerase, NANP: N-acylneuraminic acid-9-phosphatase, NANS: N-acetylneuraminidic acid synthase, PGM1: phosphoglucomutase 1, PGM3: phosphoacetylamine mutase, PMM2: phosphomannomutase 2, UAP1/2: UDP-N-acetylhexosamine pyrophosphorylase 1/2, UGDH: UDP-glucose-6-dehydrogenase, UGP1/2: UDP-glucose pyrophosphorylase 1/2 and UXS1: UDP-glucuronic acid decarboxylase.

#### 1.1.4. ER and Golgi nucleotide sugars transporters (NST)

As mentioned in Figure 4, each glycosylation reaction depends on the activity of specific GTs requiring both acceptor and donor substrates to be active. Regarding to NM/DP-sugar-dependent GTs, NM/DP-sugars need to translocate from the cytosol where they are synthesized (except CMP-Sia, Figure 7) to the ER/Golgi lumen in order to be used by GTs. This transport is mediated by specific nucleotide sugar transporters (NSTs) in both yeast and human cells. A list of human and yeast *Saccharomyces cerevisiae* NSTs is provided respectively in Table 3 and Table 4 according to NM/DP-sugar substrates and subcellular localization. Particularly, human NSTs are multi-spanning transmembrane proteins belonging to the well conserved Solute Carrier 35 (SLC35) family [88–94]. This family is divided into seven subfamilies (A to G) each of them containing one or more members. To date, only SLC35A-D have been well characterized while SLC35E-G are still referred to orphan solute carriers [93]. NSTs are antiporters that mediate the import of cytosolic NM/DP-sugar in the ER/Golgi lumen in exchange for the export of the corresponding luminal NMP. All NSTs share common kinetic properties [91,94], one of them is to be competitively inhibited by the corresponding NDP or NMP but not by the free monosaccharide. NSTs were first thought to have an absolute substrate specificity towards the NM/DP-sugar they translocate but further *in vitro* investigations revealed a multi-substrate transport activity for some of them (Table 3) [91,93]. For instance, while SLC35C1 specifically transports CMP-Sia, SLC35A2 has been shown to be a dual transporter of both UDP-GlcNAc and UDP-Gal. The other way around, a specific NM/DP-sugar can be transported by several NST such as UDP-GlcNAc which is carried out by SLC35A2, SLC35A3, SLC35B4 and SLC35D2 (Table 3). According to the higher number of NM/DP-sugars used by human GTs compared to yeast ones (Table 1), it is not surprising that human cells express a higher number of NSTs (Table 3). The crucial importance to express functional NST is dramatically illustrated in humans by the identification of four CDGs related to defects in one of the four genes encoding the corresponding NST highlighted in Table 3.

**Table 3: List of human NSTs belonging to the SLC35 family.** Transporters written in pink have been identified in CDG. Abbreviations used in this table have been previously defined in Table 1. Sub.: subcellular.

| SLC name       | Common name                     | Substrate            | Sub. localization |
|----------------|---------------------------------|----------------------|-------------------|
| <b>SLC35A1</b> | CMP-Sia transporter             | CMP-Sia              | Golgi             |
| <b>SLC35A2</b> | UDP-Gal transporter             | UDP-Gal; UDP-GlcNAc  | ER/Golgi          |
| <b>SLC35A3</b> | UDP-GlcNAc transporter          | UDP-GlcNAc           | Golgi             |
| <b>SLC35B4</b> | UDP-Xyl transporter             | UDP-Xyl; UDP-GlcNAc  | ER/Golgi          |
| <b>SLC35C1</b> | GDP-Fuc transporter             | GDP-Fuc              | Golgi             |
| <b>SLC35D1</b> | UDP-GlcA/UDP-GalNAc transporter | UDP-GlcA; UDP-GlcNAc | ER                |
| <b>SLC35D2</b> | UDP-GlcNAc/UDP-Glc transporter  | UDP-GlcNAc; UDP-Glc  | Golgi             |

In yeast *Saccharomyces cerevisiae*, only three NSTs have been identified so far: (i) Vrg4p (vanadate resistance glycosylation protein 4) [95], Yea4p [96] and Hut1p (homolog of UDP-Gal transporter protein 1) [97] (Table 4). Each of them transport one of the three NM/DP-sugars required for yeasts GTs activity *i.e.* GDP-Man, UDP-GlcNAc and UDP-Gal respectively (Table 1).

**Table 4: List of yeast *Saccharomyces cerevisiae* NSTs.** Abbreviations used in this table have been previously defined in Table 1.

| Gene/protein name | Common name            | NM/DP substrate | Subcellular localization |
|-------------------|------------------------|-----------------|--------------------------|
| <i>VRG4/Vrg4p</i> | GDP-Man transporter    | GDP-Man         | Golgi                    |
| <i>YEA4/Yea4p</i> | UDP-GlcNAc transporter | UDP-GlcNAc      | ER                       |
| <i>HUT1/Hut1p</i> | UDP-Gal transporter    | UDP-Gal         | Golgi                    |

However, it is to note that in yeast *Saccharomyces cerevisiae* no endogenous galactosyltransferases have been identified so far and very few reports demonstrated the presence of galactose residues in their glycoconjugates suggesting a lack of proper galactosylation pathway in this yeast strain. Hence, the characterization of Hut1p as a UDP-Gal transporter has been done in *Saccharomyces cerevisiae* expressing the gene *gma12<sup>+</sup>*, derived from another yeast strain (*Schizosaccharomyces pombe*) and encoding a galactosyltransferase. Overexpressing *HUT1* in such yeast background resulted in a significant increase in *in vitro* UDP-Gal transport activity together with enhanced galactosylated glycoconjugates at the cell surface assuming a role for Hut1p as a UDP-Gal transporter in the yeast *Saccharomyces cerevisiae*. Actually, the major modification in yeasts remains mannosylation, occurring during both ER and Golgi N-glycosylation, glypiation, O-glycosylation and glycosphingolipids synthesis. Besides, one of the major differences between yeast and human lies in the ability of yeast cells to import GDP-Man into the Golgi lumen to ensure Golgi mannosylation whereas human cells lack both Golgi mannosyltransferases and GDP-Man transporter.

## 1.2. Diversity of the glycosylation pathways in yeast *Saccharomyces cerevisiae* and human

In both yeast *Saccharomyces cerevisiae* and human cells, several glycosylation pathways occur simultaneously increasing the diversity of the glycans structures carried by proteins/lipids. As reported in Table 5, Table 6, Figure 8 and Figure 9, each of these glycosylation pathways (i) is initiated by a specific glycosidic linkage between the first mono/oligosaccharide and the acceptor substrate and (ii) takes place in a specific cellular environment. Three major types of glycosylation can be distinguished: (i) **N-linked glycosylation** is defined by the linkage of the oligosaccharidic precursor  $\text{Glc}_3\text{Man}_9\text{GlcNAc}_2$  to the amide group of an asparagine residue (Asn, N) belonging to the consensus

sequence Asn-X-Ser/Thr (where X can be any amino acid except proline), (ii) **O-linked glycosylation** refers to the linkage of a monosaccharide (Glc, Gal, GlcNAc, GalNAC, Man, Xyl, Fuc) to the hydroxyl group of a serine (Ser, S) a threonine (Thr, T), an hydroxyl lysine residue or the first carbon (C1) of a ceramid and (iii) **C-linked glycosylation** or C-mannosylation corresponds to the linkage of a single mannose residue to the second carbon (C2) of a tryptophan residue (Trp,W) belonging to this sequence: Trp-X-X-Trp (where X can be any amino acid). As a last type of glycosylation, **glypiation** includes the synthesis of a given glycolipid commonly named glycosylphosphatidylinositol (GPI)-anchor on which a protein is then attached. Considering one glycosylation pathway amongst other implies to take into account the specific cellular environment where glycoconjugates are synthesized. In both human and yeast cells, the ER and the Golgi apparatus are the two main hubs for protein/lipids glycosylation. Moreover, intrinsically to each glycosylation pathway, some of them are exclusively performed in the ER or in the Golgi apparatus while other, like the N-linked glycosylation process requires both organelles to be proceeded (Table 5, Table 6, Figure 8 and Figure 9). To add an extra layer of complexity, a given glycoprotein can share different glycosylated forms resulting from macro- and microheterogeneity events. Particularly well-described for the N-linked glycosylation, macroheterogeneity refers to the presence or absence of a glycan structure at a specific glycosylation site while microheterogeneity corresponds to the presence of different glycan structures at a given glycosylation site.



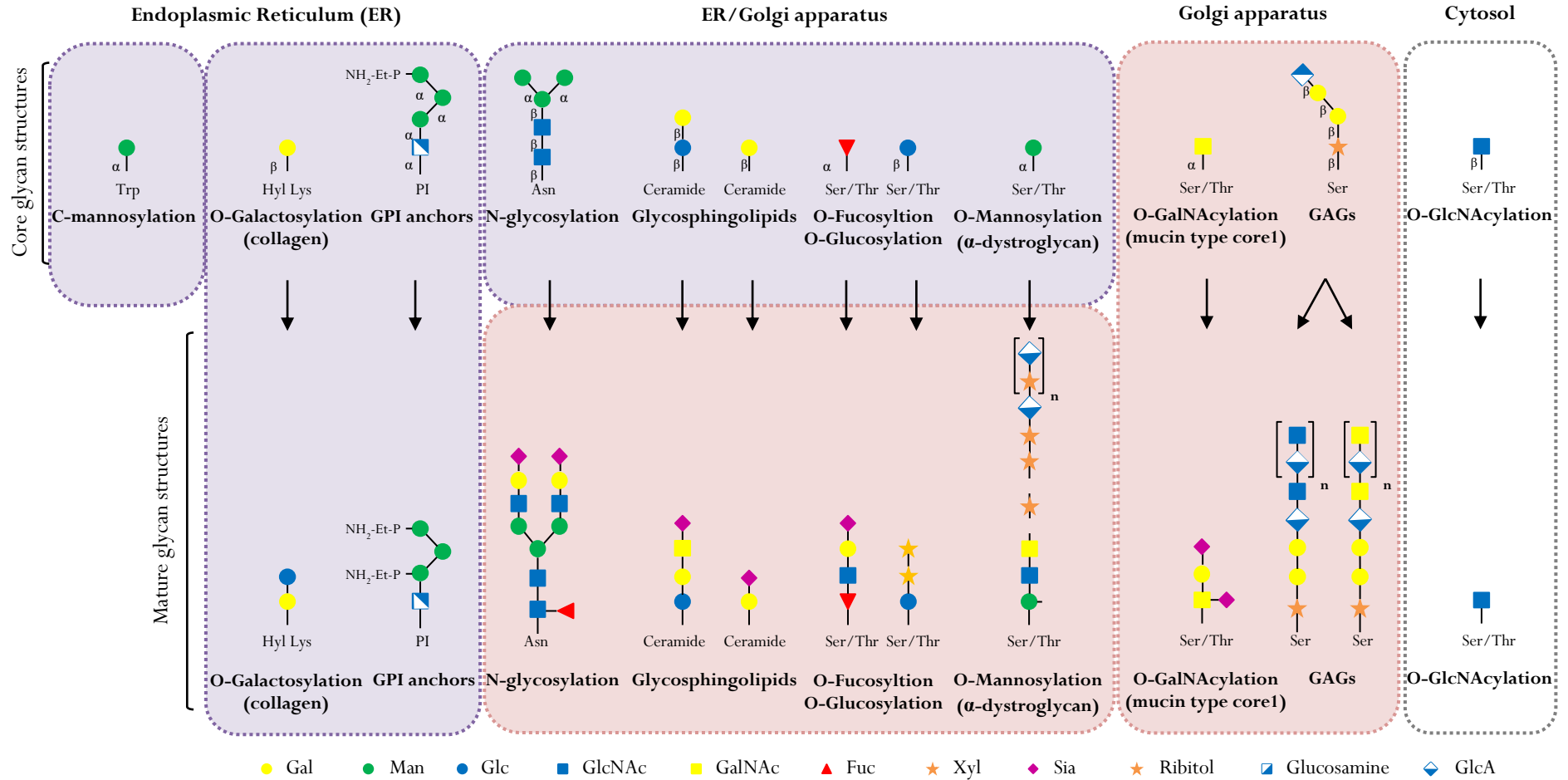


**Figure 8: Schematic representation of the initiation sites (core glycan structure, upper panel) and maturation of human glycan structures associated with the different glycosylation pathways.** ER and Golgi compartments are schematically represented by the purple and pink dotted boxes, respectively. On the right, the cytoplasmic glycosylation pathway is also shown in the gray dotted frame. The nature of the different bonds has been omitted in the lower panel representing mature glycan structures for better readability.  $\alpha$  and  $\beta$  symbolize linkage anomerism. Abbreviations used for the key have been defined in Table 1. Asn: asparagine,  $\text{NH}_2\text{-Et-P}$ : phosphatidylethanolamine, GAGs: glycosaminoglycans, GPI: glycosylphosphatidyl inositol, Hyl Lys: hydroxylysine, n: number of pattern repeats, P: phosphate, PI: inositol phosphate, Ser: serine, Thr: threonine, Trp: tryptophan.

**Table 5: Diversity of human glycosylation pathways and associated characteristics towards their first glycosidic bonds.** First glycosidic bonds between the mono/oligosaccharide and the acceptor donor are reported with the associated peptide motif, the GTs involved and the subcellular (Sub.) localization of the reaction. DPM2: dolichol phosphate-mannose biosynthesis regulatory protein, DPYL: dumpy-like, EGF: epidermal growth factor, GAGs: glycosaminoglycans, GPI: glycosylphosphatidylinositol, Hyl: hydroxyl lysine PI: phosphatidylinositol and TSR: thrombospondin type 1 repeat.

| Glycosylation pathways              | First glycosidic bond  | Peptide motif  | First glycosidic bond   |                               |
|-------------------------------------|--|--|---|-------------------------------|
|                                     |  |  | GTs involved  | Sub. localization             |
| <b>N-linked glycosylation</b>       | Glc <sub>3</sub> Man <sub>9</sub> GlcNAc <sub>2</sub> -β-Asn | Asn-X-Ser/Thr  | Oligosaccharyltransferase complex (OST)                             | ER                            |
| <b>O-linked glycosylation</b>       |  |  |   |                               |
| O-GalNAcylation<br>(mucin type)     | GalNAc-α-Ser/Thr   | Repeat domains rich in Ser, Thr, Pro, Gly,<br>Ala  | Polypeptide GalNAc transferases<br>(ppGALNTs)                       | Golgi                         |
| O-Fucosylation                      | Fuc-α-Ser/Thr  | EGF domains: Cys-X-X-X-X-Ser/Thr-Cys<br>TSR modules: Cys-X-X-X-X-Ser/Thr-Cys-<br>X-X-Gly     | Protein O-fucosyltransferases<br>(POFUT1, POFUT2)                   | ER                            |
| O-Glucosylation                     | Glc-β-Ser  | EGF modules: Cys-X-Ser-X-Pro/Ala-Cys   | Protein O-glucosyltransferase 1(POGLUT1)                            | ER                            |
| O-Mannosylation<br>(α-dystroglycan) | Man-α-Ser/Thr  | Ser/Thr-rich domains   | Protein O-mannosyltransferases (POMTs)                              | ER                            |
| O-Galactosylation<br>(collagen)     | Gal-β-Hyl  | Collagen repeats: X-Hyl-Gly  | Procollagen galactosyltransferases<br>(COLGALT1/2)                  | ER                            |
| O-GlcNAcylation                     | GlcNAc-β-Ser/Thr<br>GlcNAc-β-Ser/Thr                         | Ser/Thr-rich domains close to Pro, Val,<br>Ala, Gly<br>EGF domains of extracellular proteins | O-linked GlcNAc transferase (OGT)<br>EGF domain specific OGT (EOGT) | Cytosol/Nucleus<br>ER?        |
| GAG synthesis                       | Xyl-β-Ser  | Ser-Gly (close to acidic residues)   | Xylosyltransferases (XYLT1/2)                                       | Golgi                         |
| Glycosphingolipids synthesis        | Gal-β-Ceramide<br>Glc-β-Ceramide                             |  | Ceramide β-galactosyltransferase<br>Ceramide β-glucosyltransferase  | ER lumen<br>ER cytosolic face |
| <b>C-linked glycosylation</b>       | Man-α-C-Trp  | Trp-X-X-Trp  | C-mannosyltransferases (DPYL1-4)                                    | ER                            |
| <b>GPI anchors synthesis</b>        | GlcNAc-α-PI  |  | PI GlcNAc transferases (PIG-A, -H, -C, -Q, -<br>P, -Y), and DPM2    | Cytosol                       |



**Table 6: Diversity of yeast glycosylation pathways and associated characteristics towards their first glycosidic bonds.** First glycosidic bonds between the mono/oligosaccharide and the acceptor donor are reported with the associated peptide motif, the GTs involved and the subcellular (Sub.) localization of the reaction. Csg1p: calcium sensitive growth protein 1, GAGs: glycosaminoglycans, GPI: glycosyl phosphatidyl inositol, PI: phosphatidylinositol and Sur1p: suppressor of rvs161 and rvs167 mutations protein 1.

| Glycosylation pathways        | First glycosidic bond  | Peptide motif | First glycosidic bond  |                   |
|-------------------------------|--|---------------|--|-------------------|
|                               |  |               | GTs involved   | Sub. localization |
| <b>N-linked glycosylation</b> | Glc <sub>3</sub> Man <sub>9</sub> GlcNAc <sub>2</sub> -β-Asn | Asn-X-Ser/Thr | Oligosaccharyltransferase complex (OST)  | ER                |
| <b>O-linked glycosylation</b> |  |               |  |                   |
| O-Mannosylation               | Man-α-Ser/Thr  | Ser/Thr       | Protein mannosyltransferases (Pmt)   | ER                |
| Glycosphingolipids            | Man-α-Ceramide   |               | Mannosylinositol phosphorylceramide synthase (Sur1p/Csg1p)   | ER                |
| <b>GPI anchors synthesis</b>  | GlcNAc-α-PI  |               | GPI anchoring biosynthesis proteins (Gpi1-3p, Gpi15p, Gpi19p), ER-associated Ras inhibitor protein (Eri1p) | Cytosol           |

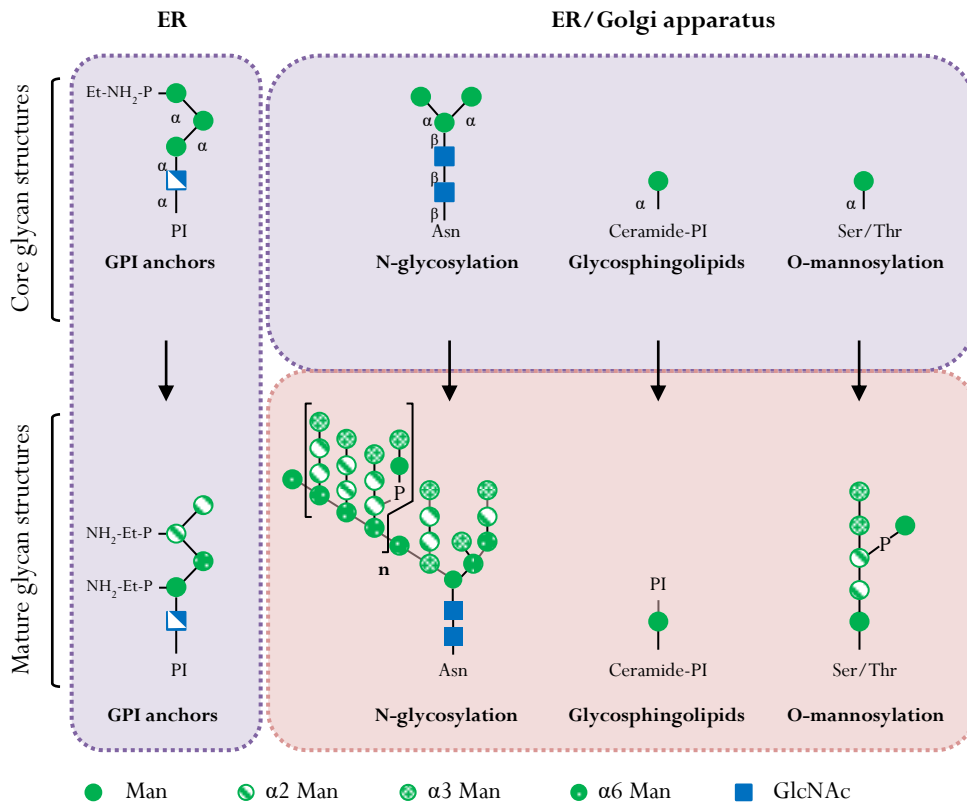


**Figure 9: Schematic representation of the initiation sites and maturation of yeast glycan structures associated with the different glycosylation pathways.** ER and Golgi compartments are schematically represented by the purple and pink dotted boxes, respectively. The nature of the different bonds has been omitted in the lower panel representing mature glycan structures and instead replaced by different green patterns for better readability.  $\alpha$  and  $\beta$  symbolize linkage anomerism. Abbreviations used for the key have been defined in Table 1. Asn: asparagine, NH<sub>2</sub>-Et-P: phosphatidylethanolamine, GPI: glycosylphosphatidyl inositol, n: number of pattern repeats, P: phosphate, PI: inositol phosphate, Ser: serine, Thr: threonine.

Thus, macro- and microheterogeneities generate the structural and functional diversity of the glycan structures carried by a given glycoprotein. Hereafter, I will briefly address the similarities and differences shared between yeast and human glycan structures before detailing the N-linked glycosylation process.

### 1.2.1. N-linked glycosylation

As mentioned above, “N-linked” glycosylation refers to the glycosidic bond formed between the oligosaccharidic precursor Dol-P-P-Glc<sub>3</sub>Man<sub>9</sub>GlcNAc<sub>2</sub> and the amide group of an Asn residue belonging to the consensus sequence Asn-X-Ser/Thr. However, this canonical sequence has been challenged over the past decades since other unusual N-linked glycosylation sites have been identified such as Asn-X-Cys (cysteine, Cys), Asn-X-Val (valine, Val) or even Asn-X-Gly (glycine, Gly) [98,99]. Of all the glycosylation pathways described so far, N-linked glycosylation is the most original one since it begins in the ER and further continues in the Golgi apparatus (detailed in section 2). Especially in yeasts and humans, the reticular steps of this process are highly conserved. However and as a major difference

between these two organisms, different maturation steps occur within the Golgi apparatus (trimming, addition, branching of monnosaccharides). While yeasts can only add mannose residues to the core glycoprotein, no further mannose can be added onto human N-glycans in the Golgi apparatus due to a lack of specific GTs and NSTs.

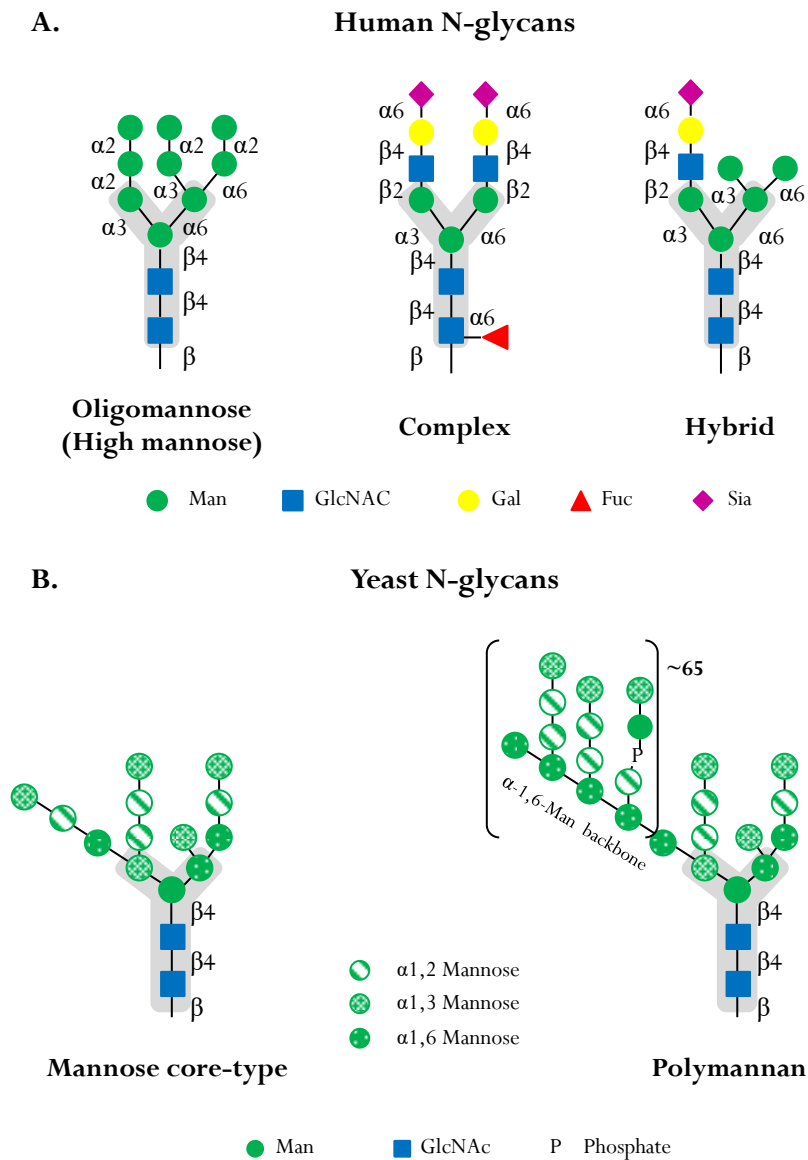


**Figure 10: Main N-glycan structures found on yeast *Saccharomyces cerevisiae* and human N-glycoproteins.** **A.** The three main types of human N-glycans found onto mature glycoproteins are oligomannose, complex and hybrid. The linkages between each monosaccharides is reported. **B.** In yeast, N-glycans are only made of GlcNAc and mannose residues. Two main N-glycans are found onto mature glycoproteins: a mannose core-type glycan and polymannans. For sake of readability, mannose linkages are symbolized by different green patterns as mentioned in the key. It is to note that both yeast and human N-glycans share the common core glycan structure  $\text{Man}_3\text{GlcNAc}_2$  (gray shape). Abbreviations used for the key have been defined in Table 1.

As depicted in Figure 10, the two types of yeast N-glycans are especially made of Man residues whereas human N-glycans exhibit additional Gal, Fuc and Sia residues increasing both diversity and complexity of the glycan structures. Three main classes of human N-glycans can be found on mature N-glycoproteins: high mannose, complex and hybrid (Figure 10A.). On the other hand, only two types of N-glycans are found in *Saccharomyces cerevisiae*: core type N-glycans and polymannans (Figure 10B.). Polymannans contain up to 150-200 mannose residues named “outer chains” that can be phosphorylated at specific positions. Yeast N-glycoproteins carrying such polymannans are mainly found expressed in walls whereas mannose core-type glycoproteins are usually retained in intracellular compartments. Hence, these huge differences between yeast and human N-glycan structures may reflect severe changes in Golgi functions during evolution from lower to higher eukaryotes.

### 1.2.2. Multiple O-linked glycosylations

Amongst the three types of glycosylation mentioned earlier (section 1.2.2), human O-linked glycans can be attached to either a protein or a lipid and be initiated by different monosaccharides. This defines and distinguishes the different O-glycosylation pathways amongst: O-linked N-acetylgalactosaminylation (O-GalNAc), O-linked N-acetylglucosaminylation (O-GlcNAc), O-linked xylosylation (O-Xyl) also referred to glycosaminoglycans (GAGs) synthesis, O-linked mannosylation (O-Man), O-linked fucosylation (O-Fuc), O-linked glucosylation (O-Glc) and O-linked glycolipid synthesis (Glc-Cer, Gal-Cer in case of glycosphingolipids) (Table 5, Figure 8). This great diversity of human O-glycan structures drastically differs from yeast ones that are limited to mannose addition onto either proteins or lipids (Table 6, Figure 9). Once again, this difference between both organisms reflects broader specialized and complex functions of the Golgi apparatus in higher eukaryotes comparing to lower ones. In the next sections of this chapter, only N-glycosylation shared by yeast and human will be further described.

## 2. N-linked glycosylation

The N-linked glycosylation process has been widely described and well documented in literature for both yeast and human cells. Considered as the “glyco-bible”, the last edition of *Essentials of Glycobiology* is an open access book on PubMed [83] that offers a panorama on glycobiology encompassing basic knowledge and further directions regarding glycosylation processes in all kingdoms of life. *Essentials of Glycobiology* was written by pioneers in the field and I highly recommend the reader to refer to this book for complementary and additional informations. In the following section, I will briefly expose the basis of N-linked glycosylation process in both yeasts and humans, relying on this book and the references it contains.

## 2.1. Initiation in the ER: from the synthesis to the transfer of the lipid-linked oligosaccharide (LLO) precursor

In both yeast *Saccharomyces cerevisiae* and human cells, the cytosolic/reticular steps initiating the N-linked glycosylation are highly conserved. Originally, this cellular process has been characterized in yeast which is a good model to study biological systems as it provides the ease of genetic manipulations to rapidly generate mutants [100]. Several strategies have been used to isolate defective yeast mutants in N-linked glycosylation. One of them is the use of [ $H^3$ ] mannose to ensure a “suicide selection” according to which mutagenized yeasts surviving radiation damage do so by virtue of a lesser uptake of radioactive mannose. This technique allowed the identification of yeast mutants with defects in both essential and non-essential genes of the dolichol pathway, universally known as *alg* mutants (asparagine-linked glycosylation). So far, almost all Alg“x”p yeast proteins have been associated to human orthologs.

### 2.1.1. Synthesis of the lipid-linked oligosaccharide precursor during the dolichol cycle

The first steps initiating the N-linked glycosylation are commonly known as the “dolichol cycle” and rely on the synthesis of a specific lipid-linked oligosaccharide (LLO) precursor whose final structure is Dol-P-P-GlcNAc<sub>2</sub>Man<sub>9</sub>Glc<sub>3</sub> (Figure 11, dashed green frame) [83]. As shown in Figure 11, the dolichol cycle begins at the cytosolic face of the ER by the transfer of a phospho-GlcNAc group onto a lipid phosphate moiety named dolichol phosphate (Dol-P). This first step is catalyzed by the dolichyl-phosphate GlcNAc phosphotransferase 1 (DPAGT1), the human ortholog of Alg7p. Then, a GlcNAc and five Man residues are sequentially added from UDP-GlcNAc and GDP-Man thanks to the successive activity of complex Alg13/14p and mannosyltransferases Alg1p, Alg2p and Alg11p to yield the dolichol pyrophosphate heptasaccharide Dol-P-P-GlcNAc<sub>2</sub>Man<sub>5</sub>. At this stage, the LLO is retrotranslocated into the luminal side of the ER, requiring the activity of the flippase Rft1p [101]. Within the ER lumen, glycan assembly continues with four mannosylation steps respectively catalyzed by Alg3p, Alg9p, Alg12p and Alg9p. Then, three terminal Glc residues are consecutively added by Alg6p, Alg8p and Alg10p to achieve the biosynthesis of the dolichol pyrophosphate tetradecasaccharide Glc<sub>3</sub>Man<sub>9</sub>GlcNAc<sub>2</sub>. Unlike the first cytosolic part of this pathway, the donor substrates in the ER lumen are the lipid-linked monosaccharides Dol-P-Man and Dol-P-Glc. Both of them are synthesized on the cytosolic face of the ER respectively by Dpm1p/DPM1-3 and Alg5p/ALG5, and then flipped into the ER lumen by an unknown mechanism (Figure 11). In addition, more attention should also be given to the biosynthetic pathway yielding the dolichol, the specific lipid moiety carrying the oligosaccharide precursor, since at least four genes encoding proteins involved in this metabolic pathway have been identified in CDG (Table 8) [102–105].

In this case, the reader has to know that the overall glycosylation defect originates from a lipid defect before the very first steps of the N-linked glycosylation process. Briefly and as shown in Figure 11, in humans, the last step of the dolichol pathway is catalyzed by the steroid 5- $\alpha$ -reductase 3 (SRD5A3) that converts polyprenol into dolichol on the cytosolic face of the ER. This newly synthesized dolichol is then phosphorylated by the dolichol kinase (DOLK) to form Dol-P, allowing then the beginning of the dolichol cycle. On the other hand, Dol-P can also originate from the recycling of Dol-P-P after the action of the dolichol diphosphatase 1 (DOLPP1). These three steps leading to the production of Dol-P are also conserved in yeast *Saccharomyces cerevisiae* with Dfg10p (defective for filamentous growth [protein 10]), Sec59p (secretory [protein 59]) and Cwh8p (calcofluor white hypersensitivity [protein 8]), the yeast orthologs of SRD5A3, DOLK and DOLPP1 (Figure 11).

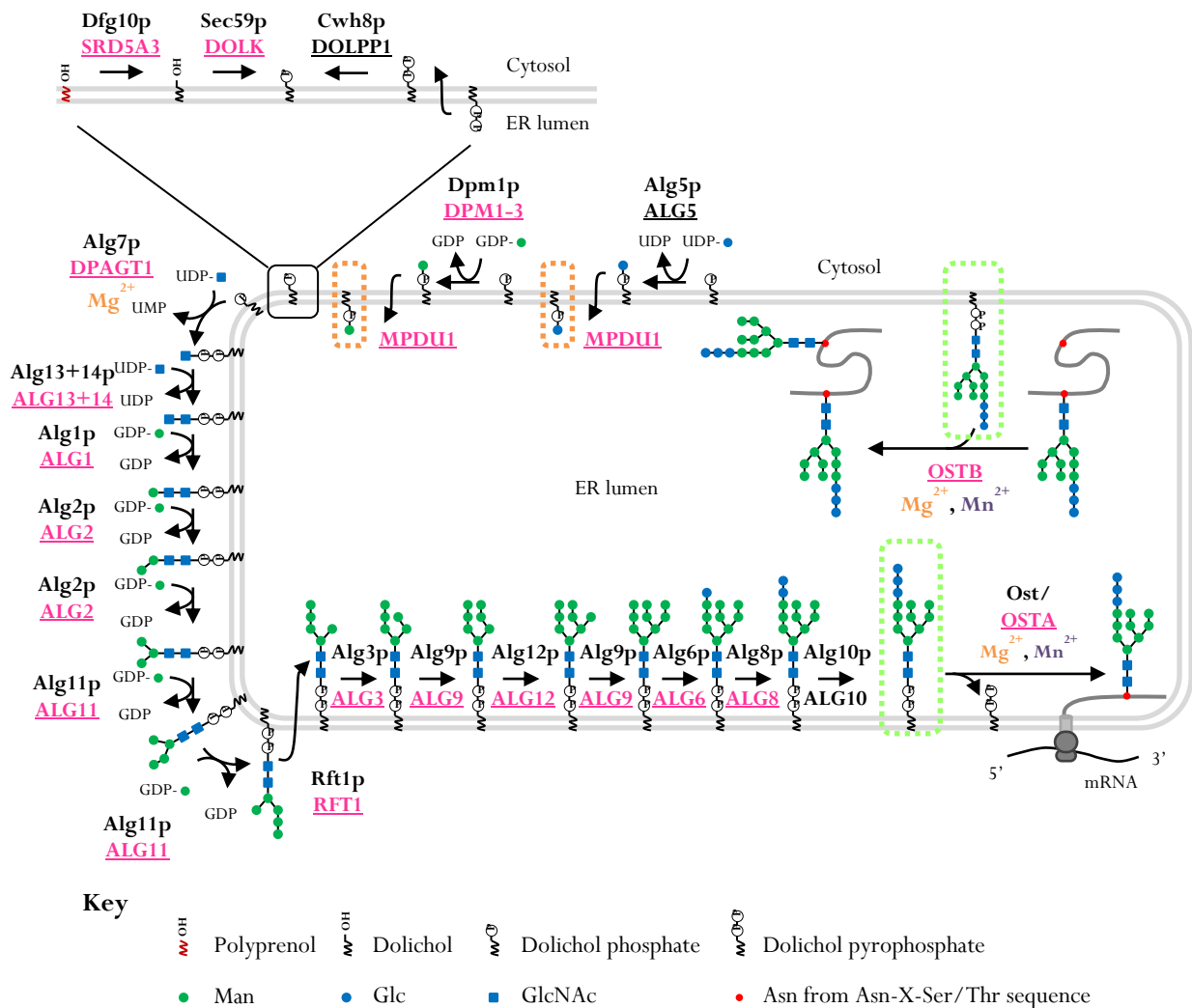


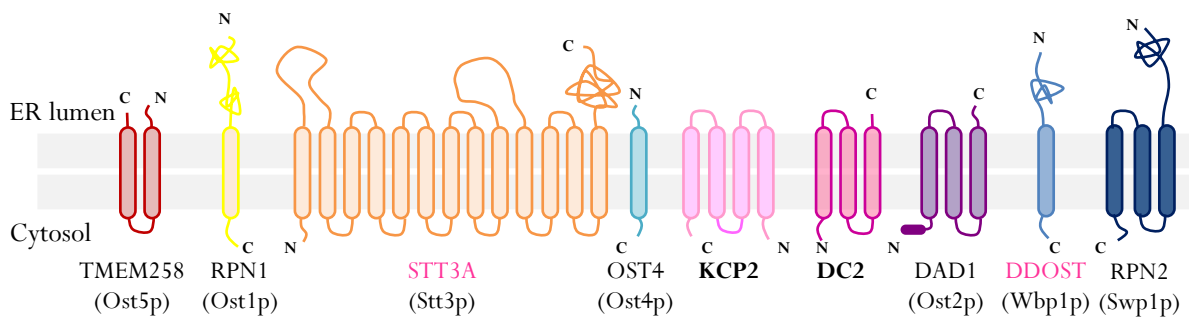
**Figure 11: Dolichol cycle initiating the N-linked glycosylation process in human and yeast *Saccharomyces cerevisiae*.** The first steps of the dolichol cycle occur at the cytosolic face of the ER membrane with the sequential addition of two GlcNAc residues and five Man residues from UDP-GlcNAc and GDP-Man to the dolichol phosphate (Dol-P). Then, the dolichol pyrophosphate heptasaccharide Dol-P-P-GlcNAc<sub>2</sub>Man<sub>5</sub> is translocated from the cytosolic to the luminal face of the ER by a still unclear process involving the flippase Rft1p/RFT1. Once in the ER lumen, glycan assembly continues with four mannosylation and three glucosylation

steps to achieve the biosynthesis of the tetradecasaccharide Dol-P-P-GlcNAc<sub>2</sub> Man<sub>9</sub>Glc<sub>3</sub> (green dashed frame). In the ER lumen, the donor substrates are the lipid-linked monosaccharides Dol-P-Man and Dol-P-Glc (orange dashed frames) synthesized on the cytosolic face of the ER by Dpm1p/DPM1-3 and Alg5p/ALG5 and then flipped into the ER lumen by an unknown mechanism. The last step of the dolichol cycle relies on the transfer of the Glc<sub>3</sub>Man<sub>9</sub>GlcNAc<sub>2</sub> from the Dol-P-P-GlcNAc<sub>2</sub>Man<sub>9</sub>Glc<sub>3</sub> onto the polypeptide. In both yeast and human, the oligosaccharyltransferase (OST) complex ensures such function. However, while yeasts possess only one Stt3p catalytic subunit, humans expressed two STT3 subunits: STT3A (OSTA complex) for co-translational glycosylation and STT3B (OSTB complex) for co- and posttranslational modification. These complexes are metal-ion dependent, requiring Mg<sup>2+</sup> and Mn<sup>2+</sup>. Yeast/human proteins are mentioned above each arrow. In case of difference between yeast and human, the underlined name refers to the human one. Human genes written in pink have been identified in CDG. Alg/ALG: asparagine-linked glycosylation protein, Cwh8p: calcofluor white hypersensitivity [protein 8], Dfg10p: defective for filamentous growth [protein 10], DOLK: dolichol kinase, DOLPP1: dolichol diphosphatase 1, DPAGT1: dolichyl-phosphate GlcNAc phosphotransferase 1, Dpm1p: dolichol phosphate mannose synthase [protein 1], DPM1-3: dolichol-phosphate mannosyltransferase subunit 1 to 3, OST: oligosaccharyltransferase, MPDU1: mannose-phosphate-dolichol utilization defect 1, Rft1p: requiring fifty three 1 protein, RFT1: oligosaccharide translocation protein RFT1, Sec59p: secretory [protein 59] and SRD5A3: steroid 5-alpha-reductase 3.

### 2.1.2. Transfer of the LLO precursor onto the protein

The last step of the dolichol cycle relies on the transfer of Glc<sub>3</sub>Man<sub>9</sub>NAc<sub>2</sub> from Dol-P-P-GlcNAc<sub>2</sub>Man<sub>9</sub>Glc<sub>3</sub> onto the nascent protein in the ER lumen. In both yeast *Saccharomyces cerevisiae* and humans, the oligosaccharyltransferase (OST) complex ensures such function [106]. OST is an enzymatic complex comprises nine non-identical protein subunits (Figure 12) with Stt3p/STT3A/STT3B as the catalytic subunit (Table 7).

#### A. OSTA complex



#### B. OSTB complex

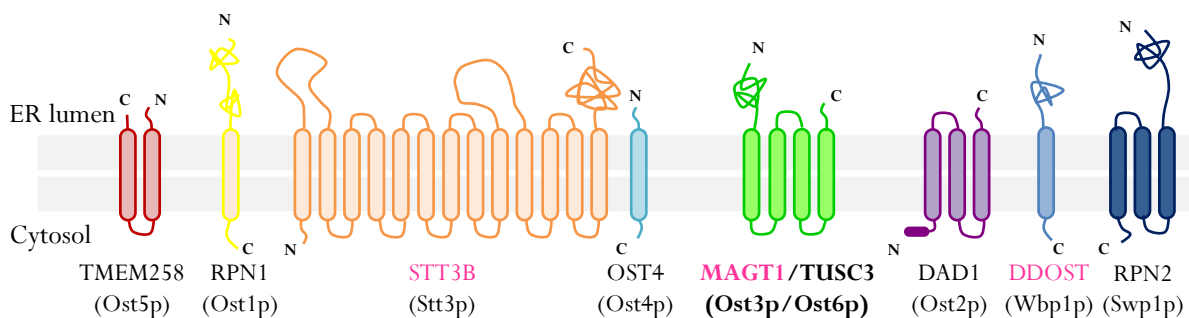


**Figure 12: Subunit organization of human and yeast *Saccharomyces cerevisiae* oligosaccharyltransferase (OST) complex.** OST complex comprises seven common subunits between yeast

and human. Mammalian protein names are indicated in capitals and corresponding yeast orthologs are mentioned into brackets. While OSTA comprises two subunits only found in mammalian cells: KCP2 and DC2 (bold names, A.), OSTB contains either mammalian MAGT1 or TUSC3 subunit or their yeast orthologs Ost3p or Ost6p (bold names, B.). Human OSTA complex is homologous to OST complex, without KCP2 and DC2 subunits. Human genes written in pink have been identified in CDG. DAD1: defense against cell death 1, DDOST: dolichyl-diphospho-oligosaccharide protein glycosyltransferase 48 kDa subunit, MAGT1: magnesium transporter 1, RPN1/2: ribophorin 1/2, STT3: staurosporine and temperature sensitive [protein 3], Swp1p: suppressor of Wbp1p mutation [protein 1], TMEM258: transmembrane protein 258, TUSC3: tumor suppressor candidate 3 and Wbp1p: wheat germ agglutinin-binding protein 1. Inspired from [106].

Yeast OST contains a single Stt3p whereas two human OST complexes exist with either STT3A (OSTA) or STT3B (OSTB), two paralogues of Stt3p. Yeast *Saccharomyces cerevisiae* possesses two functional OST isoforms comprising eight of the nine subunits and share seven common subunits: Ost1p, Ost2p, Ost4p, Ost5p, Stt3p, Swp1p and Wbp1p. Actually, the main difference between the two yeast isoforms relies on the presence of either Ost3p or Ost6p subunit. With regards to human OSTs, OSTA and OSTB share seven common subunits, all orthologous to the yeast ones: ribophorin 1 (RPN1), ribophorin 2 (RPN2), defender against cell death 1 (DAD1), dolichyl-diphospho oligosaccharide protein glycosyltransferase 48 kDa subunit (DDOST), OST 4 kDa (OST4) and transmembrane protein 258 (TMEM258) (Table 7 and Figure 12). Albeit structurally similar, OSTA and OSTB have been shown to act differently regarding to the transfer of the LLO precursor onto the protein.

**Table 7: Oligosaccharyltransferase subunits and associated functions in human and yeast *Saccharomyces cerevisiae*.** Adapted from [106]. DAD1: defense against cell death 1, DDOST: dolichyl-diphospho-oligosaccharide protein glycosyltransferase 48 kDa subunit, MAGT1: magnesium transporter 1, RPN1/2: ribophorin 1/2, STT3: staurosporine and temperature sensitive [protein 3], Swp1p: suppressor of Wbp1p mutation [protein 1], TMEM258: transmembrane protein 258, TUSC3: tumor suppressor candidate 3 and Wbp1p: wheat germ agglutinin-binding protein 1.

| Human |               | Yeast       | Function   |
|-------|---------------|-------------|--|
| OSTA  | OSTB          | OST         |  |
| STT3A | STT3B         | Stt3p       | Catalytic activity   |
|       | OST4          | Ost4p       | Maintains stability of catalytic sub-complex                           |
| -     | MAGT1/TUSC3   | Ost3p/Ost6p | Oxidoreductase activity  |
|       | TMEM258       | Ost5p       | Not clear  |
|       | RPN1          | Ost1p       | Restrains glycosylated peptide from sliding back to the catalytic site |
|       | DAD1          | Ost2p       | Not clear  |
|       | DDOST (OST48) | Wbp1p       | Possibly LLO recruitment   |
|       | RPN2          | Swp1p       |  |
| KCP2  | -             | -           | Mediates interaction with translocon channel                           |
| DC2   | -             | -           |  |



Indeed, in human OSTA, STT3A is surrounded by two accessory proteins (keratinocyte-associated protein 2 (KCP2) and DC2) that mediate the interaction between OSTA and the translocon channel (Figure 12, Table 7). This interaction enables STT3A to transfer the LLO precursor co-translationally on nascent proteins arriving into the ER lumen through the translocon channel. Conversely, OSTB is more considered as an “OSTA backup” and catch the N-linked glycosylation sites missed by OSTA on specific glycoproteins with disulfide bonds or partially folded. Instead of KCP2 and DC2, OSTB has either the magnesium transporter 1(MAGT1) or tumor suppressor candidate 3 (TUSC3) subunits, two proteins orthologous to the yeast Ost3p and Ost6p with an oxidoreductase activity allowing STT3B to access glycosylation sites (Figure 12, Table 7). Depending on the glycoprotein and the location of the missed glycosylation site, STT3B can exert its function co-translationally or post-translationally.

### 2.1.3. Congenital Disorders of Glycosylation related to cytosolic and ER initiating steps of the N-linked glycosylation process

As briefly mentioned at the end of the General Introduction, rare human genetic glycopathologies commonly known as Congenital Disorders of Glycosylation result from defective genes directly or indirectly involved in glycosylation reactions. In all the figures of this section 2.1., I mentioned in pink genes that have been identified in CDG whose encoded proteins belonging to different pathways from the cytosolic biosynthesis of the NM/DP-sugars to the transfer of the LLO precursor onto proteins in the ER lumen. All of these genes are gathered in the following Table 8 in alphabetical order according to the set of reactions described amongst: dolichol synthesis, NM/DP-sugars and Dol-P-sugars synthesis, and dolichol cycle.

**Table 8: List of human CDGs associated with genes encoding enzymes involved in (oligo)saccharide precursors synthesis and transfer onto protein during the N-linked glycosylation process.** Dol: dolichol, Dol-P: dolichol phosphate, Dol-P-P: dolichol pyrophosphate, GlcT: glucosyltransferase, LLO: lipid-linked oligosaccharide, ManT: mannosyltransferase and NM/DP-sugars: nucleotide mono/diphosphate sugars.

| Former CDG                              | Defective gene | Defective protein   | Impact                 |
|---|----------------|---|------------------------|
| <i>Dol and Dol-P synthesis</i>          |                |   |                        |
|   | <i>DHDDS</i>   | Dehydrodolichyl diphosphate synthase (DHDDS) complex                        | Dol synthesis          |
| CDG-Im                                  | <i>DOLK</i>    | Dolichol kinase   | Dol-P synthesis        |
| CDG-Iaa                                 | <i>NUS1</i>    | DHDDS complex subunit NUS1  | Dol synthesis          |
| CDG-Iq                                  | <i>SRD5A3</i>  | Steroid 5- $\alpha$ -reductase 3  | Dol synthesis          |
| <i>NM/DP- and Dol-P-sugar synthesis</i> |                |   |                        |
|   | <i>CAD</i>     | Carbamoyl phosphate synthetase/Aspartate transcarbamylase/Dihydroorotase    | NM/DP-sugar synthesis  |
|   | <i>CPS2</i>    | Carbamoylphosphate synthetase 2   | NM/DP-sugar synthesis  |
| CDG-Ie                                  | <i>DPM1</i>    | Dolichol-phosphate ManT subunit 1   | Dol-P-Man synthesis    |
|   | <i>DPM2</i>    | Dolichol-phosphate ManT subunit 2   | Dol-P-Man synthesis    |
| CDG-Io                                  | <i>DPM3</i>    | Dolichol-phosphate ManT subunit 3   | Dol-P-Man synthesis    |
|   | <i>GFPT1</i>   | GINH <sub>2</sub> fructose-6-phosphate aminotransferase 1                   | NM/DP-sugar synthesis  |
|   | <i>GMPPA</i>   | Mannose-1-phosphate guanyltransferase subunit $\alpha$                      | NM/DP-sugar synthesis  |
|   | <i>GMPPB</i>   | Mannose-1-phosphate guanyltransferase subunit $\beta$                       | NM/DP-sugar synthesis  |
|   | <i>GNE</i>     | Bifunctional UDP-GlcNAc 2' epimerase/ManNAc kinase                          | NM/DP-sugar synthesis  |
| CDG-Ib                                  | <i>MPI</i>     | Mannose phosphate isomerase   | NM/DP-sugar synthesis  |
|   | <i>NANS</i>    | N-acetylneuraminidic acid synthase  | NM/DP-sugar synthesis  |
| CDG-If                                  | <i>MPDU1</i>   | Man-P-Dol utilization defect 1  | Dol-P-sugar flippase   |
|   | <i>PGM1</i>    | Phosphoglucomutase 1  | NM/DP-sugar synthesis  |
|   | <i>PGM3</i>    | Phosphoacetylamine mutase   | NM/DP-sugar synthesis  |
| CDG-Ia                                  | <i>PMM2</i>    | Phosphomannomutase 2  | NM/DP-sugar synthesis  |
| CDG-In                                  | <i>RFT1</i>    | Protein FRT1 homolog/Man <sub>5</sub> GlcNAc <sub>2</sub> -P-P-Dol flippase | Dol-P-P-sugar flippase |
| <i>Dolichol cycle</i>                   |                |   |                        |
| CDG-Ik                                  | <i>ALG1</i>    | GDP-Man:GlcNAc <sub>2</sub> -P-P-Dol $\beta$ -1,4-ManT                      | LLO synthesis          |
| CDG-Ii                                  | <i>ALG2</i>    | GDP-Man:Man <sub>1</sub> GlcNAc <sub>2</sub> -P-P-Dol $\alpha$ -1,6-ManT    | LLO synthesis          |

|         |                 |  |               |
|---------|-----------------|--|---------------|
|         |                 | GDP-Man:Man <sub>1</sub> GlcNAc <sub>2</sub> -P-P-Dol α-1,3-ManT   |               |
| CDG-Id  | <i>ALG3</i>     | Dol-P-Man:Man <sub>5</sub> GlcNAc <sub>2</sub> -P-P-Dol α-1,3-ManT   | LLO synthesis |
| CDG-Ic  | <i>ALG6</i>     | Dol-P-Man:Man <sub>9</sub> GlcNAc <sub>2</sub> -P-P-Dol α-1,3-GlcT   | LLO synthesis |
| CDG-Ih  | <i>ALG8</i>     | Dol-P-Man:Glc <sub>1</sub> Man <sub>9</sub> GlcNAc <sub>2</sub> -P-P-Dol α-1,3-GlcT  | LLO synthesis |
| CDG-IL  | <i>ALG9</i>     | Dol-P-Man:Man <sub>6</sub> GlcNAc <sub>2</sub> -P-P-Dol α-1,2-ManT<br>Dol-P-Man:Man <sub>8</sub> GlcNAc <sub>2</sub> -P-P-Dol α-1,2-ManT | LLO synthesis |
| CDG-Ip  | <i>ALG11</i>    | Dol-P-Man:Man <sub>3</sub> GlcNAc <sub>2</sub> -P-P-Dol α-1,2-ManT<br>Dol-P-Man:Man <sub>4</sub> GlcNAc <sub>2</sub> -P-P-Dol α-1,2-ManT | LLO synthesis |
| CDG-Ig  | <i>ALG12</i>    | Dol-P-Man:Man <sub>7</sub> GlcNAc <sub>2</sub> -P-P-Dol α-1,6-ManT   | LLO synthesis |
|         | <i>ALG13/14</i> | UDP-N-GlcNAc transferase subunit ALG14 homolog   | LLO synthesis |
| CDG-Ir  | <i>DDOST</i>    | Dol-P-P-oligosaccharide:protein glycosyltransferase 48 kDa subunit   | LLO transfer  |
| CDG-Ij  | <i>DPAGT1</i>   | UDP-GlcNAc:Dolichyl-phosphate N-GlcNAc phosphotransferase  | LLO synthesis |
| CDG-Icc | <i>MAGT1</i>    | Mg <sup>2+</sup> transporter 1/Dol-P-P-oligosaccharide:protein glycosyltransferase subunit MAGT1   | LLO transfer  |
| CDG-Iw  | <i>STT3A</i>    | Dol-P-P-oligosaccharide:protein glycosyltransferase subunit STT3A  | LLO transfer  |
| CDG-Ix  | <i>STT3B</i>    | Dol-P-P-oligosaccharide:protein glycosyltransferase subunit STT3B  | LLO transfer  |
|         | <i>TUSC3</i>    | Tumor suppressor candidate 3/Dol-P-P-oligosaccharide:protein glycosyltransferase subunit TUSC3   | LLO transfer  |

---

## 2.2. Early trimming during the ER quality control for N-glycoproteins

### 2.2.1. ER quality control for human and yeast N-glycoproteins

Once  $\text{Glc}_3\text{Man}_9\text{GlcNAc}_2$  oligosaccharide precursor has been transferred from its lipid carrier Dol-P-P to the polypeptide, a series of mandatory trimming steps occur in the ER for both yeast and human N-linked glycans (Figure 13). First, ER glucosidase I (GI) cleaves the terminal  $\alpha$ -1,2-Glc residue to prevent re-binding of the processed N-linked glycan by OST [107] and rather promotes its binding to the ER lectin named malectin. This is the first checkpoint in the ER quality control for N-glycoproteins. Further investigations have then highlighted that malectin preferentially bind to misfolded proteins and drive them directly to the ER-associated degradation (ERAD) pathway [108,109]. Then, ER glucosidase II (GII) removes a second Glc residue to form the monoglucosylated structure  $\text{GlcMan}_9\text{GlcNAc}_2$ . In human, this specific glycan structure is recognized by two lectins named calnexin (CNX) and calreticulin (CRT) to be further involved in the so-called “CNX/CRT cycle” part of the ER quality control for human N-glycoproteins [110,111]. Together with chaperones, isomerases and oxidoreductases such as the protein disulfide isomerase A3 (PDIA3), CNX and CRT act in concert to help the N-glycoprotein to acquire its proper conformation with correct disulfide pairings [112]. At the end of the cycle, the last Glc residue is removed by GII to prevent the re-binding of the N-glycoprotein to the CNX/CRT-PDIA3 complex. Then, the fully deglycosylated glycan structure  $\text{Man}_9\text{GlcNAc}_2$  binds to the UDP-Glc glycoprotein glucosyltransferase (UGGT) which controls whether the protein has achieved its proper and correct native conformation. If successfully folded, N-glycoproteins are released by UGGT and ER  $\alpha$ -mannosidase I (MAN1B1) cleaves one Man residue yielding  $\text{Man}_8\text{GlcNAc}_2$ , a glycan structure that is recognized by specific lectins mediating the transport of the N-linked glycoprotein from the ER to the Golgi apparatus. Conversely, in case of misfolding, N-glycoproteins are re-glucosylated by UGGT to undergo an additional CNX/CRT cycle [113]. In some cases, N-glycoproteins are still unfolded and failed to pass the ER quality control. To avoid any accumulation of these unfolded proteins in the ER, they are subjected to the action of MAN1B1 and additional ER mannosidases belonging to the EDEM (ER degradation-enhancing  $\alpha$ -mannosidase like protein 1-3) family generating a  $\text{Man}_7\text{GlcNAc}_2$  glycan structure [114–117]. This specific sugar moiety is then recognized by the Os-9 and XTP3-B ER luminal lectins to be further degraded following the ERAD pathway (see section 2.4.1., Figure 17) [118]. With regards to yeast *Saccharomyces cerevisiae*, no proper CNX/CRT cycle has been found since yeasts lack CRT and only expressed CNX-like proteins. However, N-glycoproteins still interact with CNX-like proteins and then, GII removes the last Glc residue from  $\text{Glc}_1\text{Man}_9\text{GlcNAc}_2$ . Differing from humans, the proper ER quality control step in yeasts relies on the activity of the ER mannosidase Mns1p to cleave a Man residue and form  $\text{Man}_8\text{GlcNAc}_2$  [118]. At this stage, either the N-glycoprotein is well folded and

addressed to the Golgi apparatus or, it is mis/unfolded and targeted to the ERAD pathway. In this later case, the  $\text{Man}_8\text{GlcNAc}_2$  motif of the unfolded glycoproteins is recognized by the protein disulfide isomerase (Pdi1p) allowing the activity of Htm1p, the yeast ortholog of EDEM1, to remove an additional Man residue and form  $\text{Man}_7\text{GlcNAc}_2$  [119]. Like for human, this specific sugar moiety is then recognized by the yeast Os-9 protein (Yos9p) to be further addressed and degraded *via* the ERAD pathway [118].

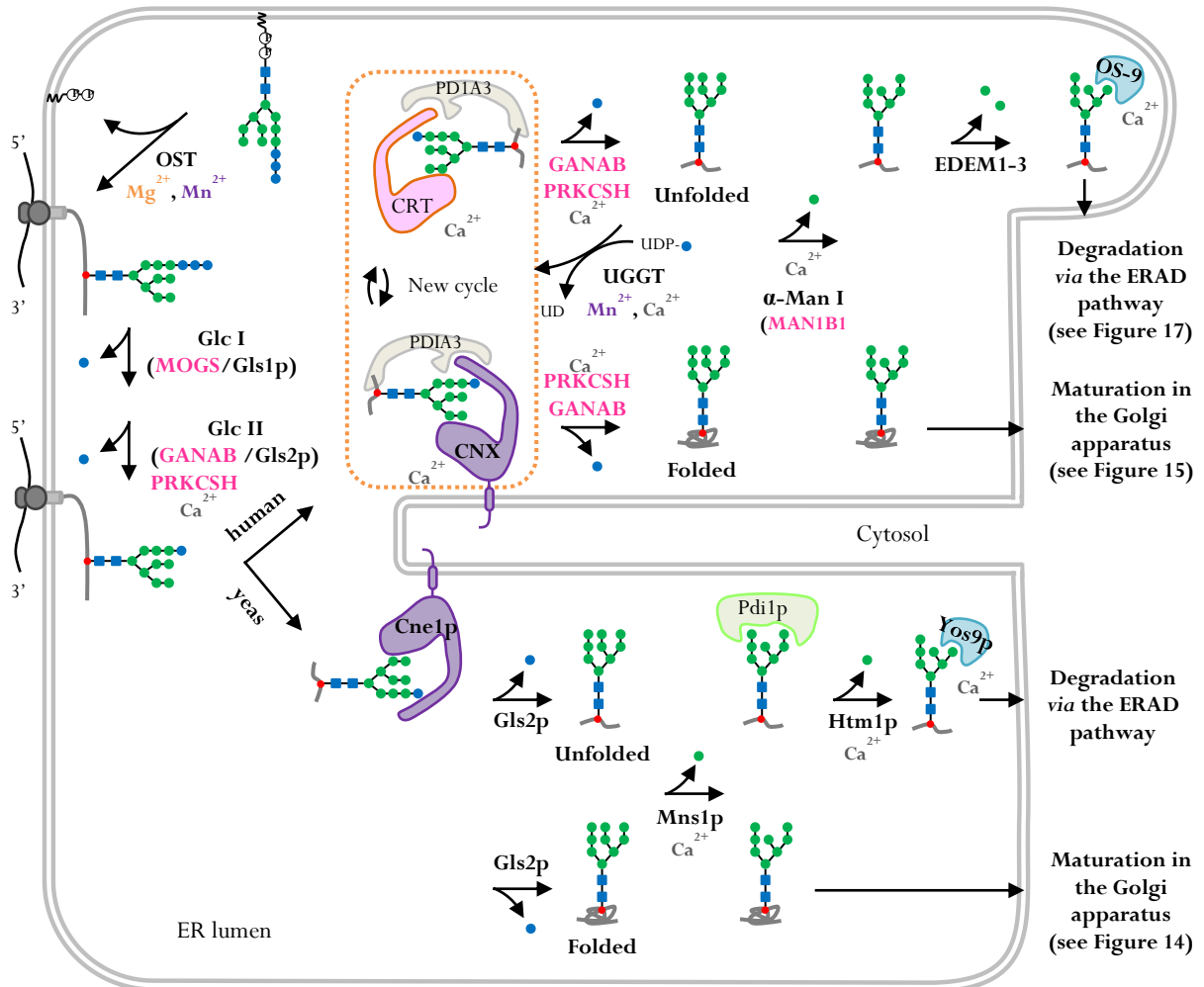


**Figure 13: ER quality control for N-glycoproteins in human and yeast *Saccharomyces cerevisiae* cells.** The two first steps are common to yeast and human and deal with the removal of the two terminal Glc from the  $\text{Glc}_3\text{Man}_9\text{GlcNAc}_2$  glycan structure through the action of glucosidase I (GI) and glucosidase II (GII). GI and GII respectively correspond to human mannosyl-oligosaccharide glucosidase (MOGS, GI) and glucosidase II  $\alpha/\beta$  subunit (GANAB/PRKCSH, GII) and yeast glucosidase 1 protein (Gls1p encoded by *CWH41* gene, GI) and glucosidase 2 protein (Gls2p encoded by *ROT2* gene, GII). Human N-glycoproteins are then involved in the calnexin/calreticulin (CNX/CRT) cycle where the two lectins together with the protein disulfide isomerase A3 (PDIA3) help the N-glycoprotein to acquire its proper folding (orange dashed frame). The last Glc residue is then released by GII followed by the action of ER  $\alpha$ -mannosidase I (MAN1B1) that removes one Man, yielding to  $\text{Man}_8\text{GlcNAc}_2$  glycan structure. Then, the N-glycoprotein is addressed to the Golgi apparatus for further glycan maturation steps. However, in case of misfolding, the N-glycoprotein can be re-glucosylated by the UDP-glucose glycoprotein glucosyltransferase (UGGT) to undergo an additional CNX/CRX cycle. If still unfolded, the N-glycoprotein is subjected to several demannosylations by MAN1B1 and additional ER mannosidases belonging to

the EDEM family to form Man<sub>7</sub>GlcNAc<sub>2</sub> structure that is recognized by the Os-9 lectin to be further degraded following the ER-associated degradation (ERAD) pathway. To the yeast side, no proper CNX/CRT cycle has been found. N-glycoproteins interact with CNX-like proteins (Cne1p: calnexin and calreticulin homolog 1 protein) and then, GII removes the last Glc residue from Glc<sub>1</sub>Man<sub>9</sub>GlcNAc<sub>2</sub>. Then, an ER mannosidase (Mns1p) removes a Man affording to Man<sub>8</sub>GlcNAc<sub>2</sub> glycan structure. Here, if the N-glycoprotein is correctly folded, it is further addressed to the Golgi apparatus. However, if the N-glycoprotein is unfolded, protein disulfide isomerase 1 (Pdi1p) recognizes the Man<sub>8</sub>GlcNAc<sub>2</sub> motif allowing the activity of the homologous EDEM1 protein (Htm1p) to remove an additional Man resulting in a Man<sub>7</sub>GlcNAc<sub>2</sub> structure. Like for human N-glycoproteins, this specific sugar moiety is then recognized by the yeast Os-9 protein (Yos9p) to be further addressed and degraded by the ERAD pathway. Human genes written in pink have been identified in CDG.

### 2.2.2. Congenital Disorders of Glycosylation related to ER trimming of human N-glycans

The ER quality control for N-linked glycoproteins is crucial for a given protein to acquire its own specific conformation that may trigger its fate in terms of subcellular localization, biological function and sorting. Any missed checkpoint(s) during this process due to a defective gene encoding one of the four proteins reported in Table 9 lead to a CDG.

**Table 9: List of human CDGs associated with genes encoding GTs and GHs directly involved in ER trimming of N-glycans.**

| Former CDG         | Defective gene | Defective protein                                      | Impact                 |
|--------------------|----------------|--|------------------------|
| <i>ER trimming</i> |                |  |                        |
|                    | <i>GANAB</i>   | Glucosidase II $\alpha$ subunit                        | N-glycoprotein folding |
|                    | <i>MAN1B1</i>  | ER mannosyl-oligosaccharide 1,2- $\alpha$ -mannosidase | N-glycoprotein folding |
| CDG-IIb            | <i>MOGS</i>    | Mannosyl-oligosaccharide glucosidase                   | N-glycoprotein folding |
|                    | <i>PRKCSH</i>  | Glucosidase II $\beta$ subunit                         | N-glycoprotein folding |

### 2.3. Maturing in the Golgi apparatus: between polymannans and complex N-glycan structures

In contrast to the well conserved core structures synthesized in the ER, final N-glycan structures processed in the Golgi apparatus highly diverged between yeast *Saccharomyces cerevisiae* and humans especially due to the non-conservation of Golgi GTs between the two organisms. While *Saccharomyces cerevisiae* only extend N-linked glycans with Man residues branched in  $\alpha$ 1,6-,  $\alpha$ 1,2- and  $\alpha$ 1,3-, human N-glycans are trimmed and processed with the addition of several different monosaccharides amongst GlcNAc, Gal, Fuc and Sia but not with Man. Despite this divergence between yeasts and humans, Golgi maturation steps for N-linked glycans are well-described in literature [83,120,121].

2.3.1. In yeast *Saccharomyces cerevisiae*, mannose exclusively!

Once N-glycoproteins exit the ER (Figure 13), Golgi processing starts on a  $\text{Man}_8\text{GlcNAc}_2$  glycan by the addition of a single  $\alpha 1,6$ -Man catalyzed by the mannosyltransferase Och1p (outer chain elongation [1 protein]) [122–124]. Then, either N-linked glycans follow the “core-type” or “polymann outer chain” pathway (both represented in Figure 14) culminating in the two distinct structures depicted in Figure 10.

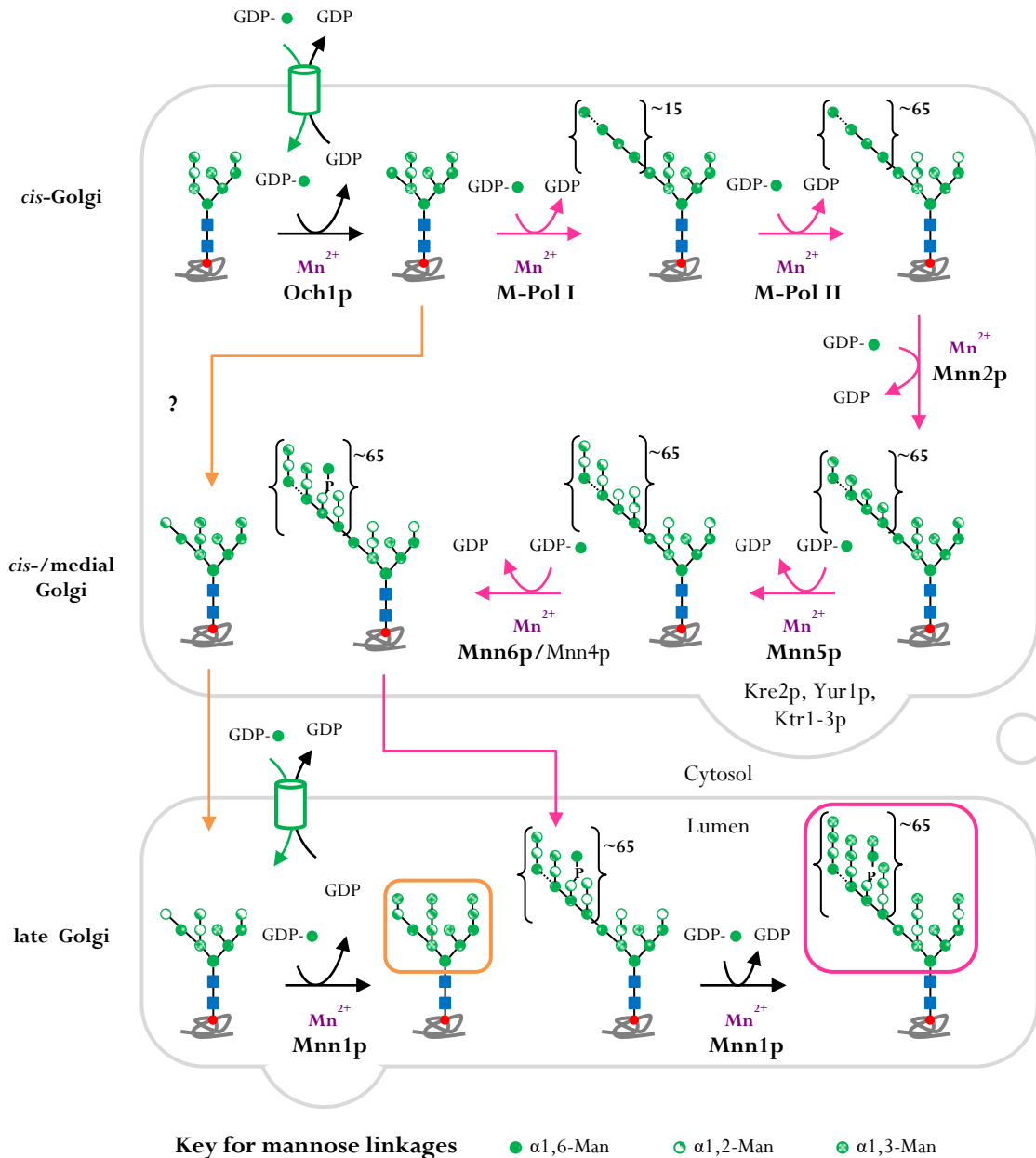


**Figure 14: Processing and maturation of yeast *Saccharomyces cerevisiae* N-glycans in the Golgi apparatus.** Golgi maturation starts on a  $\text{Man}_8\text{GlcNAc}_2$  glycan by the addition of a single  $\alpha 1,6$ -Man residue catalyzed by Och1p (outer chain elongation [1 protein]) [122–124]. Then, either the N-glycan follow the “core-type” pathway (orange arrows) or the “polymann outer chain” one (pink arrows) yielding the glycan structures framed in orange and pink, respectively. Whatever the pathway, each Golgi mannosylation steps involves  $\text{Mn}^{2+}$ -dependent mannosyltransferases.

On the one hand, core-type N-glycans only receive a  $\alpha$ 1,2-Man right after the action of Och1p and terminal  $\alpha$ 1,3-Man via the activity of Mnn1p (mannosyltransferase [1 protein]), in the late compartment of the Golgi apparatus [125,126]. On the other hand, the  $\alpha$ 1,6-Man added by Och1p is sequentially extended by two enzymatic complexes: mannosyltransferase I (M-Pol I) and mannosyltransferase II (M-Pol II) to form the  $\alpha$ 1,6-Man backbone of polymannan outer chain N-glycans [127]. M-Pol I comprises two subunits: Mnn9p and Van1p (vanadate resistance protein [1]). While Mnn9p adds the first  $\alpha$ 1,6-Man, ten to fifteen additional  $\alpha$ 1,6-Man are added in a Van1p-dependent manner [127–129]. This backbone is further elongated with up to sixty  $\alpha$ 1,6-Man by M-Pol II that contains five subunits: Mnn9p, Anp1p (aminonitrophenyl propandiol osmotic sensitive [protein 1]), Mnn10p, Mnn11p and Hoc1p (homologous to Och1p [protein 1]) [130,131]. Then,  $\alpha$ 1,2-Man are branched onto  $\alpha$ 1,6-Man by the sequential activity of the mannosyltransferases Mnn2p and Mnn5p [132], belonging to one of the two well-known family of yeast mannosyltransferases named MNN1 [133]. Additional members of second yeast mannosyltransferases family known as Kre-Two-Related (KTR): Kre2p, Yur1p and Ktr1-3p, also contribute to the addition of  $\alpha$ 1,2-Man residues [134,135]. On some branches, phosphate-Man are attached to  $\alpha$ 1,2-Man, a step that requires both activities of Mnn6p, a mannosylphosphate transferase and Mnn4p, its positive regulator [136–138]. As for core-type N-glycans, polymannan outer chains are capped by terminal  $\alpha$ 1,3-Man (onto all  $\alpha$ 1,2-Man residues) through the activity of Mnn1p, in the late Golgi [125,126]. Altogether, Golgi maturation of yeast N-glycans only requires the activity of a set of mannosyltransferases. As mentioned on Figure 14, all of these specific GTs are  $Mn^{2+}$ -dependent, suggesting that yeast Golgi  $Mn^{2+}$  homeostasis has to be tightly regulated to ensure proper Golgi mannosylation reactions. This will be further described in the next chapter of this manuscript.

### 2.3.2. In human cells, a broad variety of monosaccharides addition

After moving of the glycoprotein from the ER to the *cis*-Golgi compartment, the N-linked glycan is further trimmed by the sequential activity of three  $Ca^{2+}$ -dependent Golgi  $\alpha$ -mannosidases I ( $\alpha$ -Man I) respectively encoded by *MAN1A1*, *MAN1A2* and *MAN1C1* genes, to yield  $Man_5GlcNAc_2$ -Asn (Figure 15). These Man eliminations are required for the conversion of high mannose to complex N-glycans (Figure 10) since the use of deoxymannojirimycin, an experimental  $\alpha$ -Man I inhibitor, leads to an accumulation of  $Man_8GlcNAc_2$ -Asn and  $Man_9GlcNAc_2$ -Asn that are not further processed [139]. After the action of  $\alpha$ -Man,  $Man_5GlcNAc_2$ -Asn reach the medial-Golgi where N-acetylglucosamine transferase I (shortly GnT I) encoded by *MGAT1* adds a  $\beta$ -1,2-GlcNAc residue, initiating the first branch or antenna of the N-glycan. This GlcNAc $Man_3GlcNAc_2$  structure is then recognized by two Golgi  $\alpha$ -mannosidases II ( $\alpha$ -Man II) respectively encoded by *MAN2A1* and *MAN2A2*, generating the substrate for GnT II. It is to note that



GnT I activity is required for the action of  $\alpha$ -Man II since  $\alpha$ -Man II do not recognized  $\text{Man}_5\text{GlcNAc}_2$  glycan structures. Therefore, without the addition of  $\beta$ -1,2-GlcNAc, N-glycan processing stops and remains at the high mannose stage. In other words, the action of  $\alpha$ -Man II triggers the further production of hybrid and complex types N-glycans [140,141]. A second  $\beta$ -1,2-GlcNAc residue is then added onto the newly available Man by the GnT II (*MGAT2*) to form  $\text{GlcNAc}_2\text{Man}_3\text{GlcNAc}_2\text{-Asn}$ .

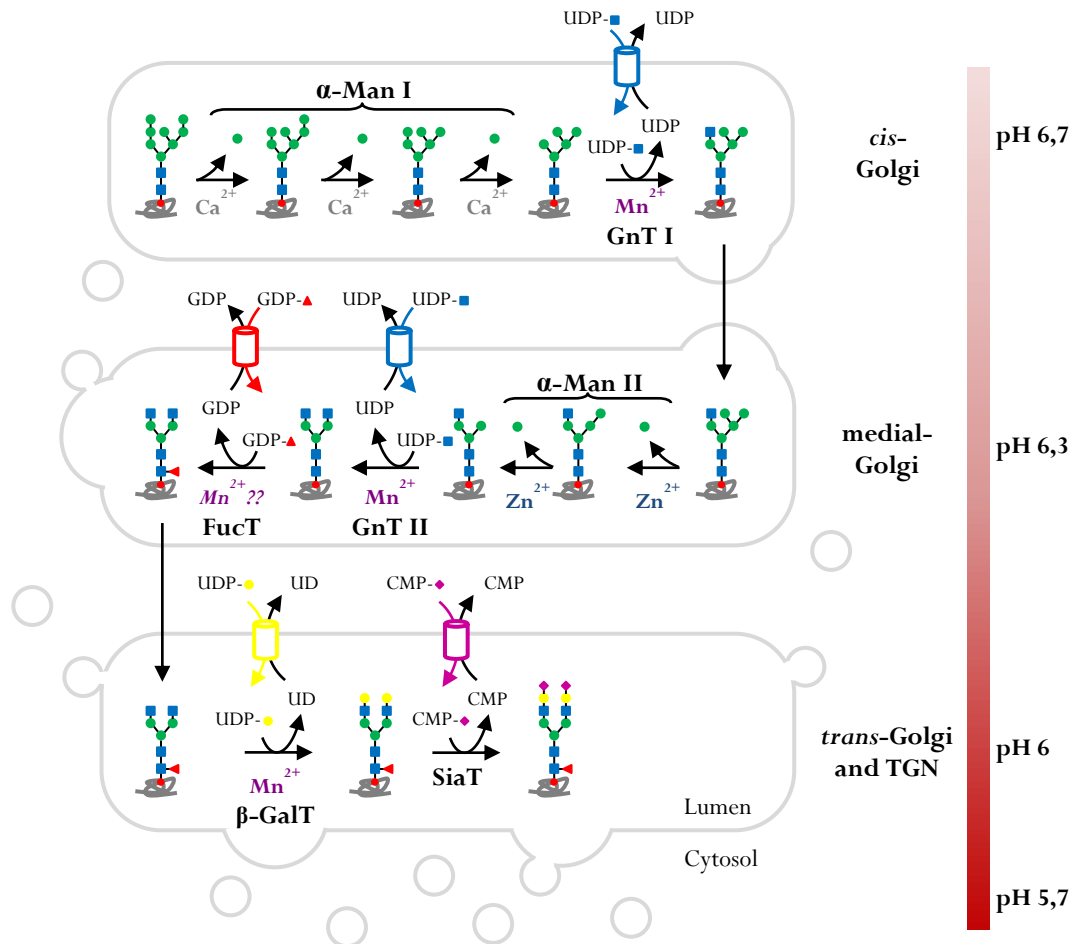


**Figure 15: Processing and maturation of a human biantennary complex N-glycan in the Golgi apparatus.** After proper folding of the glycoprotein carrying a  $\text{Man}_8\text{GlcNAc}_2$  glycan (green frame), three Man are removed in the *cis*-Golgi by  $\alpha$ -mannosidases I ( $\alpha$ -Man I) until  $\text{Man}_5\text{GlcNAc}_2$  is generated. Then, the action of the N-acetylglucosamine transferase I (GnT I) in the medial-Golgi initiates the first branch of human N-glycans. Later,  $\alpha$ -Man II removes two outer Mann generating the substrate for GnT II. The resulting biantennary N-glycan  $\text{GlcNAc}_2\text{Man}_3\text{GlcNAc}_2$  is further extended by the addition of fucose thanks to the fucosyltransferase (FucT) activity; galactose through the activity of galactosyltransferases ( $\beta$ -GalT), and sialic acid *via* the sialyltransferases (SiaT) to generate a complex N-glycan with two branches (black frame). As mentioned on the right and below each arrow, processing and maturation of human N-glycan in the Golgi apparatus require a proper ion environment in terms of pH and cation ions such as  $\text{Ca}^{2+}$ ,  $\text{Zn}^{2+}$  and  $\text{Mn}^{2+}$ .

At this stage, complex N-glycans can carry additional GlcNAc residues either bound with  $\beta$ -1,4- or  $\beta$ -1,6- linkages to yield bi-, tri-, tetra- or penta-antennary N-glycans due to the action of several GnTs (GnT III, GnT IVa-c, GnT V and GnT Vb) respectively encoded by *MAGT3*, *MAGT4A-C*, *MAGT5* and *MAGT5B* [140,141] (Figure 16). The combined actions of all of these GnTs lead to a bisected N-glycan

with five different branches. The ‘bisection’ reaction is specifically catalyzed by GnT III and corresponds to the addition of  $\beta$ -1,4-GlcNAc to the  $\beta$ -linked Man belonging to the core glycan structure  $\text{Man}_3\text{GlcNAc}_2$  (gray shape in Figure 10). Actually, the presence of this bisecting GlcNAc exerts an inhibitory effect on other GTs which in turn stops any further elongation. In order to avoid overloading Figure 15, the complexity for producing N-glycan antennae is depicted in a separate Figure 16.

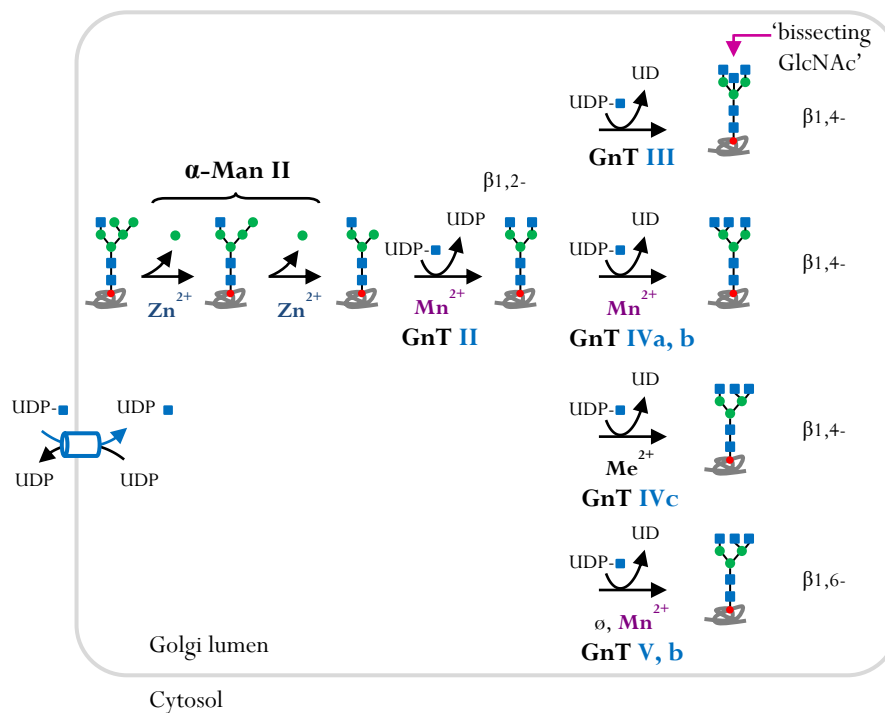


**Figure 16: Initiation of the different branches found in human complex N-glycans following the action of GnTs.**  $\emptyset$  : no divalent-metal-ion requirement,  $\text{Me}^{2+}$  : any divalent metal ion.

Keeping the example of the biantennary  $\text{GlcNAc}_2\text{Man}_3\text{GlcNAc}_2$  N-glycan, a fucosylation step may occur in the medial-Golgi onto the innermost GlcNAc residue through the activity of the  $\alpha$ -1,6-fucosyltransferase encoded by *FUT8*. The next steps occur in the *trans*-Golgi compartment, where  $\beta$ -1,4-Gal are added onto terminal GlcNAc residues through  $\text{Mn}^{2+}$ -dependent galactosylation reactions mediated by  $\beta$ -1,4-galactosyltransferase I (*B4GALT1*). Lastly, the biantennary N-glycan is capped with Sia thanks to the activity of  $\alpha$ -2,6-sialyltransferases I and II encoded by *ST6GAL1* and *ST6GAL2*.

As already mentioned, Figure 15 only illustrates the Golgi maturation steps leading to a specific and quite simple biantennary N-glycan. The diversity of the human N-glycan structures is not represented here but an overview has already been given in Figure 16, depicting additional pathways multiplying the number of antennae found in a given complex N-glycan. To add an extra layer of complexity and differing from yeast *Saccharomyces cerevisiae*, not all human Golgi GTs share the same divalent-metal-ion dependency. As reported on Figure 18, human Golgi GTs require different divalent ions amongst  $\text{Ca}^{2+}$ ,  $\text{Mn}^{2+}$  and  $\text{Zn}^{2+}$ .

### 2.3.3. Congenital Disorders of Glycosylation related to Golgi processing of human N-linked glycans

Constantly to the previous sections (2.1 and 2.2.), Table 10 lists all reported CDGs related to defective genes encoding GTs directly involved in the Golgi maturation human N-linked glycans. Compared with Table 8, only few CDG-genes encoding GTs involved in Golgi maturation steps have been identified. Actually, for more than a decade now, a new era in the CDG field has emerged with the identification of numerous genes encoding proteins not directly involved in the glycosylation reactions as defined in Figure 4; *i.e.* GTs, GHs and NST [39]. Indeed, genes encoding proteins involved in trafficking between the Golgi stacks, (ii) ionic transporters or (iii) subunits of the V-type ATPase, have been identified in type II CDG. All of these defective genes have been assumed to indirectly impact Golgi glycosylation reactions either by impacting the structural organization of the Golgi apparatus or its pH/ion homeostasis, preventing the correct localization and/or the optimal activity of specific GTs.

**Table 10: List of human CDGs associated with genes encoding GTs directly involved in Golgi maturation during the N-linked glycosylation process.** FucT: fucosyltransferase, GalT: galactosyltransferase and GlcNAcT: N-acetylglucosaminyltransferase.

| Former CDG              | Defective gene | Defective protein   | Impact              |
|-------------------------|----------------|---|---------------------|
| <i>Golgi processing</i> |                |   |                     |
| CDG-IIId                | <i>BAGALT1</i> | UDP-Gal: $\beta$ -GlcNAc $\beta$ -1,4-GalT 1                        | N-glycan elongation |
| CDG-IIa                 | <i>MGAT2</i>   | UDP-GlcNAc: $\alpha$ -1,6-mannosyl-glycoprotein 2- $\beta$ -GlcNAcT | N-glycan elongation |
| (CDGF1)                 | <i>FUT8</i>    | GDP-L-Fuc:N-acetyl- $\beta$ -D-glucosaminide $\alpha$ -1,6-FucT     | N-glycan maturation |

## 2.4. Cytosolic, proteasomal and lysosomal human N-glycans degradation

Previous sections referred to yeast and human N-glycan metabolism, from donor substrates biosynthesis (NM/DP-sugars or lipid phosphate linked-sugars) to transfer of the sugar moiety onto proteins in the ER (section 2.1.) and its maturation along the Golgi apparatus (section 2.2.). To wrap everything up, I intend here to briefly resume two main catabolism pathways for human N-linked glycans: (i) the ER-associated degradation (ERAD) pathway for mis-glycosylated/misfolded N-glycoproteins and (ii) the lysosomal degradation pathway for mature N-glycoproteins and free oligosaccharides (FOS).

### 2.4.1. ERAD pathway for mis-glycosylated/unfolded N-glycoproteins

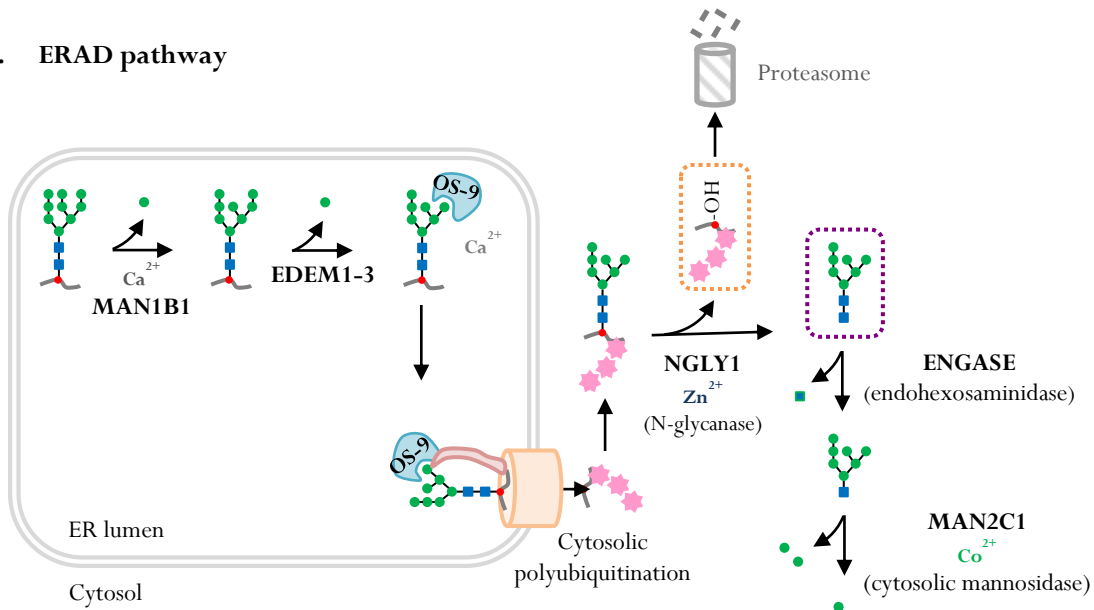
As mentioned in section 2.2.1., in some instances and despite all the checkpoints provided during ER quality control, N-glycoproteins fail to acquire their native conformation. In this case, misglycosylated or unfolded glycoproteins are subjected to the activity of EDEM ER mannosidases in addition to the first demannosylation reaction catalyzed by MAN1B1 (see Figure 13). This mannose trimming from

Man<sub>9</sub>GlcNAc<sub>2</sub> to Man<sub>5,7</sub>GlcNAc<sub>2</sub> is the signal for glycoprotein degradation *via* the ERAD pathway. ERAD is a cellular process according to which misfolded proteins are retrotranslocated from the ER lumen to the cytosol for subsequent degradation by an ubiquitin-proteasomal system (Figure 17A) [109,142]. In humans, Os-9 and XTP3-B are two luminal ER lectins that specifically bind to free terminal  $\alpha$ -1,6-Man residues found onto misfolded proteins through their mannose-6-phosphate receptor homology domains. Although in Figure 17A only the interaction with Os-9 is represented, both binding of Os-9 and XTP3-B promote the degradation of proteins by enabling their transfer to one of the numerous membrane-associated ERAD complexes. Amongst them, there is the HRD1-SLE1L ERAD complex, formed by the interaction between HRD1 and SEL1L, two ER transmembrane proteins (Figure 17A) [109]. HRD1, also known as ERAD-associated E3 ubiquitin-protein ligase, exerts an ubiquitin ligase function and polyubiquitinylates ERAD substrates on the cytosolic face of the ER. On the other hand, SLE1L interacts with different ERAD regulators such as EDEM proteins, Os-9 or XTP3-B in the ER lumen to facilitate the retrotranslocation of misfolded proteins. Once in the cytosol, the protein backbone is separated from the N-linked glycan through the action of the cytosolic endoglycosidase peptide:N-glycanase commonly known as PNGase (or even *NGLY1*, the gene encoding it), which cleaves the first glycosidic bond between GlcNAc and asparagine [143,144]. Then, the previously ubiquitin-tagged protein undergoes a proteasomal degradation while the free unconjugated N-glycan also known as free oligosaccharide (FOS) is sequentially degraded into the cytosol. From Man<sub>7</sub>GlcNAc<sub>2</sub>, endo- $\beta$ -N-acetylglucosaminidase (ENGase encoded by *ENGASE*) cleaves the innermost GlcNAc residue to yield Man<sub>7</sub>GlcNAc [145]. Two Man are then consecutively removed by the cobalt (Co<sup>2+</sup>)-dependent cytosolic  $\alpha$ -mannosidase MAN2C1 until Man<sub>5</sub>GlcNAc [146]. This specific FOS is then thought to be transported into the lysosome for further degradation by lysosomal mannosidases (Figure 17B) [147]. As shown in Figure 17, FOS released during the ERAD pathway end their degradation route into the lysosome where mature N-glycoproteins and additional glycoconjugates are also degraded.

#### 2.4.2. Lysosomal degradation of mature N-glycoproteins and FOS

All glycoconjugates (*N*-linked, *O*-linked, GAGs, glycolipids) share a common lysosomal degradation pathway enabling the recycling of their constitutive monosaccharides through the salvage pathway. In addition to make monosaccharides available again, glycoconjugates catabolism is essential to ensure lysosomal functions and appropriate homeostasis since lysosomal storage diseases have been identified. These disorders result from genetic mutations altering the function of specific glycosidases involved in such lysosomal catabolism of glycoproteins or glycolipids. Here, only the lysosomal degradation of mature *N*-linked glycoproteins will be briefly addressed, inspired from Suzuki's latest review on the topic [147] (Figure 17B).

### A. ERAD pathway



### B. Lysosomal degradation for N-glycoproteins and FOS

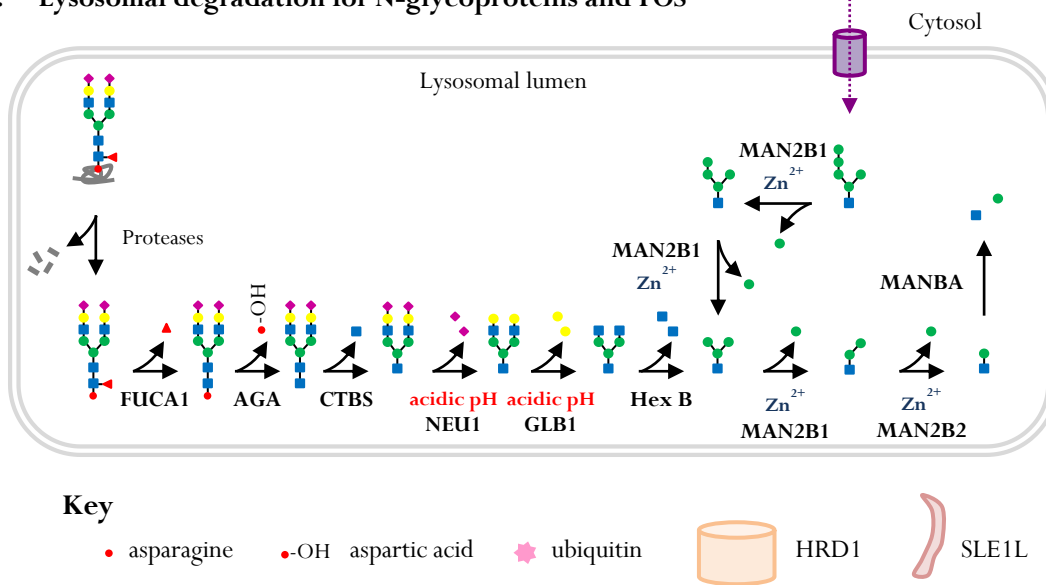


**Figure 17: Human N-glycoproteins and free oligosaccharides (FOS) catabolism.** **A.** Following the ER quality control, misfolded and/or misglycosylated N-glycoproteins are retrotranslocated into the cytosol for proteasomal degradation through the ER-associated degradation (ERAD) pathway involving here interaction of the misfolded protein with Os-9 protein and then, the HDR1-SLE1L ERAD complex. The first step of this process is to remove the N-glycan from the proteic backbone through the action of the cytosolic PNGase (encoded by *NGLY1*). Then, the proteic part (orange dashed frame) undergoes a proteasomal degradation and the FOS (purple dashed frame) are sequentially degraded into the cytosol until a  $\text{Man}_5\text{GlcNAc}$  structure. This specific FOS is then thought to be transported into the lysosome for further degradation. **B.** The different steps occurring during the lysosomal degradation of mature N-glycoproteins and FOS are inspired by Suzuki's review.

At first, a set of different lysosomal proteases act in concert to ensure proteolysis prior to glycan degradation especially due to the strict substrate specificity of the lysosomal aspartylglucosaminidase (AGA) that only cleaves the amide bond between GlcNAc and asparagine residues when this later has

free amino and carboxy ends. Following proteolysis, the lysosomal  $\alpha$ -fucosidase FUCA1 mediates defucosylation of the core fucose (*i.e.* branched onto the innermost GlcNAc residue in  $\alpha$ -1,6 linkage, Figure 10). Immediately after, AGA exerts its function, releasing aspartic acid residue and FOS. This FOS is then degraded by a series of lysosomal glycosidases as follows: N-acetylchitinase (CTBS), sialidase (NEU1),  $\beta$ -galactosidase (GLB1),  $\beta$ -hexosaminidases (HEXA/B) and  $\alpha$ -/ $\beta$ -mannosidases (MAN2B1/2, MANBA) removing one by one the monosaccharides constituent of the FOS. Briefly, CTBS cleaves the first GlcNAc residue that was previously bound to asparagine while NEU1 degrades FOS from its non-reducing ends by releasing terminal Sia residues. Once NEU1 has operated, non-reducing Gal and GlcNAc residues are sequentially removed by GLB1 and HEXA/B, respectively. Then, MAN2B1 can cleave whether on  $\alpha$ -1,2;  $\alpha$ -1,3 or  $\alpha$ -1,6-linked Man while MAN2B2 preferentially cuts  $\alpha$ -1,6-Man. Finally, the  $\beta$ -mannosidase MANBA ensures the last degradation step for N-linked glycans by breaking down the Man $\beta$ -1,4-GlcNAc disaccharide [147] (Figure 17B).

#### 2.4.3. Congenital Disorders of Glycosylation associated with N-linked glycan catabolism

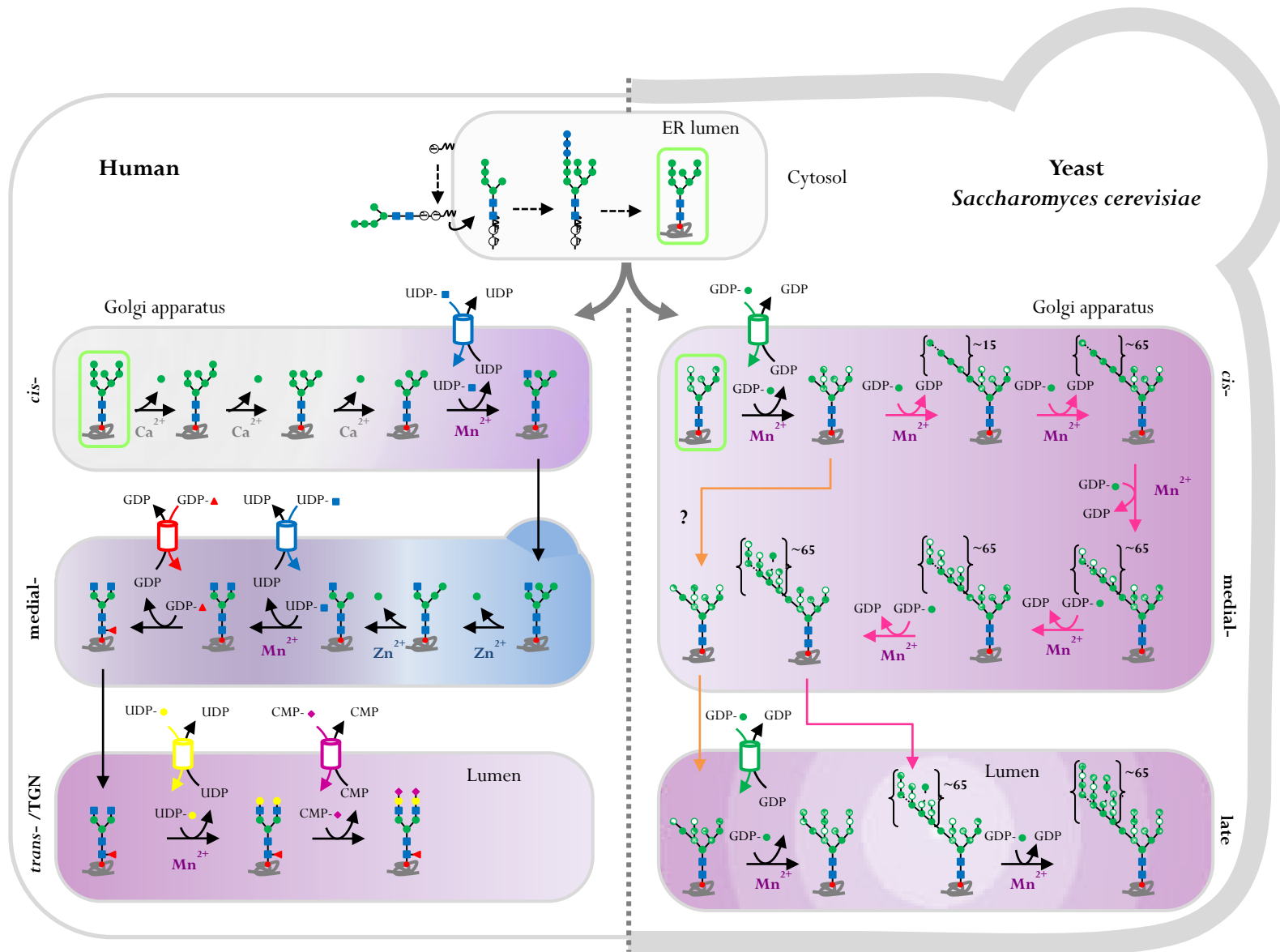
So far, no Congenital Disorders of Glycosylation have been identified associated with defective genes described in the previous sections. Nonetheless, a particular Congenital Disorder of DeGlycosylation (CDDG) has been reported for the first time in 2014 by Enns *et al.* due to pathogenic mutations in *NGLY1*, the gene encoding cytosolic PNGase [148,149].

### 3. On the ion side of the N-linked glycosylation pathway

All of the reactions described above are involved in the synthesis of glycan structures and based on sequential activities of specific enzymes adding (GTs) or removing sugar residues (GHs). As a common feature to all enzymes, pH and ion environment are crucial for them to reach an optimal activity. In particular, divalent cation ions such as  $Mn^{2+}$ ,  $Zn^{2+}$ ,  $Ca^{2+}$ ,  $Mg^{2+}$  and  $Co^{2+}$  are required as co-factors to directly act in the catalytic site of the enzyme. Hereafter, albeit all glycosylation processes imply divalent-cation-ion-dependent GTs, GHs and other proteins such as chaperones and lectins, only those related to the N-linked glycosylation process will be addressed. To have a better overview of the commonalities and differences between yeast *Saccharomyces cerevisiae* and human N-glycosylation process, the following Figure 18 summarizes this cellular process facing both organisms. In particular, Figure 18 offers a kind of ‘glyco-ion’ map of the divalent-metal-ion required during the N-linked glycosylation in both organisms. A common feature between yeasts and humans is the  $Ca^{2+}$  dependency of chaperone, GHs and lectins in the ER to ensure glycoproteins folding and transport between the ER and the Golgi apparatus. However, at the Golgi level while in yeast *Saccharomyces cerevisiae* almost all the GTs – especially mannosyltransferases – are  $Mn^{2+}$ -dependent, in mammals, the ion requirements are a bit

different. Indeed, in the early *cis*-Golgi,  $\text{Ca}^{2+}$  ions are mainly needed especially to ensure efficient activity of (i) numerous lectins involved in glycoproteins trafficking from the ER and back to it and also the activity of (ii) the first GHs, mainly mannosidases, involved in the early trimming of the N-glycans. Then, mannosidases from the *medial*-Golgi are  $\text{Zn}^{2+}$ -dependent whereas the first GTs become  $\text{Mn}^{2+}$ -dependent. Why yeast *Saccharomyces cerevisiae* GTs have evolved in an exclusive  $\text{Mn}^{2+}$ -dependent way of action is an opened question. However, since N-linked glycan maturation in the yeast mainly involved mannosyltransferases, during evolution these specific GTs may have preserved this dependency to uniform the ion requirement in the Golgi apparatus. Actually, in mammals, a more complex regulation of the ion homeostasis takes place. In the following chapter (Chapter 2), I will mainly focus on the regulation of both  $\text{Ca}^{2+}$  and  $\text{Mn}^{2+}$  homeostasis along the secretory pathway.

**Figure 18: Overview of the N-linked glycosylation pathway in human and yeast *Saccharomyces cerevisiae*.** This figure offers a clear picture of the commonalities and differences occurring during the N-linked glycosylation pathway in both human (left.) and yeast (right). For readability reason, the name of all the enzymes involved in this process has been removed in this scheme. However, the reader can refer to Figures 14 and 15 to have these complementary information. While all yeast mannosyltransferases are  $\text{Mn}^{2+}$ -dependent, the higher diversity of human GTs and GHs induces the requirement of a different Golgi cation environment. Indeed, human *cis*-Golgi mannosidases are  $\text{Ca}^{2+}$ -dependent, medial-Golgi mannosidases are  $\text{Zn}^{2+}$ -dependent and generally, all Golgi GTs using UDP-sugars as donor substrates require  $\text{Mn}^{2+}$  as a cofactor. Gradients of  $\text{Ca}^{2+}$ ,  $\text{Mn}^{2+}$  and  $\text{Zn}^{2+}$  are depicted in each Golgi cisternae with the corresponding colors: grey, purple and blue.





---

**Chapter 2:**  
**Ca<sup>2+</sup>/Mn<sup>2+</sup> homeostasis within the secretory pathway:**  
**yeast versus human**

---



Calcium (Ca) and manganese (Mn) are two elements widely found on earth and in all living organisms, with quite different abundances. While Ca ranges as the 5<sup>th</sup> most abundant element in the earth's crust, Mn is the 12<sup>th</sup>. With a stable oxidation state of +2 (Ca<sup>2+</sup>), Ca is one of the most abundant biometal in the human body. On the other hand, Mn is a trace element that commonly shares positive oxidation states ranging from +2 and +7. In physiological conditions, Mn can be found in two main forms with an oxidation state of +2 (Mn<sup>2+</sup>) or +3 (Mn<sup>3+</sup>). Biologically, Mn<sup>2+</sup> is the only active form of Mn while Mn<sup>3+</sup> is toxic, acting as a powerful oxidant. Both Ca<sup>2+</sup> and Mn<sup>2+</sup> are crucial ions involved in a broad range of cellular processes. In this chapter, a general introduction about Ca and Mn roles in yeast and human will first be addressed. Then, an overview of the different transporters involved in Ca<sup>2+</sup> and Mn<sup>2+</sup> homeostasis within the secretory pathway will be depicted.

## 1. General introduction about Ca<sup>2+</sup> and Mn<sup>2+</sup> in yeast and human

### 1.1. Ca<sup>2+</sup> and Mn<sup>2+</sup> main storage organs/organelles

#### 1.1.1. Ca<sup>2+</sup> and Mn<sup>2+</sup> stocks in human

- At the body levels (organs).

Ca is a key nutrient in the human body accounting for 1 to 2% of the body weight. Of this, 99% of the total Ca burden is stored in mineralized tissues such as bones and teeth while the remaining 1% is found in blood, extracellular fluids, and muscles (Figure 19A). The skeleton is then a major reservoir that provides Ca for both extracellular and intracellular pools. In bones, the most abundant mineralized form of Ca responsible for bone structure and density is hydroxyapatite (Ca<sub>10</sub>(PO<sub>4</sub>)<sub>6</sub>(OH)<sub>2</sub>). On the other hand, in physiological fluids, Ca is mainly found ionized (Ca<sup>2+</sup>) (50%), bound to plasma proteins (40%) or complexed with anions such as bicarbonate, lactate, citrate and phosphate (10%). For instance, in healthy individuals, total Ca concentration in plasma ranges between 2 to 2.5mM while plasma ionized Ca concentration are comprised between 1.1 and 1.35mM. [150–153]. With regards to Mn, no real Mn storage organs are actually known. However, some of them such as bones, liver, pancreas and kidneys share a higher Mn content due to their involvement in its metabolism (Figure 19A) [154,155]. More precisely, bones contain up to 40% of the total burden of Mn (1mg/kg) and the liver, being highly involved in Mn biliary excretion, contains up to 1.2mg Mn/kg. On the other hand, in healthy individuals, 0.15 to 0.46mg Mn/kg is found in the brain and this Mn level needs to be tightly regulated to prevent Mn neurotoxicity and damages. Finally, in human blood, Mn can be found in its two main ionized forms, Mn<sup>2+</sup> and Mn<sup>3+</sup>. Mn<sup>2+</sup> is predominant and mostly found in complexes with albumin, β-globulin, citrate and bicarbonate. In addition, a small fraction of Mn<sup>2+</sup> can be oxidized into Mn<sup>3+</sup> by the ceruloplasmin to especially bound transferrin (Tf) and make a stable complex.

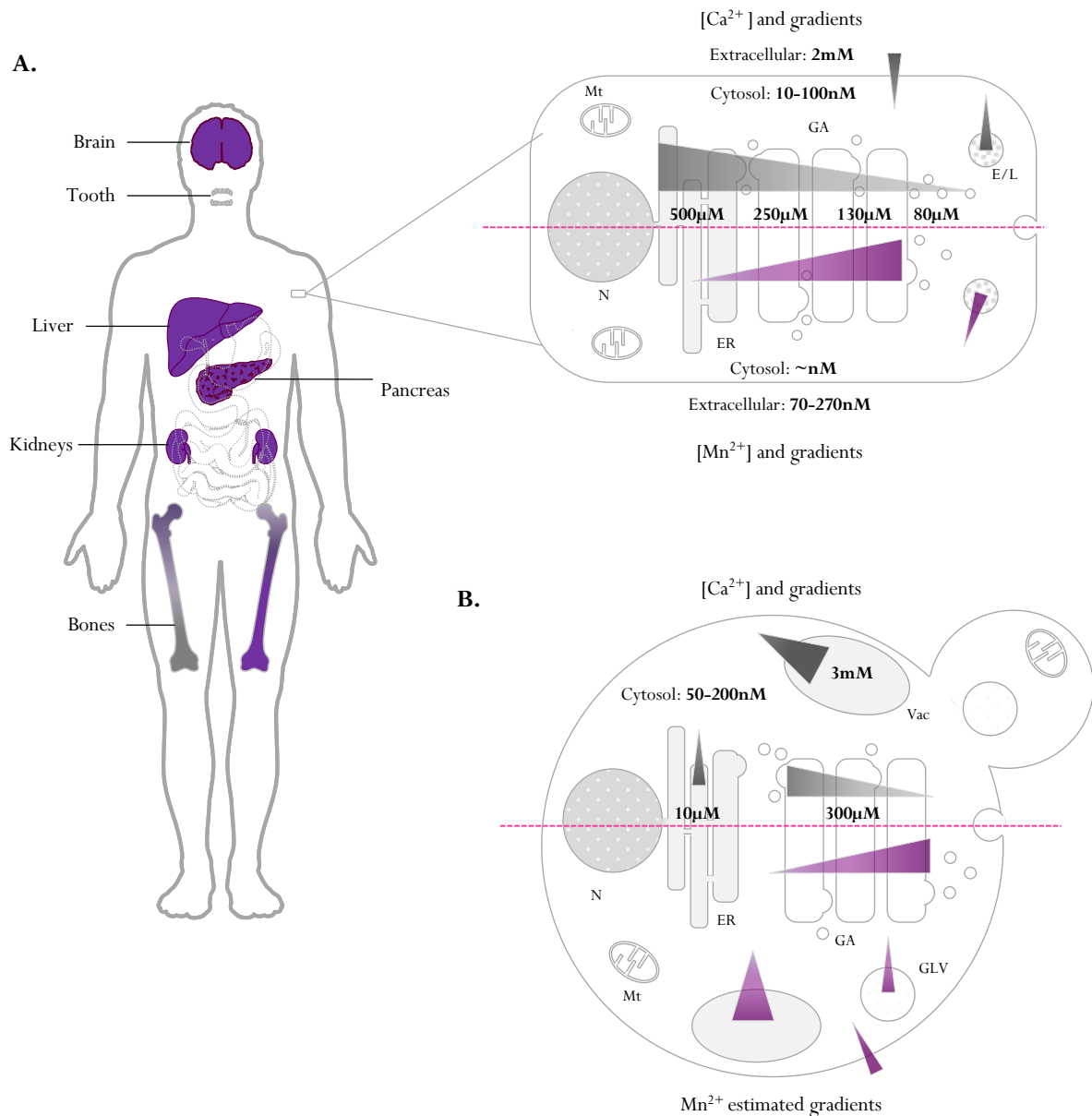


**Figure 19: Main Ca and Mn storage organs and organelles in human and yeast.** **A.** Schematic representation of the main Ca (grey) and Mn (purple) storage organs within the human body. An arbitrary zoom on the right depicts a schematic representation of a human cell. The pink dotted line artificially divides the cell in two. The main known Ca<sup>2+</sup>/Mn<sup>2+</sup> concentrations and subsequent gradients within the secretory pathway are represented respectively in grey and purple, upper and under the dotted line. **B.** Schematic representation of a yeast cell, also virtually divided in two by a pink dotted line. As for the human cell, the main known Ca<sup>2+</sup>/Mn<sup>2+</sup> concentrations and subsequent gradients within the secretory pathway are represented respectively in grey and purple, upper and under the dotted line. E/L: endo/lysosome, ER: endoplasmic reticulum, GA: Golgi apparatus, GLV: Golgi like vesicles, Mt: mitochondrion, N: nucleus and Vac: vacuole.

- Intracellular Ca<sup>2+</sup> and Mn<sup>2+</sup> stores

At the cellular level, different techniques can be used to measure intracellular Ca<sup>2+</sup> concentrations ([Ca<sup>2+</sup>]). To list some: electrophysiology based on patch clamp analysis, chemical Ca<sup>2+</sup> indicators (probes, dyes) such as Rhod-4, Fluo-4 or Fura2-AM and, genetically encoded fluorescence calcium indicators which basically correspond to the fusion of a fluorescent protein to a calcium binding protein

(such as calmodulin (GCaMP) or aequorin based assay). Whatever the technique used to determine intracellular  $[Ca^{2+}]$ , it came out that in mammalian cells,  $[Ca^{2+}]$  within the secretory pathway decreases from  $500\mu M$  in the ER to  $80\mu M$  in the secretory vesicles while cytosolic  $[Ca^{2+}]$  only ranges between 10 to  $100nM$  (Figure 19A). As well demonstrated by Pizzo *et al.*, in addition to the ER, the Golgi apparatus is one of the main  $Ca^{2+}$  store in the cell [18]. Within the Golgi apparatus itself, a decreasing  $Ca^{2+}$  gradient can be observed from the *cis*- side to the TGN. This gradient is mainly established and maintained through the presence and activity of  $Ca^{2+}$  transporters, differing from each Golgi cisternae [18].

Regarding to  $Mn^{2+}$ , no many tools are currently available to measure precisely intracellular  $[Mn^{2+}]$ , which is the reason why estimated gradients and concentrations are represented in Figure 19. However, taking advantage that  $Mn^{2+}$  can replace  $Ca^{2+}$  and bind the  $Ca^{2+}$  fluorescent indicator Fura-2, cytosolic  $Mn^{2+}$  measurement can be done. Basically,  $Mn^{2+}$  quenches Fura-2 emitted fluorescence leading to a lower signal in cells containing more Mn. To reach  $[Mn^{2+}]$  in the organelles, a detergent is then required to permeabilize membranes and release luminal  $Mn^{2+}$  to the cytosol. Very recently, Horning *et al.* developed a new selective  $Mn^{2+}$  ionophore called MESMER (Manganese Extraction Small Molecules Estimation Route). Based on  $Mn^{2+}$ -induced Fura-2 quenching, MESMER enables non-lethal quantification of cellular Mn levels. Finally, total cellular Mn detection and quantification can also be assessed through inductively coupled plasma mass spectrometry (ICP-MS) or atomic absorption spectroscopy (AAS). Based on these indirect approaches, the main intracellular  $Mn^{2+}$  stores identified in the mammalian cells are: mitochondria, ER, Golgi apparatus, lysosomes and endosomes (Figure 19A). All in all, the secretory pathway can be considered as a sink for intracellular  $Ca^{2+}/Mn^{2+}$  storage taking part in their cellular distribution. Hence, a tight regulation occurs within the secretory pathway to maintain both  $Ca^{2+}$  and  $Mn^{2+}$  homeostasis. This will be addressed in section 2.

### 1.1.2. $Ca^{2+}$ and $Mn^{2+}$ stocks in yeast

In the yeast *Saccharomyces cerevisiae*, a similar intracellular  $Ca^{2+}$  and  $Mn^{2+}$  distribution can be observed within the secretory pathway and in mitochondria (Figure 19B). However, while in mammalian cells the ER concentrates  $Ca^{2+}$  up to  $500\mu M$ , the vacuole plays this role in yeast. Indeed, 90% of the  $Ca^{2+}$  pool is found in the vacuolar compartment where it accumulates to up to  $3mM$ . This major difference between yeast and human could be due to the absence of Sarco/Endoplasmic Reticulum  $Ca^{2+}$ -ATPases (SERCA) pumps in yeasts, which are the main key players in ER  $Ca^{2+}$  storage in human. Additionally, yeast also lacks lysosomes and endosomes that are replaced by the vacuole and the Golgi like vesicles. Apart from its  $Ca^{2+}$  storage capacity, the yeast vacuole is the main organelle responsible for the sequestration of divalent heavy metals ions including  $Mn^{2+}$  then preventing their cytosolic accumulation to toxic levels.

## 1.2. $\text{Ca}^{2+}$ and $\text{Mn}^{2+}$ regulation at the body level

### 1.2.1. Main route for $\text{Ca}^{2+}$ absorption/excretion

Dietary Ca intake and absorption are essential to maintain healthy Ca body stores. In response to dietary intake, kidneys and the small intestine are the main organs required for Ca absorption and kidneys also contribute to Ca excretion. Although Ca ingestion occurs *via* the gastrointestinal tract, 65% of its absorption is done in the small intestine through passive diffusion or active transport. Once in the circulation, Ca is mostly deposited into bones not only to ensure bone formation or repairing but also to be stored. On the other hand, Ca excretion is mainly mediated by kidneys *via* urinary filtration and excretion. To have an idea, around 200mg of Ca are released in urine from healthy adults with a daily Ca intake of 1g [152]. The main foods enrich in Ca are dairy products such as milk, yogurts and cheese. However, other non-dairy sources share a high Ca content as well. These include seafood, leafy green vegetables, almonds, seeds and Ca- fortified foods, to list some. Human Ca needs vary through the different stages of life and also depends on sex gender and genetic background. In a report from the European Food Safety Authority dating back to 2015, all of these parameters have been considered to better established average Ca intake recommendations [156].

In the whole body, Ca homeostasis is controlled by its absorption/excretion and storage in the skeleton to ensure a constant plasmatic Ca concentration ( $[\text{Ca}^{2+}]_{\text{plasma}}$ ). Many complex physiological processes are involved in such  $[\text{Ca}^{2+}]_{\text{plasma}}$  regulation [150–153]. Briefly and basically described in Figure 20, three main calcitropic hormones serve to increase/decrease the entry of Ca in the extracellular space. Those hormones are the parathyroid hormone (PTH), the calcitriol and the calcitonin. In case of lower  $[\text{Ca}^{2+}]_{\text{plasma}}$ , PTH promotes both Ca release from the bones and Ca reabsorption by kidney tubules. Moreover, in concert with the calcitriol, PTH also induces Ca reabsorption in the intestine. Calcitriol is defined by the hormonal form of vitamin D, the latter being crucial for bone formation. On the other hand, calcitonin has reverse effects and inhibits both Ca release from the bones and reabsorption from the kidneys following higher  $[\text{Ca}^{2+}]_{\text{plasma}}$  [150,151].

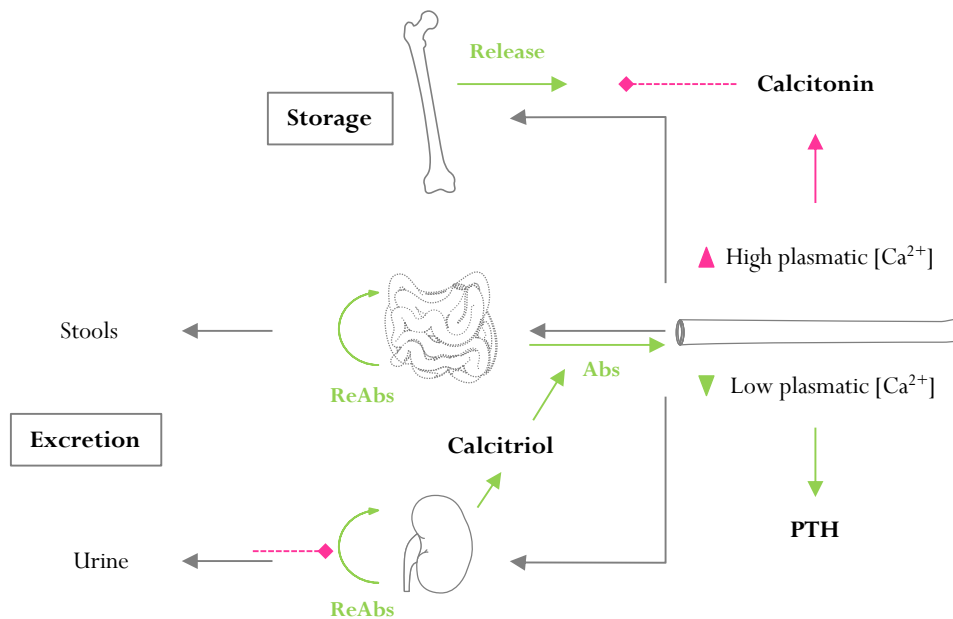


**Figure 20: Simplified representation of calcium (Ca) regulation in human.** In normal condition (grey arrows), dietary Ca is absorbed during intestinal digestion and release in the circulation. Circulating Ca is then deposited in bones for storage or excreted in urine or in stools. In case of low plasmatic Ca concentration (green arrows), PTH promotes Ca release from bones and Ca reabsorption in kidney tubules. Moreover, PTH also induces Ca reabsorption in the intestines thanks to calcitriol. In case of high plasmatic Ca concentration (dotted pink arrows), calcitonin both inhibits Ca release from bones and Ca reabsorption in kidney tubules. Abs: absorption, PTH: parathyroid hormone and ReAbs: reabsorption. Inspired by [151].

### 1.2.2. Main routes for $Mn^{2+}$ absorption/excretion

Several paths promote Mn absorption in the human body: oral consumption from diet, inhalation, dermal permeation and intravenous administration [155,157]. Amongst them, ingestion remains the most common route. Once ingested, approximately 3 to 5% of Mn is absorbed into the body through the gastrointestinal tract, especially in the intestine (Figure 21) [154,158]. Like Ca, Mn then enters cells either by passive diffusion or active transport, mostly mediated by the divalent metal transporter 1 (DMT1) [159]. Although other transporters are involved in Mn influx, none of them are Mn-specific and also regulate the import of other ions such as iron ( $Fe^{2+}$ ), calcium ( $Ca^{2+}$ ), zinc ( $Zn^{2+}$ ) and copper ( $Cu^{2+}$ ). Therefore, the presence of such ions in blood and other physiological fluids can compete with Mn and compromise its absorption. In particular, Mn interaction with iron (Fe) was well studied [160]. While Fe deficiency enhances intestinal Mn absorption, a higher intake of Fe reduces Mn blood levels. In addition, more than twenty years ago Finley *et al.* pointed out lower Mn absorption rates in healthy men than in women. This sex difference was believed to be due to Fe status variations between men and women, with a higher Mn absorption in presence of lower serum ferritin concentrations [161,162].

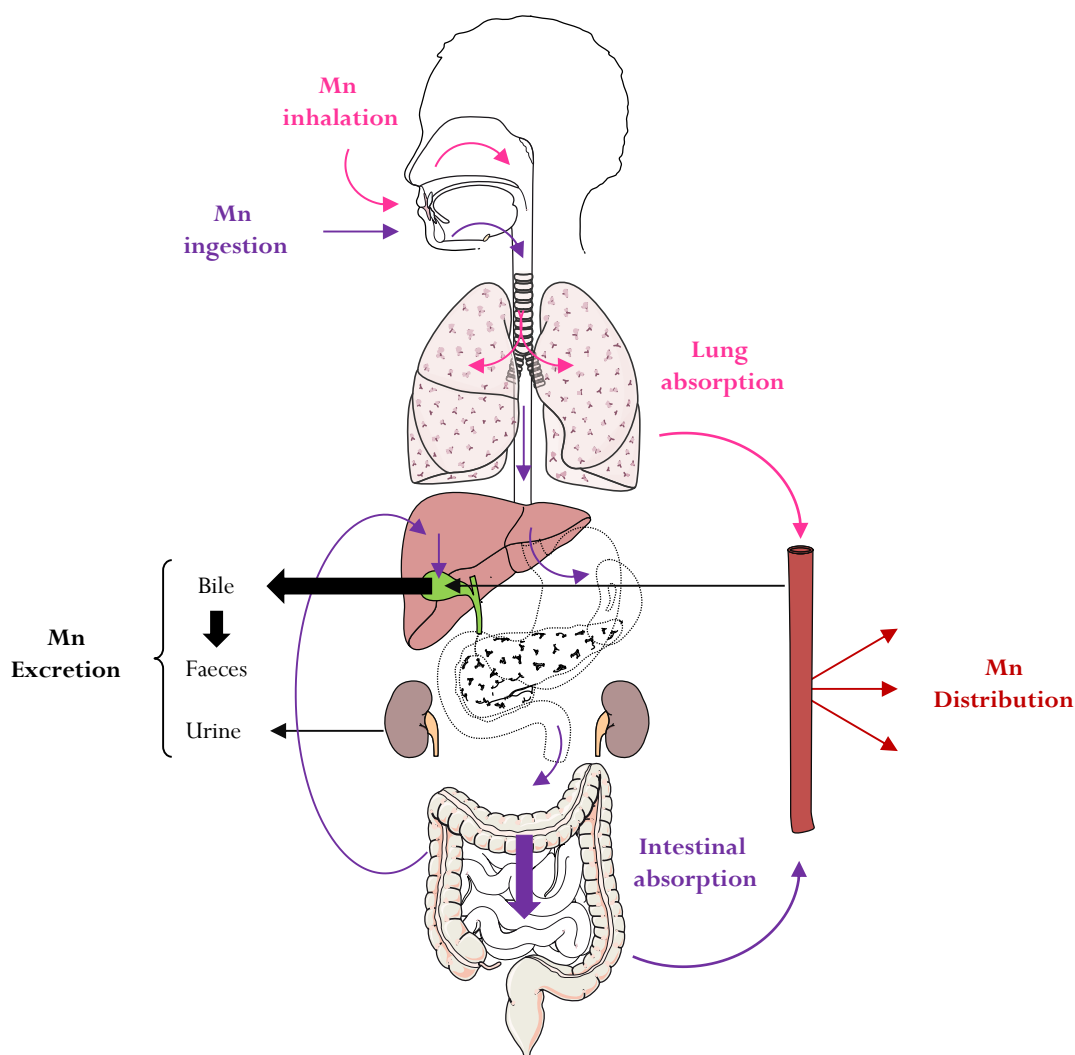


**Figure 21: Simplified representation of manganese (Mn) metabolism in human.** Mn uptake is mainly mediated by oral consumption from diet (ingestion) and inhalation. Once ingested (purple arrows), 3 to 5% of Mn is absorbed in the intestine while up to 95% is excreted via the bile (bold black arrow). Mn enters the blood stream through passive diffusion or active transport where it is then distributed to other organs. On the other hand, inhaled Mn (pink arrows) is absorbed in the lungs and bypasses the liver to enter the blood stream.

In terms of Mn elimination, the liver is the key organ ensuring such function. As depicted by bold black arrow in Figure 21, 95 to 98% of oral Mn is excreted into the small intestine through hepatobiliary secretion. Then, Mn is eliminated in the faeces while only 0.1 to 3% is excreted in urines [163,164]. Many foods are considered as rich sources of Mn and ensure its dietary uptake. To list some, high levels of Mn are found in a broad range of whole grains and nuts as well as in rice, legumes, leafy green vegetable, seafood, tea and chocolate [155]. Besides solid meals, drinking water and some beverages also contain Mn at rather high or low level. Very recently, Martins *et al.* reviewed the role of Mn in the diet with a main focus on its bioaccessibility and adequate intake [165]. This review also summarizes the average Mn intake recommendations for adults and young people depending on sex gender, established by the European Food Safety Authority in 2013 [163,165]. Apart from oral Mn consumption, Mn can be inhaled from airborne particles especially linked to particular occupational positions such as mining,



steeling, smelting, welding and battery manufacturing. Once inhaled, Mn is absorbed in the lungs and bypasses the liver to enter the blood stream (pink arrows, Figure 21). Then, circulating Mn is rapidly distributed in tissues and is believed to enter the brain through the olfactory tract (olfactory nerves). How does Mn cross the blood brain barrier is still under investigations even if DMT1 and the transferrin receptor (TfR) are suggested to play a major role in this mechanism [166–168]. Mn overexposure can lead to its accumulation in the brain, especially in the basal ganglia, which is very toxic. This will be further detailed in the section 1.4.2.

### **1.3. Ca<sup>2+</sup> and Mn<sup>2+</sup> in cellular processes**

#### **1.3.1. Ca in bone mineralization**

In the human body, the skeleton is considered as the main reservoir of Ca and phosphate. Throughout all stages of life, bones are remodeled in response to mechanical stress and physiological needs for Ca<sup>2+</sup> in extracellular fluids [169]. As defined by Clarke *et al.*, bone remodeling is a process by which bone is renewed to maintain bone strength and mineral homeostasis [169]. At the cellular level, this remodeling process is achieved by a tightly coupled group of specialized cells named osteoclasts and osteoblasts, that sequentially and respectively manage resorption of old bone and formation of new one. Basically bones are composed of 50%-70% minerals, 20%-30% organic matrix, 5%-10% water and less than 3% lipids [152,153,169]. Bone minerals are especially represented by hydroxyapatite crystals Ca<sub>10</sub>(PO<sub>4</sub>)<sub>6</sub>(OH)<sub>2</sub> with small amount of carbonate, magnesium and acid phosphate. As regards to bone organic matrix composition, it is mainly made of fiber type I collagen (90%-95%). Besides, additional and non collagenous proteins also take part in its composition such as alkaline phosphatase and osteocalcin, osteopontin and bone sialoprotein, three Ca- and phosphate-binding proteins [169]. Bone mineralization occurs throughout the formation of hydroxyapatite crystals resulting from the precipitation of Ca and phosphate. This precipitation event is not likely spontaneous and required the formation of specific matrix extracellular vesicles. Those latter contain a nucleation core made of proteins and acidic phospholipids, Ca and inorganic phosphate in complexes that promote hydroxyapatite precipitation. At the end, the amount and size of hydroxyapatite crystals are regulated by Ca- and phosphate-binding proteins [18]. Thus, Ca is a key nutrient fundamentally required in bone mineralization through the formation of hydroxyapatite crystals.

#### **1.3.2. Ca<sup>2+</sup> signaling**

At the cellular level, Ca<sup>2+</sup> ions are used to signal almost all aspects of cellular life from cell proliferation to cell death. In yeast and human cells, like in other eukaryotic cells, Ca<sup>2+</sup> is required as a second messenger in signal transduction. A dysregulation in Ca<sup>2+</sup> signaling is often associated with pathological

conditions. To avoid this, cells finely adjust  $\text{Ca}^{2+}$  levels through the activity of a broad range of pumps, transporters, carriers, channels, and calcium binding proteins (see 3.1.). Cytosolic  $[\text{Ca}^{2+}]$  ( $[\text{Ca}^{2+}]_{\text{cytosol}}$ ) increases from the nanomolar to the micromolar range following  $\text{Ca}^{2+}$  release from the Ca storage organelles (mostly the ER in human and the vacuole in yeast, Figure 19) or  $\text{Ca}^{2+}$  influx from the extracellular medium mediated at the plasma membrane [170]. Changes in  $[\text{Ca}^{2+}]_{\text{cytosol}}$  reflect the  $\text{Ca}^{2+}$  signal, that may vary in amplitude, frequency and subcellular localization according to the stimulus and the cell type, and is then converted into specific cell functions [170]. Thereafter, pumps and exchangers act in concert to restore basal  $[\text{Ca}^{2+}]_{\text{cytosol}}$  corresponding to resting conditions.

### 1.3.3. $\text{Ca}^{2+}$ and $\text{Mn}^{2+}$ as cofactors

In terms of biological relevance,  $\text{Mn}^{2+}$  plays two main roles: (i) cofactor for numerous metalloproteins embracing all type of enzymatic reactions (*i.e.* oxidoreductases, transferases, hydrolases, lyases, isomerases and ligases) and (ii) non-enzymatically removal of reactive oxygen species (ROS). Therefore,  $\text{Mn}^{2+}$  takes part in many cellular processes and is involved in a broad range of ubiquitous enzymatic reactions mainly required for the synthesis of amino acids, lipids, proteins and carbohydrates, cellular energy and host defense [38]. To list some well-known Mn-dependent enzymes, arginase is involved in urea synthesis, acetyl-CoA carboxylase is crucial for endogenous fatty acid synthesis, phosphoenolpyruvate decarboxylase and pyruvate carboxylase belong to the gluconeogenesis pathway, Mn superoxide dismutase (MnSOD or SOD2) is the mitochondrial antioxidant enzyme involved in ROS detoxification, glutamine synthetase is important for brain ammonia metabolism, and several glycosyltransferases that take part in the glycosylation processes (see Chapter 1) and in human bone health [155,157,168,171]. To the latter point,  $\text{Mn}^{2+}$  indirectly participates to bones and teeth biomineralization through the phosphorylation activity of the Mn/ATP-dependant Golgi casein kinase known as FAM20C on specific protein such as osteopontin or bone sialoprotein [172,173]. Hence, although  $\text{Mn}^{2+}$  is a trace element, its requirement is crucial for many cellular processes ensuring cell viability. On the other hand,  $\text{Ca}^{2+}$  can also act as a cofactor especially for some glycosylation enzymes such as glycosidases and sulfatases where it is required for hydrolytic activity [38]. In addition, it is to note that  $\text{Ca}^{2+}$  is not likely found as free ions in lumens but bound to so-called  $\text{Ca}^{2+}$ -binding proteins (CBP). In such binding to the protein,  $\text{Ca}^{2+}$  does not fulfill a cofactor function but rather ensures its intracellular retention. Some examples of ER and Golgi CBP will be given in section 3.1.

### 1.3.4. $\text{Mn}^{2+}$ -complexes as antioxidants

In yeast and human cells, free radical species are a by-product of an aerobic metabolism. In case of ROS accumulation, especially due to a lack of efficient protection against oxidative stress, cell damages are

observed and can lead to human diseases [174]. From yeast to human, one of the primary roles assigned to Mn is to prevent the oxidative stress response by destroying free radicals. To ensure such function, two Mn-dependent ways are possible to follow (i) the well-known enzymatic process requiring  $Mn^{2+}$  as cofactor for MnSOD activity [175–177] or, (ii) a non-enzymatically process requiring solely  $Mn^{2+}$  in complexes [178,179]. This later will be briefly discussed since  $Mn^{2+}$  in complexes with phosphate, lactate or carbonate have been shown to be very efficient to scavenge ROS [174,178,179]. In human cells, albeit no direct evidences have been provided to attest from the relevance of Mn as a non-enzymatic antioxidant, in some diseases altering MnSOD function, a tight Mn supplementation could be of interest to cope with the oxidative stress by bypassing the deficient enzymatic pathway [174]. On the other hand, in yeast lacking *SOD* genes, the growth defect associated *SOD* deletions in aerobic conditions could be suppressed by  $MnCl_2$  supplementation. Moreover, deletion of other genes encoding Mn transporters (*PMR1* and *CCC1*) in *sodA* yeasts also succeeded in restoring the aerobic growth [180–182]. This suggests that intracellular  $Mn^{2+}$  can serve as an alternative route to the enzymatic protection. Regarding to  $Mn^{2+}$ -complexes formation, environmental factors such as nutrient sensing seem to controlled their production [183]. Finally, at the structural level, the nature of some  $Mn^{2+}$ -complexes has been achieved and revealed the binding of  $Mn^{2+}$  with inorganic phosphate (Pi) and polyphosphate [184]. All in all, as well illustrated in the yeast *Saccharomyces cerevisiae*,  $Mn^{2+}$  can form non-enzymatic complexes to promote protection against oxidative stress by acting as an antioxidant. Because such function has not been reported in human cells, it is likely that higher eukaryotes may have evolved differently to manage both Mn content and oxidative stress.

## 1.4. $Ca^{2+}$ and $Mn^{2+}$ in human diseases

### 1.4.1. Ca deficiencies and bone diseases

Most of the time, Ca deficiencies are associated with a poor Ca consumption. If the dietary Ca supply is not sufficient to meet physiological requirements, Ca is resorbed from the skeleton to sustain  $[Ca^{2+}]_{plasma}$ . As mentioned above, bones are constantly remodeled at all stages of life, balancing between bone formation and bone resorption. However, by the time, unbalanced Ca release weakens bones by reducing their density and mass leading to metabolic bone diseases such as osteopenia and osteoporosis. Osteopenia is characterized by low bone density whereas osteoporosis is defined by lower bone mass and mineral content with deterioration of the bone tissues, increasing bone fragility and risk of fracture [150]. To better discriminate between osteopenia and osteoporosis, the World Health Organization recommends the measure of bone mineral density (BMD) or bone mineral content (BMC) as indicators [150,153]. Insufficient Ca intake over a long period of time can also result in osteomalacia in adults or rickets in children. These disorders are due to bone mineralization defects occurring during its

formation. Rickets affects the growing bones of children while osteomalacia impacts formed bones in adult individuals. Although osteomalacia and rickets are associated with Ca deficiency at the bone level, they usually result from a vitamin D deficiency [153].

#### 1.4.2. Impaired Mn<sup>2+</sup> regulation and diseases

- Mn toxicity and neurodegenerative diseases

Mn toxicity is associated with an excess of Mn that can be due to environmental factors or genetic disorders. Depending on the route and period of Mn exposure, its toxicity can differ. Most of the time, inhaled Mn accumulates in the brain and lead to manganism, a neurodegenerative syndrome resembling the Parkinson's disease (PD). However, while inhaled, Mn can also provoke local inflammations along the respiratory tract causing cough, bronchitis and pneumonitis [37]. On the other hand, ingested Mn from foods or drinking water also induces neurotoxicity with more subtle effects. These different degrees of Mn neurotoxicity between ingestion and inhalation are due to different ways of Mn absorption and delivery to other tissues. As already mentioned earlier, inhaled Mn is rapidly absorbed by lungs and bypasses the liver to be widely distributed in tissues -including the brain- whereas intestinal absorption from ingested Mn is a longer process in which a rather quite important amount of Mn is stored in the liver (Figure 21).

***Mn exposure due to occupational and environmental factors.*** Clinically, most cases of Mn intoxication are due to long-term Mn exposure occurring in occupational positions especially in such industrial fields: mining, smelting, welding, steeling, ceramics production and battery manufacturing. Workers exposed to high Mn-enriched dust and fumes are more subjected to Mn inhalation and breathing. However, the risk of Mn exposure is not restrictive to those workers as Mn-enriched foods or water are also sources of contamination. In addition, a current and growing public issue lies in the use of methylcyclopentadienyl manganese tricarbonyl (MMT) as a gasoline additive that might considerably increase the levels of Mn airborne particles in the atmosphere [157,167]. Another health concern lies in the intravenous injection of ephedrone also known as methcathione, a drug requiring potassium permanganate for its synthesis [186,187].

***Genetic disorders of Mn metabolism.*** Since the last decade, three mains inherited disorders of Mn metabolism have been identified. All of them are due to mutation in genes encoding putative Mn<sup>2+</sup> transporters named SLC30A10, SLC39A14 and SLC39A8 [67,188–193]. All of those proteins belong to the solute carrier (SLC) superfamily. Amongst them, SLC39A14 and SLC39A8 belong to the Zinc-regulated transporter (Zrt), Iron-regulated transporter (Irt) like protein family (ZIP) and SLC30A10 to the Zinc transporter (ZnT) family. While SLC30A10 is thought to be a plasma membrane Mn-efflux transporter, SLC39A8 and SLC39A14 are supposed to be Mn<sup>2+</sup> importers. The interplay between the

function of these three proteins is well documented [192–195] and their precise role in intracellular  $Mn^{2+}$  regulation will be further discussed in the following section 2.2.5. Briefly, mutations in *SLC30A10* and *SLC39A14* cause a Mn-induced neurotoxicity phenotype called hypermanganesemia with dystonia (HMNDYT). HMNDYT1 and HMNDYT2 are respectively associated with deficiencies in *SLC30A10* and *SLC39A14* [192]. Clinically, HMNDYT1/2 share common clinical features such as hypermanganesemia, increased Mn blood levels, dystonia and Mn deposition in the basal ganglia [192]. However, the main characteristic differentiating both disorders relies on liver damages. In patients suffering from HMNDYT1, Mn accumulation in the liver causes hepatotoxicity responsible for liver diseases ranging from mild (steatosis) to severe forms (cirrhosis). On the other hand, none of the patients with HMNDYT2 suffers from liver insufficiency. From these observations, two antagonist functions were proposed for SLC30A10 and SLC39A14 in hepatocytes and enterocytes. First, liver Mn accumulation in HMNDYT1 suggests a role for SLC30A10 in  $Mn^{2+}$  efflux. Second, the absence of Mn accumulation in liver in patients with HMNDYT2 emphasizes a role for SLC39A14 in  $Mn^{2+}$  intake for subsequent biliary excretion [195]. With regards to *SLC39A8*, mutations in this gene are associated to Mn deficiency (see next paragraph).

**Manganism.** Mechanisms of Mn-induced neurotoxicity leading to manganism are well documented in literature [154,157,165,167,168,171,196–200]. At the cellular level, Mn neurotoxicity encompasses: alteration in neurotransmission, oxidative stress associated with severe mitochondrial dysfunctions, protein misfolding and aggregation (especially  $\alpha$ -synuclein and amyloid) and neuronal inflammation culminating in cell death. This neurotoxic effect due to Mn accumulation is likely linked to its oxidation state. As for  $Fe^{3+}$  through the Fenton cycle, free  $Mn^{3+}$  is more toxic than  $Mn^{2+}$  and contributes to the generation of ROS. Several studies have reported Mn toxic effects on diverse neurotransmitter systems such as dopaminergic, cholinergic and  $\gamma$ -aminobutyric acid systems [167,200]. Those alterations have mainly behavioral consequences impairing motor coordination (bradykinesia, dystonia, rigidity...), cognitive functions (memory, learning, hyperactivity and loss of attention...) and emotional dysfunctions (apathy, depression, mood swings...) [167]. It is to note that besides manganism, Mn-induced toxicity has been linked to other major neurodegenerative diseases such as the Huntington's disease (HD), prion diseases and more indirectly, Alzheimer's disease (AD) [196].

- Mn deficiency.

In contrast to Mn neurotoxicity, Mn deficiency is not considered as a public health concern [157]. Due to the huge abundance of Mn in food and beverages, Mn dietary deficiencies are extremely rare and have never been reported yet, except under animal experimental conditions [157,168,201]. Insufficient Mn intake has been associated to birth and growth defects, skeletal abnormalities, impaired fertility and

metabolism disruptions (especially lipid and carbohydrate). In addition, some studies revealed that in a pathological context such as osteoporosis, epilepsy and pancreatic insufficiency, Mn metabolism could also be impaired resulting in lower Mn levels [157,201,202]. Furthermore, genetic disorders related to mutations in Mn transporters also result in Mn deficiency. As an example, mutations in *SLC39A8* gene, encoding a  $Mn^{2+}$  transporter at the plasma membrane, induce lower Mn blood levels associated with short stature, dwarfism, deafness, liver disease, intellectual disability and psychomotor retardation [67,188,192,193,203]. To date, twelve cases have been reported depicting four individual or grouped mutations all gathered by Winslow *et al.* and Anagianni and Tulsch [192,194]. Depending on gene mutation(s), the function of each encoded protein may vary. This could explain the discrepancy observed in Mn blood levels between patients, ranging from undetectable to normal concentrations [193]. At the cellular level, Mn deficiency mainly affects the mitochondrial and Golgi functions resulting in (i) reduced MnSOD activity leading to an increased oxidative stress [203] and (ii) reduced activity of glycosylation enzymes -such as  $\beta$ -1,4-galactosyltransferase- resulting in severe N-linked glycosylation defects [67]. For such reasons and as already described in the General Introduction, *SLC39A8* deficiency is classified as a type II CDG. Similarly, *TMEM165*-CDG is another type II CDG causing alterations in intracellular Mn concentrations [64,65]. This will be further described in Chapter 3.

## **2. Interplay between $Ca^{2+}$ and $Mn^{2+}$ import/export within the secretory pathway**

In the yeast *Saccharomyces cerevisiae*, like in mammalian cells, cytosolic free  $[Ca^{2+}]$  and  $[Mn^{2+}]$  are extremely low regarding the gradients established across the plasma membrane and across secretory organelles (Figure 19). Following the secretory pathway,  $Ca^{2+}$  and  $Mn^{2+}$  are constantly exchanged for other ions/ligands to sustain their own luminal concentrations where they contribute to numerous cellular processes. Biological membranes being lipid bilayers, they are low-permeable barriers restricting these free exchanges. Therefore, many transmembrane proteins are required to ensure their transport across membranes.  $Ca^{2+}$  and  $Mn^{2+}$  can then be transported either in an active or a passive mode. Briefly, a passive transport follows ions electrochemical gradients and is mediated by carriers or channels. On the other hand, pumps and transporters actively transport ions against their electrochemical gradients thanks to the energy from either (i) ATP hydrolysis (primary active) or (ii) transport of a coupled ion/ligand (secondary active). In the following sections, some primary active, secondary active and passive transporters involved in  $Ca^{2+}/Mn^{2+}$  transport will be described to better understand their role in  $Ca^{2+}/Mn^{2+}$  homeostasis within the secretory pathway.

## 2.1. Role of Ca<sup>2+</sup> / Mn<sup>2+</sup> P-type ATPases

### 2.1.1. General introduction

P-type ATPases are a group of primary active pumps that can be found in all domains of life from eukaryote to prokaryote and archaea [204]. According to phylogenetic studies, the P-type ATPases superfamily comprises five subfamilies (P1 to P5) classified by sequence homology and substrate specificity [29,30,204–207]. Human and yeast representatives P-type ATPases are reported in Table 11 by gene/protein names, and substrate specificities.

In this section, only P-type ATPases sharing a Ca<sup>2+</sup> and/or Mn<sup>2+</sup> transport activity will be addressed. According to Table 11, amongst all P-type subfamilies only P2 and P5 will be of interest (mentioned in pink, Table 11). In particular, the Ca<sup>2+</sup> (and Mn<sup>2+</sup>) P-type ATPases belong to the P2 subfamily. More precisely, P2A clade gathers human Sarco/Endoplasmic Reticulum Ca<sup>2+</sup>-ATPases (SERCA) and Secretory Pathway Ca<sup>2+</sup>/Mn<sup>2+</sup>-ATPases (SPCA) and yeast plasma membrane ATPase related 1 (Pmr1p) while P2B includes human Plasma Membrane Ca<sup>2+</sup>-ATPases (PMCA) and its yeast ortholog Pmc1p [29,30]. Moreover, P5 subfamily also gathers ATPases more indirectly linked to Ca<sup>2+</sup> and Mn<sup>2+</sup> homeostasis in yeast and human [208]. Although no clear substrate(s) for P5 ATPase members have been identified yet, several studies reported the involvement of P5 members in Ca<sup>2+</sup>/Mn<sup>2+</sup> homeostasis and Mn<sup>2+</sup> tolerance. Phylogenetic analysis suggested the presence of two subgroups in this family: P5A and P5B, that may have evolved differentially as P5A and P5B members display different subcellular localizations, structural conformations and subsequently, different putative functions [209,210]. What is fascinating is the very high degree of conservation during evolution for P5A members. Indeed, a recent study revealed that in fungi and animals, only a single P5A ATPase is found in each tested species [210]. The human and yeast representative members of this subgroup are respectively ATP13A1 and Spf1p, and will be further described as several studies suggest their role in Ca<sup>2+</sup>/Mn<sup>2+</sup> homeostasis along the secretory pathway. On the other hand, P5B gathers more members in human than in yeast. Indeed, four P5B ATPases isoforms can be found in human: ATP13A2-5 while the yeast *Saccharomyces cerevisiae* only possesses one, named yeast PARK9 protein (Ypk9p), referring to the human ATP13A2 (also known as PARK9) [210]. Despite none of all P-type ATPase cited above share a specificity for Ca<sup>2+</sup> and/or Mn<sup>2+</sup>, a common ions/ligands transport mechanism has been established for all P-type ATPases, based on the Post-Albers cycle [211,212].

**Table 11: List of all P-type ATPases found in human and in yeast *Saccharomyces cerevisiae*.** P1A and P2D subgroups are not represented since no human or yeast proteins belong to them. For P4 subfamily, as a new nomenclature was established very recently both new (P4A, P4B) and old (“Class”) subgroups are mentioned [213]. Human and yeast genes are written in italics with the associated proteins in brackets. When protein and gene share the same name, it is written in capital letter without italics and brackets. Subgroups indicated in pink will be further detailed as they comprise  $\text{Ca}^{2+}$  and  $\text{Mn}^{2+}$  P-type ATPases. GlcCer: glucosylceramide, GSL: glycosphingolipids, PC: phosphatidylcholine, PE: phosphatidylethanolamine, PS: phosphatidylserine. References that served to fill this table:[29,30,205–207,209,210,213–220].

| P-type ATPases |            | Gene/protein names                                 |   | Substrates   |   |    |
|----------------|------------|--|---|--|---|----|
| Subfamilies    | Subgroups  | Human  | Yeast   | Human  | Yeast   |    |
| <b>P1</b>      | P1B        | <i>ATP7A</i> (MNK)                                 | <i>PCA1</i> (Pca1p)   | $\text{Cu}^{2+}$                                   | $\text{Cu}^{2+}$                                |    |
|                |            | <i>ATP7B</i> (WND)                                 | <i>CCC2</i> (Ccc2p)   | $\text{Cu}^{2+}$                                   | $\text{Cu}^{2+}$                                |    |
| <b>P2</b>      | <b>P2A</b> | <i>ATP2A1-3</i> (SERCA1-3)                         | -   | $\text{Ca}^{2+}$                                   | -   |    |
|                |            | <i>ATP2C1-2</i> (SPCA1-2)                          | <i>PMR1</i> (Pmr1p)   | $\text{Ca}^{2+}, \text{Mn}^{2+}$                   | $\text{Ca}^{2+}, \text{Mn}^{2+}$                |    |
|                | <b>P2B</b> | <i>ATP2B1-4</i> (PMCA1-4)                          | <i>PMC1</i> (Pmc1p)   | $\text{Ca}^{2+}$                                   | $\text{Ca}^{2+}$                                |    |
| <b>P2</b>      | P2C        | <i>ATP1A1-4</i> (NaK1-4)                           | <i>PMR2/ENA1</i> (Ena1p)<br><i>PMR2/ENA2</i> (Ena2p)<br><i>ENA5</i> (Ena5p) | $\text{Na}^+/\text{K}^+$                           | $\text{Na}^+$<br>$\text{Na}^+$<br>$\text{Na}^+$ |    |
|                |            | <i>ATP4A</i><br><i>ATP12A</i>                      | -<br>-  | $\text{H}^+/\text{K}^+$<br>$\text{H}^+/\text{K}^+$ | -<br>-  |    |
| <b>P3</b>      | P3A        | -  | <i>PMA1-2</i><br>(Pma1/2p)  | -  | $\text{H}^+$                                    |    |
| <b>P4</b>      | Class 1a   | <i>ATP8A1-2</i>                                    | <i>DRS2</i> (Drs2p)   | PS>PE  | PS  |    |
|                |            | <i>ATP8B1-2</i><br><i>ATP8B3-4</i>                 | -   | PC<br>?  | -   |    |
|                | P4A        | Class 3  | -   | <i>DNF1-2</i> (Dnf1/2p)                            | -   | PC |
|                |            | Class 4  | -   | <i>DNF3</i> (Dnf3p)                                | -   | PC |
|                | Class 5    | <i>ATP10A</i>                                      | -   | -  | PC<br>?   | -  |
|                |            | <i>ATP10B</i><br><i>ATP10D</i>                     | -<br>-  | -  | GSL<br>(GlcCer)                                 | -  |
|                |            | Class 6  | <i>ATP11A-C</i>   | -  | PS>PE   | -  |
|                | P4B        | Class 2  | <i>ATP9A-B</i>  | <i>NEO1</i> (Neo1p)                                | ?   | ?  |
| <b>P5</b>      | <b>P5A</b> | <i>ATP13A1</i>                                     | <i>SPF1/COD1</i><br>(Spf1p/Cod1p)   | ?  | $\text{Mn}^{2+}, \text{Ca}^{2+},$<br>sterols ?  |    |
|                |            | <i>ATP13A2/PARK9</i>                               | <i>YOR291W/YPK9</i><br>(Ypk9p)  | Polyamines   | $\text{Mn}^{2+},$ heavy<br>metals               |    |
|                | <b>P5B</b> | <i>ATP13A3</i><br><i>ATP13A4</i><br><i>ATP13A5</i> | -<br>-<br>-   | ?<br>$\text{Ca}^{2+}$ ?<br>?                       |   |    |



First established in 1967 to characterize the active transport mechanism of sodium ( $\text{Na}^+$ ) and potassium ( $\text{K}^+$ ) (NaK) pumps, this model illustrates the four major conformational states of P-type ATPases, as depicted in Figure 22 [29,30,216,221].

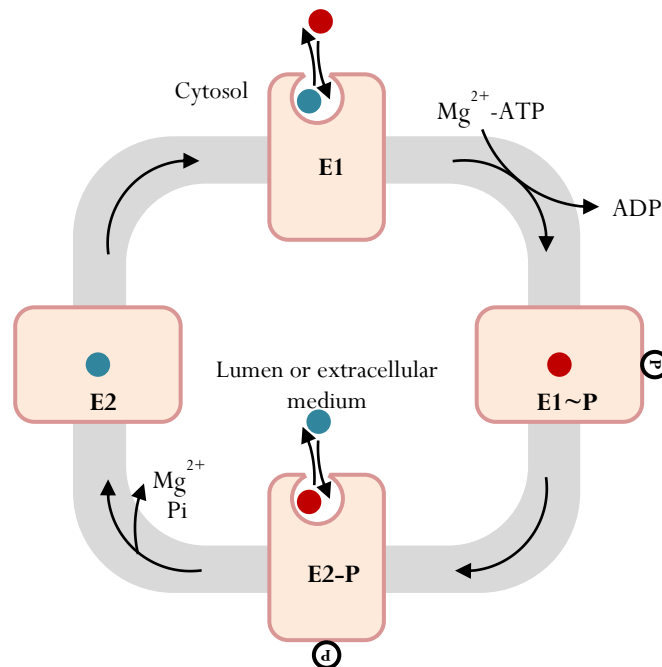


**Figure 22: Post-Albers cycle generalized for P-type ATPases.** In this cycle, a ligand (red dot) and its coupled-ligand (blue dot) are transported from one side of the membrane (cytosol) to the other (lumen or extracellular medium). In this scheme, one ligand is exported while one is imported. It is to note that the number of ligands in each direction may vary according to the nature of the P-type ATPase. This cycle illustrates the switch of P-type ATPases between two main conformational states: E1 and E2 and two intermediate conformational states E1~P and E2-P. While E1 and E1~P represent the highest ligand affinity forms, E2-P and E2 are the lowest. During transport, all P-type ATPases are subjected to reversible autophosphorylation that occurs on one of their cytosolic domains (circled « P »). Phosphorylation and dephosphorylation are mainly responsible for the closure of cytosolic and extracytosolic gates leading to the occluded intermediates E1~P and E2.

Briefly, E1 and E1~P states refer to the highest ligand affinity forms while E2-P and E2 represent the lowest affinity ones. During transport, P-type ATPases are subjected to reversible autophosphorylation that occurs on a conserved aspartate residue (Asp) in their active site. This reaction is conserved from yeast to human with quite little differences [204]. The transient transfer of phosphate onto the protein leads to the presence of the phosphorylated intermediates and is the reason of the designation “P-type ATPase” [29]. Applied to  $\text{Ca}^{2+}/\text{Mn}^{2+}$  P2 ATPases, the  $\text{Ca}^{2+}$  transport mechanism is well established for one of human SERCA isoform, named SERCA1a and serves to explain those of SPCA [29,30] and PMCA [222]. Thanks to the main contributions from Toyoshima and Nissen teams, 3D characterizations of several structural conformations of SERCA1a have been reported (see [223] for article references). More recently, Gong *et al.*, Inoue *et al.*, and Sitsel *et al.*, also provided structural conformations from PMCA1, SERCA2a and SERCA2b, respectively [224–226]. All of these structures revealed common

features shared by all P-type ATPases members that will be briefly exposed here as they have been extensively detailed in literature [29,30,204,206,207,216]. Basically, the architecture of all five classes P-type ATPase comprises six transmembrane domains (TM) forming the “core segment” and three cytosolic domains referred as an actuator domain (A), a phosphorylation domain (P) and a nucleotide-binding domain (N). According to the subfamily, additional N- and C- terminal TM can be found. For instance, to the purpose of  $\text{Ca}^{2+}/\text{Mn}^{2+}$  P2 ATPases, 10 TMD are usually found except for one member of the SERCAs, SERCA2b that possesses an additional 11<sup>th</sup> TMD [206,207,216].

After this brief and general introduction about the P-type ATPases in yeast and human, the following sections will further address the role of P2 and P5 ATPases in  $\text{Ca}^{2+}/\text{Mn}^{2+}$  transport and homeostasis within the secretory pathway.

### 2.1.2. P2-type ATPases

Dating back to more than thirty years ago, *PMCI* and *PMRI* were identified in the yeast *Saccharomyces cerevisiae* as two structural genes respectively involved in  $\text{Ca}^{2+}$  sequestration into the vacuole and secretory organelles [217,227]. Many years later, these two genes encoding the yeast proteins Pmc1p and Pmr1p are still defined as key players in  $\text{Ca}^{2+}$  homeostasis, in addition to their roles in  $\text{Mn}^{2+}$  homeostasis. To the mammalian side, PMCAs, SPCAs and SERCAs are the P-type ATPases ensuring such functions [29,30]. Of them, a main focus will be addressed on each ubiquitous protein. For additional information about other PMCA, SERCA and SPCA isoforms and protein variants, please have a look on the latest review from Chen *et al.*, including references [30].

#### ▪ P2A: SERCAs, Pmr1p and SPCAs

**SERCAs.** In humans, three separate genes *ATP2A1-3* encode for three SERCAs proteins named SERCA1-3. In addition, alternative splicing events occurring either during development or in a tissue-specific manner, introduce variations in the final protein sequence yielding the number of SERCA protein variants to eleven: SERCA1a-b, SERCA2a-b and SERCA3a-f [29,30,228,229]. Amongst them, only SERCA2b is ubiquitously expressed and then referred as the housekeeping isoform. Indeed, apart from SERCA3 whose mainly expressed in non-muscle cells, all other SERCA isoforms share a more restrictive expression pattern in muscle tissue and especially fast twitch skeletal-muscle fibers for SERCA1a (adult) and SERCA1b (neonatal), slow twitch skeletal-muscle fibers for SERCA2a and cardiomyocytes for SERCA2c [228]. All SERCAs are transmembrane proteins of the sarcoplasmic or endoplasmic reticulum (SR or ER) while some of them are also expressed in the *cis*-Golgi compartment [18]. Structurally speaking, all P2 type ATPases exhibit a similar domain organization (10 TMD, N-, P- and A-domains) and possess the key motifs for ATP hydrolysis and  $\text{Ca}^{2+}$  transport suggesting a highly

conserved mechanism for  $\text{Ca}^{2+}$  transport [29,207]. However, amongst all P2 type ATPases, only SERCA pumps contain two high-affinity  $\text{Ca}^{2+}$ -transport sites (site I and site II). As a consequence, SERCAs can transport two  $\text{Ca}^{2+}$  ions per cycle whereas PMCAs and SPCAs can only translocate one. In addition, between all SERCA isoforms,  $\text{Ca}^{2+}$  transport mechanism may be regulated by further structural features such as the presence of additional 49 amino acid residues at the C-terminus of SERCA2b, containing a 11<sup>th</sup> transmembrane domain and a luminal extension [225,230]. Hence, based on isoform-specific sequence, tissue-specific distribution and physiological requirements, each SERCA pump displays distinct kinetic properties and regulatory control on its ability to transport  $\text{Ca}^{2+}$  [29,30,228]. Regulation of SERCA isoforms will be further discussed in section 3.2.2.

The role of SERCA pumps in  $\text{Ca}^{2+}$  homeostasis has been well established and studied over the past fifty years. First identified and purified from rabbit skeletal muscle, SERCAs play a crucial role in muscle contraction/relaxation cycle. In muscle cells, the SR is analogous to the ER of non-muscle cells and can store  $\text{Ca}^{2+}$  up to hundreds of millimolar. Its main function lies in its ability to release  $\text{Ca}^{2+}$  into the cytosol through the ryanodine receptors (RyR) for muscle contraction and to actively reuptake cytosolic  $\text{Ca}^{2+}$  through SERCA pumping activity for muscle relaxation. In this context, SERCAs play two major and complementary roles (i) lowering  $[\text{Ca}^{2+}]_{\text{cytosol}}$  for muscle contraction and (ii) refilling the SR  $\text{Ca}^{2+}$  store then required for muscle relaxation [228]. In addition to such specialized function in muscle cells, the SR as well as the ER needs to maintain an adequate ion environment for proper enzymatic functions in a wide range of biological reactions such as lipid and protein synthesis, protein folding, post-translational modifications, trafficking and sorting. Thus, SERCA serves to ensure physiological  $[\text{Ca}^{2+}]$  in the ER, crucial to achieve these reactions. Beyond their ability to transport  $\text{Ca}^{2+}$ , we recently suggested that in a specific pathological context, SERCA2b would be involved in cytosolic  $\text{Mn}^{2+}$  pumping to sustain Golgi glycosylation reactions [231]. This will be further discussed in Results, Part I of this manuscript. Briefly, we have demonstrated that in HEK cells lacking the newly identified Golgi  $\text{Mn}^{2+}$  importer TMEM165 (see Chapter 3), (i) both thapsigargin and cyclopiazonic acid treatments prevent  $\text{Mn}^{2+}$ -induced glycosylation rescue and that (ii) SERCA2b overexpression partially succeed in rescuing the glycosylation profile of the heavily N-glycosylated protein LAMP2. However, this study did not provide direct evidence for  $\text{Mn}^{2+}$  transport but emphasize a potential role for SERCA2b in cytosolic  $\text{Mn}^{2+}$  pumping into the ER to then feed the Golgi apparatus. The ability of SERCA pumps to transport  $\text{Mn}^{2+}$  was already described in the past by Chiesi and Inesi [232]. Indeed, they first demonstrated that  $\text{Mn}^{2+}$  could activate SERCA pumps as  $\text{Mg}^{2+}$  could do. Then, they highlighted that  $\text{Mn}^{2+}$  was a weak competitor for  $\text{Ca}^{2+}$  and could even be transported by SERCAs instead of  $\text{Ca}^{2+}$ , at slower rates. In addition, latter evidence provided by Yonekura and Toyoshima reinforce this statement and highlight

similar  $Mn^{2+}$  and  $Ca^{2+}$  transport mechanisms for SERCA1a isoform [233]. Hence, a role of SERCA pumps in  $Mn^{2+}$  transport cannot be excluded although SERCAs mainly regulate  $Ca^{2+}$  intake in the ER and *cis*-Golgi [18].

Surprisingly and as the major difference between yeast and mammalian cells, no SERCA pumps were identified in the yeast *Saccharomyces cerevisiae*. This lack of yeast SERCA orthologs suggests a different way of regulating and storing  $Ca^{2+}$ . As illustrated in Figure 19,  $Ca^{2+}$  is mainly stored in the yeast vacuole and Golgi apparatus but not in the ER.

**Pmr1p (plasma membrane ATPase related).** Dating back to 1985, Smith et al. looked for supersecreting (*ssc*) *Saccharomyces cerevisiae* mutants in the line to pinpoint beneficial yeast mutations enabling an increased expression, production and secretion of heterologous proteins. From this study, mutations in *SSC1* gene were positively selected [234]. Couple of years later, while looking for P-type ATPases of the yeast secretory pathway, Rudolph et al. screened genes related to the plasma membrane  $Ca^{2+}$ -ATPases (PMCA) that they named plasma membrane ATPase related (PMR). Two genes came out, *PMR1* and *PMR2* among which, *PMR1* was shown to be identical to the previously identified *SSC1* [235]. *PMR1* encodes for Pmr1p, a Golgi localized transmembrane protein [236]. In *Saccharomyces cerevisiae*, Pmr1p was first described as a putative  $Ca^{2+}$ -ATPase since *pmr1Δ* strains (i) were unable to grow on low- $Ca^{2+}$  media, (ii) were highly sensitive to  $Ca^{2+}$  chelation in the culture medium (by addition of EGTA or BAPTA) and (iii) these  $Ca^{2+}$  deficiency growth defects could only be alleviated by  $Ca^{2+}$  supplementation in the culture medium and no other cations [227,235–237]. These specific phenotypes were expected from an alteration in  $Ca^{2+}$  homeostasis. Moreover, Lapinskas et al. suggested for the first time a dual involvement of Pmr1p in both  $Ca^{2+}$  and  $Mn^{2+}$  homeostasis. Indeed, they highlighted that *pmr1Δ* yeasts (i) accumulate elevated levels of intracellular Mn and (ii) exhibit a higher sensitivity to Mn-induced toxicity [180]. Hence, a physiological role for Pmr1p was assigned to  $Mn^{2+}$  transport in the Golgi apparatus to both prevent intracellular Mn accumulation to toxic levels and sustain Golgi  $Mn^{2+}$  homeostasis, especially for protein glycosylation. Further investigations then pointed out that in yeasts lacking Pmr1p, strong N- and O-linked glycosylation defects were observed on secreted glycosylated proteins such as invertase, chitinase and carboxypeptidase Y. While  $CaCl_2$  partially suppressed the Golgi glycosylation defects,  $MnCl_2$  supplementation completely succeeded [235,236,238]. From these observations that have been largely confirmed in more recent studies, Pmr1p was assumed to play a major role in Golgi  $Mn^{2+}$  homeostasis, especially to sustain the glycosylation reactions [65,239,240].

To summarize, the main function of the yeast Pmr1p is to supply the Golgi apparatus with both  $\text{Ca}^{2+}$  and  $\text{Mn}^{2+}$  and to lower cytosolic  $\text{Ca}^{2+}/\text{Mn}^{2+}$  levels upon overload. Subsequently, Pmr1p ensures Golgi  $\text{Ca}^{2+}/\text{Mn}^{2+}$  homeostasis that is required for its proper functions such as glycosylation, protein maturation, trafficking and sorting. In addition, Pmr1p is also assumed to be involved in  $\text{Mn}^{2+}$  detoxification by sequestering  $\text{Mn}^{2+}$  excess in the Golgi apparatus to then be exited from the cells through secretory vesicles.

**SPCAs.** As mentioned above, SPCAs were first identified in the yeast *Saccharomyces cerevisiae* as plasma membrane ATPases related (PMR) [235,237]. In human, two separate genes (*ATP2C1* and *ATP2C2*) encode respectively for two SPCA proteins named SPCA1 and SPCA2. Although SPCAs and SERCAs share 43% sequence similarity, SPCAs differ from SERCAs for several reasons [237]. First, as already mentioned earlier, SPCAs lack the first cation binding site (I) presents in SERCAs and thus, only transport one ion per cycle instead of two for all SERCA isoforms. Second, SPCAs can transport either  $\text{Ca}^{2+}$  or  $\text{Mn}^{2+}$  whereas SERCAs solely transports  $\text{Ca}^{2+}$ . Third, SPCAs are insensitive to well-known inhibitors of SERCAs (*i.e.* thapsigargin, 2,5-di(ter-butyl)-hydroquinone and cyclopiazonic acid, see 3.2.2.). Fourth, SERCAs and SPCA1 do not display the same subcellular localization. While SERCAs are mainly expressed in the ER, SPCA1 share multiple localizations in the latter compartments of the secretory pathways: from the *trans*-Golgi to the secretory vesicles. Thus, even evolutionarily closed, SPCAs and SERCAs differ from each other in their transport capacity, ion specificity and subcellular localizations. Albeit SPCA1 and SPCA2 share up to 63% sequence identity, only SPCA1 is ubiquitously expressed and then referred as the housekeeping  $\text{Ca}^{2+}/\text{Mn}^{2+}$  ATPase of the secretory pathway [29,30]. For such reason, a main focus on SPCA1 will be done in this section. Additional information about SPCA2 could be found in such papers and related references: [27,29,30,241–245]. As the result of splicing events in *ATP2C1* mRNA transcripts, four SPCA1 isoforms (SPCA1a-d) have been identified, only differing in their carboxyl-termini extensions [246]. Of them, SPCA1c is an inactive form and SPCA1d is the longest [246–248]. During the last twenty years, SPCA1 has been widely studied in the pathophysiological context of Hailey-Hailey disease (HHD) since the identification of disease-causing mutations in *ATP2C1* in patients suffering from HHD [249,250]. Originally described by the Hailey brothers in 1939 [251], HHD is an autosomal dominant blistering skin disorder caused by the haploinsufficiency of *ATP2C1* - meaning that one copy of the altered allele is sufficient to cause the disorder. The characteristic skin lesions observed in HHD patients are due to defects in cell-to-cell adhesion. This phenomenon, also called acantholysis, results from insufficient  $\text{Ca}^{2+}$  levels within the epidermis that weakens desmosomal connections between the cells, especially between keratinocytes [250,252]. It has been reported that cultured HHD keratinocytes have elevated  $[\text{Ca}^{2+}]_{\text{cytosol}}$  and are less

responsive to increasing extracellular  $[Ca^{2+}]$  than healthy cells suggesting that mutations in *ATP2C1* alter intracellular  $Ca^{2+}$  regulation in both resting and stimulated conditions [250,253]. So far, the mechanism by which mutations in *ATP2C1* lead to acantholysis is not elucidated yet but may be related to either abnormally elevated  $[Ca^{2+}]_{\text{cytosol}}$  or abnormally low Golgi  $Ca^{2+}/Mn^{2+}$  levels. In addition, through a specifically Golgi-targeted aequorin-based assay to measure luminal free  $[Ca^{2+}]$ , Van Baelen et al. demonstrated that in HeLa cells silenced for *ATP2C1* a lesser Golgi  $Ca^{2+}$  intake was observed [254]. Hence, apart from the ER, the Golgi apparatus also play a major role in  $Ca^{2+}$  storage especially thanks to the activity of SPCA1 in pumping cytosolic  $Ca^{2+}$  into the Golgi lumen. In other words, SPCA1 activity is essential for the regulation of cytosolic  $Ca^{2+}$  levels by storing  $Ca^{2+}$  in the Golgi apparatus. Although much attention has been focused on its  $Ca^{2+}$  pumping activity, SPCA1 also transports  $Mn^{2+}$ . This was first evidenced by heterologous expression of *ATP2C1* in yeast lacking Pmr1p. Indeed, Ton et al. demonstrated that the expression of human SPCA1 in *pmr1Δ* yeasts fully complemented both phenotypes related to hypersensitivity to  $Ca^{2+}$  chelators and  $Mn^{2+}$  toxicity [255]. Overexpression of SPCA1 in HEK cells also confers tolerance to  $Mn^{2+}$ -induced cytotoxicity by facilitating  $Mn^{2+}$  accumulation in the Golgi apparatus and secretory vesicles, thereby lowering cytosolic free  $Mn^{2+}$  levels and increasing cell viability [256]. From these observations, Leitch et al. suggested a function for SPCA1 in  $Mn^{2+}$  detoxification, especially in the liver [256]. To reinforce this statement, Mukhopadhyay and Linstedt found that a specific point mutation in SPCA1, resulting from the substitution of glutamine 747 with alanine (Q747A), preferentially enhances  $Mn^{2+}$  transport activity towards  $Ca^{2+}$  [257]. Overexpression of Q747A-SPCA1 in HeLa cells indeed result in (i) a higher degradation rate of the Golgi luminal  $Mn^{2+}$  sensor GPP130, suggesting a higher Golgi  $Mn^{2+}$  intake and (ii) an increased cell viability against  $Mn^{2+}$  toxicity [257]. Taken together, these findings highlight the importance of the Golgi apparatus in  $Mn^{2+}$  homeostasis and detoxification in mammalian cells, both mediated by SPCA1.

All in all, Pmr1p and SPCA1 share similar functions in yeast and human towards  $Ca^{2+}$  and  $Mn^{2+}$  homeostasis at the Golgi level and in cytosolic  $Mn^{2+}$  detoxification. However, while Pmr1p deficiency leads to strong glycosylation defects in yeast, no link between glycosylation and a lack have SPCA1 has been reported yet in humans. This major statement may result from additional Golgi localized  $Ca^{2+}/Mn^{2+}$  transporters in yeast and human that might differentially compensate the lack of Pmr1p/SPCA1. This will be further described Chapter 3 and in Result, Part II of this manuscript.

- P2B: Pmc1p and PMCAs

**Pmc1p (plasma membrane calcium 1 protein).** In the yeast *Saccharomyces cerevisiae*, Pmc1p shares approximately 40% identity with human PMCAs and localizes to vacuole [227,258]. In yeast lacking

Pmc1p, strong growth defects can be observed following exposure to high external  $[Ca^{2+}]$  suggesting a role for Pmc1p in  $Ca^{2+}$  tolerance [258]. Moreover, Pmc1p has been shown to transport  $Ca^{2+}$  from the cytosol to the vacuole since  $Ca^{2+}$  sequestration into the vacuole is fivefold lower in *pmc1Δ* yeasts compare to wild-type strains [258]. In addition, a similar role for Pmr1p in  $Ca^{2+}$  sequestration at the Golgi level was suggested as the overexpression of *PMR1* in *pmc1Δ* null mutant yeasts was sufficient to rescue the  $Ca^{2+}$  tolerance [227,258]. However, in response to short exposure to high  $[Ca^{2+}]$ , Pmc1p plays a minor role in lowering  $[Ca^{2+}]_{cytosol}$  while Vcx1p, the vacuolar  $H^+/Ca^{2+}$  exchanger, is responsible for  $Ca^{2+}$  sequestration into the vacuole. This will be further described in section 2.2.2. All in all, the major role for Pmc1p lie in its ability to lower  $[Ca^{2+}]_{cytosol}$  by actively pumping cytosolic  $Ca^{2+}$  into the vacuole to ensure a long term  $Ca^{2+}$  tolerance.

**PMCA.** In humans, four separate genes named *ATP2B1-4* encode for four PMCA proteins (PMCA1-4). Resulting from numerous splicing events, more than 20 PMCA isoforms have been identified so far: PMCA1a-e, PMCA2a-f, PMCA3a-c and PMCA4a-g [259]. Although all tissue expressed at least one PMCA, PMCA1 and PMCA4 are ubiquitously expressed while PMCA2 and PMCA3 exhibit a more restrictive expression pattern in the brain in addition to the lactating mammary glands for PMCA2 [30,260]. For such reasons, PMCA1 and PMCA4 are considered to fulfill a housekeeping function. Due to the greatest numbers of PMCA isoforms and their more distant involvement in  $Ca^{2+}$  homeostasis within the secretory pathway than SPCAs and SERCAs, a general presentation of the role of PMCA will be addressed here. Additional information and further description of PMCA could be found in literature [30,222,261–266]. Like other P2 type ATPases, PMCA share similar structural features and organization *i.e.* three cytosolic (N-, P- and A- domains), 10 TMD and cytosolic amino- and carboxyl-termini. Akin SPCAs, PMCA possess a single cation binding site allowing the transport of one  $Ca^{2+}$  ion per cycle. More specifically, PMCA differ from other P2 type ATPases through the presence of a calmodulin (CaM)-binding domain in their carboxyl-termini together with other protein-binding domains. These additional regulatory regions will be further discussed in section 3.2.1.

PMCA were first identified in human red blood cells where they were assumed to mediate the “ATP-dependent  $Ca^{2+}$  extrusion from red cells” in order to maintain low intracellular  $Ca^{2+}$  levels [267]. From that time, further investigations extended to other cell types also reported a common function of PMCA as  $Ca^{2+}$  exporters at the plasma membrane. However, while in erythrocytes PMCA ensure the only way to control intracellular  $Ca^{2+}$  homeostasis, in all other mammalian cells additional transmembrane pumps and transporters also take part in such intracellular  $[Ca^{2+}]$  regulation. This is even truer that the cell is excitable or not. Indeed, in non-excitable cells cytosolic  $Ca^{2+}$  levels remain low mainly thanks to the function of PMCA but in excitable cells such as (cardio)myocytes and neurons, the

solely activity of PMCA is not sufficient to rapidly and sufficiently lower  $[Ca^{2+}]_{cytosol}$  [222,263,268]. In those cells, the two main pathways for cytosolic  $Ca^{2+}$  removal are (i) reuptake into the SR/ER/Golgi apparatus through SERCAs and SPCAs activities and (ii) extrusion from the cells *via* both PMCA and the low affinity/high transport capacity  $Na^+/Ca^{2+}$  plasma membrane exchanger (NCX) activities [268,269]. Besides the involvement of PMCA in global  $Ca^{2+}$  homeostasis, those pumps also play a role in the regulation of local intracellular  $Ca^{2+}$  levels through PMCA interactions with proteins partners and recruitment into specific microenvironments [222,263–265]. PMCA share multiple protein-protein interactions especially -but not only- through its PDZ-binding domain (see 3.2.1.) that modulate their function while recruiting them into specific membrane microdomains.

To conclude, the functional relevance of P2B-type ATPases in  $Ca^{2+}$  homeostasis within the secretory pathway lies in the ability of such pumps to lower  $[Ca^{2+}]_{cytosol}$  through active sequestration in the vacuole for yeast Pmc1p or active removal across the plasma membrane for human PMCA. So far, no  $Mn^{2+}$  transport activity has been reported yet for Pmc1p and PMCA. Structurally and as a major difference between Pmc1p and PMCA, Pmc1p lacks the calmodulin (CaM)-binding domain at the carboxyl-terminus [217]. However, both PMCA and Pmc1p are respectively directly or indirectly regulated by CaM (see 3.2.1.).

### 2.1.3. P5-type ATPases

Unlike the well characterized subfamily of P2 ATPases, little is known about the function and the substrate specificity of the P5 members. However, I decided to quickly reviewed some of them, directly or indirectly related to  $Ca^{2+}$  and/or  $Mn^{2+}$  transport activity by giving the reasons that led people think of such involvement in  $Ca^{2+}/Mn^{2+}$  homeostasis along the secretory pathway.

- P5A: Spf1p and ATP13A1

**Spf1p (sensitivity to *Pichia Farinosa* killer toxin).** Also known as Cod1p (control of HMG-CoA reductase degradation), Spf1p is a transmembrane protein localized in the ER. Primary investigations led by Suzuki *et al.*, pinpointed a link between Spf1p and the glycosylation process [32]. While deciphering the resistance mechanism to the salt mediated killer toxin (SMKT), *SPF1* gene encoding the protein Spf1p was identified and characterized. From this characterization, authors pointed out the secretion of underglycosylated invertase in yeast lacking Spf1p, reflecting a N-glycosylation defect very similar to those observed in *pmr1Δ* yeast. Contrary to what was observed in *pmr1Δ*, a  $CaCl_2$  supplementation does not rescue the migration profile of the secreted invertase in *spf1Δ* yeasts. From this,  $Ca^{2+}$  was not likely considered as a substrate for the P-type ATPase Spf1p [271]. Due to its ER localization and Ca



phenotype, Spf1p was then supposed to be involved in ER  $\text{Ca}^{2+}$  homeostasis and more widely, in the secretory pathway acting in a distinct manner from Pmr1p [270–272]. In an unrelated study, Cronin et al. confirmed this hypothesis [214,273]. Indeed, while investigating the regulation of hydroxymethylglutaryl-coenzyme A (HMG-CoA) reductase degradation in the yeast *Saccharomyces cerevisiae*, authors looked for control of HMG-CoA reductase degradation (COD) genes and identified *COD1* as a candidate [273]. Although the study underlined a role for the encoded protein Cod1p as a  $\text{Ca}^{2+}$  transporter in the regulation of the yeast Hmg2p degradation, Cronin et al. also found that *COD1* was identical to *SPF1* and encodes the same protein, Cod1p/Spf1p. Thus, both studies on the same yeast P-type ATPase Cod1p/Spf1p suggested its involvement in ER  $\text{Ca}^{2+}$  homeostasis, lacking direct evidence for  $\text{Ca}^{2+}$  transport activity [214,273]. Nevertheless, a decade later, Cohen et al. emphasized a role for Spf1p in ER  $\text{Mn}^{2+}$  homeostasis [220]. Based on the fact that yeasts lacking Spf1p exhibit (i) reduced  $\text{Mn}^{2+}$  levels in microsomes, (ii) relocation of  $\text{Mn}^{2+}$  sensor proteins Smf1p and Smf2p, (iii) reduced activity of Mn-ER-dependent enzymes and (iv) increased activity of Mn-cytosolic-dependent enzymes, a role for Spf1p as a  $\text{Mn}^{2+}$  importer of the ER was suggested [220]. Although these investigations place  $\text{Ca}^{2+}$  and/or  $\text{Mn}^{2+}$  as putative substrates/ligands for Spf1p, Cronin et al., demonstrated that neither  $\text{Ca}^{2+}$  nor  $\text{Mn}^{2+}$  had stimulatory effects on Spf1p activity [66]. This was recently confirmed by Sørensen et al. that instead found that Spf1p activity was stimulated by phosphatidylinositol 4-phosphate (PI4P) [219]. In addition, in yeast lacking Spf1p an accumulation of lipid bodies together with the increased level of sterols at the plasma membrane suggested a function for Spf1p in the regulation of sterol homeostasis and trafficking between the ER and the plasma membrane. From this latest study, Spf1p was assumed to be a PI4P-stimulated flippase involved in cellular sterol homeostasis [219]. Although all of these investigations tend to elucidate the substrate for Spf1p, other studies demonstrated its role in the regulation of the Unfolded Protein Response (UPR) since (i) Spf1p is regulated by UPR and (ii) Spf1p deletion in yeast induces a constitutive activation of the UPR [274]. Hence, Spf1p is thought to be a P-type ATPase involved in UPR and ER homeostasis especially in terms of cations ( $\text{Ca}^{2+}$  /  $\text{Mn}^{2+}$ ) and sterols balance.

**ATP13A1.** To the human side, little is known about ATP13A1 since a unique study refers ATP13A1 putative function in humans [220]. In this study led in mammalian HeLa cells, Cohen et al. looked for analogous functions between yeast and human orthologs and highlighted (i) a similar ER-localization for ATP13A1, (ii) an enhanced UPR in cells silenced for *ATP13A1* and (iii) an increased activity of the glucosylceramide synthase, a Mn-cytosolic-dependent enzyme [220]. Thus, in HeLa cells silenced for *ATP13A1*, cytosolic  $[\text{Mn}^{2+}]$  are supposed to be higher than in control cells, emphasizing a role for ATP13A1 in  $\text{Mn}^{2+}$  import in the ER.

All in all, a conserved function between Spf1p and ATP13A1 has been suggested [220]. However, although the contribution of both human and yeast P5A ATPases in  $\text{Ca}^{2+}$  and  $\text{Mn}^{2+}$  homeostasis is still unclear, they remain the sole P5A ATPases enable to ensure such  $\text{Mn}^{2+}$  import function in the ER.

- P5B: Ypk9p, ATP13A2 and ATP13A4

Referring to Table 11, human ATP13A2-5 have evolved from the unique yeast Ypk9p. Of the four human isoforms, only two will be of interest in this manuscript: ATP13A2 and ATP13A4.

**Ypk9p (yeast PARK9).** Ypk9p is a transmembrane protein localized to the vacuole, the yeast organelle equivalent to the mammalian lysosomes [275,276]. Based on the work from Gitler et al. [276], Schmidt et al. [275] and Chesi et al. [277], Ypk9p was found to be involved in: (i) protection against  $\alpha$ -synuclein toxicity, (ii) resistance towards heavy metal cations ( $\text{Mn}^{2+}$ ,  $\text{Cd}^{2+}$ ,  $\text{Ni}^{2+}$  and  $\text{Se}^{2+}$ ) and (iii) protein trafficking. Regarding the role of Ypk9p in divalent heavy metals ions homeostasis and tolerance, Schmidt et al. hypothesized that the sensitivity of *ypk9Δ* yeasts to  $\text{Mn}^{2+}$ ,  $\text{Cd}^{2+}$ ,  $\text{Ni}^{2+}$  and  $\text{Se}^{2+}$  could be due to their inability to efficiently sequester these ions in the vacuole, leading to increase their cytosolic concentrations to toxic levels [275]. Hence, Ypk9p was thought to be the main  $\text{Mn}^{2+}$  (amongst other heavy metal cations) importer in the vacuole preventing its cytosolic accumulation leading to cell damages and cell death. Based on these findings in yeast, further investigations led people to think of a similar function for the human ortholog ATP13A2. Although ATP13A2 failed to rescue  $\text{Mn}^{2+}$  resistance when expressed in *ypk9Δ*, other studies led in mammalian cells overexpressing ATP13A2 highlighted their resistance to Mn-induced toxicity [278,279]. From these observations, ATP13A2 was thought to be the main lysosomal  $\text{Mn}^{2+}$  importer [216]. However, as just discussed hereafter, it turned out that this hypothesis was wrong.

**ATP13A2 and ATP13A4.** ATP13A2 is a lysosomal transmembrane protein which function has been widely studied in the pathophysiological context of neurodegenerative diseases. Mutations in *ATP13A2* (also known as *PARK9*) was indeed first identified as causal mutations in Kufor-Rakeb (KR) syndrome [280]. Then, other disease-causing mutations in *ATP13A2* were associated with a broad range of neuronal diseases including early-onset PD [281] (see [282,283] for mutations in *ATP13A2*). For many years, ATP13A2 was thought to be a lysosomal heavy metal importer as it provides a protection against  $\text{Mn}^{2+}$ ,  $\text{Zn}^{2+}$  and  $\text{Fe}^{3+}$  cytotoxicities [276,278,279,284,285]. However, the lack of direct evidence for such transport activity and the fact that neither  $\text{MnCl}_2$ ,  $\text{ZnCl}_2$  nor  $\text{FeCl}_3$  increase ATP13A2 activity assume that ATP13A2 is not likely a  $\text{Mn}^{2+}$ ,  $\text{Zn}^{2+}$  or  $\text{Fe}^{3+}$  transporter [218]. In addition, other studies suggested that polyamines and lipids could also be potential substrates for ATP13A2 [286–288]. Very recently, van Veen et al. unraveled the mystery about this substrate specificity by highlighting that ATP13A2 was a

lysosomal polyamines exporter sharing a higher affinity for spermine and spermidine [218]. To date, no correlation between polyamines transport and  $\text{Ca}^{2+}/\text{Mn}^{2+}$  homeostasis has been suggested. Nevertheless assuming that polyamines can share both positive and negative charges, one can suppose a potential role for polyamines as a  $\text{Mn}^{2+}$  chelator to prevent for its cytotoxicity. This could explain why ATP13A2 protects against  $\text{Mn}^{2+}$  and broadly heavy metals toxicity while exporting polyamines from the lysosomal lumen to the cytosol. On the other hand, ATP13A4 is an ER-localized protein mainly expressed in brain with a biological functional still under investigations [289]. ATP13A4 was first identified by Kwasnicka-Crawford *et al.* to be associated with specific language impairments, autism and Asperger syndrome since mutations in *ATP13A4* were found in patients suffering from these disorders (Table 12) [290]. At the cellular level, the same group deeper investigated the function of ATP13A4 and pinpointed its involvement in  $\text{Ca}^{2+}$  homeostasis. By overexpressing *ATP13A4* in COS-7 cells, they indeed shown that intracellular  $[\text{Ca}^{2+}]$  were increased comparing to untransfected cells [289]. From these observations, ATP13A4 could be thought to act as an ER-localized  $\text{Ca}^{2+}$  exporter. Albeit the precise role of ATP13A4 in such intracellular  $[\text{Ca}^{2+}]$  is still unclear, mutations in *ATP13A4* leading to the disruption of  $\text{Ca}^{2+}$  homeostasis may contribute to the clinical symptoms seen patients [289].

#### 2.1.4. P2/P5-type ATPase deficiencies in human related diseases

All P2/P5-type ATPases described above are directly or indirectly linked to  $\text{Ca}^{2+}/\text{Mn}^{2+}$  homeostasis within the secretory pathway. However, human pathogenic mutations have been described for nearly all of the cited genes leading to a broad range of human diseases such as skin, neurodegenerative or muscle disorders. In the recent review written by Chen *et al.*, an overview of the diseases linked to  $\text{Ca}^{2+}$ -ATPases was provided [30]. Based on this work, an updated list of human diseases related to  $\text{Ca}^{2+}/\text{Mn}^{2+}$  P-type ATPases belonging to P2 and P5 subgroups was summarized in Table 12.

**Table 12: List of human diseases related to Ca<sup>2+</sup>/Mn<sup>2+</sup>-ATPases (P2A and P2B) and P5B-ATPases deficiencies.** Adapted and updated from Chen et al. [30]. OMIM: Online Mendelian Inheritance in Man.

| Subgroups     | Genes                | Proteins   | Human diseases   | OMIM             |
|---------------|----------------------|--|--|------------------|
| <b>P2A</b>    | <i>ATP2A1</i>        | SERCA1a  | Brody disease  | 108730,          |
|               |                      | SERCA1b  | Myotonic dystrophy type 1                                    | 601003<br>160900 |
|               | <i>ATP2A2</i>        | SERCA2a  | Darier-White disease (skin disorder)                         | 124200           |
|               |                      | SERCA2b  | Heart failure  |                  |
|               |                      | SERCA2c  | Cancers  |                  |
|               | <i>ATP2A3</i>        | SERCA3a-f  | Gastric carcinoma, lung and colon cancer<br>Diabetes         | 601929           |
| <i>ATP2C1</i> | SPCA1a-d             | Hailey-Hailey disease (skin disorder)<br>Breast cancer | 169600   |                  |
| <i>ATP2C2</i> | SPCA2                | Breast cancer  | 613082   |                  |
| <b>P2B</b>    | <i>ATP2B1</i>        | PMCA1a-e   | High cardiovascular risks, preeclampsia,<br>salt sensitivity | 108741           |
|               | <i>ATP2B2</i>        | PMCA2a-f   | Hearing loss (deafness)<br>Autism                            | 108733           |
|               | <i>ATP2B3</i>        | PMCA3a-f   | X-linked cerebellar ataxia<br>Aldosterone-producing adenomas | 300014           |
|               | <i>ATP2B4</i>        | PMCA4a-g   | Familial spastic paraplegia<br>Malaria resistance            | 108732           |
| <b>P5B</b>    | <i>ATP13A2/PARK9</i> | ATP13A2  | Kufor-Rakeb syndrome<br>(neurodegenerative disorder)         | 606693           |
|               | <i>ATP13A4</i>       | ATP13A4  | Specific language impairment<br>Autism, Asperger syndrome    | 609556           |

## 2.2. Role of (un)specific transporters

### 2.2.1. General introduction

Apart from P-type ATPases, other transporters take part in the maintenance of Ca<sup>2+</sup>/Mn<sup>2+</sup> homeostasis within the secretory pathway of yeast and mammalian cells. All of them are secondary active transporters belonging to different families with their own structural features and kinetics properties. Based on the substantial work made by Legrand and Foulquier to gather all transporters involved in Ca<sup>2+</sup>/Mn<sup>2+</sup> homeostasis in mammalian cells [38], I will only focus on those involved in the secretory pathway with relevant specificity for Ca<sup>2+</sup> and/or Mn<sup>2+</sup>. Yeast orthologs will also be described. All of these transporters are listed in Table 13 by family, protein name, transport activity and subcellular localization.

**Table 13: Yeast and human Ca<sup>2+</sup>/Mn<sup>2+</sup> transporters acting in Ca<sup>2+</sup>/Mn<sup>2+</sup> homeostasis within the secretory pathway.** Yeast (Y) *Saccharomyces cerevisiae* and human (H) transporters belonging to the same family are orthologs. Atx2p: antioxydant 2 protein, CaCA: cation/Ca<sup>2+</sup> exchanger, CAX: Ca<sup>2+</sup>/H<sup>+</sup> exchanger, CDF: Cation Diffusion Facilitator, DMT1: Divalent Metal Transporter 1, DCT1: Divalent Cation Transporter 1, ER: endoplasmic reticulum, FPN: ferroportin, Gdt1: Gcr1 dependant translation factor 1 protein, NCX: Na<sup>+</sup>/Ca<sup>2+</sup> exchanger, NCKX: Na<sup>+</sup>/Ca<sup>2+</sup> K<sup>+</sup>-dependant exchanger, NRAMP: Natural Resistance-Associated Macrophage Protein, PM: plasma membrane, Rch1p: regulator calcium homeostasis 1 protein, SLCx: Solute Carrier family « x », Smf: suppressor of mitochondria import function, TFR/TfR: transferrin receptor, TMEM165: transmembrane protein 165, UPF0016: Uncharacterized Protein Family 0016, Vcx1p: Vacuolar H<sup>+</sup>/Ca<sup>2+</sup> exchanger 1 protein, ZIP: Zinc-regulated transporter (Zrt), Iron-regulated transporter (Irt) like family Protein and ZnT: Zinc Transporter.

| Superfamily      | Family         | Organism            | Protein name                       | Transported ion(s)   | Sub. localization  |
|------------------|----------------|---------------------|------------------------------------|--|--------------------|
| CaCA             | NCX            | H                   | SLC8A1-3<br>(NCX1-3)               | 3Na <sup>+</sup> :1Ca <sup>2+</sup>  | PM                 |
|                  | NCKX           | H                   | SLC2A1-5<br>(NCKX1-5)              | 4Na <sup>+</sup> :(1Ca <sup>2+</sup> + 1K <sup>+</sup> )   | PM                 |
|                  | CAX            | Y                   | Vcx1p                              | 1Ca <sup>2+</sup> :1H <sup>+</sup>   | Vacuole            |
| UPF0016          |                | H                   | TMEM165                            | Mn <sup>2+</sup> , Ca <sup>2+</sup> , H <sup>+</sup> ?   | Golgi/PM           |
|                  |                | Y                   | Gdt1p                              |  | Golgi              |
| NRAMP<br>(SLC11) |                | H                   | SLC11A1<br>(NRAMP1)                | Mn <sup>2+</sup> or Fe <sup>2+</sup> :1H <sup>+</sup>  | PM                 |
|                  |                | H                   | SLC11A2<br>(NRAMP2,<br>DTC1, DMT1) | Mn <sup>2+</sup> , Zn <sup>2+</sup> , Fe <sup>2+</sup> ,<br>Cu <sup>2+</sup> , Cd <sup>2+</sup> , Co <sup>2+</sup> ,<br>Ni <sup>2+</sup> , Pb <sup>2+</sup> or Ca <sup>2+</sup> :1H <sup>+</sup> | PM/Endosomes       |
|                  |                | Y                   | Smf1p                              | Mn <sup>2+</sup> , Zn <sup>2+</sup> , Fe <sup>2+</sup> ,<br>Cu <sup>2+</sup> , Cd <sup>2+</sup> , Co <sup>2+</sup> or  | PM                 |
|                  |                | Y                   | Smf2p                              | Ni <sup>2+</sup> :1H <sup>+</sup>  | Golgi-like vesicle |
| CDF              | TFR            | H                   | TfR                                | Mn <sup>2+</sup> , Fe <sup>2+</sup> , other  | PM                 |
|                  | ZnT<br>(SLC30) | H                   | SLC30A10<br>(ZnT10)                | Mn <sup>2+</sup> , Zn <sup>2+</sup>  | PM                 |
|                  | ZIP<br>(SLC39) | H                   | SLC39A8<br>(ZIP8)                  | Mn <sup>2+</sup> , Zn <sup>2+</sup> , Fe <sup>2+</sup> ,<br>Cd <sup>2+</sup>   | PM                 |
| H                |                | SLC39A14<br>(ZIP14) | PM                                 |  |                    |
|                  | Y              | Atx2p               | Mn <sup>2+</sup> ?                 | Golgi  |                    |
|                  | FPN<br>(SLC40) | H                   | SLC40A1<br>(Ferroportin)           | Mn <sup>2+</sup> , Fe <sup>2+</sup> , Co <sup>2+</sup> ,<br>Zn <sup>2+</sup> , Cu <sup>2+</sup>  | PM                 |
| SLC10            |                | H                   | SLC10A7                            | Unknown  | PM/Golgi/ER        |
|                  |                | Y                   | Rch1p                              | Unknown  | PM                 |

### 2.2.2. Cation/Ca<sup>2+</sup> (CaCA) exchangers superfamily

Members of the cation/Ca<sup>2+</sup> (CaCA) superfamily are key components of Ca<sup>2+</sup> signaling pathways in a broad range of species including yeast and mammals. CaCA transporters exchange cytosolic Ca<sup>2+</sup> across organellar and/or plasma membranes against its electrochemical gradient thanks to the favorable gradient of other cation ions such as Na<sup>+</sup>, H<sup>+</sup> and K<sup>+</sup> [291]. According to phylogenetic studies, the CaCA superfamily can be divided into five families: (i) K<sup>+</sup>-independent Na<sup>+</sup>/Ca<sup>2+</sup> exchangers (NCX) family, (ii) K<sup>+</sup>-dependent Na<sup>+</sup>/Ca<sup>2+</sup> exchangers (NCKX) family, (iii) Ca<sup>2+</sup>/H<sup>+</sup> exchangers (CAX) family, (iv) cation/Ca<sup>2+</sup> exchanger (CCX) family with cations other than H<sup>+</sup>, K<sup>+</sup> or Na<sup>+</sup> and (v) YRBG family gathering putative Na<sup>+</sup>/H<sup>+</sup> exchangers only found in bacteria and archaea [291]. Of them and as reported in Table 13, 3 NCX isoforms (NCX1-3) and 5 NCKX isoforms (NCKX1-5) have been described to regulate cytosolic Ca<sup>2+</sup> level in human while only one member of the CAX family (Vcx1p, vacuolar H<sup>+</sup>/Ca<sup>2+</sup> exchanger 1 protein) is involved in cytosolic Ca<sup>2+</sup> sequestration into the yeast vacuole. Hereafter, generalities will be provided for human NCX and NCKX transporters and a more detailed description of Vcx1p function in yeast Ca<sup>2+</sup>/Mn<sup>2+</sup> homeostasis will be addressed.

**NCX and NCKX.** Mammalian NCX (SLC8A) family comprises three members named NCX1-3 (SCL8A1-3), encoded by the three different genes *SLC8A1-3* [292–294]. Alternative splicing events of the primary genes *SLC8A1* and *SLC8A3* result in the generation of numerous NCX1 and NCX3 protein variants. So far, no NCX2 isoforms have been identified. All NCX proteins are found expressed in the brain with higher abundances for NCX1-2 than NCX3. While NCX1 is ubiquitously expressed with higher expression levels in the brain, the heart and the kidneys, NCX2 is only found in the brain and NCX3 shares a more restrictive expression pattern in skeletal muscle [292–294]. Depending on tissue distribution and spliced variants, NCX members contribute to the regulation of Ca<sup>2+</sup>-events in many cell type including neuronal signaling, excitation-contraction coupling in cardiomyocytes, insulin secretion in  $\beta$ -cells and Ca<sup>2+</sup> reabsorption in kidneys. In addition to PMCA, NCXs play a major role in cytosolic Ca<sup>2+</sup> removal across the plasma membrane. However, while PMCA are referred as high-affinity/low capacity systems, NCXs are low-affinity/high capacity systems, responding faster to transient changes in intracellular Ca<sup>2+</sup> levels. Basically, NCXs exchange 3 Na<sup>+</sup> for 1 Ca<sup>2+</sup> across the plasma membrane leading to the electrogenic stoichiometry of 3Na<sup>+</sup>:1Ca<sup>2+</sup>. Most of the time, NCXs mediated cytosolic Ca<sup>2+</sup> extrusion but under specific cellular conditions, they may allow extracellular Ca<sup>2+</sup> entry. Then, NCXs can operate in either a forward (Ca<sup>2+</sup>-efflux) or a reverse mode (Ca<sup>2+</sup>-entry), depending on the membrane potential and intra/extra-cellular [Na<sup>+</sup>] and [Ca<sup>2+</sup>]. Structurally, NCXs contain 10 TMD, two  $\alpha$ -repeats conserved motifs ( $\alpha_1$  and  $\alpha_2$ ) and a big cytosolic loop comprising two Ca<sup>2+</sup> binding domains (CBD1 and CBD2). These latter domains contain respectively four Ca<sup>2+</sup> binding sites (Ca1-Ca4) and two

Ca<sup>2+</sup> binding sites (CaI and CaII) with different affinities for Ca<sup>2+</sup>: low-affinity for Ca1, Ca2 and CaII, medium-affinity for CaI and high-affinity for Ca3 and Ca4 [292–294]. Impaired expression and regulation of NCXs contribute to Ca<sup>2+</sup>-homeostasis alteration in cardio-vascular diseases, diabetes and muscular dystrophy, to list some.

With regards to NCKXs, five mammalian genes *SLC2A1-5* encode for the five different NCKX1-5 proteins. The main difference between NCXs and NCKXs lie in the absolute requirement of K<sup>+</sup> for NCKXs to mediate Na<sup>+</sup>/Ca<sup>2+</sup> exchange. NCKXs are also referred as low-affinity/high capacity systems and mediate the exchange of 4 Na<sup>+</sup> against 1Ca<sup>2+</sup> plus 1K<sup>+</sup>, leading to the transport stoichiometry 4Na<sup>+</sup>:(1Ca<sup>2+</sup> + 1K<sup>+</sup>). Under normal physiological conditions, the inward Na<sup>+</sup> and outward K<sup>+</sup> established gradients promote cytosolic Ca<sup>2+</sup> extrusion across the plasma membrane. However, like NCXs, upon specific (intra)cellular conditions in which Na<sup>+</sup> and K<sup>+</sup> gradients would be reversed, the direction of Ca<sup>2+</sup> transport would also change and NCKXs would mediate Ca<sup>2+</sup> entry into the cell [295–297]. While NCKX1-4 are localized to the plasma membrane, NCKX5 was recently thought to be more likely expressed in the TGN. According to tissue distribution, NCKX1 is restricted found in the rod photoreceptors, NCKX2 is specifically expressed in neurons including cone photoreceptors, NCKX3 and NCKX4 are predominantly expressed in brain but also in other tissues and NCKX5 shares restrictive expression pattern in some specific areas of the brain. Hence, it has been shown that NCKXs play major roles in retinal rod (NCKX1) and cone (NCKX2) photoreceptors, olfactory neurons (NCKX4), epidermal melanocytes (NCKX5) and in brain for motor learning and memory (NCKX2). Due to the abundance of NCKX proteins in the brain and neurons, it has been suggested that NCKX represent the main mechanism of neuronal Ca<sup>2+</sup> clearance [296]. At the structural level, NCKXs and NCXs share similarities including two groups of 5 TMD separated by a big cytosolic and hydrophilic loop and the presence of  $\alpha_1$ - and  $\alpha_2$ -repeats motifs. Besides their crucial role in neuronal Ca<sup>2+</sup> homeostasis, only few human disease-causing mutations have been associated with *NCKX* genes. They concern mutations in (i) *NCKX1*, leading to non-degenerative retinal disease, (ii) *NCKX4* causing amelogenesis imperfecta, a defective enamel mineralization disease and (iii) *NCKX5* associated with oculocutaneous albinism type VI, a severe hypopigmentation condition (see [296] for references).

**Vcx1p.** In yeast, Ca<sup>2+</sup> exchanges over the vacuolar membrane is mediated by two proteins: the P-type Ca<sup>2+</sup>-ATPase Pmc1p already described in section 2.1.2. and the low-affinity/high capacity Ca<sup>2+</sup>/H<sup>+</sup> transmembrane antiporter Vcx1p. Vcx1p, also known as Hum1p (high copy number undoes manganese) belongs to the CAX family and uses the vacuolar pH gradient established by the V-type H<sup>+</sup>-ATPase to import cytosolic Ca<sup>2+</sup> into the vacuole. With regards to Pmc1p, Vcx1p responds faster to brief exposure to high external Ca<sup>2+</sup> levels [298]. Originally, Hum1p was identified for its ability to confer Ca<sup>2+</sup> or

Mn<sup>2+</sup> tolerance when overexpressed in either wild type strains or yeast lacking functional calcineurin (*cnb1Δ*, yeast deleted for *CNB1*, the gene encoding calcineurin regulatory subunit) [299]. However and surprisingly, no Ca/Mn phenotypes were associated with *HUM1* deletion, unless other genes implicated in Ca<sup>2+</sup> signaling were also deleted (*PMR1*, *PMC1*, *CNB1*) [299,300]. In particular, (i) in the double mutant *hum1Δpmc1Δ*, Ca<sup>2+</sup> sensitivity was enhanced together with lower accumulation of intracellular Ca<sup>2+</sup> levels suggesting a role for both Hump1 and Pmc1p in Ca<sup>2+</sup> sequestration and (ii) Ca<sup>2+</sup> tolerance was shown to be lower in strains with functional calcineurin than those lacking calcineurin activity suggesting a calcineurin-dependent inhibition of Vcx1p function [300]. While Vcx1p Ca<sup>2+</sup> transport activity has been confirmed, no direct Mn<sup>2+</sup> transport was shown [300]. However, two particular Vcx1p mutants (Vcx1-M1p and Vcx1-D1p) have been described for their ability to confer a higher Mn<sup>2+</sup> tolerance when overexpressed [301,302]. Vcx1-M1p (S204A/L208P) acts in Mn<sup>2+</sup> tolerance in a calcineurin-dependent manner and such activity does not depend on Pmr1p or Pmc1p [301]. In contrast, Vcx1-D1p (M383I) confers a calcineurin-independent Mn<sup>2+</sup> tolerance that respectively completely and partially depends on Pmr1p and Pmc1p activities [301,302]. All in all, the yeast CAX member Vcx1p functions in Ca<sup>2+</sup> homeostasis by rapidly sequestering cytosolic Ca<sup>2+</sup> into the vacuole in response to burst of [Ca<sup>2+</sup>]. In addition, while the wild-type form of Vcx1p is poorly involved in Mn<sup>2+</sup> tolerance, two Vcx1p mutants have been identified to play a role in Mn<sup>2+</sup> homeostasis in either a calcineurin-dependent or -independent manner.

### 2.2.3. Uncharacterized Protein Family 0016 (UPF0016)

The Uncharacterized Protein Family 0016 (UPF0016) can be divided in twelve subfamilies, gathering members from all branches of life [303]. Although the function of such members is still unknown, evidence from several living organisms (yeast, cyanobacteria, plants, humans) suggest a role in Ca<sup>2+</sup>/H<sup>+</sup>/Mn<sup>2+</sup> homeostasis (see Chapter 3, section 2.2.). As reported in Table 13, TMEM165 and Gdt1p are respectively the human and yeast orthologs of the UPF0016. Both proteins are secondary active transporters involved in Ca<sup>2+</sup> and Mn<sup>2+</sup> homeostasis and will be further and deeply detailed in the next chapter (Chapter 3). Briefly, TMEM165 and Gdt1p were first identified as new Golgi-localized Ca<sup>2+</sup>/H<sup>+</sup> antiporters, forming a novel Ca<sup>2+</sup> transporter family differing from the CaCA superfamily for sequence homology reasons [239,303–305]. Next, further investigations highlighted a role for TMEM165 and Gdt1p in Golgi Mn<sup>2+</sup> homeostasis where both proteins could act as Mn<sup>2+</sup>/Ca<sup>2+</sup> antiporters referring them as the newcomers in the regulation of Ca<sup>2+</sup>/Mn<sup>2+</sup> homeostasis along the secretory pathway [28,65,240,306,307].



#### 2.2.4. Natural Resistance-Associated Macrophage Protein (NRAMP) family

Historically, the first members of the NRAMP family were cloned in 1992 from the yeast *Saccharomyces cerevisiae* and called SMF for suppressor of mif (mitochondria import function) [308]. A year later, the first mammalian member of the family (Nramp1) was identified in mouse macrophages where it conferred resistance and defense against mycobacteria invasion [309]. This primary function gave its name to the family that has been renamed Solute Carrier family 11 (SLC11). NRAMP orthologs have been found in all kingdoms of life and this family of metal transporters is highly conserved from bacteria to human [310,311]. Basically, SLC11 proteins are referred as secondary metal-ions/H<sup>+</sup> transporters, most of them being symporters. Functional studies on various orthologs reflected similar function, substrate and transport mechanism shared by all NRAMP family members. Hence, they have been shown to mediate various biometals exchange across plasma/organelle membrane such as Fe<sup>2+</sup>, Mn<sup>2+</sup>, Zn<sup>2+</sup>, Co<sup>2+</sup>, Ca<sup>2+</sup>, Cu<sup>2+</sup>, Ni<sup>2+</sup>, Cd<sup>2+</sup> and Pb<sup>2+</sup> placing them as key players in the regulation of cytosolic (may toxic) biometal homeostasis [311]. In addition, related SLC11 proteins shared conserved structural features including (i) an hydrophobic core composed of 10 TMD, (ii) several charged amino acid residues conserved within the TMD, (iii) two invariant histidine residues in the 6<sup>th</sup> predicted TMD which are thought to be involved in H<sup>+</sup> transport mechanism and (iv) a group of N-glycosylation sites in lesser conserved regions of the 7<sup>th</sup> and 8<sup>th</sup> predicted TMD [310,312]. As reported in Table 13, two human and two yeast orthologs of the NRAMP family have been identified and will be promptly described afterwards.

**SLC11A1 and SLC11A2.** In humans, two separate genes encode for SLC members: *SLC11A1* and *SLC11A2*. While both encoded proteins SLC11A1 and SLC11A2 share common transport mechanism for Fe<sup>2+</sup> and Mn<sup>2+</sup> [313], SLC11A2 has been widely reported for its contribution in Mn<sup>2+</sup> transport and will be further detailed. Also known as NRAMP2, DCT1 (Divalent Cation Transporter 1) or even DMT1 (Divalent Metal Transporter 1), SLC11A2 was functionally characterized in *Xenopus laevis* and in mammalian cells where it mediates the transport of a broad range of divalent metal ions in a pH-dependent manner, including Mn<sup>2+</sup> and Fe<sup>2+</sup> [314–319]. In particular, Garrick et al. reported that Mn<sup>2+</sup> was preferentially transported by DMT1 with the following order of affinity: Mn<sup>2+</sup>>Cd<sup>2+</sup>>Fe<sup>2+</sup>>Pb<sup>2+</sup>~Co<sup>2+</sup>~Ni<sup>2+</sup>>Zn<sup>2+</sup> [319]. *SLC11A2* produces, by alternative splicing events, two main protein variants named as DMT1-I and DMT1-II, differing in their carboxyl-termini. While DMT1-I possesses an iron regulatory element (IRE), DMT1-II lacks this domain [320,321]. Moreover, an additional alternative use of DMT1 promoters leads to the production of two other transcripts that differ, at the protein level, in the amino-terminal region (DMT1-A and DMT1-B) [322,323]. Together, DMT1 exhibits four protein isoforms described as DMT1-AI/II and DMT1-BI/II. Although DMT1 is

ubiquitously expressed, some higher specific isoform abundance can be found in the duodenum (DMT1-AI/II), kidneys (DMT1-AI), the reticuloendothelial system (DMT1-BI) and the brain [315,322,324]. At the cellular level, DMT1 is predominantly expressed at the plasma membrane and also share an isoform specific distribution linked to cations requirement. While isoforms possessing IRE domain are expressed at the apical membrane of epithelial cells (DMT1-AII) or in the late endosomes/lysosomes (DMT1-BI), the others devoided of IRE domain localize in recycling endosomes (DMT1-A/BII) [159,323,325,326]. In addition, it has been shown that the two N-glycan structures carried by DMT1 influence its strictly apical redistribution in polarized cells since mutations in both N-linked glycosylation sites (S338A and T351A) result in equal distribution of the protein at both the apical and basolateral surfaces of the cell [325]. All in all, DMT1 expression appears to be regulated at several levels depending on tissue specificity, glycosylation status, cell-type and Mn/iron (Fe) dependency. To date, DMT1 was the first mammalian Fe transporter to be characterized. Its biological function in both Fe and Mn homeostasis has been originally determined in microcytic anemia mice and Belgrade rats [327–329]. These two animals with Fe deficiency share the same missense mutation in *SLC11A2* leading to the substitution of glycine 185 to arginine (G185R) at the protein level which reduces by 35-fold the Fe transport activity of DMT1 [330]. In human, mutations in *SLC11A2* also cause hypochromic microcytic anemia suggesting a conservation of function between several mammals [159]. In addition to Fe deficiency, Belgrade rats described by Chua and Morgan also display alterations in Mn metabolism [327]. An overall decrease in Mn uptake was observed in reticulocytes and organs such as the brain, kidneys and femurs along with a reduced Mn absorption from the duodenum. Hence, authors emphasized that Mn uptake and transport could be mediated by DMT1 and in case of mutation in *SLC11A2*, DMT1 loss-of-function could result in Mn metabolism impairments [327]. This hypothesis was later reinforced by similar results obtained by Knopfel and Garrick in the same Belgrade rat animal models and suggest an important role played by DMT1 in  $Mn^{2+}/Fe^{2+}$  cellular uptake, independently from their binding and entry *via* the transferrin/transferrin receptor (Tf-TfR) pathway [331]. So far, DMT1 has been established as a key player in Mn and Fe cellular uptake with two possible ways of action. On the one hand, DMT1 can mediate the direct uptake of extracellular  $Mn^{2+}$  and  $Fe^{2+}$  across the plasma membrane upon acidic conditions -especially in the duodenum- where it acts as a  $H^+-Mn^{2+}/Fe^{2+}$  symporter in a Tf/TfR-independent pathway. On the other hand, DMT1 was shown to export  $Mn^{2+}/Fe^{2+}$  from the endosomal lumen to the cytosol in a Tf/TfR-dependent pathway. Briefly, like  $Fe^{2+}$ , plasmatic Mn is oxidized from  $Mn^{2+}$  to  $Mn^{3+}$  by ceruloplasmin that can be carried by the Tf. Then,  $Mn^{3+}$ -Tf binds the TfR at the plasma membrane and an endocytosis-mediated internalization within the endosomes ensues. In the endosomal compartment, the dissociation of  $Mn^{3+}$  from the Tf/TfR complex occurs upon acidification by the V-ATPase, leading to the subsequent reduction of  $Mn^{3+}$  into  $Mn^{2+}$  by the ferrireductase. Here, endosomal

Mn<sup>2+</sup> is released in the cytosol through DMT1 activity, DMT1 being localized in the endosomes. It is to note that these two Tf/TfR and DMT1 mediated Mn transports are the primary routes for Mn transport across the blood brain barrier. Hence, apart from being key players in Mn<sup>2+</sup> homeostasis at the cellular level, both Tf/TfR and DMT1 are particularly involved in case of long term Mn exposure and may contribute to facilitate Mn accumulation in specific areas of the brain, leading to Mn cytotoxicity and the development of neurodegenerative diseases such as manganism.

**Smf1p and Smf2p.** In the yeast *Saccharomyces cerevisiae*, there are three known NRAMP orthologs Smf1p, Smf2p and Smf3p respectively encoded by *SMF1*, *SMF2* and *SMF3* genes [308,332]. Structurally, all Smfpps possess 11 TMD and lack the IRE domain found in human DMT1. Moreover, a similar “transport sequence” is shared by human and yeast orthologs implying functional similarities between Smfpps and DMT1 [159]. However, albeit the presence of three yeast homologs, only two of them (Smf1p and Smf2p) have been reported to act in Mn<sup>2+</sup> transport and homeostasis [333]. Indeed, dating back to 1996, Supek et al. first demonstrated the Mn transport activity of Smf1p across the plasma membrane where it is localized [334]. While *SMF1* deletion induces a significant decrease in Mn<sup>2+</sup> uptake, Smf1p overexpression increased by 5 times the observed Mn<sup>2+</sup> transport activity suggesting that Smf1p is a high-affinity Mn<sup>2+</sup> transporter [334]. Like other NRAMP members, Smf1p transport activity was later shown not to be Mn<sup>2+</sup> specific but extend to other divalent metal ions such as Zn<sup>2+</sup>, Fe<sup>2+</sup>, Cu<sup>2+</sup> and Cd<sup>2+</sup>. With regards to Smf2p and Smf3p, Cohen et al. demonstrated that in the triple mutant *smf1Δsmf2Δsmf3Δ*, only the overexpression of Smf1p and Smf2p rescued Mn uptake. Hence, Smf3p function may differ from those of Smf1p and Smf2p towards Mn<sup>2+</sup> transport ability [333]. This was confirmed in the comparative study led by Portnoy et al., highlighting a role for Smf3p in Fe homeostasis through its vacuolar storage [332]. Yet, even if Smf1p and Smf2p are involved in Mn uptake and regulated by Mn levels, both proteins are not redundant. Several lines of evidence pinpointed a distinct role for both proteins in Mn uptake and cellular trafficking, in physiological conditions. First, yeasts lacking Smf1p display a greater sensitivity to metal chelators than *smf2Δ* strains [333]. Second, Smf1p is a more effective H<sup>+</sup>-coupled/Mn<sup>2+</sup> symporter than Smf2p suggesting a higher Mn<sup>2+</sup> affinity for Smf1p than for Smf2p. Third, Smf1p and Smf2p do not share similar subcellular localizations under physiological grown conditions. While Smf1p localizes to the plasma membrane, Smf2p was shown to be expressed in intracellular vesicles (Golgi-like vesicles) [334,335]. Fourth, *SMF2* deletion causes greater alterations in overall Mn<sup>2+</sup> homeostasis and distribution within the different organelles than *SMF1* deletion. Indeed, in yeast lacking Smf1p only subtle changes in intracellular Mn levels were observed together with normal functioning of Mn-dependent enzymes such as the mitochondrial Sod2p and the Golgi glycosyltransferases, especially mannosyltransferases (ManT) [334–336]. In contrast, *smf2Δ* mutant

exhibit (i) a global decrease in cellular and mitochondrial Mn levels, (ii) an impaired mitochondrial Sod2p activity and (iii) an altered Golgi glycosylation process reflected by the enhanced gel mobility of the secreted invertase [335]. Together, these observations shed light on the crucial role for Smf2p -but not Smf1p- in Mn delivery to the cytosol and its subsequent redistribution in the different organelles to ensure Mn-dependent reactions such as mitochondrial Sod2p activity and Golgi glycosylation process. While the mitochondrial Mn<sup>2+</sup> importer still needs to be identified, Mn<sup>2+</sup> entry at the Golgi level required Pmr1p activity [335,336]. Hence, the accurate distribution of Mn<sup>2+</sup> in the secretory pathway implies both Smf2p and Pmr1p functions. It is to note that in extreme cases of Mn excess or starvation, Smf1p and Smf2p are subjected to Mn regulation occurring at the post-translational level, driving their protein stability and trafficking. This will be better discussed in section 3.3.1.

#### 2.2.5. Zinc transporter family (ZnT) and Zinc-regulated transporter, Iron-regulated transporter like protein family (ZIP)

Besides their name, some human Zn transporters also contribute to Mn<sup>2+</sup> homeostasis at both the organism and cellular levels. This was evidenced during the last decade through the identification of three inherited disorders of Mn metabolism resulting from mutations in genes encoding Zn transporter proteins known as SLC39A8 (or ZIP8), SLC39A14 (or ZIP14) and SLC30A10 (or ZnT10) [194]. Basically and based on their predictive membrane topology, Zn transporters can be found in two major families named as Zinc-regulated transporter (Zrt), Iron-regulated transporter (Irt) like family Protein (ZIP, also referred as SLC39 family) and Zinc Transporter family (ZnT, also known as SLC30 family). ZIP and ZnT especially mediated the transport of Zn<sup>2+</sup> (but also Mn<sup>2+</sup> which is of interest in this manuscript) in opposite directions. While ZIP members transport Zn<sup>2+</sup> from the extracellular medium and/or intracellular compartments to the cytosol, ZnT members carry Zn<sup>2+</sup> from the cytosol to the extracellular medium and/or organellar lumens [337]. To date, ZIP/SLC39 family contains 14 members and ZnT/SLC30 family, 10 [35,338,339]. Of them, SLC39A8, SLC39A14 and SLC30A10 will be further detailed, being directly involved in Mn<sup>2+</sup> homeostasis (Table 13 and Table 14).

**SLC30A10.** In 2008, Tuschl et al. first reported a clinical case from a 17 years old girl with hepatic cirrhosis associated with elevated liver Mn levels, hypermanganesemia (~10-fold increase in Mn blood levels), polycythemia, dystonia and a MRI revealed Mn deposition in the basal ganglia [340]. This patient was later shown to carry homozygous mutation in *SLC30A10* and was included in the second study led by the same group in 2012, reporting twelve additional cases of patients harboring disease-causing mutations in *SLC30A10* [191].

**Table 14: SLC30A10, SLC39A14 and SLC39A8: from systemic to intracellular regulation of Mn homeostasis.** ECM: extracellular medium, ER: endoplasmic reticulum and HMDYT: hypermanganesemia with dystonia, Sub.: subcellular.

| Protein         | Sub. localization                                   | Consequences in case of deficiency   | Mn <sup>2+</sup> transport                        |
|-----------------|---|--|---|
| <b>SLC30A10</b> | Plasma membrane, apical side (polarized cells)      | <ul style="list-style-type: none"> <li>▪ Higher Mn blood levels</li> <li>▪ Liver disease</li> <li>▪ Polycythemia</li> <li>▪ Parkinsonism</li> <li>▪ Dystonia</li> </ul>  | <b>HMNDTY1</b> <b>Export</b><br>(cytosol to ECM)  |
| <b>SLC39A14</b> | Plasma membrane, basolateral side (polarized cells) | <ul style="list-style-type: none"> <li>▪ Higher Mn blood levels</li> <li>▪ Lower hepatic Mn blood</li> <li>▪ Parkinsonism</li> <li>▪ Dystonia</li> </ul>   | <b>HMNDTY2</b> <b>Import</b><br>(ECM to cytosol)  |
| <b>SLC39A8</b>  | Plasma membrane, Golgi apparatus, ER                | <ul style="list-style-type: none"> <li>▪ Lower to undetectable Mn blood levels</li> <li>▪ Liver disease</li> <li>▪ Deafness</li> <li>▪ Skeletal anomalies, short seizure, dwarfism</li> <li>▪ Congenital Disorders of Glycosylation</li> <li>▪ Mitochondrial <b>Leigh-like</b> syndrome</li> </ul> | <b>Import</b><br>(ECM/organelle lumen to cytosol) |

In a companion study, Quadri et al. also identified in 2012 five patients from two different families with familial Mn-induced neurotoxicity due to mutations in *SLC30A10* [190]. Although SLC30A10 was first assumed to be a Zn efflux transporter [341], the clinic from patients strongly suggested a role for SLC30A10 in Mn homeostasis through a Mn-efflux activity. This was deeply investigated in different cultured cell lines [342–346]. To summarize these findings, authors demonstrated that (i) SLC30A10 is a transmembrane protein expressed at the plasma membrane [342], (ii) SLC30A10 overexpression 1) blocks the Mn-induced degradation of GPP130 upon MnCl<sub>2</sub> treatment suggesting either an increased Mn influx or an inhibition of Mn uptake, 2) lowers intracellular Mn level in favor for a higher Mn efflux activity mediated by SLC30A10, 3) protects against Mn-induced cytotoxicity [342,345] and (iii) patient mutations 1) impair SLC30A10 trafficking (ER-localization) [342] and 2) alter SLC30A10 efflux activity leading to Mn accumulation in the Golgi apparatus [342,346]. Moreover, Zogzas et al. pointed out the involvement of specific amino acid residues in both TMD (second and fifth) and cytoplasmic domains responsible for Mn<sup>2+</sup> transport capacity instead of Zn<sup>2+</sup> [344,345]. According to tissue specificity, SLC30A10 is mainly expressed in the liver, the brain and the gastrointestinal tract [190,347,348]. In a

very recent study led in mice knock-out for *Slc30a10* (whole-body and tissue specific knock-out), it has been shown that under physiological conditions, brain Mn levels were mainly regulated through the activity of Slc30a10 localized in the liver and in the gastrointestinal tract while in case of Mn exposure, Slc30a10 Mn-efflux activity in the brain protects from Mn cytotoxicity [348].

**SLC39A14.** In addition to SLC30A10, Tuschl et al. reported in 2016 that homozygous mutations in *SLC39A14* also lead to a human disorder of Mn metabolism [189]. Clinically, except for polycythemia and liver damages that have not been associated with *SLC39A14* mutations, SLC30A10 and SLC39A14 deficiencies result in the similar condition of hypermanganesemia with dystonia (HMDYT) [192]. In contrast to SLC30A10, SLC39A14 belongs to the ZIP family and is assumed to transport metal in the reverse mode, *i.e.* from the extracellular compartments to the cytosol. Before it was hypothesized to act in Mn<sup>2+</sup> homeostasis, previous *in vitro* studies evidenced that SLC39A14 could transport Mn<sup>2+</sup>, Fe<sup>2+</sup> and Cd<sup>2+</sup> in addition to Zn<sup>2+</sup> [349–352]. In fact, the biological and physiological functions of SLC39A14 in Mn homeostasis became clear with the identification of human mutations and the use of *SLC39A14* knock-out animal models (zebrafish and mice) and cultured cell lines [189,194,353]. Ubiquitously expressed with a higher abundance in liver and the small intestine, SLC39A14 is a cell surface Mn<sup>2+</sup> importer which plays a significant role in both Mn cellular and systemic homeostasis. Based on the fact that *SLC39A14* deficiency in human, zebrafish and mice led to (i) higher Mn accumulation in the brain, (ii) unaffected nay lower hepatic Mn levels and (iii) elevated blood Mn level, SLC39A14 was first thought to act as the main Mn importer into the hepatocytes facilitating Mn clearance through biliary excretion. However, in specific *Slc39a14*-liver knock-out mice, it turned out that even if Mn levels in liver were lowered, no other Mn accumulation was observed – either in blood or in the brain [353]. Hence, the lack of functional SLC39A14 in the liver is not solely responsible for Mn accumulation in other tissues. Because SLC39A14 is also highly expressed in the small intestine, further investigations led in *SLC39A14* depleted Caco-2 cells shed light on a significant increase in the apical-to-basolateral Mn transport meaning that a lack of SLC39A14 in the small intestine may result in a higher Mn absorption and subsequent accumulation. This hypothesis was then confirmed in specific *Slc39a14*-intestine knock-out mice [354]. Indeed, in contrast to the previous *Slc39a14*-liver knock-out mice, increased Mn levels in both the liver and brain were observed in *Slc39a14*-intestine knock-out mice [354]. All in all and as summarized in Table 14, SLC39A14 is assumed to be the main cell surface Mn importer in both hepatocytes and enterocytes (basolateral localization) with a crucial role in maintaining the systemic Mn homeostasis from its intestine localization [194,354].

**SLC39A8.** The last  $Mn^{2+}$  transporter identified to actively contribute in both cellular and systemic Mn homeostasis is SLC39A8. It is to note that historically, the function of SLC39A8 was linked to its  $Cd^{2+}$  transport activity, especially in rat testis [355]. During the following century and taking advantage of new technologies, *SLC39A8* was then described as a causal gene in numerous human disorders before being prone to be a key player in Mn systemic regulation [355]. Akin SLC39A14, SLC39A8 is a transmembrane protein belonging to the ZIP family and able to transport several cation biometals including  $Cd^{2+}$ ,  $Mn^{2+}$ ,  $Se^{4+}$  and  $Fe^{2+}$  in addition to  $Zn^{2+}$  [350,351,356–358]. Identification of human mutations in *SLC39A8* gave rise to new insights in the understanding of both biological and physiological functions of the transporter. In 2015, two clinical studies from separate groups reported heterozygous compound and recurrent homozygous mutations in *SLC39A8* leading to an overall systemic Mn deficiency associated with liver disease, skeletal abnormalities (short seizures, dwarfism), deafness and intellectual disability [67,188,192,193]. In addition to these reported cases, Riley et al. identified some patients presenting with Leigh-like syndrome, which is a disease related to mitochondrial impairments [203]. At the cellular level, alterations in both Golgi and mitochondrial functions reflected intracellular Mn deficiency resulting in (i) reduced activity of glycosylation enzymes -such as  $\beta$ -1,4-galactosyltransferase- causing severe N-linked glycosylation defects and (ii) reduced activity of the mitochondrial superoxidismutase (MnSOD) leading to an increased oxidative stress [67,203]. For such reasons, human SLC39A8 deficiency is classified as a Congenital Disorders of Glycosylation associated or not with a Leigh-like syndrome, depending on the causal mutations [67,68,203]. In addition, to better characterize SLC39A8  $Mn^{2+}$  transport activity, HeLa cells were transfected with either the wild-type or four pathogenic mutation forms of *SLC39A8*. In this study, Choi et al. demonstrated that (i) wild-type SLC39A8 is expressed at the cell surface where it mediates  $^{54}Mn$  uptake, (ii) SLC39A8 mutants are trapped in the ER and (iii) failed to enhance  $^{54}Mn$  uptake. Hence, the mislocalization of disease-causing SLC39A8 mutants revealed the mutations may alter its proper folding/targeting and subsequently, its function [359].

Altogether, Table 14 gathers general information about SLC30A10, SLC39A14 and SLC39A8 subcellular localization, direction of  $Mn^{2+}$  transport and systemic consequences in case of deficiency that was at the basis of the understanding of their role in Mn homeostasis at the cellular level. Also, Figure 23 depicts the current interplay between SLC30A10, SLC39A14 and SLC39A8 in Mn cellular homeostasis especially in enterocytes and hepatocytes.

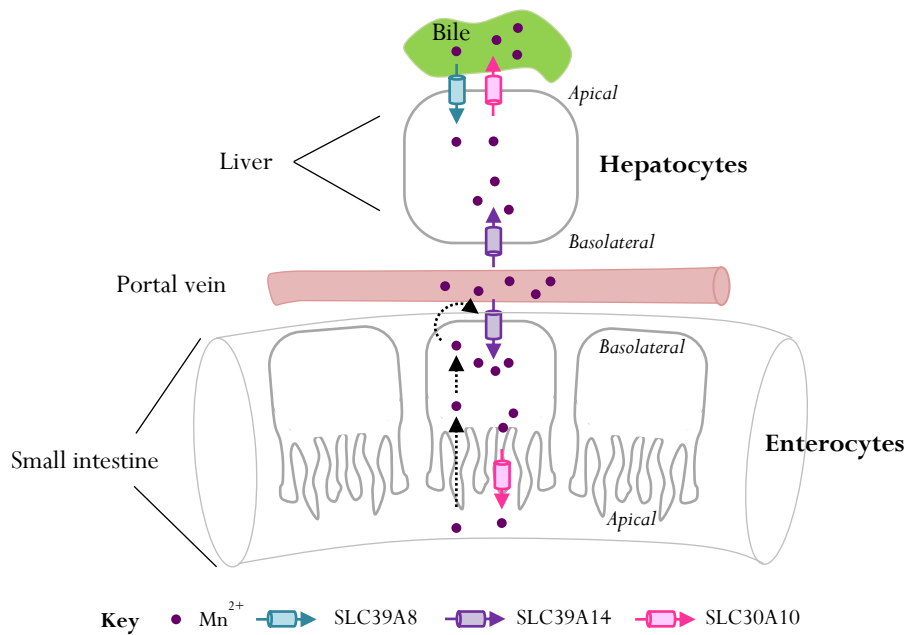


**Figure 23: Interconnection between SLC30A10, SLC39A14 and SLC39A8 functions in regulating Mn homeostasis in enterocytes and hepatocytes.** Both liver and intestines play a central role in regulating systemic Mn metabolism. On the one hand, liver is the main organ clearing Mn from the blood and secreting it into the bile for two purposes: intestinal resorption or fecal excretion. In liver and particularly in hepatocytes, SLC39A14 imports circulating Mn from the blood at the basolateral surface while SLC30A10 extrudes Mn into the bile at the apical side of the cell. In addition, localized at the apical side of hepatocytes, SLC39A8 mediates Mn import from the bile to increase Mn storage. On the other hand, Mn can be transported from the blood to the intestinal lumen *via* a two-step process within the enterocytes. First, SLC39A14 imports Mn from the blood at the basolateral membrane. Second, SLC30A10 releases intracellular Mn into the intestinal lumen. It is to note that Mn can directly be absorbed in enterocytes from the intestinal lumen *via* an unknown mechanism (dashed arrows) and released at the basolateral membrane where it can be reuptake by SLC39A14 (circled dashed arrow).

**Atx2p.** According to the Transporter Classification Database (TCDB), Atx2p (Antioxidant 2 protein) is referred as a yeast ortholog of the ZIP family with a putative function in  $Mn^{2+}$  homeostasis at the Golgi level [360]. Historically, Atx2p was discovered in the search for yeast antioxidant genes (*ATX*), able to compensate the loss of *SOD1* [361]. In the primary and solely study mentioning Atx2p, Lin and Culotta demonstrated that (i) the yeast Atx2p is a Golgi-localized transmembrane protein, (ii) yeasts overexpressing *ATX2* tends to accumulate higher intracellular levels of Mn, (iii) *ATX2* deletion induces a decrease in cytosolic Mn levels and (iv) *ATX2* deletion in a *pmr1Δ* background reduces the  $Mn^{2+}$  sensitivity associated to *PMR1* deletion [361]. Together, these observations led the authors thinking about an antagonist function between Pmr1p and Atx2p to control  $Mn^{2+}$  homeostasis. While Pmr1p imports cytosolic  $Mn^{2+}$  into the Golgi lumen, Atx2p would export luminal  $Mn^{2+}$  to the cytosol. However, no direct  $Mn^{2+}$  transport activity has been shown for Atx2p since no “metal binding site(s)” have been reported in the structure of the protein [361]. Hence, Atx2p involvement in  $Mn^{2+}$  homeostasis at the Golgi level remains indirect.



### 2.2.6. Additional solute carriers (SLC): SLC40A1 and SLC10A7/Rch1p

**SLC40A1.** Ferroportin (Fpn), also known as iron-regulated protein (IREG1), metal transporter protein (MTP1) or SLC40A1, was reported twenty years ago by three independent studies as a key player in Fe homeostasis, mediating the export of cellular  $\text{Fe}^{2+}$  into the blood stream [362–364]. Encoded by *FPN1*, Fpn is the solely member of the SLC40 family (SLC40A1) and possesses 12 TDM, an intracellular amino-terminus, an extracellular carboxyl-terminus and several predicted N-linked glycosylation and phosphorylation sites [365]. This iron-regulated protein is mainly expressed in tissues involved in both Mn and Fe homeostasis including the brain, the liver and the duodenum. Human mutations in *FPN1/SLC40A1* cause an autosomal dominant form of hemochromatosis type IV, a disorder of Fe metabolism associated with Fe overload (Table 15). At the cellular level, Fpn localizes to the basolateral membrane of polarized epithelial cells such as enterocytes [362–365]. From these primary studies, (i) mouse *Mtp1* overexpression reduces intracellular Fe levels [362], (ii) *Mtp1*-deficient mice tend to accumulate higher levels of Fe in enterocytes, macrophages and hepatocytes [366], (iii) when expressed in *Xenopus laevis* oocytes, Fpn enhances Fe efflux [364] and (iv) Fpn is found regulated by Fe contents (overload or deficiency) at both mRNA and protein levels [362,364]. Hence, Fpn has been suggested to actively contribute to Fe homeostasis as a plasma membrane  $\text{Fe}^{2+}$  extruder. To date, no other mammalian  $\text{Fe}^{2+}$  exporter has been identified. However, since Mn and Fe share very close physical and chemical properties, it is not surprising that Fpn has later been reported to also function as a  $\text{Mn}^{2+}$  exporter [367]. Originally in search for mammalian mechanisms of Mn efflux, Yin et al. hypothesized that ferroportin could be involved in such cellular Mn clearance since it fulfills this function for Fe. Using both *in vitro* and *in vivo* approaches, they demonstrated that (i)  $\text{MnCl}_2$  exposure induces endogenous Fpn protein expression in HEK293T as well as in mouse cerebellum, (ii) Fpn overexpression in HEK293T cells lowers intracellular Mn accumulation and (iii) reduces Mn-induced cytotoxicity [368]. Although no direct evidence of  $\text{Mn}^{2+}$  transport activity was provided at the time, these observations support a Mn-efflux function for SLC40A1 [368]. In a later study, Madejczyk and Ballatori further investigate this putative Mn transport activity of SLC40A1 using *Xenopus laevis* oocytes injected with human FPN1 complementary RNA [367]. Amongst other things, they demonstrated that more  $^{54}\text{Mn}$  was exported by Fpn-expressing oocytes comparing to control while no differences were observed in  $^{54}\text{Mn}$  uptake, suggesting that Fpn mediates cellular Mn export. In addition, in Fpn-expressing oocytes,  $^{54}\text{Mn}$  export was shown to be (i) [ $^{54}\text{MnCl}_2$ ]-dependent, (ii) reduced by acidic pH, and (iii) partially inhibited by other divalent metals ( $\text{Fe}^{2+}$ ,  $\text{Co}^{2+}$  and  $\text{Ni}^{2+}$ ) [367]. Altogether, this study allows the characterization of Mn export mediated by SLC40A1 and provides direct *in vitro* evidences of  $\text{Mn}^{2+}$  transport activity and substrate specificity. Then, to link this function of  $\text{Mn}^{2+}$  exporter and biological relevance, Choi et al. highlighted that human disease-causing mutation in *FPN1* impact Mn

accumulation and subsequent toxicity [369]. In this *in vitro* study, HEK293T cells were transiently transfected with wild-type Fpn and pathogenic mutations in *FPN1* leading to Fpn loss-of-function (LOF) or gain-of-function (GOF). In these conditions, authors demonstrated that upon  $[\text{MnCl}_2]$  exposure, intracellular Mn levels decreased in cells overexpressing wild-type and GOF Fpn while a huge Mn accumulation was observed in cells overexpressing LOF Fpn. In addition, Mn-induced degradation of GPP130 was only shown in control cells and cells overexpressing LOF Fpn but not in cells overexpressing wild-type or GOF Fpn suggesting that wild-type and GOF Fpn functions result in Mn depletion while LOF Fpn exhibit an altered  $\text{Mn}^{2+}$  export activity [369]. Additional experiments confirm this claim. Altogether, these findings may help to redefine the proper hemochromatosis type IV with both Fe and Mn homeostasis impairments. However, the lack of *in vivo* evidences of such altered Mn homeostasis weakens the previous statement. Indeed, a recent study led in mice suggests that Fpn1 only exerts a minor role in systemic Mn homeostasis [370]. Briefly, mice depleted for the transmembrane serine protease 6 (TMPRSS6) expressed very low levels of Fpn due to constitutive overexpression of hepcidin. In this specific background, Fe homeostasis is hugely impaired (reduced dietary Fe absorption and Fe levels in tissues) while Mn homeostasis remains unaffected [370]. Hence, authors emphasized that Fpn contribution in Mn homeostasis could be neglected comparing to other transporters. All in all, while *in vitro* studies clearly demonstrate Fpn ability to export cytosolic  $\text{Mn}^{2+}$ , the biological relevance of such function *in vivo* is not so clear and still need to be further investigated.

**SLC10A7 and Rch1p (regulator of calcium homeostasis 1 protein).** As a last member of the human SLC family, SLC10A7 was recently reported to be a negative regulator of Store Operated Channels (SOCs) that mediate  $\text{Ca}^{2+}$  entry at the plasma membrane [371]. Prior to human SLC10A7, a similar function was assigned for its yeast ortholog Rch1p, suggesting a conservation of function between yeasts and humans [372]. To date, no direct evidence proves any  $\text{Ca}^{2+}$  and/or  $\text{Mn}^{2+}$  transport activity for SLC10A7/Rch1p. Despite their contribution in  $\text{Ca}^{2+}$  homeostasis remain likely indirect, I decided to further discuss on these two proteins since mutations in *SLC10A7* cause a CDG very close to TMEM165-CDG [373]. Based on literature, we speculated that SLC10A7 could somehow be involved in ER/Golgi ionic homeostasis, driving Golgi glycosylation. Briefly, SLC10A7 belongs to the SLC10 family which contains six additional members SLC10A1-6 [374]. Although it shares homology with other members of the family through its sodium bile acid symporter family (SBF) domain, SLC10A7 also displays distinctive features in terms of (i) genomic organization (12 exons instead of 1 to 6 for other members), (ii) protein topology (10 predictive TMD instead of 7) and (iii) proper function (not related to bile transport). In addition, while all other SLC10 members are exclusively found in vertebrates, SLC10A7 has orthologs in other species including bacteria, plants and yeasts [374]. In particular, two yeast

orthologs have been found: one in *Candida albicans* known as CaRch1p and the other in *Saccharomyces cerevisiae* named ScRch1p (or Rch1p in this manuscript) [372,375]. Originally, CaRch1p was first characterized and later investigations in *Saccharomyces cerevisiae* demonstrated that ScRch1p was its functional homolog [372,375]. Although *CaRCH1* and *ScRCH1* deletions did not result in the same Ca phenotypes, both yeast homologs have been characterized as negative regulators of cytosolic Ca<sup>2+</sup> homeostasis. Moreover, both protein expressions are subjected to the Ca<sup>2+</sup>-CaM/calcineurin regulatory pathway - that will be further detailed in section 3.3.2., Figure 34 - but contrary to CaRch1p which is constitutively expressed, ScRch1p is only expressed and only localizes to the plasma membrane in response to high external Ca levels [372,375]. To the human side, consistent with yeast studies, SLC10A7 is also assumed to be a negative regulator of Ca<sup>2+</sup> entry at the plasma membrane since (i) intracellular Ca<sup>2+</sup> levels are higher in cells knock-out for SLC10A7 and lower in cells overexpressing SLC10A7, and (ii) a higher Ca<sup>2+</sup> influx is observed upon thapsigargin treatment in SLC10A7 knock-out cells suggesting a higher SOCE response in absence of SLC10A7. For such reasons and others, SLC10A7 was even proposed to be renamed RCAS for regulator of intracellular calcium signaling [371]. However, SLC10A7 is still considered as an orphan solute carrier since transport studies failed to identify a specific substrate and subsequent transport activity for the protein [374]. At last, it is to note that two years ago, pathogenic mutations in human *SLC10A7* were identified in two unrelated studies using whole-exome sequencing in individuals presenting with skeletal dysplasia, amelogenesis imperfecta and glycosylation defects [373,376]. To the latter point, glycomics were performed on patient samples and revealed (i) a decrease in sialylation, (ii) an increase in the proportion of high mannose glycan structures and also in (iii) glycans lacking GlcNAc residues [373]. From these observations, SLC10A7 deficiency was classified as a new type II CDG, SLC10A7-CDG. However, further investigations are needed to potentially link SLC10A7 biological function in Ca<sup>2+</sup> homeostasis and an alteration of the glycosylation processes. This is an ongoing project in the team.

#### 2.2.7. Two other yeast transporters: Pho84p and Ccc1p

In yeast, apart from Smf1p and Smf2p, two additional transporters have been shown to play a role in cellular Mn<sup>2+</sup> homeostasis: Pho84p and Ccc1p.

**Pho84p (phosphate metabolism 84 protein).** Pho84p, a high affinity inorganic phosphate transporter localized at the plasma membrane was indeed thought to act as a low affinity metal transporter. In the yeast *Saccharomyces cerevisiae*, *PHO84* deletion results in (i) a Mn<sup>2+</sup>-resistant phenotype and (ii) an altered biometals accumulation upon exposure to high concentrations -not only restrictive to Mn<sup>2+</sup> but also to Zn<sup>2+</sup>, Co<sup>2+</sup> and in a lesser extend to Cu<sup>2+</sup>. In particular, in *pho84Δ* mutants grown

under  $[\text{MnCl}_2]$  ranging from 0 to  $25\mu\text{M}$ , no Mn accumulation was observed for any concentrations suggesting that the ensued  $\text{Mn}^{2+}$ -resistance was due a reduced  $\text{Mn}^{2+}$  uptake. In contrast, in the wild-type strain, yeasts accumulate cellular Mn in excess and proportionally to the extracellular  $[\text{MnCl}_2]$ . Hence, Pho84p was assumed to be responsible for cellular Mn accumulation especially in case of Mn excess (see Figure 33) and subsequently to act as a low affinity  $\text{Mn}^{2+}$  transporter at the plasma membrane. Further experiments indeed demonstrated the contribution of Pho84p in  $\text{Mn}^{2+}$  uptake at the plasma membrane separately from Smf1p. In addition, it has been shown that Mn transported by Pho84p was biologically active as it not only contributes to cell toxicity but also to Mn-dependent reactions and can be incorporated into Mn-dependent enzymes such as Sod2p [377]. All in all, Pho84p is an inorganic phosphate transporter able to mediate  $\text{Mn}^{2+}$  import at the plasma membrane with a low affinity and especially in case of Mn excess.

**Ccc1p (cross-complements  $\text{Ca}^{2+}$  phenotype of *csg1* [ $\text{Ca}^{2+}$  sensitive growth] 1 protein).**

Originally and as referred by its name, *CCC1* was positively screened in the search for genes able to suppress the  $\text{Ca}^{2+}$ -sensitive phenotype due to mutations in the *CSG1* gene, emphasizing a role for Ccc1p in  $\text{Ca}^{2+}$  homeostasis [378]. Two years after Fu's discovery, Lapinskas et al. identified *CCC1* as a suppressor of  $\text{Mn}^{2+}$  sensitivity due to mutations in *PMR1* [181]. In such yeast background, it came out that *CCC1* overexpression in both wild-type or *PMR1*-mutated strains (i) reduces the  $\text{Mn}^{2+}$ -induced cytotoxicity without lowering total Mn content and (ii) restricts the cytosolic  $\text{Mn}^{2+}$  bioavailability since yeasts lacking the cytosolic copper/zinc superoxydismutase (SOD) 1 protein (Sod1p) became Mn-dependent. In addition, *CCC1* deletion increases the  $\text{Mn}^{2+}$ -sensitivity of the wild-type strain. Hence Ccc1p was thought to be a Mn transporter involved in  $\text{Mn}^{2+}$  sequestration elsewhere than in the cytosol, protecting yeasts from  $\text{Mn}^{2+}$  cytotoxicity [181]. Like Pmr1p, Ccc1p was assumed to serve a dual function in  $\text{Ca}^{2+}$  and  $\text{Mn}^{2+}$  homeostasis which has been confirmed by others that identify Ccc1p as a suppressor of  $\text{Mn}^{2+}$  sensitivity in yeasts with non-functional calcineurin [299]. Similarly to Pmr1p, Ccc1p was found localized in the Golgi apparatus then raising the question of Pmr1p/Ccc1p functional redundancy. As already mentioned, yeasts lacking Pmr1p exhibit Golgi glycosylation defects, that are not observed in *ccc1Δ* mutants. In addition, *CCC1* overexpression in a *pmr1Δ* background failed to reverse the glycosylation defects, meaning that Ccc1p could not provide sufficient  $\text{Mn}^{2+}$  to the Golgi enzymes [181]. In fact, in a later study led on Ccc1p, Li et al. demonstrated the vacuolar localization of the protein [379]. This confirms the non-redundant function of Pmr1p and Ccc1p in  $\text{Mn}^{2+}$  sequestration within the secretory pathway as Pmr1p acts at the Golgi level while Ccc1p functions in the vacuolar compartment. Moreover, in addition to its contribution to  $\text{Ca}^{2+}$  and  $\text{Mn}^{2+}$  homeostasis, Ccc1p was shown to play a crucial role in  $\text{Fe}^{2+}$  homeostasis through  $\text{Fe}^{2+}$  sequestration into the vacuole [379,380].

*CCC1* was again positively screened to suppress a specific phenotype associated with *YFH1* deletion. Yfh1p refers to yeast Frataxin homologue 1 protein, an ortholog of the mammalian Frataxin known to be involved in the development of human Friedreich's ataxia, a neurodegenerative disorder. Insights into the function of Frataxin pass through the characterization of its yeast ortholog. In *Saccharomyces cerevisiae*, a lack of *YFH1* results in a loss of respiratory activity due to toxic accumulation of mitochondrial  $\text{Fe}^{2+}$  levels [380]. In such yeast model of Friedreich's ataxia, *CCC1* overexpression sustained the respiratory function by preventing excessive accumulation of mitochondrial  $\text{Fe}^{2+}$  [380]. Later investigations by the same group highlighted that *CCC1* overexpression (i) lowers cytosolic  $\text{Fe}^{2+}$  levels and (ii) increases both  $\text{Mn}^{2+}$  and  $\text{Fe}^{2+}$  accumulation into the vacuole. Inversely, in case of *CCC1* deletion, yeasts are subjected to increased  $\text{Mn}^{2+}$  and  $\text{Fe}^{2+}$  sensitivities [379]. Hence, by sequestering  $\text{Fe}^{2+}$  into the vacuole, Ccc1p hampers the accumulation of mitochondrial  $\text{Fe}^{2+}$  by lowering cytosolic  $\text{Fe}^{2+}$  levels. Altogether, Ccc1p has been shown to play a role in  $\text{Ca}^{2+}$ ,  $\text{Mn}^{2+}$  and  $\text{Fe}^{2+}$  homeostasis, acting as a suppressor of  $\text{Ca}^{2+}$ -,  $\text{Mn}^{2+}$ - and  $\text{Fe}^{2+}$ -sensitivities associated with specific gene deletions. Ccc1p is now assumed to be a vacuolar  $\text{Mn}^{2+}/\text{Fe}^{2+}$  transporter acting in  $\text{Mn}^{2+}$  and  $\text{Fe}^{2+}$  sequestration into the vacuole to avoid their cytosolic accumulation to toxic levels.

#### 2.2.8. $\text{Ca}^{2+}/\text{Mn}^{2+}$ transporters deficiencies in human related diseases

Mutations in nearly all of the genes encoding the human  $\text{Ca}^{2+}/\text{Mn}^{2+}$  transporters mentioned above have been described in human disorders, reflecting the crucial importance of such functional transporters to maintain both intracellular and systemic  $\text{Ca}^{2+}$  and  $\text{Mn}^{2+}$  homeostasis. The following table (Table 15) lists human diseases linked to deficiency in some of them.

**Table 15: List of human diseases related to  $\text{Ca}^{2+}/\text{Mn}^{2+}$  transporters deficiencies.** This table compiles the main disorders associated with deficiency in one of the  $\text{Ca}^{2+}/\text{Mn}^{2+}$  transporters mentioned above. CDG: Congenital Disorders of Glycosylation, NCKX:  $\text{Na}^+/\text{Ca}^{2+} \text{K}^+$ -dependant exchanger, NRAM: Natural Resistance-Associated Macrophage Protein, OMIM: Online Mendelian Inheritance in Man, SLCx: Solute Carrier family « x », UPF0016: Uncharacterized Protein Family 0016, ZIP: Zinc-regulated transporter (Zrt), Iron-regulated transporter (Irt) like family Protein and ZnT: Zinc Transporter.

| Family       | Gene                            | Human diseases   | OMIM   |
|--------------|---------------------------------|--|--------|
| NCKX         | <i>NCKX1</i>                    | Congenital stationary night blindness  | 613830 |
|              | <i>NCKX4</i>                    | Amelogenesis imperfecta  | 615887 |
|              |                                 | Skin/hair/eye pigmentation variation 6   | 210750 |
| <i>NCKX5</i> | Oculocutaneous albinism type VI | 113750   |        |
| UPF0016      | <i>TMEM165</i>                  | TMEM165-CDG (CDG-IIIc)   | 614727 |
| NRAMP        | <i>SLC11A2</i>                  | Hypochromic microcytic anemia with iron overload-1 (AHMIO1)                                    | 206100 |
| ZnT          | <i>SLC30A10</i>                 | Hypermanganesemia with dystonia (HMDYT1)   | 613280 |
| ZIP          | <i>SLC39A8</i>                  | SLC39A8-CDG (CDG-IIIn)   | 616721 |
|              |                                 | Leigh-like syndrome  | 256000 |
|              | <i>SLC39A14</i>                 | Hypermanganesemia with dystonia (HMDYT2)   | 617013 |
|              | <i>FPN1</i>                     | Hemochromatosis type IV  | 606069 |
| SLC          | <i>SLC10A7</i>                  | Short stature, amelogenesis imperfecta, skeletal dysplasia with scoliosis/SLC10A7-CDG (CDG-II) | 618363 |

### 2.3. Role of (un)specific channels

#### 2.3.1. General introduction

This latter family of proteins gathers passive transporters commonly named ion channels. Ion channels can be classified according to their structural organization, the type of ions passing through them (*e.g.* calcium  $\text{Ca}^{2+}$ , potassium  $\text{K}^+$ , sodium  $\text{Na}^+$ , chloride  $\text{Cl}^-$ ), the factors influencing their gating (membrane potential for the voltage-gated channels, ligand, second messenger, temperature, mechanical changes) and their tissue distribution. Basically, all of these channels exist in one of the three states described in Figure 24: opened, inactivated closed and resting closed. Most of the ion channels are formed by several subunits, each of them being encoded by a different gene leading to a great number and diversity for these channels. Amongst them, only those involved in  $\text{Ca}^{2+}$  and/or  $\text{Mn}^{2+}$  transport will be briefly addressed. In humans, more than 30 different channels are referred as  $\text{Ca}^{2+}$  channels. Of them, 15 share a strict specificity for  $\text{Ca}^{2+}$  encompassing the six following families: (i)  $\text{Ca}^{2+}$  Release Activated  $\text{Ca}^{2+}$  (CRAC) channels, (ii) Voltage-gated Ion Channel (VIC), (iii) Ryanodine-Inositol 1,4,5-triphosphate Receptor  $\text{Ca}^{2+}$  Channel (RIR-CaC), (iv) Calcium Transporter A (CaTA), (v) Flower (Synaptin Vesicle-Associated  $\text{Ca}^{2+}$  channel) and (vi) Presenlin (Presenlin ER  $\text{Ca}^{2+}$  channel) [38].

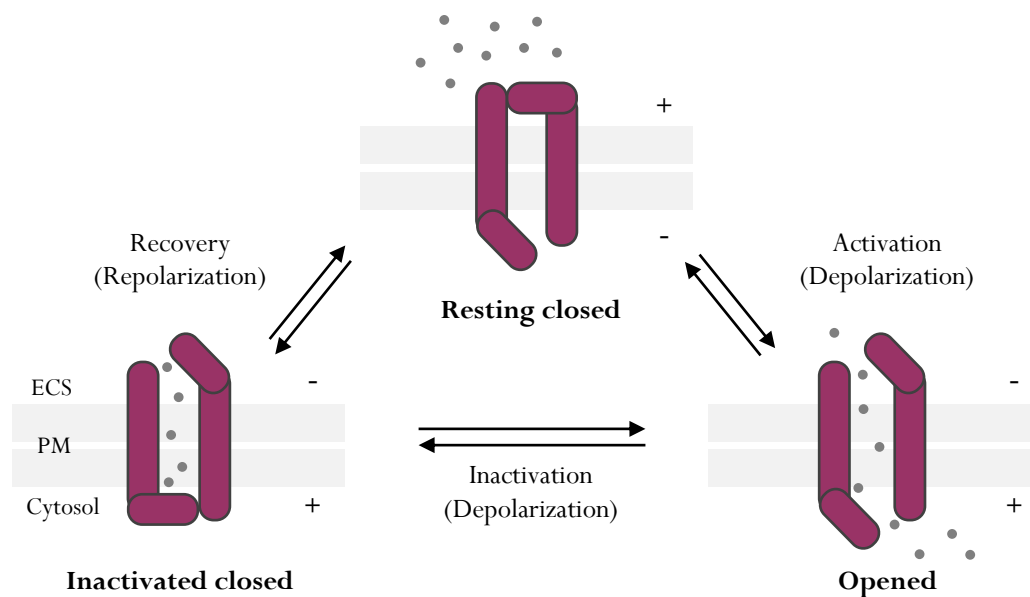


**Figure 24: Schematic diagram illustrating the three states of an ion channel (here, a voltage-gated ion channel).** In physiological or resting conditions, the channel is in a closed conformation (**resting closed**). Changes in membrane potential initiate the transition between the three states. First, depolarization of membrane potential triggers activation (**opened**) and subsequent inactivation of the channel (**inactivated closed**) that cannot be opened anymore. Second, upon repolarization of the membrane potential, the channel recovers its resting closed conformation. ECS: extracellular space and PM: plasma membrane.

All the other have been considered as non-selective  $\text{Ca}^{2+}$  channels, meaning that they can transport other additional ions than  $\text{Ca}^{2+}$ . Of interest in this manuscript, three  $\text{Ca}^{2+}$ -permeable channels are able to transport  $\text{Mn}^{2+}$ : TRPML1 and TRPM7, two members of the Transient Receptor Potential (TRP) superfamily and CACNA1H that belong to the VIC family [38]. To the yeast point of view, some orthologs can be found, mainly belonging to the VIC and TRP families. In the following sections, only few mammals and yeast  $\text{Ca}^{2+}/\text{Mn}^{2+}$  channels will be described, as listed in Table 16. Additional information will be provided through referred reviews.

### 2.3.2. Calcium Release-Activated Calcium (CRAC) channels

In mammals,  $\text{Ca}^{2+}$  release-activated  $\text{Ca}^{2+}$  (CRAC) channels are part of the primary route for  $\text{Ca}^{2+}$  entry in many cell types including both excitable and non-excitable cells. More than thirty years ago, James W. Putney Jr was the first to propose a model of  $\text{Ca}^{2+}$  entry activation upon store-depletion of intracellular  $\text{Ca}^{2+}$  reservoirs such as the ER [381]. This concept was named “Capacitative  $\text{Ca}^{2+}$  Entry” (CCE) and is now referred as Store-Operated  $\text{Ca}^{2+}$  Entry (SOCE). During the past twenty years, electrophysiological studies revealed the fingerprint of the CRAC channels in terms of biophysical and pharmacological properties, distinguishing them from other  $\text{Ca}^{2+}$  channels. In particular, CRAC channels are (i) activated by ER  $\text{Ca}^{2+}$  store depletion, (ii) have a high  $\text{Ca}^{2+}$  selectivity, (iii) an extremely low conductance (termed  $I_{\text{CRAC}}$ ), and (iv) are subjected to  $\text{Ca}^{2+}$ -dependent inactivation [382].

**Table 16: Yeast and human Ca<sup>2+</sup> channels acting in Ca<sup>2+</sup>/Mn<sup>2+</sup> homeostasis within the secretory pathway.** Yeast (Y) *Saccharomyces cerevisiae* and human (H) Ca<sup>2+</sup> channels belonging to the same family are orthologs. CRAC: Ca<sup>2+</sup> release-activated Ca<sup>2+</sup>, ER: endoplasmic reticulum, HACS: high-affinity Ca<sup>2+</sup> uptake system, LACS: low-affinity Ca<sup>2+</sup> uptake system, PM: plasma membrane, RIR-CAC: ryanodine-inositol-1, 3, 4-triphosphate receptor Ca<sup>2+</sup> channel, TRP: transient receptor potential, VGCC: voltage-gated Ca<sup>2+</sup> channels.

| Family  | Organism | Proteine name                | Function                 | Subcellular localization |
|---------|----------|------------------------------|--------------------------|--------------------------|
| CRAC    | H        | Orai1                        | Ca <sup>2+</sup> entry   | PM                       |
|         |          | STIM1                        |                          | ER, ER-to-PM junctions   |
| TRPC    | Y        | Yvc1p                        | Ca <sup>2+</sup> entry   | Vacuole                  |
| VGCC    | H        | Ca <sub>v</sub> 1.1-4        | Ca <sup>2+</sup> entry   | PM                       |
|         |          | Ca <sub>v</sub> 2.1-3        |                          |                          |
|         |          | Ca <sub>v</sub> 3.1-3        |                          |                          |
|         |          | α <sub>1</sub> subunits      |                          |                          |
| HACS    | Y        | α <sub>2</sub> δ1-4 subunits | Ca <sup>2+</sup> entry   | PM                       |
|         |          | β1-4 subunits                |                          |                          |
|         |          | γ 1-8 subunits               |                          |                          |
| LACS    | Y        | Cch1p (~ α <sub>1</sub> )    | Ca <sup>2+</sup> entry   | PM                       |
|         |          | Mid1p (~ α <sub>2</sub> δ)   |                          | PM                       |
|         |          | Ecm7p (~ γ)                  |                          | PM?                      |
| RIR-CAC | H        | IP <sub>3</sub> R            | Ca <sup>2+</sup> release | ER, cis-Golgi            |
|         |          | RyR                          |                          | ER, Golgi                |

CRAC channels are composed of two molecular key players: STromal Interaction Molecules (STIM) and Orai proteins. Since their initial identification in 2005 [383,384] and 2006 [385–388] by several unrelated groups, substantial works have been done to decipher the molecular and cellular mechanism driving the STIM-Orai interaction. Reviews on the subject can be read for additional information as I will only briefly exposed such mechanism without going into details: [266,382,389–395]. Basically, CRAC channels are part of the Store-Operated Ca<sup>2+</sup> (SOC) channels as they become activated when ER [Ca<sup>2+</sup>] are lower than its resting level of ~400μM. Physiologically, this occurs through the activation of Ca<sup>2+</sup> release signals involving either IP<sub>3</sub>R or RyR. Ca<sup>2+</sup> release from the ER is sensed by STIM1, driving its relocalization from the ER to ER-to-plasma membrane junctions where it interacts with the plasma membrane CRAC channel subunit Orai1. From this interaction, Orai1 opens what triggers Ca<sup>2+</sup> entry (Figure 25). Many regulators of either STIM1 or Orai1 exist, modulating the SOCE response. Some of them act by direct protein-protein interactions while other are biochemical compounds and will be further detailed in section 3.3.4. It is to note that post-translational modifications inherent to STIM1/Orai1 as well as spliced variants can also regulate STIM1/Orai1 interaction and subsequent function in SOCE.



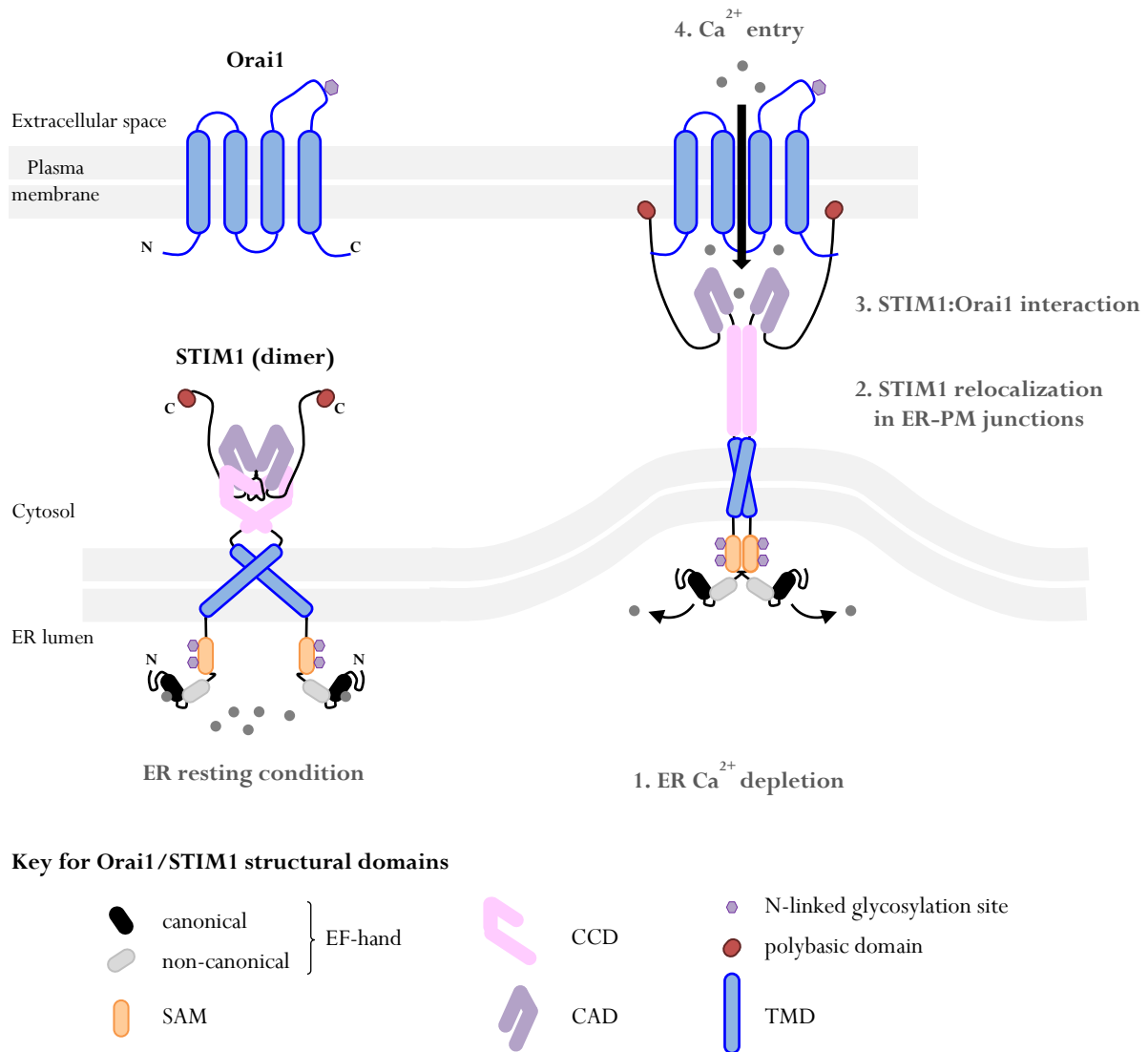


**Figure 25 : The CRAC channel STIM1/Orai1: structure and simplified mechanism of activation.** **Left.** Schematic representation of Orai1 and STIM1 highlighting their key structural domains. In this cartoon, STIM1 is shown as a dimer in resting conditions. **Right.** STIM1-Orai1 interaction following (1.) ER  $\text{Ca}^{2+}$  store depletion, (2.) STIM1 relocalization and (3.) Orai1 activation for subsequent (4.)  $\text{Ca}^{2+}$  entry. CAD: CRAC activation domain, CCD: coiled-coil domains, CRAC:  $\text{Ca}^{2+}$  release-activated  $\text{Ca}^{2+}$ , ER: endoplasmic reticulum, ER-PM: ER-to-plasma membrane, SAM: sterile  $\alpha$ -motif, TMD: transmembrane domain.

**STIM.** In mammalian cells, two isoforms of STIM are expressed, STIM1 and STIM2, sharing up to 60% identity. The STIM protein family also gathers splice variants for both STIM1 (STIM1L) and STIM2 (STIM 2.1 or STIM2 $\beta$ , STIM 2.2 or STIM2 $\alpha$ , STIM2.3). At the cellular level, STIM are predominantly expressed in the ER and can also be found in a lesser extend at the plasma membrane and in acidic compartments such as lysosomes. Of these multiple subcellular localizations, STIM proteins expressed in the ER have a role in the activation of CRAC channels by binding to Orai proteins in specific ER-to-plasma membrane junctions. Structurally, STIM1 and STIM2 share a similar organization with common features and domains. Basically, STIM proteins possess (i) a luminal amino-terminus including the  $\text{Ca}^{2+}$ -sensing region, (ii) a single TMD and (iii) a cytosolic carboxyl-terminus region containing the CRAC

activation domain (CAD, also known as STIM-Orai activation region (SOAR)). As depicted in Figure 25, the luminal part of STIM proteins possesses both a canonical and non-canonical EF-hand domain that are involved in  $\text{Ca}^{2+}$  binding and a sterile  $\alpha$ -motif (SAM) domain known to promote protein homo-/hetero-oligomerization. In this specific SAM domain, two N-linked glycosylation sites have been identified for STIM1 (N<sub>131</sub> and N<sub>171</sub>) while STIM2 only possesses one (N<sub>135</sub>). Another difference between STIM1 and STIM2 through this SAM region is the presence of additional non-polar residues for STIM2 increasing its stability in a  $\text{Ca}^{2+}$ -bound state. On the other hand, the cytosolic part contains three coiled-coil domains including CAD and at the very carboxyl-terminus, a lysine rich region defines the polybasic domain that interacts with the plasma membrane. Early studies led on STIM proteins first identified them as potential tumor growth suppressors. Later, STIM were identified as key players in  $\text{Ca}^{2+}$  signaling by two different groups through RNA interference screens in search for inhibitors of the thapsigargin-induced  $\text{Ca}^{2+}$  entry mediated by SOCs (also known SOCE) [383,384]. In mammalian cultured cells knockdown for *STIM1*, SOCE was suppressed and current associate to CRAC function ( $I_{\text{CRAC}}$ ) was no more detectable [383]. The later identification of Orai1 as the pore-forming unit of the CRAC channels then defined the STIM1:Orai1 interaction underlying the basis of the SOCE mechanism. Apart from Orai1, STIM1 also activates some channels belonging to the canonical transient receptor potential (TRPC) family such as TRPC1 [396–398]. STIM1 activity can be regulated by post-translational modifications such as N-linked glycosylation and phosphorylation [399–401]. Mutations of the N-linked glycosylation sites in STIM1 can result in either an increase or a decrease in SOCE, likely due to mis-oligomerization of the protein [402]. With regards to its phosphorylation status, STIM1 has been suggested to be phosphorylated during mitosis [401,403]. This phosphorylation step prevents its relocalization from the ER to ER-to-plasma membrane junctions suppressing SOCE during mitosis. In particular, Smyth et al. identified two “mitosis-specific” phosphorylation sites, S<sub>486</sub> and S<sub>668</sub>, that rescue mitotic SOCE when mutated into alanine [401].

**Orai.** In the human genome, three Orai homologs have been identified Orai1-3 also known as CRAC modulators 1-3 (CRACM1-3). Of them, Orai1 is the most studied and best-characterized protein originally characterized by similarities with the unique Orai protein from *Drosophila* (dOrai). Structurally, Orai1 contains four transmembrane domains and intracellular amino- and carboxyl-termini (Figure 25). In human, the Orai1 story began in early 1990s when several individuals presented with severe combined immunodeficiency (SCID), linked to defective SOCE response and CRAC channel activity [404]. Although SCID patients’ T cells express normal and functional levels of STIM1, this was not sufficient to mediate CRAC activation, suggesting that other components may contribute to the SOCE mechanism. Further investigations led by Feske et al. identified that patients suffering from SCID

were homozygous for a single missense mutation in Orai1 (substitution of arginine 91 by tryptophan, R91W) [405]. This specific mutation has been shown responsible for the inactivation of the CRAC channels since transformation of patients' T cells with wild-type *ORAI1* rescued both SOCE and the CRAC current ( $I_{\text{CRAC}}$ ) [405]. Additional knockdown and overexpression experiments in either *Drosophila* S2 cells or mammalian cells (HEK293 and Jurkat) further characterized the involvement of Orai1 in the SOCE response [386]. While a knockdown completely inhibits  $I_{\text{CRAC}}$ , *ORAI1* overexpression with *STIM1* increases this current up to 100 times. It is to note that the solely overexpression of *ORAI1* is not sufficient to enhance  $I_{\text{CRAC}}$  in either HEK293 or Jurkat cells [386]. Hence, Orai1 contributes to CRAC activation but is not sufficient in itself to increase the SOCE response. It has even been shown that overexpression of Orai1 alone tend to reduce rather than enhance the SOCE [406]. This was explained by the unbalanced stoichiometry between Orai1 and STIM1, leading to reduce STIM1-Orai1 interactions. While further investigating STIM1:Orai1 stoichiometry, CRAC channels were first thought to act as tetramers of Orai1 subunits each bound to two STIM1 (or a STIM1 dimer) [406]. However, since the crystal structure of dOrai1 revealed a hexameric organization for the *Drosophila* CRAC channel [407], human CRAC channels were also supposed to be hexamers of Orai1 subunits. This is further discussed by Yen and Lewis in a quite recent review [393]. Despite this specific homomeric rearrangement, Orai1 is also known to form heteromultimers with Orai3 leading to specific STIM1-dependent  $\text{Ca}^{2+}$  channels regulated by either arachidonic acid (ARC channels) or leukotriene  $\text{C}_4$  (LRC channels) [408]. It is to note that even STIM1-dependent, these latter channels are store-independent  $\text{Ca}^{2+}$  channels. In other cases, Orai1 activation can be mediated by either SPCA1 or SPCA2 leading to store-independent  $\text{Ca}^{2+}$  entry (SICE) [244,245,409,410]. This will be further detailed in section 3.3.4., being a kind of specific regulation of Orai1 by other proteins than STIM1. Another way of regulating Orai1 activity passes through post-translational modifications such as N-linked glycosylation. Orai1 possesses a unique N-linked glycosylated site ( $\text{N}_{223}$ ) that has been shown to be differentially glycosylated according to cell-type [411]. Dörr *et al.* indeed demonstrated that depending on its glycosylation status, Orai1 influenced the SOCE response. For instance, mutation of Orai1  $\text{N}_{223}$  enhanced the SOCE response in mammalian Jurkat cells while it failed to alter either SOCE or  $I_{\text{CRAC}}$  in mammalian HEK293 cells. It was suggested that in Jurkat T cells as well as in SCID patients' T cells, Orai1 glycosylation could have an inhibitory effect on the SOCE [411]. Extend to other diseases such as cancers and immune disorders, it was hypothesized that Orai1 glycosylation may contribute to their pathophysiological  $\text{Ca}^{2+}$  signaling.

In yeast, contrary to mammalian cells, the main  $\text{Ca}^{2+}$  storage organelle is the vacuole and not the ER (Figure 19). While looking for such SOCE-like process in yeast, it appears that  $\text{Ca}^{2+}$  depletion from the

vacuole did not trigger a  $\text{Ca}^{2+}$  influx response [412]. Indeed, yeasts lacking both vacuolar  $\text{Ca}^{2+}$  transporters Pmc1p and Vcx1p are depleted of vacuolar  $\text{Ca}^{2+}$  and yet do not exhibit higher  $\text{Ca}^{2+}$  influx rates at the plasma membrane [298]. Actually, a SOCE-like mechanism has been proposed in response to  $\text{Ca}^{2+}$  depletion from the ER and/or the Golgi apparatus in yeast lacking Pmr1p which implied the activation of a high-affinity  $\text{Ca}^{2+}$  uptake system homologous to the mammalian voltage-gated  $\text{Ca}^{2+}$  channels (VGCC) rather than a SOCE component ortholog [413].

### 2.3.3. Transient Receptor Potential (TRP)

The transient receptor potential (TRP) channels superfamily defines non-selective cation channels acting as signal transducer by either altering membrane potential or intracellular  $\text{Ca}^{2+}$  levels. TRP channels are found expressed in a broad range of living organisms including yeasts and mammals [414,415]. The mammalian TRP superfamily can be divided into six families: (i) the canonical TRP (TRPC) family, (ii) the vanilloid TRP (TRPV) family, (iii) the melastatin TRP (TRPM) family, (iv) the ankyrin TRP (TRPA) family, (v) the polycystin TRP (TRPP) family and the (vi) the mucolipin TRP (TRPML) family. Of them, the first four families are gathered in group 1 and the two later constitute the group 2. Altogether, 28 mammalian TRP exist with only few of them known to transport either  $\text{Ca}^{2+}$  and/or  $\text{Mn}^{2+}$ : TRPC1/2, TRPML1/2 and TRPM7. Because of this huge diversity and poor ion selectivity in mammals, I will no longer describe these channels. In contrast, in the yeast *Saccharomyces cerevisiae*, only one member of the TRP family is expressed and will be further detailed.

**Yvc1p (yeast vacuolar conductance 1 protein).** To date, Yvc1p is the solely TRP member expressed in the yeast *Saccharomyces cerevisiae*. Encoded by the yeast vacuolar conductance (*YVCI*) gene, Yvc1p was first identified and cloned by Palmer et al. in 2001 [416]. Structurally, Yvc1p contains six TMD and both cytosolic amino- and carboxyl-termini [416–419]. Although its homology with mammalian TRP, Yvc1p is not expressed at the cell surface but rather and specifically into the vacuole [416–418]. Linking its function with Ca homeostasis, Yvc1p was described as a cation-selective channel able to conduct  $\text{Ca}^{2+}$ ,  $\text{Na}^+$  and  $\text{K}^+$ . Through patch-clamp experiments, Yvc1p has been shown to be activated by millimolar  $[\text{Ca}^{2+}]$  or by physiological  $[\text{Ca}^{2+}]_{\text{cytosol}}$  in the presence of the reducing agent dithiothreitol (DTT) [416]. Although no specific growth phenotype was associated with *YVCI* deletion, its overexpression results in  $\text{Ca}^{2+}$  sensitivity according to  $[\text{CaCl}_2]$  in the culture medium [417]. A year later, Denis and Cyert investigated the effect a hypertonic shock on  $\text{Ca}^{2+}$  signaling in yeast. Using a combination of single/double yeast mutants for *PMCI* and *VCX1*, they first showed (i) that cytosolic  $\text{Ca}^{2+}$  levels increased in response to hypertonic shocks and that (ii) this transient increase in  $[\text{Ca}^{2+}]_{\text{cytosol}}$  originate from the vacuole [417]. Because no other candidate than Yvc1p was known to effect vacuolar  $\text{Ca}^{2+}$  release, similar  $\text{Ca}^{2+}$  response to hypertonic shocks were performed in yeasts lacking Yvc1p or

overexpressing it. While *ycv1Δ* yeasts exhibit no significant increase in cytosolic  $\text{Ca}^{2+}$  levels, Yvc1p overexpression massively increases  $[\text{Ca}^{2+}]_{\text{cytosol}}$  in response to hyperosmolarity compare to the wild-type strain. These results combined to other from Denis and Cyert study demonstrated that Yvc1p mediates the  $\text{Ca}^{2+}$  release from the vacuole into the cytosol in response to hypertonic conditions [417]. In a later study, Zhou et al. described the mechanosensitivity of Yvc1p allowing the channel to open independently from  $\text{Ca}^{2+}$  activation [420]. Under hypertonic conditions, water is expelled from the cytosol and then from the vacuole causing an osmotic pressure across the vacuolar membrane. Its subsequent deformation activates Yvc1p through channel opening [420]. Lastly, in 2018, two additional studies led by Hamamoto et al. and Ruta et al., further investigated Yvc1p function and regulation using both *in vitro* and *in vivo* approaches [419,421]. Renamed TRPY1 for transient receptor potential yeast channel, they demonstrated that in addition to its mechanosensitivity, TRPY1 activity could be regulated by cytosolic  $\text{Ca}^{2+}$  and  $\text{Mn}^{2+}$  levels, by the presence of reducing agent in the cytosol (such as DTT or  $\beta$ -mercaptoethanol), by phosphatidylinositol-3-phostate and by luminal  $\text{Zn}^{2+}$  and  $\text{Ca}^{2+}$  levels. From these studies, TRPY1 was assumed to act in response to both external changes in osmolarity and oxidative stress. To the latter point, Ruta et al. showed that TRPY1 activity was enhanced by increased  $[\text{Mn}^{2+}]_{\text{cytosol}}$  [421]. All in all, TRPY1 is the solely yeast TRP channel able to modulate cytosolic  $\text{Ca}^{2+}$  levels through vacuolar  $\text{Ca}^{2+}$  release to maintain intracellular  $\text{Ca}^{2+}$  homeostasis.

#### 2.3.4. Voltage-Gated Calcium Channels (VGCC)

Voltage-gated  $\text{Ca}^{2+}$  channels (VGCC) are part of the Voltage-gated ions channels (VIC) family. First discovered in crustacean muscles by Fatt and Katz, VCGC play major roles in both physiological and pathophysiological cellular processes [422]. In mammals, voltage-activated  $\text{Ca}^{2+}$  currents were first identified in rabbit skeletal cells and then extend to all other excitable tissues. Basically, all VGCC are plasma membrane permeable channels for both  $\text{Na}^+$  and  $\text{Ca}^{2+}$  with a greater affinity for  $\text{Ca}^{2+}$  than for  $\text{Na}^+$ . Physiologically, they are found in a closed conformation but upon depolarization of the membrane potential, they become activated and share an opened conformation. Because  $\text{Ca}^{2+}$  levels are higher extracellularly than intracellularly, VGCC activation results in a  $\text{Ca}^{2+}$  influx that will contribute to several cellular processes such as muscular contraction, hormone secretion, or neurotransmitters release, according to cell specificity. Thanks to electrophysiological recordings, distinct characteristic were assigned to these voltage-activated  $\text{Ca}^{2+}$  currents depending on the membrane potentials needed to open channels. Hence, two major classes of VGCC were identified and classified as either low- or high-voltage-activated (LVA or HVA) channels. The LVA channels, also known as T-type channels, (i) have a small conductance, (ii) respond to small variations from the resting membrane potential and (iii) are rapidly inactivated. In contrast, HVA channels (i) display higher conductances, (ii) require stronger

depolarization of the membrane potential and (iii) can be differentially inactivated. Four types of HVA channels have been identified so far, named as L-type, N-type, R-type and P/Q-type and differing from each other according to pharmacology, kinetics and cellular distribution. It is to note that pharmacology contributes a lot in the identification and characterization of all of these  $\text{Ca}^{2+}$  channels [423–426]. Structurally and as depicted in Figure 26, VGCC are formed as a complex of five different components termed  $\alpha_1$ ,  $\alpha_2$ ,  $\delta$ ,  $\beta$  and  $\gamma$  [427,428]. Of them,  $\alpha_1$  constitute the pore-forming subunit of the channel responsible for its biophysical and pharmacological properties. These properties can be modified by the two main auxiliary subunits  $\alpha_2\delta$  (disulfides bonds between  $\alpha_2$  and  $\delta$ ) and  $\beta$ , involved in channel folding, driving their proper sorting to the cell surface.

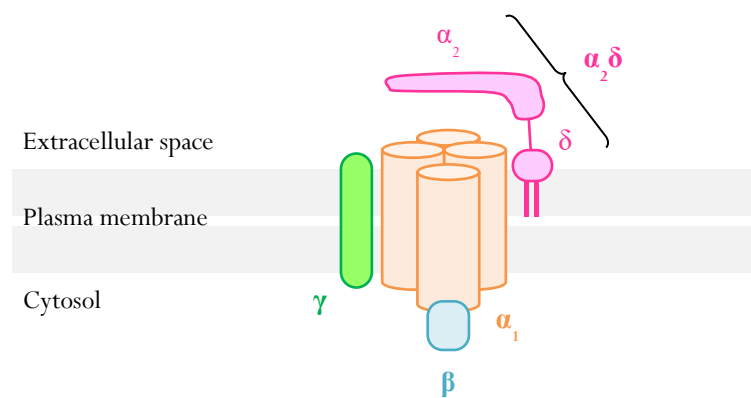


**Figure 26: Schematic representation of the mammalian VGCC.** Basically, mammalian VGCC share a similar structure made of five components:  $\alpha_1$ ,  $\alpha_2$ ,  $\delta$ ,  $\beta$  and  $\gamma$ .  $\alpha_1$ , the pore-forming subunit of the channel, contains four domains (I-IV, orange barrels) each composed of six transmembrane domains. One of the auxiliary subunits,  $\alpha_2\delta$  is formed by the covalent binding (disulfide bonds) between the highly glycosylated  $\alpha_2$  subunit and the GPI-anchored  $\delta$  protein. The last component of the mammalian VGCC, the  $\gamma$  subunit is expressed according to tissue specificity.

Of these three  $\alpha_1$ ,  $\alpha_2\delta$  and  $\beta$  subunits, many isoforms and spliced variants were further identified and characterized, massively increasing the number and functional diversity of the mammalian VGCC [423]. In particular, in the mammalian genome, ten separate genes (*CACNA1A-1* and *-5*) encode for  $\alpha_1$  proteins (Table 17), four separate genes (*CACNB1-4*) encode for  $\beta_{1-4}$  subunits and four other separate genes (*CACNA2D1-4*) encode for  $\alpha_2\delta_{1-4}$  subunits.

**Table 17: Classification of the mammalian VGCC.** In the « Proteins » column, both new and old nomenclatures are indicated. The old nomenclature is mentioned into brackets. HVA: high-voltage-activated and LVA: low-voltage-activated.

| Electrophysiology | Types | Genes          | Proteins                           |
|-------------------|-------|----------------|------------------------------------|
| HVA               | L     | <i>CACNA1S</i> | Ca <sub>v</sub> 1.1 ( $\alpha$ 1S) |
|                   |       | <i>CACNA1C</i> | Ca <sub>v</sub> 1.2 ( $\alpha$ 1C) |
|                   |       | <i>CACNA1D</i> | Ca <sub>v</sub> 1.3 ( $\alpha$ 1D) |
|                   |       | <i>CACNA1F</i> | Ca <sub>v</sub> 1.4 ( $\alpha$ 1F) |
|                   | P/Q   | <i>CACNA1A</i> | Ca <sub>v</sub> 2.1 ( $\alpha$ 1A) |
| LVA               | N     | <i>CACNA1B</i> | Ca <sub>v</sub> 2.2 ( $\alpha$ 1B) |
|                   | R     | <i>CACNA1E</i> | Ca <sub>v</sub> 2.3 ( $\alpha$ 1E) |
|                   | T     | <i>CACNA1G</i> | Ca <sub>v</sub> 3.1 ( $\alpha$ 1G) |
|                   |       | <i>CACNA1H</i> | Ca <sub>v</sub> 3.2 ( $\alpha$ 1H) |
|                   |       | <i>CACNA1I</i> | Ca <sub>v</sub> 3.3 ( $\alpha$ 1I) |

Association with the auxiliary subunits  $\alpha_2$ ,  $\delta$  and  $\beta$

Furthermore, according to cellular distribution, an additional  $\gamma$  subunit takes part in the structure of the VGCC. This has been shown true for skeletal VGCC but not for neuronal and cardiac Ca<sup>2+</sup> channels albeit several other  $\gamma$  subunits have been cloned. Facing this huge diversity of mammalian VGCC, I will not further describe them. To have a better understanding and a good overview on their discovery, pharmacology and role in both physiological and pathophysiological conditions, please refer to these reviews and references: [423,424,426,429].

As previously mentioned, in the yeast *Saccharomyces cerevisiae*, a plasma membrane Ca<sup>2+</sup> influx occurs in response to Ca<sup>2+</sup> depletion from the ER/Golgi apparatus that was originally underlined in *PMR1*-deficient yeasts exhibiting higher Ca<sup>2+</sup> influx rates and higher cytosolic Ca<sup>2+</sup> levels [413]. In this pioneer study, Locke et al. demonstrated the existence of a yeast SOCE-like mechanism to refill Ca<sup>2+</sup> stores within the secretory pathway through the activation of a high-affinity Mg<sup>2+</sup>-resistant Ca<sup>2+</sup> uptake system later known as high-affinity Ca<sup>2+</sup> uptake system (HACS) under low-Ca<sup>2+</sup> condition [413]. A screen for yeast mutants specifically defective in the HACS response revealed two genes: *CCH1* (calcium channel homolog 1) and *MID1* (mating pheromone-induced death), that were both previously identified in Ca<sup>2+</sup> influx response to mating pheromones [430,431]. *CCH1* or *MID1* single deletion in a *pmr1Δ* background specifically abolished Ca<sup>2+</sup> entry. This HACS inhibition was shown to be similar in the double mutant *cch1Δmid1Δ* suggesting that both Cch1p and Mid1p are required to act in the HACS response [413]. Further investigations pinpointed that both Cch1p and Mid1p were constitutively expressed at the plasma membrane where they physically interact to form the HACS or Cch1p/Mid1p channel. Hence, unlike mammalian SOCE that requires STIM1 re-localization from the ER to ER-to-plasma membrane

junction upon ER  $\text{Ca}^{2+}$  depletion, Cch1p/Mid1p stimulation after  $\text{Ca}^{2+}$  depletion of the secretory pathway may involve other regulatory processes than protein delocalization. In a search for additional subunits and regulators of Cch1p/Mid1p channel, Martin *et al.* identified *ECM7* (extracellular mutant) as a gene involved in  $\text{Ca}^{2+}$  entry after exposure to mating pheromone or tunicamycin, in the presence or absence of the calcineurin inhibitor FK506 [432]. *ECM7* deletion leads to similar phenotypes associated with *MID1* or *CCH1* deletions regarding  $\text{Ca}^{2+}$  entry in response to tunicamycin and mating pheromones and markedly reduces  $\text{Ca}^{2+}$  entry in yeast lacking calcineurin [432,433]. Albeit no direct evidence was provided to confirm a physical interaction between Cch1p, Mid1p and Ecm7p, Ecm7p was shown stabilized by Mid1p which is itself stabilized by Cch1p in non-stimulated cells [432]. Because Mid1p and Cch1p interact together [413], this result emphasized a physical interaction between the three proteins. Structurally, the Cch1p/Mid1p/Ecm7 channel is considered as the yeast homolog of the mammalian VGCC with homologous  $\alpha_1$ ,  $\alpha_2\delta$  and  $\gamma$  subunits, respectively. Indeed, Cch1p is a transmembrane protein that contains four repeated membrane domains each showing strong similarities with the  $\alpha_1$  subunit [413]. Mid1p is a plasma membrane N-glycoprotein similar to the  $\alpha_2\delta$  subunit [431]. Ecm7p is also a transmembrane protein sharing four transmembrane domains, a big extracellular loop and both cytosolic amino- and carboxyl-termini referring to the structural organization is of mammalian VGCC  $\gamma$  subunit [433]. It is to note that in addition to HACS, a low-affinity  $\text{Ca}^{2+}$  uptake system (LACS) also exists in yeast. Shown to be  $\text{Mg}^{2+}$ -sensitive, its molecular components still need to be better identified [413]. To date, the plasma membrane protein Fig1p (factor induced gene 1 protein) was proposed to be either the  $\text{Ca}^{2+}$  channel itself or its regulator since the protein facilitates both  $\text{Ca}^{2+}$  influx and cell-cell fusion step during mating [434,435]. Like Ecm7p, Fig1p contains four TMDs that are structurally similar to the  $\gamma$  subunit of mammalian VGCC. Altogether, the yeast *Saccharomyces cerevisiae* expresses a kind of VGCC that differs from mammalian one through its activation mechanism relying of  $\text{Ca}^{2+}$  store depletion that is associated to mammalian CRAC and TRP channels through the SOCE response [412].

#### 2.3.5. Ryanodine-Inositol-1,4,5-triphosphate Receptor $\text{Ca}^{2+}$ Channels (RIR-CAC)

The ryanodine-inositol-1, 4, 5-triphosphate ( $\text{IP}_3$ ) receptor  $\text{Ca}^{2+}$  channel (RIR-CaC) family comprises both ryanodine receptors (RyR) and  $\text{IP}_3$  receptors ( $\text{IP}_3\text{R}$ ), two mammalian  $\text{Ca}^{2+}$ -release channels of the SR/ER and the Golgi apparatus.

**$\text{IP}_3\text{R}$ .** Three isoforms  $\text{IP}_3\text{R}$  are encountered in mammalian cells, with  $\text{IP}_3\text{R1}$  being the most studied. First described in the SR/ER,  $\text{IP}_3\text{R}$  is also found in the Golgi apparatus where it acts as the major  $\text{Ca}^{2+}$ -release channel in non-excitable cells. Structurally,  $\text{IP}_3\text{R}$  and RyR share common features such as a tetramer organization and the presence of a large cytosolic loop where many regulatory partners can bind to modulate their function. Basically,  $\text{IP}_3\text{R}$  releases free  $\text{Ca}^{2+}$  from the SR/ER and Golgi lumens to



the cytosol following the recognition of its ligand, IP<sub>3</sub>. IP<sub>3</sub> is a second messenger originated from phosphatidylinositol diphosphate (PIP<sub>2</sub>) hydrolysis mediated by the phospholipase C through the activation of G-protein coupled receptors (GCPR). Several molecules interact directly or not with IP<sub>3</sub>R leading to its activation. For instance, ATP can enhance IP<sub>3</sub>-mediated Ca<sup>2+</sup> release from the ER by binding to a GCPR, triggering the production of IP<sub>3</sub> and increasing its binding to IP<sub>3</sub>R to enhance its Ca<sup>2+</sup> release activity. IP<sub>3</sub>R can also be activated by a thiol modification and was also shown to be phosphorylated [436].

**RyR.** In mammals, three RyR isoforms are expressed, RyR1-3, and shared a tissue specific expression pattern. While RyR1 and RyR2 are mainly expressed in skeletal and cardiac muscles, RyR3 is predominantly found in the thalamus, hippocampus, corpus striatum and smooth muscle. Hence, RyR are mainly expressed in excitable cells. At the cellular level, all three isoforms localized to the SR/ER and in some cisternae of the Golgi apparatus. Depending on [Ca<sup>2+</sup>]<sub>cytosol</sub>, RyR are either activated or inhibited. It has been established that when [Ca<sup>2+</sup>]<sub>cytosol</sub> is around 1μM, RyR is active and releases intracellular Ca<sup>2+</sup> to raise cytosolic Ca<sup>2+</sup> level. In contrast, when [Ca<sup>2+</sup>]<sub>cytosol</sub> is sufficient and reaches 1mM, RyR is inhibited [436]. Many proteins can bind to RyR, especially in its cytosolic loop, to regulate its function. This is the case of some Ca<sup>2+</sup>-binding proteins such as calmodulin, S100A and calsequestrin. In the latter case, calsequestrin modulates RyR in the ER lumen through its interaction with two additional proteins named junction and triadin. Cytosolic Ca<sup>2+</sup>, caffeine and ATP are also known to activate RyR while free Mg<sup>2+</sup> is a strong inhibitor of the channel, acting as a competitive Ca<sup>2+</sup> antagonist at a specific site of the protein (*A*-site) [436,437]. Together, mammalian RyR and IP<sub>3</sub>R act in concert to release Ca<sup>2+</sup> from the SR/ER and Golgi lumens in response and to spread Ca<sup>2+</sup> signaling.

In *Saccharomyces cerevisiae*, old studies identified an ER-localized transmembrane protein known as calcium sensitive growth protein 2 (Csg2p) involved in Ca<sup>2+</sup> sequestration in a non-vacuolar compartment, likely the ER [438–440]. Functionally, Csg2p primarily named Cls2p for calcium sensitive mutant protein 2 (i) confers Ca<sup>2+</sup> resistance, (ii) regulates Ca<sup>2+</sup> compartmentalization elsewhere than in the vacuole and (iii) contributes to enhance calcineurin activity. For such reasons, authors suggest a crucial function for Csg2p in regulating ER Ca<sup>2+</sup> level through a Ca<sup>2+</sup> efflux activity from the ER. Hence, albeit yeasts lack both SERCA and RIR-CaC orthologs, Csg2p was considered as the main ER Ca<sup>2+</sup> extruder. Further investigations then identified Csg2p as a Ca<sup>2+</sup>-binding protein involved in the synthesis of complex sphingolipids (mannosylinositol phosphorylceramide (MIPC)) being a regulatory unit of the MIPC synthase [441]. To date, no RyR and IP<sub>3</sub>R orthologs have been found in yeast, suggesting another way to release Ca<sup>2+</sup> from the intracellular compartments. In fact, when ER and Golgi [Ca<sup>2+</sup>] are higher than their resting concentrations (10μM and 300μM, respectively (Figure 19)),

$\text{Ca}^{2+}$  is thought to be removed *via* the secretory pathway. Hence, as in case of  $\text{Mn}^{2+}$  excess, the main mechanism to deeply reduce intracellular levels of  $\text{Ca}^{2+}$  and  $\text{Mn}^{2+}$  in yeast ER and Golgi lumens is exocytosis [442].

### 2.3.6. $\text{Ca}^{2+}/\text{Mn}^{2+}$ channel deficiencies and human related diseases

Commonly, human diseases related to ion channel deficiency/dysfunction are called channelopathies and can be due to either genetic or acquired factors [443]. Channelopathies are not restricted to  $\text{Ca}^{2+}$  channels and also affect potassium ( $\text{K}^+$ ), sodium ( $\text{Na}^+$ ), chloride ( $\text{Cl}^-$ ) and cholinergic channels, to list some. Consistent with their tissue distribution along the human body, a broad range of disorders have been reported resulting from ion channels deficiency encompassing myopathy, cardiac arrhythmia, epilepsy, migraine, deafness and blindness. Of interest in this manuscript, only human disorders due to deficiency in  $\text{Ca}^{2+}$  channels are listed in Table 18, only referring to those described previously.

**Table 18: List of human  $\text{Ca}^{2+}$  channelopathies.** This table gathers the main human related disorders associated with deficiencies in one of the  $\text{Ca}^{2+}$  channels cited in section 2.3. Only deficiencies linked to the different  $\alpha 1$  pore-forming subunits of human VGCC are mentioned in this table. Additional information about mutations in other VGCC subunits leading to human disorders can be found here [429]. CRAC:  $\text{Ca}^{2+}$  release-activated  $\text{Ca}^{2+}$ , OMIM: Online Mendelian Inheritance in Man, RIR-CAC: ryanodine-inositol-1, 4, 5-triphosphate receptor  $\text{Ca}^{2+}$  channel, VGCC: voltage-gated  $\text{Ca}^{2+}$  channels.

| Family         | Gene   | Human diseases                              | OMIM             |
|----------------|--|---|------------------|
| CRAC           | <i>ORAI1</i>   | Tubular aggregate myopathy 2                | 615883           |
|                |  | Immunodeficiency 9                          | 612782           |
|                | <i>STIM1</i>   | Tubular aggregate myopathy 1                | 160565           |
|                |  | Immunodeficiency 10<br>Stormorken syndrome  | 612783<br>185070 |
| VGCC           | <i>CACNA1A</i>   | Early infantile epileptic encephalopathy 42 | 617106           |
|                |  | Episodic ataxia type 2                      | 108500           |
|                |  | Familial hemiplegic migraine type 1         | 141500           |
|                |  | Spinocerebellar ataxia 6                    | 183086           |
| <i>CACNA1B</i> | Neurodevelopmental disorder with seizures and non-epileptic hyperkinetic movements | 618497                                      |                  |
| <i>CACNA1C</i> | Brugada syndrome 3   | 611875                                      |                  |
|                | Timothy syndrome   | 601005                                      |                  |
|                | Long QT syndrome 8   | 618447                                      |                  |
| <i>CACNA1D</i> | Primary aldosteronism, seizures, and neurologic abnormalities                      | 615474                                      |                  |
|                | Sinoatrial node dysfunction and deafness   | 614896                                      |                  |
| <i>CACNA1E</i> | Early infantile epileptic encephalopathy 69  | 618285                                      |                  |

|                |  |        |
|----------------|--|--------|
| <i>CACNA1F</i> | Aland Island eye disease   | 300600 |
|                | X-linked cone-rod dystrophy type 3   | 300476 |
|                | X-linked congenital stationary night blindness type 2A                           | 300071 |
| <i>CACNA1G</i> | Spinocerebellar ataxia 42  | 616795 |
|                | Early onset spinocerebellar ataxia 42 with neurodevelopmental deficits           | 618087 |
| <i>CACNA1H</i> | Susceptibility to childhood absence epilepsy type 6                              | 611942 |
|                | Familial hyperaldosteronism type IV  | 617127 |
| <i>CACNA1S</i> | Susceptibility to malignant hyperthermia 5                                       | 601887 |
|                | Susceptibility to thyrotoxic periodic paralysis 1                                | 170400 |
| <i>IP3R</i>    | Gillepsie syndrome   | 206700 |
|                | Spinocerebellar ataxia 15  | 606658 |
|                | Congenital non-progressive spinocerebellar ataxia 29                             | 117360 |
| <b>RIR-CAC</b> | Central core disease, congenital neuromuscular disease with uniform type 1 fiber | 117000 |
|                | King-Denborough syndrome   | 145600 |
|                | Minicore myopathy with external ophthalmoplegia                                  | 255320 |
| <i>RYR2</i>    | Arrhythmogenic right ventricular dysplasia 2                                     | 600996 |
|                | Ventricular tachycardia, catecholaminergic polymorphic 1                         | 604772 |

#### 2.4. Overview of $Mn^{2+}$ and $Ca^{2+}$ key transporters within the secretory pathway

Given the great diversity of biometals found in every living organisms [38], this manuscript only offered a small and narrowed overview on the regulation of two cation homeostasis ( $Ca^{2+}$  and  $Mn^{2+}$ ) in two organisms, human and yeast *Saccharomyces cerevisiae*. At the cellular level, this study only focuses on the secretory pathway (from ER to the plasma membrane) excluding other organelles such as mitochondria, nucleus or even the peroxisomes although they are also sites of many biological reactions requiring adequate ion homeostasis. As a summary from the three sections above (2.1., 2.2. and 2.3.), Figure 27 and Figure 28 replace the main human and yeast key players in  $Mn^{2+}$  and  $Ca^{2+}$  homeostasis along the secretory pathway. Apart from  $Ca^{2+}$  and  $Mn^{2+}$ , a plethora of other biometals are essential for cellular life including magnesium ( $Mg^{2+}$ ), iron ( $Fe^{2+}$ ), copper ( $Cu^{2+}$ ), zinc ( $Zn^{2+}$ ), nickel ( $Ni^{2+}$ ) and cobalt ( $Co^{2+}$ ) [38], whose homeostasis are also finely regulated by a set of pumps, transporters and channels. Nonetheless, according to physico-chemical properties, some biometals can behave very similarly to other and can either compete, be recognized and even replace them. This is the case for Mn and Fe that are both recognized by transferrin (Tf) and then internalized through the Tf receptor pathway.

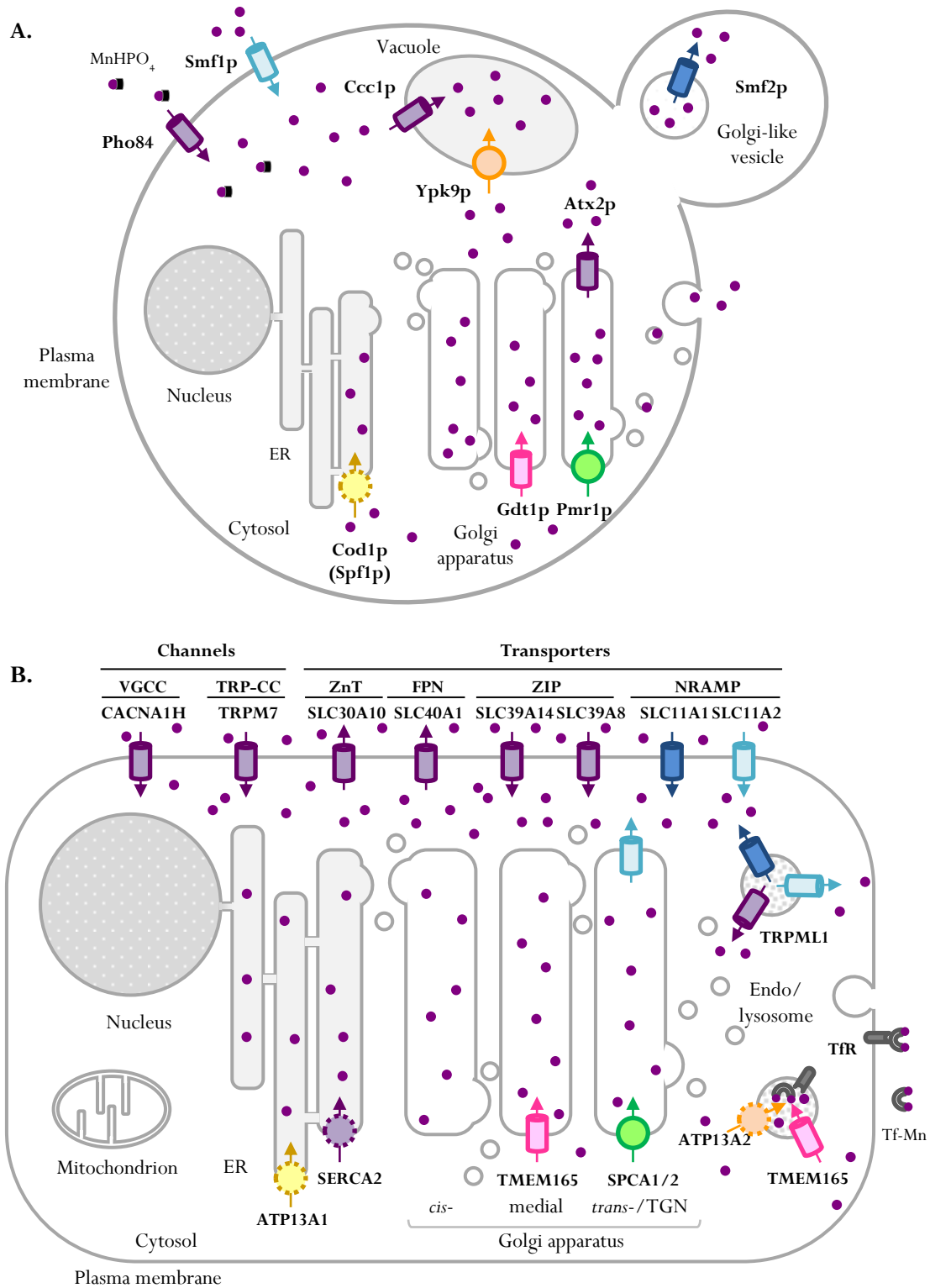


**Figure 27: Subcellular localization of the main actors involved in  $Mn^{2+}$  homeostasis in yeast (*Saccharomyces cerevisiae*) and humans.** Channels and transporters (symporters and/or antiporters) are represented by a barrel whereas a disc refers to P-ATPase pumps. Purple is the default color referring to any  $Mn^{2+}$  import or export. A similar color between yeast (A) and human (B) suggests that the two proteins are orthologs. Arrows indicate the direction of the flux (influx or efflux). Purple dots refer to free manganese ( $Mn^{2+}$ ) whereas bound manganese is explicited ( $MnHPO_4$  and  $Mn^{3+}$  bound to transferrin (Tf-Mn)). ER: endoplasmic reticulum, Tf: transferrin, TfR: transferrin receptor and TGN: *trans*-Golgi network.

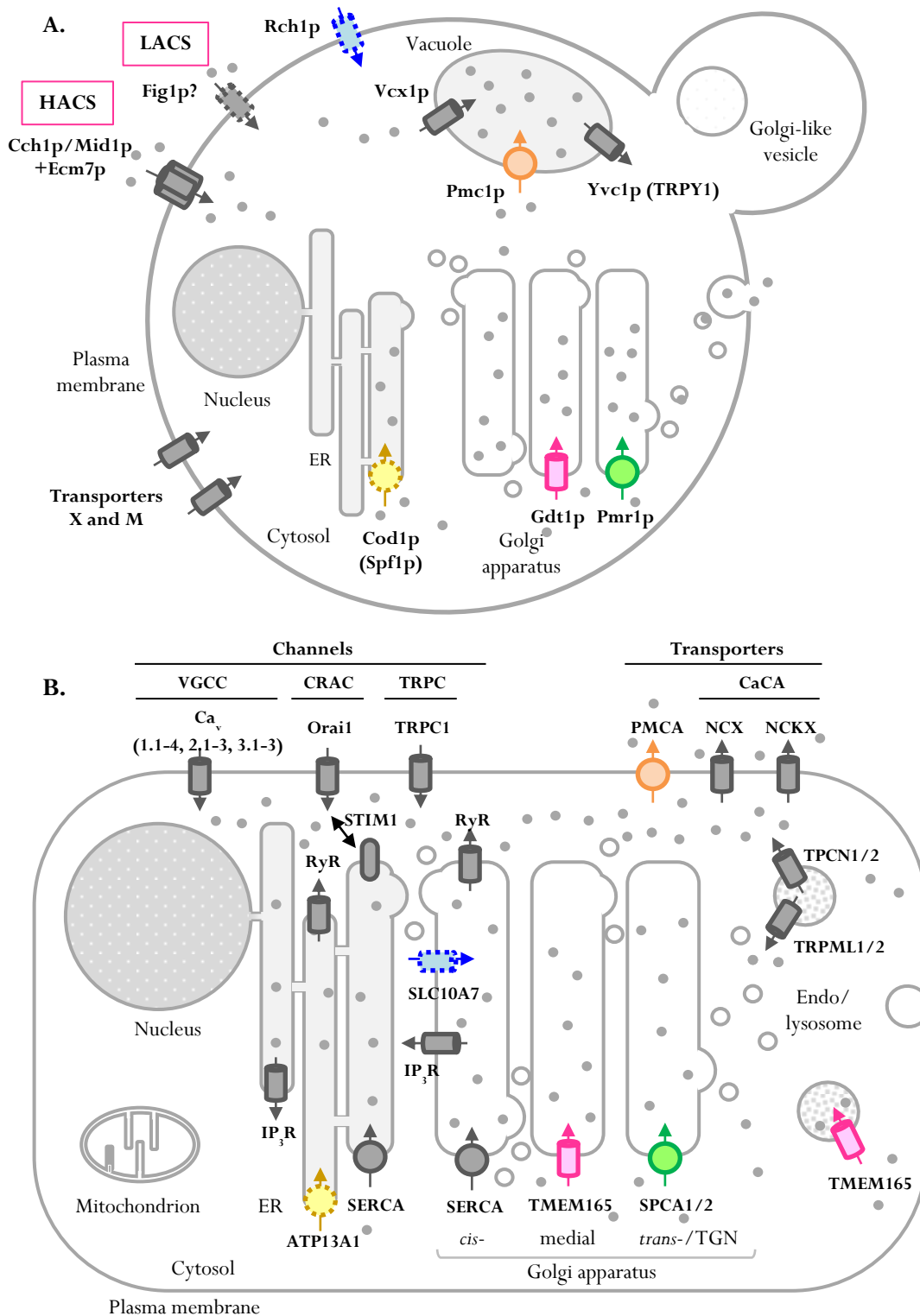


**Figure 28: Subcellular localization of the main actors involved in  $\text{Ca}^{2+}$  homeostasis in yeast (*Saccharomyces cerevisiae*) and humans.** Channels and transporters (symporters and/or antiporters) are represented by a barrel whereas a disc refers to P-ATPase pumps. Grey is the default color referring to any  $\text{Ca}^{2+}$  import or export. A similar color between yeast (A) and human (B) suggests that the two proteins are orthologs. Arrows indicate the direction of the flux (influx or efflux). Grey dots refer to free calcium ( $\text{Ca}^{2+}$ ). ER: endoplasmic reticulum, HACS: high affinity calcium uptake systems, LACS: low affinity calcium uptake systems and TGN: *trans*-Golgi network.

### 3. Intracellular Ca<sup>2+</sup> and Mn<sup>2+</sup> regulation

This section will deal with “regulation” of intracellular Ca<sup>2+</sup>/Mn<sup>2+</sup> transporters. To my mind and to clarify, talking about such regulation implies regulatory mechanisms leading to their degradation, stabilization, overexpression and/or re-localization in response to Ca<sup>2+</sup>/Mn<sup>2+</sup> deficiency or excess. *In fine*, these mechanisms serve to the proper expression and functionality of each actor involved in Ca<sup>2+</sup>/Mn<sup>2+</sup> homeostasis ensuring the maintenance of such homeostasis.

#### 3.1. Calcium binding proteins

Apart from active or passive transport, another way to regulate cellular Ca<sup>2+</sup> content lies in its ability to be bound to specific proteins so-called Ca<sup>2+</sup>-binding proteins (CBP). CBP can be found in the cytosol, in organellar lumens (Golgi apparatus, ER/SR, mitochondria) and also in extracellular spaces. Their main function within the organelles is to keep/retain Ca<sup>2+</sup> in the lumens to (i) ensure the Ca<sup>2+</sup> reservoir capacity of such compartments, (ii) act as Ca<sup>2+</sup> sensors and drive Ca<sup>2+</sup> uptake and release, (iii) contribute to cellular process by providing Ca<sup>2+</sup> and (iv) fulfill a proper function of chaperone for some of them. Within the secretory pathway, several human CBP have been identified in the SR/ER and the Golgi apparatus. To list some: (i) endoplasmic reticulum chaperone protein (BiP), glucose-regulated protein 94 (Grp94), protein disulfide isomerase (PDI), calreticulin and calnexin are Ca<sup>2+</sup>-dependent chaperones in the ER, (ii) calsequestrin acts as a SR luminal Ca<sup>2+</sup> sensor for skeletal or cardiac RyR through its interaction with the junction-triadin complex, and (iii) Ca<sup>2+</sup>-binding protein of 45kDa (Cab45), reticulocalbin, ER Ca<sup>2+</sup>-binding protein of 55kDa (ERC-55), crocalbin and calumenin define the CREC family of low-affinity CBP sharing multiple EF-hands [444,445]. Structurally, EF-hand domains consist of two  $\alpha$ -helices oriented perpendicularly to each other and separated by a loop where Ca<sup>2+</sup> or Mg<sup>2+</sup> can bind (helix-loop-helix). Besides the CREC family, other CBP possess EF-hand domains like calmodulin (CaM) and calcineurin, two cytosolic key components of the Ca<sup>2+</sup> signaling pathway and CALNUC, the second but most abundant CBP identified in the Golgi apparatus [18]. In contrast, additional proteins are defined as CBP with other Ca<sup>2+</sup> binding domains than EF hand, C2 domain for instance. A better overview on CBP function and structural features can be found in the following reviews: [266,444–446].

#### 3.2. Regulation of intracellular Ca<sup>2+</sup>/Mn<sup>2+</sup>-ATPases

A very recent review written by Chen et al. addressed some of the regulatory mechanisms assigned for each Ca<sup>2+</sup>/Mn<sup>2+</sup>-ATPase [30]. The following sections will resume few of them regarding to the modulation of PMCA, SERCA and SPCA activities, in humans (and yeast when applied). For additional and complementary information about such regulations, please referred to [29,30,222,263,447,448].

### 3.2.1. PMCA

- Protein-protein interactions

As already mentioned, PMCA's differ from SERCA's and SPCA's by the presence of numerous regulatory domains in their structural organization that modulate their activities (Figure 29) [259]. Of them and best characterized, a CaM-binding domain is found at the carboxyl-terminus and exerts an autoinhibitory control. In absence of CaM, PMCA's display a closed conformation also known as "autoinhibited state" resulting from the interaction between the CaM-binding domain and two cytosolic inhibitory regions (Figure 29). Such interaction blocks the ATP-binding site and dramatically lowers PMCA's affinity for  $\text{Ca}^{2+}$ . In contrast, upon elevation of  $[\text{Ca}^{2+}]_{\text{cytosol}}$ , CaM binds to free  $\text{Ca}^{2+}$  ( $\text{CaM-Ca}^{2+}$ ) and then interacts with the CaM-binding domain, which (i) relieves the autoinhibition and (ii) raises PMCA's  $\text{Ca}^{2+}$  affinity. According to PMCA isoforms,  $\text{CaM-Ca}^{2+}$  binds to its domain with a rather high or low affinity. For instance,  $\text{CaM-Ca}^{2+}$  binds with a 5 to 10-fold higher affinity to neuronal isoforms (PMCA2 and PMCA3) compared with the ubiquitous PMCA1 and PMCA4 [263].

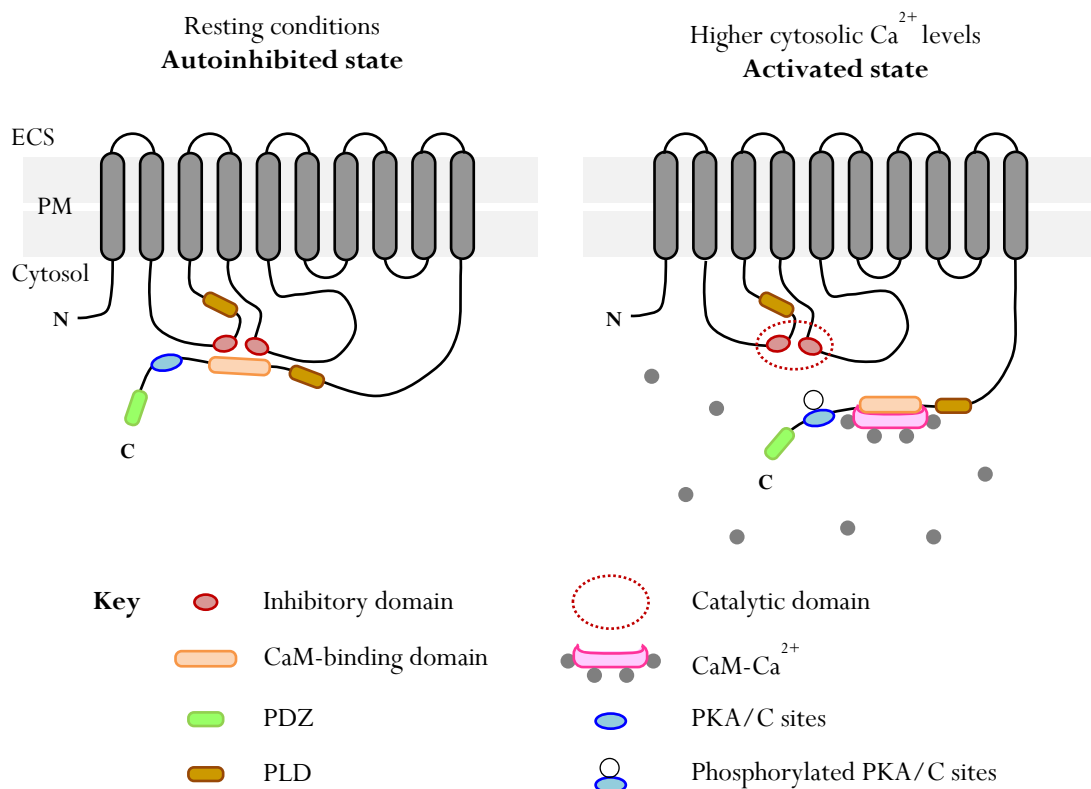


**Figure 29: Simplified representation of PMCA autoinhibited and activated states mediated by CaM-binding domain and elevation of cytosolic  $\text{Ca}^{2+}$  levels.** **Left.** At resting  $[\text{Ca}^{2+}]_{\text{cytosol}}$ , PMCA displays an autoinhibited state since CaM-binding domain interacts with two cytosolic inhibitory regions part of the catalytic domain preventing both  $\text{Ca}^{2+}$  binding and transport. **Right.** Upon elevation of  $[\text{Ca}^{2+}]_{\text{cytosol}}$ ,  $\text{Ca}^{2+}$ -CaM binds to the autoinhibitory CaM-binding domain which induces a conformational change releasing the catalytic domain and allowing  $\text{Ca}^{2+}$  transport. Additional regulatory domains are depicted in this cartoon such as two phospholipid-binding domains (PLD), a protein-protein binding domain (PDZ) and protein kinases (PKA/PKC) phosphorylation sites in the carboxyl-terminus.

Besides this CaM-binding domain, PMCAs mediate additional protein-protein interactions at their carboxyl-terminus thanks to a PDZ-binding domain (Figure 29). PDZ is an acronym referring the three first proteins sharing the domain: Post-Synaptic Density-95 (PSD95), Drosophila discs-large-1 tumor suppressor (Dlg) and Zonula Occludens-1 (ZO-1) [449]. Numerous PDZ proteins have been found directly bound to the PMCAs. Of them, proteins of the membrane-associated guanylate kinase (MAGK) family, the Ca<sup>2+</sup>/CaM-dependent serine protein kinase (CASK), the Na<sup>+</sup>/H<sup>+</sup> exchanger regulatory factor 2 (NHERF2) and the neuronal nitric oxide synthase (nNOS) [263–265]. Such PDZ-PMCA binding enables the protein to be specifically integrated into signaling complexes concentrated into microdomains like caveolae or lipid rafts. These interactions have been shown to be isoform specific and further discriminate between PMCA splice variants activity [264,265]. In addition to PDZ proteins, numerous other proteins have been shown to specifically interact with PMCA including: signaling and trafficking proteins (*e.g.* calcineurin A, syntaxin), scaffolding and cytoskeletal proteins (*e.g.* actin) and membrane receptors and sensors (*e.g.* STIM1). These protein-protein interactions between PMCAs and partners fine tune their activity according to isoforms' specificity and cell type by (i) modulating their affinity for Ca<sup>2+</sup>, CaM and ATP, (ii) relieving the autoinhibition state, (iii) lowering PMCAs number at the plasma membrane or (iv) altering their integration into signaling complexes [264].

- Protein-lipid interactions

Apart from protein-protein interaction, all PMCAs mediate protein-lipid interactions through two phospholipids binding sites: one before the third TMD and the second within the carboxyl-tail (Figure 29). Dating back to 1981, Niggli *et al.* first demonstrated that specific lipids were able to modulate PMCAs activity [450]. Several acidic phospholipids such as phosphatidylserine, phosphatidylinositol, and phosphatidic acid indeed stimulated PMCA activity by increasing its  $V_{max}$  and decreasing its  $K_M$  for Ca<sup>2+</sup>. Unsaturated fatty acids such as oleic and linoleic acid also shown similar stimulatory effect whereas zwitterionic ones (phosphatidylcholine, sphingomyelin and phosphatidylethanolamine) had no effect on these constants. In addition, the lipid environment surrounding PMCAs (*i.e.* composition of the plasma membrane or microdomains such as lipid rafts) also modulates their activities [30,222,450].

- Carboxyl-terminus

Post-translational modifications occurring in the carboxyl-region of PMCAs have also been shown to modulate their activity. More particularly, PMCAs are subjected to phosphorylation by two protein kinases, protein kinase A (PKA) and protein kinase C (PKC). PKA was first identified to phosphorylate a serine residue belonging to the CaM-binding domain of PMCA1 increasing its affinity for Ca<sup>2+</sup>. With regards to PKC, many groups confirmed the stimulation of PMCA under PKC phosphorylation but this



effect was shown to be isoform-dependent since phosphorylated sequences are not conserved between all PMCA protein variants [268]. Additional studies revealed that PMCA could also be phosphorylated by tyrosine kinase, enhancing their activity [451]. At least, PMCA activity can also be modulated by proteolytic cleavages ensured by two types of proteases: calpain and caspases [30,222].

### 3.2.2. SERCA

- Pharmacological SERCA inhibitors

To date, many pharmacological SERCA inhibitors have been identified ranging from vanadate oxoanions ( $\text{VO}_4^{3-}$ ) to small hydrophobic molecules. Originally, SERCA inhibitors were addressed to better characterize their mechanistic and kinetic properties. Years later, the use of inhibitors helped to determine the different conformational structures of the pumps that change according to the different states during the Post-Albers cycle (*i.e.* E1, E1~P, E2~P and E2; see Figure 22) [29,452,453]. Amongst all SERCA inhibitors that have been identified so far, most of them exert their inhibitory effect at very low concentrations ranging from micromolar to nanomolar [452]. Given the diversity of the inhibitory molecules and their high-affinity to bind the pump, only a limited number of binding sites exist and can overlap between different compounds. Of them, thapsigargin is the most widely used SERCA inhibitor. Thapsigargin is a plant-derived molecule extracted from *Thapsia garganica* that binds all mammalian SERCA proteins (SERCA1-3) in the same binding pocket defined by interactions between three TMDs: TMD3, TMD5 and TMD7. As a result, thapsigargin stabilizes SERCA pumps in the low  $\text{Ca}^{2+}$ -affinity E2 conformational state preventing  $\text{Ca}^{2+}$  transport activity. Although thapsigargin binds all mammalian SERCA proteins with a rather high affinity (nanomolar range), its inhibitory effect is slightly different according to protein variants. While SERCA1 is the most sensitive to thapsigargin ( $K_i = 0.2 \text{ nM}$ ), SERCA2 and SERCA3 share lowest affinities ( $K_i = 1 \text{ nM}$  and  $12 \text{ nM}$ , respectively) [452]. In addition, at these very low concentrations, thapsigargin was shown to only and specifically inhibit SERCA pumps since the other mammalian  $\text{Ca}^{2+}$ -ATPases PMCA and SPCA were not inhibited [29,452]. As second and third most widely used pharmacological SERCA inhibitors, cyclopiazonic acid (CPA) and 2,5-di(tert-butyl) hydroquinone (DBHQ) both bind specifically to SERCA pumps with lower affinity than thapsigargin. CPA is a mycotoxin produced by some strains of *Penicillium* and *Aspergillus* while DBHQ is a synthetic compound. Like thapsigargin, both molecules stabilize SERCA pumps in an E2-like conformational state. CPA and DBHQ share the same binding site that differs from that of thapsigargin since crystal structures of SERCA1 bound to both thapsigargin and DBHQ revealed two distinct binding pockets. CPA and DBHQ are assumed to bind at the cytosolic ends of TMD1-4, preventing the cytosolic  $\text{Ca}^{2+}$  access to the pumps [29,452]. As already mentioned, many of SERCA inhibitors have been

identified so far. Nowadays, in addition to serve the mechanistic and structural aspects of the pumps, the search for isoform-specific SERCA inhibitors is valuable as new therapeutic approaches in some diseases such as cancers. On the other hand, in some pathological conditions such as heart failure or diabetes, an altered function of the pumps has been reported. In these cases, SERCA activators could be of interest to stimulate SERCA activity up to physiological range [453].

- Protein-protein interactions

Apart from pharmacological inhibitors, all SERCA pumps are regulated by a family of small transmembrane proteins (STMP) that modulate their  $\text{Ca}^{2+}$  affinity by direct protein-protein interactions. Most of these STMPs interact with specific SERCA isoforms and often mirror they expression pattern. In Table 19, a list of the main STMPs is given, according to SERCA isoform specificity, tissue distribution and regulatory effect on SERCAs activity.

**Table 19: List of the main small transmembrane proteins (STMP) regulating SERCA pumps activity by direct binding.**

| STMP                         | SERCA isoform      | Tissue distribution   | Effect    |
|------------------------------|--------------------|---|-----------|
| <b>Phospholamban (PLN)</b>   | 1a, 2a, 2b         | Ventricular and atrial cardiac muscles, slow-twitch skeletal and smooth muscles |           |
| <b>Sarcolipin (SLN)</b>      |                    | Atrial cardiac and fast-twitch skeletal muscles                                 |           |
| <b>Myoregulin (MLN)</b>      | 1a, 2a             | Skeletal muscles  | Inhibitor |
| <b>Endoregulin (ELN)</b>     | 2b, 3a             | Endothelial and epithelial tissues, non muscle tissues                          |           |
| <b>Another-regulin (ALN)</b> |                    | Non muscle tissues  |           |
| <b>DWORF</b>                 | 1a, 2a, 2b, 3a, 3b | Cardiac and slow-twitch skeletal muscles  | Activator |

Briefly, phospholamban (PLN) was the first STMP identified to specifically inhibit SERCA2a activity [454]. PLN is a 52 amino acid protein that mirrors the expression pattern of SERCA2a, being mainly expressed in cardiac muscles (ventricular and atrial regions), slow-twitch skeletal muscles and smooth muscles. PLN directly binds on SERCA2a as a monomer resulting in a decrease of its apparent  $\text{Ca}^{2+}$  affinity. In addition, PLN has been shown to interact and inhibit the activities of other SERCA isoforms amongst SERCA1a, 2a and 2b. However, SERCA inhibition by PLN is reversible and can be relieved by phosphorylation of the protein or upon elevated cytosolic  $\text{Ca}^{2+}$  levels. A second STMP is sarcolipin (SLN), a structural and functional homolog of PLN acting in skeletal muscles rather than cardiac tissues. SLN interacts with SERCA isoforms at the same binding site that PLN resulting in a similar reduced  $\text{Ca}^{2+}$

affinity. This inhibition can also be relieved by SLN phosphorylation but not upon elevation of  $\text{Ca}^{2+}$  levels. Myoregulin (MLN), endoregulin (ELN) and another-regulin (ALN) are three other STMPs structurally related to PLN and SLN. All three proteins directly bind to SERCA isoforms, using the same site as PLN and SLN. MLN has been defined as a skeletal muscle specific regulator of both SERCA1a and 2a while ELN and ALN both follow the ubiquitous expression pattern of SERCA2b in non-muscle tissues in addition to that of SERCA3a in endothelial and epithelial tissues. As a last member of the STMPs, DWARF open reading frame (DWORF) is a specific one. Indeed, DWORF does not reduce SERCA apparent  $\text{Ca}^{2+}$  affinity but rather enhance it by displacing endogenous inhibitors such as PLN. For such reason, DWORF can be considered as a SERCA activator. Additional information about STMP can be found in the following recent review [221].

- Carboxyl-terminus

As already mentioned, in mammalian cells, three separate genes encode for three SERCA proteins named SERCA1-3. Additional splicing events yield the total number of SERCA pumps to more than ten (see 2.1.2.). Of them, the housekeeping SERCA2b particularly differs from all others in its carboxyl-terminus (C-tail). Comparing with SERCA2a isoform, SERCA2b exhibits a 49 amino acids extended C-tail forming an additional 11<sup>th</sup> TMD and a luminal extension [455]. This specific “2b-tail” confers unique biochemical properties to the pump such as a two-fold higher  $\text{Ca}^{2+}$  affinity and a two-fold lower turnover rate compared to SERCA2a [455]. Further investigations demonstrated that these properties were also given to SERCA1a when the 2b-tail was fused to protein, leading to the chimera SERCA1a2b [230]. It has been shown that these two structural features, the 11<sup>th</sup> TMD and the luminal extension, control themselves the apparent  $\text{Ca}^{2+}$  affinity of the pump by interacting with other structural motifs [230]. This 2b-tail is then a potent activator of SERCA pumps and could be a potential target to increase  $\text{Ca}^{2+}$  affinity of SERCA isoforms with altered function in some pathological conditions.

### 3.2.3. SPCAs/Pmr1p

- Protein-protein interactions

To date, SPCA1 and SPCA2 have been shown to both interact with Orai1, the plasma membrane CRAC channel, independently from depletion in intracellular  $\text{Ca}^{2+}$  stores or STIM1 relocalization. These specific SPCA-Orai1 couplings are part of the store-independent  $\text{Ca}^{2+}$  entry (SICE) pathway and were first demonstrated by Feng *et al.* for SPCA2-Orai1 in mammary tumors [409]. In such breast cancer context, SPCA2 was shown to be up-regulated and its absence significantly reduces both basal  $\text{Ca}^{2+}$  levels and tumorigenesis [409]. From these observations, authors have demonstrated that SPCA2 mediated the increased  $\text{Ca}^{2+}$  entry through its interaction with Orai1, without involving its own  $\text{Ca}^{2+}$

ATPase activity or depletion of ER  $\text{Ca}^{2+}$  stores. Instead, SPCA2 was shown to directly bind to Orai1 through its amino-terminus, rendering the two proteins close enough to allow an additional interaction of SPCA2 thanks to its carboxyl-terminus enabling Orai1 activation and  $\text{Ca}^{2+}$  entry (Figure 30) [409].

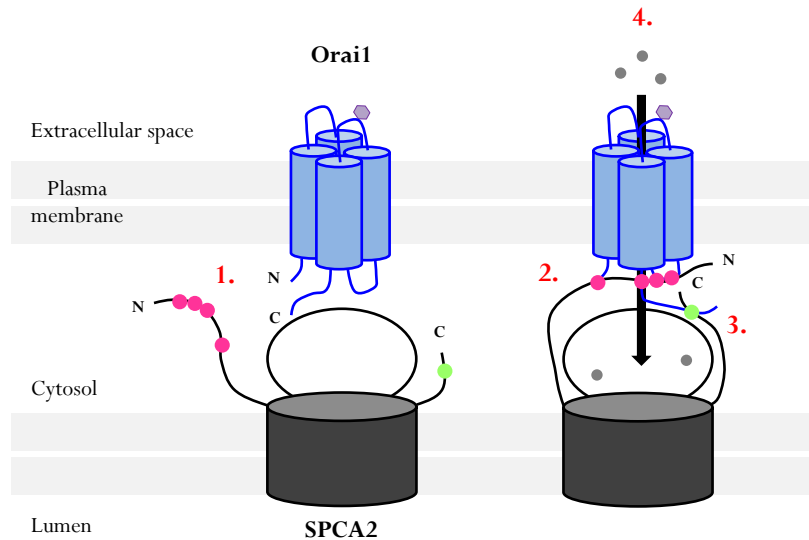


**Figure 30: Schematic representation of SPCA2-Orai1 interaction.** Four residues (pink circles) in the amino-terminus of SPCA2 are assumed to directly bind to cytosolic regions of Orai1 (1.). Once bound (2.), the interaction between Orai1 and the carboxyl-terminus of SPCA2 (3.; green circle) activates the channel, leading to  $\text{Ca}^{2+}$  entry (4.). The model is inspired by [448].

Later investigations then evaluated the physiological relevance of such interaction and confirmed this model in mouse mammary glands in lactation where SPCA2-Orai1 coupling promotes basolateral  $\text{Ca}^{2+}$  influx into the cells to support  $\text{Ca}^{2+}$  transport requirement for milk secretion [244]. In another study, Smaardjik *et al.* demonstrated that both SPCA2 amino- and carboxyl-termini directly interacting with Orai1 were also responsible for SPCA2 activation, enhancing its  $\text{Ca}^{2+}$  pumping activity into the Golgi apparatus [410]. This Orai1-mediated  $\text{Ca}^{2+}$ -influx and SPCA2-mediated  $\text{Ca}^{2+}$  uptake into the Golgi apparatus and/or the secretory pathway was even thought to possibly take place within microdomains [245]. Couple of years later, the same group identified that like SPCA2, SPCA1 could also interact with Orai1 to mediate a SICE response [410]. In addition, authors wondered whether this functional coupling between SPCA1 and Orai1 would be affected in Hailey-Hailey disease (HHD), the skin disorder resulting from SPCA1 haploinsufficiency. Amongst other things, they found that all of the tested HHD-mutations impaired the  $\text{Ca}^{2+}$  content of the non-ER stores while some of them only altered Orai1 activation or  $\text{Ca}^{2+}$  transport. Hence, this new SICE pathway might be affected in HHD.

Apart from binding Orai1, SPCA1 has been found to be activated by a couple of cytosolic proteins interacting with its phosphorylation domain in order to mediate the secretory cargo sorting at the TGN [456,457]. These two cytosolic proteins are the actin-depolymerizing factor (ADF) and the cofilin 1.

From this study, it has been shown that  $\text{Ca}^{2+}$  uptake into the TGN was mediated by ADF/cofilin 1 interaction with SPCA1 and that this SPCA1  $\text{Ca}^{2+}$  pumping activity was required for protein sorting and secretion since the knockdown of both ADF and cofilin1 resulted in (i) reduced  $\text{Ca}^{2+}$  import in the TGN and (ii) mis-sorting events [456]. In fact, part of the mechanism beyond this involved the  $\text{Ca}^{2+}$  binding protein Cab45. In response to the local increase of luminal  $\text{Ca}^{2+}$  mediated by SPCA1, Cab45 polymerizes and subsequently interacts with cargo molecules to ensure their secretion [457–459]. A simple representation of this mechanism is depicted in Figure 31, adapted from [457–459].

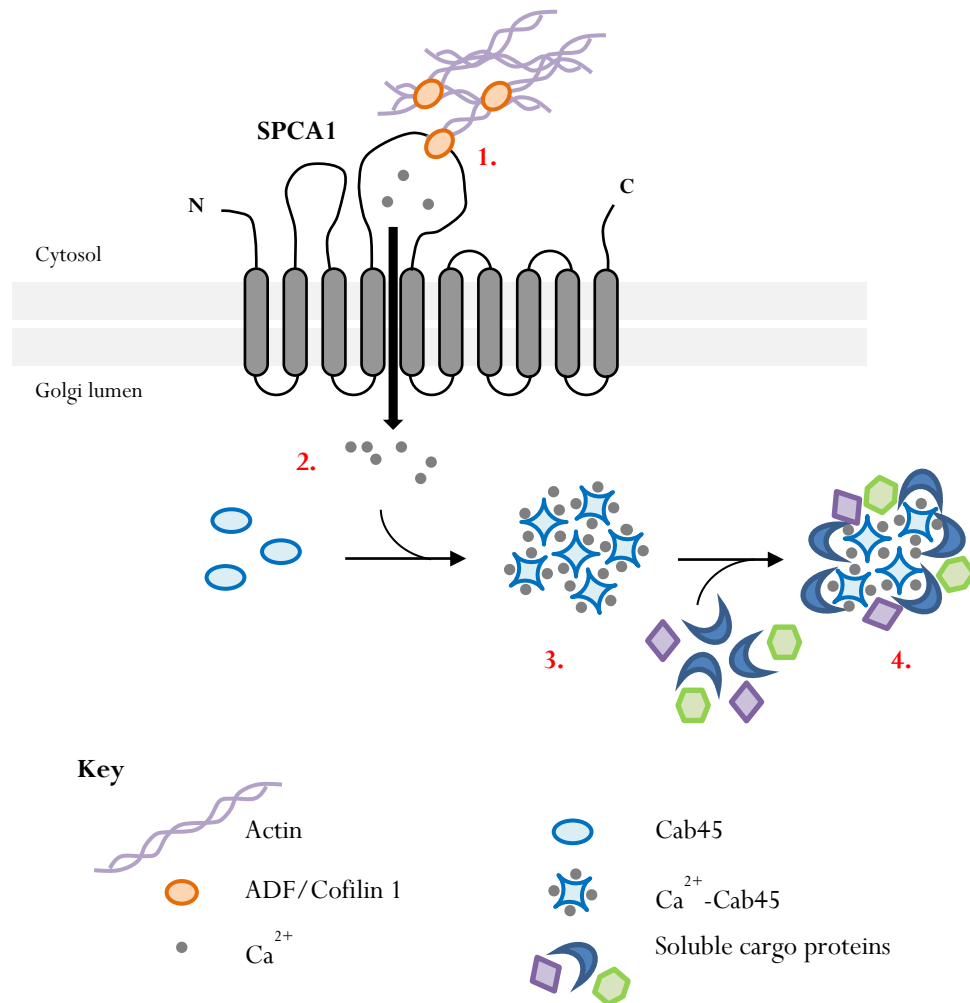


**Figure 31: Schematic representation of SPCA1 interaction with ADF/Cofilin 1 for subsequent Cab45-dependent sorting at the TGN.** Upon ADF/Cofilin 1 interaction, SPCA1 is activated and pumps  $\text{Ca}^{2+}$  into the TGN lumen (1.) inducing a transient  $\text{Ca}^{2+}$  increase (2.). This local  $\text{Ca}^{2+}$  elevation triggers the oligomerization of Cab45, a soluble  $\text{Ca}^{2+}$  binding protein (3.) which then binds to specific soluble cargo proteins (4.). These secretory cargoes are then sorted into vesicles while Cab45 remains in the Golgi apparatus to ensure new sorting cycles. Adapted from [457–459].

To add an extra-layer of complexity, the same group recently identified that SPCA1 activity was also sphingomyelin-dependent and that local lipid synthesis in the TGN could  $\text{Ca}^{2+}$  import in the TGN, driving protein sorting and secretion [460].

At last but not least, in our lab, we recently highlighted a functional link between SPCA1 and TMEM165. In both fibroblasts from HHD patients and in SPCA1 KO cell lines (HeLa and Hap1 cells), we clearly demonstrated that SPCA1 ion pumping activity governs the stability of TMEM165 [461,462]. This will be further discussed in the Result, Part II of this manuscript together with the comparison of such link between the yeast orthologs Pmr1p and Gdt1p, respectively [240].

- Amino- and carboxyl-termini

**Amino-terminus (N-ter).** Both yeast Pmr1p and human SPCA1 possess an EF-hand-like motif at their amino-terminus that has been shown to bind  $\text{Ca}^{2+}$  and modulate the  $\text{Ca}^{2+}$  transport activity of both proteins. This was well established for Pmr1p [463] and more recently proven for SPCA1 [464]. Shortly, twenty years ago, Wei et al. investigated the role of Pmr1p EF-hand-like motif and demonstrated its  $\text{Ca}^{2+}$  binding property that was shown to be lowered in excess of  $\text{Mn}^{2+}$  but unaffected in presence of  $\text{Mg}^{2+}$ . This first revealed that  $\text{Mn}^{2+}$  could compete with  $\text{Ca}^{2+}$  for binding. Second, the introduction of point mutations within the EF-hand-like domain at position 51 and 53 (two aspartic acid substituted by alanine, D51A and D53A), increased the apparent  $K_M$  for  $\text{Ca}^{2+}$  transport resulting in lower  $\text{Ca}^{2+}$  transport and affinity. In addition, D51A mutation reduces  $\text{Mn}^{2+}$  tolerance while D53A did not suggesting a higher  $\text{Mn}^{2+}$  pumping activity for Pmr1p carrying the D53A mutation. Altogether, these observations led to a model in which altered ion ( $\text{Ca}^{2+}$  or  $\text{Mn}^{2+}$ ) affinity at this N-terminal region result in subsequent changes in Pmr1p ion pumping activity:  $\text{Ca}^{2+}$  over  $\text{Mn}^{2+}$  or *vice versa* [463]. In human, two SPCA proteins exist, SPCA1 and SPCA2. Of them, only SPCA1 possesses an EF-hand-like motif. In a study comparing SPCA1a biochemical properties to that of SPCA2, specific differences in both  $\text{Ca}^{2+}/\text{Mn}^{2+}$  affinities and turnover rates were observed [464]. These differences between the two proteins were found to be partially dependent on the  $\text{Ca}^{2+}$ -binding EF-hand-like domain in SPCA1a amino-terminus that is absent in SPCA2 [464].

All in all, the amino-terminus of both Pmr1p and SPCA1a contains an EF-hand-like domain that seems to play a regulatory role in  $\text{Ca}^{2+}/\text{Mn}^{2+}$  ion selectivity and transport. With regards to SPCA2, instead an EF-hand-like motif, the corresponding sequence was found responsible for Orai1 binding [410]. Indeed, specific residues in the amino-terminus of SPCA2 were identified to coordinate the interaction with Orai1, ensuring a close proximity between the two proteins, required for Orai1 activation through a specific region of SPCA2 carboxyl-terminus (Figure 30) [245,409].

**Carboxyl-terminus (C-ter).** In humans, SPCA1 isoforms result from splicing events leading to the four protein variants SPCA1a-d. While SPCA1a, b and d are functional, SPCA1c is not. Each isoform differs from the other in their carboxyl-terminus sequence that is thought to be important for their own

functionality [246,247]. Many regulatory roles could be assigned to these carboxyl-termini such as sorting to reach a specific subcellular localization or specific protein interaction regulating Golgi cation homeostasis. So far, only human SPCA2 has been shown to contain specific binding domain at its carboxyl-terminus. A dileucine motif and putative PDZ binding domains were indeed reported to potentially drive the subcellular localization of the protein [448]. In addition, residues in the carboxyl-terminus of SPCA2 have been identified to specifically interact with Orai1, ensuring its activation leading to  $\text{Ca}^{2+}$  entry through the SICE pathway [245,409].

### 3.3. Regulation of intracellular $\text{Ca}^{2+}/\text{Mn}^{2+}$ transporters and some channels

#### 3.3.1. Regulation of the NRAMP family members

- Yeast Smf1p/Smf2p regulation upon changes in  $\text{Mn}^{2+}$  levels

As well established by Culotta and co-workers [332,336,465–468], in the yeast *Saccharomyces cerevisiae*, Smf1p and Smf2p are two  $\text{Mn}^{2+}$  transporters post-translationally regulated by Mn levels. To go deeper in this mechanism, three distinct conditions need to be defined: (i) “resting conditions” refers to laboratory conditions when yeast are grown in standard enriched or minimal medium containing sufficient Mn levels (around 1 and 5  $\mu\text{M}$ ) -Mn is available but does not reach toxic concentrations-, (ii) “manganese starvation” corresponds to yeast grown with  $[\text{MnCl}_2]$  in the culture medium below 1  $\mu\text{M}$ , leading to low Mn availability and (iii) “manganese excess” implies a condition in which yeast are grown upon toxic Mn levels.

As depicted in Figure 32 and Figure 33, Smf1p and Smf2p are subjected to relocalization or vacuolar degradation depending on changes in surrounding Mn levels. In resting conditions when Mn levels are sufficient, Smf1p and Smf2p are poorly expressed at the plasma membrane and the Golgi-like vesicles but continuously addressed to the vacuole for subsequent degradation by vacuolar proteases (Figure 32A and Figure 33, middle). This vacuolar targeting of Smf1p and Smf2p relies on Bsd2p activity and is summarized in Figure 32. Bsd2p was originally screened in the search for genes able to bypass SOD1 defect [469]. Mutations in *BSD2* result in higher Mn accumulation that was correlated with Smf1p and Smf2p overexpression since in yeast lacking Bsd2p, Smf1p and Smf2p failed to reach to vacuole [469]. Bsd2p is a transmembrane protein sharing multiple localizations within the secretory pathway (ER, prevacuolar compartments and vacuole) where it drives misfolded proteins to the vacuole for degradation. As described in Figure 32, Bsd2p only recognizes Smf1p when  $\text{Mn}^{2+}$  is sufficient suggesting that Smf1p interaction with  $\text{Mn}^{2+}$  may change its conformation. Once bound to Smf1p, Bsd2p recruits the E3 ubiquitin ligase Rsp5 to ubiquitinate Smf1p (Ub-Smf1p). This ubiquitin tag is then responsible for Smf1p targeting at the vacuole (Figure 32A) [332,466,467]. Since Smf1p and Smf2p are able to interact

with other toxic ions than  $Mn^{2+}$ , their vacuolar degradation may have a protective effect, limiting the influx of toxic ions that can be deleterious and engage cell survival.

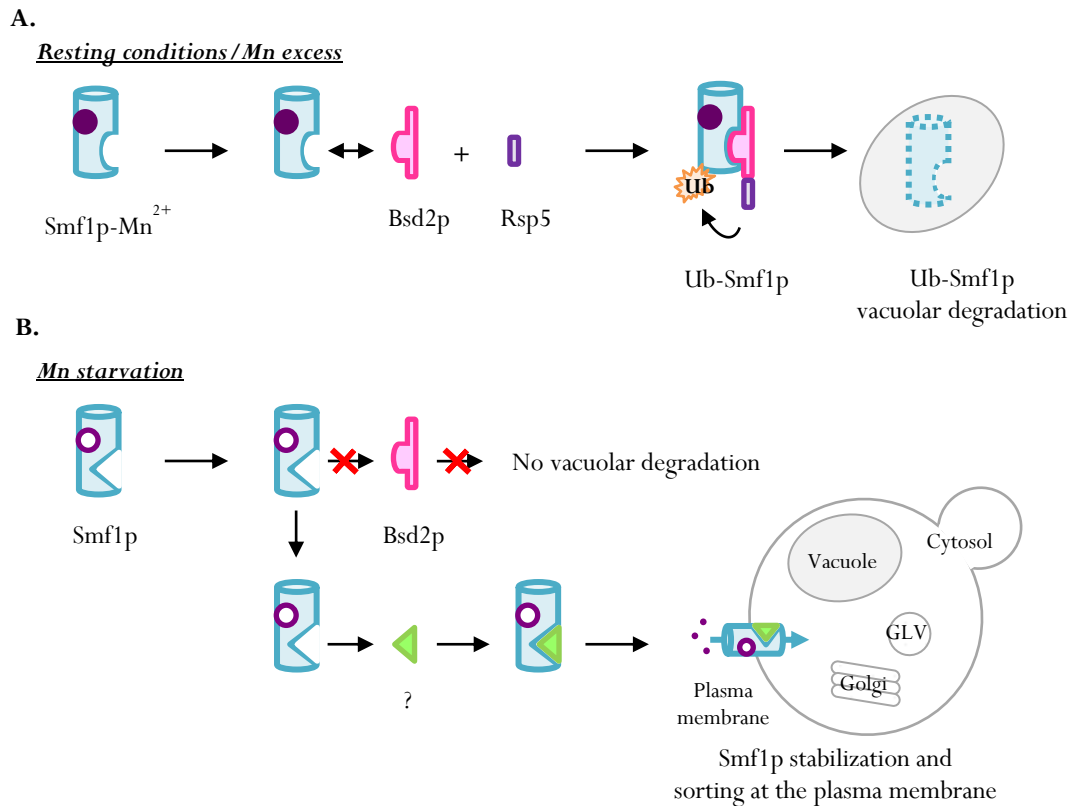


**Figure 32: Schematic representation of Smf1p regulation and relocalization mediated by changes in Mn levels (inspired by Culotta et al. [336]).** **A.** In resting conditions, when Mn availability is not limited, Smf1p is assumed to interact with  $Mn^{2+}$  and adopt a specific conformation (Smf1p- $Mn^{2+}$ ) that can be recognized by Bsd2p-dependent machinery. This recognition leads to Smf1p ubiquitination (Ub-Smf1p) through the activity of Rsp5, an E3 ubiquitin ligase. Ub-Smf1p is then targeted to the vacuole for subsequent degradation by vacuolar proteases and never reaches the plasma membrane. **B.** In case of Mn starvation, Smf1p does not likely interact with  $Mn^{2+}$  and exhibits a distinct conformation (Smf1p) that is not recognized by Bsd2p. Hence, Smf1p is not subjected to ubiquitination and no longer degraded because it fails to reach the vacuolar compartment. Instead, Smf1p may be recognized by other protein trafficking factor(s) (?) that may address the protein to the plasma membrane.

However, in case of Mn starvation, yeast has developed a mechanism by which Smf1p and Smf2p failed to reach to vacuole and are instead overexpressed at the plasma membrane (Smf1p) or in intracellular vesicles (Smf2p) (Figure 32 and Figure 33, left). Under low Mn availability, Smf1p is thought to adopt another conformation that is no more recognized by Bsd2p. Instead, another set of trafficking proteins seems to be required for Smf1p targeting at the plasma membrane (green triangle ?, Figure 32B). Hence, Smf1p is stabilized in case of Mn starvation due the shift in its subcellular localization from the vacuole to the plasma membrane [332,465–467]. Similar conclusions can be addressed for Smf2p with a relocalization from the vacuole to Golgi-like vesicles. Increasing the number of  $Mn^{2+}$  transporters in case of low Mn availability is supposed to promote  $Mn^{2+}$  uptake and its redistribution to ensure essential Mn-



dependent biological reactions. Similar mechanisms have also been reported in yeast starved for other biometals such as  $\text{Fe}^{2+}$ ,  $\text{Cu}^{2+}$  or  $\text{Zn}^{2+}$ . However, while mRNA levels of the corresponding transporters were upregulated, in case of Smf1p and Smf2p regulation by  $\text{Mn}^{2+}$ , the overexpression not likely occurs at the mRNA levels but take place post-translationally (Figure 32) [336].

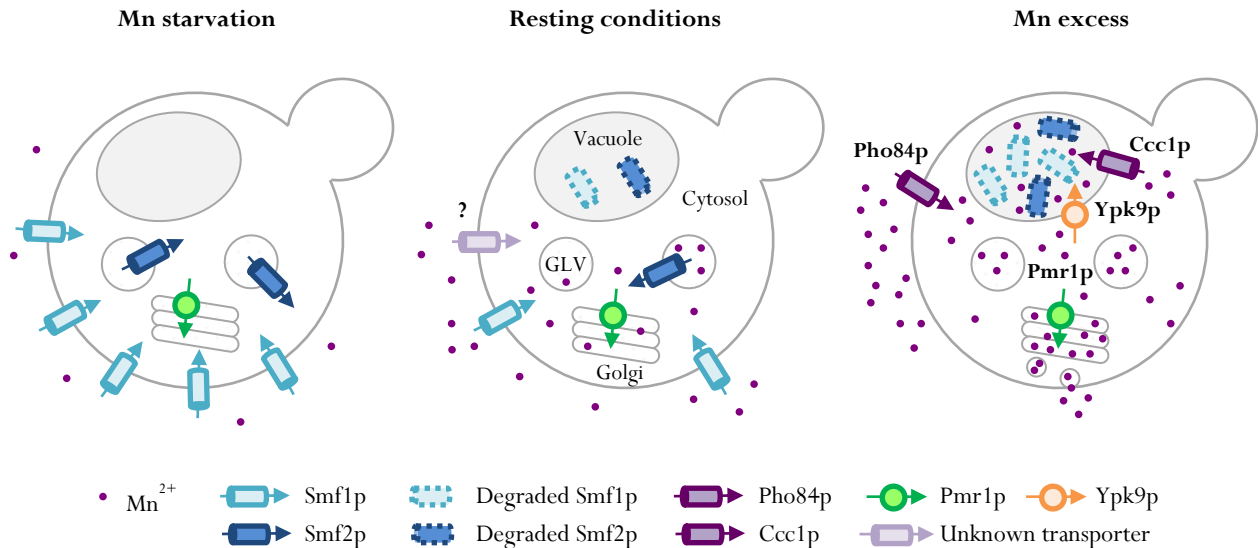


**Figure 33: Simplified overview of Smf1p and Smf2p localization and redistribution upon surrounding changes in Mn levels.** These three schemes illustrate the regulation of Smf1p and Smf2p in case of Mn starvation (low  $\text{Mn}^{2+}$  availability), resting conditions ( $\text{Mn}^{2+}$  sufficiency) and Mn excess (toxic  $\text{Mn}^{2+}$  levels). **Left.** When yeasts are starved for  $\text{Mn}^{2+}$ , Smf1p and Smf2p adopt a specific conformation allowing them to reach the plasma membrane and the Golgi-like vesicles (GLV) where they are overexpressed to promote Mn uptake for physiological requirements. **Middle.** In resting conditions, Smf1p and Smf2p are localized to the plasma and the GLV where they respectively mediate  $\text{Mn}^{2+}$  uptake and redistribution in the secretory pathway. Other undetermined transporters may take part in  $\text{Mn}^{2+}$  uptake at the cell surface (?) while  $\text{Mn}^{2+}$  redistribution in the secretory pathway is mainly achieved by Pmr1p at the Golgi level. It is to note that Smf1p and Smf2p are down-regulated comparing to « Mn starvation » condition in order to prevent from  $\text{Mn}^{2+}$  overload. **Right.** In case of Mn excess, while Smf1p and Smf2p are subjected to vacuolar degradation mediated by Bsd2p to prevent  $\text{Mn}^{2+}$  accumulation to toxic levels, Pho84p is mainly responsible for Mn entry ( $\text{MnHPO}_4$ ). In these conditions, (i) Pmr1p act in cytosolic  $\text{Mn}^{2+}$  detoxification by  $\text{Mn}^{2+}$  pumping in the Golgi and subsequent secretion *via* the secretory vesicles and (ii) both Ypk9p and Ccc1p sequester  $\text{Mn}^{2+}$  into the vacuole.

In the latter case of Mn excess leading to Mn cytotoxicity (Figure 33, right), Smf1p and Smf2p are subjected to vacuolar degradation to prevent Mn entry and intracellular accumulation to toxic levels. However, in such conditions, the low-affinity  $\text{Mn}^{2+}$  transporter Pho84p has been shown to be responsible for Mn entry placing it as the main  $\text{Mn}^{2+}$  transporter contributing to Mn cytotoxicity [377]. To avoid cell death in response to such increase in intracellular Mn levels, a detoxification pathway is needed. In yeast *Saccharomyces cerevisiae*, two main routes are known for Mn detoxification [174]. A first one involves Pmr1p  $\text{Mn}^{2+}$  pumping activity from the cytosol to the Golgi lumen to then be extruded from the cell *via* the secretory pathway and secretory vesicles. A second route for Mn detoxification lies in  $\text{Mn}^{2+}$  sequestration in the vacuole thanks to the transport activities of both Ccc1p and Ypk9p (Figure 33, right).

- DMT1 regulation in human cells

In mammals, DMT1 expression has been shown to be regulated by either (i) mRNA stabilization through the binding of Iron Regulatory Proteins (IRP) to the IRE domain [321] and/or (ii) protein degradation *via* the proteasomal pathway [470]. This latter involves an ubiquitination-dependent mechanism. In the case of DMT1, two different ubiquitin ligases (E3 ligases) are required: Parkin or E3 ligase from the neuronal precursor cell-expressed developmentally downregulated 4 (Nedd4) family which often use the additional accessory proteins referred as Nedd4 family interacting proteins 1 and 2 (Ndfip1-2) to ubiquitinate the targeted protein [471–473]. DMT1 proteasomal degradation was thought to occur in an isoform specific manner since Parkin only ensures the ubiquitination of DMT1-B and Nedd4/Ndfip1-2 was assumed to ubiquitinate DMT1 in the duodenum where the main expressed isoform is DMT1-AI [470]. In addition, two studies revealed contradictory conclusions about changes in DMT1 mRNA levels upon  $MnCl_2$  treatment. While in cultured choroidal (Z310) cells Wang *et al.* reported an increase in both mRNA levels and protein expression after 24h to 48h of  $MnCl_2$  exposure (100 -200 $\mu$ M) [474], Li *et al.* recently evidenced a decreased in DMT1 mRNA levels in Caco-2 cells following 800 $\mu$ M  $MnCl_2$  exposure for 2h [475]. Then two antagonist hypotheses may arise from these observations. First, upon  $MnCl_2$  exposure,  $Mn^{2+}$  may stabilize DMT1 mRNA by promoting IRP binding to the IRE domain. The subsequent increased in DMT1 protein expression would then facilitate  $Mn^{2+}$  transport across the blood brain barrier (BBB), which may contribute to Mn-induced neurodegenerative disease through Mn accumulation. In this case, such Mn-induced overexpression of DMT1 is against all biological relevance. Second and more likely, the down-regulation of DMT1 transcription in case of Mn excess would prevent  $Mn^{2+}$  uptake across the BBB and subsequently avoid its toxic accumulation. Comparing yeast and human NRAMP regulation, it appears that in both cases, an ubiquitination-dependent mechanism is involved for Smf1/2p and DMT1 degradations. Moreover, both yeast and human ortholog protein expressions are intimately linked to Mn/Fe levels driving mRNA or protein stabilization and/or degradation. Hence, it appears that a conserved regulation occurs in yeast and human NRAMP orthologs.

### 3.3.2. $Ca^{2+}$ regulation in yeast: calcineurin-dependent and independent pathways

- $Ca^{2+}$ -CaM/Calcineurin/Crz1p pathway

For a better and simple overview of this signaling pathway, please have a look on the review written by Espeso [442]. Here, I will only summarize the  $Ca^{2+}$ -CaM/Calcineurin/Crz1p pathway involving Pmc1p, Pmr1p, Vcx1p and Rch1p, previously described in the above sections. To contextualize, yeasts are subjected to diverse environmental conditions that can be seen as many stimuli impacting free cytosolic

Ca<sup>2+</sup> levels. If yeasts are able to grow upon extremely low to high external Ca<sup>2+</sup> levels, it is because they rapidly adapt to such variations. The signaling cascade involving Ca<sup>2+</sup>-CaM/Calcineurin/Crz1p pathway is part of their adaptation process and result in a transcriptional response to cope with excess of cytosolic Ca<sup>2+</sup> levels. These variations in [Ca<sup>2+</sup>]<sub>cytosol</sub> trigger the Ca<sup>2+</sup> signal that is then sensed, transduced and translated into a transcription factor named calcineurin-response zinc finger (Crz1p) through the CaM/calcineurin pathway.

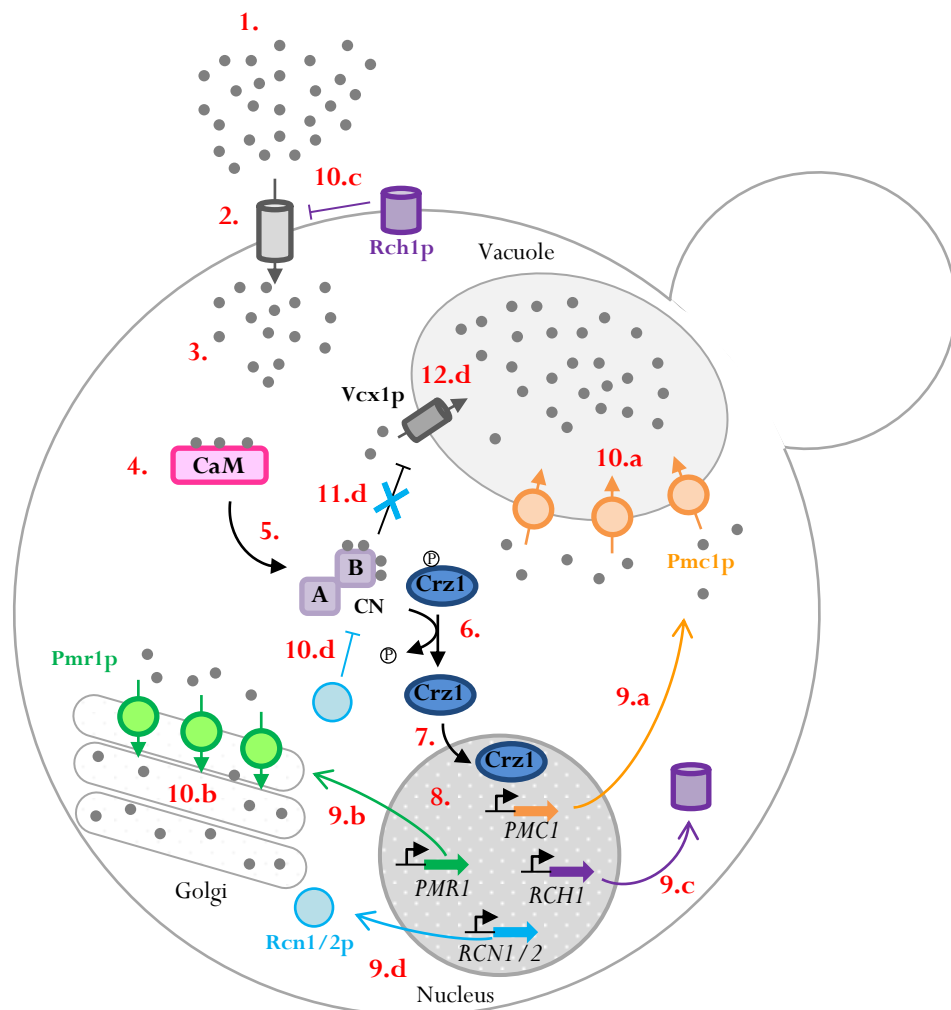


**Figure 34: Simplified illustration of the Ca<sup>2+</sup>-CaM/Calcineurin/Crz1p pathway involving Pmc1p, Pmr1p, Rch1p and Vcx1p.** Basically, **1.** upon elevation of extracellular Ca<sup>2+</sup> levels ([Ca<sup>2+</sup>]<sub>extracellular</sub>), **2.** Ca<sup>2+</sup> massively enters the cell leading to **3.** increase cytosolic Ca<sup>2+</sup> levels ([Ca<sup>2+</sup>]<sub>cytosol</sub>). **4.** Free Ca<sup>2+</sup> binds to calmodulin (CaM) which then **5.** activates calcineurin (CN). **6.** Subsequently, Crz1p is dephosphorylated by CN and **7.** sent to the nucleus where it binds to specific DNA sequence to regulate **8.** genes transcription. In response, **9.** Pmc1p, Pmr1p and Rch1p are up-regulated and addressed to **9.a.** the vacuole, **9.b.** the Golgi apparatus and **9.c.** the plasma membrane, respectively. In addition, **9.d.** CN regulators Rcn1/2p are also positively regulated by Crz1p leading to **10.d.** CN inhibition that **11.d.** relieves Vcx1p inhibition and **12.d.** rescues Vcx1p Ca<sup>2+</sup> pumping activity. **10.a.** Pmc1p and **10.b.** Pmr1p sequester cytosolic Ca<sup>2+</sup> into the vacuole and the Golgi lumen and **10.c.** Rch1p negatively regulates Ca<sup>2+</sup> entry to lower [Ca<sup>2+</sup>]<sub>cytosol</sub>.

The main purpose of this regulatory pathway is to lower  $[Ca^{2+}]_{\text{cytosol}}$  via a transcriptional response providing (i) higher number of intracellular transporters dissipating the excess of cytosolic  $Ca^{2+}$  into the vacuole or the Golgi lumens and (ii) regulators to modulate the signaling cascade (Figure 34). Briefly and as depicted in Figure 34, upon elevation of external  $[Ca^{2+}]$ , a massive  $Ca^{2+}$  entry occurs, increasing  $[Ca^{2+}]_{\text{cytosolic}}$ . In response to such excess of cytosolic  $Ca^{2+}$ , free  $Ca^{2+}$  binds to the cytosolic CBP calmodulin (CaM or Cmd1p in yeast) that then activates the serine/threonine phosphatase calcineurin. Calcineurin is also a cytosolic protein that binds  $Ca^{2+}$  in its regulatory subunit (subunit B) while exerting a phosphatase activity through its catalytic subunit (subunit A). In response to  $Ca^{2+}$ -CaM activation, calcineurin dephosphorylates the Crz1p transcription factor that is consequently sent to the nucleus. Once in the nucleus, Crz1p binds to specific DNA sequences named CDRE for calcineurin-dependent regulatory elements and positively/negatively modulates gene transcription subjected to this regulation. Amongst them, *PMR1*, *PMC1* and *RCH1* are transcriptionally up-regulated leading to an increase in the encoded proteins expression. While Pmr1p and Pmc1p activities would contribute to dissipate excess of cytosolic  $Ca^{2+}$  into the Golgi apparatus and the vacuole, Rch1p would prevent  $Ca^{2+}$  entry by a negative feedback regulation. In addition, Crz1p indirectly impacts calcineurin activity through the transcription and translation of regulator of calcineurin (*RCN1/2*) genes. One of the main purposes of such calcineurin inhibition is to relieve its inhibitory effect exerted on the vacuolar  $Ca^{2+}/H^+$  transporter Vcx1p to enhance the  $Ca^{2+}$  sequestration in the vacuole together with Pmc1p activity.

- $Mg^{2+}$ -sensitive  $Ca^{2+}$  influx pathway.

In response to  $[Ca^{2+}]_{\text{external}}$  elevation, free cytosolic  $Ca^{2+}$  increases and predominantly binds to CaM to ensure the previously described calcineurin-dependent signaling cascade (Figure 34). However, the rapidity of such calcineurin feedback on Pmr1p and Pmc1p expressions appeared not to be physiologic during the first minutes following the  $Ca^{2+}$  burst, suggesting another calcineurin-independent pathway to inhibit/limit  $Ca^{2+}$  influx [476]. By means of single to multiple deletions of genes encoding proteins involved in  $Ca^{2+}$  regulation (*i.e.* *PMC1*, *PMR1*, *VXC1*, *CNBI*, *YVC1*, *MID1* and *CCH1*) Cui et al. demonstrated that extracellular  $Mg^{2+}$  increased  $IC_{50}$  for  $CaCl_2$  associated to single to all gene deletions [476]. Hence,  $Mg^{2+}$  suppresses  $Ca^{2+}$  toxicity independently from all known  $Ca^{2+}$  transporters (Pmc1p, Pmr1p, Vcx1p, Yvc1p and Mid1p/Cch1p) suggesting that  $Mg^{2+}$  could inhibit additional and unknown  $Ca^{2+}$  influx pathways at the plasma membrane [476]. Combining these experimental data to a mathematical model of  $Ca^{2+}$  entry and sequestration in which Pmc1p, Pmr1p and Vcx1p are not subjected to calcineurin feedback, two  $Mg^{2+}$ -sensitive  $Ca^{2+}$  influx transporters have been identified, named transporter X and transporter M. While both of them contribute to  $Ca^{2+}$  entry, in case of high  $[Mg^{2+}]_{\text{extracellular}}$ , transporter X is dispensable. In addition, transporter M was described as a low affinity

Ca<sup>2+</sup> transporter competitively inhibited by extracellular MgCl<sub>2</sub> levels [476]. It is to note that this model is only valid for short periods (up to 3 minutes) after Ca<sup>2+</sup> burst and voluntarily omits CaM/calcineurin feedback. Further experimental data are needed to confirm such model.

### 3.3.3. Mn-induced degradation of Mn<sup>2+</sup> transporters

- TMEM165/Gdt1p from the UPF0016 family

Widely investigated by our group and collaborators, we have demonstrated that both TMEM165 and Gdt1p were specifically degraded upon high Mn<sup>2+</sup> exposure [65,307,477]. The mechanism of such degradation in yeast still needs to be elucidated. However, in human cultured cell lines, Mn-induced TMEM165 degradation is better understood and will be further described in Chapter 3.

- SLC39A14 from the ZIP family

As described before, SLC39A14 is mainly expressed in liver where its biological function is to ensure Mn<sup>2+</sup> import in hepatocytes for subsequent biliary excretion. In a recent study using a human-derived and polarized hepatocytoma cell line named HepaRG, authors characterized Mn uptake in hepatocytes and looked for SLC39A14 contribution [478]. While <sup>54</sup>Mn uptake was shown to be time- and temperature-dependent, a reduced Mn uptake after Mn exposure (50μM for 4h and 16h) was also evidenced. This loss of Mn transport activity was emphasized to be correlated with a decrease in SLC39A4 protein expression. SLC39A14 expression was indeed shown to be specifically decreased upon MnCl<sub>2</sub> treatment in a dose-dependent manner while other hepatocyte Mn transporters (*i.e.* SLC39A8, SLC30A10 and SLC40A1) protein expression remained stable. Moreover and similarly to TMEM165, the observed Mn-induced degradation of SLC39A14 addresses the protein to the endo/lysosomal compartment since bafilomycin A1 treatment (i) blocks the phenomenon and (ii) increases SLC39A14 expression in LAMP1 positive vesicles [478]. Besides no structural motifs or specific amino acid residues have been identified to be involved in such Mn-induced degradation of SLC39A14, this mechanism aims at decreasing the number of SLC39A14 cell surface Mn importers to limit Mn entry and protect the cells from Mn cytotoxicity. However, it is to note that oldest investigations first identified a proteasomal-mediated degradation route for SLC39A14 involving protein endocytosis, extraction from membranes, ubiquitination and deglycosylation prior to degradation [479]. In such study, not Mn but Fe levels were shown to induce SLC39A14 proteasomal degradation. Furthermore, one of the three N-linked glycosylation sites of the protein (N<sub>102</sub>) was shown to be critical for both Fe sensitivity and membrane extraction required for subsequent degradation of the protein. Altogether, SLC39A14 protein expression seems to be regulated by specific biometals (Mn and Fe) that engage the protein into specific degradatory pathways (lysosomal and proteasomal, respectively).

#### 3.3.4. Regulation of mammalian CRAC channels

- CRAC channels inhibitors

The use of CRAC channel inhibitors allowed both the identification and function of such channels in different tissues. Many CRAC channel inhibitors exist, although most of them share a poor selectivity to specifically block the channels. To date, the trivalent lanthanide ions lanthanum ( $\text{La}^{3+}$ ) and gadolinium ( $\text{Gd}^{3+}$ ) are the most potent inhibitors of such channels, blocking  $I_{\text{CRAC}}$  with a high affinity. Nevertheless, these ions can not be considered as specific CRAC channel inhibitors since they inhibit other plasma membrane  $\text{Ca}^{2+}$  channels such as VGCC and TRP channels. Lanthanides have been shown to physically interact with CRAC channels, defining them as “pore blockers”. Another widely used molecule is BTP2, a chemical compound which inhibits the SOCE response after a thapsigargin treatment and  $I_{\text{CRAC}}$ . While BTP2 exhibits specificity for CRAC channels over  $\text{K}^+$  channels and VGCC, it also inhibits some TRPC channels and even stimulates the  $\text{Na}^+$ -permeable channel TRPM4. Additional widely used inhibitors are reported in this review [382], arguing for new insights in their mode of action conferring their inhibitory effect.

- Protein-protein interactions

As described earlier, both mammalian SOCE and SICE responses are mediated by Orai1. While SOCE is a STIM1-dependent process, SICE is a STIM1-independent pathway culminating in  $\text{Ca}^{2+}$  entry through Orai1 activation by SPCA isoforms (SPCA1 and SPCA2) (see 3.2.3.). However, apart from being activated by SPCA, the CRAC channel activity can be regulated by additional protein-protein interactions known either activate or inhibit  $\text{Ca}^{2+}$  entry [382]. Amongst them, some only interact with STIM1 (STIM1-binding proteins) such as Junctate [480], SOCE-associated regulatory factor (SARAF) [481] and calnexin [482], other only bind Orai1 like SPCA1 [410] and SPCA2 [244,245,409] and finally, some interaction partners both interact with STIM1 and Orai1 such as partner of STIM1 (POST) [483], CaM [484], CRAC regulatory protein 2A (CRACR2A) [485] and SLC10A7 [371]. Amongst the diversity and complexity of the regulatory pathways involving protein-protein interaction between Orai1 and/or STIM1, additional information can be found in the original publications and in the following review [382].

---

**Chapter 3:**  
**TMEM165 and Gdt1p: between glycosylation and**  
**Ca<sup>2+</sup>/Mn<sup>2+</sup>/H<sup>+</sup> homeostasis:**  
**what would be their biological function(s)?**

---





Since the identification of *TMEM165* in 2012, the yeast model *Saccharomyces cerevisiae* played a crucial role in our current understanding of *TMEM165* function in human through the characterization of Gdt1p, its yeast ortholog. Therefore, in this chapter, both functions of *TMEM165* and Gdt1p will be discussed, often in a “mirror” manner.

## 1. *TMEM165* at the genomic level

### 1.1. *TMEM165* gene

*TMEM165* gene is located on chromosome 4, portion q12 (4q12) and spans over 37kb. As shown in Figure 35, *TMEM165* coding sequence can be divided into 6 exons leading to the production of a 1312 bp mRNA transcript [64,486]. This latter is then referred as “WT-*TMEM165*” as it is the most abundant transcript to be translated into the 324 amino acids *TMEM165* protein. However, alternative spliced isoforms have recently been identified, leading to translation of shorten *TMEM165* isoforms [486] that will briefly be described in the next paragraph.

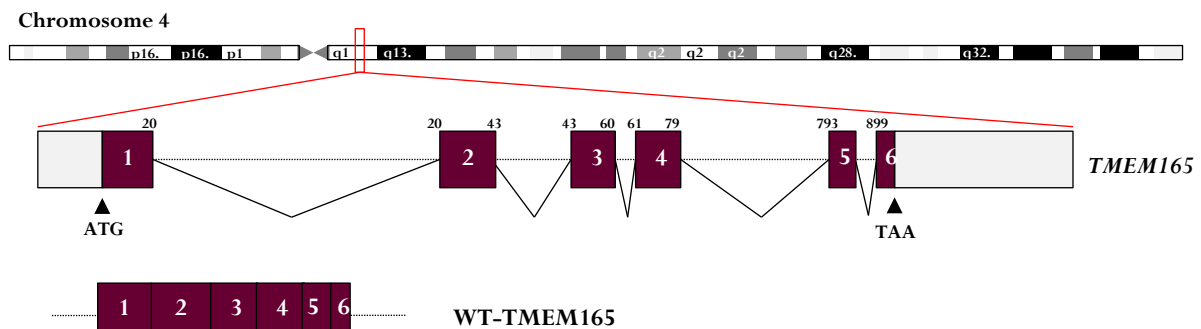


**Figure 35: *TMEM165* genomic localization and organization leading to WT-*TMEM165* transcript.** Chromosome 4 is schematically represented to highlight the portion q12 where *TMEM165* is located. *TMEM165* coding sequence is divided into 6 exons (whited numbered purple boxes). Left black arrow indicates the starting point (ATG) and right black arrow refers to the stop codon (TAA). The numbering above each exon is based on coding nucleotides. Adapted from Foulquier et al., 2012 [64].

To date, no pseudo-genes have been identified yet in the human genome. In addition, *TMEM165* sequence is highly conserved during evolution as witnessed a phylogenetic study highlighting homologous sequences in more than 400 eukaryotes organisms and 900 different species of bacteria [303].

### 1.2. *TMEM165* splicing leading to *TMEM165* isoforms

*TMEM165* is mainly translated into the 324 amino acids *TMEM165* full length protein. However, the EST (Expressed Sequence Tags) data base revealed three different EST corresponding to *TMEM165* transcripts and differing from the WT one according to alternative splicing events. Further investigations

have been done to highlight TMEM165 isoforms and two of them have been characterized: a long-form (LF) and a short-form (SF) [486]. Looking at the splicing event, LF corresponds to a 1124 bp mRNA transcript missing exon 2 and containing an additional truncated exon named E3' (Figure 356). This transcript is then translated into a 259 amino acids and has been shown to be only expressed in a specific region of the human brain: the temporal lobe. On the other hand, a 713 bp mRNA transcript containing exons 1, 5 and 6 corresponds to the SF isoform (Figure 36). This transcript is one of those already identified in the EST data base and referred as "BI457666". The translated protein is made of 129 amino acids. Although SF seems to be expressed in a broad range of samples from diverse organs, this isoform is predominantly expressed in the human brain. Moreover, SF expression levels are rather low comparing with those of WT TMEM165. Owing to tissue specificity and low expression levels of both SF and LF isoforms, they won't be further detailed in this manuscript.

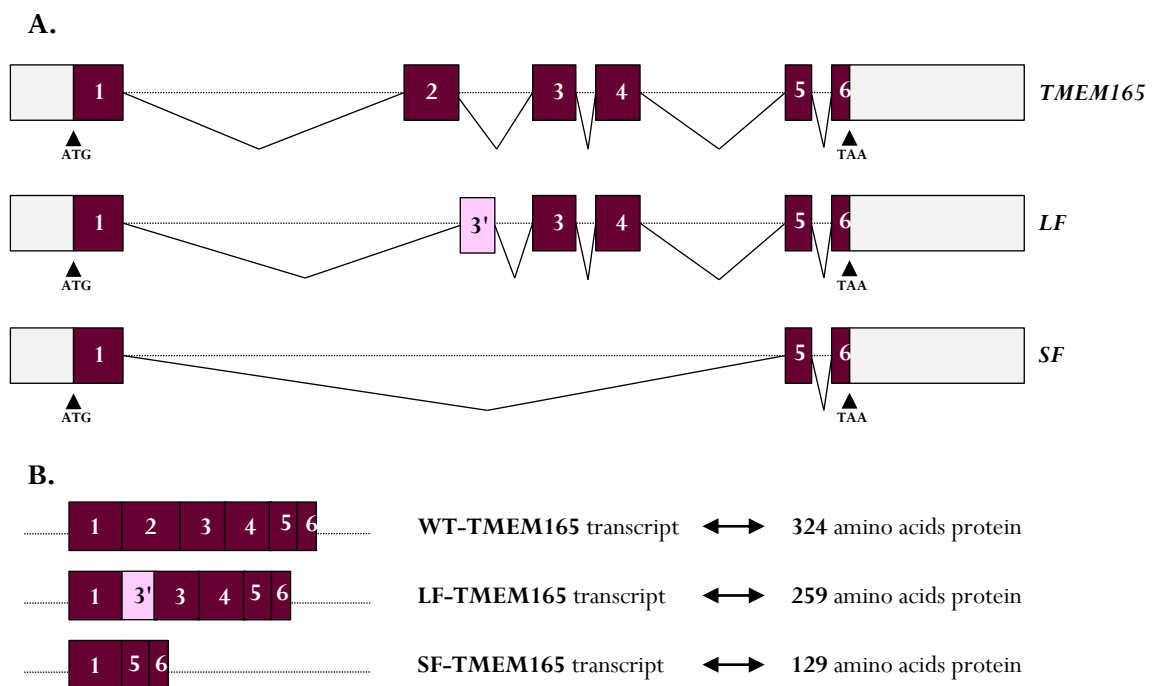


**Figure 36: *TMEM165* alternative splicing variants generating the short-form (SF) and long-form (LF) isoforms of *TMEM165*.** **A.** *TMEM165* genomic splicing events leading to the transcript of *TMEM165* short form (SF) and long form (LF) isoforms. **B.** WT, SF and LF –*TMEM165* transcripts and associated amino acids content translated proteins. Adapted from Krzewinski et al., 2017 [486].

### 1.3. *TMEM165* patients' mutations

In 2012, mutations in *TMEM165* have been reported to be pathogenic, leading to a CDG (see section 3.2). To date, four different mutations have been identified and carried amongst seven reported patients [64,487]. All of those mutations are listed in Table 20.

**Table 20: List of reported *TMEM165* patients' mutation causing TMEM165-CDG**

| Mutations             |                       |   |   | Reported<br>TMEM165-CDG<br>patients |
|-----------------------|-----------------------|---|---|-------------------------------------|
| Origin                | Gene location         | Subsequent effects                        | Protein changes                             |                                     |
| Homozygous            | c.792+182G>A          | Activation of a cryptic splice donor site | WT-TMEM165<br>+ 94 aa shorten TMEM165       | 3 (P1, P2, P3)                      |
| Homozygous            | c.377G>A              |   | p.ARG126His (R126H)                         | 1 (P4)                              |
| Compound heterozygous | c.377C>T and c.910G>A | Missense                                  | p.Arg126Cys (R126C) and p.Gly304Arg (G304R) | 1 (P5)                              |
| Homozygous            | c.323A>G              |   | p.Glu108Gly (E108G)                         | 2 (P6 and P7)                       |

First identified by Foulquier et al. in 2012, the homozygous mutation in *TMEM165* leading to the activation of a cryptic splice donor (c.792+182 G>A) is shared by three out of the seven mentioned patients. Although two of them are siblings, the third patient is not related to them. The three other mutations found in *TMEM165* are missense mutations. One is again shared by siblings (c.323 A>G) whereas the two others are carried by unrelated individuals. All missense mutations enable the production of the associated and mutated *TMEM165* transcripts and proteins. In contrast, the most common mutation (c.792+182 G>A) leads to the transcript of wild-type *TMEM165* and another one in which exon 4 is replaced by an additional 117 bp intronic sequence. At the protein level, it would lead to the synthesis of wild-type TMEM165 and a truncated protein, shorten by 94 amino acids.

## 2. TMEM165 and Gdt1p at the protein level

### 2.1. TMEM165 and Gdt1p topologies

TMEM165 is a 324 amino acids hydrophobic protein ubiquitously expressed in human. According to diverse predictions, TMEM165 is made of six or seven transmembrane domains, a putative luminal N-tail and a 52 amino acids cytosolic loop organized in a coiled-coil domain (Figure 37) [64,488]. These uncertainties lie on the predictive signal-peptide cleavage site at position 33, including the whole first transmembrane domain (black arrow, Figure 37). Although it has not been clearly identified, if this signal peptide is removed, six transmembrane domains and a luminal N-tail are predicted [64]. Compared to human TMEM165, the yeast ortholog Gdt1p is a 280 amino acids protein matching 38% amino acids identity with TMEM165 (protein sequence alignment adapted from [66] are shown in Figure 38). Slight topological differences can be observed between TMEM165 and Gdt1p: (i) Gdt1p lacks the first 55 human amino acids and subsequently, the first transmembrane domain and (ii) the central cytosolic loop is 10 amino acids longer in the yeast protein. Except the number of transmembrane domains that may vary between TMEM165 and Gdt1p, both proteins belong to the UPF0016 family by sharing two copies of the hydrophobic motif E-Ø-G-D-(KR)-(ST) (Ø any

hydrophobic residue) and a cytosolic loop containing acidic amino acid residues (see 2.2.). Those features are respectively highlighted in Figure 38 by pink boxes and colored asterisks. As depicted in Figure 37, apart from these UPF0016 signature motifs, TMEM165 also possesses two putative lysosomal targeting signals in two cytosolic loops: (i)  $Y_{124}NRL_{127}$  is located in the first small cytosolic loop and is part of the conserved tyrosine-based sorting motif  $YXX\emptyset$  whereas (ii) the di-leucine motif  $L_{209}L_{210}$  belonging to the non-canonical  $[DE]XXXL[LI]$  sequence is located in the second cytosolic loop [488].

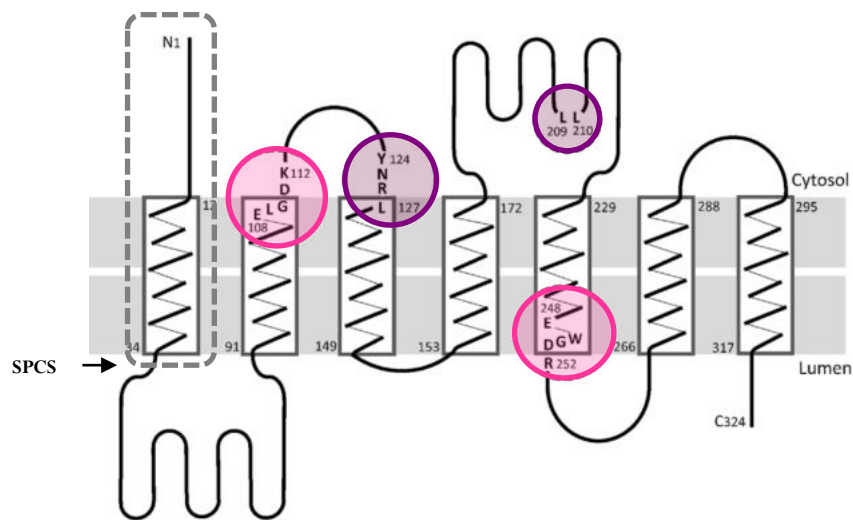


**Figure 37: TMEM165 predicted topology highlighting its conserved domains.** TMEM165 transmembrane domains and signal peptide cleavage site were previously predicted using respectively TMHMM software and SignalP. Black arrow indicates the putative signal-peptide cleavage site (SPCS) removing the first transmembrane domain represented in the gray dotted box. Pink circles highlight the two signature motifs of the UPF0016 family:  $E-\emptyset-G-D-(KR)-(ST)$  ( $\emptyset$  any hydrophobic residue). Purple circles indicate the two putative lysosomal targetting sequences:  $YXX\emptyset$  and the di-leucine motif belonging to the  $[DE]XXXL[LI]$  sequence. Adapted from Dulary et al., 2017 [66].

In TMEM165 the position of the aspartic residue ( $D_{201}$ ) is too far from the first leucine residue ( $L_{209}$ ), not allowing the recognition of the  $[DE]XXXL[LI]$  sequence. Thus,  $L_{209}L_{210}$  motif is not required in any targeting of TMEM165 to the lysosomes. On the other hand, in the  $Y_{124}NRL_{127}$  motif, both  $Y_{124}$  and  $R_{126}$  residues are involved in TMEM165 traveling from the Golgi apparatus to the plasma membrane where it could be then internalized [488].

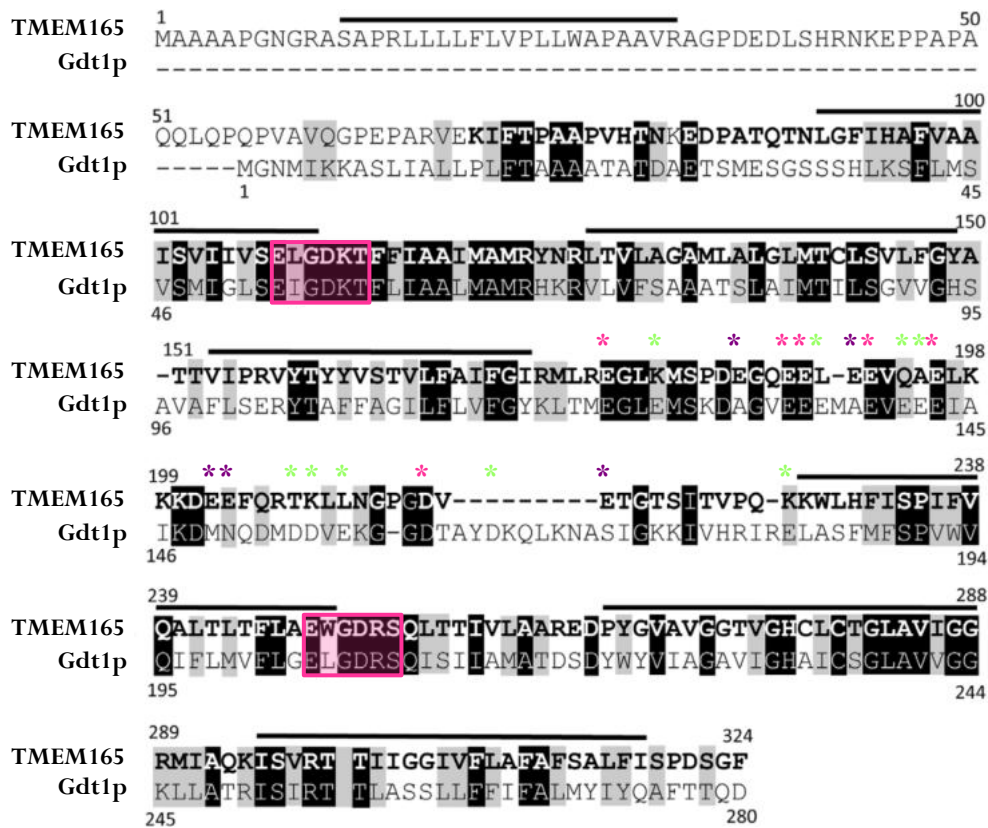


**Figure 38: Protein sequence alignment of TMEM165 and Gdt1p, adapted from [66].** Black boxes indicate identical amino acid residues in both sequences whereas grayed boxes underline homologous amino acid residues. Black horizontal bars gather the amino acid stretches predicted as potential transmembrane domains (TMHMM v2.0 server tool). Light pink boxes highlight the two hydrophobic motifs E-Ø-G-D-(KR)-(ST) (Ø any hydrophobic residue) shared by both proteins. Pink asterisks show the conserved acidic amino acid residues belonging to the cytosolic loop. Purple and green asterisks indicate acidic amino acid residues belonging to the cytosolic loop respectively found in TMEM165 and Gdt1p.

## 2.2. The Uncharacterized Protein Family 0016 (UPF0016)

TMEM165 and Gdt1p are respectively the human and yeast members of the UPF0016 family (Pfam PF01169). UPF0016 is a highly conserved family of membrane proteins with unknown functions. Members of this family share strong sequence homologies across a broad range of species. Based on a phylogenetic approach, two phylogenetic trees have been drawn revealing twelve subfamilies for this family. The first tree corresponds to prokaryotic species and gathers subfamilies I to VI. This tree identified members of the UPF0016 family in every bacterial phylum except for Bacillales and Lactobacillales. A second phylogenetic tree was assigned to eukaryotic organisms and encompassed subfamilies VII to XII. In this tree, plants are represented by subfamily IX and show the highest protein diversity as reflecting by the number of paralogs found per genome (2 to 5) [303]. Amongst the twelve subfamilies, two main features characterize UPF0016 members (i) the presence of one or two copies of the hydrophobic motifs E-Ø-G-D-(KR)-(ST) (Ø any hydrophobic residue) and (ii) the presence of six predicted transmembrane domains. Those latter are supposed to play a crucial role for protein folding,

stability, localization and/or function. Because TMEM165 and Gdt1p respectively belong to the Metazoa and Fungi eukaryotic subfamilies X and XI, the common predicted topology of both proteins is schematically represented in Figure 39.

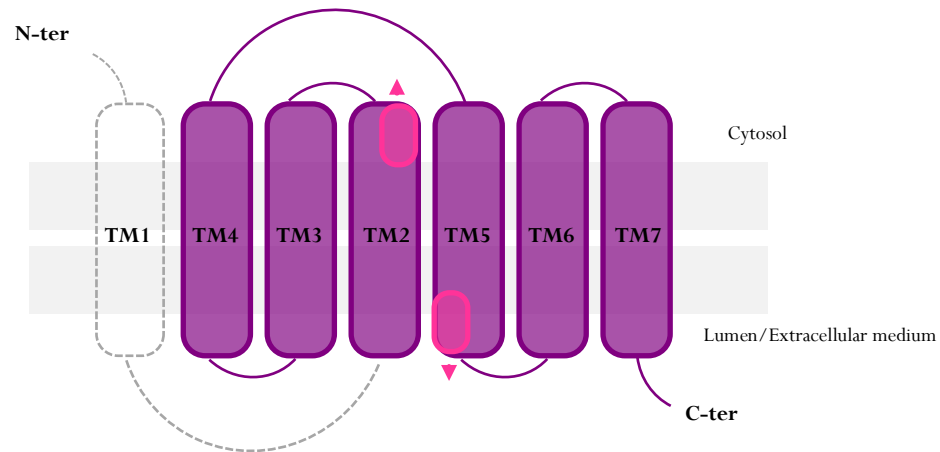


**Figure 39: Common predicted topology of the Metazoa and Fungi eukaryotic UPF0016 subfamilies X and XI.** Transmembrane domains (TM) and signal peptide cleavage site were predicted using respectively TMHMM and SignalP. Gray dotted box and lines show the putative first transmembrane domain. Pink circles highlight the location of hydrophobic motifs on the second and fifth transmembrane domain. Associated pink arrows show the orientation of both domains. Inspired by Demaegd *et al.*, 2014 [303] and Potelle *et al.*, 2017 [307].

The growing interest for this family has emerged in 2012, when Foulquier *et al.* discovered that TMEM165, its human member, was genetically implicated in Congenital Disorders of Glycosylation [64]. Since then, study of UPF0016 family members is on-going in various species such as mammals (TMEM165), yeast *Saccharomyces cerevisiae* (Gdt1p) [303,304], plant *Arabidopsis thaliana* (PAM71, CMT1, PML3-5) [489–492], cyanobacterium *Synechocystis* (SymPAM71) [493,494] and bacterium *Vibrio cholerae* (MneA) [495,496]. So far, all of these UPF0016 members have been assigned a function of cations transporter and more precisely,  $Mn^{2+}$  transporter with additional  $Ca^{2+}$  and/or  $H^{+}$  transport activities for some of them, which will be further detailed in section 2.2.3. Amongst these five species, all UPF0016 orthologs are required for  $Mn^{2+}$  homeostasis in addition to lactation in mammals,  $Ca^{2+}$  signaling in yeast and photosynthesis in plants and cyanobacteria. To ensure such transport function activity(ies) and meet physiological requirements, UPF0016 family members share specific subcellular localization being embedded in the membrane of the Golgi apparatus in yeast and mammals, in the thylakoid and chloroplast envelope in plants, in the thylakoid and at the plasma membrane in cyanobacteria and at the plasma membrane in bacteria (see section 2.2.3.). Given the number of on-going studies providing new insights into the biological functions on UPF0016 members, this family is no more considered as uncharacterized since it has been recently renamed “Gdt1p family” [497].

### 2.2.1. E-Ø-G-D-(KR)-(ST) motif during evolution and N-tail extension variability

Eukaryotic members of the UPF0016 possess two copies of the hydrophobic E-Ø-G-D-(KR)-(ST) domain oriented in an antiparallel manner which is a common feature for secondary cation transporter. This specific orientation results from an ancient gene-duplication event as demonstrated by Demaegd *et al.* [303] based on bacterial UPF0016 members. Briefly, bacterial orthologs can be found in three main forms resulting from (i) singleton genes encoding homodimer of single-domain proteins, (ii) pairs of adjacent genes each encoding heterodimers of single-domain proteins and (iii) genes encoding two-domain proteins resulting from an internal gene duplication and subsequent genes fusion. On the other hand, amongst the twelve subfamilies, the highest variability and heterogeneity lie in the N-terminal region of the proteins. Its length varies from no extension to a hundred of amino acids, without any conservation between species. In the latter case, a seventh transmembrane domain is predicted and often supposed to be cleaved by the presence of a signal peptide cleavage site. This is typically the case for TMEM165 (see Figure 37). Moreover, other cleaved signal peptides have been identified in the N-tail of many orthologs. For instance, TMEM165 plants orthologs CMT1 (Chloroplast Manganese Transporter 1) and PAM71 (Photosynthesis Affected Mutant 71) possess putative chloroplast transit peptides of around 70 amino acids and are both localized in the chloroplast (thylakoid membrane and chloroplast envelope, respectively). Hence, the N-terminal extension of the eukaryotic UPF0016 members may have an impact in their targeting to reach their proper final destination [303,491]. Because of this great variability of the N-terminal region, the conserved function of UPF0016 members is not likely depending on it.

### 2.2.2. UPF0016 and cation/Ca<sup>2+</sup> superfamily (CaCA) similarities

Except for the number of transmembrane domains, TMEM165 and Gdt1p share the exact topology defined for the CaCA family members *i.e.* two hydrophobic regions (named  $\alpha$ -repeats) oriented in an antiparallel manner and spaced by a huge hydrophilic loop containing acidic residues [291]. In addition, both hydrophobic domains are surrounding by serine and threonine residues. Those latter polar amino acids may help to create a hydrophilic pocket required for Ca<sup>2+</sup> transport. At last, the presence of glycine and alanine residues in those hydrophobic regions can provide more flexibility to allow conformational changes [304]. Besides UPF0016 members share tight similarities with the CaCA superfamily members, no primary sequence homology was found. In this way, these two families have to be considered independently. In the last decade, many studies aiming to decipher the biological functions of both TMEM165 and Gdt1p have been done. New insights into those protein functions will be addressed and discussed in the last section on this chapter (3.).

### 2.2.3. Other studied UPF0016 orthologs

Many UPF0016 orthologs can be found in databases but only few of them are under study. Amongst them, human and yeast orthologs are the most studied and will be described in the last section of this chapter. Mouse and zebrafish orthologs will also be further discussed as *TMEM165* knockout mice and zebrafish models have been generated to study TMEM165 function (see section 3.2.1.). Hence, in the following sections only plants and cyanobacteria orthologs will be addressed. At last, all UPF0016 orthologs described in this manuscript are listed in Table 21

**Table 21: List of studied UP0016 ortholgs presented in this manuscript.** For each UPF0016 member, organisms, gene and encoded protein are mentioned. Name indicated in brackets are previous one. Names separated by a slash are both used.

| Organisms     | Gene name         | Encoded protein (name; length)      |
|---------------|-------------------|-------------------------------------|
| Human         | <i>TMEM165</i>    | TMEM165; 324 aa                     |
| Yeast         | <i>GDT1</i>       | Gdt1p; 280 aa                       |
| Mouse         | <i>Tmem165</i>    | TMEM165; 323 aa                     |
| Zebrafish     | <i>tmem165</i>    | Tmem165/GDT1 family protein; 305 aa |
| Plants        | <i>At1g64150</i>  | PAM71/BICAT1; 370 aa                |
|               | <i>At4g13590</i>  | CMT1 (PAM71-HL)/BICAT2; 359 aa      |
|               | <i>At5g36290</i>  | PML3; 293 aa                        |
|               | <i>At1g25520</i>  | PLM4; 230 aa                        |
|               | <i>Atg1g68650</i> | PLM5; 228 aa                        |
| Cyanobacteria | <i>sl10615</i>    | SynPAM71/Mnx; 206 aa                |

- Plant orthologs: PAM71, CMT1 and PML3-5

As already mentioned above, plants (subfamily IX) represented the highest diversity of UPF0016 orthologs by sharing up to 5 paralogs per genome. In this section, only *Arabidopsis thaliana* UPF0016 orthologs will be described. To date, five genes encode for UPF0016 orthologs in *Arabidopsis thaliana* [303,491]. In the order of their discoveries, they are: PAM71 [489], CMT1 (previously PAM71-HL) [490] and three PAM71 like proteins (PML) PML3, PML4 and PML5 [492].

Among them, PAM71 and its closest homolog CMT1 share the most identity with human TMEM165 and yeast Gdt1p. Sequences alignment confirm the presence of the two hydrophobic signature motifs, the big cytosolic loop and six to seven predicted transmembrane domains [489,490]. Both PAM71 and CMT1 possess an extended N-tail containing a putative chloroplast transit signal peptide allowing their proper localization to the chloroplast [489,490]. From Schneider et al. and Eisenhut et al. studies, both *PAM71* and *CMT1* knockouts lead to a similar phenotype including (i) severe growth defects associated with (ii) an alteration of the photosystem II (PSII) function and reduced photosynthesis, both being (iii)



suppressed by manganese supplementation. At the cellular level, *pam71* deletion causes a mis-sequestration of  $\text{Ca}^{2+}$  and  $\text{Mn}^{2+}$  within the chloroplast. As a result,  $\text{Ca}^{2+}$  accumulates in the thylakoid lumen while  $\text{Mn}^{2+}$  accumulates in the stroma. Then, PAM71 was first supposed to act as a  $\text{Mn}^{2+}/\text{H}^+$  exchanger, importing  $\text{Mn}^{2+}$  from the stroma to the thylakoid lumen (Figure 40). Consequently to its accumulation in the stroma, a depletion of  $\text{Mn}^{2+}$  in the thylakoids has been observed in *pam71* mutants. Plants mainly required manganese in the Oxygen Evolving Complex (OEC), a  $\text{Mn}_4\text{CaO}_5$  cluster part of PSII. Hence, a manganese deficiency in the thylakoid lumen leads to a reduced function of the PSII and a decrease in the photosynthesis yield. Growing *pam71* in an enriched manganese medium suppresses the photosynthesis defect and then suggests a role for PAM71 in manganese tolerance. To better confirm its involvement in manganese transport, PAM71 heterologous expression was performed in the manganese sensitive *pmr1Δ* yeast. As a result, PAM71 protein expression compensates the loss of Pmr1p by suppressing the manganese sensitivity of *pmr1Δ*, demonstrating its function as a manganese transporter. All in all, PAM71 functions as a manganese importer of the thylakoid lumen and thus, contributes to manganese homeostasis in the chloroplast.

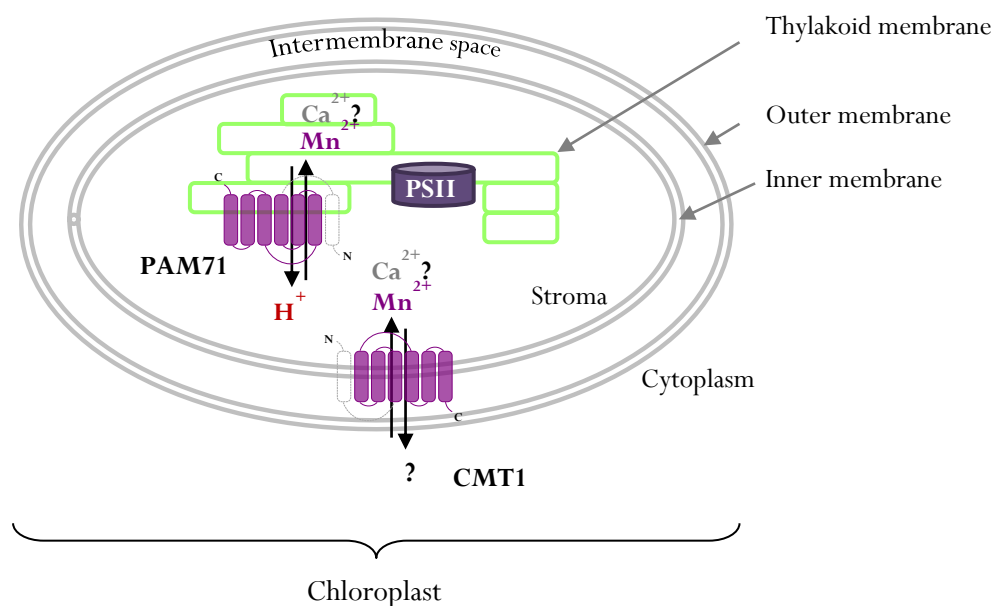


**Figure 40: Subcellular localization and putative function of PAM71 and CMT1 in the regulation of  $\text{Mn}^{2+}/\text{Ca}^{2+}$  homeostasis within the chloroplast.** Simplified representation of a chloroplast. Black arrows indicate the direction of ions transport. Uncertainties are indicated by “?”. PSII: photosystem II. Inspired by [497].

Concerning CMT1, this 359 amino acids protein is localized in the chloroplast envelope. At the cellular level, *cmt1* deletion lowers manganese concentration within the chloroplast. As for *pam71* mutants, a direct consequence of manganese deficiency in the chloroplast lies in the loss of manganese binding to the PSII altering its function in photosynthesis. In addition, chloroplast ultrastructures were completely disorganized in *cmt1*. To highlight CMT1 function in manganese transport, complementation study in

the sensitive *pmr1Δ* yeast was also performed. As for PAM71, CMT1 alleviates manganese sensitivity suggesting its role as a manganese transporter. Hence, due to its subcellular localization and manganese deficiency in *cmt1* chloroplast, CMT1 was supposed to act as a  $Mn^{2+}$  importer at the chloroplast envelope (Figure 40). Then, *Arabidopsis thaliana* expresses two homologs of the UPF0016 family, both involved in manganese homeostasis in the chloroplast. One can wonder if there is any redundant activity. Analyzing single *cmt1* and double *pam71 cmt1* mutants, CMT1 appears to be the limiting step in manganese delivery to the chloroplast suggesting that it should act before PAM71. To conclude, both PAM71 and CMT1 are involved in chloroplast manganese homeostasis through its correct delivery from the cytoplasm to the thylakoid lumen.

In addition, PAM71 and CMT1 functions are neither redundant nor competitive but sequential according to their proper localizations (Figure 40). First,  $Mn^{2+}$  import from the cytosol to the stroma is achieved through the activity of CMT1, being localized in the chloroplast envelope. Second, manganese reaches the thylakoid lumen thanks to PAM71 activity, being properly localized in the thylakoid membrane. However, in a very recent study, Frank et al. assigned a major role for both proteins in calcium homeostasis [498]. In this study, PAM71 and CMT1 were renamed respectively BICAT1 and BICAT2 for Bivalent Cation Transporter 1 and 2 and were found well localized both in the thylakoid membrane (BICAT1/PAM71) and in the chloroplast envelope (BICAT2/CMT1). By means of heterologous expression of both proteins in either *Escherichia coli* or yeast lacking Gdt1p and/or Pmr1p,  $Ca^{2+}$  transport activities were assigned to BICAT1/2. Thus, BICAT1 would import  $Ca^{2+}$  within the thylakoid lumen whereas BICAT2 would import cytosolic  $Ca^{2+}$  to the stroma. Then, further investigations need to be done to better determine the role of both proteins in either calcium or manganese homeostasis within the chloroplast.

In contrast, the three PAM71 homologs recently described by Hoecker et al., PML3, PML4 and PML5 display different subcellular localizations and are not restrictively expressed in photosynthetic cells [492]. Those proteins share respectively 38%, 32% and 32% identical amino acids with PAM71. Although both predictive transmembrane domains and signature motifs are conserved between PAM71 and PML, their functions are poorly understood. PML are not crucial neither for plant growth nor development and may be linked to manganese homeostasis according to their subcellular localizations. Authors suggested a role for PML3 in balancing excess of manganese at the Golgi apparatus level. As regard to PML4 and PML5, a putative role in manganese import in the ER lumen has been hypothesized based on their ER localization.

- Cyanobacterium ortholog: SynPAM71/Manganese exporter (Mnx)

Following the identification of PAM71 as an integral thylakoid manganese importer in *Arabidopsis thaliana*, Gandini *et al.* looked for PAM71 ortholog(s) in the cyanobacterium *Synechocystis* PCC6803 [493]. Based on previous phylogenetic studies [303] combined to sequence alignment, a unique PAM71 homolog was identified in *Synechocystis* and named SynPAM71. The same year, Brandenburg *et al.*, working in the same field also identified SynPAM71 as unique PAM71 homolog but called it Mnx for Manganese exporter [494]. Then, both SynPAM71 and Mnx refer to the same protein. By homology, SynPAM71/Mnx was suggested to play a role in  $Mn^{2+}$  homeostasis. This was confirmed in  $\Delta$ SynPAM71/*mnx* mutant in whom SynPAM71/Mnx loss-of-function leads to manganese sensitivity and manganese toxicity symptoms. Those latter are characterized by reduced levels of chlorophyll, PSI accumulation, altered PSII function and cytosolic manganese accumulation. Indeed, a  $^{54}Mn$  chase experiment conducted in *mnx* mutants highlight their inability to release internal manganese pool out of the cyanobacteria resulting in manganese intracellular accumulation. Thus, a manganese exporter function was proposed for SynPAM71/Mnx (Figure 41).

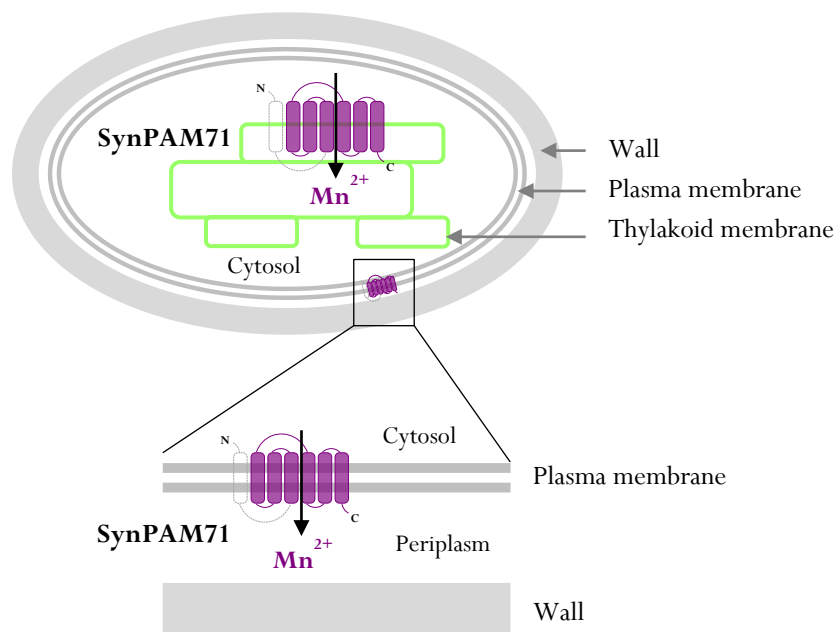


**Figure 41: Subcellular localization(s) and function of SynPAM71 in the regulation of  $Mn^{2+}$  homeostasis.** Simplified representation of a cyanobacterium highlighting a thylakoid. According to two separate studies, SynPAM71 was found expressed either in the thylakoid membrane or in both the thylakoid membrane and the plasma membrane. Black arrows indicate the direction of  $Mn^{2+}$  transport.

To further identify the role of Mnx in manganese transport, Mnx heterologous expression was performed in *pmr1Δ* yeast. As for PAM71 and CMT1, Mnx expression compensates Pmr1p loss-of-function and suppresses *pmr1Δ* manganese sensitivity. According to the subcellular localization, Gandini *et al.*, found SynPAM71 preferentially expressed at the plasma membrane with a small proportion in the

thylakoid membrane [493] whereas, Brandenburg *et al.* only found Mnx localized in the thylakoid membrane [494]. Despite this difference in SynPAM71/Mnx subcellular localization, both groups characterized SynPAM71/Mnx as a  $Mn^{2+}$  exporter, mediating its transport from the cytoplasm to the periplasm or other luminal compartments (Figure 41). Such function protects the cytoplasm from manganese excess and toxicity.

### **2.3. TMEM165 and Gdt1p subcellular localization(s)**

#### **2.3.1. TMEM165 and Gdt1p: two Golgi localized proteins**

First visualized in fibroblasts, TMEM165 is a Golgi localized protein. To fine tune its localization within the Golgi apparatus (at the cisternae level), a nocodazole treatment combined with Golgi markers stainings allowed the identification of TMEM165 in the *trans*-Golgi subcompartment by co-localization with the  $\beta$ -1,4-galactosyltransferase [64]. With regards to Gdt1p, sucrose gradient fractioning and Golgi markers stainings highlighted its expression in the early Golgi stacks, respectively co-localizing with the *cis*- and medial Golgi proteins Sed5p and Gos1p [304]. Hence, TMEM165 and Gdt1p are both Golgi-localized proteins, the human ortholog being mainly expressed in the late Golgi and the yeast ortholog in the early Golgi.

#### **2.3.2. Other subcellular localizations for TMEM165**

Although 95% of endogenous TMEM165 is Golgi-localized, a small proportion of the protein is also found in the late endosomes/lysosomes and at the plasma membrane [304,307,488]. This is even truer in case of TMEM165 overexpression. Indeed, transient transfection of tagged versions of the protein in HeLa cells (RFP- or GFP-TMEM165) display a cell surface localization [304,488]. This was then confirmed in a later study by cell surface biotinylation indicating that 5% of endogenous TMEM165 is expressed at the plasma membrane in HEK cells [307]. According to the late endosomes/lysosomes localization, cell fragmentation of control and patients' fibroblasts allowed the detection of endogenous TMEM165 in the Golgi apparatus and in acidic compartments [488]. Therefore, TMEM165 shares multiple subcellular localizations within the late compartments of the secretory pathway: from the Golgi apparatus to the plasma membrane.

### **2.4. TMEM165 and Gdt1p stabilities**

Described by Potelle, Dulary *et al.* for the first time, TMEM165 and Gdt1p are two proteins extremely sensitive to high manganese concentration [307]. Amongst other tested ions, only  $Mn^{2+}$  leads to TMEM165 and Gdt1p-cMyc protein degradation. More precisely, 4h of treatment with 500 $\mu$ M  $MnCl_2$  (or  $MnSO_4$ ) in the culture medium are enough to specifically target TMEM165 to the lysosomes. This  $Mn^{2+}$ -induced lysosomal degradation was then confirmed by using leupeptin and chloroquine, two

molecules interfering with lysosomal protease activities. In case of both  $\text{MnCl}_2$  and chloroquine treatments, TMEM165 protein expression and lysosomal subcellular localizations were recovered [307]. Then, taking advantage of patients' missense mutations already described (*i.e.* R126H, R126C+G304R and E108G), TMEM165 sensitivity to  $\text{Mn}^{2+}$  was assessed in patients' fibroblasts of two of them (R126H and E108G) [307]. While R126H-TMEM165 variant is highly sensitive to  $\text{Mn}^{2+}$ , E108G-TMEM165 was described as  $\text{Mn}^{2+}$  resistant. This first evidenced the importance of glutamic acid residue E108 in TMEM165  $\text{Mn}^{2+}$  sensitivity.

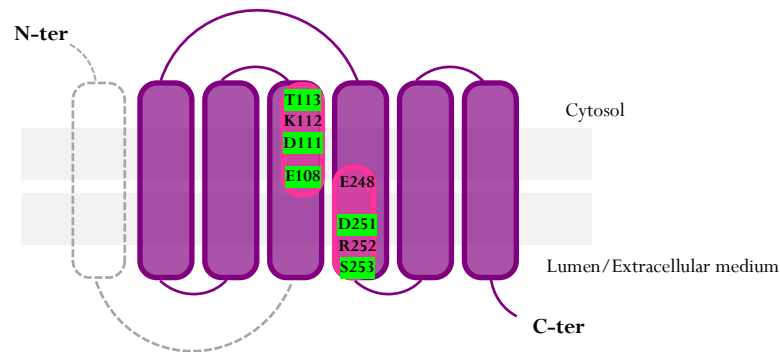


**Figure 42: Site-directed mutagenesis of TMEM165.** The residues targeted for glycine substitution are the eight amino acids that compose the two repeated conserved motifs E-Ø-G-D-(KR)-(ST). The acidic and polar residues in the repeated motifs were found to be important for manganese sensitivity of TMEM165 (colored in green).

As E108 is part of one of the consensus motif E-Ø-G-D-(KR)-(ST), point mutations were extended to other amino acids in these domains:  $E_{108}$ ,  $D_{111}$ ,  $K_{112}$ ,  $T_{113}$  and  $E_{248}$ ,  $D_{251}$ ,  $R_{252}$ ,  $S_{253}$  (Figure 42) [477]. TMEM165 KO HEK cells were transfected with TMEM165 variants and expressed for 24h before being subjected to  $\text{MnCl}_2$  treatment. The study led by Lebretonchel *et al.* suggests that most of the acidic and polar mutated residues ( $E_{108}$ ,  $D_{111}$ ,  $T_{113}$ ,  $D_{251}$ , and  $S_{253}$ ) are resistant to  $\text{MnCl}_2$  treatment (except  $E_{248}$ ) while basic mutated residues ( $K_{112}$  and  $R_{252}$ ) confer TMEM165  $\text{Mn}^{2+}$  sensitivity (Figure 42).

Due to this  $\text{Mn}^{2+}$  sensitivity, TMEM165 was then considered as a new Golgi localized manganese sensor in addition to the *cis*-Golgi phosphoprotein of 130 kDa (GPP130) previously described by Mukhopadhyay *et al.* [499]. However, some differences distinguish TMEM165 and GPP130. First, TMEM165 was shown to be more sensitive to  $\text{MnCl}_2$  than GPP130 suggesting different manganese binding affinity and/or degradation routes for these two proteins [307]. Second and very recently, we demonstrated that TMEM165 is a cytoplasmic  $\text{Mn}^{2+}$  sensor while GPP130 is a Golgi luminal  $\text{Mn}^{2+}$  sensor [461]. Third, although TMEM165 and GPP130 are targeted to the lysosomes for their degradation, a faster mechanism seems to occur for TMEM165. Indeed, contrary to GPP130, TMEM165 was never seen in punctate structures after  $\text{Mn}^{2+}$  exposure [307,499]. Moreover, Venkat *et al.* have recently demonstrated that  $\text{Mn}^{2+}$ -induced turnover and trafficking of GPP130 and TMEM165

were mediated by sortilin [500]. Unfortunately, we were unable to reproduce this result for TMEM165 suggesting a different pathway addressing the protein to the lysosomes after  $Mn^{2+}$  treatment. Although the molecular mechanism beyond this  $Mn^{2+}$ -induced TMEM165 lysosomal degradation is still unclear, the  $Mn^{2+}$ -induced degradation of Gdt1p-cMyc in yeast demonstrated a conserved mechanism during evolution [307]. From these observations, one can suppose that TMEM165 and Gdt1p need to be degraded upon high  $Mn^{2+}$  exposure to prevent manganese toxicity leading to cell damages and cell death. Their role in manganese homeostasis will be further addressed in section 3.1.3.

### 3. Insights into TMEM165 and Gdt1p biological functions

Gathering previous studies from the team and collaborators to the working hypothesis assumed when I started my PhD, this section will retrace evidence elucidating TMEM165 and Gdt1p biological functions.

#### 3.1. TMEM165 and Gdt1p involvements in pH and $Mn^{2+}/Ca^{2+}$ homeostasis

Based on their belonging to the UPF0116 family, TMEM165 and Gdt1p are thought to be cation exchangers. In particular, the antiparallel orientation of the two E-Ø-G-D-(KR)-(ST) motifs suggests a cation antiporter function for both proteins (see above 2.1.). Several studies on TMEM165, Gdt1p and other orthologs, pointed out the involvement of UPF0016 members in  $H^+$ ,  $Ca^{2+}$  and  $Mn^{2+}$  homeostasis.

##### 3.1.1. TMEM165 and Gdt1p in calcium regulation

- Gdt1p is involved in both calcium tolerance and supply

The first studies on TMEM165 and Gdt1p suggested a role for both proteins in calcium homeostasis [304]. In yeast lacking Gdt1p (*gdt1Δ*), a strong growth defect was observed in the presence of high calcium ( $CaCl_2$ ) concentrations in the culture medium (ranging from 500 to 700mM) [304]. This first evidenced a role for Gdt1p in calcium tolerance. Further comparisons between single *gdt1Δ*, *pmr1Δ* and double *gdt1Δ/pmr1Δ* mutants grown with either high or low calcium (15mM EGTA) concentrations highlighted more severe growth defects when both Gdt1p and Pmr1p were lacking (*gdt1Δ/pmr1Δ*). In addition, while *pmr1Δ* sensitivity to EGTA was already known [238], *gdt1Δ* was not affected by the presence of EGTA. Therefore, Gdt1p function in calcium homeostasis is not required when Pmr1p is expressed but become essential when Pmr1p is absent. All in all, Gdt1p plays a crucial role in both calcium tolerance and calcium supply within the secretory pathway when Pmr1p is lacking.

- Truncated TMEM165 acts in calcium tolerance in yeast

The conservation of function from yeast to human was then assessed. *gdt1Δ* null mutant was transformed with human *TMEM165* and grown under 750mM  $CaCl_2$ . While full length TMEM165 failed to rescue

the calcium sensitivity in *gdt1Δ*, a truncated TMEM165 ( $\Delta^{55}$ TMEM165) partially succeeded [304]. This shortened TMEM165 lacks the first 55 amino acids of the human protein that are absent in the yeast ortholog (see 2.1, Figure 38). Thereby,  $\Delta^{55}$ TMEM165 better corresponds to Gdt1p topology, resulting in a similar function for both Gdt1p and  $\Delta^{55}$ TMEM165 in calcium tolerance. Hence and as already suggested above, the conserved function between TMEM165 and Gdt1p does not lie in the N-terminal region of both orthologs. Here, TMEM165 N-tail extension may impact its proper localization in yeast, altering and/or preventing its function. Altogether, both Gdt1p and  $\Delta^{55}$ TMEM165 play a role in calcium tolerance in yeast.

- Truncated TMEM165 and Gdt1p  $\text{Ca}^{2+}$  transport activities

The next step linking Gdt1p/TMEM165 biological functions and calcium homeostasis was to demonstrate their calcium transport activities. First evidence came from an *in vitro* study of the human ortholog. RFP-TMEM165 was stably expressed in HeLa cells and its rather high expression at the cell surface allowed patch-clamp experiments. Compared to untransfected cells, a significant outward current was measured at the plasma membrane of cells overexpressing TMEM165, highlighting TMEM165 function in cation transport. Since this current was inhibited by the addition of EGTA in the external medium, a transport of  $\text{Ca}^{2+}$  was suggested. Moreover, using the  $\text{Ca}^{2+}$  probe Fura-2, basal cytosolic calcium concentrations and thapsigargin-induced calcium released were reduced in cells overexpressing RFP-TMEM165. Thus, TMEM165 is also involved in intracellular calcium homeostasis [304]. To strengthen this result, Stribny *et al.* recently expressed another truncated form of TMEM165 ( $\Delta^{78}$ TMEM165) in the bacterial host *Lactococcus lactis* and measured *in vivo* its apparent  $K_M$  for  $\text{Ca}^{2+}$  ( $21 \pm 4\mu\text{M}$ ) [28]. With regards to its yeast ortholog, the calcium activity of Gdt1p was first demonstrated by heterologous expression of truncated *GDT1* in *Lactococcus lactis* [239]. In bacteria expressing  $\Delta^{23}$ Gdt1p, increasing external  $[\text{Ca}^{2+}]$  resulted in an increase of intracellular  $[\text{Ca}^{2+}]$ . This was not observed in the control strain and suggests that  $\Delta^{23}$ Gdt1p can mediate calcium influx from extracellular medium to the cytoplasm.  $\Delta^{23}$ Gdt1p corresponds to Gdt1p lacking the first 23 amino acids forming the peptide signal, not necessary when expressed in a bacterial model. In a later study from the same group,  $\Delta^{23}$ Gdt1p  $\text{Ca}^{2+}$  affinity was measured *in vivo*, still in *Lactococcus lactis* and evaluated with a  $K_M$  of  $15.6 \pm 2.6\mu\text{M}$  [306]. Moreover, this calcium pumping activity at the plasma membrane depends on the pH gradient existing between the cytoplasm and the external medium [239].

In addition, Gdt1p  $\text{Ca}^{2+}$  activity coupled to the pH gradient established by the V-ATPase was demonstrated in the yeast *Saccharomyces cerevisiae* [501] and will be described in the next section (3.1.2.).

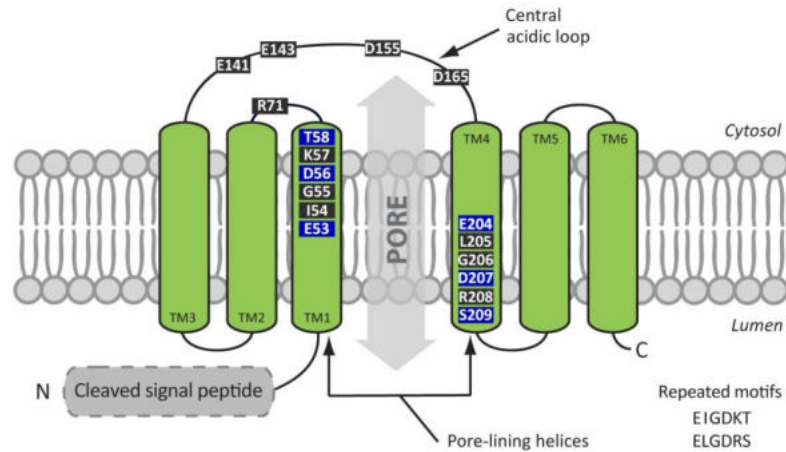


**Figure 43: Site-directed mutagenesis of Gdt1p.** The topology model of Gdt1p was predicted using the Memsat-SVM tool (Nugent *et al.*, 2012). The residues targeted for alanine substitution are the twelve amino acids that compose the two repeated motifs within the predicted TM1 and TM4, four conserved acidic residues of the cytosolic loop, and the arginine R71 found mutated in some patients suffering from TMEM165-CDG. The acidic and hydrophilic residues in the repeated motifs were found to be important for calcium tolerance and transport activity of Gdt1p (colored in blue). **Colinet et al.**, 2017 [305].

Lastly, Colinet *et al.* demonstrated the crucial involvement of six amino acids residues in the consensus motifs of Gdt1p for its  $\text{Ca}^{2+}$  transport activity (blue squared in Figure 43) [305]. Using site-directed mutagenesis, seventeen point mutations were generated in Gdt1p including twelve amino acids within the two consensus motifs E-Ø-G-D-(KR)-(ST) (Figure 43). Gdt1p mutants were screened in the yeast strain lacking both Gdt1p and Pmr1p (*gdt1Δ/pmr1Δ*) for (i)  $\text{Ca}^{2+}$  tolerance and (ii)  $\text{Ca}^{2+}$  response to saline stress. Amongst all Gdt1p mutations, four acidic residues (E<sub>53</sub>, D<sub>56</sub>, E<sub>204</sub> and D<sub>207</sub>) and two uncharged polar residues (T<sub>58</sub> and S<sub>209</sub>) affected both *gdt1Δ/pmr1Δ* growth under high  $\text{CaCl}_2$  concentration and  $\text{Ca}^{2+}$  response after a saline stress. Thus, the  $\text{Ca}^{2+}$  binding pocket of Gdt1p seems to be likely made of these acidic and polar amino acid residues found in the repeated consensus motif share by all UPF0016 members. Further investigations in TMEM165 could be of interest to reinforce the conservation of function for both proteins.

From these studies, TMEM165 and Gdt1p were supposed to be part of a novel family of Golgi-localized  $\text{Ca}^{2+}/\text{H}^+$  antiporters, differing from the well-known CaCA superfamily for sequence homology reasons. Further studies in TMEM165-CDG patients' cells, yeast and conditional mouse knockout for TMEM165 then strengthened the link between TMEM165/Gdt1p and pH regulation.



### 3.1.2. TMEM165 and Gdt1p in pH regulation

- Over acidification of the Golgi apparatus and acidic compartments in TMEM165-depleted cells

From the pioneering study on TMEM165, Foulquier *et al.* suggested a role for TMEM165 as a proton ( $H^+$ ) transporter based on its topology [64]. Although no direct link between TMEM165 and Golgi pH homeostasis was demonstrated, TMEM165 deficiency results in pH disruption of the acidic compartments. Indeed, using pH-sensitive probes (LysoTracker and LysoSensor green DND189), a general decrease in the pH of late endosomes and lysosomes was observed in TMEM165-CDG patients' fibroblasts as well as in *siTMEM165* HeLa cells [304]. Moreover, a very recent study provides more evidences for TMEM165  $H^+$  transport activity. Using *in situ* fluorescent and photoacoustic imaging of Golgi pH, an acidification of the Golgi apparatus was observed in TMEM165-depleted HL7702 cells [502]. To reinforce TMEM165 involvement in  $H^+$  exit from the Golgi apparatus, HL7702 cells were treated with both thapsigargin and calcium in order to increase cytosolic calcium concentration. Thereby, this should favor the transport of cytosolic  $Ca^{2+}$  to the Golgi lumen in exchange for luminal  $H^+$  export, mediated by TMEM165. Compared to control cells, Golgi pH was again more acidic in *siTMEM165* HL7702, providing stronger evidences for TMEM165 involvement in Golgi pH homeostasis and  $H^+$  transport activity [502].

- Gdt1p involvement in Golgi  $H^+$  homeostasis in yeast

As described earlier, when expressed in *Lactococcus lactis*,  $\Delta^{23}$ Gdt1p mediates  $Ca^{2+}$  influx from the external medium to the cytoplasm across the plasma membrane, depending on pH gradient. Interestingly, such  $H^+$ -dependent  $Ca^{2+}$  activity for Gdt1p was further investigated during the Golgi glycosylation process - back in the yeast model *Saccharomyces cerevisiae* [501]. Basically, most of the GT involved in a glycosylation reaction use nucleotide sugar diphosphate as donors and release the free associated nucleotide diphosphate. This latter is then converted to nucleotide monophosphate plus inorganic phosphate (Pi) and  $H^+$  as byproducts of the reaction. Although luminal nucleotide monophosphate is exchanged to cytoplasmic nucleotide sugar *via* the same nucleotide sugar transporter, little is known about the recycling of Pi and  $H^+$ . In this context, Snyder *et al.* demonstrated the contribution of Erd1p and Gdt1p in these two recycling mechanisms. On the one hand, Erd1p would export Pi from the Golgi lumen to the cytosol. On the other hand, Gdt1p would remove  $H^+$  from the Golgi while importing cytosolic  $Ca^{2+}$  to the Golgi lumen [501]. It is to note that Gdt1p could also work in a reverse mode according to pH variations between the cytosol and the Golgi lumen. Indeed, in case of deletion of the V-ATPase proton pump, an increased cytosolic  $Ca^{2+}$  concentration was observed

suggesting that Gdt1p might import cytosolic  $H^+$  to acidify the Golgi apparatus by releasing  $Ca^{2+}$  to the cytoplasm [501]. Thus, this study points out a reverse role for Gdt1p in  $Ca^{2+}$  import (export) to the Golgi lumen (cytoplasm) depending on the pH gradient established by the V-ATPase. Gdt1p could then be considered as a key player in both  $Ca^{2+}$  and  $H^+$  regulations at the Golgi level.

- TMEM165 involvement in lactose biosynthesis during milk production

In mammals, milk production occurs during mammary glands lactation and involves the biosynthesis of lactose and the formation of  $Ca^{2+}$ -casein enriched micelles. Calcium is highly concentrated in milk, ranging between 30 and 80mM whereas its concentration in human blood only reaches 2 to 2.5mM. Many  $Ca^{2+}$  transporters, channels and binding proteins are involved in its transport from/within the mammary epithelial cells into milk. Acting as a  $Ca^{2+}/H^+$  exchanger in the Golgi apparatus, TMEM165 could be an additional  $Ca^{2+}$  transporter in lactating mammary gland cells. First, according to the Gene Expression Omnibus at NCBI, TMEM165 mRNA levels are found 7-times upregulated during the secretory phase of lactation [503,504]. At the protein level, TMEM165 expression is increased by 25-fold in mammary glands in lactation, especially in the alveolar epithelial cells where it displays a Golgi localization [503,504]. Second, TMEM165 is upregulated in PMCA2-deficient mice, which is a hallmark of many  $Ca^{2+}$  transporters during lactation [503]. Therefore, in line with its subcellular localization and its function as a  $Ca^{2+}/H^+$  antiporter, TMEM165 was thought to parallel SPCA1 by importing cytosolic  $Ca^{2+}$  within the Golgi lumen while removing  $H^+$  excess especially due to the high rates of lactose synthesis during milk production (Figure 44).

Lactose synthesis is indeed achieved in the Golgi apparatus, from glucose and UDP-galactose through the activity of an enzymatic complex named lactose synthase. This complex includes two subunits, each of them requiring a cation as a cofactor ( $Mn^{2+}$ ) or nutrient ( $Ca^{2+}$ ) for maximal activity: a Mn-dependent  $\beta$ -1,4-galactosyltransferase and a Ca-binding protein  $\alpha$ -lactalbumin. During the transfer of galactose from UDP-galactose onto glucose, a first  $H^+$  is released in the Golgi lumen. Then, a second  $H^+$  is generated with  $P_i$  following the hydrolysis of UDP to UMP. Thus, two  $H^+$  are released in the Golgi lumen for one lactose moiety (Figure 44). In case of milk production, lactose concentration can reach up to 100mM in the Golgi lumen, increasing massively the release of  $H^+$ .

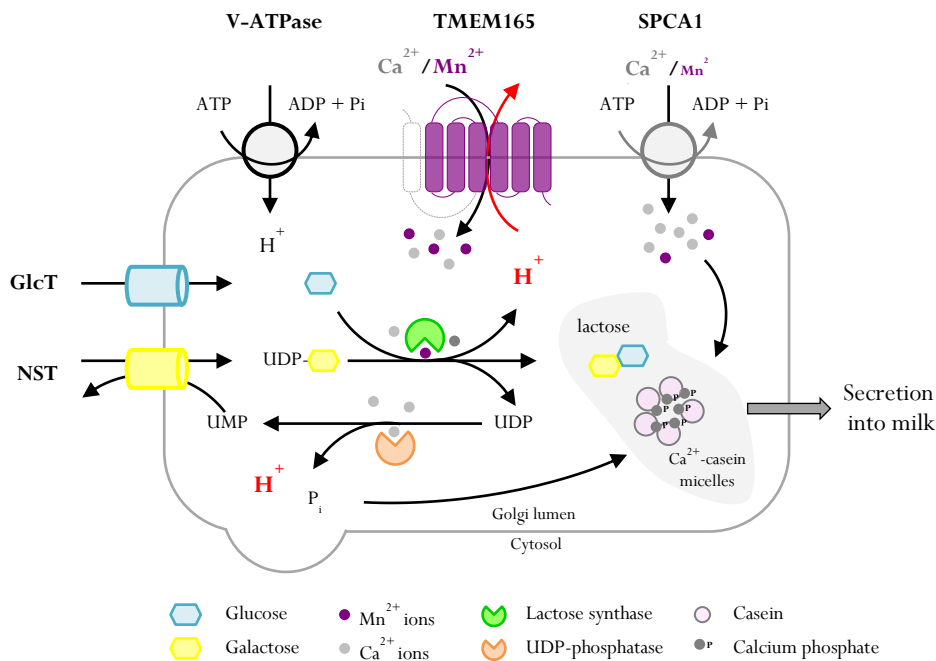


**Figure 44: Putative involvement of TMEM165 as a Ca<sup>2+</sup>, Mn<sup>2+</sup> and H<sup>+</sup> transporter supporting lactose biosynthesis during milk production in mammary glands in lactation.** Lactose biosynthesis occurs in the Golgi lumen and requires both UDP-galactose transport by a nucleotide-sugar transporter (NST) and glucose import by a glucose transporter (GlcT). Then, the Mn<sup>2+</sup>/Ca<sup>2+</sup>-dependent lactase synthase (green pacman) transfers UDP-galactose onto glucose, releasing UDP and a first proton (H<sup>+</sup>). UDP is then hydrolyzed into UMP and Pi by a Ca<sup>2+</sup>-dependent UDP-phosphatase (orange pacman), releasing a second H<sup>+</sup>. Both Pi and H<sup>+</sup> need to be recycled in order to prevent lactose synthase inhibition. Pi can complex with Ca<sup>2+</sup>, Mg<sup>2+</sup> and casein to form Ca<sup>2+</sup>-casein micelles and then be secreted into milk. On the other hand, luminal H<sup>+</sup> are thought to be exchanged by TMEM165 for Ca<sup>2+</sup> and/or Mn<sup>2+</sup> to sustain lactose biosynthesis and prevent Golgi acidification. In such context, TMEM165 indeed parallels SPCA1, the latter being mainly involved in Ca<sup>2+</sup> import. Inspired by Snyder et al. [504].

To prevent both acidification of the Golgi apparatus and lactose synthase inhibition, a passive transport of luminal H<sup>+</sup> to the cytosol may occur. This was the first hypothesized function for TMEM165 [64], reiterate by Reinhardt et al. [503] and Snyder et al. in a more recent study [504]. Using conditional *Tmem165* knockout mice, strong defect in milk quality from TMEM165-deficient dams were observed. Lower lactose, calcium and manganese levels were measured in this milk, not allowing the proper feeding and growing of the pups nursed by TMEM165-deficients mice [504]. Although *in vitro* lactose synthase activities were similar between TMEM165-depleted and control mammary gland cells, the *in vivo* activity was thought to be severely reduced in cells lacking TMEM165. Assuming that TMEM165 could export luminal H<sup>+</sup> in exchange for cytoplasmic Mn<sup>2+</sup> or Ca<sup>2+</sup>, in case of TMEM165 deficiency, a more acidic Golgi lumen and a lower availability for Mn<sup>2+</sup> and Ca<sup>2+</sup> may alter lactose synthase activity. Thus, as depicted in Figure 44, TMEM165 should play a crucial role in lactose biosynthesis during milk production, supporting lactose synthase activity by importing both cytosolic Mn<sup>2+</sup> and Ca<sup>2+</sup> to the Golgi lumen of professional secretory cells in exchange for H<sup>+</sup>.

Altogether, these studies shed light on TMEM165 and Gdt1p involvement in pH homeostasis and  $H^+$  transport activities. This is even truer in the context of Golgi glycosylation where  $H^+$  is a byproduct of the reaction that need to be recycle. However, these roles for TMEM165 and Gdt1p as  $Ca^{2+}/H^+$  exchangers are not restricted as already evoked in the section above. In the light of further investigations, strong evidences link TMEM165/Gdt1p and Golgi manganese homeostasis which is easily conceivable regarding to the function of other UPF0016 members in manganese homeostasis in plants and cyanobacteria (see 2.2.3.).

### 3.1.3. TMEM165 and Gdt1p in manganese (Mn) homeostasis

- TMEM165 and Gdt1p deficiencies alter Golgi  $Mn^{2+}$  homeostasis

A first clue linking TMEM165 deficiency and Golgi  $Mn^{2+}$  homeostasis was given through the observation that GPP130  $Mn^{2+}$  sensitivity was altered in shTMEM165 HEK cells [65]. Indeed, 4hr of treatment with 500 $\mu$ M  $MnCl_2$  induces a loss of 70% of expression in control cells while GPP130 remains quite stable in shTMEM165 (90% left). Thus, GPP130 is almost insensitive to  $MnCl_2$  treatment in TMEM165 depleted cells. Assuming that GPP130 stability strictly depends on Golgi  $Mn^{2+}$  concentration, it was then hypothesized that TMEM165 could play a role in  $Mn^{2+}$  import from the cytosol to the Golgi lumen [65]. This  $Mn^{2+}$  import would require the export of a counter ion which nature is still unclear. One can suppose that the  $Ca^{2+}$  gradient within the Golgi lumen established through the activity of SPCA could be used by TMEM165 to import  $Mn^{2+}$ . On the other hand, if SPCA pumps more cytosolic  $Mn^{2+}$  than  $Ca^{2+}$ , the gradient would be reversed and a  $Ca^{2+}$  import by TMEM165 is then conceivable (Figure 45).

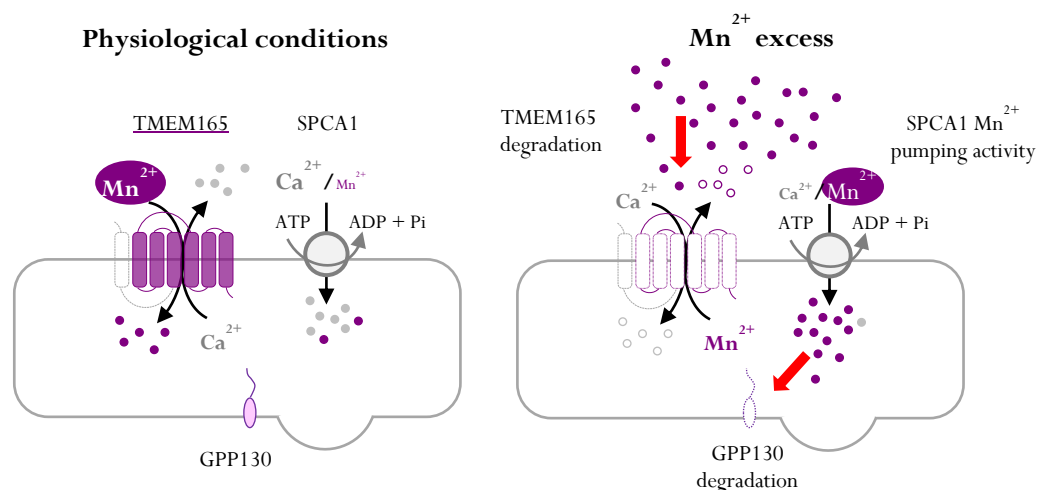


**Figure 45: Putative role of TMEM165 in Golgi  $Mn^{2+}$  homeostasis in physiological conditions and in case of  $Mn^{2+}$  excess.** In physiological conditions, TMEM165 would import cytosolic  $Mn^{2+}$  against luminal  $Ca^{2+}$  thanks to the  $Ca^{2+}$  gradient established by SPCA1. In contrast, in case of  $Mn^{2+}$  excess, SPCA1 would preferentially pump  $Mn^{2+}$  and create a  $Mn^{2+}$  gradient that could be used by TMEM165 to transport  $Mn^{2+}$  back to the cytosol. In such conditions, TMEM165 is also degraded (dotted protein) probably to prevent this phenomenon leading to cell death. Purple and gray dots respectively represent  $Mn^{2+}$  and  $Ca^{2+}$  ions.

However, although plausible, these two related models exclude the H<sup>+</sup> transport activity of TMEM165 [65,66]. To conclude, albeit indirectly evidenced, TMEM165 play a role in Golgi Mn<sup>2+</sup> homeostasis. With regards to the yeast ortholog Gdt1p, its involvement in Mn<sup>2+</sup> homeostasis will be further described in the section 3.2.3, also assessing its role in Golgi glycosylation.

- Truncated TMEM165 and Gdt1p.Mn<sup>2+</sup> transport activities

As for Ca<sup>2+</sup> transport activity (see 3.1.1.), both *TMEM165* and *GDT1* were expressed in the bacterial host *Lactococcus Lactis* to determine their abilities to transport Mn<sup>2+</sup> [28,306]. These two independent studies from the same group took advantage of the Mn<sup>2+</sup>-induced quenching of Ca<sup>2+</sup> probe Fura-2 emitted fluorescence to highlight a Mn<sup>2+</sup> influx across the plasma membrane mediated by  $\Delta^{78}$ TMEM165 or  $\Delta^{23}$ Gdt1p in bacteria expressing either  $\Delta^{78}$ TMEM165 or  $\Delta^{23}$ Gdt1p. This technique allowed the determination of their apparent K<sub>M</sub> for Mn<sup>2+</sup>: 170 ± 30μM for  $\Delta^{78}$ TMEM165 and 83.2 ± 9.8μM for  $\Delta^{23}$ Gdt1p. Further experiments demonstrated a competition effect between Mn<sup>2+</sup> and Ca<sup>2+</sup> transport resulting in a higher affinity of both proteins for Ca<sup>2+</sup> than Mn<sup>2+</sup>. Thus, TMEM165 and Gdt1p can mediate Ca<sup>2+</sup> and Mn<sup>2+</sup> transport through the plasma membrane in *Lactococcus lactis* with a higher affinity for Ca<sup>2+</sup>. Lastly, in *gdt1Δ* and *gdt1Δ/pmr1Δ* yeasts, authors further investigate such Mn<sup>2+</sup> transport activity and highlighted their role in Mn<sup>2+</sup> tolerance [28,306]. Therefore, these two studies place TMEM165 and Gdt1p as novel proteins involved in Ca<sup>2+</sup> and Mn<sup>2+</sup> intracellular yeast/human homeostasis. More precisely, TMEM165 and Gdt1p would (i) feed the Golgi apparatus with Ca<sup>2+</sup> and Mn<sup>2+</sup> and (ii) act in concert with Pmr1p in cytosolic detoxifying in case of Mn<sup>2+</sup> excess.

#### 3.1.4. TMEM165 and Gdt1p transport activities: Why choosing? Ca<sup>2+</sup>, Mn<sup>2+</sup> and H<sup>+</sup> all at once!

Since a decade, the functions of TMEM165 and Gdt1p, amongst other UPF0016 members, have been deeply investigated [28,239,304,306,307,501–504]. TMEM165 and Gdt1p are both secondary active antiporters embedded in the membrane of the Golgi apparatus. First identified as Ca<sup>2+</sup>/H<sup>+</sup> exchangers, TMEM165 and Gdt1p were then thought to be Ca<sup>2+</sup>/Mn<sup>2+</sup> transporters. Both TMEM165 and Gdt1p Ca<sup>2+</sup> and Mn<sup>2+</sup> transport activities were assessed through *in vivo* experiments in the bacterial strain *Lactococcus Lactis* [28,239,306]. From this, both proteins were described as Mn<sup>2+</sup>-Ca<sup>2+</sup>/H<sup>+</sup> exchangers, sharing a higher affinity for Ca<sup>2+</sup> than for Mn<sup>2+</sup>. The same function was assigned for TMEM165 in lactating mammary gland cells to support lactose biosynthesis during milk production (Figure 44) [501,503,504].

Regarding to the amino acid residues involved in the ion transport activity of both proteins, Colinet et al. first highlighted six amino acids (E<sub>53</sub>, D<sub>56</sub>, T<sub>58</sub>, E<sub>204</sub>, D<sub>207</sub> and S<sub>209</sub>) crucial for Gdt1p Ca<sup>2+</sup> transport function [305]. On the other hand, in the human ortholog, Lebredonchel et al. recently shown that the conserved threonine and serine residues (T<sub>113</sub> and S<sub>253</sub>) were important for TMEM165 function in glycosylation and especially in Mn<sup>2+</sup> transport activity [477]. Thus, from yeast to human, these two specific polar residues are well conserved and are essential for the cation transport activity of TMEM165 and Gdt1p. To add a layer of complexity, as secondary active antiporters transport an ion against its electrochemical gradient powered by the transport of a coupled ion following its electrochemical gradient, TMEM165 and Gdt1p can also work in a reverse mode according to Ca<sup>2+</sup>, Mn<sup>2+</sup> and H<sup>+</sup> gradients established between the Golgi lumen and the cytosol. This was already evidenced for Gdt1p, whose Ca<sup>2+</sup> pumping activity could be reversed by a pH disruption [501]. Hence, the nature of the ionic driving force required for TMEM165 and Gdt1p for exchanging Ca<sup>2+</sup> to Mn<sup>2+</sup> or Ca<sup>2+</sup> and/or Mn<sup>2+</sup> to H<sup>+</sup> may change according to cell conditions. To conclude, depending on cell physiology and numerous other transporters, both proteins play a role in all three homeostasis at the Golgi level: H<sup>+</sup>, Ca<sup>2+</sup> and Mn<sup>2+</sup>, acting either as Ca<sup>2+</sup>/Mn<sup>2+</sup> or Ca<sup>2+</sup> and/or Mn<sup>2+</sup>/H<sup>+</sup> exchangers.

## 3.2. TMEM165 and Gdt1p involvements in glycosylation

### 3.2.1. TMEM165-CDG

- TMEM165-CDG reported cases

As already mentioned earlier, four patients' mutations have been reported and carried by seven patients (section 1.3., Table 20). Most of them were identified and characterized in 2012 by the same research group (P1 to P5) [64,505] and the two last were identified in 2016 (P6 and P7) [487]. As for many CDG, all TMEM165-CDG patients harbor a broad range of clinical features: growth and psychomotor retardations, failure to thrive, facial dysmorphism, muscular weakness, fat excess and abnormal distribution, joint laxity and some of them have liver disorder, epilepsy and fever episodes. Despite this heavy clinical picture, the main phenotype distinguishing TMEM165-CDG from others lies in the severe skeletal anomalies shared by most of the patients. Indeed, four TMEM165-CDG patients present a short stature associated with dwarfism, scoliosis, and severe osteoporosis with very thin bone cortex and dysplastic vertebrae, ribs and toenails. Clinically speaking, bone defects observed in TMEM165-CDG can be classified as spondylo-epi-(meta)-physeal dysplasia [505]. Linking *TMEM165* mutation and skeletal anomalies, patients carrying the splice mutation present the more severe defects.

- Mutated TMEM165 expression pattern

*TMEM165* patients' mutations cause changes in the encoded protein as described in Table 20. Mutated *TMEM165* protein expression and subcellular localization were assessed by western blot and immunofluorescence analyses in patients' fibroblasts. Compare to control, *TMEM165* protein expression is dramatically decreased in patients (P1-3) sharing the splicing mutation (c.792+182 G>A). Almost no full length and either no truncated protein expression was observed. For P4 harboring the missense mutation R126H, mutated *TMEM165* was reported to be unstable as only 25% of protein expression left. A stable expression of *TMEM165* was only seen in P5, even if this protein contains two point mutations (R126C and G304R). With regards to the subcellular localization, in all five patients *TMEM165* is Golgi-localized. However, different intensities were observed: the highest for P5, then P4 and a very weak signal was observed for P1-3 [64]. To further characterize *TMEM165* patients' mutations, Rosnoblet *et al.* reproduced them and transiently expressed WT-, R126H-, R126C-, G304R- and both R126C/G304R-*TMEM165* constructs in HeLa cells [488]. As observed in patients' cells, the splicing mutation completely prevents the expression of *TMEM165* after transient expression in HeLa cells. Moreover, while WT-*TMEM165* was equally expressed in the *trans*-Golgi and in lysosomes/endosomes, R126H- and R126C-*TMEM165* were reversely more localized in the lysosomes/endosomes than in the Golgi apparatus. Thus, both point mutations lead to the mislocalization of the protein in the late acidic compartments of the secretory pathway. As regards for G304R- and both R126C/G304R-*TMEM165*, proteins were well Golgi-localized. Hence, G304R point mutation seems to retain *TMEM165* in the Golgi apparatus. All in all, mutations identified in *TMEM165* leading to a CDG-II affect both stability and subcellular localization of the protein that may affect *TMEM165* function.

- *TMEM165* deficiency and glycosylation defects

*TMEM165* identification in a CDG implies somehow a glycosylation defect. All patients were diagnosed as type II CDG based on serum-transferrin isoelectric focusing (sTf-IEF). Type II CDG results in a Golgi glycosylation defects due to either N-glycans, O-linked glycans, GAGs and/or glycolipids biosynthesis defect. To fine tune Golgi glycosylation in *TMEM165*, diverse approaches were used. First, siRNA, shRNA and finally *TMEM165* KO HEK cells were generated to further studied the impact of *TMEM165* on Golgi glycosylation [64–66,506]. Then, *TMEM165* mutants were generated and transfected into HEK cells to pursue this goal [477]. Many tools were used to perform Golgi glycosylation studies and especially (i) mass spectrometry to analyze N-glycans, O-glycans and glycolipids from either engineered cells, patients sera or patients fibroblasts and (ii) western blot to look at the migration profile of two glycoproteins markers LAMP2 and TGN46.

Mass spectrometry analysis of total N-glycans from patients' sera highlighted an increase of abnormal N-glycans lacking both galactose and sialic acid residues [64]. Later, this lack of Golgi maturation was confirmed in shTMEM165 HEK cells through the accumulation of truncated agalactosylated and consequently asialylated N-glycans. Moreover, the absence of complex glycan structures attests from a severe Golgi processing defect in absence of TMEM165 [65]. Those results were reproducible in TMEM165 KO HEK cells [506] and highlight a strong galactosylation defect, a mild GlcNAcylation defect and a slight sialylation defect associated with a lack of TMEM165. Regarding the O-glycosylation, no clear defects in O-glycan structures were observed in both sera from patients and TMEM165 deficient cells [64]. This is consistent with the normal ApoC-III profile and suggests that TMEM165 deficiency may not impact the O-glycosylation process. However, in a later study, the undersialylation of O-glycan structures from patients' sera suggests a potential involvement of TMEM165 in the O-glycosylation process [507]. Nevertheless, further investigations need to be done to strengthen this link between TMEM165 and O-glycosylation. However, recent unpublished data highlight a significant VVL-FITC staining in TMEM165 KO HEK cells which was not observed in control cells. *Vicia villosa* lectin (VVL) recognizes preferentially  $\alpha$ - terminal GalNAc residue linked to serine or threonine in a polypeptide. This first GalNAc residue (also called Tn antigen) initiates the mucin type O-glycans and is supposed to be further substituted. Hence, VVL recognition in TMEM165 KO HEK cells suggests the presence of truncated O-glycan structures and may linked TMEM165 and impaired O-glycosylation. Next, looking at glycolipids, a decrease in glycosphingolipids (GLS) synthesis was observed in TMEM165 KO HEK cells. Only few traces of GM2 and GM3 were observed in those cells suggesting that a lack of TMEM165 impairs Gal/GalNAc transfer onto GSL [506]. Finally, TMEM165 deficiency also impacts GAG synthesis as depicted in morpholino *tmem165* zebrafish model where chondroitin sulfate (CS) proteoglycans expression is impaired [508].

All in all, TMEM165 deficiency leads to strong glycosylation defects in multiple pathways including N-glycosylation, GAG, and glycolipids synthesis. So far, no strong evidence linked TMEM165 deficiency with altered O-glycosylation.

- TMEM165-CDG animal models

As mentioned above in Table 21 (2.2.3), a mouse and a zebrafish model both lacking *Tmem165/tmem165* expression were generated to further study TMEM165 function. In mouse (*mus musculus*), *Tmem165* gene is located on chromosome 5 and encoded for a 323 amino acids protein that shares 92% of identity with human TMEM165. First mentioned by Reinhardt et al. in 2014 [503], C57BL/6 *Tmem165* knockout mice were reported online by the International Mouse Genotyping Consortium and the Infrafrontier



websites, both giving complementary data about their genotype and phenotype. Surprisingly, these mice failed to reproduce the severe skeletal abnormalities found in human TMEM165-CDG patients. Instead, they exhibited eye defects (abnormal cornea and iris morphologies) and an increased mean corpuscular volume. At that time, mouse lactation phenotype was not investigated. Then, in a later study still including Reinhardt, Snyder et al.[504] used conditional *Tmem165* deficient mice to further investigate the function of TMEM165 in lactating mammary glands (see 3.2.1.). *Tmem165* depletion only occurs in milk-producing alveolar epithelial cells at the rather high level of 85%. A more detailed methodology giving birth to these mice is well described in the experimental procedures section of the associated paper [504]. Thus, although mice model lacking *Tmem165* expression are sharing only few clinical features with human TMEM165-CDG patients, a better understanding of the role of TMEM165 during lactose synthesis was highlighted (see 3.2.1.).

With regards to the zebrafish (*Danio rerio*), a single ortholog for TMEM165 was found. Encoded by *tmem165* gene, *Tmem165* shares 79% identity with human TMEM165. Moreover, *Tmem165* expression is stable during early development *i.e.* the first week post-fertilization [508]. Therefore, using a morpholino approach, Bammens et al., reported the developmental impact of *tmem165* deficiency in zebrafish [508]. Briefly, *tmem165* morphants exhibited strong skeletal defects reflected by shorter seizure, craniofacial abnormalities and altered cartilage and bones formation. All of these skeletal anomalies are consistent with those observed in human TMEM165-CDG patients [64,505]. Besides, the human patient mutation R126H was reproduced in the zebrafish, leading to R106H replacement and failed to rescue the cartilage alterations observed in the morphants. Therefore, the pathogenicity of such human mutation is also pathogenic for the zebrafish. At the cellular level, using different markers of chondrogenesis, *tmem165* deficiency impairs the latter stage of chondrocyte maturation. Moreover, bone mineralization defects were also shown in those morphants resulting from a disrupted osteoblast maturation. All in all, *tmem165* zebrafish morphants mirror *TMEM165* human deficiency and linked for the first TMEM165 function to skeletal anomalies. This model should allow further investigations on the function of TMEM165 in both physiological and pathophysiological conditions.

### 3.2.2. Gdt1p involvement in glycosylation under high external [CaCl<sub>2</sub>] and in yeast lacking Pmr1p

Many years ago Antebi and Fink [236] followed by Dürre et al. [238] found that yeast lacking Pmr1p, the only Ca<sup>2+</sup>/Mn<sup>2+</sup> Golgi ATPase, presented N- and O-linked glycosylation abnormalities. These results were based on the faster gel mobility of N-glycosylated invertase and O-glycosylated chitinase. At the time, both Ca<sup>2+</sup> and Mn<sup>2+</sup> requirements were assigned to sustain the glycosylation as either CaCl<sub>2</sub> or MnCl<sub>2</sub> supplementations partially rescued those defects [236,238].

More recently, Gdt1p was described as a new Golgi localized  $\text{Ca}^{2+}$ - $\text{Mn}^{2+}/\text{H}^+$  transporter. As already mentioned, the yeast null mutant *gdt1Δ* exhibits a strong growth defect when cultured in the presence high external  $\text{CaCl}_2$  concentrations [304]. To address whether this growth deficiency was linked to glycosylation abnormalities, N- and O-linked glycosylation were assessed thanks to the migration profile of different glycosylation markers (secreted invertase, carboxypeptidase Y (CPY) and Gas1p), in parallel with those obtained in *pmr1Δ* [65,239,240]. While secreted invertase and CPY are only highly N-glycosylated, Gas1p possesses both N- and O-linked glycans. In line with previous studies, in *pmr1Δ* yeast all three proteins migrates faster reflecting a lack of N- and/or O-linked glycans. Increasing  $\text{CaCl}_2$  concentrations in the culture medium altered the migration profiles of the three proteins in *gdt1Δ* whereas those migration profiles were partially rescued in *pmr1Δ* [65,239,240]. Moreover, in the double yeast mutant *gdt1Δ/pmr1Δ*, glycosylation defects were also observed without  $\text{CaCl}_2$  excess and couldn't be restored by  $\text{CaCl}_2$  complementation. This was confirmed at the structural level *via* NMR experiments on total mannans in wild-type, *gdt1Δ*, *pmr1Δ* and *gdt1Δ/pmr1Δ*. In resting conditions, wild-type and *gdt1Δ* strains exhibit similar mannosylation patterns whereas both *pmr1Δ* and *gdt1Δ/pmr1Δ* possess lesser branched mannans mostly lacking  $\alpha$ -1,2-mannose substitutions and  $\alpha$ -1,3-mannose terminations [240]. On the other hand, in the presence of 500 $\mu\text{M}$   $\text{CaCl}_2$ , this branching mannans defect was induced in *gdt1Δ* and *gdt1Δ/pmr1Δ* while it was abolished in *pmr1Δ* [240]. All in all, Gdt1p is required to sustain both N- and O-glycosylation (i) under high external  $\text{CaCl}_2$  concentrations and (ii) in yeast lacking Pmr1p through its ability to transport  $\text{Ca}^{2+}$ .

### 3.2.3. Link between TMEM165 and Gdt1p function in glycosylation and $\text{Mn}^{2+}$ homeostasis

To the yeast side, a first clue linking Gdt1p function in glycosylation and  $\text{Mn}^{2+}$  homeostasis was given by the observation that addition of 50 $\mu\text{M}$   $\text{MnCl}_2$  to the Ca-enriched medium of *gdt1Δ* suppressed the observed glycosylation defects [65,239]. In addition, comparing *gdt1Δ*, *pmr1Δ* and *gdt1Δ/pmr1Δ* yeast mutants,  $\text{MnCl}_2$  complementation rescues all the glycosylation defects due to Pmr1p deficiency or both Gdt1p and Pmr1p deficiencies [23,31]. At the structural level, this  $\text{MnCl}_2$  supplementation resulted in the suppression of the branching mannan defects [240]. Therefore, a lack of Gdt1p and/or Pmr1p would alter the Golgi  $\text{Mn}^{2+}/\text{Ca}^{2+}$  homeostasis then impairing the activity of Golgi mannosyltransferases (ManT), most of them being Mn-dependent (*i.e.* Mnn1p, Mnn2p, Mnn5p and Mnn6p). Hence, Gdt1p is required for its activity in both  $\text{Mn}^{2+}$  and  $\text{Ca}^{2+}$  homeostasis to sustain the glycosylation process in absence of Pmr1p. This shed light on a functional link between Gdt1p and Pmr1p in Golgi glycosylation that will be further discussed in the Results, Part II of this manuscript.

In mammalian cells, a similar study was done in TMEM165 KO cells by analyzing the migration profile of two heavily glycosylated proteins (LAMP2 and TGN46) and by mass spectrometry analysis of the total N-glycans [65,231,506,509]. MnCl<sub>2</sub> supplementation ranging from 100nM to 50μM rescued the gel mobility of LAMP2 and TGN46 and abolished the galactosylation defects associated with the lack of TMEM165. Thus, TMEM165 deficiency would also affect Golgi Mn<sup>2+</sup> homeostasis, therefore altering the Golgi glycosylation process by impairing the activity of Mn-dependent glycosyltransferases such as galactosyltransferases (GalT).

These observations highlight three major differences between yeast and human. First, TMEM165 deficiency leads to severe glycosylation defects while a lack of Gdt1p only affect the glycosylation process when exposed to high external CaCl<sub>2</sub> concentrations. This suggests distinct involvements for TMEM165 and Gdt1p in glycosylation. Second, strong glycosylation abnormalities characterized the yeast null mutant *pmr1Δ* while in human, no direct link between glycosylation and SPCA1 (Pmr1p human ortholog) deficiency has been done yet. Third, further investigations demonstrate that Gdt1p function in glycosylation was Pmr1p-dependent [240].

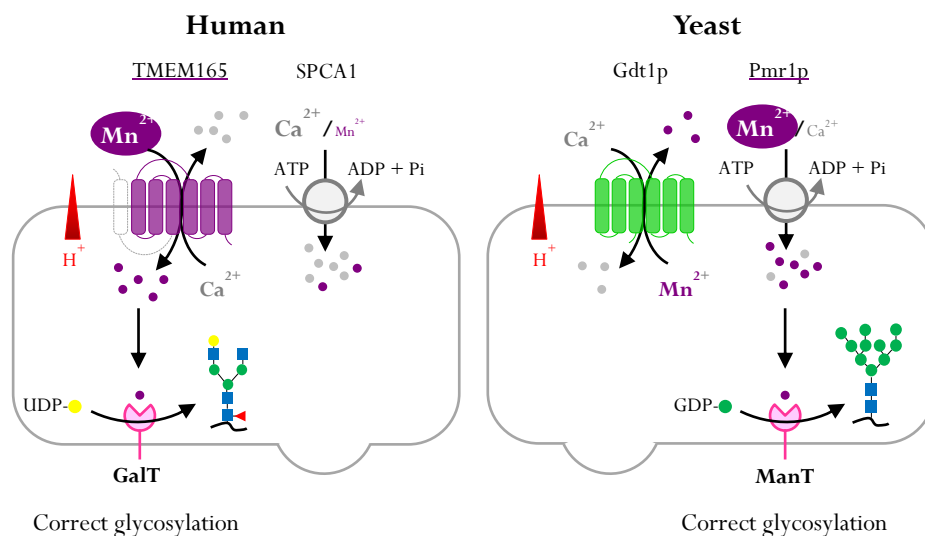


**Figure 46: Comparison between TMEM165 and Gdt1p function in Golgi glycosylation and Mn<sup>2+</sup> homeostasis.** To the human side, TMEM165 is considered as the major Golgi localized Mn<sup>2+</sup> transporter supposed to exchange cytosolic Mn<sup>2+</sup> for luminal Ca<sup>2+</sup> and/or H<sup>+</sup>. In human cells, TMEM165 involvement in Golgi Mn<sup>2+</sup> homeostasis drives the Golgi glycosylation by feeding the Golgi apparatus with Mn<sup>2+</sup>, crucial cofactors of many galactosyltransferases (GalT). On the other hand, in the yeast *Saccharomyces cerevisiae*, Gdt1p plays a minor role in Golgi Mn<sup>2+</sup> homeostasis. The main Golgi Mn<sup>2+</sup> importer is Pmr1p whose function is crucial in Golgi glycosylation as mannosyltransferases (ManT) require Mn<sup>2+</sup> as cofactor to be fully active.

In mammalian cells, although a functional link between TMEM165 and SPCA1 has been established, it does not rely on their function in glycosylation but on TMEM165 stability regarding SPCA1 ion pumping activity [461]. This will be further discussed in the Results, Part II of this manuscript.

All in all, these differences between yeast and human led us to support the following hypotheses: (i) in human cells, TMEM165 mainly transports cytosolic  $Mn^{2+}$  to feed the Golgi apparatus and sustain the glycosylation process while (ii) in yeast, Gdt1p  $Mn^{2+}$  activity is only required when those of Pmr1p is lacking.

#### 3.2.4. MnCl<sub>2</sub> and/or D-galactose supplementation suppress the glycosylation defects associated with TMEM165 deficiency

As mentioned above, slight exogenous  $MnCl_2$  concentrations are sufficient to suppress the N-glycosylation defects observed in TMEM165 KO cells. In particular, the severe galactosylation abnormalities resulting from a lack of TMEM165 were completely suppressed by such  $MnCl_2$  treatment [65,506]. The molecular mechanisms behind this  $Mn^{2+}$ -induced glycosylation rescue in absence of TMEM165 remains unclear and will be further developed in the Results, Part I of the manuscript. However, this *in vitro* beneficial  $MnCl_2$  effect gives a glimpse of a potential therapeutic approach to treat TMEM165-CDG patients as it has already been done for SLC39A8-CDG, another CDG in which Golgi  $Mn^{2+}$  homeostasis is also impaired [67,68]. Back to the strong galactosylation defects associated with TMEM165 deficiency, another way to suppress them was to increase the GalT substrate, *i.e.* UDP-galactose, to enhance its galactosylation activity. This was first achieved *in vitro* by treating TMEM165 KO cells with D-galactose. Mass spectrometry analysis of total N-glycans indeed demonstrate the positive effect of such treatment by restoring complex galactosylated and sialylated glycan structures. As D-galactose was already used to treat other CDG such as SLC39A8-CDG or PGM1-CDG [82], this treatment was rapidly developed for TMEM165-CDG patients. A clinical trial involving two patients confirmed the beneficial effect of a daily dose of 1g/kg of D-galactose [506]. Biochemical and clinical parameters improved during the galactose therapy such as the increased of sialylated forms of the transferrin and the decrease of hypogalactosylation total N-glycan structures. From this study, the use of D-galactose was therapeutically recommended for TMEM165-CDG patients [506]. Again, the precise mechanism by which oral galactose supplementation significantly suppresses the N-glycosylation defects in TMEM165 deficient cell is still unclear. Some arguments will be further developed in the Results, Part I of this manuscript, in addition to explanations about the efficacy of combined D-galactose and  $MnCl_2$  supplementation already obtained *in vitro*.

## PhD objectives

Since almost a decade now, substantial work has been done by our lab to unravel the biological function of TMEM165 and its proper role in Golgi glycosylation. Given that *TMEM165* does not encode for a GT nor a NST, the glycosylation defects associated to its deficiency are secondary. At the beginning of my PhD, a link between TMEM165 and  $Mn^{2+}$  homeostasis was established since (i) the lack of TMEM165 alters Golgi  $Mn^{2+}$  homeostasis, (ii) TMEM165 is a  $Mn^{2+}$ -sensitive protein and (iii) N-glycosylation defects observed in TMEM165 deficient cells can be suppressed by  $MnCl_2$  supplementation. However, the mechanisms beyond these observations were far from being elucidated.

Therefore, the **first objective** of my PhD was to provide new insights into the mechanisms of  $Mn^{2+}$ -induced glycosylation rescue in TMEM165 deficient cells. Then, as a **second objective**, my PhD project focused on the potential functional links between TMEM165/Gdt1p and SPCA1/Pmr1p, two key players acting in the regulation of the secretory pathway ionic homeostasis in humans and yeast *Saccharomyces cerevisiae*, respectively.

Altogether, the ultimate goal of this PhD was to understand the molecular mechanisms of Golgi ion homeostasis maintenance to sustain Golgi glycosylation reactions in both yeast *Saccharomyces cerevisiae* and human cells.



---

## Results

---





## 1. - Part I -

---

### **Insights into the Mn<sup>2+</sup>-induced Golgi glycosylation rescues in TMEM165 KO HEK cells.**

---

**Paper 1:** Involvement of thapsigargin and cyclopiazonic acid sensitive pumps in the Mn<sup>2+</sup>-induced LAMP2 glycosylation rescue in TMEM165 KO HEK cells

**Paper 2:** Fetal Bovine Serum impacts the observed N-glycosylation defects in TMEM165 KO HEK cells

# **1. Paper 1: Involvement of thapsigargin and cyclopiazonic acid sensitive pumps in the Mn<sup>2+</sup>-induced LAMP2 glycosylation rescue in TMEM165 KO HEK cells**

## **1.1. Introduction**

As just described in the last introductory chapter (Chapter 3), substantial work has been done to decipher the biological function(s) of TMEM165. At the beginning of my PhD, two publications from the team highlighted that (i) Golgi glycosylation defects due to TMEM165 deficiency resulted from a disrupted Golgi Mn<sup>2+</sup> homeostasis (February 2016) [65] and (ii) both D-galactose or MnCl<sub>2</sub> supplementations in the culture medium could rescue the Golgi glycosylation defects observed on N-glycan structures in TMEM165 KO cells (December 2016) [506]. Hence, at the time, the state-of-the-art had just linked TMEM165 function and Golgi Mn<sup>2+</sup> homeostasis. However, the molecular mechanism by which exogenous MnCl<sub>2</sub> led to the suppression of the N-glycosylation defects associated with TMEM165 deficiency was unknown and actually defined the starting point of my PhD. As the main objective of this work, we wondered: how does extracellular MnCl<sub>2</sub> rescue the N-glycosylation defects in absence of TMEM165? Using control and isogenic TMEM165 KO HEK cells, I first developed a qualitative biochemical tool to easily assess the cellular N-linked glycosylation status using the electrophoretic migration profile of the lysosomal glycoprotein LAMP2 as a “glycomarker”. Then, assuming that extracellular MnCl<sub>2</sub> can either enter the cell by crossing the plasma membrane through a plethora of (un)specific transporters or channels or, be internalized *via* endocytosis, I further investigated the intracellular pathway(s) by which cytosolic MnCl<sub>2</sub> could reach the Golgi lumen. At the time, current knowledge on the regulation of human Golgi Mn<sup>2+</sup> homeostasis pointed out the potential role of SPCA1, the only known Golgi Ca<sup>2+</sup>/Mn<sup>2+</sup> P-type ATPase.

## **1.2. Publication**

# Involvement of thapsigargin and cyclopiazonic acid-sensitive pumps in the rescue of TMEM165-associated glycosylation defects by Mn<sup>2+</sup>

Marine Houdou,\* Elodie Lebredonchel,\* Anne Garat,<sup>†</sup> Sandrine Duvet,\* Dominique Legrand,\* Valérie Decool,<sup>†</sup> André Klein,\* Mohamed Ouzzine,<sup>‡</sup> Bruno Gasnier,<sup>§</sup> Sven Potelle,<sup>\*,1</sup> and François Foulquier<sup>\*,1,2</sup>

\*Centre National de la Recherche Scientifique (CNRS), Unité Mixte de Recherche (UMR) 8576, Unité de Glycobiologie Structurale et Fonctionnelle (UGSF), <sup>†</sup>Centre Hospitalier Universitaire (CHU) Lille, Institut Pasteur de Lille, Equipe d'Accueil (EA) 4483, Impact de l'Environnement Chimique sur la Santé Humaine (IMPECS), University of Lille, Lille, France; <sup>‡</sup>UMR 7365, Centre National de la Recherche Scientifique (CNRS)–Université de Lorraine, Biopôle-Faculté de Médecine, Vandoeuvre-lès-Nancy, France; and <sup>§</sup>Neurophotonics Laboratory, CNRS UMR 8250, Paris Descartes University, Sorbonne Paris Cité, Paris, France

**ABSTRACT:** Congenital disorders of glycosylation are severe inherited diseases in which aberrant protein glycosylation is a hallmark. Transmembrane protein 165 (TMEM165) is a novel Golgi transmembrane protein involved in type II congenital disorders of glycosylation. Although its biologic function is still a controversial issue, we have demonstrated that the Golgi glycosylation defect due to TMEM165 deficiency resulted from a Golgi Mn<sup>2+</sup> homeostasis defect. The goal of this study was to delineate the cellular pathway by which extracellular Mn<sup>2+</sup> rescues N-glycosylation in TMEM165 knockout (KO) cells. We first demonstrated that after extracellular exposure, Mn<sup>2+</sup> uptake by HEK293 cells at the plasma membrane did not rely on endocytosis but was likely done by plasma membrane transporters. Second, we showed that the secretory pathway Ca<sup>2+</sup>-ATPase 1, also known to mediate the influx of cytosolic Mn<sup>2+</sup> into the lumen of the Golgi apparatus, is not crucial for the Mn<sup>2+</sup>-induced rescue glycosylation of lysosomal-associated membrane protein 2 (LAMP2). In contrast, our results demonstrate the involvement of cyclopiazonic acid- and thapsigargin (Tg)-sensitive pumps in the rescue of TMEM165-associated glycosylation defects by Mn<sup>2+</sup>. Interestingly, overexpression of sarco/endoplasmic reticulum Ca<sup>2+</sup>-ATPase (SERCA) 2b isoform in TMEM165 KO cells partially rescues the observed LAMP2 glycosylation defect. Overall, this study indicates that the rescue of Golgi N-glycosylation defects in TMEM165 KO cells by extracellular Mn<sup>2+</sup> involves the activity of Tg and cyclopiazonic acid-sensitive pumps, probably the SERCA pumps.—Houdou, M., Lebredonchel, E., Garat, A., Duvet, S., Legrand, D., Decool, V., Klein, A., Ouzzine, M., Gasnier, B., Potelle, S., Foulquier, F. Involvement of thapsigargin and cyclopiazonic acid-sensitive pumps in the rescue of TMEM165-associated glycosylation defects by Mn<sup>2+</sup>. *FASEB J.* 33, 000–000 (2019). [www.fasebj.org](http://www.fasebj.org)

**KEY WORDS:** manganese homeostasis · congenital disorders of glycosylation · Golgi apparatus

**ABBREVIATIONS:** BCA, bichoninic acid; CDG, congenital disorders of glycosylation; CPA, cyclopiazonic acid; CQ, chloroquine; DPBS, Dulbecco's phosphate-buffered saline; ER, endoplasmic reticulum; ICP-MS, inductively coupled plasma mass spectrometry; KO, knockout; LAMP2, lysosomal-associated membrane protein 2; MBCD, methyl- $\beta$ -cyclodextrin; SERCA, sarco/endoplasmic reticulum Ca<sup>2+</sup>-ATPase; siRNA, small interfering RNA; SPCA1/2, secretory-pathway Ca<sup>2+</sup>-ATPase 1/2; TBS-T, Tris-buffered saline with Tween 20; Tg, thapsigargin; TMEM165, transmembrane protein 165

<sup>1</sup> These authors contributed equally to this work.

<sup>2</sup> Correspondence: Centre National de la Recherche Scientifique (CNRS), UMR 8576, Unité de Glycobiologie Structurale et Fonctionnelle (UGSF), University of Lille, Villeneuve D'Ascq, F-59000 Lille, France. E-mail: [francois.foulquier@univ-lille1.fr](mailto:francois.foulquier@univ-lille1.fr)

doi: 10.1096/fj.201800387R

This article includes supplemental data. Please visit <http://www.fasebj.org> to obtain this information.

In 2012, we identified the transmembrane protein 165 (TMEM165) gene as a new gene involved in congenital disorders of glycosylation (CDG) (OMIM entry 614727) (1). TMEM165-CDG patients present a peculiar clinical phenotype, including major skeletal dysplasia, osteoporosis, and dwarfism (2). They also present hyposialylation and hypogalactosylation of their sera N-glycoproteins. TMEM165 is a Golgi transmembrane protein belonging to an uncharacterized family of transmembrane proteins named UPF0016 (uncharacterized protein family 0016; Pfam PF01169). Even if TMEM165 is highly conserved during evolution from yeast to human, its biologic function is still a controversial issue. TMEM165 was first described as a Golgi cation antiporter by sequence analogy

with other members of the family (3). In addition, we recently demonstrated that the Golgi glycosylation defect due to TMEM165 deficiency in patients and in TMEM165 knockout (KO) cells resulted from a defect in Golgi Mn<sup>2+</sup> homeostasis, thus linking TMEM165 with Mn<sup>2+</sup> homeostasis and suggesting it may import Mn<sup>2+</sup> into the Golgi stacks (4). This is reinforced by the thylakoid Mn<sup>2+</sup> import *via* photosynthesis-affected mutant 71 transporter, the *Arabidopsis thaliana* ortholog of TMEM165 (5). In addition, we highlighted that only 1 μM Mn<sup>2+</sup> supplementation was sufficient to rescue a normal glycosylation.

Manganese is considered to be a trace element, but it is still essential for several cellular processes. It is involved in the catalytic domain of many enzymes, such as mitochondrial enzymes, RNA and DNA polymerase, and Golgi glycosyltransferases. Although the link between Golgi glycosylation and Mn<sup>2+</sup> has long been known (6), it has only recently been shown that a decrease in cellular Mn<sup>2+</sup> could cause CDG. In addition to our study showing that TMEM165 deficiency was linked with Golgi Mn<sup>2+</sup> homeostasis (4), Park *et al.* (7) have shown that mutations in SLC39A8, a putative plasma membrane manganese transporter, lead to severe glycosylation defects.

The question we address here is how does extracellular Mn<sup>2+</sup> supplementation rescue the glycosylation in TMEM165 KO cells? Extracellular Mn<sup>2+</sup> could reach the Golgi lumen one of two ways: first, it might be internalized by endocytosis and subsequently reach the Golgi lumen through endosome-to-trans-Golgi network retrograde trafficking (8); and second, it might cross the plasma membrane and eventually the Golgi membrane through unspecific channels or transporters. In the latter case, current knowledge suggests that Mn<sup>2+</sup> supply in the Golgi is achieved *via* the action of the secretory pathway Ca<sup>2+</sup>-ATPases (SPCA1 and SPCA2) (9–12), which mediates the import of Ca<sup>2+</sup> and Mn<sup>2+</sup> into the Golgi lumen. Thus, the aim of this study was to decipher by which pathways 1 μM MnCl<sub>2</sub> supplementation leads to glycosylation rescue in TMEM165 KO HEK293 cells.

## MATERIALS AND METHODS

### Antibodies and other reagents

Anti-TMEM165 and anti-β-actin antibodies were purchased from MilliporeSigma (Burlington, MA, USA). Anti-LAMP2 antibodies were purchased from Santa Cruz Biotechnology (Dallas, TX, USA). Anti-SPCA1 antibodies were purchased from Abcam (Cambridge, United Kingdom) for immunofluorescence staining and from Abnova (Taipei City, Taiwan) for Western blot analysis. Anti-GM130 antibody was from BD Biosciences (Franklin Lakes, NJ, USA). Anti-GPP130 antibody was purchased from Covance (Princeton, NJ, USA), and anti-sarco/endoplasmic reticulum Ca<sup>2+</sup>-ATPase (SERCA) 2 antibody was purchased from MilliporeSigma. Polyclonal goat anti-rabbit or goat anti-mouse horseradish peroxidase-conjugated Igs were purchased from Agilent Technologies (Santa Clara, CA, USA). Polyclonal goat anti-rabbit or goat anti-mouse conjugated with Alexa Fluor were purchased

from Thermo Fisher Scientific (Waltham, MA, USA). Manganese (II) chloride tetrahydrate was from Riedel-de-Haën (Seelze, Germany). All other chemicals were from MilliporeSigma, unless otherwise specified.

### Cell culture, drug treatments, and transfections

Control and TMEM165 KO HEK293 cells were maintained in DMEM (Lonza, Basel, Switzerland) supplemented with 10% fetal bovine serum (Dutscher, Brumath, France) at 37°C in a humidity-saturated 5% CO<sub>2</sub> atmosphere. For drug treatments, cells were incubated either with 1 μM MnCl<sub>2</sub> and/or 10 μM chloroquine (CQ), 300 nM nocodazole, 50 nM Tg, 100 μM cyclopiiazonic acid (CPA), 5 mM methyl-β-cyclodextrin (MBCD), 500 μM CaCl<sub>2</sub>, 1mM sodium pyruvate for different treatment times. Transfections were performed using Lipofectamine 2000 (Thermo Fisher Scientific) according to the manufacturer's instructions. Human SERCA2b plasmid (pcDNA3.1+) was purchased from Addgene (Cambridge, MA, USA), and human siATP2C1 from Dharmacon (Horizon Discovery, Lafayette, CO, USA).

### Immunofluorescence staining

Cells were seeded on coverslips for 12 to 4 h, treated as indicated in each figure, washed twice in PBS (Euromedex, Souffelweyersheim, France), and fixed with 4% paraformaldehyde in PBS pH 7.3, for 30 min at room temperature. Coverslips were then washed 3 times with PBS, and cells were permeabilized with 0.5% Triton X-100 in PBS for 10 min before being washed 3 times with PBS. Coverslips were then incubated for 1 h in blocking buffer [0.2% gelatin, 2% bovin serum albumin, 2% fetal bovine serum (Lonza) in PBS] and then for 1 h with primary antibody diluted either at 1:100 or 1:300 in blocking buffer. After 3 washings with PBS, cells were incubated for 1 h with Alexa Fluor 488- or Alexa Fluor 568-conjugated secondary antibody (Thermo Fisher Scientific) diluted at 1:600 in blocking buffer. After 3 washings with PBS, coverslips were mounted on glass slides with Mowiol. Fluorescence was detected by an inverted Zeiss LSM780 or LSM700 Confocal Microscope. Acquisitions were done using ZEN Pro 2.1 software (Carl Zeiss GmbH, Jena, Germany).

### Image analyses

Immunofluorescence images were analyzed using TisGolgi, an in-house made ImageJ plugin (National Institutes of Health, Bethesda, MD, USA; <http://imagej.nih.gov/ij>) developed by the local TisBio (<http://tisbio.wixsite.com/tisbio>) facility.

### Western blot analysis

Cells were scraped in Dulbecco's phosphate-buffered saline (DPBS) and then centrifuged at 4000 g, 4°C for 10 min. Supernatant was discarded, and cells were then resuspended in RIPA buffer (Tris/HCl 50 mM pH 7.9, NaCl 120 mM, NP40 0.5%, EDTA 1 mM, Na<sub>3</sub>VO<sub>4</sub> 1 mM, NaF 5 mM) supplemented with a protease cocktail inhibitor (Roche Diagnostics, Rotkreuz, Switzerland). Cell lysis was done either by passing the cells several times through a syringe with a 26-gauge needle or by a sonication bath for 2 min followed by incubation on ice for 10 min. Cells were centrifuged 20,000 g, 4°C for 30 min. Protein concentration contained in the supernatant was estimated with the micro bicinchoninic acid (BCA) Protein Assay Kit (Thermo Fisher Scientific). Ten or 20 μg of total protein lysate was mixed with NuPAGE LDS sample buffer (Thermo Fisher

Scientific), pH 8.4, supplemented with 4%  $\beta$ -mercaptoethanol (Fluka; MilliporeSigma). Samples were heated 10 min at 95°C (excepted for TMEM165, SPCA1 and SERCA2), then separated on 4 to 12% Bis-Tris gels (Thermo Fisher Scientific) and transferred to nitrocellulose membrane Hybond ECL (GE Healthcare, Little Chalfont, United Kingdom). Membranes were blocked in blocking buffer [5% milk powder in TBS-T (1× TBS with 0.05% Tween 20)] for 1 h at room temperature, then incubated overnight with the primary antibodies (used at a dilution of 1:1000) in blocking buffer and washed 3 times for 5 min in TBS-T. Membranes were then incubated with peroxidase-conjugated secondary goat anti-rabbit or goat anti-mouse antibodies (used at a dilution of 1:10,000 or 1:20,000; Agilent Technologies) in blocking buffer for 1 h at room temperature and later washed 3 times for 5 min in TBS-T. Signal was detected with chemiluminescence reagent (ECL 2 Western blotting substrate or SuperSignal West Pico Plus Chemiluminescent Substrate; Thermo Fisher Scientific) on imaging film (GE Healthcare).

### Mass spectrometry

Two T75 flasks at 90% confluence, treated as indicated in each figure, were used. Cells were then scraped in DPBS at 4°C and centrifuged at 4000 *g*, 4°C for 5 min. Then, supernatant was discarded, and cells were resuspended in PBS and washed 4 times by centrifugation (4000 *g*, 4°C for 10 min). Before the last wash, an aliquot of the resuspended cells in PBS was kept (1:10) in order to estimate the total protein concentration of the sample. The resting pellets were resuspended in lysis buffer (1% Triton-X100 in BS) after a sonication bath at 4°C for 1 h and centrifuged at 20,000 *g*, 4°C for 10 min. Supernatants were then transferred into new tubes. Next, dithiothreitol (MilliporeSigma) was added to a final concentration of 10 mM and incubated 45 min at 56°C followed by the addition of 50 mM iodoacetamide (Bio-Rad, Hercules, CA, USA) for 1 h at 37°C, protected from light. The reduced and acylated proteins were precipitated with a final concentration of 10% trichloroacetic acid and incubated for 30 min at -20°C. After a centrifugation at 20,000 *g*, 4°C for 10 min, supernatants were discarded. Protein pellets were then washed by the addition of iced acetone and centrifuged at 20,000 *g*, 4°C for 10 min. This step was repeated. Washed protein pellets were dried at room temperature for 30 min. Then trypsin at 2 mg/ml (MilliporeSigma) was added overnight and up to 48 h at 37°C in 50 mM ammonium bicarbonate (MilliporeSigma) with a 5:1 ratio. The reaction was stopped by heating samples 10 min at 100°C. *N*-glycans were released from the proteins by addition of 10 U of PNGase F (Roche Diagnostics) overnight at 37°C. *N*-glycans were then purified by a C18 Sep-Pak chromatography (Water, Guyancourt, France). The column was washed with 100% acetonitrile and 100% 2-propanol, and then equilibrated with 5% acetic acid in water. Samples were loaded onto the C18 Sep-Pak, and the bound peptides were eluted 3 times with 5% acetic acid in water. *N*-glycans in 5% aqueous acetic acid were lyophilized overnight. They were permethylated and spotted onto a matrix-assisted desorption plate and analyzed by matrix-assisted desorption ionization–time of flight mass spectrometry on a 4800 Proteomics Analyzer Mass Spectrometer (Applied Biosystems; Thermo Fisher Scientific), as described by Delannoy *et al.* (13). Each spectrum resulted from the accumulation of 10,000 spectra and shows glycans structures from *m/z* 1500 up to 3000.

### Whole cell Mn measurement

#### Sample preparation

After the indicated treatments, cells were washed twice in DPBS at 4°C. Cells were then collected and centrifuged at

4000 *g*, 4°C for 10 min. Supernatant was discarded, and cells were then resuspended in 1 ml of PBS; 200  $\mu$ l was kept for protein dosage, and 800  $\mu$ l was kept for Mn measurement by inductively coupled plasma mass spectrometry (ICP-MS). Both were centrifuged at 4000 *g*, 4°C for 10 min. The cell pellet for protein dosage was resuspended in RIPA buffer, and cell lysis was performed. Protein concentration contained in the supernatant was estimated with the micro-BCA Protein Assay Kit (Thermo Fisher Scientific). Cell pellet for ICP-MS analysis was resuspended in deionized water and then sonicated for 30 s. A chloroform/methanol/water (ratio 2:1:3) extraction was then done to separate lipids, proteins, and soluble material. The upper phase containing soluble material was kept and dried under nitrogen flux or with a vacuum concentrator (Eppendorf Concentrator 5301). Samples were then dissolved in 500  $\mu$ l of deionized water.

### Instrumentation and analysis

Samples were diluted 50 times with 1.5% (v/v) nitric acid (ultrapure quality 69.5%; Carlo Erba Reagents, Val de Reuil, France) solution in ultrapure water (PurElab Option-Q; Veolia Water, Antony, France) containing 0.1% Triton X-100 (Euromedex), 0.2% butan-1-ol (VWR Chemicals, Fontenay-sous-Bois, France), and 0.5  $\mu$ g/L rhodium (Merk, Darmstadt, Germany). Assays were performed on an ICP-MS Thermo ICap Q device (Thermo Fisher Scientific). The limit of quantification was 0.2  $\mu$ g/L.

### Statistical analysis

Comparisons between groups were performed by the Student's *t* test for 2 variables with equal or different variances, depending on the result of the *F* test.

## RESULTS

### Time course of lysosomal-associated membrane protein 2 glycosylation rescue by Mn<sup>2+</sup>

Our previous studies demonstrated that supplementation with low Mn<sup>2+</sup> concentrations could completely suppress lysosomal-associated membrane protein 2 (LAMP2) glycosylation defects in TMEM165 KO cells (4). This has, however, been observed for long treatments (48 h). The time course of the Mn<sup>2+</sup> effect was not evaluated. To answer this point, a concentration of 1  $\mu$ M of MnCl<sub>2</sub> was applied to the cells for increasing times (1–64 h), and LAMP2 glycosylation was assessed by Western blot analysis (Fig. 1A). The results showed that after Mn<sup>2+</sup> treatment of TMEM165 KO cells, fully glycosylated forms of LAMP2 appear after 8 h of Mn<sup>2+</sup> treatment, yet most LAMP2 remain underglycosylated. Relative quantification of underglycosylated and fully glycosylated LAMP2 (Fig. 1B) indicate that fully glycosylated LAMP2 progressively increases from 10% after 8 h to 97% after 64 h of Mn<sup>2+</sup> treatment. This result is consistent with the slow turnover of LAMP2 estimated to 48 h. In further experiments, cells were treated with 1  $\mu$ M MnCl<sub>2</sub> for 8 and/or 16 h.

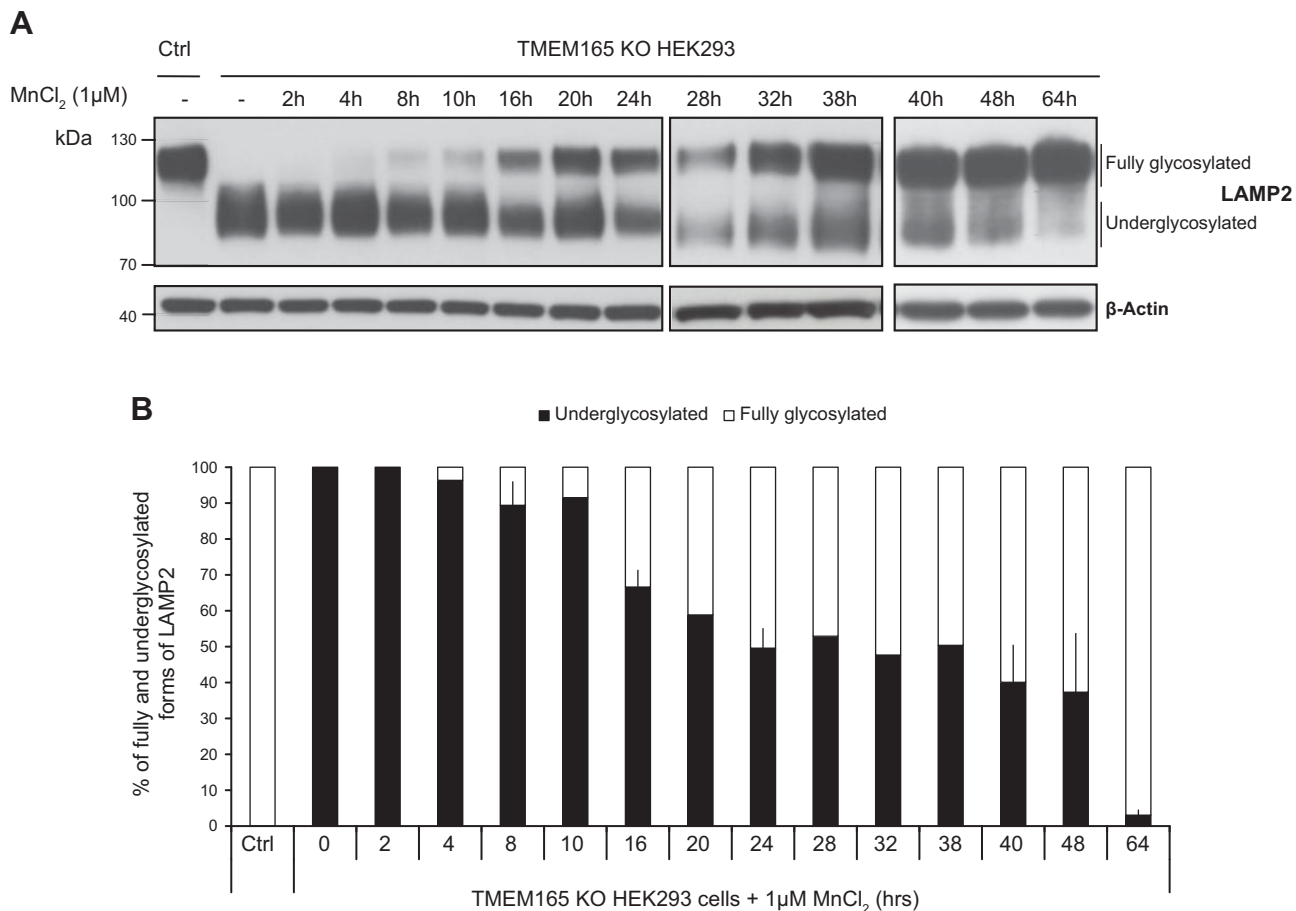


**Figure 1.** Time course of Mn<sup>2+</sup>-induced LAMP2 glycosylation rescue. *A*) Control and TMEM165 KO HEK293 cells were cultured with 1 μM MnCl<sub>2</sub> during indicated times. Cell culture medium was renewed every 16 h. Total cell lysates were prepared, then subjected to SDS-PAGE and Western blot with indicated antibodies. *B*) Relative quantification of fully and underglycosylated forms of LAMP2 (*n* = 2).

### Blocking endocytosis in TMEM165 KO cells does not prevent rescue of LAMP2 glycosylation by Mn<sup>2+</sup>

The pathways by which Mn<sup>2+</sup> enters cells after MnCl<sub>2</sub> exposure are unknown. Two different ways are possible, either by permeating membranes using specific and/or unspecific transporters or *via* endocytosis and endosome-to-trans-Golgi network retrograde trafficking (8). To discriminate between these possibilities, cells were treated with different drugs known to interfere with endocytosis such as CQ (14), a weak base raising the pH of acidic compartments, MBCD, that depletes cholesterol from plasma membrane and nocodazole, a microtubule depolymerizing agent (15) (Fig. 2 and Supplemental Figs. S1 and S2). We first checked the potential effects of these drugs on both the steady-state glycosylation status of LAMP2 in control HEK293 cells and its subcellular localization. No changes in the LAMP2 electrophoresis mobility could be observed in control HEK293 cells after these drug treatments (Supplemental Figs. S1A and S2A), suggesting no major alteration of its glycosylation. Moreover, neither nocodazole nor MBCD nor CQ disrupted the lysosomal localization of LAMP2 (Supplemental Figs. S1B and S2B).

We also checked the effects of those drugs on the morphology of the Golgi apparatus. Immunofluorescence staining of Golgi proteins GPP130 and GM130 were performed, followed by confocal microscopy analyses (Supplemental Figs. S1B and S2B). As already known from the literature, nocodazole fragmented the Golgi apparatus, but CQ and MBCD had no effect on its morphology.

The LAMP2 glycosylation profile in TMEM165 KO HEK293 cells after treatment with or without a combination of those drugs and MnCl<sub>2</sub> was then assessed (Fig. 2 and Supplemental Fig. S2C). The observed LAMP2 mobility in TMEM165 KO cells after 1 μM MnCl<sub>2</sub> treatment was comparable to the one observed in Fig. 1. Ten percent of LAMP2 was found to be normally glycosylated after 8 h of Mn<sup>2+</sup> treatment and 33% after 16 h. Cells were then treated with CQ or MBCD in the presence or absence of 1 μM MnCl<sub>2</sub> for 8 and 16 h (Fig. 2). The results show that CQ and MBCD did not prevent the rescue of LAMP2 glycosylation after Mn<sup>2+</sup> supplementation because 22 and 32% of fully glycosylated forms, respectively, were observed after 16 h treatment. Similar results were obtained with nocodazole (Supplemental Fig. S1C, D).

These results clearly highlight that none of these drugs prevents the rescue of LAMP2 glycosylation by Mn<sup>2+</sup> in TMEM165 KO cells. This suggests that at the extracellular

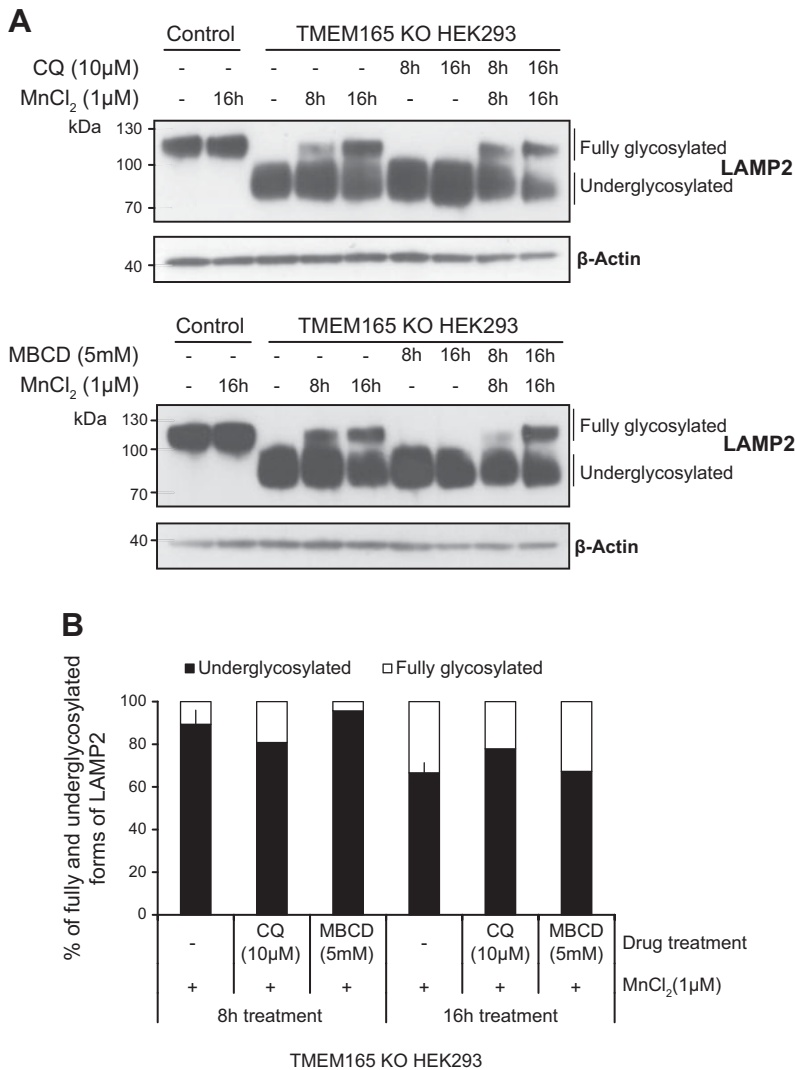


**Figure 2.** Mn<sup>2+</sup> entry into TMEM165 KO HEK293 cells does not rely on endocytosis. **A)** Control and TMEM165 KO HEK293 cells were cultured with CQ (10  $\mu$ M) or MBCD (5mM) in combination or not with 1  $\mu$ M MnCl<sub>2</sub> for 8 or 16 h. Total cell lysates were prepared, then subjected to SDS-PAGE and Western blot with indicated antibodies. **B)** Relative quantification of fully and underglycosylated forms of LAMP2 ( $n = 2$ ).

concentration used in our study (1  $\mu$ M), Mn<sup>2+</sup> enters TMEM165-defective HEK293 cells through plasma membrane transporters rather than by endocytosis.

### Is Golgi pump SPCA1 involved in Mn<sup>2+</sup>-induced rescue of LAMP2 glycosylation?

After entering TMEM165-defective cells, cytosolic Mn<sup>2+</sup> should reach the Golgi lumen to correct the glycosylation defects. Besides TMEM165, which acts as a key determinant for Golgi Mn<sup>2+</sup> homeostasis (4), the SPCA pumps (SPCA1 and -2) are known to be the main suppliers of Mn<sup>2+</sup> in the Golgi lumen (11). Because SPCA2 is poorly expressed in our cell line, we tested the contribution of SPCA1 by silencing its gene, *ATP2C1* (Fig. 3). The small interfering RNA (siRNA) knockdown was very efficient, as 95% of the protein was depleted compared to untreated cells. Surprisingly, the knockdown of *ATP2C1* did not prevent the rescue of LAMP2 glycosylation by Mn<sup>2+</sup>. Thirty-seven percent of LAMP2 was fully glycosylated after 16 h Mn<sup>2+</sup> treatment in si*ATP2C1*-treated cells, a level similar to that observed without *ATP2C1* knockdown. SPCA1 is thus not involved in

the glycosylation rescue induced by Mn<sup>2+</sup> supplementation in TMEM165 KO HEK293 cells.

### Golgi glycosylation rescue induced by Mn<sup>2+</sup> supplementation requires Tg and CPA-sensitive pumps

Given the previous results, we next considered whether the endoplasmic reticulum (ER) could play a role in the observed glycosylation rescue. It had indeed been shown that SERCA pumps are able, in certain conditions, to transport Mn<sup>2+</sup> into the ER lumen in addition to Ca<sup>2+</sup> (16–18). We thus hypothesized that SERCA pumps might be involved in the Mn<sup>2+</sup> supplementation effect. To address this point, LAMP2 glycosylation status was evaluated by Western blot analysis in cells treated with CPA or Tg, two specific SERCA inhibitors, in the presence or absence of 1  $\mu$ M MnCl<sub>2</sub> (Fig. 4). CPA and Tg did not induce any glycosylation defect on LAMP2 in control HEK293 cells; nor did this occur after 8 or 16 h of treatment (Supplemental Fig. S3). Remarkably, in TMEM165 KO HEK293 cells treated with CPA and 1  $\mu$ M MnCl<sub>2</sub>, the treatment strongly delayed the rescue of LAMP2 glycosylation by Mn<sup>2+</sup>, as only 4% of LAMP2 was fully glycosylated

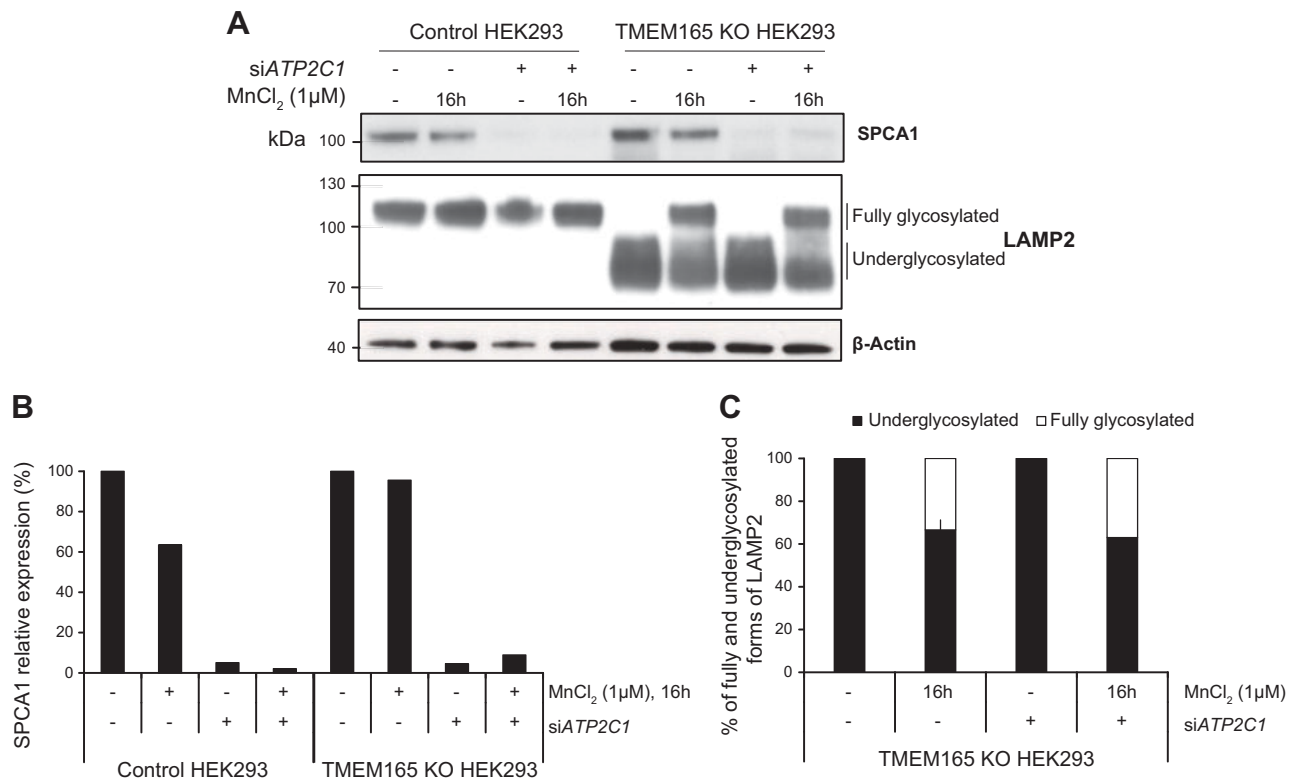


**Figure 3.** *ATP2C1* knockdown does not prevent Mn<sup>2+</sup>-induced rescue glycosylation of LAMP2 in TMEM165 KO HEK293 cells. *A*) Control, TMEM165 KO, and siATP2C1 HEK293 cells were cultured with 1 μM MnCl<sub>2</sub> for 16 h. Total cell lysates were prepared, and then subjected to SDS-PAGE and Western blot analyses with indicated antibodies. *B*) Quantification of SPCA1 protein expression after normalization with actin. *C*) Relative quantification of fully and underglycosylated forms of LAMP2.

after 8 h and 29% after 16 h of Mn<sup>2+</sup> treatment. To reinforce this result, stronger effects were obtained after Tg treatment (Fig. 4A, B). To confirm these results at the structural level, mass spectrometry of total *N*-glycans was performed (Fig. 5). TMEM165 KO HEK293 cells were treated or not with 1 μM MnCl<sub>2</sub> and with or without Tg/CPA. Consistent with our previous studies, a pronounced hypogalactosylation was seen in TMEM165 KO HEK293 cells, with the accumulation of agalactosylated glycan structures detected at *m/z* 1661, 1835, 2081, and 2326. Consistent with our previous studies, MnCl<sub>2</sub> treatment rescues the general glycosylation defect, as indicated by the decreased abundance of the structures *m/z* 1835, 2081, and 2326 (54% decrease, Supplemental Fig. S4). Although Tg and CPA treatments in KO TMEM165 cells slightly increase the abnormal agalactosylated glycan structures, such treatments fully prevent the total rescue of TMEM165-associated glycosylation defects by Mn<sup>2+</sup>, as indicated by the remaining high abundance of the structures *m/z* 1661, 1835, 2081, and 2326 (Supplemental Fig. S4).

To validate these results, we tested whether CPA or Tg treatment acted by indirectly altering Mn<sup>2+</sup> entry into the cells. Therefore, the total cellular Mn concentration in presence and absence of CPA or Tg was evaluated by ICP-MS after MnCl<sub>2</sub> supplementation. The results showed that after Mn<sup>2+</sup> supplementation, the amount of Mn is comparable in cells treated or not with CPA or Tg (Supplemental Fig. S3C). This demonstrated that neither CPA nor

Tg prevented the cellular Mn<sup>2+</sup> entry after MnCl<sub>2</sub> supplementation.

In parallel, the effects of CPA and Tg on the morphology of the Golgi apparatus were investigated by confocal immunofluorescence analysis of the Golgi proteins GPP130 and GM130 (Fig. 4C and Supplemental Fig. S3A). No effect was observed on the Golgi apparatus morphology after CPA treatment, and only a slight dilatation of the Golgi was shown after Tg treatment. Moreover, LAMP2 localization was not disrupted by either Tg or CPA.

Overall, these results provide pharmacologic evidence for the involvement of Tg- and CPA-sensitive pumps in the Golgi *N*-glycosylation rescue induced by Mn<sup>2+</sup> supplementation in TMEM165 KO HEK293 cells.

### Potential involvement of SERCA pump in the Mn<sup>2+</sup>-induced rescue of LAMP2 glycosylation

The observed Tg and CPA sensitivity led us to investigate the potential role of ER SERCA pump in the Mn<sup>2+</sup> supplementation effect. Among all SERCA proteins, the SERCA2b isoform is the main form expressed in HEK293 cells. SERCA2b was overexpressed for 48 h in TMEM165 KO HEK293 cells, and LAMP2 glycosylation status was assayed by Western blot analysis. The correct SERCA2b expression was checked by immunofluorescence (data not shown) and by Western blot analyses in both TMEM165



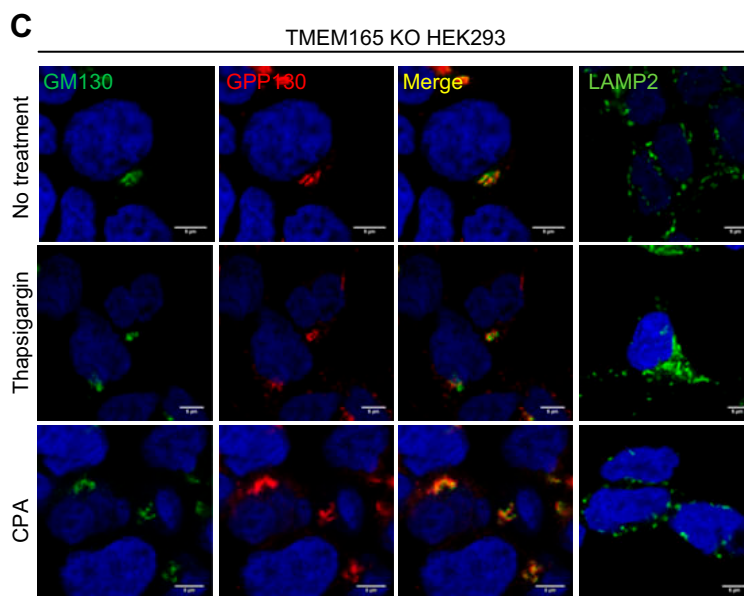
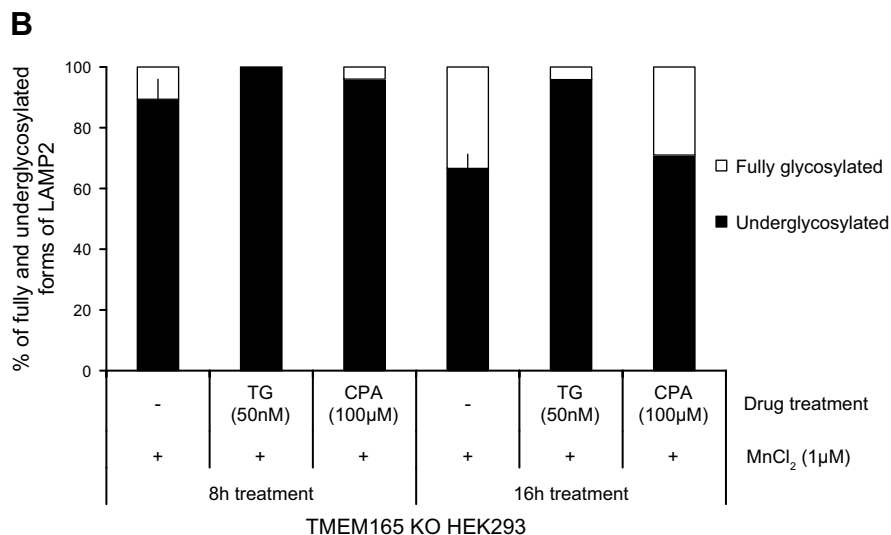
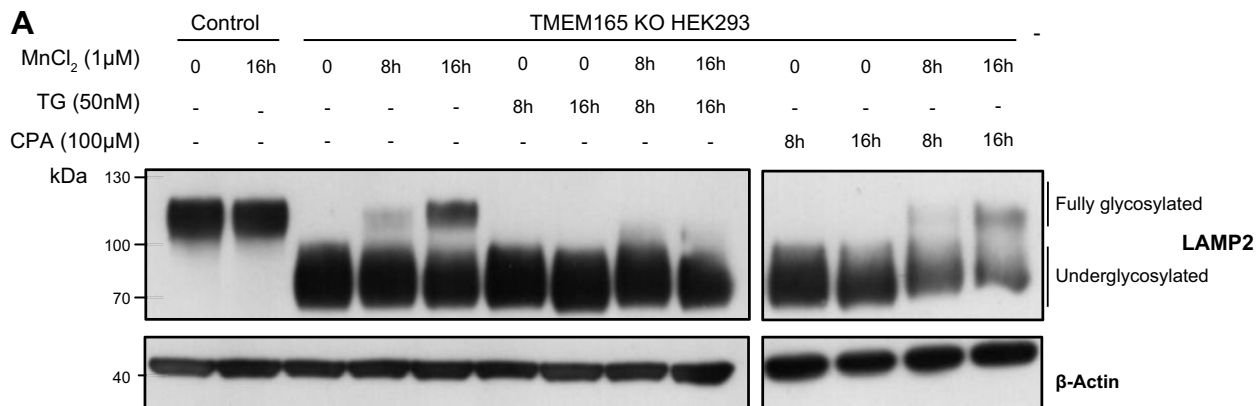


**Figure 4.** Involvement of Tg- and CPA-sensitive pumps in Mn<sup>2+</sup>-induced rescue of LAMP2 glycosylation. *A*) Control and TMEM165 KO cells were cultured with either Tg (50 nM) or CPA (100 μM), 2 SERCA inhibitors, in combination or not with 1 μM MnCl<sub>2</sub> for 8 or 16 h. Total cell lysates were prepared, then subjected to SDS-PAGE and Western blot with indicated antibodies. *B*) Relative quantification of fully and underglycosylated forms of LAMP2 (*n* = 2). *C*) Immunofluorescence analysis. TMEM165 KO HEK293 cells were incubated with either Tg (50 nM) or CPA (100 μM) for 16 h, fixed, permeabilized, and labeled with antibodies against GM130, GPP130, and LAMP2 before confocal microscopy visualization. DAPI staining (blue) was performed, showing nuclei. Scale bars, 5 μm.

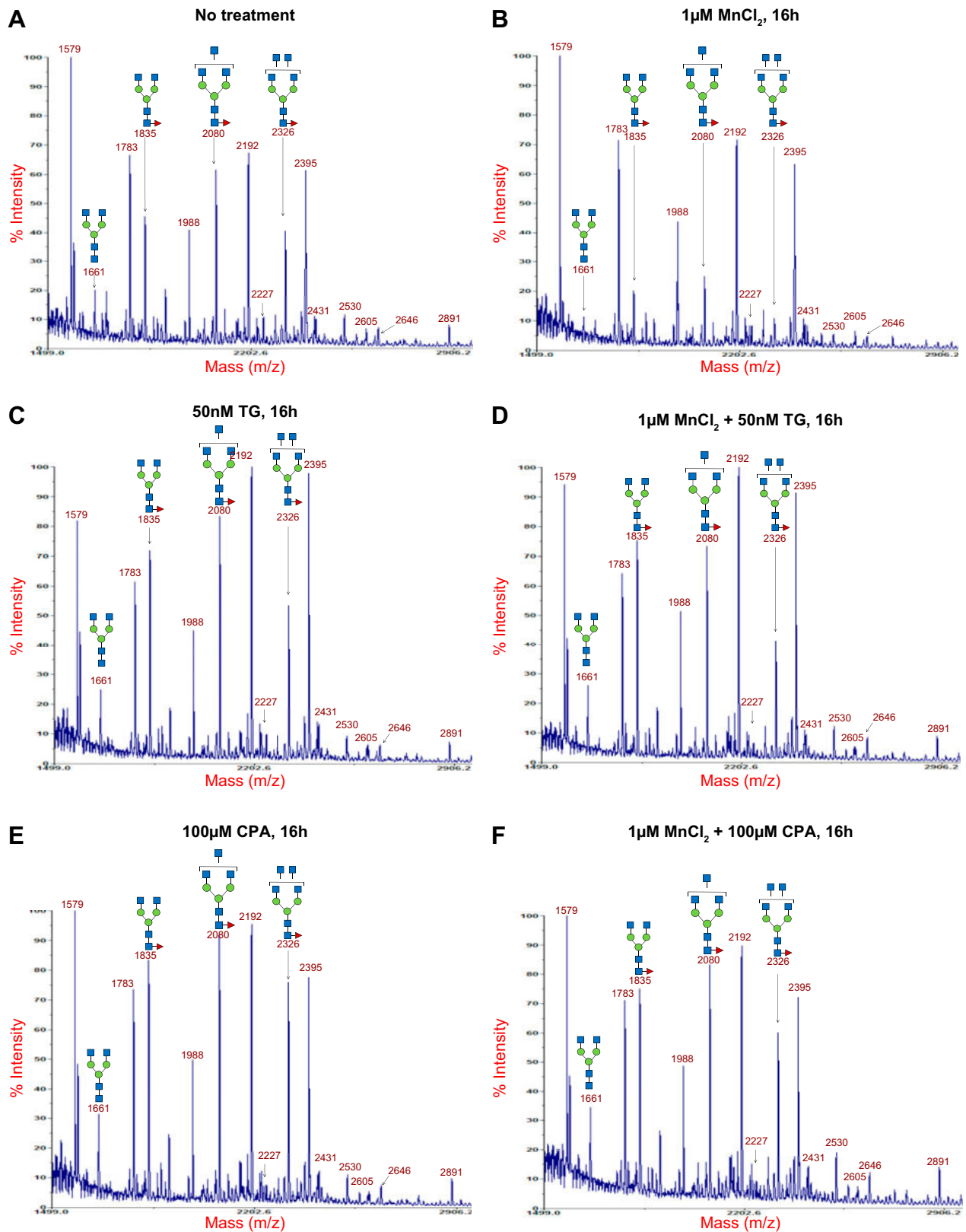


**Figure 5.** *N*-glycosylation defects observed in TMEM165 KO HEK293 cells treated with Tg or CPA are not rescued by Mn<sup>2+</sup> supplementation. Matrix-assisted desorption/ionization–time of flight mass spectrometry spectra of permethylated *N*-glycans from TMEM165 KO HEK293 cells after different treatments. No treatment (A), TMEM165 KO HEK293 cells treated with 1  $\mu$ M MnCl<sub>2</sub> for 16 h (B), TMEM165 KO HEK293 cells treated with 50 nM Tg, in combination or not with 1  $\mu$ M MnCl<sub>2</sub> for 16 h (C, D), TMEM165 KO HEK293 cells treated with 100  $\mu$ M CPA in combination or not with 1  $\mu$ M MnCl<sub>2</sub> for 16 h (E, F). Symbols represent sugar residues as follows: blue square, *N*-acetylglucosamine; green circle, mannose; yellow circle, galactose; purple diamond, sialic acid; red triangle, fucose. Linkages between sugar residues have been removed for simplicity.

KO and control HEK293 cells (Fig. 6). Compared to untransfected cells, LAMP2 glycosylation profile is slightly restored in TMEM165 KO HEK293 cells overexpressing SERCA2b (Fig. 6). In order to prove that this slight rescue was not due to potential ER/Golgi  $\text{Ca}^{2+}$  homeostasis changes, the overexpressing cells were treated with 500  $\mu\text{M}$   $\text{CaCl}_2$  and 1 mM sodium pyruvate. LAMP2 glycosylation rescue is identical to the one obtained without such treatment and suggests that the observed shift is likely not the cause of the SERCA2b  $\text{Ca}^{2+}$  pumping activity. Taken together, these results suggest the potential involvement of SERCA2b pump in the  $\text{Mn}^{2+}$  rescued glycosylation of LAMP2.

## DISCUSSION

TMEM165 deficiency was recently found to lead to a type II CDG associated with strong Golgi glycosylation abnormalities (1). Our previous work has shown that these glycosylation abnormalities in TMEM165 KO cells could result from a lack of Golgi  $\text{Mn}^{2+}$  (4). Many Golgi glycosyltransferases using UDP sugars as a donor substrate, such as UDP-Gal:*N*-acetylglucosamine  $\beta$ -1,4-galactosyltransferase I (B4GALT1; EC 2.4.1.22) and UDP-Gal:*N*-acetylglucosamine  $\beta$ -1,4-galactosyltransferase II (B4GALT2; EC 2.4.1.22), are indeed known to require  $\text{Mn}^{2+}$  in their catalytic site to be fully active. Indeed, as it has been well described by Ramakrishnan *et al.* (19),  $\text{Mn}^{2+}$  first needs to bind the enzyme in a so-called open conformation to then allow the binding of the nucleotide sugar. Once in this enzyme- $\text{Mn}^{2+}$ -nucleotide sugar conformation, the acceptor substrates bind it, and the catalysis can start. Remarkably, we have demonstrated that 1  $\mu\text{M}$   $\text{MnCl}_2$  supplementation was sufficient to completely suppress the glycosylation defects in TMEM165 KO cells. The underlying mechanism of this glycosylation rescue by  $\text{Mn}^{2+}$  was however unknown.

To address this point, LAMP2 was used as a reporter glycoprotein to finely study the  $\text{Mn}^{2+}$ -induced mechanism of Golgi glycosylation rescue. We have clearly shown that after 8 h 1  $\mu\text{M}$   $\text{MnCl}_2$  treatment, newly synthesized LAMP2 was already fully glycosylated in TMEM165 KO cells. Moreover, and in line with its turnover, half of LAMP2 is fully glycosylated after 24-h treatment, and almost all LAMP2 is fully glycosylated

after 64-h treatment. This showed that LAMP2 could be used to study glycosylation kinetics and that 1  $\mu\text{M}$   $\text{MnCl}_2$  was able to totally suppress the glycosylation defect observed on LAMP2 in TMEM165 KO HEK293 cells.

The first step of this glycosylation rescue induced by 1  $\mu\text{M}$   $\text{MnCl}_2$  is the  $\text{Mn}^{2+}$  uptake at the plasma membrane. This can be done either by endocytosis or through transporters. Using CQ, nocodazole, and MBCD, 3 drugs known to disrupt endocytosis (14), we have demonstrated that none of these drugs prevented the glycosylation rescue after 1  $\mu\text{M}$   $\text{MnCl}_2$  exposure in TMEM165 KO cells, thus suggesting that  $\text{Mn}^{2+}$  does not enter into cells *via* endocytosis. This can easily be explained by the presence of several plasma membrane transporters known to import  $\text{Mn}^{2+}$ . This includes the divalent metal transporter 1 (DMT1/NRAMP2/SLC11A2) (20, 21), NRAMP1 (22), transferrin, and transporters SLC30A10/ZNT8 (23), SLC39A8/ZIP8 (7) and SLC30A14/ZIP14 (24, 25). As a consequence, we reasonably think that  $\text{Mn}^{2+}$  can use a wide set of transporters to directly enter into cells, thus making the identification of the involved transporters difficult, with possibly different answers depending on the cell type.

Once in the cytosol,  $\text{Mn}^{2+}$  needs to reach the Golgi lumen to suppress the Golgi glycosylation defect induced by a lack of TMEM165. In the absence of TMEM165, it is likely that the  $\text{Mn}^{2+}$  supply in the Golgi is achieved *via* the action of SPCA pumps (SPCA1 and SPCA2) (9, 11, 26). Overexpression of SPCA1 has indeed been shown to increase  $\text{Mn}^{2+}$  accumulation into the Golgi after high  $\text{Mn}^{2+}$  concentrations exposure (27). Given that SPCA2 is not expressed in HEK cells, we have depleted SPCA1 by siRNA and analyzed the status of LAMP2 glycosylation in TMEM165 KO cells in the presence or absence of 1  $\mu\text{M}$   $\text{MnCl}_2$ . The results unequivocally showed that  $\text{Mn}^{2+}$  supplementation could rescue a normal LAMP2 glycosylation in siATP2C1 TMEM165 KO-treated cells. This demonstrates that somehow SPCA1 is not involved in the glycosylation rescue induced by  $\text{Mn}^{2+}$  in TMEM165 KO cells. However, because 5% of SPCA1 still remains after siRNA treatment, we cannot completely exclude the notion that the remaining SPCA1 is sufficient to efficiently transport  $\text{Mn}^{2+}$  from the cytosol to the Golgi apparatus to rescue glycosylation.

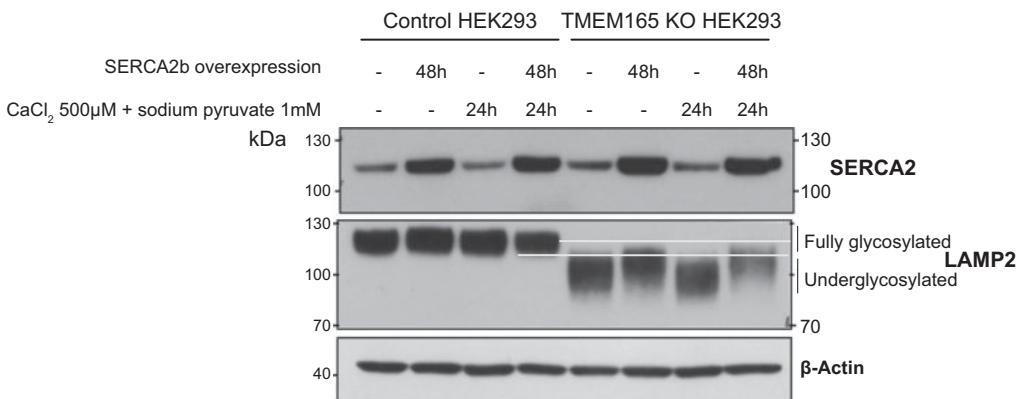


**Figure 6.** Potential involvement of SERCA2b pump in  $\text{Mn}^{2+}$  supplementation effect. Effect of SERCA2b overexpression in control and TMEM165 KO HEK293 cells treated or not with 500  $\mu\text{M}$   $\text{CaCl}_2$  and 1 mM sodium pyruvate on LAMP2 glycosylation. Total cell lysates were prepared, and then subjected to SDS-PAGE and Western blot with indicated antibodies.

We then investigated the hypothesis that  $Mn^{2+}$  could reach the ER before being transported to the Golgi compartment. The effects of specific inhibitors of sarcoplasmic reticulum calcium ATPase, Tg, and CPA were investigated. Interestingly, we did demonstrate that  $Mn^{2+}$  supplementation could not rescue a correct LAMP2 glycosylation in cells treated with CPA (100  $\mu$ M) or Tg (50 nM). Importantly, these used concentrations of CPA and Tg did not inhibit the activity of SPCA1. Indeed, Chen *et al.* (28), recently showed that SPCA1 inhibition by either CPA or Tg occurred from 182 to 7  $\mu$ M, respectively. As we demonstrated using ICP-MS, neither CPA nor TG treatment prevented the cellular  $Mn^{2+}$  entry; our results suggest that the observed Golgi glycosylation rescue induced by  $Mn^{2+}$  supplementation could come from ER/Golgi uptake *via* Tg and CPA sensitive proteins. To address the potential involvement of SERCA pumps, SERCA2b (the main isoform expressed in HEK cells) overexpression in TMEM165 KO HEK293 cells was performed. Although partial, the LAMP2 glycosylation profile is clearly enhanced, which suggests the involvement of SERCA2b protein in the  $Mn^{2+}$  rescued glycosylation of LAMP2.

The importance of SERCA pumps in the observed Golgi glycosylation rescue was quite unexpected, and the molecular mechanisms by which SERCA pumps are involved in the  $Mn^{2+}$  rescued Golgi glycosylation in TMEM165 KO cells remain unknown. One can expect that under  $Mn^{2+}$  supplementation, cytosolic  $Mn^{2+}$  is directly pumped by SERCA into the ER. Such role has already been documented in the literature. Chiesi and Inesi (17) showed in sarcoplasmic reticulum vesicles that a  $Ca^{2+}$  ATPase could indeed be activated by  $Mn^{2+}$  and was even able to import  $Mn^{2+}$  instead of  $Ca^{2+}$ , but at slower rate. It was also confirmed, many years ago, that SERCA1a was able to transport  $Mn^{2+}$  instead of  $Ca^{2+}$  with similar activation energies using the same mechanism but with a much lower affinity (18). Another hypothesis that we cannot exclude would be the crucial importance of ER/Golgi  $Ca^{2+}$  homeostasis in the  $Mn^{2+}$ -induced Golgi glycosylation rescue. Some Golgi glycosyltransferases, and particularly the Golgi  $\beta$ 4GalT1 (EC 2.4.1.38) enzyme, possesses 2 metal binding sites. Site I binds  $Mn^{2+}$  with high affinity, and site II binds diverse metal ions including  $Ca^{2+}$  (18). It could be possible that a decrease in ER/Golgi  $Ca^{2+}$  homeostasis completely inhibits, *in cellulo*, the activity of  $\beta$ 4GalT1 even under  $Mn^{2+}$  supplementation.

Overall, our results shed light on the involvement of Tg- and CPA-sensitive pumps, most likely SERCA pump, in the rescue of TMEM165-associated glycosylation defects by  $Mn^{2+}$ .

## ACKNOWLEDGMENTS

The authors are indebted to D. Legrand [Federation of Research Structural and Functional Biochemistry of Biomolecular Assemblies (FRABio), University of Lille] for providing the scientific and technical environment conducive to achieving this work. The authors thank the staff of the BioImagingCenter of Lille, especially C. Slomianny and E. Richard, for the use of the Leica LSM700 and LSM780

devices. The authors are indebted to D. Mouajjah (Centre National de la Recherche Scientifique Unités Mixte de Recherche 8576, University of Lille) for her helpful assistance in mass spectrometry experiments, and D. Allorge (Centre Hospitalier Universitaire Lille, EA 4483) for her kind assistance in ICP-MS experiments. This work was supported by the French National Research Agency (SOLV-CDG to F.F.) and the Mizutani Foundation for Glycoscience (to F.F.). The authors declare no conflicts of interest.

## AUTHOR CONTRIBUTIONS

S. Potelle and F. Foulquier designed the research; M. Houdou, E. Lebretonchel, and V. Decool performed the experiments; M. Houdou, S. Duvet, and S. Potelle analyzed data; M. Houdou, S. Potelle, and F. Foulquier wrote the manuscript; A. Garat developed and optimized the ICP-MS analysis and kindly gave access to the platform for the experiments; and D. Legrand, A. Klein, M. Ouzzine, and B. Gasnier helped edit the manuscript and provided useful advice.

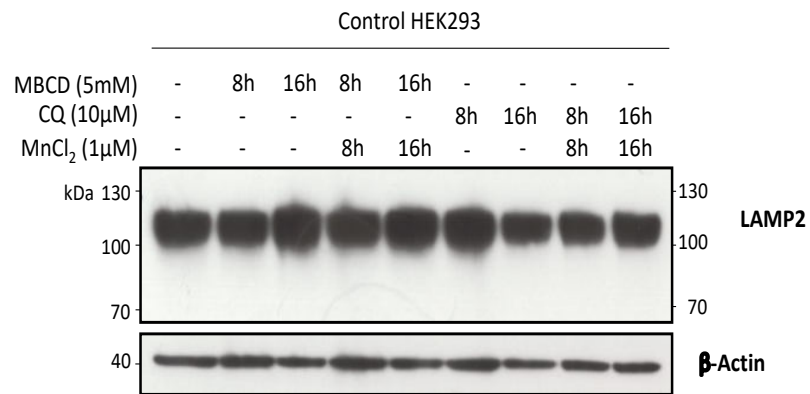
## REFERENCES

1. Foulquier, F., Amyere, M., Jaeken, J., Zeevaert, R., Schollen, E., Race, V., Bammens, R., Morelle, W., Rosnoblet, C., Legrand, D., Demaegd, D., Buist, N., Cheillan, D., Guffon, N., Morsomme, P., Annaert, W., Freeze, H. H., Van Schaftingen, E., Vikkula, M., and Matthijs, G. (2012) TMEM165 deficiency causes a congenital disorder of glycosylation. *Am. J. Hum. Genet.* **91**, 15–26
2. Zeevaert, R., de Zegher, F., Sturiale, L., Garozzo, D., Smet, M., Moens, M., Matthijs, G., and Jaeken, J. (2013) Bone dysplasia as a key feature in three patients with a novel congenital disorder of glycosylation (CDG) type II due to a deep intronic splice mutation in TMEM165. *JIMD Rep.* **8**, 145–152
3. Demaegd, D., Foulquier, F., Colinet, A.-S., Gremillon, L., Legrand, D., Mariot, P., Peiter, E., Van Schaftingen, E., Matthijs, G., and Morsomme, P. (2013) Newly characterized Golgi-localized family of proteins is involved in calcium and pH homeostasis in yeast and human cells. *Proc. Natl. Acad. Sci. USA* **110**, 6859–6864
4. Potelle, S., Morelle, W., Dulary, E., Duvet, S., Vicogne, D., Spriet, C., Krzewinski-Recchi, M.-A., Morsomme, P., Jaeken, J., Matthijs, G., De Bettignies, G., and Foulquier, F. (2016) Glycosylation abnormalities in Gdt1p/TMEM165 deficient cells result from a defect in Golgi manganese homeostasis. *Hum. Mol. Genet.* **25**, 1489–1500
5. Schneider, A., Steinberger, I., Herdean, A., Gandini, C., Eisenhut, M., Kurz, S., Morper, A., Hoecker, N., Rühle, T., Labs, M., Flügge, U.-I., Geimer, S., Schmidt, S. B., Husted, S., Weber, A. P. M., Spetea, C., and Leister, D. (2016) The evolutionarily conserved protein photophosphorylation mutant71 is required for efficient manganese uptake at the thylakoid membrane in Arabidopsis. *Plant Cell* **28**, 892–910
6. Powell, J. T., and Brew, K. (1976) Metal ion activation of galactosyltransferase. *J. Biol. Chem.* **251**, 3645–3652
7. Park, J. H., Högberg, M., Grüneberg, M., DuChesne, I., von der Heiden, A. L., Reunert, J., Schlingmann, K. P., Boycott, K. M., Beaulieu, C. L., Mhanni, A. A., Innes, A. M., Hörtnagel, K., Biskup, S., Gleixner, E. M., Kurlmann, G., Fiedler, B., Omran, H., Rutsch, F., Wada, Y., Tsiakas, K., Santer, R., Nebert, D. W., Rust, S., and Marquardt, T. (2015) SLC39A8 deficiency: a disorder of manganese transport and glycosylation. *Am. J. Hum. Genet.* **97**, 894–903
8. Bonifacino, J. S., and Rojas, R. (2006) Retrograde transport from endosomes to the trans-Golgi network. *Nat. Rev. Mol. Cell Biol.* **7**, 568–579
9. He, W., and Hu, Z. (2012) The role of the Golgi-resident SPCA  $Ca^{2+}/Mn^{2+}$  pump in ionic homeostasis and neural function. *Neurochem. Res.* **37**, 455–468
10. Micaroni, M., Perinetti, G., Berrie, C. P., and Mironov, A. A. (2010) The SPCA1  $Ca^{2+}$  pump and intracellular membrane trafficking. *Traffic* **11**, 1315–1333; erratum: 12, 789
11. Van Baelen, K., Dode, L., Vanoevelen, J., Callewaert, G., De Smedt, H., Missiaen, L., Parys, J. B., Raeymaekers, L., and Wuytack, F. (2004) The  $Ca^{2+}/Mn^{2+}$  pumps in the Golgi apparatus. *Biochim. Biophys. Acta* **1742**, 103–112

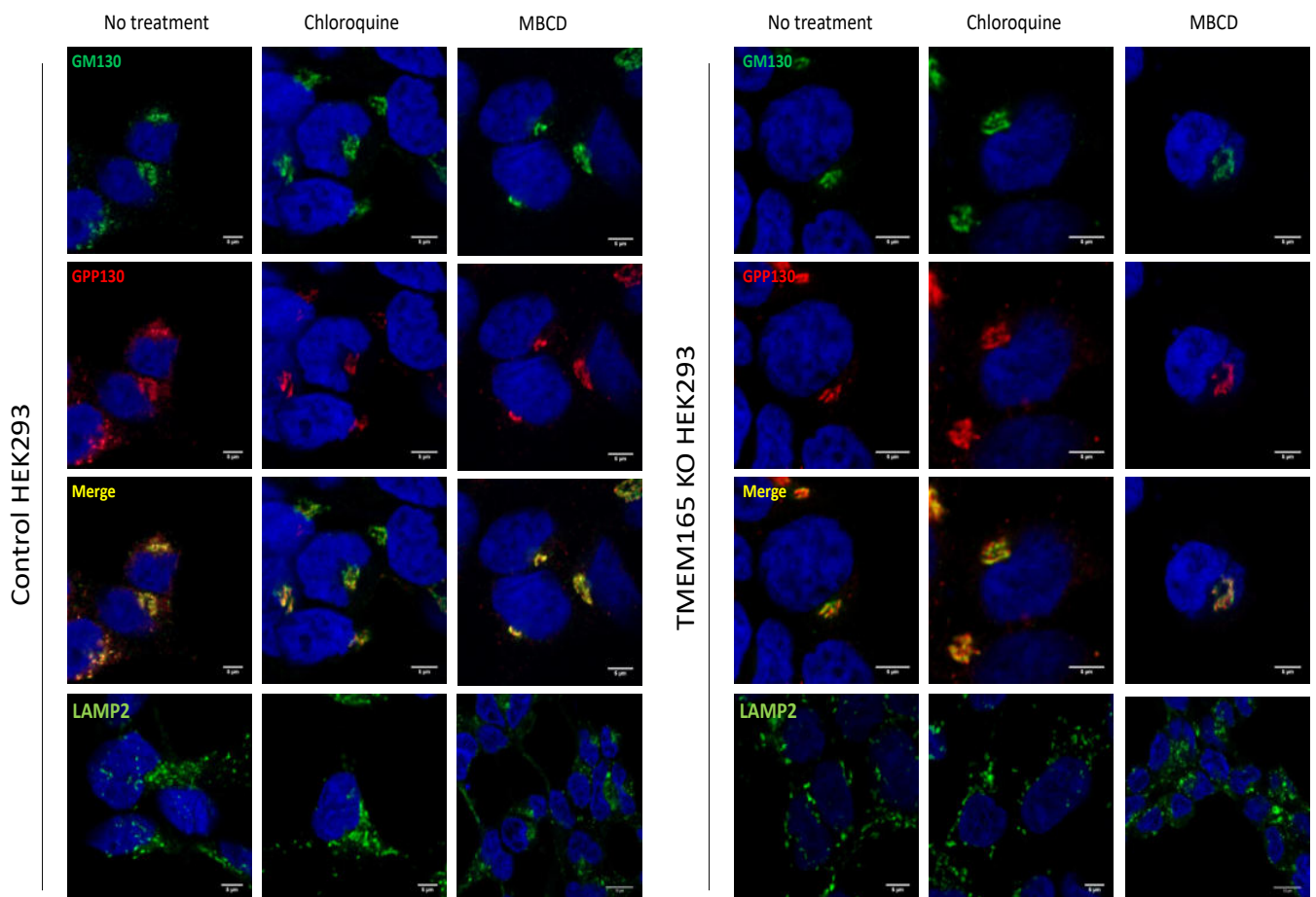
12. Roth, J. A. (2006) Homeostatic and toxic mechanisms regulating manganese uptake, retention, and elimination. *Biol. Res.* **39**, 45–57
13. Delannoy, C. P., Rombouts, Y., Groux-Degroote, S., Holst, S., Coddeville, B., Harduin-Lepers, A., Wuhrer, M., Ellass-Rochard, E., and Guérardel, Y. (2017) Glycosylation changes triggered by the differentiation of monocytic THP-1 cell line into macrophages. *J. Proteome Res.* **16**, 156–169
14. Dutta, D., and Donaldson, J. G. (2012) Search for inhibitors of endocytosis: intended specificity and unintended consequences. *Cell. Logist.* **2**, 203–208
15. Bayer, N., Schober, D., Prchla, E., Murphy, R. F., Blaas, D., and Fuchs, R. (1998) Effect of bafilomycin A1 and nocodazole on endocytic transport in HeLa cells: implications for viral uncoating and infection. *J. Virol.* **72**, 9645–9655
16. Chiesi, M., and Inesi, G. (1980) Adenosine 5'-triphosphate dependent fluxes of manganese and hydrogen ions in sarcoplasmic reticulum vesicles. *Biochemistry* **19**, 2912–2918
17. Chiesi, M., and Inesi, G. (1981) Mg<sup>2+</sup> and Mn<sup>2+</sup> modulation of Ca<sup>2+</sup> transport and ATPase activity in sarcoplasmic reticulum vesicles. *Arch. Biochem. Biophys.* **208**, 586–592
18. Yonekura, S.-I., and Toyoshima, C. (2016) Mn<sup>2+</sup> transport by Ca<sup>2+</sup>-ATPase of sarcoplasmic reticulum. *FEBS Lett.* **590**, 4650; erratum: 2086–2095
19. Ramakrishnan, B., Ramasamy, V., and Qasba, P. K. (2006) Structural snapshots of beta-1,4-galactosyltransferase-I along the kinetic pathway. *J. Mol. Biol.* **357**, 1619–1633
20. Au, C., Benedetto, A., and Aschner, M. (2008) Manganese transport in eukaryotes: the role of DMT1. *Neurotoxicology* **29**, 569–576
21. Garrick, M. D., Dolan, K. G., Horbinski, C., Ghio, A. J., Higgins, D., Porubcin, M., Moore, E. G., Hainsworth, L. N., Umbreit, J. N., Conrad, M. E., Feng, L., Lis, A., Roth, J. A., Singleton, S., and Garrick, L. M. (2003) DMT1: a mammalian transporter for multiple metals. *Biometals* **16**, 41–54
22. Forbes, J. R., and Gros, P. (2003) Iron, manganese, and cobalt transport by Nramp1 (Slc11a1) and Nramp2 (Slc11a2) expressed at the plasma membrane. *Blood* **102**, 1884–1892
23. Chen, P., Bowman, A. B., Mukhopadhyay, S., and Aschner, M. (2015) SLC30A10: a novel manganese transporter. *Worm* **4**, e1042648
24. Chen, P., Chakraborty, S., Mukhopadhyay, S., Lee, E., Paoliello, M. M. B., Bowman, A. B., and Aschner, M. (2015) Manganese homeostasis in the nervous system. *J. Neurochem.* **134**, 601–610
25. Girijashanker, K., He, L., Soleimani, M., Reed, J. M., Li, H., Liu, Z., Wang, B., Dalton, T. P., and Nebert, D. W. (2008) SLC39A14 gene encodes ZIP14, a metal/bicarbonate symporter: similarities to the ZIP8 transporter. *Mol. Pharmacol.* **73**, 1413–1423
26. Vandecaetsbeek, I., Vangheluwe, P., Raeymaekers, L., Wuytack, F., and Vanoevelen, J. (2011) The Ca<sup>2+</sup> pumps of the endoplasmic reticulum and Golgi apparatus. *Cold Spring Harb. Perspect. Biol.* **3**, a004184
27. Mukhopadhyay, S., and Linstedt, A. D. (2011) Identification of a gain-of-function mutation in a Golgi P-type ATPase that enhances Mn<sup>2+</sup> efflux and protects against toxicity. *Proc. Natl. Acad. Sci. USA* **108**, 858–863
28. Chen, J., De Raeymaecker, J., Hovgaard, J. B., Smaardijk, S., Vandecaetsbeek, I., Wuytack, F., Møller, J. V., Eggermont, J., De Maeyer, M., Christensen, S. B., and Vangheluwe, P. (2017) Structure/activity relationship of thapsigargin inhibition on the purified Golgi/secretory pathway Ca<sup>2+</sup>/Mn<sup>2+</sup>-transport ATPase (SPCA1a). *J. Biol. Chem.* **292**, 6938–6951

Received for publication February 26, 2018.  
Accepted for publication September 17, 2018.

A.

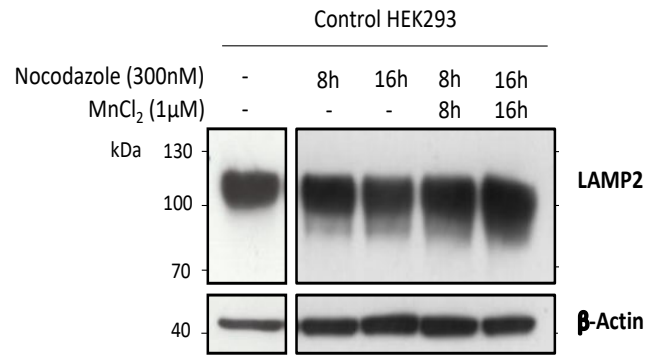


B.

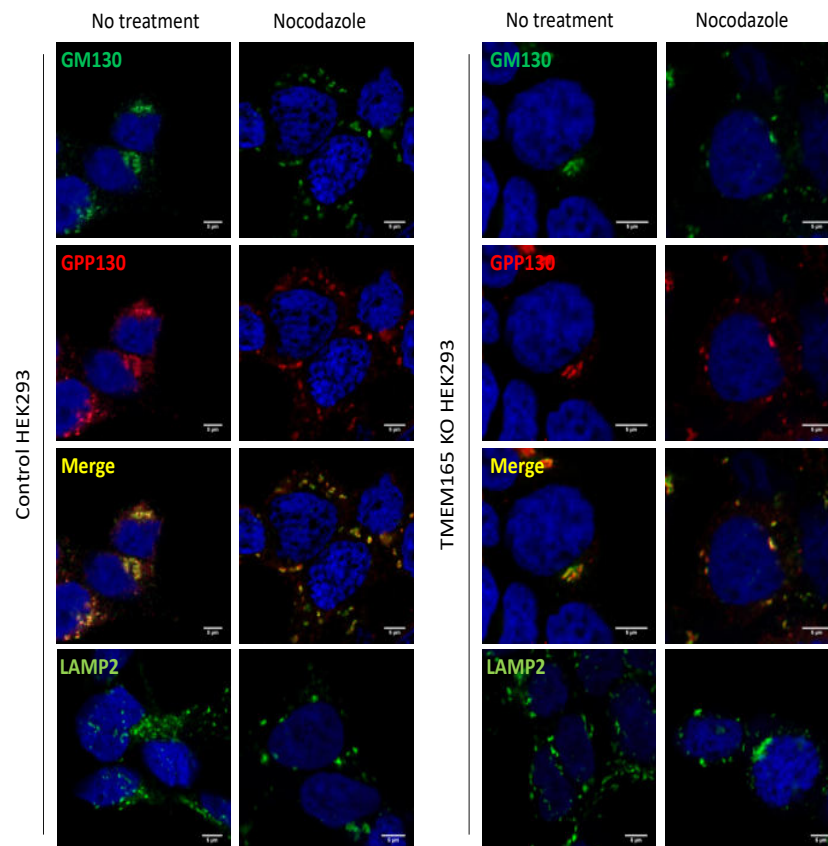


**Supplementary figure 1: Effect of chloroquine (CQ) and methyl- $\beta$ -cyclodextrin (MBCD) on Golgi morphology, LAMP2 subcellular localization and glycosylation profile.** A. Control HEK293 cells were incubated with CQ (10 $\mu$ M) or MBCD (5mM) for 8h or 16h, in combination or not with 1 $\mu$ M MnCl<sub>2</sub>. Total cell lysates were prepared, subjected to SDS-PAGE and western blot with the indicated antibodies. B. Immunofluorescence analysis. Control and TMEM165 KO HEK293 cells were incubated with CQ (10 $\mu$ M) or MBCD (5mM) for 16h, fixed, permeabilized and labeled with antibodies against GM130, GPP130 and LAMP2 before confocal microscopy visualization. DAPI staining (blue) was performed, showing nuclei.

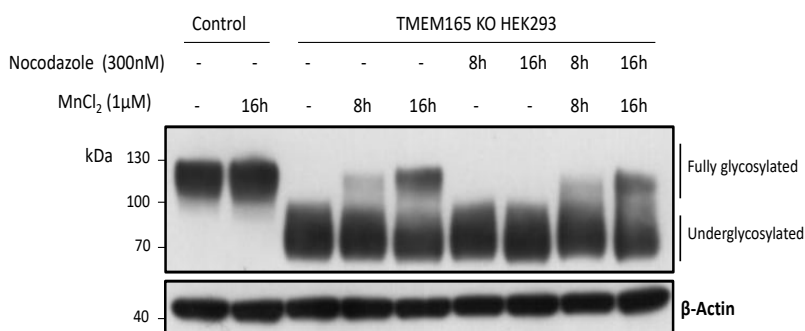
A.



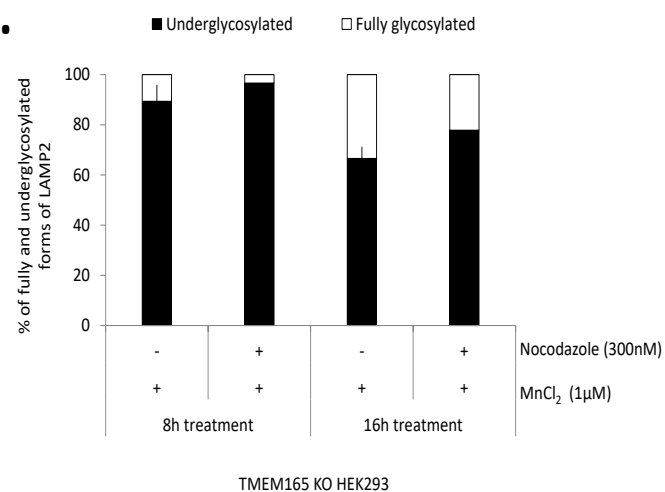
B.



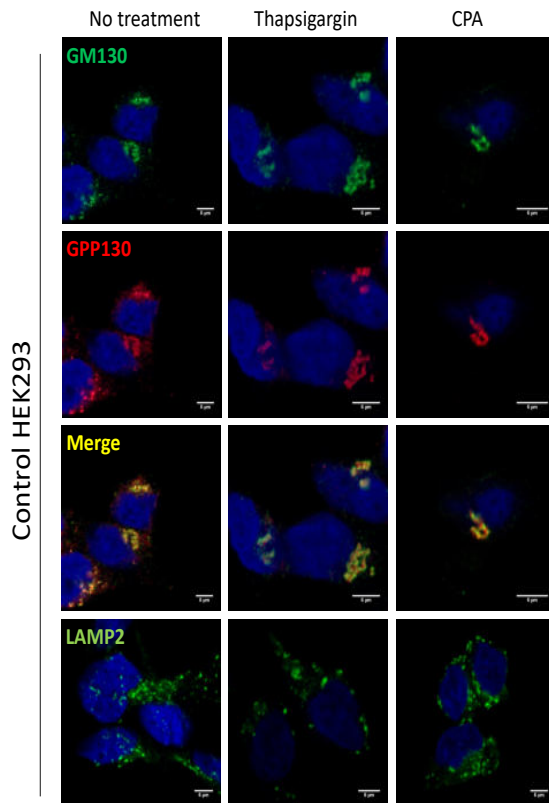
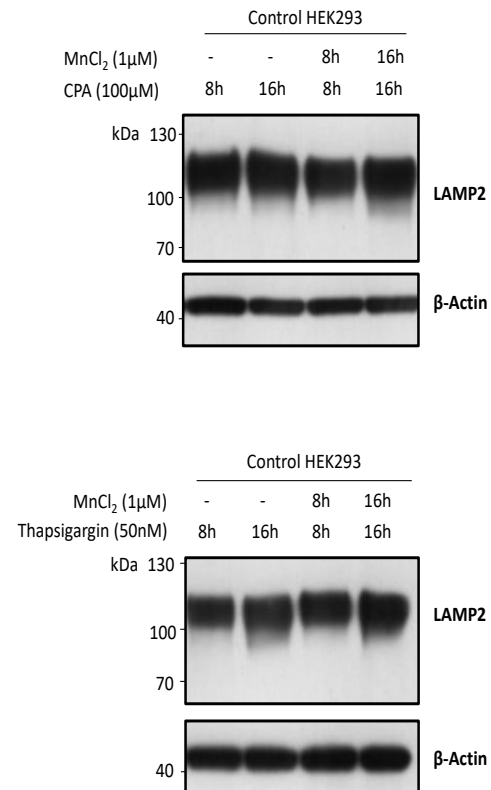
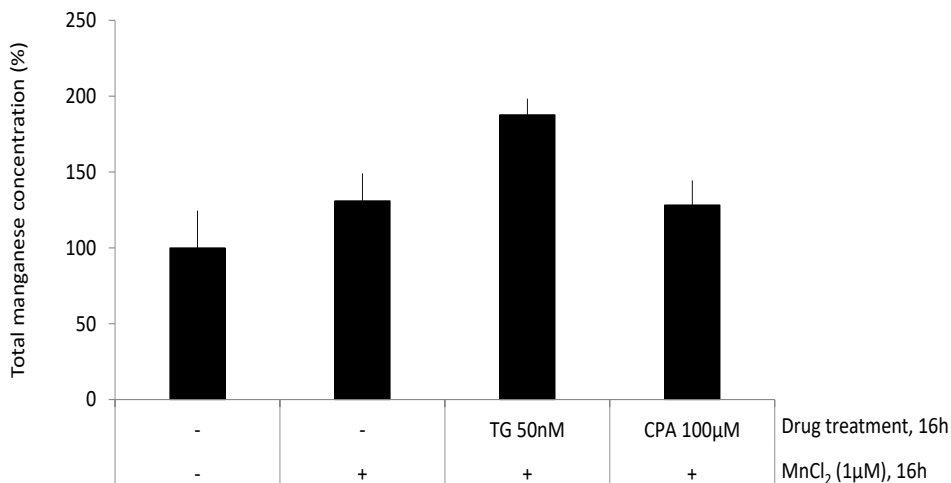
C.



D.



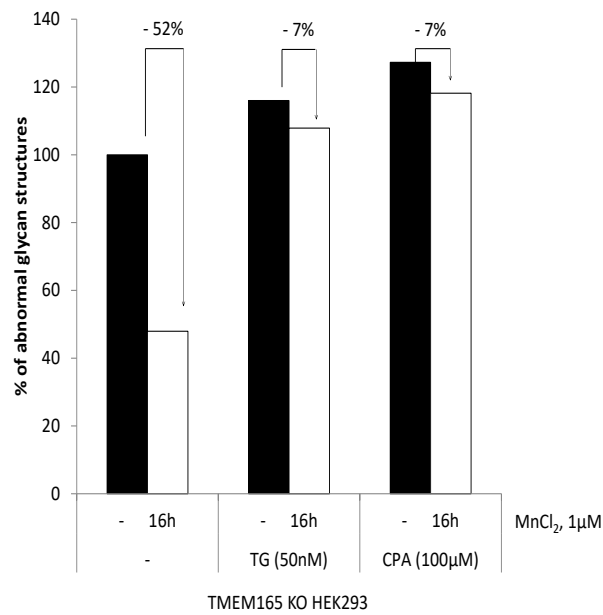
**Supplementary figure 2: Effect of nocodazole on Golgi morphology, LAMP2 subcellular localization and glycosylation profile.** A. and C. Control and TMEM165 KO HEK293 cells were incubated with nocodazole (300nM) for 8h or 16h, in combination or not with 1μM MnCl<sub>2</sub>. Total cell lysates were prepared, subjected to SDS-PAGE and western blot with the indicated antibodies. B. Immunofluorescence analysis. Control and TMEM165 KO HEK293 cells were incubated with nocodazole (300nM) for 16h, fixed, permeabilized and labeled with antibodies against GM130, GPP130 and LAMP2 before confocal microscopy visualization. DAPI staining (blue) was performed, showing nuclei. D. Relative quantification of fully and underglycosylated forms of LAMP2 (N, number of experiments = 2).

**A.****B.****C.**

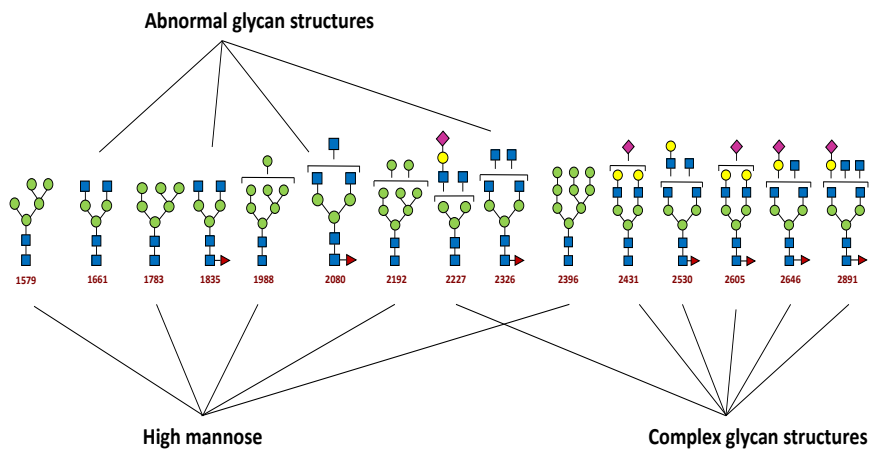
**Supplementary figure 3: Effect of thapsigargin (TG) and cyclopiazonic acid (CPA) on Golgi morphology, LAMP2 subcellular localization and glycosylation profile and manganese uptake.** **A.** Immunofluorescence analysis. Control cells were incubated with either TG (50nM) or CPA (100μM) for 16h, fixed, permeabilized and labeled with antibodies against GM130, GPP130 and LAMP2 before confocal microscopy visualization. DAPI staining (blue) was performed, showing nuclei. **B.** Control HEK293 cells were incubated with either TG (50nM) or CPA (100μM) for 8h or 16h, in combination or not with 1μM MnCl<sub>2</sub>. Total cell lysates were prepared, subjected to SDS-PAGE and western blot with the indicated antibodies. **C.** TMEM165 KO HEK293 cells were cultured with either TG (50nM) or CPA (100μM) in combination with 1μM MnCl<sub>2</sub> for 16h. Total cell lysates were prepared as described in Material and Methods section for ICP-MS analysis and total manganese concentration was measured (N = 2, n, number of samples = 4).



A.



B.



**Supplementary figure 4: Quantification of the abnormal structures found in TMEM165 KO HEK293 cells treated with TG or CPA and with or without Mn<sup>2+</sup>.** **A.** Quantification of abnormal glycan structures observed in TMEM165 KO HEK293 cells following the different indicated treatments. **B.** Representative glycan structures took into account for the quantification (abnormal glycan structures with mass-per-charge ratios (m/z) 1661, 1835, 2080 and 2326; high mannose structures with mass-per-charge ratios (m/z) 1579, 1783, 1988, 2192 and 2396; complex glycan structures mass-per-charge ratios m(z) 2227, 2431, 2530, 2605, 2646 and 2891). Symbols represent sugar residues as follow: blue square, N-acetylglucosamine; green circle, mannose; yellow circle, galactose; purple diamond, sialic acid; red triangle, fucose. Linkages between sugar residues have been removed for simplicity.

### 1.3. Complementary results

#### 1.3.1. Multiplicity of the routes of entry for extracellular MnCl<sub>2</sub>

Assuming that neither CQ, nocodazole, methyl- $\beta$ -cyclodextrine nor dynasore prevents the entry of extracellular MnCl<sub>2</sub>, we reasoned that MnCl<sub>2</sub> could be transported from the extracellular medium to the cytosol through the transport activity of (un)specific transporters or channels. Before standing for it, we did perform siRNA based experiments to knockdown the expression of genes encoding for putative plasma membrane Mn<sup>2+</sup> importers, mainly *SLC11A2* and *SLC39A14*. However, as shown below in Figure 47, none of the two siRNA seemed to prevent the Mn<sup>2+</sup>-induced rescue of LAMP2 in TMEM165 KO HEK cells. Moreover, the lack of efficient antibodies against SLC11A2 and SLC39A14 did not allow us to warrant siRNA efficiency.

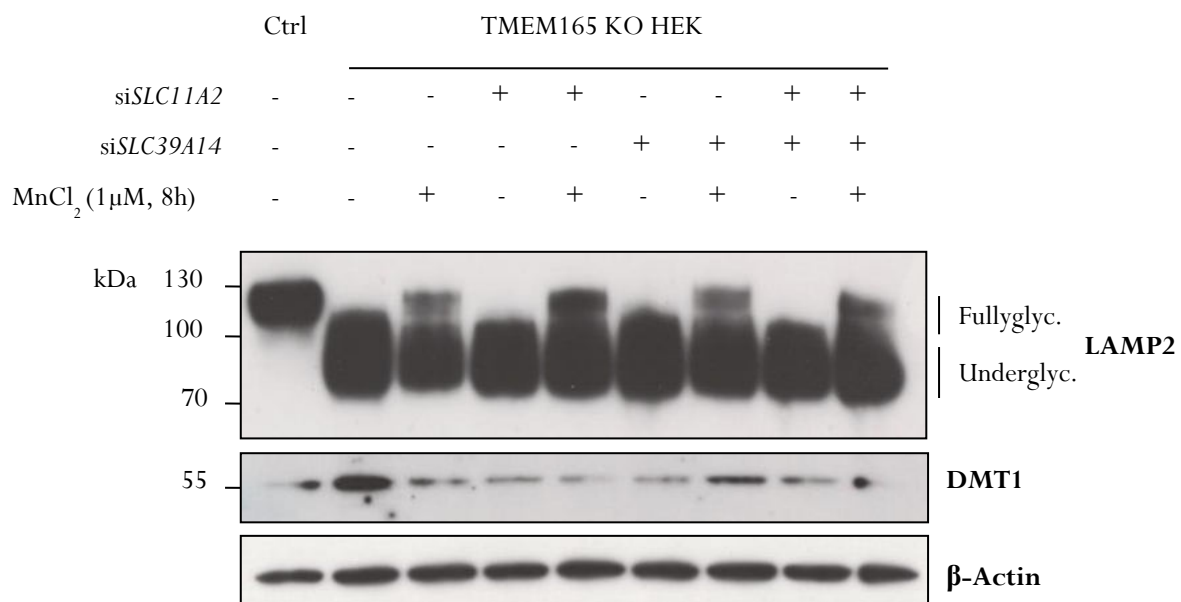


**Figure 47: Impact of *SLC11A2* and *SLC39A14* silencing by siRNA on the rescue of LAMP2 glycosylation defect induced by MnCl<sub>2</sub> supplementation.** TMEM165 KO HEK293 cells were transfected with si*SLC11A2* and si*SLC39A14* and incubated or not with 1 $\mu$ M MnCl<sub>2</sub> for 8h. Total cell lysates were prepared, subjected to SDS-PAGE and western blot with the indicated antibodies.

Hence, facing the multiplicity of the putative Mn<sup>2+</sup> plasma membrane transporters (see Chapter 2, Figure 27), we therefore admit that Mn<sup>2+</sup> could enter the cells using one or several of them.

#### 1.3.2. SERCA2 as “thapsigargin and cyclopiazonic acid sensitive pumps”?

As suggested from the title of this publication, “thapsigargin and cyclopiazonic acid sensitive pumps” have been identified to play a role in the Mn<sup>2+</sup>-induced N-glycosylation rescue in absence of TMEM165. This particular caution relies on the fact that we lacked evidence to clearly identify SERCA2. Although we highlighted that SERCA2b overexpression slightly rescues LAMP2 glycosylation status in TMEM165 KO HEK cells, we failed to demonstrate that *ATP2A2* silencing prevents the Mn<sup>2+</sup>-induced glycosylation

rescue on LAMP2. Using a siRNA strategy, TMEM165 KO HEK cells were silenced for *ATP2A2* and treated or not with 1  $\mu$ M  $MnCl_2$  for 8h. As shown in Figure 48, *ATP2A2* silencing was not sufficient to prevent the  $Mn^{2+}$ -induced glycosylation rescue on LAMP2. Although the good efficiency of the si*ATP2A2* (more than 90% extinction), we reasoned that this result may come from “off-target” effects due to the endogenous expression of additional SERCA protein variants (SERCA1 and SERCA3).

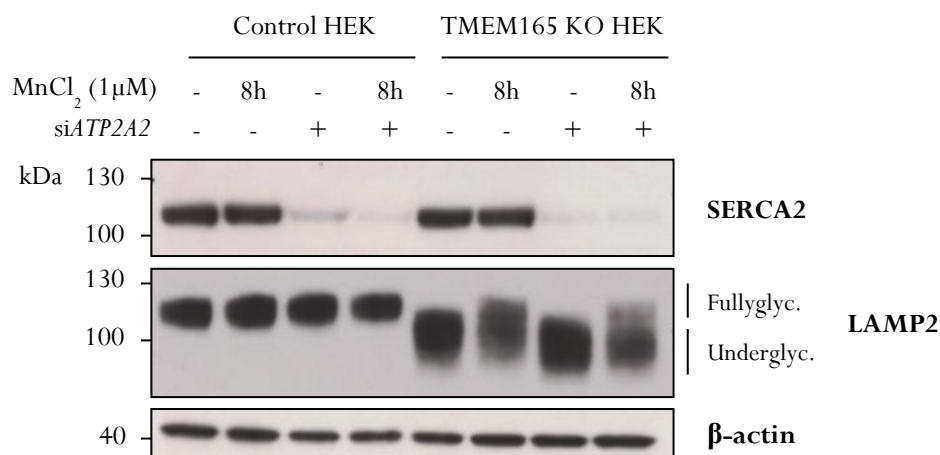


**Figure 48: Effect of *ATP2A2* silencing by siRNA on the rescue of LAMP2 glycosylation defect induced by  $MnCl_2$  supplementation.** Control and TMEM165 KO HEK293 cells were transfected with si*ATP2A2* and incubated or not with 1  $\mu$ M  $MnCl_2$  for 8h. Total cell lysates were prepared, subjected to SDS-PAGE and western blot with the indicated antibodies.

Indeed, as mentioned in the Introduction part of this manuscript (Chapter 2, section 2.1.2.), SERCA pumps are encoded by three separate genes *ATP2A1*, *ATP2A2* and *ATP2A3* that are all expressed in HEK cells (with different expression levels). In addition, splicing events in each of the corresponding mRNA yield the total number of SERCA protein variants to more than ten. Hence, it is likely that the silencing of only one isoform, although the ubiquitous one (SERCA2b), is not sufficient to prevent the  $Mn^{2+}$ -induced mechanism in TMEM165 KO cells which could be compensate or rely on the activity of other SERCA protein variants and/or isoforms. Nonetheless, the remaining SERCA2 protein expression over siRNA could also contribute to the slight rescue on LAMP2 migration profile upon  $MnCl_2$  supplementation. These “off-target” effects are not seen with the use of pharmacological agents such as thapsigargin and CPA that completely inhibit the activity of all SERCA proteins.

## 1.4. Conclusion

In this first study, we aimed at demonstrating that exogenous supplementation of the cell culture medium with 1  $\mu$ M  $MnCl_2$  for 8h was sufficient to correct Golgi N-linked glycosylation in TMEM165 KO HEK cells. Although the mechanism beyond this observation still needs to be clarified, we shed light on a completely new and unknown mechanism by which the ER would feed the Golgi apparatus with

Mn<sup>2+</sup> ions, through the activity of likely SERCA pumps to sustain Golgi glycosylation reactions in absence of TMEM165. This concept is summarized below in Figure 49 and will be discussed further in the General Discussion of this manuscript.

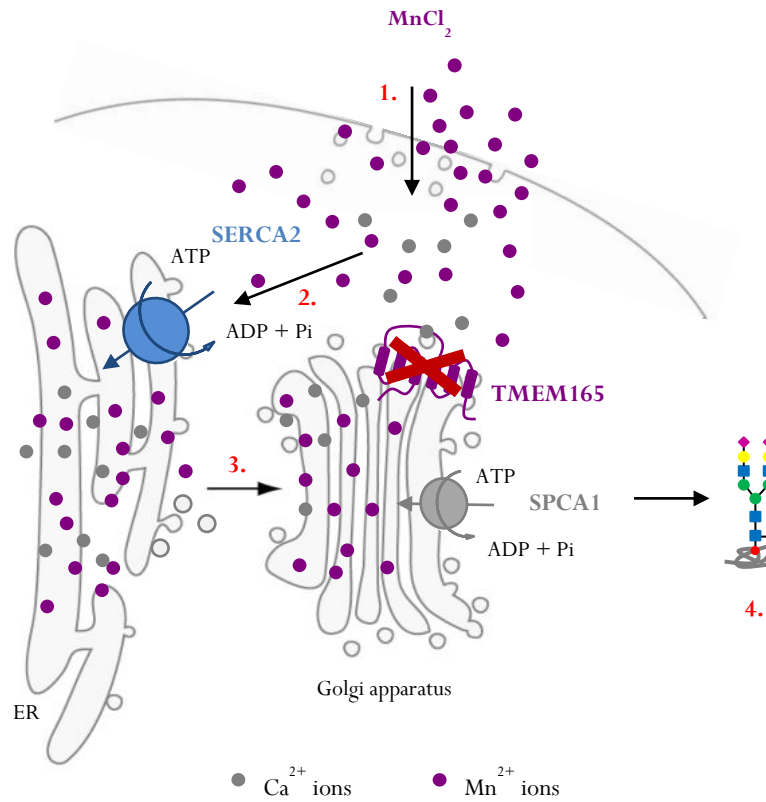


**Figure 49: Potential involvement of SERCA2 pumps in cytosolic Mn<sup>2+</sup> pumping to sustain the Golgi glycosylation process in TMEM165 KO cells.** Schematic representation of the concept arose from our observations. **1.** Entry of extracellular MnCl<sub>2</sub>. **2.** Cytosolic Mn<sup>2+</sup> pumping by SERCA2 in the ER. **3.** Mn<sup>2+</sup> redistribution into the Golgi lumen to sustain the Golgi glycosylation. **4.** Glycoprotein correctly glycosylated.

## 2. Paper 2: Fetal Bovine Serum impacts the observed N-glycosylation defects in TMEM165 KO HEK cells

### 2.1. Introduction

This study is directly linked to Paper 1. To contextualize, during the reviewing of the previous publication, I did experience a so-called cruel joke. While I spent almost a year to demonstrate that  $MnCl_2$  supplementation was triggering Golgi glycosylation rescue in TMEM165 deficient cells, in a couple of months, I found out that Golgi glycosylation defects were spontaneously suppressed in TMEM165 KO HEK cells without any  $MnCl_2$  supplementation. I first checked TMEM165 expression in those TMEM165 KO HEK cells to be sure that the mistake was not coming from a potential crossed contamination, resulting in a mixed population of TMEM165 KO and control cells that might have explained the unexpected LAMP2 migration profile. However, as shown in Figure 50, this was not likely: cells were not contaminated and still, the result was there.

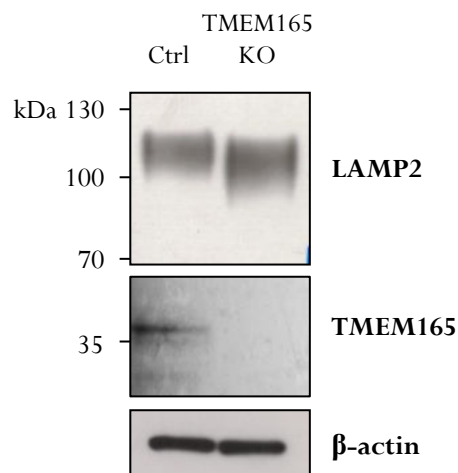


**Figure 50: LAMP2 glycosylation defect observed in TMEM165 KO cells is no more detectable.** TMEM165 KO and HEK cells were thawed and cultured in DMEM Lonza with 10% FBS\* for several weeks. Total cell lysates were prepared, subjected to SDS-PAGE and western blot with the indicated antibodies.

Trying to figure it out, I then looked for potential changes in cell culture conditions and pinpointed that both cell culture media and fetal bovine serum (FBS) had changed, in the same period of time, apart from early 2018. Actually, (i) we were running out of FBS1 (Dutscher, batch n° S10536S1810), *i.e.* batch number could not have been the same anymore due to end of production and (ii) the firm from which we were purchasing DMEM cell culture media (Lonza) had a contamination on its production chain supply, forcing us to find another supplier (Biowest) to overcome the lack of media and sustain cell culture activities. Taking these two major modifications into account, I decided to further investigate from where the issue originates.

First, I cultured TMEM165 KO and control HEK cells in three different media we had at the time: DMEM from Lonza (batch n°0000704255), UltraMEM from Lonza (batch n°6MB140) and two different batches of DMEM from Biowest (n°S17337L0104 and n°S17436L0104), all supplemented with 10% of FBS from Corning (batch n°35079002), named FBS\*.

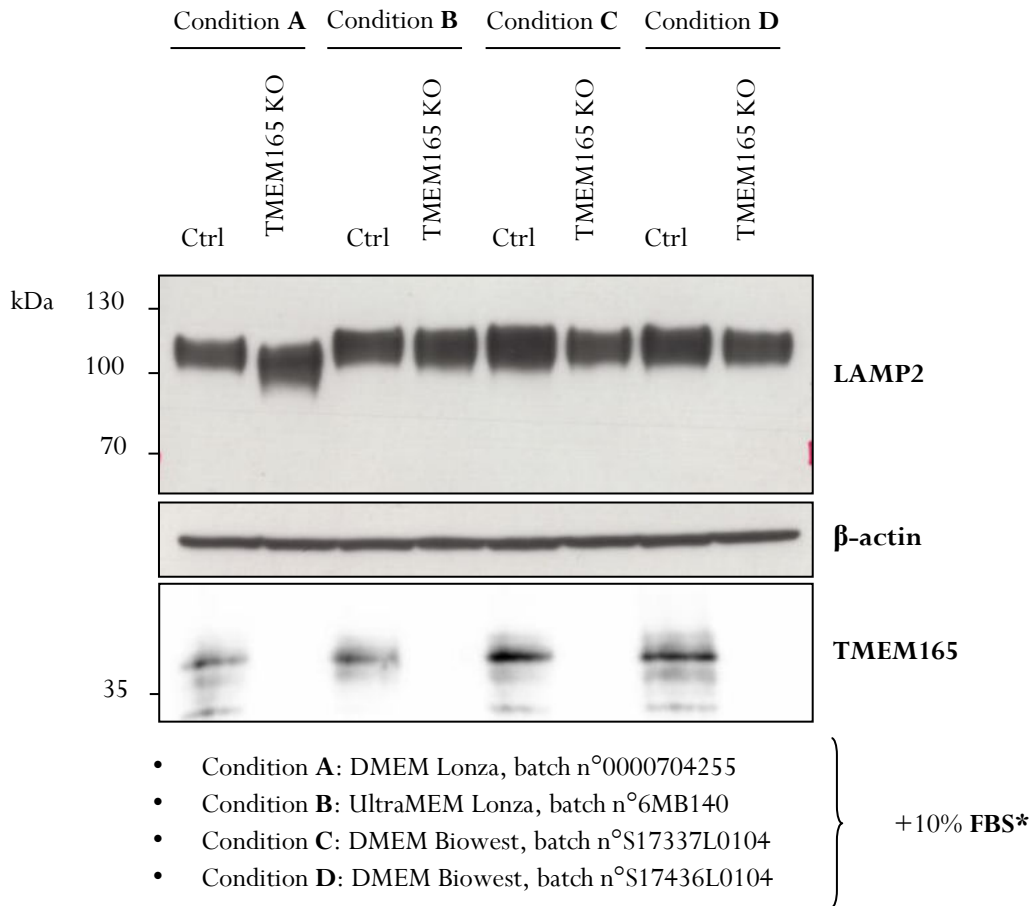


**Figure 51: Changes in cell culture conditions impact Golgi glycosylation defects associated with TMEM165 deficiency.** TMEM165 KO and control (ctrl) cells were cultured in four different conditions for 72h with medium renewal every 24h hours. FBS\* refers to FBS from Corning, batch n°35079002. Total cell lysates were prepared, subjected to SDS-PAGE and western blot with the indicated antibodies.

The hypothesis beyond these treatments was to evaluate whether the composition of the different media could interfere with the observed spontaneous Golgi glycosylation rescue seen on LAMP2 in TMEM165 KO HEK cells. As shown in Figure 51, after 72h in the different cell culture media, a rather slight shift in LAMP2 gel mobility was observed in TMEM165 KO HEK cells cultured in the usual medium (DMEM Lonza) complemented with new FBS\* (condition A). In contrast, no more differences in the migration profile of LAMP2 were noticed between TMEM165 KO and control cells in the three other conditions (Figure 51, conditions B, C and D). From these observations, it was likely that LAMP2 glycosylation rescue originated from a component of the FBS\* since in condition A compared to usual and old conditions, only FBS has changed (from FBS1 to FBS\*).

To strengthen this observation and better visualize discrepancies in LAMP2 gel mobility, I then re-loaded a SDS-PAGE with old (September 2016) and fresh (April 2018) TMEM165 KO cell lysates coming from cells cultivated in DMEM Lonza with 10% of either old FBS Dutscher (FBS1) or new FBS Corning (FBS\*) (Figure 52). Unambiguously, the more TMEM165 KO HEK cells are cultured with FBS\*, the slightest shift in LAMP2 gel mobility is observed. In other words, the more TMEM165 deficient cell are incubated with FBS\*, the better the Golgi glycosylation rescue can be observed.

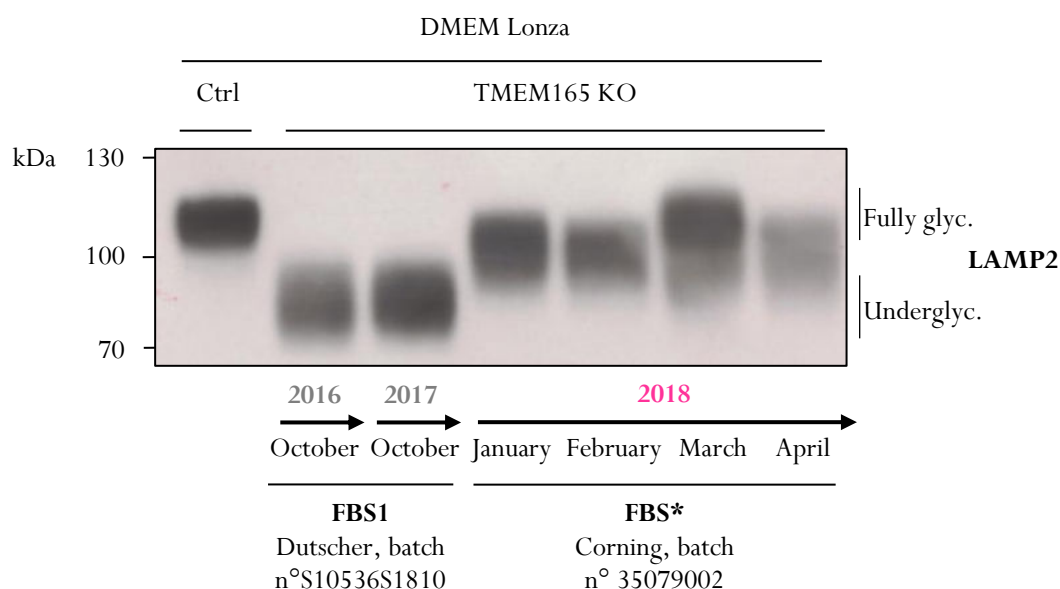



**Figure 52: Suppression of LAMP2 glycosylation defect in TMEM165 KO cells induced by change in FBS used for cell culture.** Control and TMEM165 KO HEK cells were cultured in DMEM Lonza supplemented with 10% FBS1 or \*. Total cell lysates were prepared, subjected to SDS-PAGE and western blot with the indicated antibody.

All of these introductive results defined the starting point for further investigations on the influence of different FBS onto N-linked glycosylation process in TMEM165 KO HEK cells and led to Paper 2.

## 2.2. Publication

# Fetal bovine serum impacts the observed N-glycosylation defects in TMEM165 KO HEK cells

Dorothee Vicogne<sup>1</sup> | Marine Houdou<sup>1</sup> | Anne Garat<sup>2,3</sup> | Leslie Climer<sup>4</sup> | Vladimir Lupashin<sup>5</sup> | Willy Morelle<sup>1</sup> | François Foulquier<sup>1</sup> 

<sup>1</sup>CNRS, UMR 8576, Unité de Glycobiologie Structurale et Fonctionnelle (UGSF), Université de Lille, Lille, France

<sup>2</sup>EA 4483, IMPact de l'Environnement Chimique sur la Santé humaine (IMPECS), Université de Lille, Lille, France

<sup>3</sup>CHU Lille, Unité Fonctionnelle de Toxicologie, Lille, France

<sup>4</sup>Department of Biology, Baylor University, Waco, Texas

<sup>5</sup>Department of Physiology and Biophysics, College of Medicine, University of Arkansas for Medical Sciences, Little Rock, Arkansas

## Correspondence

François Foulquier, CNRS, UMR 8576, Unité de Glycobiologie Structurale et Fonctionnelle (UGSF), Université de Lille, F-59000 Lille, France.  
Email: francois.foulquier@univ-lille.fr

**Communicating Editor:** Eva Morava

## Funding information

Agence Nationale de la Recherche, Grant/Award Number: SOLV-CDG; H2020 European Research Council, Grant/Award Number: 643578

## Abstract

TMEM165 is involved in a rare genetic human disease named TMEM165-CDG (congenital disorders of glycosylation). It is Golgi localized, highly conserved through evolution and belongs to the uncharacterized protein family 0016 (UPF0016). The use of isogenic TMEM165 KO HEK cells was crucial in deciphering the function of TMEM165 in Golgi manganese homeostasis. Manganese is a major cofactor of many glycosylation enzymes. Severe Golgi glycosylation defects are observed in TMEM165 Knock Out Human Embryonic Kidney (KO HEK) cells and are rescued by exogenous manganese supplementation. Intriguingly, we demonstrate in this study that the observed Golgi glycosylation defect mainly depends on fetal bovine serum, particularly its manganese level. Our results also demonstrate that iron and/or galactose can modulate the observed glycosylation defects in TMEM165 KO HEK cells. While isogenic cultured cells are widely used to study the impact of gene defects on proteins' glycosylation patterns, these results emphasize the importance of the use of validated fetal bovine serum in glycomics studies.

## KEYWORDS

FBS, manganese level, N-glycosylation defects, TMEM165

## 1 | INTRODUCTION

Congenital disorders of glycosylation (CDG) are a rapidly growing and heterogeneous group of rare genetic diseases.<sup>1-5</sup> The deficiencies observed in CDG affect the biosynthesis of glycoproteins leading to macro- and/or micro-heterogeneity of the protein glycosylation status. They show heterogeneous phenotypes comprising mostly neurological involvement and dysmorphism.<sup>6,7</sup> A new era in CDG is started with the identification of defects in genes not directly linked to glycosylation but involved in vesicular Golgi trafficking<sup>8-14</sup> and Golgi homeostasis.<sup>15</sup> In order to understand the molecular mechanisms that fine-tune the glycosylation machinery to physiological

requirements, several cellular and animal models were created. Regarding CDG, isogenic cell lines represent an interesting toolset to better understand the molecular and cellular mechanisms of the glycosylation process itself. This was used to find out the function of TMEM165 in Golgi glycosylation. Indeed, in 2012 we identified *TMEM165* as a gene involved in a novel CDG-II, TMEM165-CDG (OMIM entry #614727).<sup>16,17</sup> TMEM165 is a 324 amino acids transmembrane Golgi protein belonging to the uncharacterized protein family 0016 (UPF0016; Pfam PF01169). The cellular and molecular functions of the UPF0016 family members remain controversial. Our previous results unambiguously demonstrated a link between TMEM165 and Golgi Mn<sup>2+</sup> homeostasis<sup>18</sup> through



the rescue of Golgi glycosylation defects observed in TMEM165 Knock Out Human Embryonic Kidney (KO HEK) cells by  $MnCl_2$  supplementation.<sup>18,19</sup> Recently, we noticed that suppression of these glycosylation defects depends on cell culture conditions. In this study, we investigate the effects of different fetal bovine sera (FBS) on Golgi glycosylation defects in TMEM165 KO HEK cells.

## 2 | MATERIAL AND METHODS

### 2.1 | Antibodies and other reagents

Anti-LAMP2 antibody was purchased from Santa Cruz Biotechnology (Dallas). Polyclonal goat anti-mouse immunoglobulins HRP conjugated were purchased from Dako (Glostrup, Denmark). D-(+)-Galactose, zinc chloride ( $ZnCl_2$ ) and nickel sulfate hexahydrate ( $NiSO_4$ ) were purchased from Sigma (Saint Louis), manganese(II) chloride tetrahydrate ( $MnCl_2$ ) was from Riedel-de-Haën (Seelze, Germany), calcium chloride ( $CaCl_2$ ) and iron(III) chloride ( $FeCl_3$ ) were from ACROS Organics (New Jersey), copper(II) sulfate ( $CuSO_4$ ) was from Prolabo (France), lithium chloride ( $LiCl$ ) was from Bio Basic Canada (Canada), magnesium chloride ( $MgCl_2$ ) was from Euromedex (Souffelweyersheim, France) and iron(II) tetrahydrate ( $FeCl_2$ ) was purchased from WVR Chemicals (Germany).

### 2.2 | Cell culture, drug treatments and transfections

Control and TMEM165 KO HEK/HeLa-GalT cells were generated as previously described in Reference 23. Briefly, TMEM165 was knocked out using CRISPR/Cas9-mediated deletion with guide RNAs targeting the first exon (target sequence: TCCAGGGAACGGCCGCGCAT). Clones were first screened for lack of detection of TMEM165 protein with TMEM165 antibodies in western blot and immunofluorescence experiments and then by sequencing. Clones were analyzed by PCR using genomic DNA as a template and primers F7 (tggaggaagcagaagtga) and R4 (ctaattcctctgcttctaag) producing an amplicon length around 1200 bp. Sequencing of KO clones showed a deletion of 347 bp. Control cells were from a clone that went through the screening process but was immunoreactive with TMEM165 antibodies and showed no mutations by sequencing. Cells were maintained in Dulbecco's modified Eagle's medium (DMEM; Lonza, Basel, Switzerland) supplemented with either 10% FBS from animal origin from Dutscher (France), Corning (France) or PAN Biotech (Germany), or 10% synthetic serum substitute (Panexin) from PAN Biotech (Germany) at 37°C in humidity-saturated 5%  $CO_2$  atmosphere. To simplify both writing and reading, we named the different FBS from animal origin as follow: FBS 1 for FBS from Dutscher (old batch, lot no. S10536S1810), FBS 2 for FBS from Dutscher (new batch, lot no. S15642S1810), FBS 3 for FBS from Corning

(lot no. 35079011) and FBS 4 for FBS from PAN (lot no. P170602). When used, the cells have been cultured for at least 9 days with the different sera.

### 2.3 | Western blotting

Cells were scraped in DPBS and then centrifuged at 6000 rpm, 4°C for 10 minutes. Supernatant was discarded and cells were then resuspended in RIPA buffer (Tris/HCl 50 mM pH 7.9, NaCl 120 mM, NP40 0.5%, EDTA 1 mM,  $Na_3VO_4$  1 mM, NaF 5 mM) supplemented with a protease cocktail inhibitor (Roche Diagnostics, Penzberg, Germany). Cell lysis was done by passing the cells several times through a syringe with a 26G needle. Cells were centrifuged for 30 minutes, 4°C at 14 000 rpm. Protein concentration contained in the supernatant was estimated with the micro BCA Protein Assay Kit (Fisher Scientific, Waltham). Total protein lysate of 10  $\mu$ g was mixed with NuPAGE LDS sample buffer (Fisher Scientific) pH 8.4 supplemented with 4%  $\beta$ -mercaptoethanol (Sigma). Samples were heated 10 minutes at 95°C then separated on 4 to 12% Bis-Tris gels (Fisher Scientific) and transferred to nitrocellulose membrane Hybond ECL (GE Healthcare, Little Chalfont, UK). Membranes were blocked in blocking buffer (5% milk powder in TBS-T [ $\times 11X$  TBS with 0.05% Tween20]) for 1 hour at room temperature, then incubated overnight with the primary antibody (used at a dilution of 1:2000) in blocking buffer and washed three times for 5 minutes in TBS-T. Membranes were then incubated with the peroxidase-conjugated secondary anti-mouse antibody (Dako; used at a dilution of 1:20 000) in blocking buffer for 1 hour at room temperature and later washed five times for 5 minutes in TBS-T. Signal was detected with chemiluminescence reagent (Super Signal West Pico PLUS chemiluminescent Substrate, Thermo Scientific, Courtaboeuf, France) on imaging film (GE Healthcare).

### 2.4 | Glycan analysis by mass spectrometry

Cells were sonicated in extraction buffer (25 mM Tris, 150 mM NaCl, 5 mM EDTA and 1% CHAPS, pH 7.4) and then dialyzed in 6 to 8 kDa cut-off dialysis tubing in an ammonium bicarbonate solution (50 mM, pH 8.3) for 48 hours at 4°C and lyophilized. The proteins/glycoproteins were reduced and carboxyamidomethylated followed by sequential tryptic and peptide N-glycosidase F digestion and Sep-Pak purification. Permethylated of the freeze-dried glycans and MALDI-TOF-MS of permethylated glycans were performed as described elsewhere.<sup>24</sup>

### 2.5 | Mn measurement by ICP-MS

#### 2.5.1 | Instrumentation and analysis

Serum samples were diluted 50 times with 1.5% (v/v) nitric acid (ultrapure quality 69.5%, Carlo Erba Reagents, Val de

Reuil, France) solution in ultrapure water (Purelab Option-Q, Veolia Water, Antony, France) containing 0.1% TritonX-100 (Euromedex, Souffelweyersheim, France), 0.2% butan-1-ol (VWR Chemicals, Fontenay-sous-Bois, France) and 0.5 µg/L rhodium (Merk, Darmstadt, Germany). Assays were performed on an ICP-MS THERMO ICAP Q (Thermo Scientific). The limit of quantification was 0.2 µg/L.

### 3 | RESULTS

#### 3.1 | Serum impacts the observed Golgi glycosylation defects in TMEM165 KO HEK cells

We previously reported that LAMP2 glycosylation defects found in TMEM165 KO HEK cells were totally suppressed by the addition of exogenous MnCl<sub>2</sub> in the culture medium. This was observed from 8 hours of incubation with 1 µM MnCl<sub>2</sub>.<sup>18,19</sup> We recently observed that this suppression could appear without any supplementation of MnCl<sub>2</sub> probably due to cell culture conditions (data not shown). This urged us to investigate the effects of different sources of FBS on the appearance and/or rescue of the N-glycosylation defects in TMEM165 KO HEK cells. To investigate this, LAMP2 glycosylation profile was assessed by western blot in TMEM165 KO HEK cells grown in medium supplemented with six different FBS: four from animal origin (FBS 1, 2, 3 and 4 in this study) and two synthetic serum substitutes. After a few passages, HEK cells (controls and TMEM165 KO) did not survive when cultured with the synthetic serum substitutes (data not shown). Regarding the sera from animal origin, differential gel mobilities of LAMP2 can be easily seen after 9 days of culture (Figure 1). When cells were grown with FBS 3, LAMP2 gel mobility was less pronounced compared to cells cultured with FBS 1 or FBS 2. Intriguingly, a very pronounced gel mobility arguing for a severe LAMP2 N-glycosylation defect was observed with FBS 4 (Figure 1). Similar results were observed with TMEM165 KO HeLa-GalT cells cultured with FBS 4 (Figure S1). This suggests that

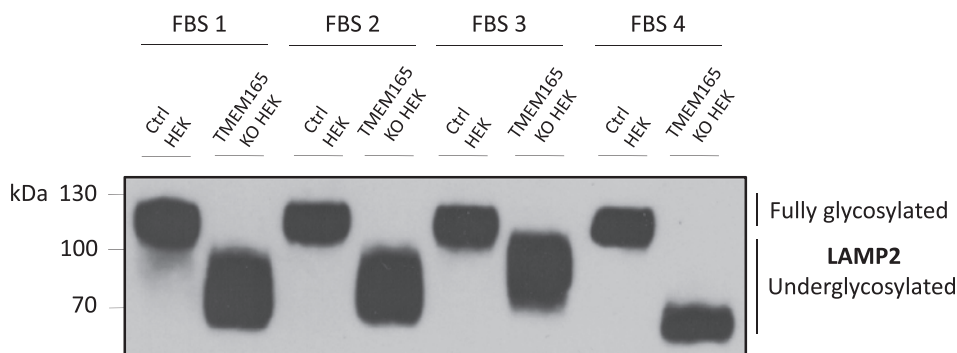
the severity of the observed glycosylation defects depends on the source of the serum used for cell culture.

To confirm these results and pinpoint the potential differences in N-glycosylation that result from the use of each FBS, mass spectrometry analysis of total N-glycans was performed in the different cell culture conditions. For control cells, no significant changes in N-glycan structures were observed with any serum tested (Figure 2, panels A-D). Similar to our previously published analyses,<sup>18,20</sup> TMEM165 KO HEK cells showed massive hypogalactosylation in all tested conditions with the accumulation of agalactosylated glycan structures detected at mass-per-charge (*m/z*) ratios of 1591, 1836, 2081 and 2326 (Figure 3, panels E-H). Interestingly, the proportion of these abnormal glycan structures found was totally dependent upon the FBS chosen for cell growth (see Table 1). On one hand, the proportion of these abnormal glycan structures was comparable, and found in rather low quantity to control cells when TMEM165 KO HEK cells were cultured with FBS 2 or 3 (Table 1). On the other hand, they largely increased in abundance in TMEM165 KO HEK cells cultured with FBS 1 or 4 (24% general increase of abnormal glycan structures compared to FBS 2/3). The mass spectrometry analyses not only confirmed the results obtained from LAMP2 gel mobility, but also highlighted the crucial importance of the use of validated FBS in analyzing the Golgi glycosylation defects and/or rescue observed in TMEM165 KO HEK cells.

#### 3.2 | Independently of the serum used for cell growth, Mn<sup>2+</sup> supplementation suppresses the glycosylation defects in TMEM165 KO HEK cells

As we have previously shown that Mn<sup>2+</sup> supplementation could rescue the observed N-glycosylation defects in TMEM165 KO HEK cells, we wondered whether Mn<sup>2+</sup> supplementation would overcome the issues we have observed with regard to FBS. First, each culture medium was supplemented with 1 µM MnCl<sub>2</sub>, and LAMP2 glycosylation was assessed by western blot. Such treatment partially suppressed

**FIGURE 1** The appearance of LAMP2 glycosylation defects in TMEM165 KO HEK cells depends on the FBS used for cell culture. Control and TMEM165 KO HEK cells were cultured in DMEM supplemented with 10% FBS 1, 2, 3 or 4. Total cell lysates were prepared, subjected to sodium dodecyl sulfate polyacrylamide gel electrophoresis (SDS-PAGE) and western blot with the indicated antibody



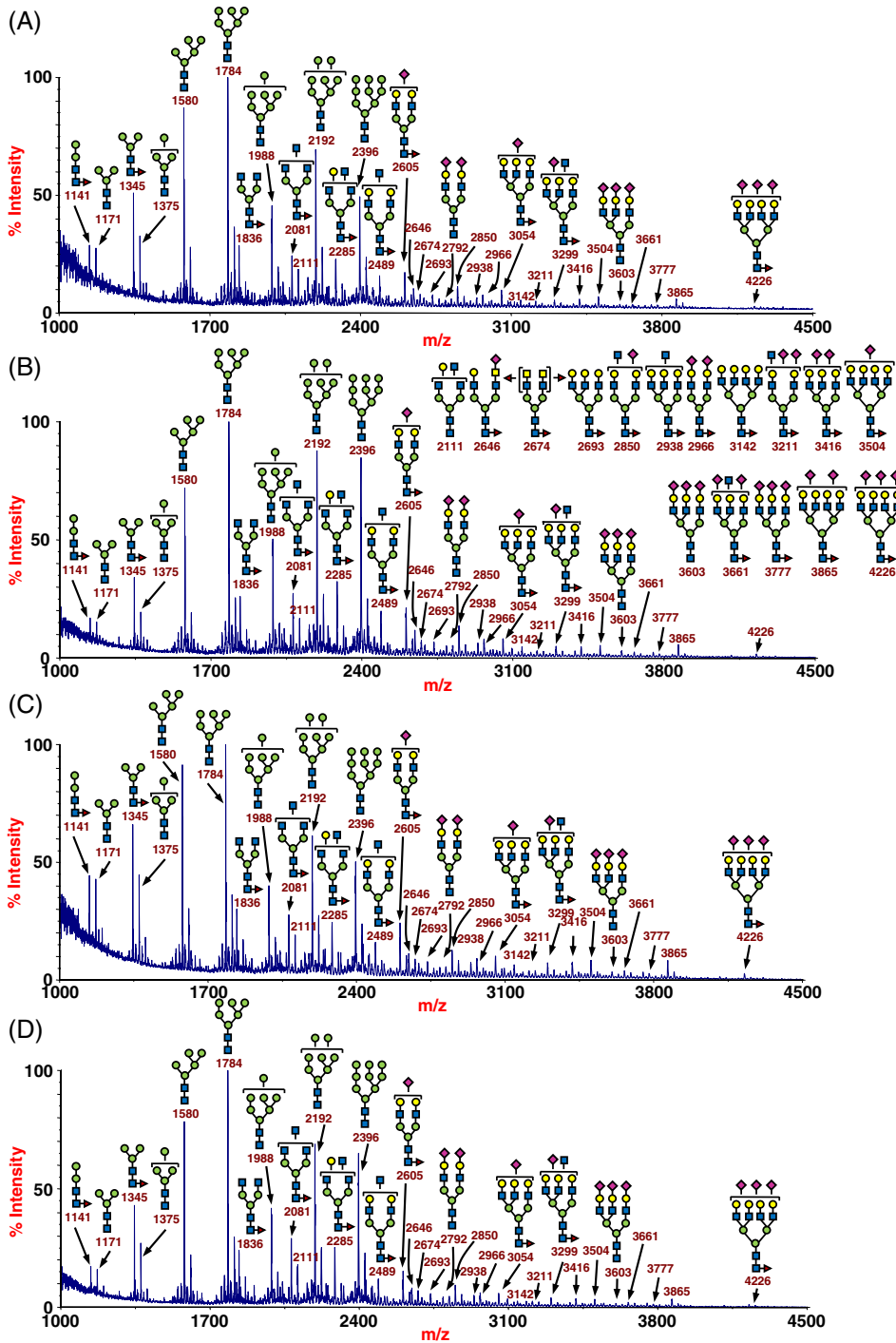
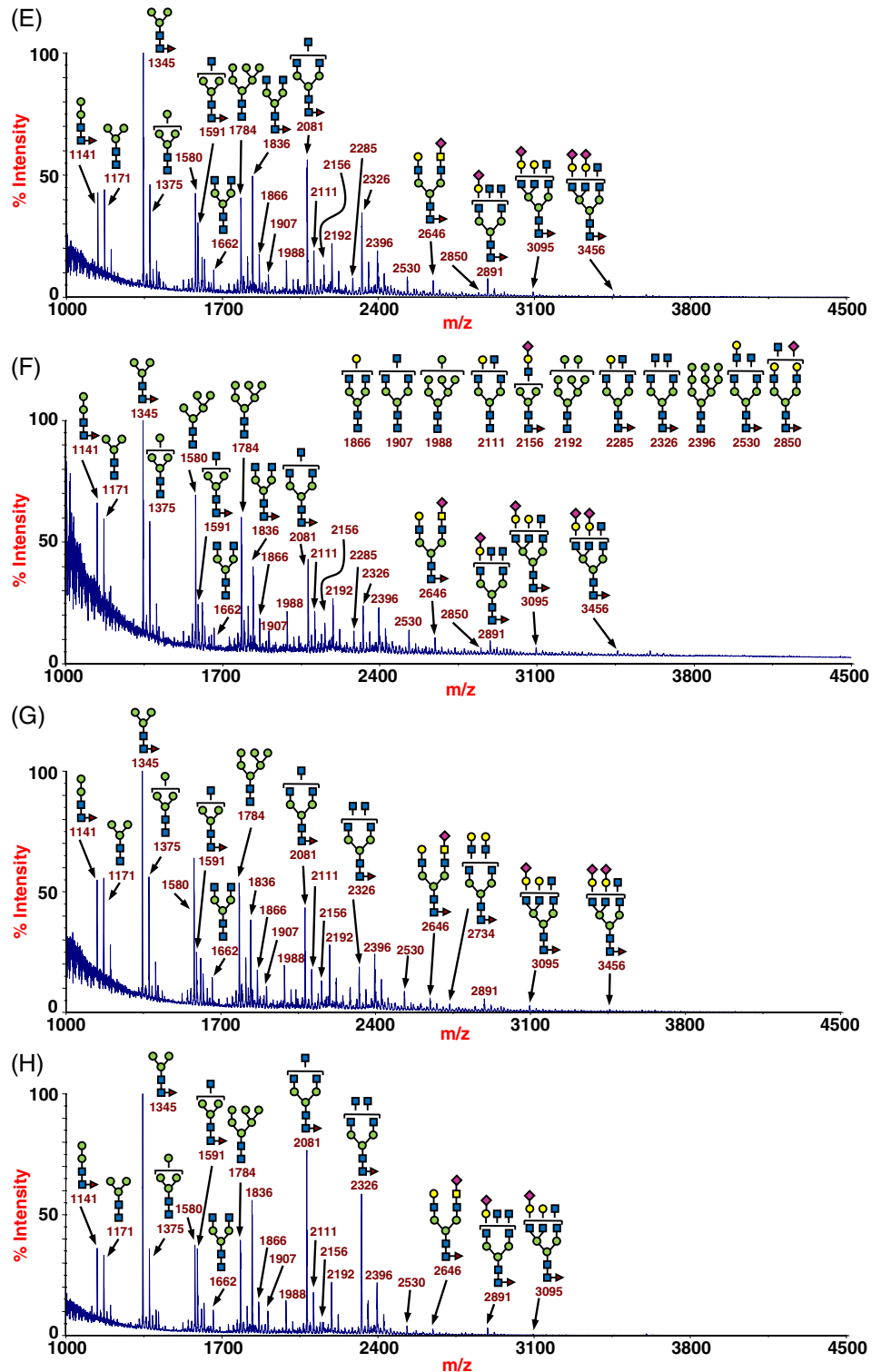


**FIGURE 2** The *N*-glycosylation defects severity observed in TMEM165 KO HEK cells depends on the FBS used for cell culture. MALDI-TOF-MS spectra of the permethylated *N*-glycans from control cells following different cell culture conditions. A to D. HEK control cells were cultured in DMEM supplemented with 10% FBS 1 (A) or 2 (B) or 3 (C) or 4 (D). Symbols represent sugar residues as follow: blue square, N-acetylglucosamine; green circle, mannose; yellow circle, galactose; purple diamond, sialic acid; red triangle, fucose. Linkages between sugar residues have been removed for simplicity

the increased gel mobility observed with FBS 1, 2 and 3 (Figure 4). However, this was not the case for the condition with FBS 4 where only a slight decrease in LAMP2 gel mobility was seen (Figure 4). This last condition was retested with increased amounts of  $MnCl_2$ , 5 and 10  $\mu M$ , in addition to FBS 4. Very interestingly, a pronounced suppression of LAMP2 glycosylation defect could be seen for these two  $Mn^{2+}$  concentrations with a significant increase in the fully glycosylated forms of LAMP2 (Figure 5). Nevertheless, a significant fraction of underglycosylated LAMP2 remained after treatment.

Therefore, 5  $\mu M$   $MnCl_2$  was applied to the cells cultured in FBS 4 for 72 hours with cells harvested at multiple time points (Figure 6). The results showed that fully glycosylated forms of LAMP2 started to appear after 8 hours of  $Mn^{2+}$  treatment and progressively increased until 72 hours, while underglycosylated LAMP2 forms decreased from 2 to 72 hours (Figure 6). These results demonstrated that the fraction of underglycosylated LAMP2 observed under  $Mn^{2+}$  supplementation depends on LAMP2 turnover,  $Mn^{2+}$  concentration and incubation time. Altogether, these results strongly suggest that the observed

**FIGURE 3** The N-glycosylation defects severity observed in TMEM165 KO HEK cells depends on the FBS used for cell culture. MALDI-TOF-MS spectra of the permethylated N-glycans from TMEM165 KO HEK cells following different cell culture conditions. (E-H) TMEM165 KO HEK cells were cultured in DMEM supplemented with 10% FBS 1 (E) or 2 (F) or 3 (G) or 4 (H). Symbols represent sugar residues as follow: blue square, N-acetylglucosamine; green circle, mannose; yellow circle, galactose; purple diamond, sialic acid; red triangle, fucose. Linkages between sugar residues have been removed for simplicity



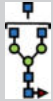



glycosylation defect in TMEM165 KO HEK cells certainly depends on  $Mn^{2+}$  level in the different FBS used for cell culture.

To test this hypothesis, manganese levels of each FBS were quantified by inductively coupled plasma-mass spectrometry (ICP-MS). As observed in Figure 7, manganese levels vary between sources of FBS. In synthetic serum substitutes, the manganese level was extremely low,

between 0.03 and 0.05  $\mu M$ . In the four other sera from animal origin, our results showed that the concentration is between 0.56 and 0.61  $\mu M$  for FBS 1 and FBS 4 and 1.08 and 1.21  $\mu M$  for FBS 2 and FBS 3 (Figure 7). This result confirms that the observed differences in severity of the glycosylation defects in TMEM165 KO HEK cells may be correlated with the manganese level present in the FBS used for cell culture.

**TABLE 1** Comparison of the relative intensity of specific ions ( $m/z$ ) observed in control and TMEM165 KO HEK cells cultured with different fetal bovine serum (FBS)

|                   | Ion at $m/z$ 1591<br> | Ion at $m/z$ 1836<br> | Ion at $m/z$ 2081<br> | Ion at $m/z$ 2326<br> |
|-------------------|--|--|--|--|
| A (Ctrl FBS 1), % | 27   | 29   | 25   | 13   |
| B (Ctrl FBS 2), % | 19   | 26   | 27   | 13   |
| C (Ctrl FBS 3), % | 29   | 30   | 28   | 13   |
| D (Ctrl FBS 4), % | 22   | 24   | 28   | 10   |
| E (KO FBS 1), %   | 31   | 50   | 56   | 34   |
| F (KO FBS 2), %   | 24   | 39   | 42   | 23   |
| G (KO FBS 3), %   | 24   | 38   | 43   | 18   |
| H (KO FBS 4), %   | <b>36</b>  | <b>56</b>  | <b>77</b>  | <b>58</b>  |

Symbols represent sugar residues as follow: blue square, N-acetylglucosamine; green circle, mannose; red triangle, fucose. Linkages between sugar residues have been removed for simplicity.

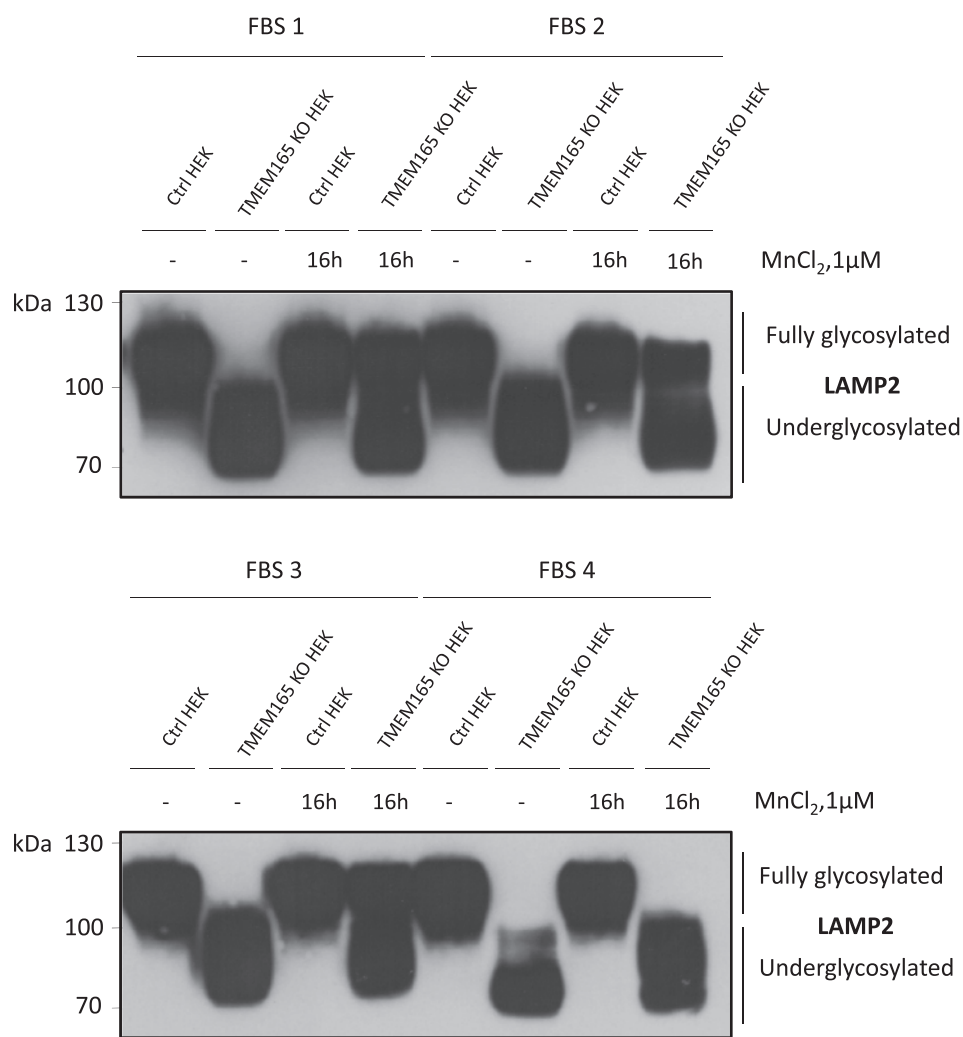


**FIGURE 4** The suppression of LAMP2 glycosylation defect by  $Mn^{2+}$  supplementation in TMEM165 KO HEK cells depends on the FBS used for cell culture. Control and TMEM165 KO HEK cells were cultured in DMEM supplemented with 10% FBS 1, 2, 3 or 4. Cells were incubated with or without  $1 \mu M$   $MnCl_2$  for 16 hours. Total cell lysates were prepared, subjected to sodium dodecyl sulfate polyacrylamide gel electrophoresis (SDS-PAGE) and western blot with the indicated antibody

**FIGURE 5** Increasing concentrations of  $MnCl_2$  are required to rescue LAMP2 glycosylation defect in TMEM165 KO HEK cells cultured with FBS 4. Control and TMEM165 KO HEK cells were cultured in DMEM supplemented with 10% FBS 4. Cells were incubated with either 1, 5 or 10  $\mu M$   $MnCl_2$  for 16 hours. Total cell lysates were prepared, subjected to sodium dodecyl sulfate polyacrylamide gel electrophoresis (SDS-PAGE) and western blot with the indicated antibody

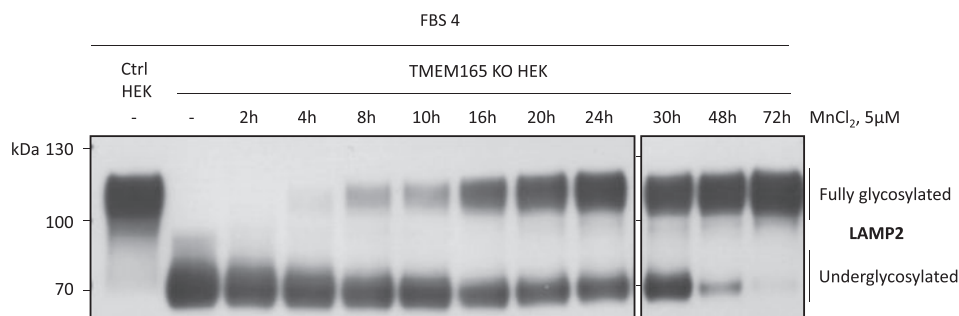
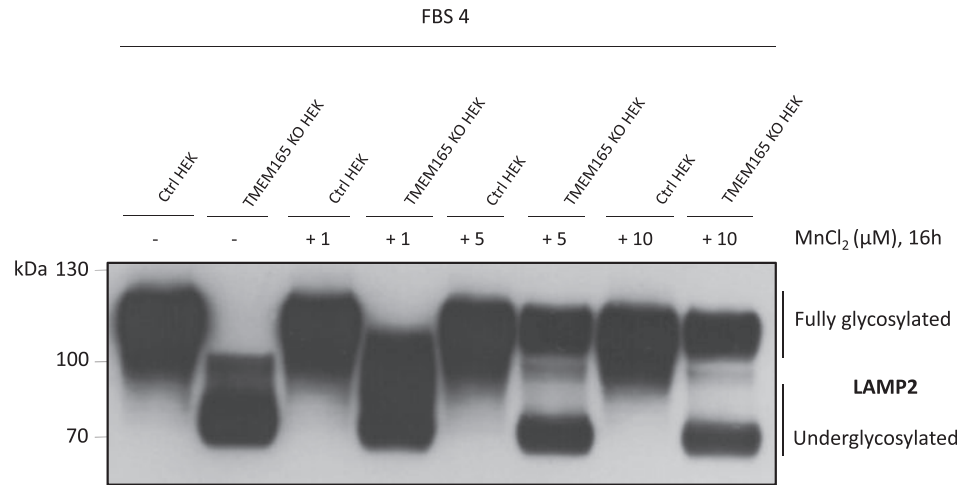


**FIGURE 6** Time course of the  $Mn^{2+}$ -induced LAMP2 glycosylation rescue in FBS 4. Control and TMEM165 KO HEK cells were cultured in DMEM supplemented with 10% FBS 4. Cells were incubated with 5  $\mu M$   $MnCl_2$  during indicated times. Cell culture medium was renewed every 16 to 24 hours. Total cell lysates were prepared, subjected to sodium dodecyl sulfate polyacrylamide gel electrophoresis (SDS-PAGE) and western blot with the indicated antibody

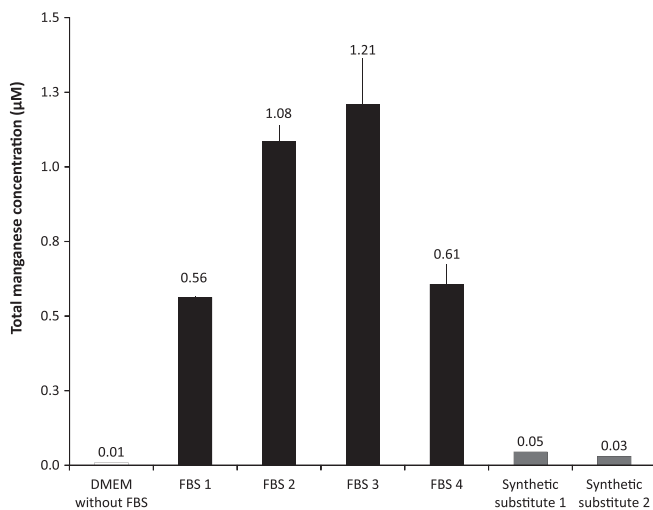


**FIGURE 7** Inductively coupled plasma-mass spectrometry (ICP-MS) Mn levels differ according to different FBS sources. 500  $\mu L$  of DMEM and 500  $\mu L$  of each FBS were prepared as described in Material and Methods section for ICP-MS analysis and total manganese concentration was measured

### 3.3 | Iron supplementation can also suppress the glycosylation defects in TMEM165 KO HEK cells

While our results clearly support that the serum Mn level is an important factor to take into consideration, it cannot by itself explain the observed differences in the suppression of the glycosylation defects. This suggests that additional factors within sera could also affect the glycosylation in TMEM165 KO cells. To tackle this point, the culture medium of TMEM165 KO HEK cells grown in FBS 4 was supplemented with 100  $\mu M$  of many different ions, and LAMP2 glycosylation was assessed by western blot (Figure S2). Interestingly, we observed that in addition to  $Mn^{2+}$ ,  $Fe^{3+}$  was also capable of rescuing the abnormal LAMP2 glycosylation profile. To assess the sensitivity of glycosylation to  $Fe^{3+}$ , a similar experiment was performed with a reduced  $Fe^{3+}$  concentration of 5  $\mu M$ . In addition,  $Fe^{2+}$  was also tested. As shown in Figure 8, while fully glycosylated forms of LAMP2 appeared under  $Mn^{2+}$  supplementation, this was not the case under  $Fe^{2+}$  and  $Fe^{3+}$  supplementation where

only partially LAMP2 glycosylated forms were observed. Altogether these results suggest that iron is also capable of rescuing Golgi glycosylation in a TMEM165 KO background but not in the same concentration range as manganese.

### 3.4 | Galactose supplementation enhances the Mn<sup>2+</sup> effect in TMEM165 KO HEK cells grown in FBS 4

Our previous work showed that galactose supplementation could suppress some glycosylation defects of TMEM165-CDG.<sup>20</sup> We then wondered whether this suppression could also depend on

the source of FBS. To tackle this point, TMEM165 KO HEK cells were cultured in two different FBS (FBS 2 or FBS 4) and supplemented with 1 μM MnCl<sub>2</sub>, 1 mM galactose or 1 μM MnCl<sub>2</sub> + 1 mM galactose. Intriguingly, all treatments resulted in fully glycosylated forms of LAMP2 in TMEM165 KO HEK cells cultured in FBS 2 (Figure 9A). The result was completely different in cells grown in FBS 4 (Figure 9B). In the latter condition, galactose or Mn<sup>2+</sup> supplementation poorly rescued LAMP2 glycosylation (Figure 9B). However and very interestingly, a combination of these two factors rescued fully glycosylated forms of LAMP2 (Figure 9B). This result demonstrates that depending on the source of the FBS, Mn<sup>2+</sup> can enhance the

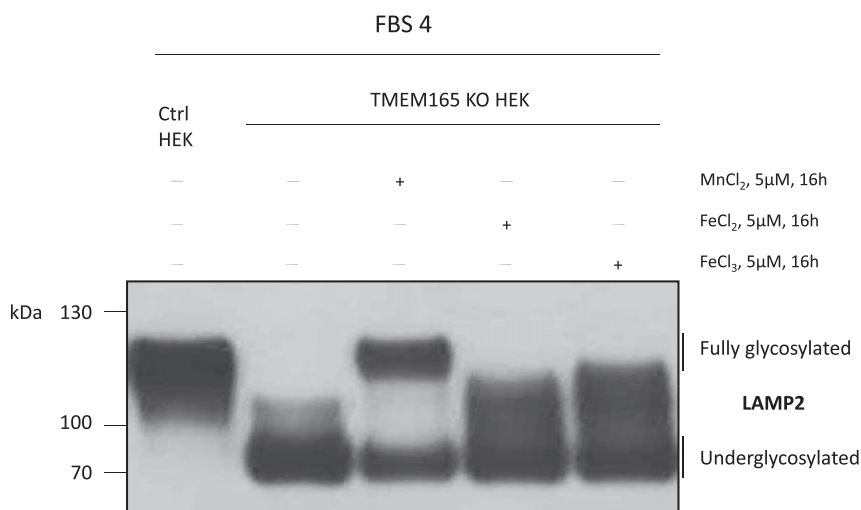


**FIGURE 8** Comparative efficacy of Mn<sup>2+</sup>, Fe<sup>2+</sup> and Fe<sup>3+</sup> addition on the suppression of LAMP2 glycosylation defect. Control and TMEM165 KO HEK cells were cultured in DMEM supplemented with 10% FBS 4. Cells were incubated with or without 5 μM MnCl<sub>2</sub>, 5 μM FeCl<sub>2</sub> and 5 μM FeCl<sub>3</sub> for 16 hours. Total cell lysates were prepared, subjected to sodium dodecyl sulfate polyacrylamide gel electrophoresis (SDS-PAGE) and western blot with the indicated antibody

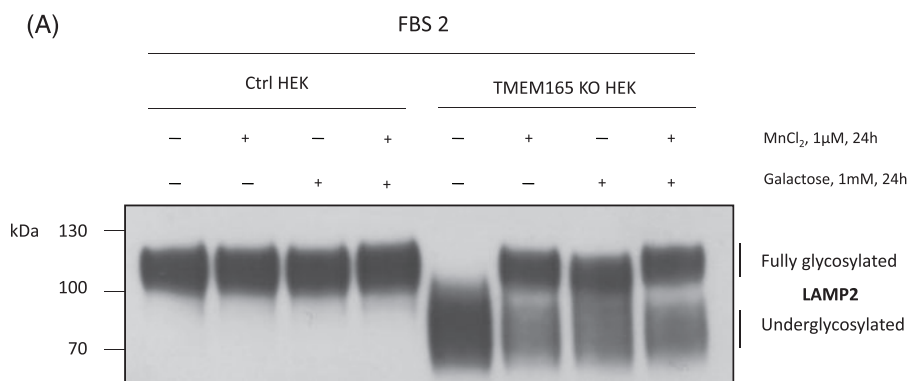
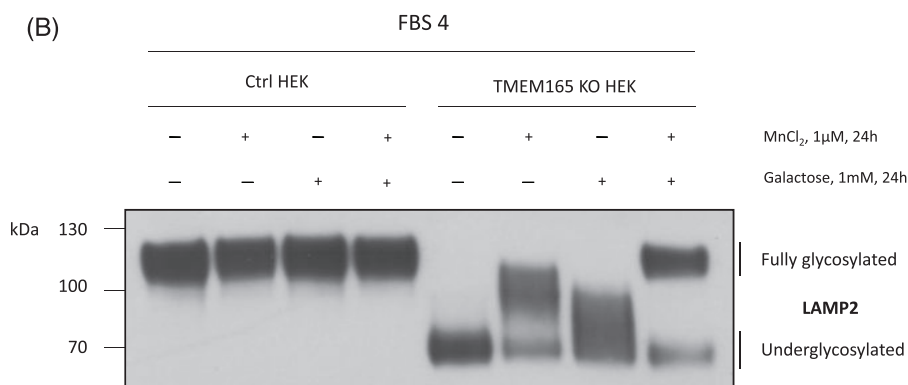


**FIGURE 9** The suppression of LAMP2 glycosylation defect by galactose supplementation depends on the FBS used for cell culture. Control and TMEM165 KO HEK cells were cultured in DMEM supplemented with 10% FBS 2 (panel A) or 4 (panel B). Cells were incubated with or without 1 μM MnCl<sub>2</sub> and 1 mM galactose for 24 hours. Total cell lysates were prepared, subjected to sodium dodecyl sulfate polyacrylamide gel electrophoresis (SDS-PAGE) and western blot with the indicated antibody



galactose effect (or vice versa) on the suppression of LAMP2 glycosylation defect. These results reinforce the extreme importance of serum content on glycomics' results.

## 4 | DISCUSSION

Isogenic TMEM165 KO HEK cells are a powerful model for studying the function of TMEM165 in  $Mn^{2+}$ -mediated regulation of the Golgi glycosylation process. TMEM165 KO HEK cells present strong Golgi glycosylation defects affecting different classes of Golgi glycosylation (N- and O-glycosylation and glycolipid glycosylation).<sup>18,20</sup> The hypothesis that TMEM165 is crucial in regulating Golgi manganese homeostasis, a major cofactor of many glycosylation enzymes,<sup>21,22</sup> came from the observation that low  $Mn^{2+}$  concentrations (100 nM-1  $\mu$ M) in the culture medium were sufficient to suppress the observed Golgi glycosylation defects.<sup>18,19</sup> In the present study, we examined the contribution of fetal bovine serum on these observed Golgi glycosylation defects. This came from the observation that Golgi glycosylation defects could be suppressed depending on culture conditions. In this study, we demonstrate that the manganese content in serum is a crucial factor to take into account when analyzing Golgi glycosylation defects in TMEM165 KO cells. Although logical, this finding is quite unexpected as manganese is found in serum at a very low concentration between 0.56  $\mu$ M and 1.21  $\mu$ M. We calculate that the final manganese concentration in the culture media is between 56 and 121 nM. Our results suggest that slight  $Mn^{2+}$  variations in FBS can have huge impacts on the mature N-glycan structures. This result is also in accordance with the observation that only 100 nM  $Mn^{2+}$  supplementation could rescue the observed LAMP2 glycosylation defects in TMEM165 KO HEK cells in our previous work.<sup>18</sup> While our results clearly support that serum Mn levels are an important factor to take into consideration, we have demonstrated that galactose and/or iron can also affect the observed glycosylation defects in TMEM165 deficient cells. Since 5  $\mu$ M  $MnCl_2$  was able to rescue a significant portion of LAMP2 glycosylation, we can guess that serum that is under/over supplemented with other ions could alter the efficiency of the glycosylation machinery.

At a fundamental level, and as isogenic cultured cells and patients' cells are widely used to study the impact of gene defects on proteins' glycosylation patterns, our results point out that glycomics results, obtained with cultured cells, crucially depend on the level of  $Mn^{2+}$  and other factors in FBS. This study emphasizes the importance of the use of validated FBS in glycosylation analysis.

## ACKNOWLEDGMENTS

We acknowledge Dr Dominique Legrand for the Research Federation FRABio (Univ. Lille, CNRS, FR 3688,

FRABio, Biochimie Structurale et Fonctionnelle des Assemblages Biomoléculaires) and for providing the scientific and technical environment conducive to achieving this work.

## CONFLICT OF INTEREST

The authors declare no potential conflict of interest.

## AUTHOR CONTRIBUTIONS

D.V. and M.H. performed the cell biology experiments. A.G. contributed to ICP-MS analysis. L.C. and V.L. generated the KO cell lines and took part in the writing. W.M. performed and analyzed the mass spectrometry data. F.F. designed the study and wrote the paper.

## ORCID

François Foulquier  <https://orcid.org/0000-0001-5084-4015>

## REFERENCES

1. Freeze H. Congenital disorders of glycosylation: CDG-I, CDG-II, and beyond. *Curr Mol Med*. 2007;7:389-396. <https://doi.org/10.2174/156652407780831548>.
2. Jaeken J. Congenital disorders of glycosylation. *Handb Clin Neurol*. 2013;113:1737-1743.
3. Jaeken J, Matthijs G. Congenital disorders of glycosylation: a rapidly expanding disease family. *Annu Rev Genomics Hum Genet*. 2007;8:261-278. <https://doi.org/10.1146/annurev.genom.8.080706.092327>.
4. Schachter H, Freeze HH. Glycosylation diseases: quo vadis? *Biochim Biophys Acta*. 2009;1792:925-930. <https://doi.org/10.1016/j.bbadis.2008.11.002>.
5. Scott K, Gadomski T, Kozicz T, Morava E. Congenital disorders of glycosylation: new defects and still counting. *J Inherit Metab Dis*. 2014;37:609-617. <https://doi.org/10.1007/s10545-014-9720-9>.
6. Jaeken J, Péanne R. What is new in CDG? *J Inherit Metab Dis*. 2017;40:569-586. <https://doi.org/10.1007/s10545-017-0050-6>.
7. Péanne R, de Lonlay P, Foulquier F, et al. Congenital disorders of glycosylation (CDG): quo vadis? *Eur J Med Genet*. 2017;61:643-663. <https://doi.org/10.1016/j.ejmg.2017.10.012>.
8. Foulquier F. COG defects, birth and rise! *Biochim Biophys Acta*. 2009;1792:896-902. <https://doi.org/10.1016/j.bbadis.2008.10.020>.
9. Foulquier F, Ungar D, Reynders E, et al. A new inborn error of glycosylation due to a Cog8 deficiency reveals a critical role for the Cog1—Cog8 interaction in COG complex formation. *Hum Mol Genet*. 2007;16:717-730. <https://doi.org/10.1093/hmg/ddl476>.
10. Foulquier F, Vasile E, Schollen E, et al. Conserved oligomeric Golgi complex subunit 1 deficiency reveals a previously uncharacterized congenital disorder of glycosylation type II. *Proc Natl Acad Sci*. 2006;103:3764-3769. <https://doi.org/10.1073/pnas.0507685103>.



11. Kranz C, Ng BG, Sun L, et al. COG8 deficiency causes new congenital disorder of glycosylation type IIIh. *Hum Mol Genet.* 2007;16:731-741. <https://doi.org/10.1093/hmg/ddm028>.
12. Paesold-Burda P, Maag C, Troxler H, et al. Deficiency in COG5 causes a moderate form of congenital disorders of glycosylation. *Hum Mol Genet.* 2009;18:4350-4356. <https://doi.org/10.1093/hmg/ddp389>.
13. Reynders E, Foulquier F, Leão Teles E, et al. Golgi function and dysfunction in the first COG4-deficient CDG type II patient. *Hum Mol Genet.* 2009;18:3244-3256. <https://doi.org/10.1093/hmg/ddp262>.
14. Wu X, Steet RA, Bohorov O, et al. Mutation of the COG complex subunit gene COG7 causes a lethal congenital disorder. *Nat Med.* 2004;10:518-523. <https://doi.org/10.1038/nm1041>.
15. Kornak U, Reynders E, et al. Impaired glycosylation and cutis laxa caused by mutations in the vesicular H<sup>+</sup>-ATPase subunit ATP6V0A2. *Nat Genet.* 2008;40:32-34. <https://doi.org/10.1038/ng.2007.45>.
16. Foulquier F, Amyere M, Jaeken J, et al. TMEM165 deficiency causes a congenital disorder of glycosylation. *Am J Hum Genet.* 2012;91:15-26. <https://doi.org/10.1016/j.ajhg.2012.05.002>.
17. Zeevaert R, de Zegher F, Sturiale L, et al. Bone dysplasia as a key feature in three patients with a novel congenital disorder of glycosylation (CDG) type II due to a deep Intronic splice mutation in TMEM165. In: Zschocke J, Gibson KM, Brown G, et al., eds. *JIMD Reports—Case and Research Reports, 2012/5*. Berlin, Heidelberg: Springer; 2012:145-152.
18. Potelle S, Morelle W, Dulary E, et al. Glycosylation abnormalities in Gdt1p/TMEM165 deficient cells result from a defect in Golgi manganese homeostasis. *Hum Mol Genet.* 2016;25:1489-1500. <https://doi.org/10.1093/hmg/ddw026>.
19. Houdou M, Lebretonchel E, Garat A, et al. Involvement of thapsigargin- and cyclopiazonic acid-sensitive pumps in the rescue of TMEM165-associated glycosylation defects by Mn<sup>2+</sup>. *FASEB J.* 2019;33:2669-2679. <https://doi.org/10.1096/fj.201800387R>.
20. Morelle W, Potelle S, Witters P, et al. Galactose supplementation in patients with TMEM165-CDG rescues the glycosylation defects. *J Clin Endocrinol Metab.* 2017;102:1375-1386. <https://doi.org/10.1210/jc.2016-3443>.
21. Powell JT, Brew K. Metal ion activation of galactosyltransferase. *J Biol Chem.* 1976;251:3645-3652.
22. Ramakrishnan B, Ramasamy V, Qasba PK. Structural snapshots of β-1,4-Galactosyltransferase-I along the kinetic pathway. *J Mol Biol.* 2006;357:1619-1633. <https://doi.org/10.1016/j.jmb.2006.01.088>.
23. Potelle S, Dulary E, Duvet S, et al. Manganese-induced trafficking and turnover of TMEM165. *Biochem J.* 2017;474:1481-1493. <https://doi.org/10.1042/BCJ20160910>.
24. Morelle W, Michalski J-C. Analysis of protein glycosylation by mass spectrometry. *Nat Protoc.* 2007;2:1585-1602.

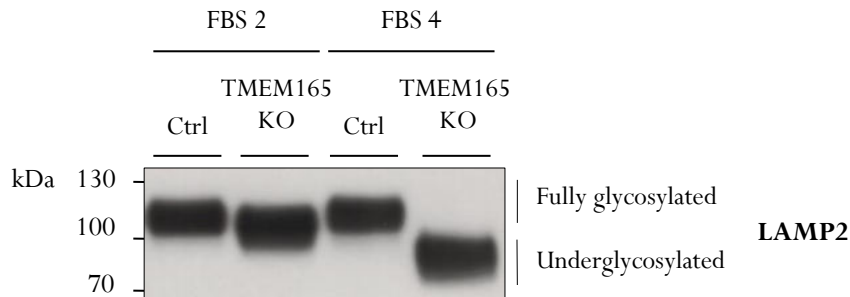
## SUPPORTING INFORMATION

Additional supporting information may be found online in the Supporting Information section at the end of this article.

**How to cite this article:** Vicogne D, Houdou M, Garat A, et al. Fetal bovine serum impacts the observed N-glycosylation defects in TMEM165 KO HEK cells. *J Inherit Metab Dis.* 2019;1–10. <https://doi.org/10.1002/jimd.12161>

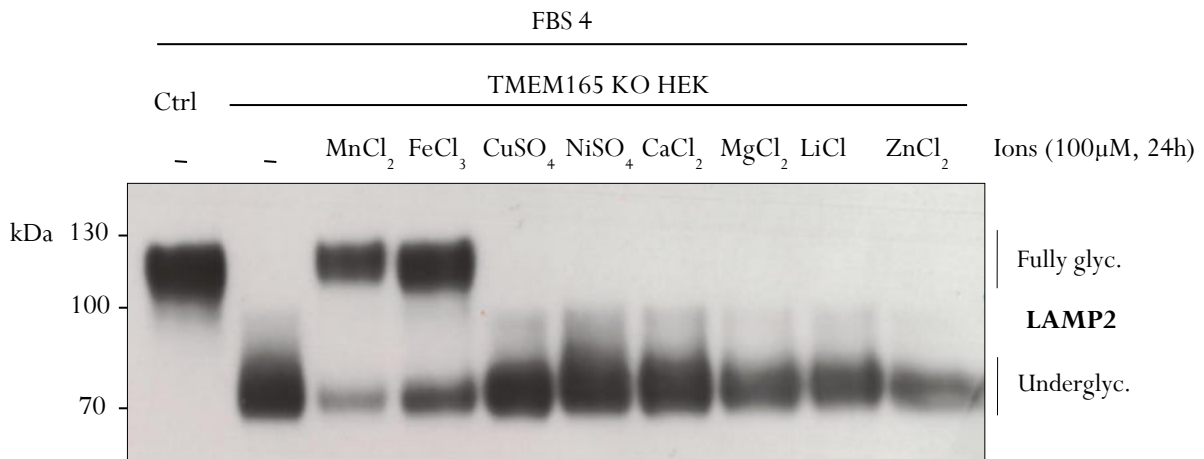
## 2.3. Supplementary data associated with the publication

### 2.3.1. Supplementary Figure 1



**Supplementary Figure 1: The appearance of LAMP2 glycosylation defects in CRISPR-TMEM165 KO HeLa-GalT cells depends also on the FBS used for cell culture.** Control and CRISPR-TMEM165 KO HeLa-GalT cells were cultured in DMEM supplemented with 10% FBS 2 or 4. Total cell lysates were prepared, subjected to SDS-PAGE and western blot with the indicated antibody.

### 2.3.2. Supplementary Figure 2



**Supplementary Figure 2: Impact of different ions supplementation on the suppression of LAMP2 glycosylation defects.** Control and TMEM165 KO HEK cells were cultured in DMEM supplemented with 10% FBS 4. Cells were then incubated with 100 μM of different ions for 24h. Total cell lysates were prepared, subjected to SDS-PAGE and western blot with the indicated antibody.

## 2.4. Conclusion

All in all, this study conducted in TMEM165 KO HEK cells revealed the crucial importance to be consistent with cell culture conditions when doing glycomics. We clearly demonstrated the versatility of our results while changing cell culture conditions. However, based on our strong expertise in the field and the overall understanding of TMEM165 deficient system, we faced this issue. Indeed, based on previous work from the team, we already knew that exogenous MnCl<sub>2</sub> or D-galactose supplementations could enhance Golgi glycosylation in TMEM165 KO cells, culminating in the complete suppression of N-linked glycosylation defects depending on MnCl<sub>2</sub>/D-galactose concentration and/or incubation time.

We therefore hypothesized that Mn content in the FBS might be different from one FBS to the other and could be behind the spontaneous observed Golgi glycosylation rescue in TMEM165 KO HEK cells. Through the quantification of total Mn levels in four FBS from animal origin, we indeed correlated variations in FBS Mn levels to the severity of the observed glycosylation defects in TMEM165 KO cells. Although this study particularly focused on Mn levels in FBS, one can imagine that under/over supplemented sera with other components might positively or negatively affect the glycosylation machinery of other isogenic cell lines knockout for specific gene-CDG. A good alternative to cope up with variations in the composition of FBS from animal origin could be the use of synthetic substitutes with a controlled chemical composition. Unfortunately, in our case, TMEM165 KO HEK cell did not survive in culture medium complemented with such synthetic substitutes. Other components from animal origin were probably missing in these chemically controlled sera and might be detrimental to cell survival and proliferation. All in all, although each laboratory has its own cell culture guidelines, we unambiguously demonstrated that the nature of the FBS used for cell culture has to be validated and consistent over the time to enable proper identification of glycosylation abnormalities in isogenic cell lines mimicking specific CDG glycosylation phenotypes. The lack of uniformed protocols to (i) culture isogenic cell lines, (ii) collect and (iii) prepare samples for further glycomics analyses appears as a plague that we all need to be aware of and stands for the take home message of this study.



---

## **General discussion and perspectives on Part I**

---



Altogether, Paper 1 and Paper 2 unveiled some mechanistic aspects of the  $Mn^{2+}$ -induced Golgi glycosylation rescue in TMEM165 KO HEK cells as well as its sensitivity to specific cell culture conditions. These two studies corroborated each other and are complementary to previous publications from the team. Besides  $Mn^{2+}$ , we also reported that D-Galactose (Gal) supplementation results in Golgi N-linked glycosylation recovery [506]. Hereafter, I will discuss some additional and unpublished results I obtained during my PhD, highlighting commonalities and differences between  $Mn^{2+}$  and Gal-induced glycosylation rescues in a TMEM165-deficient background.

## 1. Unraveling Gal-induced Golgi N-linked glycosylation rescue in TMEM165 KO cells

As the main achievement of Paper 1, we have demonstrated that thapsigargin or cyclopiazonic acid treatment prevented the  $Mn^{2+}$ -induced glycosylation rescue in TMEM165 KO HEK cells. However, we did not evaluate the effect of such treatments on the Gal-induced N-linked glycosylation rescue in TMEM165 KO HEK cells. Since Gal,  $Mn^{2+}$  and  $Ca^{2+}$  are required for the optimal activity of specific GTs such as the  $\beta$ -1,4-galactosyltransferase 1 (B4GALT1), we then hypothesized that  $Ca^{2+}$  homeostasis in the ER/Golgi may be crucial to contribute to the Gal supplementation effect, culminating in the suppression of the main galactosylation defects observed in TMEM165 deficient cells. To tackle this point, TMEM165 KO HEK cells were pre-treated with either thapsigargin (50nM) or cyclopiazonic acid (100 $\mu$ M) for 2h and then incubated together with 1mM Gal and/or 2,5 $\mu$ M  $MnCl_2$  for 16h. To summarize Figure 53, what we did observe is that either  $MnCl_2$  or Gal supplementation alone is not sufficient to induce any glycosylation rescue in TMEM165 KO HEK cells pre-treated with thapsigargin or cyclopiazonic acid. Surprisingly, the combination of  $MnCl_2$  and Gal overcomes SERCA inhibition and sustains correct Golgi glycosylation reactions. Based on these observations, several hypotheses can be raised: (i) to the “ $Mn^{2+}$ ” point of view, SERCA inhibition using thapsigargin or cyclopiazonic acid likely restricts cytosolic  $Ca^{2+}$  and  $Mn^{2+}$  pumping in the ER for further redistribution in the Golgi apparatus, preventing  $Mn^{2+}$  beneficial effect on Golgi glycosylation and/or proper  $Ca^{2+}$  gradient between ER and Golgi. (ii) To the “Gal” point of view, assuming that there is no direct link between SERCA activity and Gal uptake at the Golgi level, one can suggest that, due to the disrupted Golgi  $Mn^{2+}$  homeostasis in TMEM165 KO HEK cells, Gal supplementation may require a proper ER/Golgi  $Ca^{2+}$  homeostasis to ensure optimal activity for galactosyltransferases. In case of SERCA inhibition, this  $Ca^{2+}$  gradient may be disrupted leading to improper/slower galactosylation reactions. However, the synergic effect observed in presence of  $MnCl_2$  and Gal in TMEM165 KO HEK cells pre-treated or not with SERCA inhibitors is still not understood. How such combined incubation of  $MnCl_2$  and Gal overcomes the effect of thapsigargin and cyclopiazonic acid is an opened question.

One can supposed that either Gal treatment in combination with  $MnCl_2$  may facilitate  $Mn^{2+}$  entry and subsequent redistribution to reach together the Golgi lumen (bypassing SERCA requirement) where they favor galactosyltransferases catalytic activity or,  $MnCl_2$  treatment in combination with Gal boosts UDP-sugar biosynthesis (UDP-Glc, UDP-GlcNAc and UDP-Gal) yielding to increase the pool of donor substrates for subsequent higher glycosyltransferase activities.

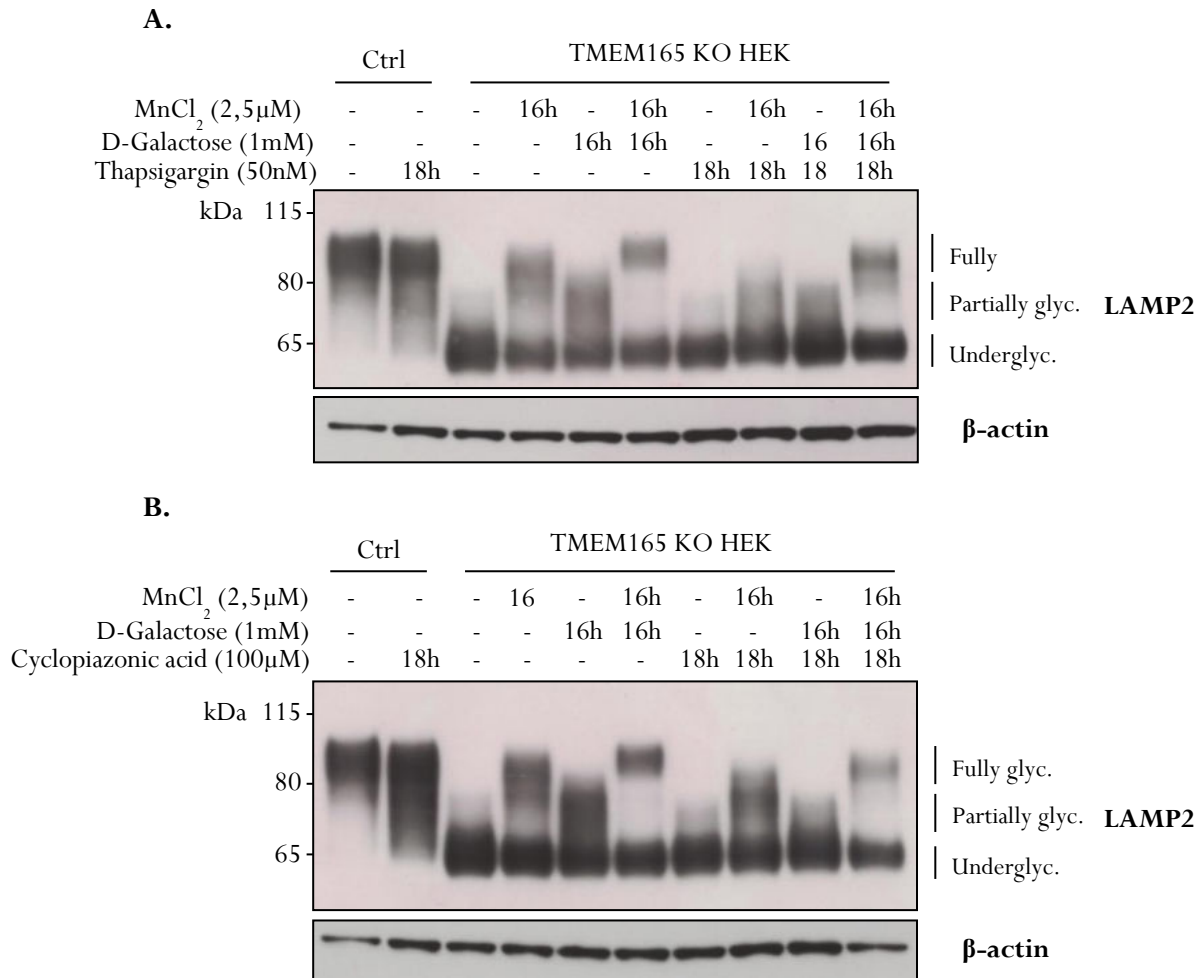


**Figure 53: Involvement of thapsigargin- and cyclopiazonic acid-sensitive pumps in Gal-induced rescue of LAMP2 glycosylation.** Control (ctrl) and TMEM165 KO HEK293 cells were incubated with either thapsigargin (A.) or cyclopiazonic acid (B.) in combination or not with  $MnCl_2$  and/or D-Galactose for 16h to 18h. Total cell lysates were prepared, subjected to SDS-PAGE and western blot with the indicated antibodies.

To test whether Gal treatment may increase  $Mn^{2+}$  uptake, we evaluated  $Mn^{2+}$  entry at the plasma membrane in TMEM165 KO HEK cells pre-treated with 1mM Gal for 48h using an indirect method called “ $Mn^{2+}$ -quenching”. Basically, Fura-2 is a ratiometric dye with a strong  $Ca^{2+}$  binding affinity allowing the measure of cellular  $Ca^{2+}$  concentrations. However, at its isoblastic point (365nm) and in presence of 100μM  $MnCl_2$ , Fura-2 can rather bind  $Mn^{2+}$  instead of  $Ca^{2+}$ , resulting in a decreased emitted



fluorescence. This is what we called Fura-2  $Mn^{2+}$  quenching. The more  $Mn^{2+}$  enters the cells, the steeper the quenching slope is. Here, as shown in Figure 54, we first observed that  $Mn^{2+}$  quenching is higher in control cells than in TMEM165 KO HEK cells suggesting a functional role of TMEM165 in  $Mn^{2+}$  entry at the plasma membrane. Nonetheless, we also highlighted that Gal treatment in both control and TMEM165 KO HEK cells resulted in steeper  $Mn^{2+}$  quenching compared to untreated cells.

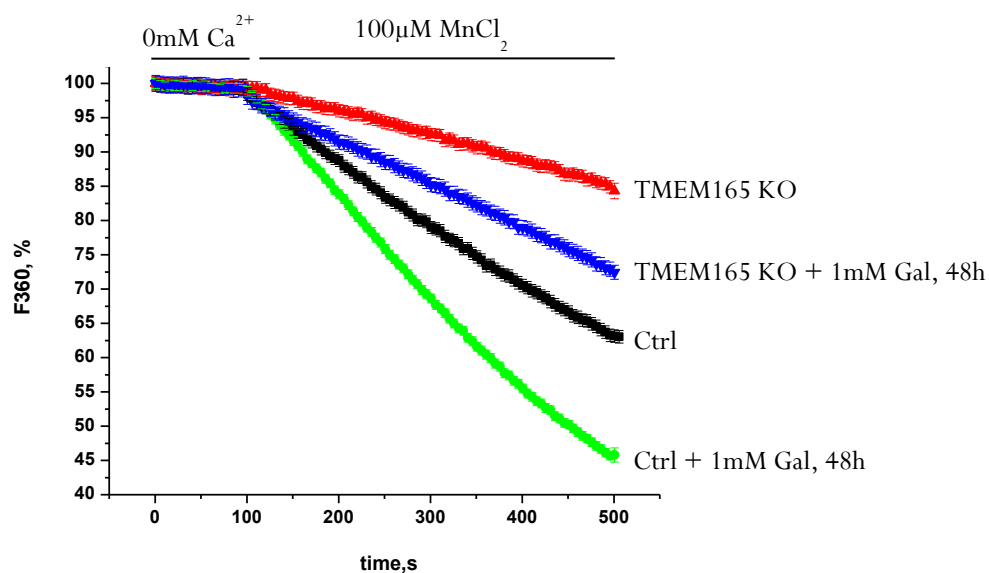


**Figure 54: Gal pre-treatment influences  $Mn^{2+}$  quenching observed in both control and TMEM165 KO HEK cells.** Control (Ctrl) and TMEM165 KO HEK cells were loaded with Fura2/AM probe and subjected to calcium imaging experiment. Data are presented as representative of three independent experiments.

Albeit the experimental conditions are different between  $Mn^{2+}$  quenching and  $Mn^{2+}$ -Gal-induced glycosylation rescue experiments, this result suggests that independently of TMEM165 presence/absence, Gal enhances  $Mn^{2+}$  uptake at the plasma membrane. Another way to evaluate the higher  $Mn^{2+}$  entry in presence of Gal would be to quantify by ICP-MS the total Mn level in cells treated with either  $MnCl_2$ , Gal or both  $MnCl_2$  and Gal.

We have also evaluated the effect of either  $MnCl_2$  or Gal supplementations on UDP-sugar biosynthesis in control and TMEM165 KO HEK cells. This has been done in collaboration with Dr Christian Thiel. As shown in Figure 55, no significant difference can be observed for UDP-Gal and UDP-Glc pools between control and KO TMEM165 HEK cells. Moreover, both  $MnCl_2$  and Gal supplementations have comparable impacts on UDP-Glc and UDP-Gal pools on both cell lines.  $MnCl_2$  supplementation similarly slightly increases the pool of UDP-Gal in both cell types (x1.15 in control cells and x1.16 in TMEM165 KO cells) and slightly reduces the accumulation of UDP-Glc (x0.84 in control cells and x0.90 in TMEM165 KO cells).

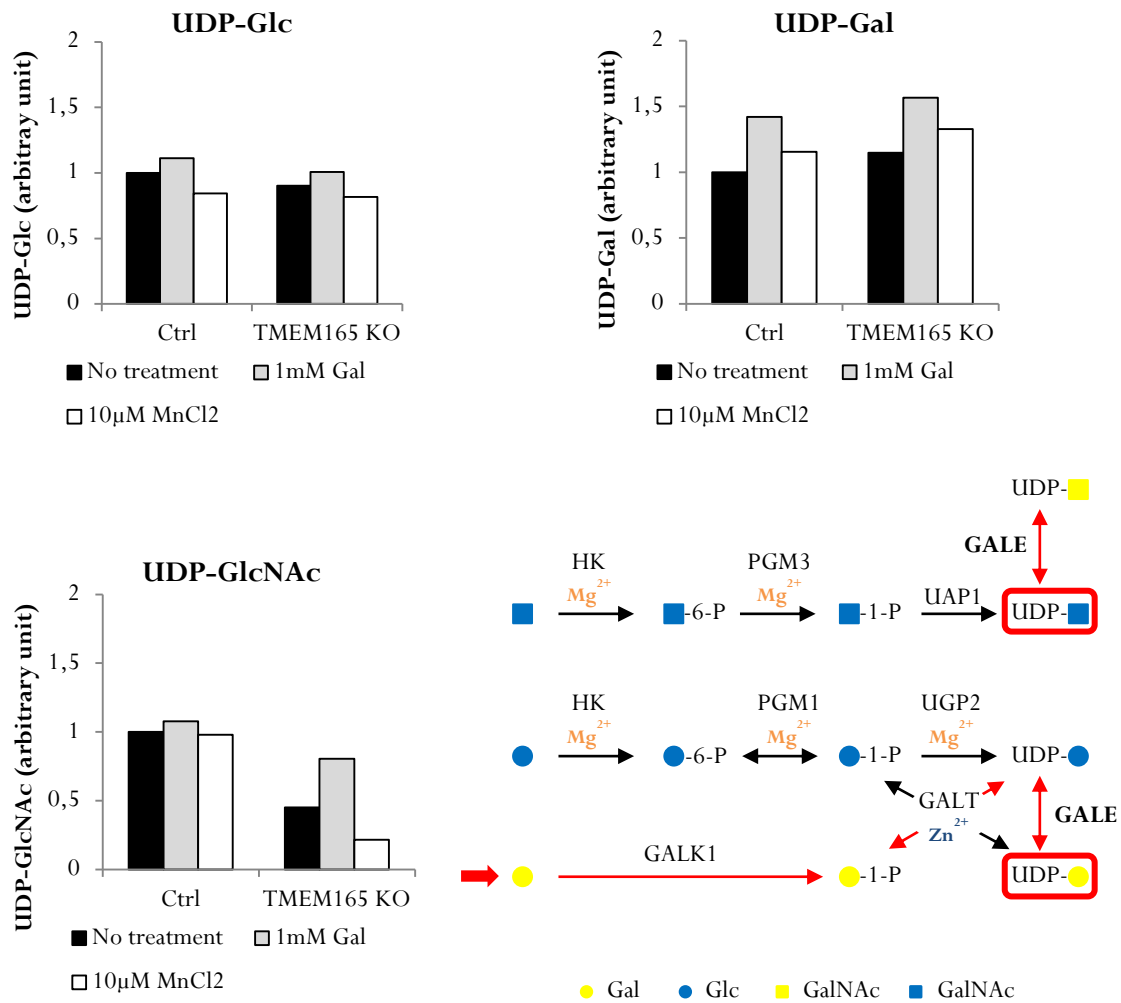


**Figure 55: Impact of Gal and MnCl<sub>2</sub> supplementations on UDP-sugar pools in control versus TMEM165 KO HEK cells.** Level of cytosolic UDP-Glc, UDP-Gal and UDP-GlcNAc were quantified in control and TMEM165 KO HEK cells treated or not with 1Mm Gal or 10µM MnCl<sub>2</sub> for 48h. On the right bottom corner, a simplified overview of UDP-sugar biosynthesis pathway is depicted. Red arrow symbolizes Gal supplementation.

With regards to the pool of UDP-GlcNAc, half less is found in TMEM165 deficient cells compared to control cells. Furthermore, while Gal supplementation only induces a slight increase in the total amount of UDP-GlcNAc found in control cells (x1.07), this effect is stronger in TMEM165 KO cells (x1.78). At last, MnCl<sub>2</sub> supplementation drastically reduces the pool of UDP-GlcNAc in TMEM165 KO cells (x0.47) whereas no significant impact of MnCl<sub>2</sub> was observed in control cells (x0.98). All in all, Gal supplementation leads to the accumulation of UDP-Gal in both control and TMEM165 KO cells that might be beneficial to sustain the incorporation of Gal residues in N-linked glycans by increasing the bioavailability of galactosyltransferases donor substrates. Moreover, MnCl<sub>2</sub> supplementation also promotes the accumulation of cytosolic UDP-Gal in TMEM165 KO cells which seems to be detrimental for the level of UDP-Glc and might be explained by a higher interconversion rate from UDP-Glc to UDP-Gal catalyzed by GALE (Figure 55). More intriguingly, the lack of TMEM165 (in)directly but

drastically affects the pool of UDP-GlcNAc suggesting that somehow, TMEM165 function is required to ensure proper UDP-GlcNAc biosynthesis. In addition,  $\text{MnCl}_2$  supplementation lowers by half the pool of UDP-GlcNAc in TMEM165 KO cells suggesting that potential cytosolic accumulation of  $\text{Mn}^{2+}$  (or any other ions/factors) may inhibit specific enzymes involved in the biosynthetic pathway of UDP-GlcNAc (Figure 55). One explanation could be that excess of  $\text{Mn}^{2+}$  may replace  $\text{Mg}^{2+}$  in the catalytic domain of UPA1, the enzyme catalyzing the formation of UDP-GlcNAc from UTP and GlcNAc-1-phosphate, and inhibit its function. In yeast *Saccharomyces cerevisiae*, UPA1 ortholog reaches 100% activity in presence of  $\text{Mg}^{2+}$  while  $\text{Mn}^{2+}$  reduces this activity to 49% [510]. In addition, excess of  $\text{Mg}^{2+}$  inhibits UPA1. Therefore, a similar inhibition could be set up in case of cytosolic  $\text{Mn}^{2+}$  accumulation that would be detrimental to preserve sufficient UDP-GlcNAc levels. If this hypothesis is true, a higher  $\text{Mn}^{2+}$  accumulation in the cytosol of TMEM165 KO HEK cells is then expected and could also be quantify by ICP-MS.

Although pieces of the puzzle are missing to establish the mechanism by which Gal supplementation correct the N-linked glycosylation defects in TMEM165 KO cells, I formulated hypotheses that need to be deeper investigated. To add an extra layer of complexity, by analyzing additional glycosylation pathways than N-linked glycosylation, we found that exogenous  $\text{MnCl}_2$  could suppress glycosylation defects associated to TMEM165 deficiency in multiple glycosylation pathways including glycosphingolipids, O-linked mucin types and GAGs biosynthesis whereas Gal supplementation appeared to be more restrictive to the N-linked glycosylation process (Table 22). This is the main focus on the next section.

## **2. Impact of $\text{MnCl}_2$ and/or Gal supplementations on other glycosylation pathways in a TMEM165 defective background**

As introduced in Chapter 3, glycosphingolipids and GAG biosynthesis have also been reported affected by TMEM165 deficiency in patients suffering from TMEM165-CDG [64,487,65,506,511], in TMEM165 morpholino zebrafish [508] and TMEM165 KO model cell lines [64,65,506]. In addition and very recently, I obtained preliminary results standing for O-linked mucin type defects in TMEM165 KO HEK cells using an indirect fluorescently labeled lectin staining strategy. In this study, *Vicia villosa* lectin (VVL) coupled to the green fluorescein isothiocyanate (FITC) was used. VVL preferentially recognizes  $\alpha$ -terminal GalNAc residue linked with O-glycosidic bond to serine or threonine in a polypeptide (Figure 56A). This first GalNAc residue (also called Tn antigen) initiates the mucin type O-linked glycans and is supposed to be further substituted by Gal and additional monosaccharides, in the Golgi apparatus (Figure 56A). As a positive control, VVL-FITC staining was first performed in HEK cells

lacking COSMC, the C1GALT1-specific chaperone 1 required for the proper activity of core 1 synthase galactosyltransferase 1 (C1GALT1) that catalyzes the transfer of Gal from UDP-Gal onto the first GalNAc residue (Figure 56A). As shown in Figure 56B, a significant green signal associated to VVL-FITC is detectable in COSMC KO HEK cells, reflecting higher VVL binding to free terminal O-GalNAc residues expressed at the plasma membrane comparing to control cells. Nonetheless, basal green fluorescence intensity is also observed in control HEK cells. Therefore, we cannot exclude that either control cells expressed a small proportion of unsubstituted terminal O-GalNAc at the plasma membrane or, this fluorescence reflects unspecific VVL binding, defining an aspecific background.

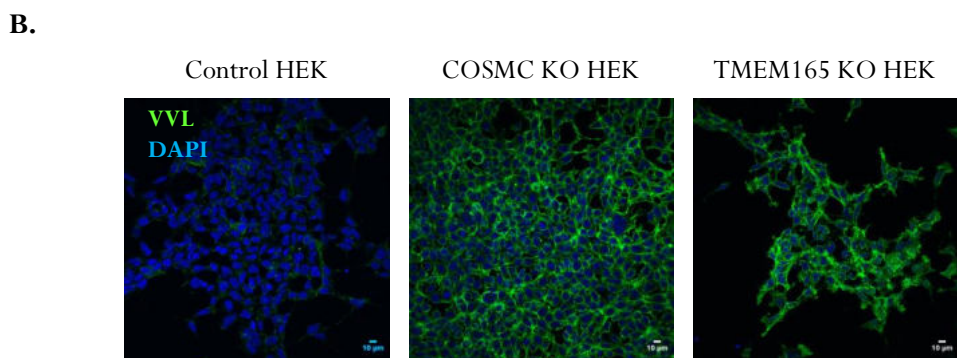
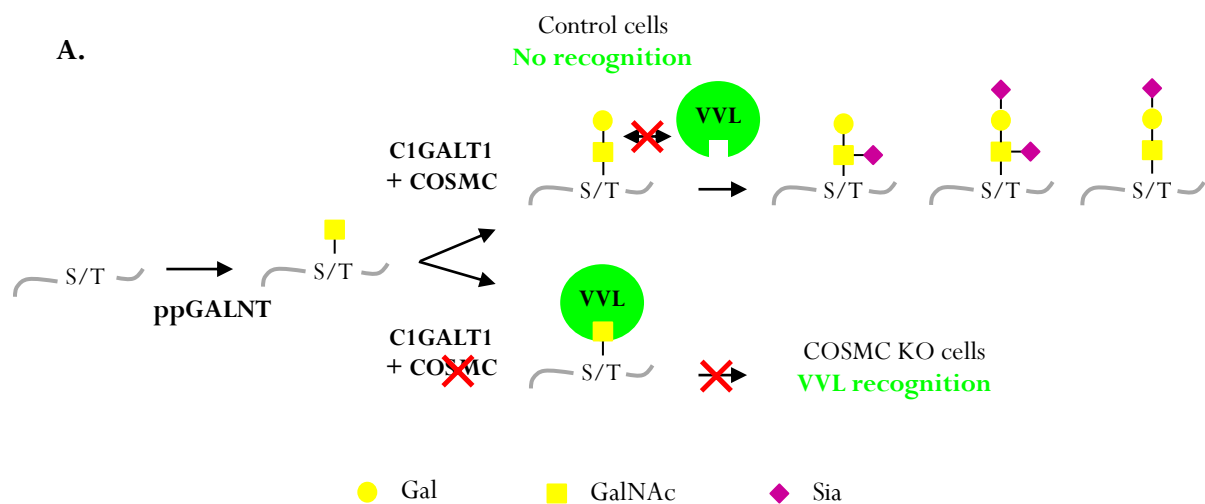


**Figure 56: Indirect evidence for O-linked mucin type defects in TMEM165 KO HEK cells. A.** Schematic representation of core 1 mucin type initiating steps. A first GalNAc residue is linked to the hydroxyl group of a serine (S) or threonine (T) within a polypeptide *via* the activity of several peptidyl GalNAc transferases (ppGALNT). Then, the galactosyltransferase C1GALT1 catalyzes the addition of a Gal onto GalNAc for further elongation by Sia. C1GALT1 requires the chaperone COSMC to be fully functional and both proteins are  $Mn^{2+}$  and  $Ca^{2+}$ -dependent. VVL only recognizes free terminal GalNAc residues. In case of COSMC deficiency, GalNAc are no longer substituted allowing VVL recognition. In our study, this binding between VVL-FITC and GalNAc is reflected by a green fluorescence signal. **B.** VVL-FITC staining in control, TMEM165 KO and COSMC KO HEK cells. Cells were fixed and labeled with VVL-FITC before confocal microscopy visualization. DAPI staining (blue) was performed, showing nuclei.

Interestingly, in TMEM165 KO HEK cells a significant green staining is also detected (Figure 56B) suggesting the presence of truncated O-linked mucin type in TMEM165 KO HEK cells. This VVL-FITC recognition in TMEM165 deficient cells may link for the first time TMEM165 function in O-linked glycosylation. However the mechanism beyond this O-linked glycosylation defect is not known. Since both COSMC and C1GALT1 require  $Mn^{2+}$  and  $Ca^{2+}$  to be fully active, we reasoned that the disrupted Golgi  $Mn^{2+}$  homeostasis in TMEM165 KO HEK cells may alter the function of both proteins resulting in improper transfer of Gal from UDP-Gal onto the GalNAc residue.

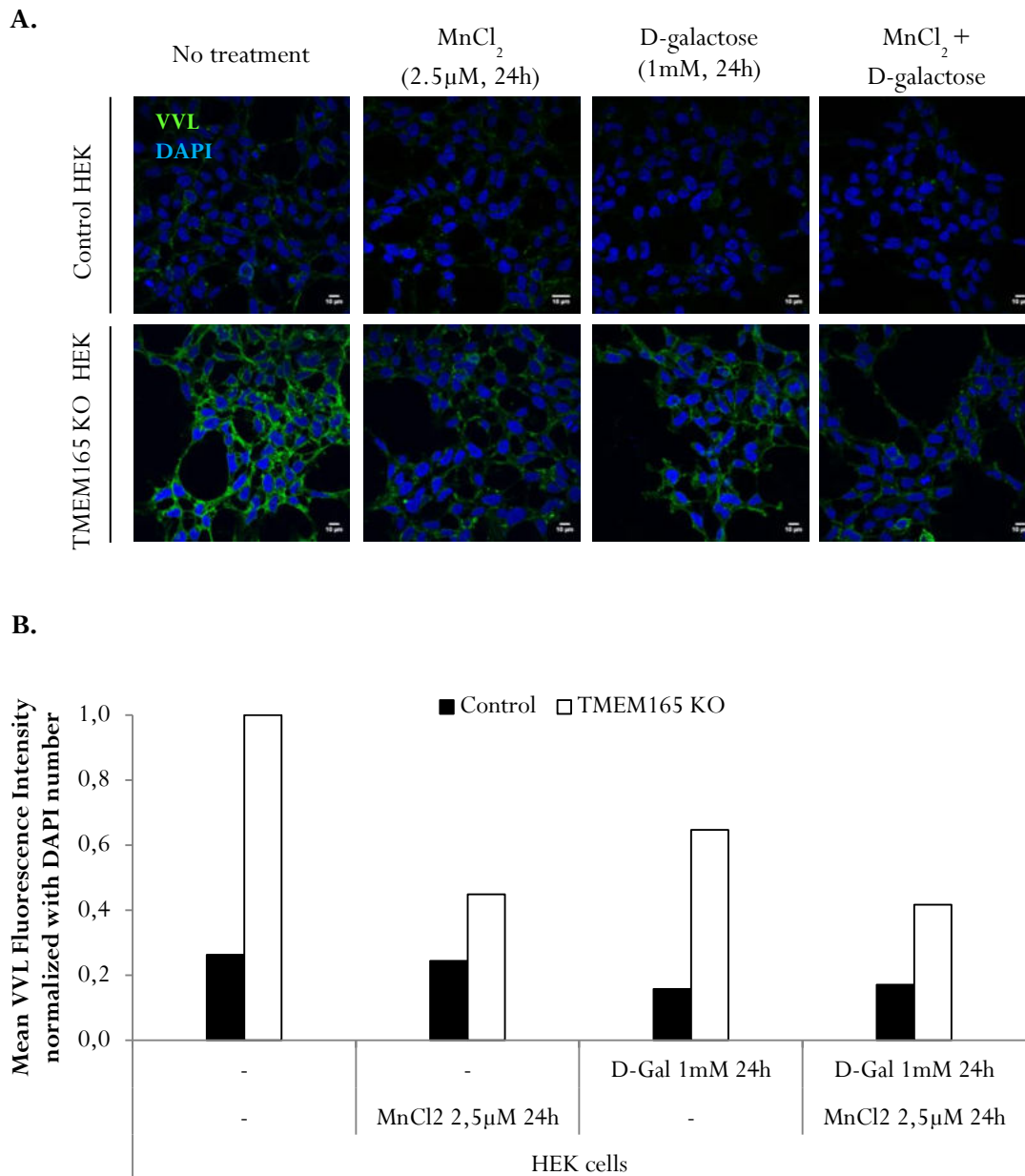


**Figure 57: Influence of  $MnCl_2$  and/or Gal supplementations on VVL-FITC staining in TMEM165 KO HEK cells.** **A.** Cells were fixed and labeled with VVL-FITC before confocal microscopy visualization. DAPI staining (blue) was performed, showing nuclei. **B.** Quantification of VVL-FITC signal has been normalized to the number of DAPI. Arbitrary mean fluorescence intensity (MFI) of 1 has been assigned to TMEM165 KO cells.

To test whether  $\text{MnCl}_2$  and/or Gal supplementations would correct this defect, control and TMEM165 KO HEK cells were treated with  $2.5\mu\text{M}$   $\text{MnCl}_2$  and/or  $1\text{mM}$  Gal for 24h. As depicted in Figure 57, differences between the three treatments are observed in both control and TMEM165 KO cells with a higher impact on VVL-FITC mean fluorescence intensity (MFI) in TMEM165 KO HEK cells. In both cell lines, all treatments resulted in a decreased MFI associated to VVL-FITC suggesting that O-GalNAc residues were more likely substituted following  $\text{MnCl}_2$  or Gal treatment. However, it is to note that Gal supplementation is less efficient (MFI: 0.65) than  $\text{MnCl}_2$  addition alone (MFI: 0.45) or even  $\text{MnCl}_2$  in combination with Gal (MFI: 0.42). Therefore, the hypothesis according to which an impaired Golgi  $\text{Mn}^{2+}$  homeostasis in TMEM165 deficient cell would affect the activity of key enzymes in the early initiation of O-linked mucin type glycans is still valid and relevant. Nevertheless, these results need to be repeated to be strengthened as this experiment has only been done once. All in all, we indirectly shed light on the presence of truncated mucin type likely harboring unsubstituted terminal O-GalNAc in TMEM165 KO HEK cells that seems to be further substituted and processed upon  $\text{MnCl}_2$  and/or Gal supplementations.

Lastly, additional unpublished data also revealed a  $\text{Mn}^{2+}$ -induced glycosylation rescue on proteoglycans synthesis in TMEM165 KO ATDC5 cells, a chondrogenic mouse-derived cell lines. In contrast, Gal supplementation still failed to suppress both GAGs defects found onto decorin and syndecan. These results will no longer be discussed since they have been obtained by a collaborator and will soon be incorporated into a publication.

All in all, Table 22 gathers the current state-of-the-art regarding glycosylation pathways altered due to TMEM165 deficiency and the beneficial effects of  $\text{MnCl}_2$  and/or Gal supplementations to recover proper glycan structures. From these observations, we and collaborators have clearly demonstrated that  $\text{MnCl}_2$  supplementation completely suppress all glycosylation defects due to TMEM165 deficiency. Actually, as well described for N-linked glycosylation, all glycosylation reactions are catalyzed by enzymes that mainly require divalent metal ion as cofactors to be fully active. In both yeast and human Gdt1p/TMEM165 deficient cells, we have demonstrated that Golgi glycosylation defects originate from a disrupted Golgi  $\text{Mn}^{2+}$  homeostasis [65]. Conceptually, providing defective cells with the missing/required ions made sense and all the results we obtained prove the efficiency of such treatment. Mechanistically, we reasoned that  $\text{MnCl}_2$  addition boosts glycosylation reactions by enhancing proper glycosyltransferases activities, especially UDP-sugar GTs that are all divalent-metal-ion-dependent but not only (see Table 23). Thanks to the above publication (Paper 1), we have provided new insights in the mechanism of such  $\text{Mn}^{2+}$ -induced glycosylation rescue with regards to N-linked glycosylation.

**Table 22: Current state-of-the-art about glycosylation defects associated with TMEM165 deficiency and effects of MnCl<sub>2</sub> and/or Gal supplementation as glycosylation suppressors.** CS: chondroitin sulfate, GAGs: glycosaminoglycans, GM2/3: monosialotri/dihexosyl ganglioside, GlcNH<sub>2</sub>: glucosamine, GSLs: glycosphingolipids, HS: heparan sulfate, m/z: masse per charge ratio, LAMP2: lysosomal associated-membrane protein 2, N/A: not applicable because not performed, TGN46: trans-Golgi network glycoprotein 46 and VVL: *Vicia villosa* lectin.

| Glyco-pathway                          | Supplementation and effective suppression of glycosylation defects                      |   |  |  |
|--|---|---|--|--|
|  | No treatment  | MnCl <sub>2</sub>   | Gal  | MnCl <sub>2</sub> + Gal  |
| <b>N-linked</b><br>[64,65,231,506,508] | Accumulation of agalactosylated and asialyated glycan structures                        | Complete recovery   | Complete recovery  | Complete recovery  |
| <b>N- and O-linked</b><br>[65,231,506] | LAMP2 and TGN46 glycosylation defects reflect by altered electrophoretic gel mobilities | Specific and complete recovery (same effect with MnSO <sub>4</sub> , no effect of other ions: CaCl <sub>2</sub> , CuSO <sub>4</sub> , NiSO <sub>4</sub> , MgCl <sub>2</sub> , FeCl <sub>2</sub> , ZnCl <sub>2</sub> , LiCl) | Specific but partial recovery on LAMP2 (no effect of GlcNAc nor GlcNH <sub>2</sub> )<br>No effect on TGN46 | Specific and complete recovery (no effect of GlcNAc nor GlcNH <sub>2</sub> combined with MnCl <sub>2</sub> ) |
| <b>GSLs</b><br>[506]                   | Few GSLs expressed at rather low levels: GM3 and GM2                                    | Complete recovery of GM3 and GM2 levels   | Partial recovery of GM3 but no effect on GM2 levels  | N/A  |
| <b>GAGs</b><br>[unpublished]           | Defect in proteoglycans synthesis: decorin (CS) and syndecan (HS)                       | Complete recovery   | No effect  | N/A  |
| <b>Mucin type</b><br>[unpublished]     | High VVL lectin staining reflecting free O-GalNAc ends                                  | Signal diminution by 55%  | Signal diminution by 35%   | Signal diminution by 58%   |

However, we need to keep in mind that Mn<sup>2+</sup> can be as beneficial as toxic for cells and organisms since Mn<sup>2+</sup> deficiency leads to CDGs (TMEM165-CDG and SLC39A8-CDG) whereas Mn<sup>2+</sup> overload or chronic exposure results in the development of Parkinson-like syndromes (HMDYT1, HMDTY2) (see Chapter 2, section 1.4.2.). In that way and because TMEM165-CDG patients had normal Mn blood levels, a clinical trial based on MnCl<sub>2</sub> therapy enrolling TMEM165-CDG patients was much more difficult to set up than the one with Gal administration that was safer [506]. Nonetheless, manganese supplementation (MnSO<sub>4</sub>-H<sub>2</sub>O) has been successfully reported for two patients suffering from SLC39A8-CDG with very low to undetectable Mn blood. In a clinical trial lead by Park et al., therapeutic MnSO<sub>4</sub>-H<sub>2</sub>O doses of 200mg (20mg/kg) and 600mg (15mg/kg) were established to be beneficial to both patients despite they were considerably higher than the recommended daily Mn intake of 1 to 2mg. At these doses, MnSO<sub>4</sub>-H<sub>2</sub>O supplementation has been carefully monitored with cranial MRI examinations that did not reveal any symptom of Mn-induced toxicity [68]. In contrast, beneficial effects of such Mn administration led to major clinical improvements and correct all biochemical abnormalities. It is to note that in a previous study from Park et al., Gal supplementation was also

shown to normalize glycosylation defects observed on serum transferrin from SLC39A8-CDG patients [67] and we demonstrated couples of year later a similar Gal effect for TMEM165-CDG [506]. However, in both studies Gal supplementation was only partial compared to Mn [68,506]. In fact, in both disorders, glycosylation abnormalities originate from a primary disorder of Mn metabolism which can be alleviated by restoring physiological Mn levels in body fluids and intracellular compartments thanks to  $\text{MnCl}_2/\text{MnSO}_4\text{-H}_2\text{O}$  supplementations. Here, Gal only seems to boost the activity of specific GTs by increasing cytosolic and Golgi concentrations of UDP-Gal, its donor substrate.

Nonetheless, oral administrations of monosaccharide are increasingly used in CDG and are seen as simplest and safer treatments. For instance, Gal therapies have been prove to be successful in the treatment of PGM1-CDG and SLC35A2-CDG; L-fucose has been used for SLC35C1-CDG and D-mannose for MPI-CDG [82,512,513]. All of these examples suggest that increasing the Golgi-cytoplasmic gradient of UDP-sugars can improve its import and further incorporation into glycoconjugates. However, this increased transport remains to be demonstrated *in vitro*. From what we observed, although Gal supplementation increases the pools of UDP-Gal, UDP-Glc and UDP-GlcNAc (Figure 55), it does not seem to be sufficient to lead to a better Gal incorporation into other glycoconjugates than N-linked glycans. As already mentioned earlier, we cannot exclude that Gal supplementation may induce  $\text{Mn}^{2+}$  uptake from the extracellular medium that would in fact enhance/potentiate the proper “Gal effect”. In this case, one can easily imagine that Gal-induced glycosylation rescue may correlate variations of cellular  $\text{Mn}^{2+}$  levels. This is what we observed in TMEM165 KO cells cultured with FBS containing different levels of Mn (Paper 2, repeated in Figure 58A, B) [509]. When cells were cultured with a FBS containing low Mn levels (FBS4), Gal effect was drastically reduced compared to TMEM165-deficient cells cultured with FBS containing higher amounts of Mn (FBS2). In addition, contrary to  $\text{MnCl}_2$  supplementation which is time- and concentration-dependent [231,509], no such effect have been observed for Gal-induced glycosylation rescue on LAMP2 in TMEM165 KO HEK cells cultured with FBS4 (Figure 58C). Together, these results strongly suggest that Gal-induced LAMP2 glycosylation rescue in TMEM165 (i) highly depends on external Mn availability in the culture medium and (ii) is potentiated by  $\text{MnCl}_2$  co-incubation.

### **3. Deciphering LAMP2 and TGN46 major post-translational modifications**

To add an extra layer of complexity, Gal-induced glycosylation rescue was only seen for LAMP2 and not for TGN46, another glycoprotein carrying both N- and O-linked glycans. As shown in Figure 59A, while  $\text{MnCl}_2$  supplementation completely suppresses the electrophoretic gel mobility of TGN46 in TMEM165 KO HEK cells, Gal has no effect unless it is combined to  $\text{MnCl}_2$ .



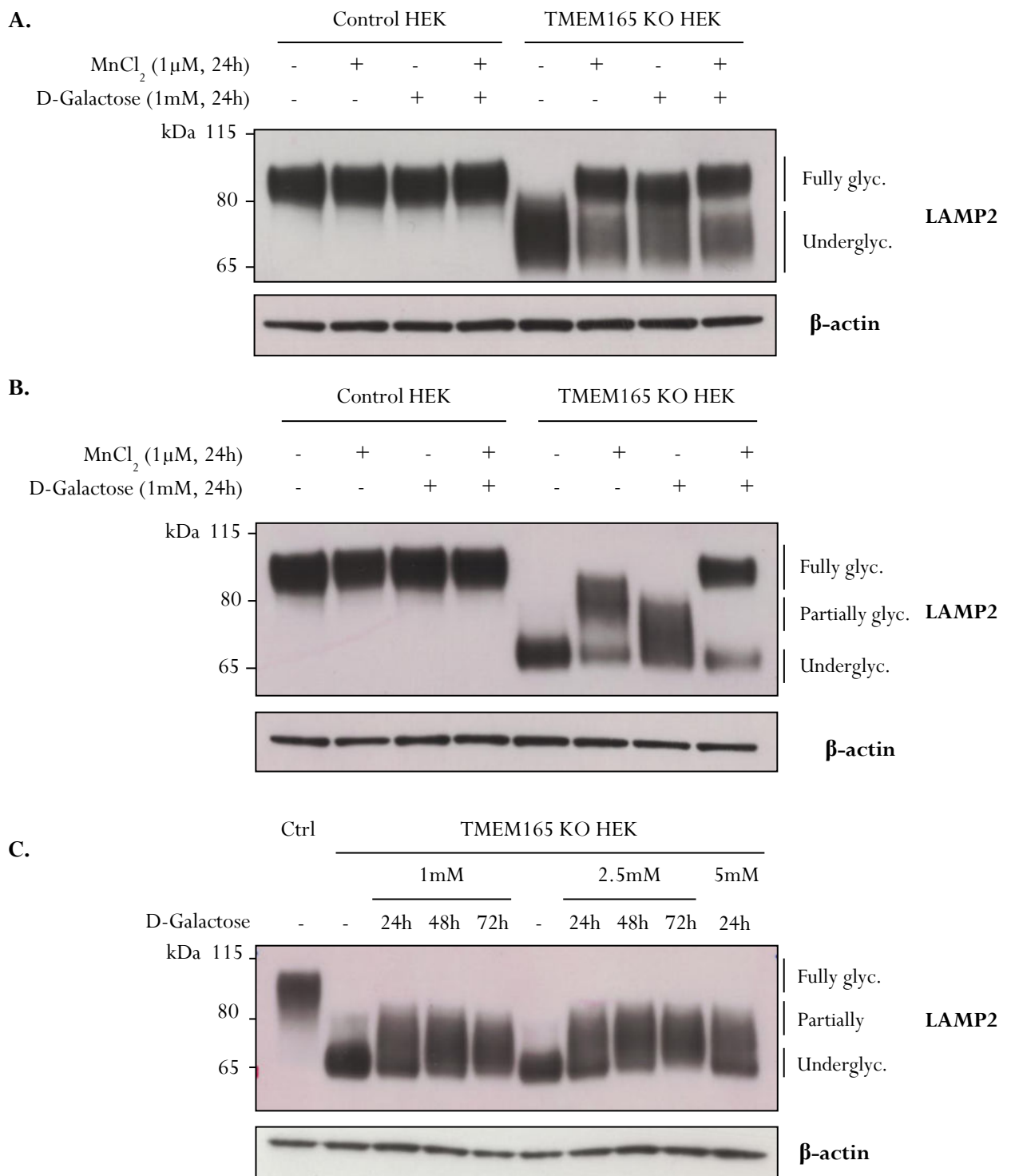


**Figure 58: Gal supplementation efficiency depends on external Mn availability. A. and B.** correspond to Figure 9, Paper 2. **The suppression of LAMP2 glycosylation defect by Gal supplementation depends on the FBS used for cell culture.** Control and TMEM165 KO HEK cells were cultured in DMEM supplemented with 10% FBS2 (**A.**) or 4 (**B.**). Cells were incubated with or without 1μM MnCl<sub>2</sub> and 1mM Gal for 24h. Total cell lysates were prepared, subjected to SDS-PAGE and western blot with the indicated antibodies. **C. The suppression of LAMP2 glycosylation defect by Gal supplementation is not time-/concentration-dependent.** Control (Ctrl) and TMEM165 KO HEK cells were cultured in DMEM supplemented with 10% FBS4 and incubated with or without 1mM to 5mM galactose for 24 to 72 hours. Total cell lysates were prepared, subjected to SDS-PAGE and western blot with the indicated antibodies.

In addition, increasing either Gal concentration (from 1mM to 5mM) or the incubation time (from 24h to 72h) has no impact on TGN46 migration profile (Figure 59B). This intriguing result pushed us to further assess the nature of the main glycan structures carried by LAMP2 and TGN46. According to Table 22, we suggested that the main difference between LAMP2 and TGN46 could rely on the number and/or nature of glycan structures they carry or additional post-translational modification (PTM) such as phosphorylation or ubiquitination.

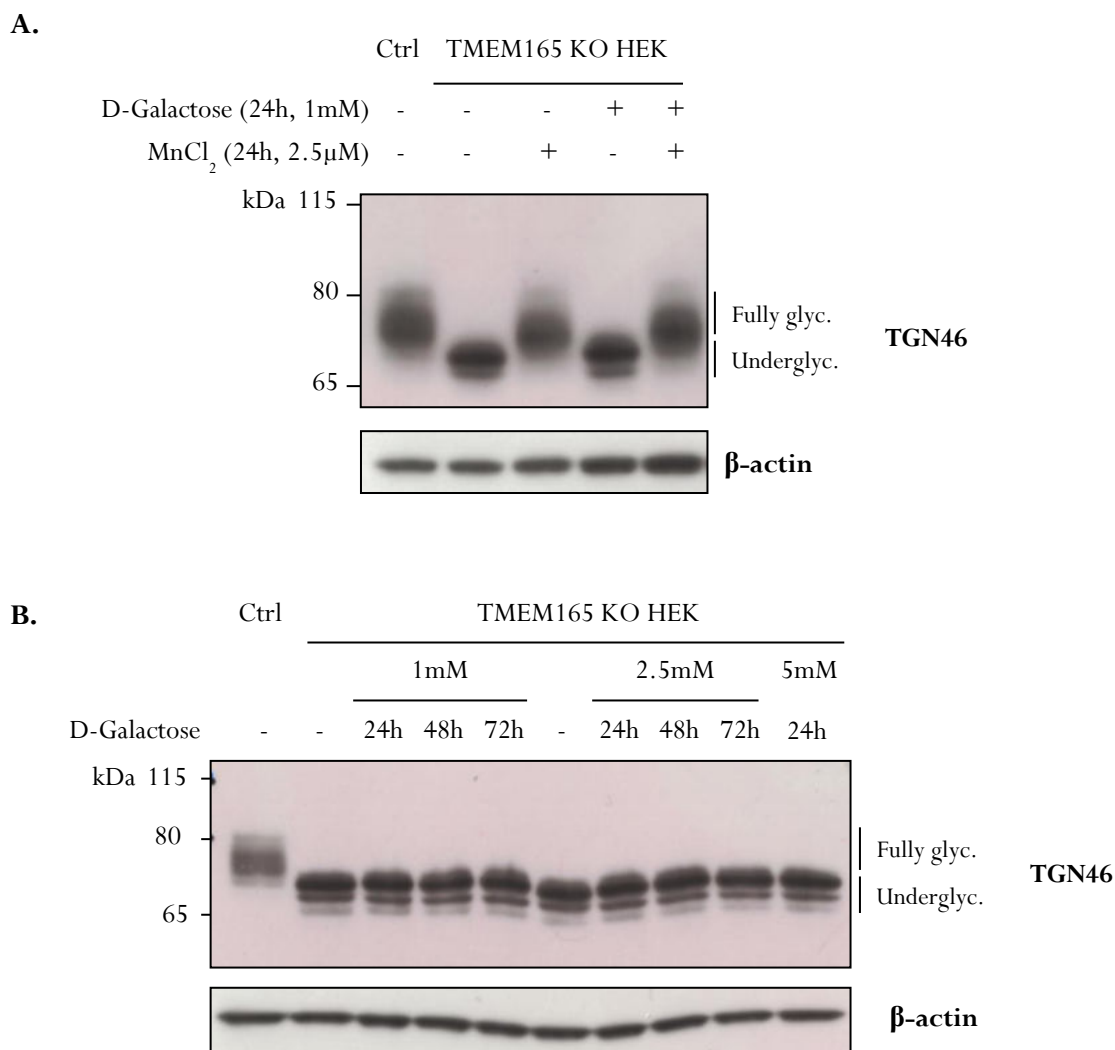


**Figure 59: Gal supplementation fails to rescue TGN46 electrophoretic gel mobility in TMEM165 KO HEK cells.** **A.** Control (Ctrl) and TMEM165 KO HEK cells were cultured in DMEM supplemented with 10% FBS4 and incubated with or without 2.5μM MnCl<sub>2</sub> and/or 1mM galactose for 24h. Total cell lysates were prepared, subjected to SDS-PAGE and western blot with the indicated antibodies. **B.** Control (Ctrl) and TMEM165 KO HEK cells were cultured in DMEM supplemented with 10% FBS4 and incubated with or without 1mM to 5mM galactose for 24 to 72h. Total cell lysates were prepared, subjected to SDS-PAGE and western blot with the indicated antibodies.

From literature, it is well established that LAMP2 and TGN46 are heavily glycosylated proteins with high number of N- and O-linked glycosylation sites. In the early 90's, Carlsson *et al.* identified 16 N-linked and 10 O-linked glycosylation sites on LAMP2 [514,515]. After protein purification and

proteolysis, both N- and O-linked glycans were characterized by lectin affinity and gel filtration, and further peptide sequencing allows the identification of precise N- and O-linked glycosylation sites. In terms of glycan structures, poly-N-acetylglucosamine N-glycans were assigned to three asparagine (N) and more recently, Tan *et al.* identified complex N-glycan structures thanks to a mass spectrometry approach on total N-glycans released from purified LAMP2 proteins [516]. With regards to O-linked glycans, after a sialidase treatment to favor lectin binding, two main structures were found: disaccharide O-GalNAc-Gal and poly-N-acetylglucosamine tetrasaccharide O-GalNAc-Gal-GlcNAc-Gal, in smaller proportion. Altogether and depending on the glycosylation sites, LAMP2 either possesses polyglucosaminoglycans (N- and O-linked) or complex N-glycans. However, according to the cell type, variations in polyglucosamine chains length can be observed resulting in subtle differences for LAMP2 electrophoretic migration profile at a steady state level. A simplified representation of the protein with its glycans is provided in Figure 60.

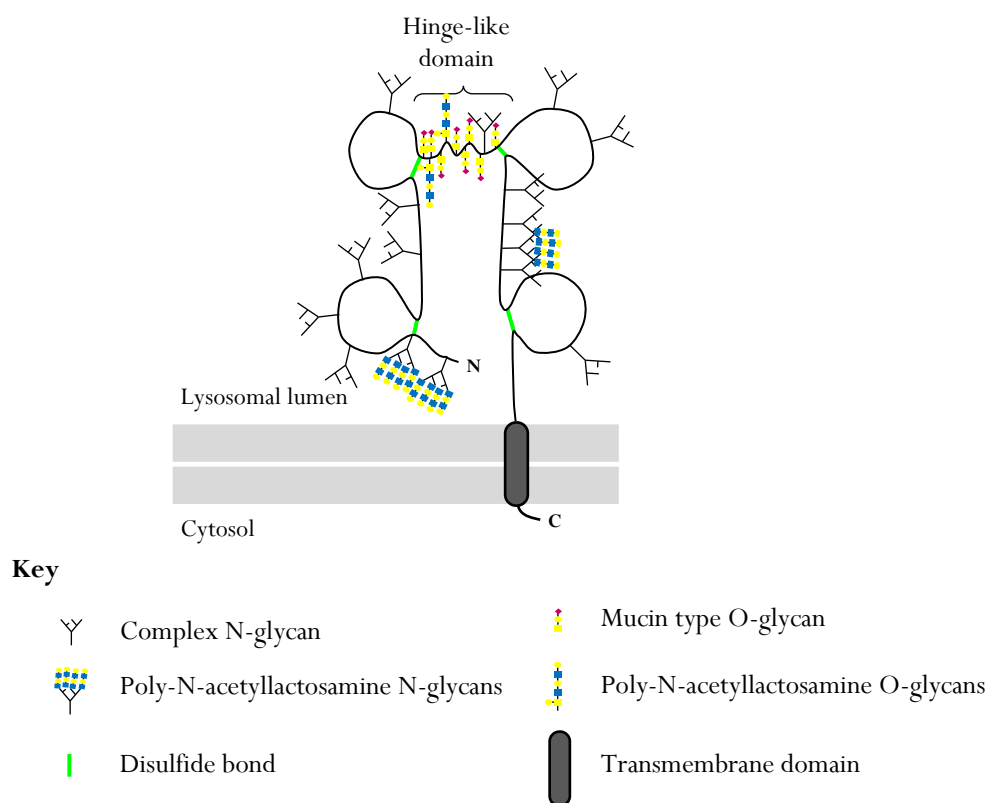


**Figure 60: Schematic representation of LAMP2 highlighting its different glycosylation sites.** LAMP2 is a single transmembrane protein with a very short cytosolic carboxy-terminus tail (C). N-linked glycosylation sites are represented by antennae (distinction between complex and polyglucosaminoglycans is explained in the key). O-linked glycosylation sites are gathered in the hinge-like domain (distinction between mucin type and polyglucosaminoglycans is explained in the key). Inspired from [517].

On the other hand, little is known about TGN46 post-translational modifications, including N- and O-linked glycans. In the UniprotKB Database, TGN46 is predicted to have 9 N-linked glycosylation and 5 phosphorylation sites while PhosphoSitePlus® software assigned more than 20 phosphorylation sites and

around 25 O-GalNAcylation sites to TGN46. Since phosphorylation and O-GalNAcylation both occur through the hydroxyl group from serine, threonine and tyrosine amino acid residues, it is more difficult to discriminate one from the other. Then, we decided to perform a deglycosylation experiment to better understand the electrophoretic migration profile of TGN46 that we observed in TMEM165 KO HEK cells.

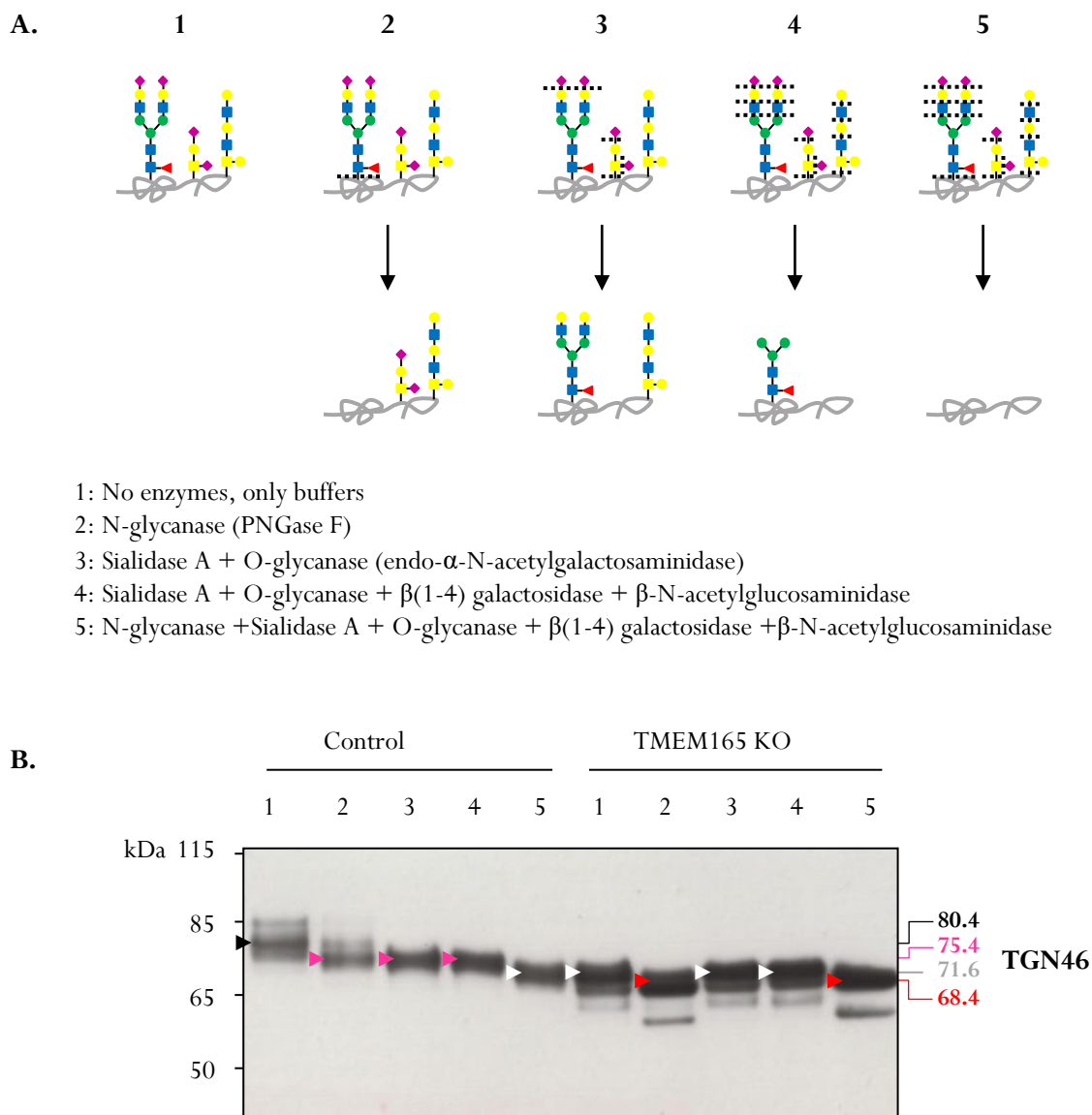


**Figure 61: Insights into the nature of TGN46 glycosylation sites.** **A.** Schematic representation of N-linked and O-linked glycan structures following enzymatic deglycosylation associated to each experimental condition (1 to 5). Specific cutting sites are indicated with dashed lines. **B.** Control and TMEM165 KO HEK cell lysates were prepared for the different enzymatic digestions following guidelines and protocol provided by the manufacturer. Then, samples were loaded onto SDS-PAGE and western blot with TGN46 antibody. Black, pink, white and red arrows indicate different shifts in the electrophoretic migration of TGN46 and associated molecular weights are reported on the right.

Using different glycosidases amongst N-glycanase (PNGase F), O-glycanase (endo- $\alpha$ -N-acetylgalactosaminidase),  $\beta$ (1,4)galactosidase,  $\beta$ -N-acetylglucosaminidase and sialidase A, we analyzed TGN46 migration profile by western blot in both control and TMEM165 KO cells. Results are presented in Figure 61B. In control cells, comparing lanes 1 and 2, the shift in TGN46 electrophoretic migration profile from 80.4 to 75.4 kDa revealed that N-glycans have been removed by PNGase F assuming that TGN46 is an N-linked glycoprotein. Then, an identical migration profile is observed between lane 3 and 4 (75.4 kDa), both shifting compared to lane 1, suggesting the removal of O-linked glycans. Hence, in addition to be N-glycosylated, TGN46 is also O-glycosylated. This is corroborated in lane 5, where the shift in TGN46 electrophoretic migration is the highest comparing to lane 1 (71.6 kDa). Actually, the trickiest part to analyze in these first five lanes is the very similar molecular weight of TGN46 in lanes 2, 3 and 4 around 75.4 kDa. It appears that all N-linked glycan(s) and all O-linked glycan(s) carried by TGN46 have a similar molecular weight. In other words, removing either all N-glycans or all O-glycans results in a similar molecular weight loss. On the other hand, in TMEM165 KO HEK cells, identical electrophoretic migrations of TGN46 are observed in lanes 1, 3 and 4, corresponding to lane 5 of control cells (75.4 kDa). This observation implies that TGN46 is likely under N- and O-glycosylated in case of TMEM165 deficiency. However, although no differences between condition without treatment (lane 1) and conditions with O-glycanase (lanes 3 and 4) are observed, treatment with PNGase F (lanes 2 and 5) induces an additional and similar shift (68.4 kDa) compared to lanes 1, 3, and 4. This suggests that TGN46 is likely N-glycosylated in TMEM165 KO HEK cells and probably possesses truncated N-glycans that would explain the smaller shift between lanes 1 and 2 in control cells and lanes 1 and 2 in TMEM165 KO cells. The fact that TGN46 migrates faster in TMEM165 deficient cells in lanes 2 and 5 (68.4 kDa) compared to all other lanes may be explained by additional PTM on the protein such as phosphorylation that might also be affected due to TMEM165 deficiency. What could be interesting to perform in the future would be to (i) repeat these deglycosylation reactions after  $\text{MnCl}_2$  and/or Gal supplementation, (ii) further analyze LAMP2 and TGN46 glycan structures *via* a mass spectrometry approach following protein purification and glycan release and (iii) explore TGN46 potential phosphorylation sites through western blot and mass spectrometry based proteomics.

#### 4. Conclusion and introduction of Results, Part II

All in all, in case of TMEM165 deficiency,  $Mn^{2+}$  supplementation broadly acts on all glycosylation pathways since  $Mn^{2+}$  will enhance/rescue/stimulate the activity of all enzymes requiring  $Mn^{2+}$  as cofactor and will not only trigger the activity of one specific galactosyltransferase that requires both Gal and  $Mn^{2+}$  to be fully active. In my opinion, there is no proper Gal-induced glycosylation rescue. From all our results, I strongly believe that Gal effect is intimately dependent on (intra)cellular  $Mn^{2+}$  levels that might vary when Gal is uptaken from the extracellular medium.

Actually, this  $Mn^{2+}$ -induced Golgi glycosylation rescue was also observed in yeast *Saccharomyces cerevisiae* lacking TMEM165 yeast ortholog named Gdt1p. However, differing from human cells, yeasts lacking *GDT1* only exhibit strong Golgi glycosylation defect in presence of high external  $CaCl_2$  concentrations (> 500mM), suggesting that Gdt1p and TMEM165 function may have evolved during evolution. As mentioned in Chapter 2, Figure 27 and Figure 28, many different proteins are involved in the regulation of Golgi  $Ca^{2+}$  homeostasis in yeast and mammals. Amongst them one is particularly conserved between the two organisms: the  $Ca^{2+}/Mn^{2+}$  Golgi P-type ATPase SPCA1 in mammals and Pmr1p, the yeast ortholog. Interestingly, yeast lacking *PRM1* display severe Golgi glycosylation defects associated with altered protein trafficking whereas no link has been established between *ATP2C1* deficiency and glycosylation reactions in humans. Assuming that TMEM165/Gdt1p and SPCA1/Pmr1p are key players in the regulation of Golgi  $Ca^{2+}/Mn^{2+}$  homeostasis, the second aspect of my PhD was to further investigate the potential functional link between these two Golgi proteins, in yeast *Saccharomyces cerevisiae* and mammalian cell lines (HeLa and Hap1 cells).

## 2. - Part II -

---

### Investigating the functional links between TMEM165/Gdt1p and SPCA1/Pmr1p

---

**Paper 3:** Investigating the function of Gdt1p in yeast glycosylation

**Paper 4:** Investigating the functional link between TMEM165 and SPCA1





### 3. Paper 3: Investigating the function of Gdt1p in yeast glycosylation

#### 3.1. Introduction

At the early beginning of my PhD, I was trained to handle yeast *Saccharomyces cerevisiae*, particularly to end up the reviewing of this Paper 3. My major contribution to this work relies on the generation of supplementary Figures, required to satisfy reviewers and ensuring the publication of the study. At the time, right after the discovery that Golgi glycosylation defects observed in TMEM165/Gdt1p deficient cells were due to an altered Golgi  $Mn^{2+}$  homeostasis [65], we further investigated (i) mechanism of  $Mn^{2+}$ -induced glycosylation rescue in mammalian TMEM165 KO cells (Paper 1) and (ii) Gdt1p function in yeast Golgi glycosylation (Paper 3) in two separate studies. As already summarized in Chapter 3, almost thirty years ago Antebi and Fink [236] followed by Dürr *et al.* [238] first established a link between glycosylation and Golgi  $Ca^{2+}/Mn^{2+}$  homeostasis in yeast lacking Pmr1p (*pmr1Δ*), the Golgi  $Ca^{2+}/Mn^{2+}$  ATPase. At the time, both  $Ca^{2+}$  and  $Mn^{2+}$  requirements were assigned to sustain glycosylation reactions since both  $CaCl_2$  and  $MnCl_2$  supplementations partially rescued those defects. More recently, in 2016, these findings were updated by our team [65] and collaborators [239] with the identification of severe N-linked Golgi glycosylation defects in yeast lacking Gdt1p (*gdt1Δ*) exposed to high extracellular  $CaCl_2$  concentrations (>500 mM). Following the characterization of *gdt1Δ*, we found that addition of 50μM  $MnCl_2$  to the Ca-enriched medium suppressed the observed glycosylation defects [65,239].

**Table 23: Summary about Gdt1p/TMEM165 and Pmr1p/SPCA1 involvement in Golgi glycosylation.**

|                                 | Golgi N-linked glycosylation defects?        | Suppressed by...      |
|---------------------------------|--|-----------------------|
| <i>Saccharomyces cerevisiae</i> |  |                       |
| Wild-type                       | No   |                       |
| <i>gdt1Δ</i>                    | Yes, in excess of $[CaCl_2]_{extracellular}$ | $MnCl_2$              |
| <i>pmr1Δ</i>                    | Yes  | $CaCl_2$ , $MnCl_2$   |
| <i>gdt1Δ/pm1Δ</i>               | Yes  | $MnCl_2$              |
| Mammalian cells                 |  |                       |
| Control                         | No   |                       |
| TMEM165 KO                      | Yes  | D-Galactose, $MnCl_2$ |
| SPCA1 KO                        | No   |                       |

Then, the first link between Gdt1p function in Golgi glycosylation and  $Mn^{2+}$  was established. Table 23 draws up the start-of-the-art of the indirect contribution of Gdt1p/TMEM165 and Pmr1p/SPCA1 in Golgi glycosylation and  $Mn^{2+}/Ca^{2+}$  homeostasis. As mentioned in Table 23, while Golgi glycosylation defects due to *PMR1* deletion can be suppressed by either  $CaCl_2$  or  $MnCl_2$  supplementation, only  $MnCl_2$  addition can rescue the glycosylation defects observed in the double mutant *gdt1Δ/pmr1Δ*. Surprisingly,  $CaCl_2$  supplementation failed to rescue Golgi glycosylation in *gdt1Δ/pmr1Δ* assuming that Gdt1p functionality might be required during the  $Ca^{2+}$ -induced glycosylation rescue in yeast lacking Pmr1p. This unexpected finding highly suggests a functional link between Pmr1p and Gdt1p in Golgi glycosylation that was therefore further investigated in the following study (Paper 3). Hence, we took advantage of three mutated forms of Pmr1p, specifically defective for transport of either  $Ca^{2+}$  (Pmr1p-D53A),  $Mn^{2+}$  (Pmr1p-Q783A) or both  $Ca^{2+}$  and  $Mn^{2+}$  (Pmr1p-D778A) (Figure 62).

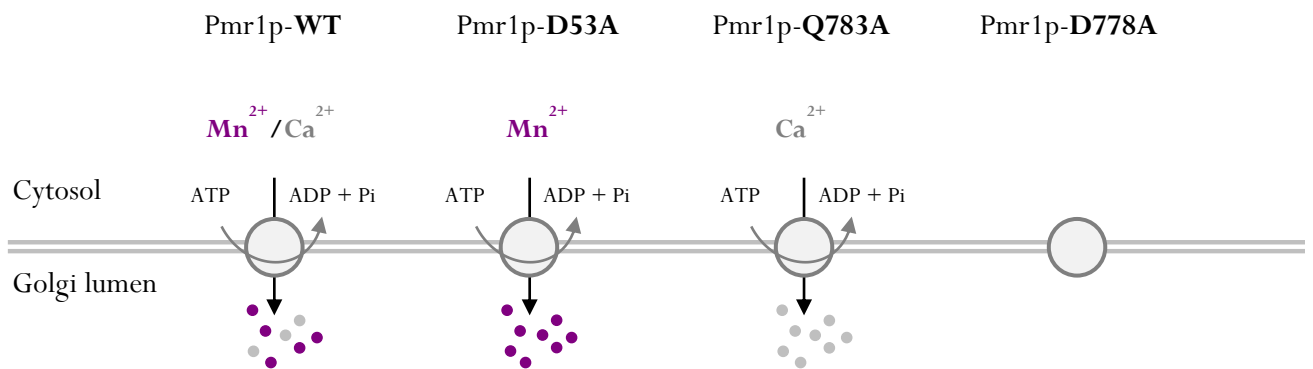


**Figure 62: Pmr1p defective mutants and associated ion pumping capacity used in the study.**

The idea was to better discriminate the role of Pmr1p and Gdt1p in Golgi glycosylation by evaluating the contribution of Gdt1p in *pmr1Δ* strains expressing different forms of Pmr1p.

### 3.2. Publication

# Investigating the function of Gdt1p in yeast Golgi glycosylation

Eudoxie Dulary<sup>a,b,1</sup>, Shin-Yi Yu<sup>a,1</sup>, Marine Houdou<sup>a,b,1</sup>, Geoffroy de Bettignies<sup>a,b</sup>, Valérie Decool<sup>c</sup>, Sven Potelle<sup>a,b</sup>, Sandrine Duvet<sup>a,b</sup>, Marie-Ange Krzewinski-Recchi<sup>a,b</sup>, Anne Garat<sup>c</sup>, Gert Matthijs<sup>b,d</sup>, Yann Guerardel<sup>a</sup>, François Foulquier<sup>a,b,\*</sup>

<sup>a</sup> Univ. Lille, CNRS, UMR 8576 – UGSF - Unité de Glycobiologie Structurale et Fonctionnelle, F-59000 Lille, France

<sup>b</sup> LIA GLYCOLAB4CDG France/Belgium (International Associated Laboratory “Laboratory for the Research on Congenital Disorders of Glycosylation – from cellular mechanisms to cure”, France

<sup>c</sup> Univ. Lille, CHU Lille, Institut Pasteur de Lille, EA 4483 – IMPECS – IMPact de l’Environnement Chimique sur la Santé humaine, F-59000 Lille, France

<sup>d</sup> Center for Human Genetics, KU Leuven, Leuven, Belgium

## ARTICLE INFO

### Keywords:

Gdt1p  
Pmr1p  
Golgi glycosylation  
Mn<sup>2+</sup> homeostasis  
Ca<sup>2+</sup> homeostasis

## ABSTRACT

The Golgi ion homeostasis is tightly regulated to ensure essential cellular processes such as glycosylation, yet our understanding of this regulation remains incomplete. Gdt1p is a member of the conserved Uncharacterized Protein Family (UPF0016). Our previous work suggested that Gdt1p may function in the Golgi by regulating Golgi Ca<sup>2+</sup>/Mn<sup>2+</sup> homeostasis. NMR structural analysis of the polymannan chains isolated from yeasts showed that the *gdt1Δ* mutant cultured in presence of high Ca<sup>2+</sup> concentration, as well as the *pmr1Δ* and *gdt1Δ/pmr1Δ* strains presented strong late Golgi glycosylation defects with a lack of α-1,2 mannoses substitution and α-1,3 mannoses termination. The addition of Mn<sup>2+</sup> confirmed the rescue of these defects. Interestingly, our structural data confirmed that the glycosylation defect in *pmr1Δ* could also completely be suppressed by the addition of Ca<sup>2+</sup>. The use of Pmr1p mutants either defective for Ca<sup>2+</sup> or Mn<sup>2+</sup> transport or both revealed that the suppression of the observed glycosylation defect in *pmr1Δ* strains by the intraluminal Golgi Ca<sup>2+</sup> requires the activity of Gdt1p. These data support the hypothesis that Gdt1p, in order to sustain the Golgi glycosylation process, imports Mn<sup>2+</sup> inside the Golgi lumen when Pmr1p exclusively transports Ca<sup>2+</sup>. Our results also reinforce the functional link between Gdt1p and Pmr1p as we highlighted that Gdt1p was a Mn<sup>2+</sup> sensitive protein whose abundance was directly dependent on the nature of the ion transported by Pmr1p. Finally, this study demonstrated that the aspartic residues of the two conserved motifs E-x-G-D-[KR], likely constituting the cation binding sites of Gdt1p, play a crucial role in Golgi glycosylation and hence in Mn<sup>2+</sup>/Ca<sup>2+</sup> transport.

## 1. Introduction

In 2012, we highlighted TMEM165 as the first member of the Uncharacterized Protein Family 0016 (UPF0016) related to human diseases. Defects in TMEM165 lead to a rare inherited disorder named CDG for Congenital Disorders of Glycosylation in which Golgi glycosylation process is affected. Found in bacteria, archaea, yeast, plants and animals, members of the UPF0016 family share two highly conserved regions as signature motifs: E-x-G-D-[KR] [1]. Many evidences show that these two motifs form the pore of the protein and thus regulate the functionality of the UPF0016 members. Currently, the precise cellular functions of these proteins remain to be fully characterized and are under debate. In yeasts, it was previously reported that Gdt1p was involved in Ca<sup>2+</sup> transport then playing an important role in Ca<sup>2+</sup>

signaling and Golgi protein glycosylation thereby supporting the hypothesis that Gdt1p would act as Ca<sup>2+</sup>/H<sup>+</sup> antiporter in the Golgi apparatus [2,3]. The role of TMEM165 as a Golgi Ca<sup>2+</sup>/H<sup>+</sup> antiporter can however be questioned. We recently highlighted that the observed glycosylation defect due to TMEM165 deficiencies resulted from a defect in Golgi Mn<sup>2+</sup> homeostasis [4]. Moreover, we demonstrated that TMEM165 was a novel Golgi protein sensitive to Mn<sup>2+</sup> as exposition to high Mn<sup>2+</sup> concentrations lead to lysosomal degradation of TMEM165 [5]. These data reinforced the hypothesis of TMEM165 as being involved in Mn<sup>2+</sup> transport. This is also currently emphasized by several other studies. In *Arabidopsis thaliana*, the homologous protein photosynthesis affected mutant 71 PHOTOSYNTHESIS AFFECTED MUTANT 71 (PAM71) has been shown to be required for efficient Mn<sup>2+</sup> uptake at the thylakoid membrane [6]. Moreover, the Mnx protein of the

\* Corresponding author at: Univ. Lille, CNRS, UMR 8576 – UGSF - Unité de Glycobiologie Structurale et Fonctionnelle, F-59000 Lille, France.

E-mail address: francois.foulquier@univ-lille1.fr (F. Foulquier).

<sup>1</sup> These authors have equally contributed.

cyanobacterial model strain *Synechocystis* sp. PCC 6803, also belonging to the UPF0016 family, was recently demonstrated as a Mn exporter [7]. Altogether these data cast doubt about the substrate specificity of the UPF0016 members. From a general point of view, the mechanisms by which yeast cells regulate Golgi  $\text{Ca}^{2+}$  and  $\text{Mn}^{2+}$  homeostasis, both critical for many cellular processes and in particular Golgi glycosylation, are not completely deciphered yet.

In this report we have investigated into details the contribution of Gdt1p, Pmr1p and both in Golgi glycosylation processes. We have demonstrated that inactivation of Pmr1p led to strong Golgi glycosylation defects fully reversed by the addition of both  $\text{Ca}^{2+}$  and  $\text{Mn}^{2+}$ . Interestingly, in the *gdt1Δ/pmr1Δ* double knock-out strain, only the addition of  $\text{Mn}^{2+}$  was capable to suppress the observed Golgi glycosylation defect thus pointing the critical role of Gdt1p in suppressing the Golgi glycosylation defect in *pmr1Δ* strains supplemented with  $\text{Ca}^{2+}$ . We have also shown that the abundance and function of Gdt1p in Golgi glycosylation was dependent on the function of Pmr1p. By using mutants of Pmr1p specifically defective for transport of either  $\text{Ca}^{2+}$  ions (Pmr1pD53A),  $\text{Mn}^{2+}$  ions (Pmr1pQ783A) or both (Pmr1pD778A), our results evidenced that in the case where Pmr1p only transport  $\text{Ca}^{2+}$  from the cytosol to the Golgi lumen, Gdt1p was necessary to import  $\text{Mn}^{2+}$  inside the Golgi lumen to suppress the observed Golgi glycosylation defect. Finally, this report demonstrates that the acidic residues of the two conserved motifs E-x-G-D-[KR] of Gdt1p are involved in Golgi glycosylation.

## 2. Material and methods

### 2.1. Yeast strains and media

Yeast strains used for the experiments are all derivatives of BY4741 and BY4742 and are listed below:

Wild-type (WT) - Mata his3Δ1 leu2Δ0 ura3Δ0  
*pmr1Δ* - Mata his3Δ1 leu2Δ0 ura3Δ0 *pmr1Δ::KanMX4*  
*gdt1Δ* - Mata his3Δ1 leu2Δ0 ura3Δ0 *gdt1Δ::KanMX4*  
*gdt1Δ/pmr1Δ* - Mata his3Δ1 leu2Δ0 ura3Δ0 *gdt1Δ::KanMX4*  
*pmr1Δ::KanMX4*

All strains were obtained by backcrossing *pmr1Δ* (Y04534) and *gdt1Δ*(Y13327) strains provided by Euroscarf.

Yeast was cultured at 30 °C. Cultures in liquid media are done under a light shaking. Rich media, named YEP media, contains yeast extract (10 g·L<sup>-1</sup>, Difco), Bacto-peptone (20 g·L<sup>-1</sup>, Difco). YPD media is a YEP media supplemented with 2% D-glucose (Sigma-Aldrich). YPR is YEP media supplemented with 2% raffinose (Euromedex). Selection antibiotics were added at 100 μg·mL<sup>-1</sup> for nourseothricine, 200 μg·mL<sup>-1</sup> for G418 and 300 μg·mL<sup>-1</sup> for hygromycin.

### 2.2. Constructs, vector engineering and mutagenesis

All the constructs allowing *GDT1* (wt (wt-HA) or mutant (mutant-HA)) expression are pRS41H derivatives. First a 1473 bp fragment starting 417pb before the Start of *GDT1* was amplified from genomic DNA by PCR and cloned between *KpnI* and *XmaI* sites of pRS41H. Mutant and/or HA-tagged versions of *GDT1* (E53G, D56G, E204G, L205W and D207G) were created from this vector using PCR directed mutagenesis by Ezyvec (Lille, France). The HA tag was inserted in the cytoplasmic loop in between the aa 171–172. All the constructs allowing *PMR1* (wt (wt-Myc) or mutant (mutant-Myc)) expression are pRS41N derivatives. First a 4004 bp fragment starting 999 pb before the Start of *PMR1* was amplified from genomic DNA by PCR and cloned between *EagI* and *SacI* sites of pRS41N. Mutant and/or N-Myc-tagged versions of *PMR1* (D53A, D778A and Q783A) were created from this vector using PCR directed mutagenesis by Ezyvec (Lille, France). All constructs were checked by Sanger sequencing of the full insert.

### 2.3. Extraction and isolation of mannan from yeast

The equivalent of 50 g yeast was suspended in 300 mL of 0.02 M citrate buffer (pH 7), autoclaved at 125 °C, 90 min. The solid pellet was then removed by centrifugation and the supernatant collected. An equivalent volume of Fehling solution was added to the supernatant and stirred at room temperature until precipitates form. The precipitates are collected and dissolved with 100 mL of 3 N HCl. 300 mL of ethanol are then added to precipitated mannan. The mannan are then dissolved in 50 mL water and dialyzed (MWCO 3500) against water overnight at 4 °C. The dialyzed mannans are then dried and lyophilized.

### 2.4. Invertase glycosylation analysis

Before any analysis, a preculture in YPD media is done and a volume equivalent to 15 OD600nm units is centrifuged for 3 min at 3500g. The supernatant is discarded and the pellet is suspended in YPR media to induce invertase expression. Calcium, manganese and other ions were added at this step at the indicated concentration. After a 20 h culture in YPR, yeasts were centrifuged for 5 min at 3500g. Supernatant was discarded and the pellet was kept frozen at -20 °C. The cells were then resuspended and lysed by glass-bead agitation in cold TBP buffer (5.52 g of diethylbarbituric acid and 1 g of Tris base per liter of water, pH 7.0; to 100 mL, add 1 mL of stock PMSF (0.174 g of phenylmethanesulfonyl fluoride in 10 mL of absolute ethanol) just before use]. 3 μL of the supernatant are loaded on native gel. For the revelation of the invertase activity, the gel is then soaked into a 4 °C sucrose solution (0.1 M pure sucrose in 0.1 M sodium acetate, pH 5.1) for 10 min and then immediately transferred into a 37 °C sucrose solution for 10 min to hydrolyze the substrate. The gel is then quickly rinsed twice with water and transferred to a Pyrex dish containing 50 mL of TTC (50 mg of 2,3,5-triphenyltetrazolium chloride (TTC) in 50 mL of 0.5 M NaOH). The dish is boiled until the color appears. To stop the coloration and neutralize the NaOH, the gel is washed with water and stored in 10% acetic acid until imaging.

### 2.5. Western blotting

Yeasts were centrifuged for 5 min at 3500g. Supernatant was discarded and cells were then resuspended in TBP buffer supplemented with a protease cocktail inhibitor (Roche Diagnostics, Penzberg, Germany). Cell lysis was induced by vortexing the cells with beads 1 h at 4 °C. Cells were centrifuged for 5 min at 3500g. The protein concentration of supernatant was estimated with the micro BCA Protein Assay Kit (Thermo Scientific). 20 μg of total protein lysates were dissolved in NuPAGE LDS sample buffer (Invitrogen) pH 8.4 supplemented with 4% β-mercaptoethanol (Fluka). Samples were heated 10 min at 95 °C and then separated on 4%–12% Bis-Tris gels (Invitrogen) and transferred to nitrocellulose membrane Hybond ECL (GE Healthcare, Little Chalfont, UK). The membranes were incubated in blocking buffer (5% milk powder in TBS-T [1X TBS with 0.05% Tween20]) for 1 h at room temperature, then incubated overnight with the anti-HA (Santa Cruz; clone Y-11 used at a dilution of 1:200) or anti-c-myc(Santa Cruz, clone 9E10 used at a dilution of 1:200) or anti-CPY (Abcam; clone 10A5B5 used at a dilution of 1:2000) in blocking buffer, and washed three times for 5 min in TBS-T. The membranes were then incubated with the peroxidase-conjugated secondary goat anti-rabbit (Dako; used at a dilution of 1:10,000) in blocking buffer for 1 h at room temperature and later washed three times for 5 min in TBS-T. Signal was detected with chemiluminescence reagent (ECL 2 Western Blotting Substrate, Thermo Scientific) on imaging film (GE Healthcare, Little Chalfont, UK).

### 2.6. Whole cell Mn measurement by ICP-MS

Yeasts were grown in YPD medium and a volume equivalent to 15

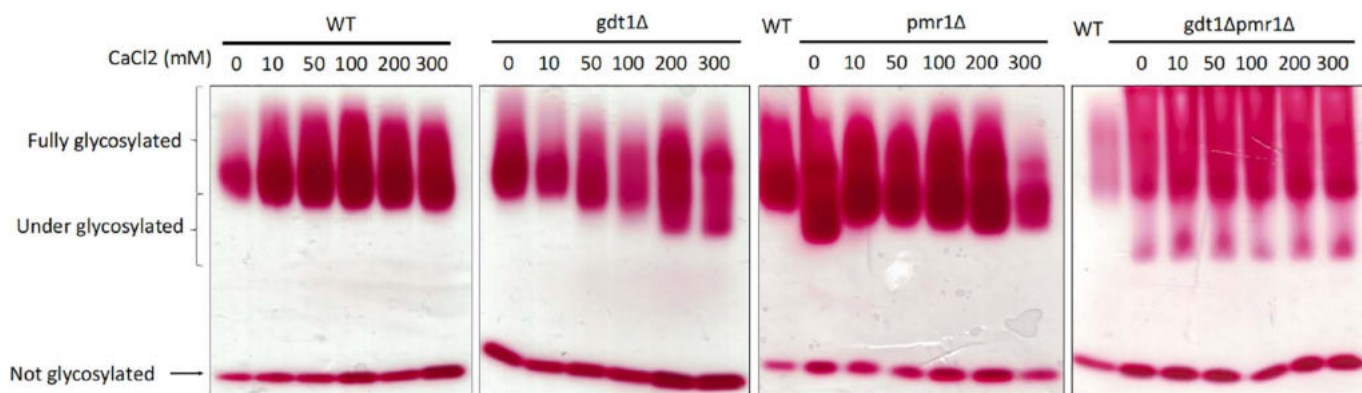


**Fig. 1.** The suppression of the glycosylation defect in *pmr1Δ* strains supplemented with  $\text{Ca}^{2+}$  is dependent of the activity of Gdt1p. Wild-type (WT), *gdt1Δ*, *pmr1Δ* and *gdt1Δ/pmr1Δ* yeasts mutants were grown to an OD600 of 0.8 in a YPD medium. Afterwards, yeasts were transferred in YPR medium with an increase of the indicated  $\text{CaCl}_2$  concentrations to induce invertase secretion. N-glycosylated invertase secreted was analyzed in a native gel as indicated by Ballou et al. [15].

OD600nm units was centrifuged for 3 min at 3500g. The supernatant was discarded and the pellet was suspended in YPD media containing or not 50  $\mu\text{M}$   $\text{MnCl}_2$ . After 20 h, a volume equivalent to 25 OD600nm units is centrifuged for 3 min at 3500g. Yeasts are washed twice with EDTA 1  $\mu\text{M}$  and 3 times with water. Yeasts were suspended in 500  $\mu\text{L}$  of  $\text{HNO}_3$  30% and heat at 65  $^\circ\text{C}$  in a light shaking during 20 h. 500  $\mu\text{L}$  of water were added to the mixture. 300  $\mu\text{L}$  were analyzed by ICP-MS (Inductively Coupled Plasma - Mass Spectrometer). Mn analyses were done in the Toxicology Laboratory of the Lille University Hospital. Samples were diluted 50 times with 1.5% (v/v) nitric acid (ultrapure quality 69.5%, Carlo Erba Reagents, Val de Reuil, France) solution in ultrapure water (Purelab Option-Q, Veolia Water, Antony, France) containing 0.1% triton<sup>®</sup>X-100 (Euromedex, Souffelweyersheim, France), 0.2% butan-1-ol (VWR Chemicals, Fontenay-sous-Bois, France), and 0.5  $\mu\text{g/L}$  rhodium (Merk, Darmstadt, Germany). Assays were performed on an ICP-MS THERMO ICAPTM Q (Thermo Scientific, Courtaboeuf Cedex, France). The limit of quantification was 0.2  $\mu\text{g/L}$ .

## 2.7. NMR analyses

All NMR experiments were acquired on Avance II Bruker spectrometer equipped with BBO 5 mm probe resonating at 400 MHz for  $^1\text{H}$ , 100.6 MHz for  $^{13}\text{C}$ . Mannans were dissolved in 500  $\mu\text{L}$   $^2\text{H}_2\text{O}$  (99.96%  $^2\text{H}$ , Eurisotop<sup>®</sup>), and then transferred into 5 mm Shigemi tubes (Allision Park, USA). NMR experiments were performed at 293 K. The  $^1\text{H}$  chemical shifts were expressed in ppm. Related to the methyl signal of acetone ( $\delta$   $^1\text{H}$  2.225 and  $\delta$   $^{13}\text{C}$  31.55 ppm) as internal standards. The COSY90- $^1\text{H}/^{13}\text{C}$ -HSQC experiments were performed by using Bruker standard sequences and optimized for each experiment.

## 2.8. Monosaccharide analyses

10  $\mu\text{g}$  of inositol (taken as internal standard) and 10  $\mu\text{g}$  of target mannan were mixed. The monosaccharide composition was established by GC and GC/MS as alditol-acetate derivatives. Briefly, samples were hydrolyzed in 4 M trifluoroacetic acid (TFA) for 4 h at 100  $^\circ\text{C}$  and then reduced with sodium borohydride (10 mg/mL) in 0.05 M NaOH for 4 h. Reduction was stopped by dropwise addition of acetic acid until pH 6 was reached and borate salts were co-distilled by repetitive evaporation in dry methanol. Peracetylation was performed in acetic anhydride at 100  $^\circ\text{C}$  for 2 h. The derivatized monosaccharides were dissolved in 1 mL of chloroform, and 1  $\mu\text{L}$  of sample was injected into GC-MS (TRACE GC Ultra, Thermo Fisher Scientific). The capillary column is SOLGEL-1MS (Part No. 054795, 30 m  $\times$  0.25 mm  $\times$  0.25  $\mu\text{m}$ ). The initial oven temperature was held at 120  $^\circ\text{C}$ , increased to 230  $^\circ\text{C}$  at 3  $^\circ\text{C}/\text{min}$ , and then, 270  $^\circ\text{C}$  for 10 min. The derivatized monosaccharides were separated into individual peaks, and identified by MS. However, the signal

of GlcNAc was very low due to low percentage of GlcNAc in mannan. Therefore, selected ion monitor (SIM) was applied to increase sensitivity and quantify Man and GlcNAc. Ions at  $m/z$  168, 187, and 144 were used as indicative fragment ions for inositol, Man, and GlcNAc, respectively. The size of isolation window was set 0.2 Da, and the scan time of selected ion was 0.2 s. The response factor of inositol was set to 1. In this system, response factors of Man and GlcNAc were established to 0.48 and 0.28, respectively. The amount ( $\mu\text{g}$ ) of mannose in different Mannan samples was calculated by the formula [(Peak area of selected ion at  $m/z$  187 for Man/0.48)/Peak area of selected ion at  $m/z$  168 for inositol  $\times$  10]. Similar calculation was applied to GlcNAc, which is [(Peak area of selected ion at  $m/z$  144 for GlcNAc/0.28)/Peak area of selected ion at  $m/z$  168 for inositol  $\times$  10]. We assumed that most of mannan is located on N-glycans. Therefore, the number of Man per N-glycan was established as [molar of Man/(molar of GlcNAc  $\times$  2)].

## 3. Results

### 3.1. The suppression of the glycosylation defect in *pmr1Δ* strains supplemented with $\text{Ca}^{2+}$ is dependent on the activity of Gdt1p

We have previously reported that the increased mobility of secreted invertase activity by zymography (in native polyacrylamide gel) was a good reporter of Golgi N-glycosylation deficiency in yeast [4]. Using this technique, we have demonstrated that the Golgi N-glycosylation defect in *gdt1Δ* strains observed on invertase cultured in presence of high  $\text{Ca}^{2+}$  concentration could efficiently be suppressed by the addition of  $\text{Mn}^{2+}$ . This was also observed for *pmr1Δ* and *gdt1Δ/pmr1Δ* double knock-out strains [4]. Although we demonstrated that high environmental  $\text{Ca}^{2+}$  concentration in *gdt1Δ* led to strong glycosylation defects, we established here that the addition of  $\text{Ca}^{2+}$  rescues the glycosylation defect in *pmr1Δ*. Indeed, 10 mM  $\text{Ca}^{2+}$  treatment is sufficient to greatly reduce the invertase mobility to a normal value (Fig. 1). Since Gdt1p and Pmr1p are two Golgi proteins involved in the regulation of the Golgi  $\text{Ca}^{2+}/\text{Mn}^{2+}$  homeostasis, glycosylation defect in *gdt1Δ/pmr1Δ* double knock-out strains was analyzed in the absence and the presence of increasing  $\text{Ca}^{2+}$  concentrations (from 10 mM  $\text{Ca}^{2+}$  to 300 mM) (Fig. 1). Although the invertase mobility is strongly affected in the *gdt1Δ/pmr1Δ* double knock-out strains, the  $\text{Ca}^{2+}$  treatment does not restore it to a normal value (Fig. 1). By contrast and as previously observed, the addition of 50  $\mu\text{M}$   $\text{Mn}^{2+}$  is sufficient to fully restore the Golgi N-glycosylation in the different yeast strains (Supplementary Fig. 1).

These results points to the crucial requirement of Gdt1p activity in the restoration of the glycosylation in *pmr1Δ* strains supplemented with  $\text{Ca}^{2+}$ . Altogether these results strongly suggest a functional link between Gdt1p and Pmr1p in maintaining Golgi glycosylation

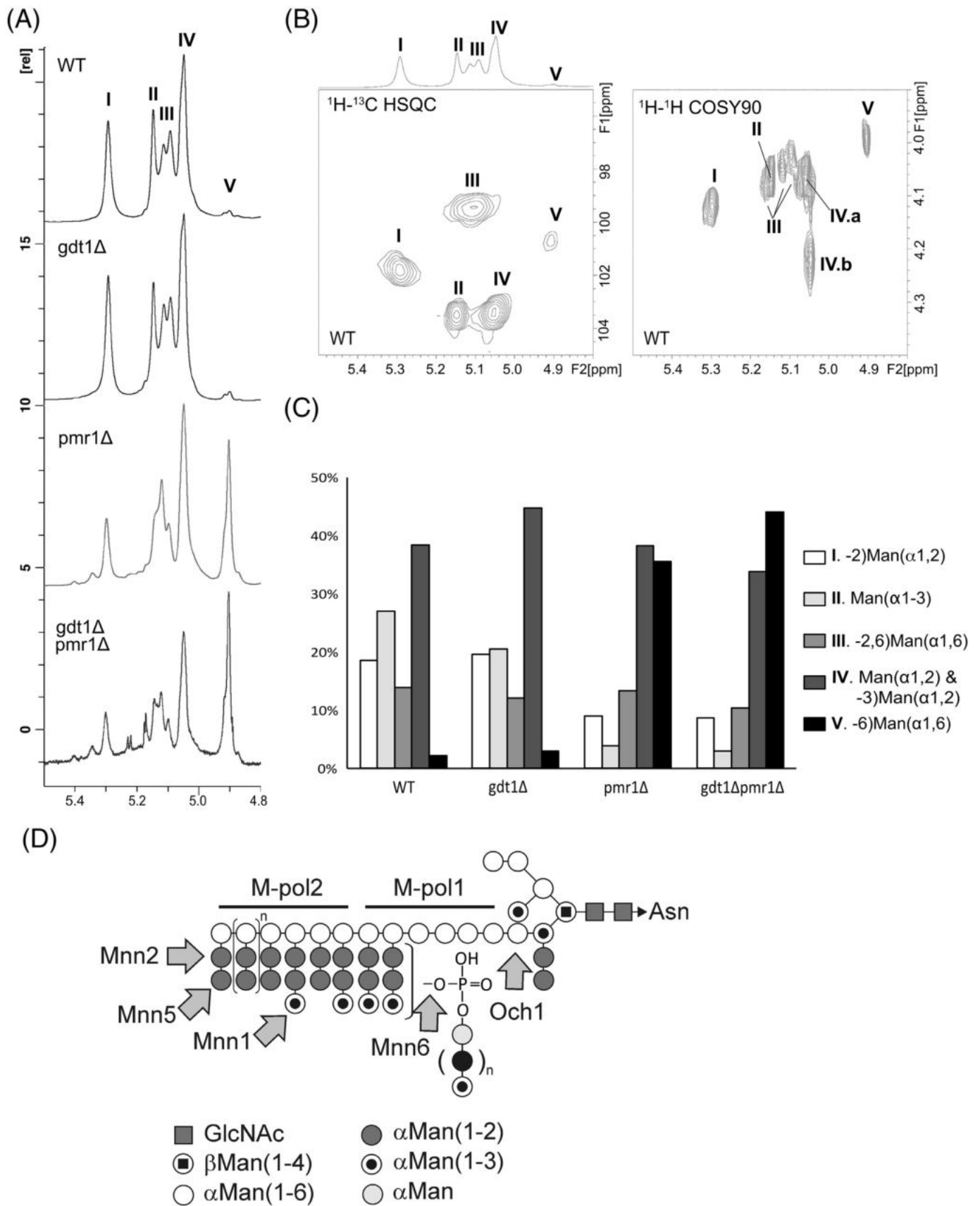


**Fig. 2.** Structural analysis of the mannans from *S. cerevisiae* strains depleted or not in Gdt1p and Pmr1p. (A) Comparison of the anomeric regions of  $^1\text{H}$  NMR spectra from WT, *gdt1Δ*, *pmr1Δ* and *gdt1Δ/pmr1Δ* strains; (B) details of the  $^1\text{H}$ - $^{13}\text{C}$  HSQC and  $^1\text{H}$ - $^1\text{H}$  COSY spectra from WT mannan showing the anomeric positions of mannose residues I-V; (C) relative quantifications of mannose residues based on NMR signals intensities. (D) Protein mannosylation pathway in *S. cerevisiae*. The structures of the N-linked glycans of *S. cerevisiae* are schematized. The arrows indicate the function of the different mannosyltransferases.

homeostasis.

### 3.2. General structural analysis of the mannans from wild type and different mutants under different supplement of $\text{Ca}^{2+}/\text{Mn}^{2+}$

In order to further delineate the nature of the observed overall Golgi *N*-glycosylation defects, total mannans were isolated from yeast strains cultured under different  $\text{Ca}^{2+}/\text{Mn}^{2+}$  conditions, followed by detailed structural analyses. So called mannans from most yeasts share similar overall architectures. They are made of  $\text{Man}_8\text{GlcNAc}_2$  *N*-linked glycans extended by a  $\alpha$ -linked polymannoside containing around 200 mannose residues. In *S. cerevisiae*, the polymannoside is composed of a long stretch of  $(\alpha-1,6)$ -linked  $\text{D}$ -mannopyranose units substituted in C2 positions by short side chains of  $(\alpha-1,2)$ -linked mannose units that may be further capped by terminal  $\text{Man}(\alpha-1,3)$  residues [8]. So called acid-labile mannan domain is further attached to the  $(\alpha-1,2)$ -oligomannosides through phospho-di-ester bonds [9]. In a first step, we established the structural features of the mannan isolated from WT strain by 1D  $^1\text{H}$  NMR experiment (Fig. 2A). Due to its polymeric nature, it is not possible to assign the signals corresponding to all individual monosaccharide residues of mannans. However, five broad signals annotated as I, II, III, IV, V could be detected in the 5.5–4.8 ppm anomeric region, which natures were established by observing their spin systems by  $^1\text{H}$ - $^1\text{H}$  COSY, TOCSY and  $^1\text{H}$ - $^{13}\text{C}$  HSQC experiments, based on literature ([10] (Fig. 2B)). They were assigned to five major epitopes (I), internal  $-2)\text{Man}(\alpha-1,2)$  residues; (II), terminal  $\text{Man}(\alpha-1,3)$  residues; (III),  $-2,6)\text{Man}(\alpha-1,6)$  branched residues; (IV), terminal  $\text{Man}(\alpha-1,2)$  and  $-3)\text{Man}(\alpha-1,2)$  residues; (V), unbranched  $-6)\text{Man}(\alpha-1,6)$  residues. Furthermore, terminal  $\text{Man}(\alpha-1,2)$  (IV.a, H2 at 4.06 ppm) and  $-3)\text{Man}(\alpha-1,2)$  residues (IV.b, H2 at 4.22 ppm) could be differentiated by COSY90 spectrum as shown in Fig. 2B. Relative quantification of NMR signals I to V provides reliable snapshot of the overall mannan structural features. As shown in Fig. 2C, mannan isolated from WT strain is characterized by a high proportion of  $(\alpha-1,2)$  substitution on the  $(\alpha-1,6)$ -mannoside stretch [ $2,6)\text{Man}/6)\text{Man} = 6,4$ ], leaving few unsubstituted  $-6)\text{Man}(\alpha-1,6)$  residues.

In a second step, we compared the structures of mannans isolated from all four strains grown in normal conditions by homo- and heteronuclear NMR. 1D  $^1\text{H}$  NMR spectra, of mannans isolated from wild type and *gdt1Δ* established that these two strains exhibit very similar mannosylation patterns (Fig. 2A). In contrast, distinctive features were observed in the structures of mannans isolated from *pmr1Δ* and *gdt1Δ/pm1Δ* strains compared to WT, as shown by 1D  $^1\text{H}$  NMR spectra (Fig. 2A) and relative quantification of  $^1\text{H}$ - $^{13}\text{C}$  HSQC NMR signals (Fig. 2C). The two most salient features of mannans from *pmr1Δ* and *gdt1Δ/pm1Δ* strains were (i) a sharp decrease in the proportion of internal  $(\alpha-1,2)$  oligomannoside side chains and of  $(\alpha-1,3)$  capping mannose residues, which correlated with (ii) a large increase in the proportion of unbranched  $(\alpha-1,6)$  polymannoside backbone. Indeed, the proportion of unbranched  $6)\text{Man}(\alpha-1,6)$  residues in *pmr1Δ* and *gdt1Δ/pm1Δ* strains increased by 17 and 28 times compared to WT mannan. Additionally, COSY90 spectra showed an increased proportion of terminal  $\text{Man}(\alpha-1,2)$  residues on mannans from *pmr1Δ* and *gdt1Δ/pm1Δ* strains, which is correlated with a decreased proportion of terminal  $\text{Man}(\alpha-1,3)$  (data not shown). Altogether, these experiments show that a lack of *pmr1p* and both *gdt1p/pm1p* lead to a drastic reduction of the branching pattern of  $(\alpha-1,6)$  polymannoside domain of the mannan.

In a third step, we screened by 1D  $^1\text{H}$  NMR experiments the structural variability of mannans isolated from all four strains following supplementation with 0.5 M  $\text{Ca}^{2+}$ , 0.05 mM  $\text{Mn}^{2+}$  and 0.5 M  $\text{Ca}^{2+}/0.05$  mM  $\text{Mn}^{2+}$  with a special focus on their branching patterns (Supplementary Fig. 1) expressed as a % of unbranched  $-6)\text{Man}(\alpha-1,6)$  residues compared with total residues by quantifying signal V (Fig. 3A). In accordance with the above results, WT and *gdt1Δ* grown in normal condition contained less than 2% of  $-6)\text{Man}(\alpha-1,6)$  residues,

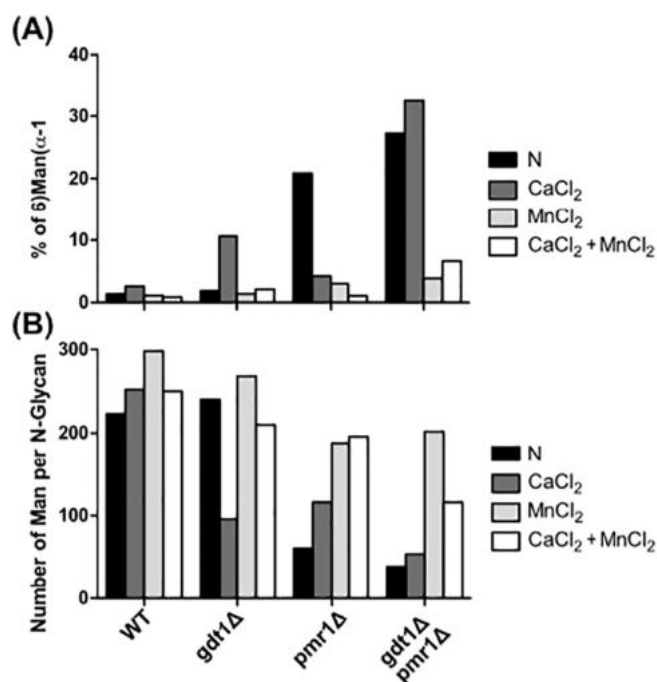
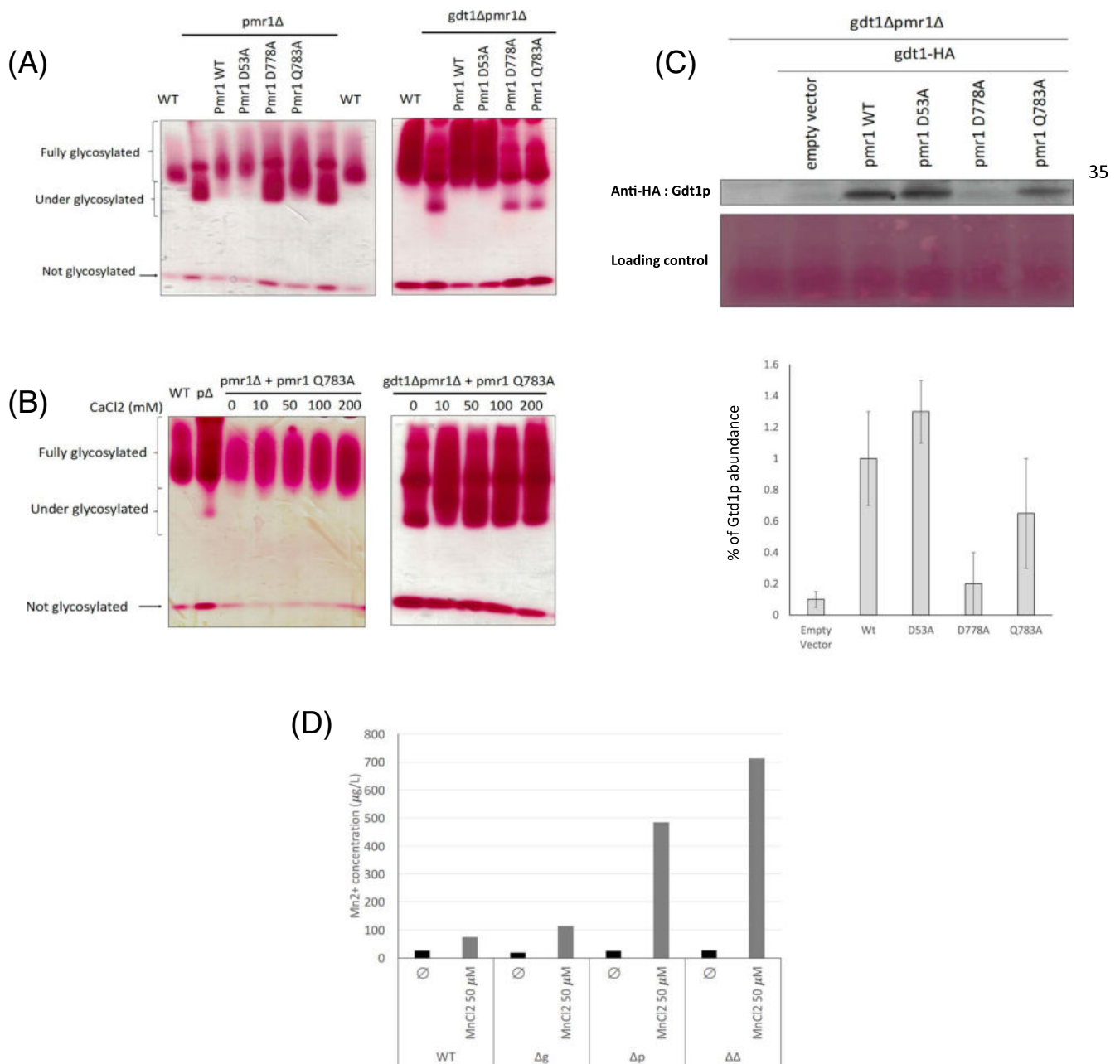


Fig. 3. Comparison of mannans isolated from yeasts grown in various conditions: N, non-supplemented;  $\text{CaCl}_2$ , supplemented with 0.5 M  $\text{CaCl}_2$ ;  $\text{MnCl}_2$ , supplemented with 0.05 mM  $\text{MnCl}_2$ ;  $\text{CaCl}_2 + \text{MnCl}_2$ , supplemented with  $\text{CaCl}_2$  0.5 N and  $\text{MnCl}_2$  0.05 mM. (A) The branching pattern of the 1,6-linked mannan backbone is expressed as the proportion of  $6)\text{Man}(\alpha-1,6)$  residues in mannans and calculated from the relative integration of signal V from  $^1\text{H}$  NMR spectra (see Supplementary Fig. 1). Its increases is indicative a defect in the synthesis of  $2)\text{Man}(\alpha-1,2)$  side chains. (B) The overall size of mannans was established as a number of mannose residues per *N*-glycans. The reduction in the size of mannans correlates with the defect in the synthesis of  $2)\text{Man}(\alpha-1,2)$  side chains.

whereas mannans from *pmr1Δ* and *gdt1Δ/pm1Δ* contained 21 and 27% of  $-6)\text{Man}(\alpha-1,6)$  residues, respectively (Fig. 3A). This branching defect was fully restored in *pmr1Δ* by the addition of any divalent cation,  $\text{Ca}^{2+}$  or  $\text{Mn}^{2+}$ . Contrarily, the glycosylation defect of *gdt1Δ/pm1Δ* strain which is almost entirely restored in presence of  $\text{Mn}^{2+}$  and both  $\text{Ca}^{2+} + \text{Mn}^{2+}$  (4% and 7%), is not restored in the sole presence of  $\text{Ca}^{2+}$ . Then, *gdt1Δ* cultured in presence of 0.5 M  $\text{Ca}^{2+}$  showed an increased proportion of unbranched  $-6)\text{Man}(\alpha-1,6)$  backbone, as well as a decreased number of  $(\alpha-1,3)$  mannose capping (data not shown). However, these defects were also completely restored by the addition of  $\text{Mn}^{2+}$ .

NMR analysis established that a lack of *Pmr1p* leads to strong defects in the mannan synthesis through the decrease of terminal  $\text{Man}(\alpha-1,3)$  capping, the decrease of side chains  $(\alpha-1,2)$  mannosylation and the increase of the proportion of unbranched  $6)\text{Man}(\alpha-1,6)$ . These characteristics should result in the change of mannan size. In order to determine the average size of mannan domain of *N*-glycans, we quantified Man and GlcNAc residues in all samples by GC/MS analysis, and deduced the average number of mannose per *N*-glycan based on the presence of the chitobiose core. As shown in Fig. 3B, *N*-glycans isolated from WT and *gdt1Δ* strains grown in normal conditions contained an average of 220–250 Man residues. However, we observed that the size of mannan domain of *gdt1Δ* strains under  $\text{Ca}^{2+}$ , as well as *pmr1Δ* and *gdt1Δ/pm1Δ* strains in normal conditions and under  $\text{Ca}^{2+}$  are drastically reduced (Fig. 3A) down to about 40 Man residues. Under  $\text{Mn}^{2+}$  supplementation, the size of mannans from *pmr1Δ* and *gdt1Δ/pm1Δ* was restored to average sizes. Altogether, structural analysis by NMR and GC/MS showed that the glycosylation defects are due to a reduced synthesis of  $-2)\text{Man}(\alpha-1,2)$  side chains that results in the synthesis of polymannosylated *N*-glycans of smaller size compared to that of WT strains.

This suggests that a lack of *Pmr1p* and/or *Gdt1p* would affect late



**Fig. 4.** The function and abundance of Gtd1p in glycosylation is dependent on the Pmr1p function (A) The Glycosylation defect in *pmr1p* mutants depends on its function. Pmr1 $\Delta$  and *gdt1Δ/pmr1Δ* strains were transformed with pRS41N-*pmr1p* mutants (*pmr1p*-WT, *pmr1p*-D53A, *pmr1p*-D778A and *pmr1p*-Q783A). Yeasts were grown in YPR media and *N*-glycosylated invertase profile was performed (B)  $\text{Ca}^{2+}$  uptake by *pmr1p* influences the  $\text{Mn}^{2+}$  uptake by Gtd1p. Yeasts were grown in YPR media supplemented with an increase of the indicated  $\text{CaCl}_2$  concentrations in the medium and invertase profile was analyzed. (C) Abundance of Gtd1p depends on the Pmr1p function. *gdt1Δpmr1Δ* strains were transformed with pRS41H-Gtd1p-HA and with pRS41N-*Pmr1p* mutants (*pmr1p*-WT, *pmr1p*-D53A, *pmr1p*-D778A and *pmr1p*-Q783A). Yeasts were grown in YPD medium and *GDT1* expression was performed by western Blot using an anti-HA. Quantification of Gtd1p protein after normalization on ponceau red (N = 3). (D) Cytosolic manganese detoxification needs Pmr1p. Wild-type (WT), *gdt1Δ*, *pmr1Δ* and *gdt1Δ/pmr1Δ* yeasts mutants were grown to an OD600 of 0.8 in a YPD medium and transferred to a media containing no  $\text{Mn}^{2+}$  or 50  $\mu\text{M}$   $\text{MnCl}_2$ . Total  $\text{Mn}^{2+}$  concentrations were analyzed by ICP-MS. Quantification of the cellular  $\text{Mn}^{2+}$  concentration (N = 2).

Golgi glycosyltransferases such as MMN2/MMN5/MNN. 1 Altogether, these results demonstrate (i) the crucial requirement of Gtd1p in maintaining Golgi glycosylation when cells are cultured in presence of  $\text{Ca}^{2+}$  and (ii) that the suppression of the glycosylation defect by the  $\text{Ca}^{2+}$  in *pmr1Δ* strains is strictly dependent on the activity of Gtd1p.

### 3.3. The abundance and function of Gtd1p in glycosylation is dependent on the Pmr1p function

To further investigate the contribution of  $\text{Ca}^{2+}$  versus  $\text{Mn}^{2+}$  transport activity of Pmr1p to the observed *N*-glycosylation defect, we

first transfected *PMR1*-deficient cells with three point mutants of Pmr1p that were defective for transport of either  $\text{Ca}^{2+}$  ions (Pmr1pD53A),  $\text{Mn}^{2+}$  ions (Pmr1pQ783A) or both (Pmr1pD778A) [11,12]. Although both Pmr1pD53A and Q783A can restore the observed initial glycosylation defect, differences can be observed (Fig. 4A). The restoration is total with Pmr1pWT and the Pmr1pD53A and only partial with Pmr1pQ783A (Fig. 4A, left panel). To assess the potential role of Gtd1p in this glycosylation rescue, *gdt1Δ/pmr1Δ* strains were transfected with the same Pmr1p mutants. While the expression of the D53A completely restored the glycosylation, the Q783A clearly did not (Fig. 4A, right panel). To confirm these results, the invertase mobility in the *pmr1Δ*



and *gdt1Δ/pmr1Δ* double knock-out strains transfected with the Pmr1pQ783A in the presence of increasing  $\text{Ca}^{2+}$  concentrations was evaluated. In the *pmr1Δ* yeast strains transfected with the *pmr1Q783A*, the invertase mobility is strongly reduced both in absence of  $\text{Ca}^{2+}$  and under increasing  $\text{Ca}^{2+}$  concentrations (Fig. 4B, left panel). We demonstrated that this effect was due to the activity of Gdt1p, as the  $\text{Ca}^{2+}$  treatment in the *gdt1Δ/pmr1Δ* double knock-out strains transfected with the *pmr1Q783A* does not suppress the observed glycosylation defect (Fig. 4B, right panel). These results have also been confirmed by glycosylation analysis on carboxypeptidase Y (CPY) and fully support those from the invertase assay experiments (Supplementary Fig. 2). We then wondered whether the suppression of the glycosylation defect in *pmr1Δ* strains supplemented with  $\text{Ca}^{2+}$  could result from Gdt1p expression changes. The cellular abundance of Gdt1p was then evaluated by Western blotting using specific antibodies directed against Gdt1p in *pmr1Δ* strains, transfected or not with the different Pmr1p mutants defective for transport of either  $\text{Ca}^{2+}$  ions (Pmr1pD53A),  $\text{Mn}^{2+}$  ions (Pmr1pQ783A) or both (Pmr1pD778A). This experiment showed that the abundance of Gdt1p was directly linked to the transport function of Pmr1p. In *pmr1Δ*, the abundance of Gdt1p was greatly reduced ( $\sim 80\%$  compared to WT) (Fig. 4C). Remarkably, the expression of Pmr1WT in *pmr1Δ* strains restored the Gdt1p abundance. Interestingly, while the expression of the Pmr1pD53A also completely rescued the Gdt1p level, the Pmr1pD778 mutant had no effects on Gdt1p abundance (Fig. 4C and Supplementary Fig. 3). A slight rescue can be seen with the Pmr1pQ783A mutant. The expression of Pmr1p mutant proteins was confirmed by using myc-tagged versions. As seen in Supplementary Fig. 3, all Pmr1p mutants are expressed. Altogether, these results prove that the abundance of Gdt1p is dependent of the transport function of Pmr1p.

To go further, we then evaluated the total cellular  $\text{Mn}^{2+}$  concentration in the different yeast strains under different conditions by ICP-MS. While under physiological conditions the total cellular  $\text{Mn}^{2+}$  concentration is similar in the different mutants, a huge increase is observed following  $\text{Mn}^{2+}$  supplementation in all investigated mutants compared to WT (Fig. 4D). After  $\text{Mn}^{2+}$  supplementation, a 10-fold increase in  $\text{Mn}^{2+}$  concentration is observed in the *gdt1Δ/pmr1Δ* double knock-out mutant, a 5 fold increase in the *pmr1Δ* mutant and a 2 fold increase in the *gdt1Δ* mutant. These results support the fact that both Pmr1p and Gdt1p are involved in total cellular  $\text{Mn}^{2+}$  homeostasis maintenance.

Our results demonstrate that (i) the Golgi glycosylation defect observed in *pmr1p* deficient cells results from a lack of Golgi intraluminal  $\text{Mn}^{2+}$ , (ii) that the rescue of the glycosylation defect in *pmr1Δ* strains by the intraluminal Golgi  $\text{Ca}^{2+}$  requires the activity of Gdt1p.

### 3.4. Acidic residues of the conserved motifs of Gdt1p are involved in Golgi glycosylation

As previously published [1,13,14], members of the UPF0016 family contain two highly conserved consensus motifs E-φ-G-D-[KR]-[TS], predicted to be involved in the transport function of UPF0016 members. Recently these motifs have been shown to be part of the regulatory  $\text{Ca}^{2+}$  binding domains. In order to evaluate the importance of these two motifs in the maintenance of Golgi glycosylation homeostasis, mutated versions of Gdt1p have been generated (E53G, D56G, E204G, L205W and D207G) and used to complement the observed glycosylation defect in *gdt1Δ* strains cultured in presence of high  $\text{Ca}^{2+}$  concentrations. The expression level of Gdt1 mutant proteins was first assessed by western blot using the HA-tagged mutated version of Gdt1p (Supplementary Fig. 4). Although the D56G, D207G and L205W were found expressed, the E53G and E204G were surprisingly not. Interestingly none of the mutated Gdt1p, except L205W mutation, complements the observed glycosylation defect on invertase and CPY (data not shown) then demonstrating that the aspartic amino acids are essential for the function of Gdt1p in Golgi glycosylation (Fig. 5 and

Supplementary Fig. 4). We then wondered whether the activity of Gdt1p was required in the case where Pmr1p would only transport  $\text{Mn}^{2+}$ . For that, the same mutated versions were expressed in *gdt1Δ/pmr1Δ* strains transformed with Pmr1pD53A and the invertase mobility was assessed. As shown in Fig. 5, the glycosylation was completely restored for all the mutated versions of Gdt1p, demonstrating that, Gdt1p is dispensable when Pmr1p exclusively transports  $\text{Mn}^{2+}$ . Similar experiment was then performed in *gdt1Δ/pmr1Δ* strains transformed with Pmr1pQ783A. Although the expression of Gdt1p wt partially rescues the invertase glycosylation defect, none of the mutated version suppresses the glycosylation defect (Fig. 5). This result clearly demonstrates that the requirement of Gdt1p for Golgi glycosylation depends on the nature of the ion transported by Pmr1p.

## 4. Discussion

The regulation of  $\text{Ca}^{2+}$  and  $\text{Mn}^{2+}$  concentrations in the Golgi apparatus is crucial for many cellular processes particularly the secretion of proteins and the maintenance of Golgi glycosylation. One of the main supplier/regulator of  $\text{Ca}^{2+}/\text{Mn}^{2+}$  Golgi homeostasis is the Golgi localized P-type ATPase Pmr1p. Our previous work raised the possibility that Gdt1p may also play a crucial role in Golgi ion homeostasis and Golgi glycosylation. Although the precise cellular function of Gdt1p in the Golgi remains unsolved, results cast doubt about its precise function in the transport of substrates. In this work we show that Gdt1p is a functionally important Golgi protein playing a unique role in Golgi glycosylation. Compared to mammalian cells, yeasts further matureate the N-linked glycans with the addition of outer chains that may contain up to  $\sim 300$  mannose residues [8]. These hypermannosylated structures consist in backbones of  $\alpha$ -1,6-linked mannose residues substituted with  $\alpha$ -1,2-linked mannose residues themselves branched with terminal  $\alpha$ -1,3-linked mannose residues (Fig. 2D). Many Golgi mannosyltransferase complexes are involved in generating these specific structures. In this paper we assessed and compared by using NMR the structural details of polymannan chains of the different yeast strains (*gdt1Δ*, *pmr1Δ* and *gdt1Δ/pmr1Δ* strains) under different conditions. The NMR experiments showed strong alteration of the Golgi N-linked glycosylation in the different yeast strains under various conditions. While the backbone of  $\alpha$ -1,6-linked mannose residues is not altered, strong defects in  $\alpha$ -1,3- and  $\alpha$ -1,2- branching are mainly observed in *gdt1Δ* strains cultured in presence of high  $\text{Ca}^{2+}$  concentration, *pmr1Δ* and *gdt1Δ/pmr1Δ* strains. We also confirmed that the addition of  $\text{Mn}^{2+}$  was sufficient to completely restore the observed branching defects. Interestingly, our data clearly demonstrated that the suppression of the Golgi glycosylation defects by the  $\text{Ca}^{2+}$  in *pmr1Δ* yeast strains was dependent on the activity of Gdt1p. Based on the structural analysis of the polymannan chains, we deduced that the defects mainly affected medial and late Golgi glycosylation as only the  $\alpha$ -1,2 substitution- and the  $\alpha$ -1,3 termination are affected. This points toward an alteration of Mnn2p/Mnn5p/Mnn6p and/or Mnn1p activities (Fig. 2D). The  $\alpha$ -1,6 initiation/elongation seems not to be altered in our analysis. Taken together, our structural analysis data showed Gdt1p as well as Pmr1p to be critical participants in medial and late Golgi glycosylation functions.

The identity of Gdt1p as a potential Golgi transporter controlling both Golgi  $\text{Ca}^{2+}/\text{Mn}^{2+}$  homeostasis arose from our studies and others [3,4,14]. In this work we further evaluated the potential role of Gdt1p in importing  $\text{Mn}^{2+}$  from the cytosol to the Golgi lumen. As first pointed by us [1] and others [6,7,13] members of the UPF0016 family contain two highly conserved consensus motifs E-φ-G-D-[KR]-[TS], predicted to be involved in the transport function of UPF0016 members. Our results show that mutations of the aspartic amino acids of these two conserved motifs (D56A, and D207A) completely abolish the rescue of the glycosylation. Interestingly we did observe that the glutamic amino acids mutated versions of Gdt1p were not expressed then raising the possibility that these two mutated forms are highly sensitive to the availability of  $\text{Mn}^{2+}$  in the Golgi lumen or in the cytosol. We did also

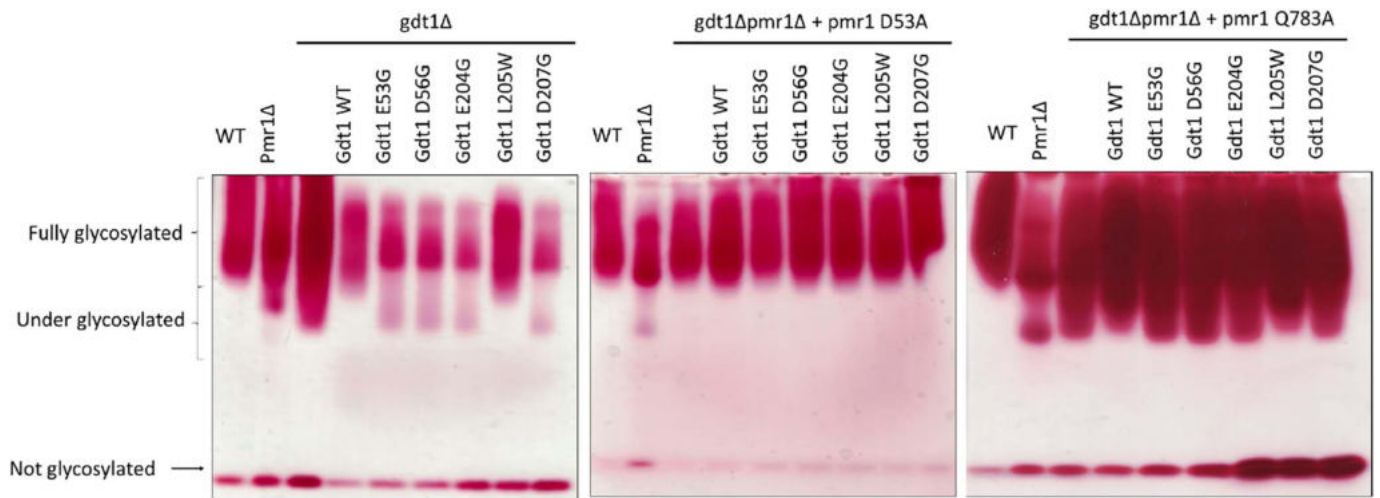


Fig. 5. Acidic residues of the conserved motifs of Gdt1p are involved in Golgi glycosylation. *gdt1Δ/pmr1Δ* strains were transformed with pRS41N-*pmr1pD53A* (middle panel) and pRS41N-*pmr1p-Q783A* (right panel) and with pRS41H-*gdt1p* mutants (Gdt1p-E53G, Gdt1p-D56G, Gdt1p-E204G, Gdt1p-L205 W and Gdt1p-D207G). Yeasts were grown in YPR medium. *gdt1Δ* strains were transformed with pRS41H-*gdt1p* mutants (Gdt1p-E53G, Gdt1p-D56G, Gdt1p-E204G, Gdt1p-L205W and Gdt1p-D207G) (right panel) and yeasts were grown in a YPR media supplemented with 200 mM CaCl<sub>2</sub>.

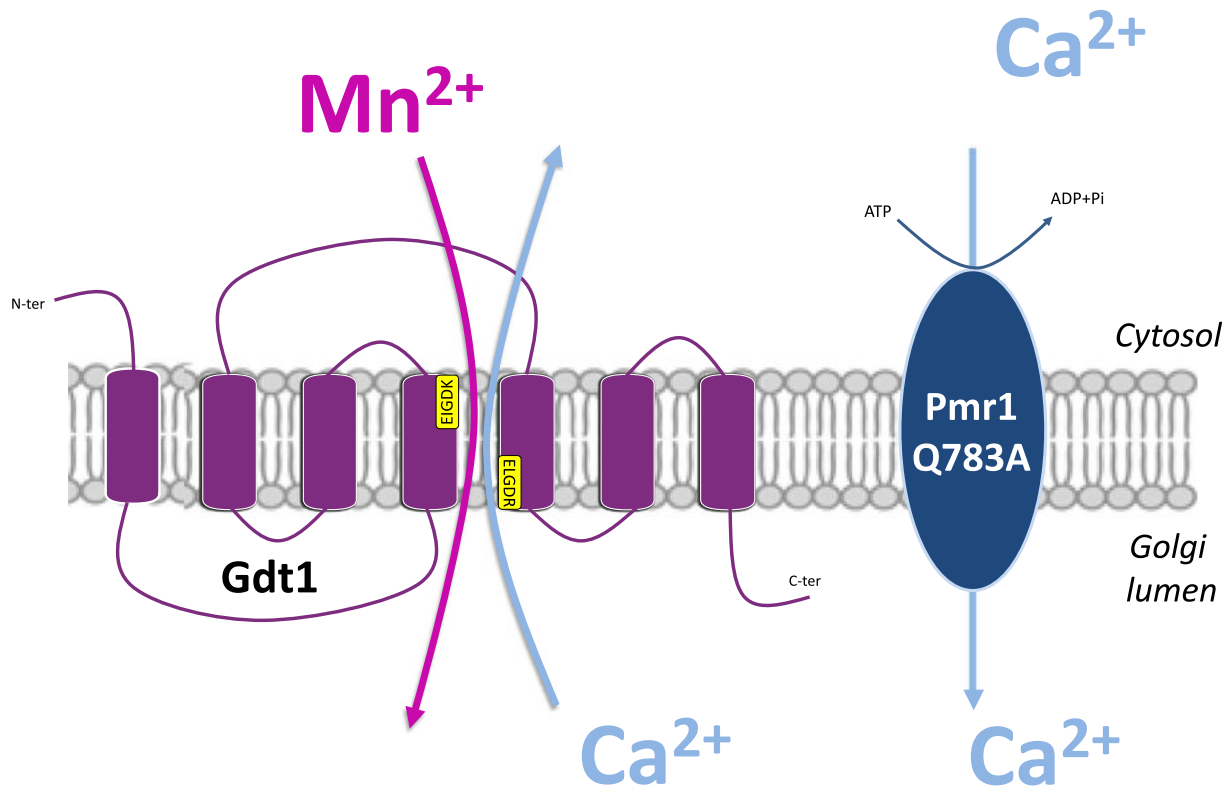


Fig. 6. Proposed model for the function of Gdt1p in regulating Golgi Mn<sup>2+</sup> together with the Ca<sup>2+</sup>/Mn<sup>2+</sup> ATPase Pmr1p. In this model, Gdt1p would be a Mn<sup>2+</sup>/Ca<sup>2+</sup> antiporter whose functions depend on Pmr1p. When Pmr1p would exclusively import Ca<sup>2+</sup> to the Golgi lumen, Gdt1p is crucial to import Mn<sup>2+</sup> inside the Golgi lumen by exchanging Ca<sup>2+</sup>.

demonstrate that an active form of Gdt1p was exclusively required in case where Pmr1p mainly transports Ca<sup>2+</sup>. When Pmr1p mainly imports Mn<sup>2+</sup> inside the Golgi lumen, our results show that Gdt1p is completely dispensable for the Golgi glycosylation. We propose that the aspartic amino acids are part of the cation binding sites of Gdt1p (one for Ca<sup>2+</sup> and one for Mn<sup>2+</sup>). We can assume that mutations in any of these amino acids completely abolish the transport function of Gdt1p by impairing cation affinity or conformation changes of the pocket.

Moreover, the use of different Pmr1p mutants defective for transport of either Ca<sup>2+</sup> ions (Pmr1pD53A), Mn<sup>2+</sup> ions (Pmr1pQ783A) or both (Pmr1pD778A) [11,12] showed that the observed Golgi

glycosylation defect in the *gdt1Δ/pmr1Δ* strains only resulted from a lack of intraluminal Golgi Mn<sup>2+</sup> and not Ca<sup>2+</sup>. Our data suggest that the activity of Gdt1p in Golgi glycosylation becomes essential only when Pmr1p transports Ca<sup>2+</sup>. It should also be noted that the suppression of the glycosylation defect is more efficient in *pmr1Δ* strains complemented with Pmr1pQ783A under Ca<sup>2+</sup> supplementation. Given the fact that the observed Golgi glycosylation defect was due to a lack of intraluminal Golgi Mn<sup>2+</sup>, our results strongly suggest that when Pmr1p only transports Ca<sup>2+</sup> from the cytosol to the Golgi lumen, Gdt1p is necessary to import Mn<sup>2+</sup> inside the Golgi lumen by exchanging Ca<sup>2+</sup> (Fig. 6). This model also explains why high environmental Ca<sup>2+</sup>

concentrations in *gdt1Δ* lead to strong *N*-glycosylation deficiencies. When cytosolic  $\text{Ca}^{2+}$  concentration increases, Pmr1p favors the transport of  $\text{Ca}^{2+}$  in place of  $\text{Mn}^{2+}$ . The Golgi luminal pool of  $\text{Mn}^{2+}$  is then rapidly depleted if Gdt1p is not there to efficiently import  $\text{Mn}^{2+}$  inside the Golgi lumen. Given the fact that a lack of Pmr1p leads to strong Golgi glycosylation defects, our results suggest that in physiological conditions, Pmr1p preferentially imports  $\text{Mn}^{2+}$  rather than  $\text{Ca}^{2+}$  into the Golgi lumen. In such conditions, the role of Gdt1p, at least in Golgi glycosylation, is completely dispensable. Would that suggest that Gdt1p use the Golgi  $\text{Mn}^{2+}$  gradient generated by Pmr1p to import cytosolic  $\text{Ca}^{2+}$  inside the Golgi lumen? The question is completely open. As many antiport transporters can work in reverse if the gradient concentration of the driving ion is reversed, we can reasonably postulate that Gdt1p may also work in both directions. As our results show that the requirement of Gdt1p in Golgi glycosylation depends on the nature of the ion transported by Pmr1p, we propose that Gdt1p would be the leak channel of Pmr1p.

### Transparency document

The <http://dx.doi.org/10.1016/j.bbagen.2017.11.006> associated with this article can be found, in online version.

### Acknowledgements

This work was supported by grants from Agence Nationale de la Recherche (SOLV-CDG project to F.F., N° ANR-15-CE14-0001-01), Mizutani Grant (N° 150155 to F.F.) and EURO-CDG-2 that has received funding from the European Union's Horizon 2020 research and innovation program under the ERA-NET Cofund action No 643578. We are also indebted to Dr. Dominique Legrand for the Research Federation FRABio (Univ. Lille, CNRS, FR 3688, FRABio, Biochimie Structurale et Fonctionnelle des Assemblages Biomoléculaires) for providing the scientific and technical environment conducive to achieving this work.

### Conflict of interests

None.

### Appendix A. Supplementary data

Supplementary data to this article can be found online at <https://doi.org/10.1016/j.bbagen.2017.11.006>.

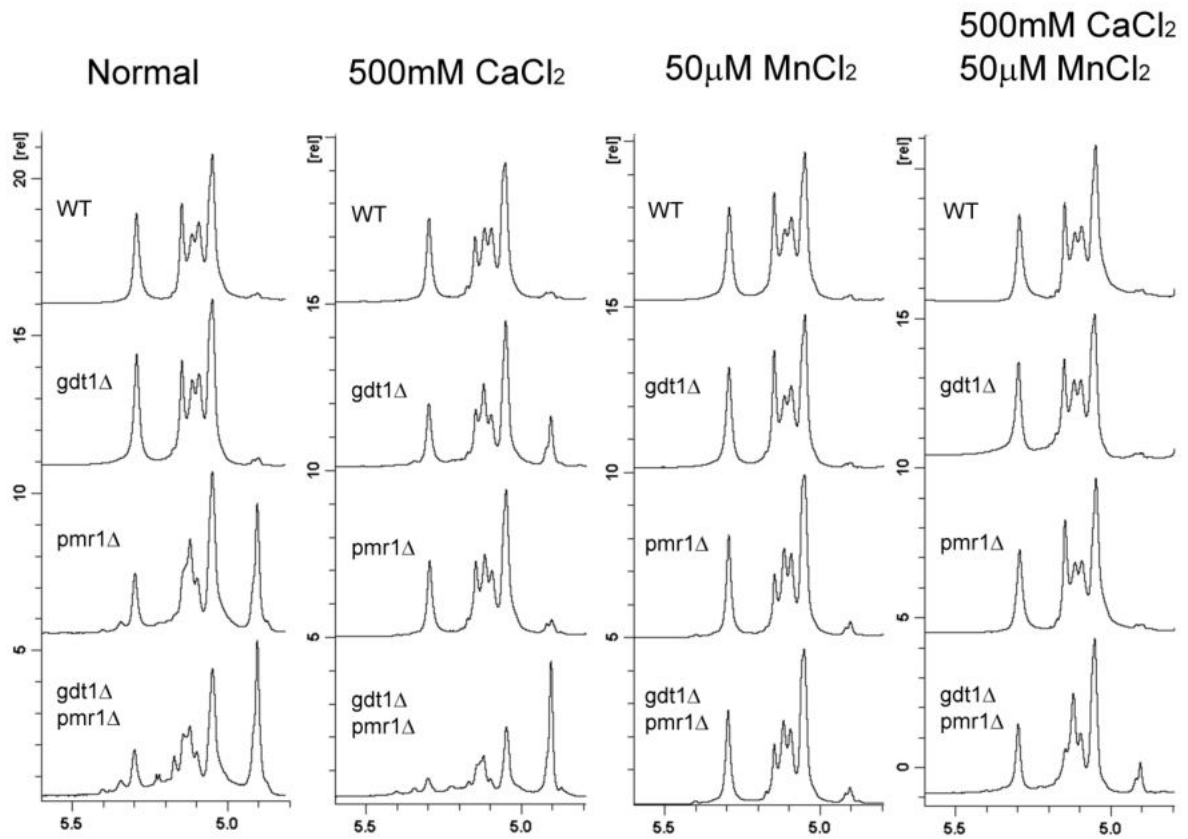
### References

[1] F. Foulquier, M. Amyere, J. Jaeken, R. Zeevaert, E. Schollen, V. Race, R. Bammens,

- W. Morelle, C. Rosnoblet, D. Legrand, D. Demaegd, N. Buist, D. Cheillan, N. Guffon, P. Morsomme, W. Annaert, H.H. Freeze, E. Van Schaftingen, M. Vikkula, G. Matthijs, TMEM165 deficiency causes a congenital disorder of glycosylation, *Am. J. Hum. Genet.* 91 (2012) 15–26, <http://dx.doi.org/10.1016/j.ajhg.2012.05.002>.
- [2] D. Demaegd, F. Foulquier, A.-S. Colinet, L. Gremillon, D. Legrand, P. Mariot, E. Peiter, E. Van Schaftingen, G. Matthijs, P. Morsomme, Newly characterized Golgi-localized family of proteins is involved in calcium and pH homeostasis in yeast and human cells, *Proc. Natl. Acad. Sci. U. S. A.* 110 (2013) 6859–6864, <http://dx.doi.org/10.1073/pnas.1219871110>.
- [3] A.-S. Colinet, P. Sengottaiyan, A. Deschamps, M.-L. Colsoul, L. Thines, D. Demaegd, M.-C. Duchêne, F. Foulquier, P. Hols, P. Morsomme, Yeast Gdt1 is a Golgi-localized calcium transporter required for stress-induced calcium signaling and protein glycosylation, *Sci. Rep.* 6 (2016) 24282, <http://dx.doi.org/10.1038/srep24282>.
- [4] S. Potelle, W. Morelle, E. Dulary, S. Duvet, D. Vicogne, C. Spriet, M.-A. Krzewinski-Recchi, P. Morsomme, J. Jaeken, G. Matthijs, G. De Bettignies, F. Foulquier, Glycosylation abnormalities in Gdt1p/TMEM165 deficient cells result from a defect in Golgi manganese homeostasis, *Hum. Mol. Genet.* 25 (2016) 1489–1500, <http://dx.doi.org/10.1093/hmg/ddw026>.
- [5] S. Potelle, E. Dulary, L. Climer, S. Duvet, W. Morelle, D. Vicogne, E. Lebedonchelle, M. Houdou, C. Spriet, M.-A. Krzewinski-Recchi, R. Peanne, A. Klein, G. DE Bettignies, P. Morsomme, G. Matthijs, T. Marquardt, V. Lupashin, F. Foulquier, Manganese-induced turnover of TMEM165, *Biochem. J.* (2017), <http://dx.doi.org/10.1042/BCJ20160910>.
- [6] A. Schneider, I. Steinberger, A. Herdean, C. Gandini, M. Eisenhut, S. Kurz, A. Morper, N. Hoecker, T. Rühle, M. Labs, U.I. Flügge, S. Geimer, S.B. Schmidt, S. Husted, A.P.M. Weber, C. Spetea, D. Leister, The evolutionarily conserved protein PHOTOSYNTHESIS AFFECTED MUTANT71 is required for efficient manganese uptake at the thylakoid membrane in arabidopsis, *Plant Cell* (2016) tpc.00812.2015, <http://dx.doi.org/10.1105/tpc.15.00812>.
- [7] F. Brandenburg, H. Schoffman, S. Kurz, U. Krämer, N. Keren, A.P.M. Weber, M. Eisenhut, The synechocystis manganese exporter Mnx is essential for manganese homeostasis in cyanobacteria, *Plant Physiol.* 173 (2017) 1798–1810, <http://dx.doi.org/10.1104/pp.16.01895>.
- [8] S. Munro, What can yeast tell us about *N*-linked glycosylation in the Golgi apparatus? *FEBS Lett.* 498 (2001) 223–227, [http://dx.doi.org/10.1016/S0014-5793\(01\)02488-7](http://dx.doi.org/10.1016/S0014-5793(01)02488-7).
- [9] R.D. Nelson, N. Shibata, R.P. Podzorski, M.J. Herron, Candida mannan: chemistry, suppression of cell-mediated immunity, and possible mechanisms of action, *Clin. Microbiol. Rev.* 4 (1991) 1–19.
- [10] E. Vinogradov, B. Petersen, K. Bock, Structural analysis of the intact polysaccharide mannan from *Saccharomyces Cerevisiae* yeast using 1H and 13C NMR spectroscopy at 750 MHz, *Carbohydr. Res.* 307 (1998) 177–183.
- [11] Y. Wei, V. Marchi, R. Wang, R. Rao, An *N*-terminal EF hand-like motif modulates ion transport by Pmr1, the yeast Golgi  $\text{Ca}^{2+}/\text{Mn}^{2+}$ -ATPase, *Biochemistry (Mosc)* 38 (1999) 14534–14541.
- [12] D. Mandal, T.B. Woolf, R. Rao, Manganese selectivity of pmr1, the yeast secretory pathway ion pump, is defined by residue gln783 in transmembrane segment 6. Residue Asp778 is essential for cation transport, *J. Biol. Chem.* 275 (2000) 23933–23938, <http://dx.doi.org/10.1074/jbc.M002619200>.
- [13] D. Demaegd, A.-S. Colinet, A. Deschamps, P. Morsomme, Molecular evolution of a novel family of putative calcium transporters, *PLoS One* 9 (2014) e100851, <http://dx.doi.org/10.1371/journal.pone.0100851>.
- [14] E. Dulary, S. Potelle, D. Legrand, F. Foulquier, TMEM165 deficiencies in Congenital Disorders of Glycosylation type II (CDG-II): Clues and evidences for roles of the protein in Golgi functions and ion homeostasis, *Tissue Cell* (2016), <http://dx.doi.org/10.1016/j.tice.2016.06.006>.
- [15] C.E. Ballou, Yeast cell wall and cell surface, in: J.N. Strathern, E.W. Jones, J.R. Broach (Eds.), *The Molecular Biology of the Yeast Saccharomyces: Metabolism and Gene Expression*, Cold Spring Harbor Laboratories, Cold Spring Harbor, N.Y., 1982, pp. 335–360.

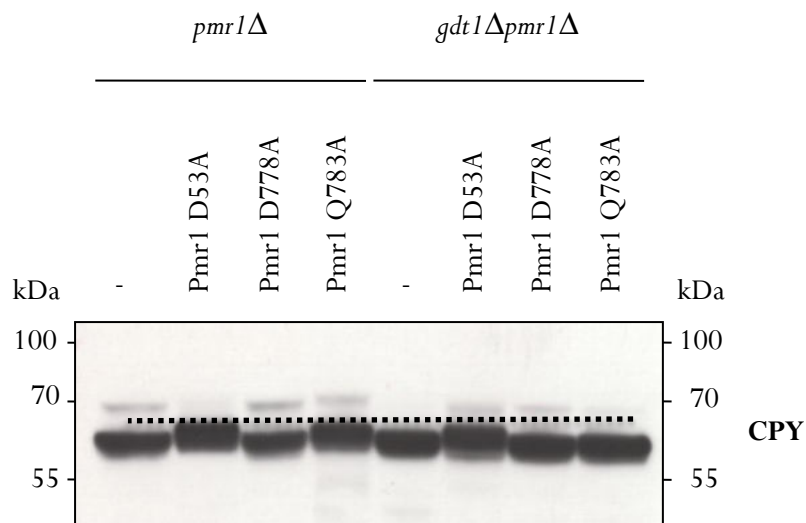
### 3.3. Supplementary data associated with the publication

#### 3.3.1. Supplementary Figure 1



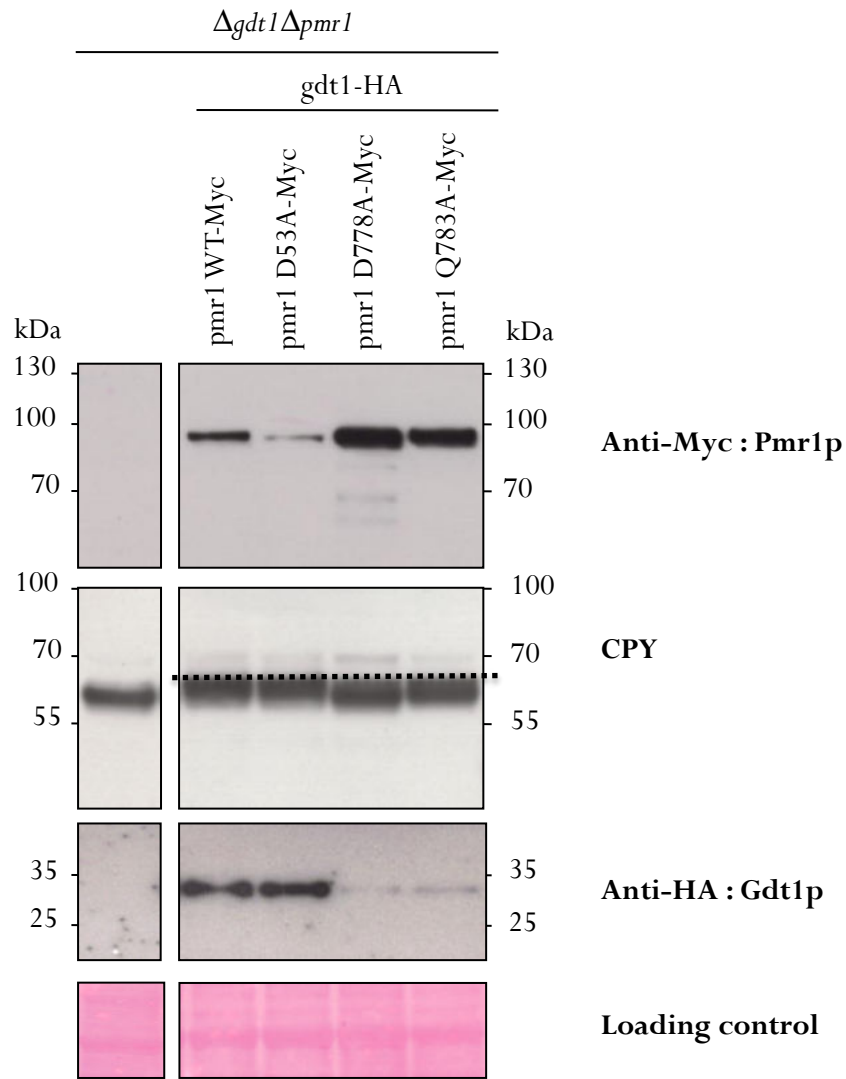
SUPP FIGURE 1

#### 3.3.2. Supplementary Figure 2



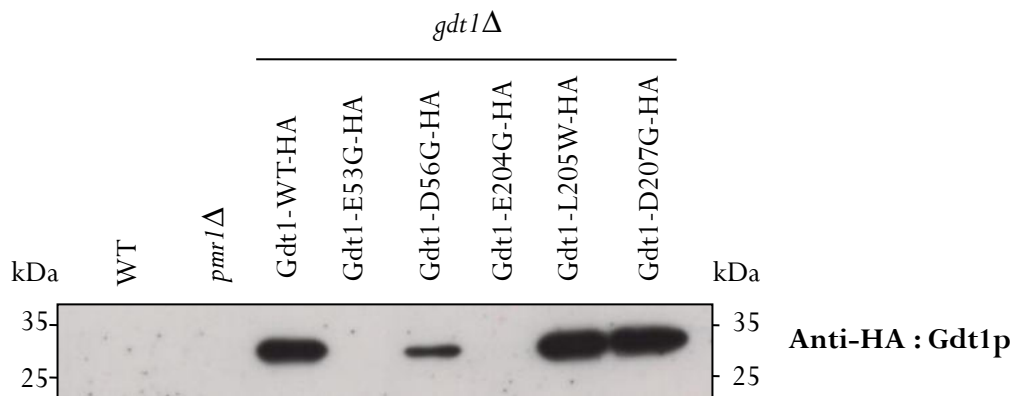
SUPP FIGURE 2

3.3.3. Supplementary Figure 3



SUPP FIGURE 3

3.3.4. Supplementary Figure 4



SUPP FIGURE 4

### 3.4. Conclusion

In this study, we have investigated the contribution of Gdt1p, Pmr1p and both in Golgi glycosylation. We have demonstrated that either  $\text{CaCl}_2$  or  $\text{MnCl}_2$  could rescue the Golgi glycosylation defect associated to Pmr1p deficiency, whereas only  $\text{MnCl}_2$  supplementation could suppress these defects in the double mutant *gdt1Δ/pmr1Δ*. From these observations, we pointed out the crucial role of Gdt1p in suppressing the Golgi glycosylation defect in yeast lacking Pmr1p and supplemented with  $\text{CaCl}_2$ . Using a set of different mutated forms of Pmr1p, we also revealed both crucial and dispensable roles of Gdt1p in Golgi glycosylation depending on the presence/ion transport capacity of Pmr1p. As resumed in Figure “Big Yeast”, in *pmr1Δ* yeast, Gdt1p is found degraded as its protein expression is reduced by almost 80%. Only a complementation with either Pmr1p-WT or Pmr1p-D53A rescues Gdt1p stability. The hypothesis beyond these observations would be that both Pmr1p-WT and D53A are able to transport cytosolic  $\text{Mn}^{2+}$  into the Golgi lumen, lowering cytosolic  $\text{Mn}^{2+}$  levels responsible for constitutive degradation of Gdt1p into the vacuole. This is also corroborated by the suppression of glycosylation defects in the two complemented yeast strains, likely thanks to  $\text{Mn}^{2+}$  entry in the Golgi apparatus *via* Pmr1p-WT and Pmr1p-D53A. In contrast, complementations with Pmr1p-Q783A or Pmr1p-D778A neither rescue glycosylation defects associated to Pmr1p deficiency nor Gdt1p protein expression suggesting that no cytosolic  $\text{Mn}^{2+}$  ions are pumped into the Golgi lumen to either sustain glycosylation reactions or rescue Gdt1p protein expression. Hence, we established that Gdt1p abundance depends on Pmr1p capacity to import  $\text{Mn}^{2+}$  into the Golgi apparatus and also proposed that Gdt1p would be the leak channel of Pmr1p to ensure its function in Golgi glycosylation.

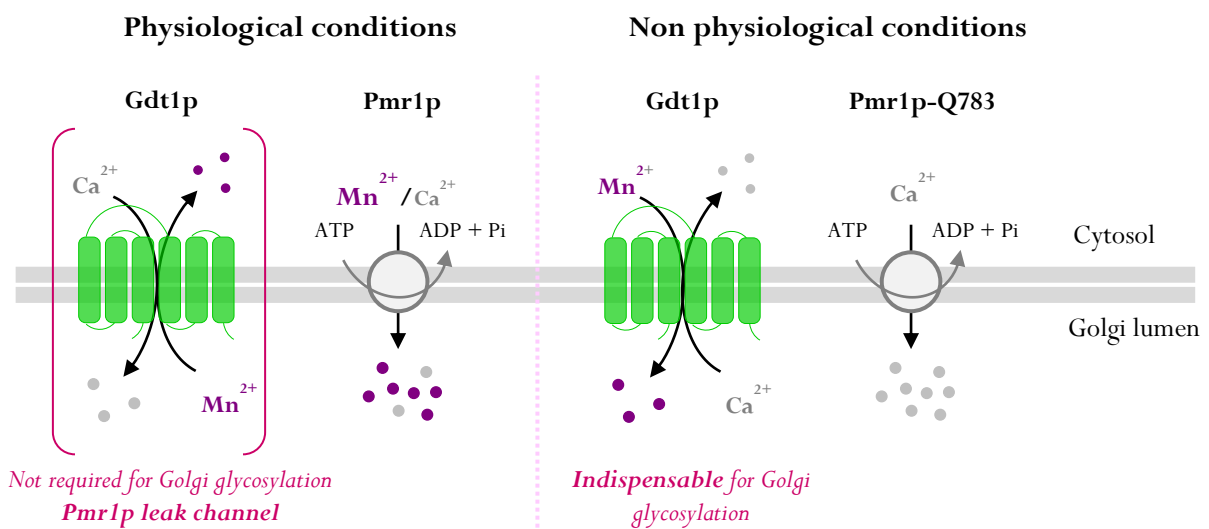
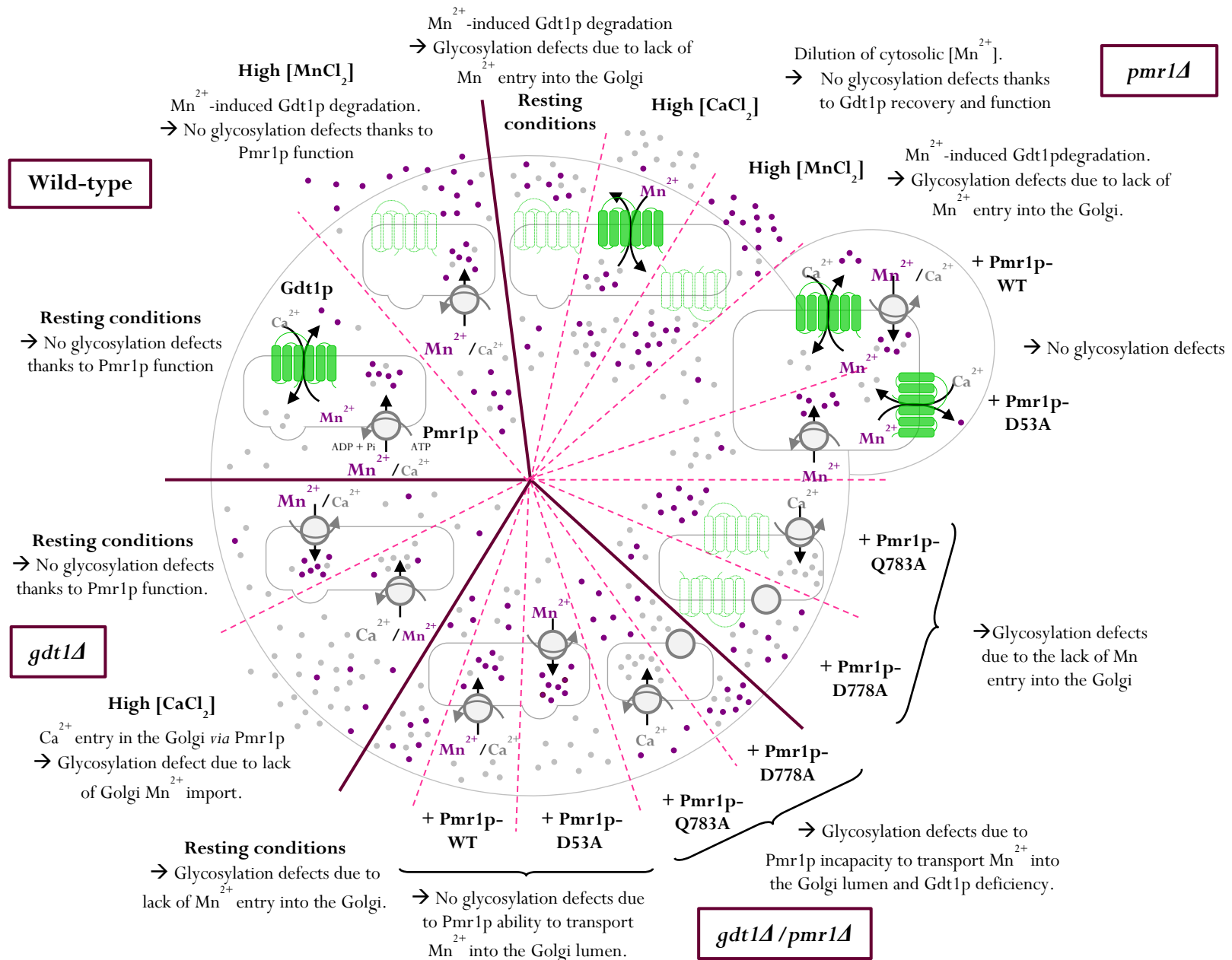


**Figure 63: Current model proposed for Gdt1p and Pmr1p function in Golgi glycosylation.** In physiological conditions Pmr1p is assumed to be the main Golgi  $\text{Mn}^{2+}$  importer and Gdt1p its leak channel, probably using the gradient established by Pmr1p to import  $\text{Ca}^{2+}$  into the Golgi. In contrast, when Pmr1p only transports  $\text{Ca}^{2+}$ , Gdt1p becomes crucial to import  $\text{Mn}^{2+}$  into the Golgi lumen and sustain glycosylation reactions.



All in all, in yeast *Saccharomyces cerevisiae*, Gdt1p would act as a main Golgi (i)  $\text{Ca}^{2+}$  importer when Pmr1p is expressed and able to transport  $\text{Mn}^{2+}$  into the Golgi lumen and (ii)  $\text{Mn}^{2+}$  importer when Pmr1p is only able to import  $\text{Ca}^{2+}$  into the Golgi apparatus (Figure 63). Gdt1p and Pmr1p are then connected through a functional link to ensure proper Golgi glycosylation reactions and regulate  $\text{Ca}^{2+}$  and  $\text{Mn}^{2+}$  intracellular homeostasis in yeast *Saccharomyces cerevisiae*. Because both Gtd1p and Pmr1p have conserved human orthologs (respectively, TMEM165 and SPCA1), the aim of the following publication (Paper 4) was to investigate the potential functional link between TMEM165 and SPCA1.



## 4. Paper 4: Investigating the functional link between TMEM165 and SPCA1

### 4.1. Introduction

Given the previous study in yeast *Saccharomyces cerevisiae* highlighting a functional link between Gdt1p and Pmr1p in Golgi glycosylation maintenance, we next wondered whether a similar link could have been conserved/preserved between the human orthologs, TMEM165 and SPCA1. Although our previous results rather identified SERCA-like proteins as key players in Golgi glycosylation maintenance in human cells lacking TMEM165, we assumed that SPCA1 and TMEM165 could be linked by their function in the regulation of Golgi  $\text{Ca}^{2+}/\text{Mn}^{2+}$  homeostasis. Since no obvious changes in SPCA1 protein expression have been observed in TMEM165 KO HEK cells, we presumed that both physical and functional lack of TMEM165 do not interfere with SPCA1 stability. However, in the other way around, we did not know whether TMEM165 stability could depend on the physical/functional presence of SPCA1.

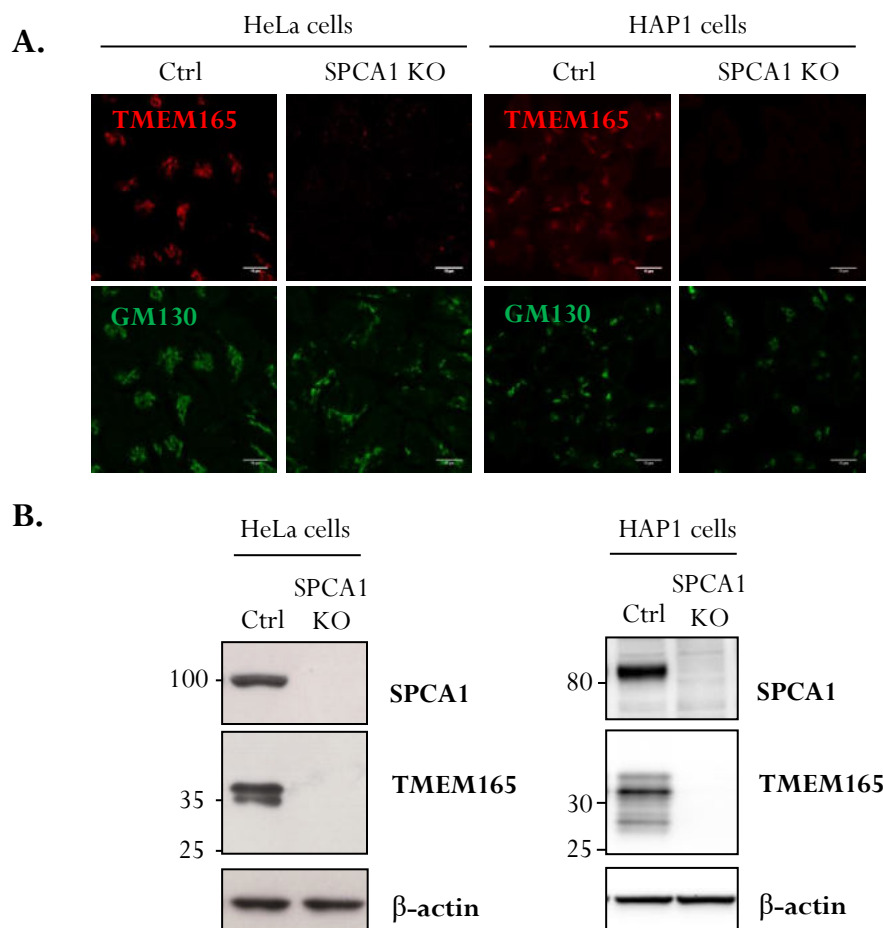


**Figure 64: TMEM165 protein expression in SPCA1 KO HeLa and HAP1 cells.** **A.** TMEM165 subcellular localization in SPCA1 KO HeLa (left) and HAP1 (right) cells. Cells were fixed, permeabilized and labeled with antibodies against TMEM165 and GM130. **B.** TMEM165 protein expression. Total cell lysates were prepared, subjected to SDS-PAGE and western blot with the indicated antibodies.

Thanks to a collaboration with Pr Charles Rice, we took advantage of two mammalian cell lines defective for SPCA1 (HeLa and Hap1 cells) and looked for TMEM165 protein expression. Surprisingly, as shown in Figure 64, in two different cell lines, the lack of SPCA1 led to a nearly complete loss of TMEM165 protein expression, using both western blot and immunofluorescence approaches. This first convincing preliminary result steered us to further explore whether TMEM165 degradation was due to a lack of physical or functional interaction with SPCA1. Actually, like for Pmr1p in yeast, we hypothesized that SPCA1 may influence the protein abundance and stability of TMEM165, according to its ion pumping activity. Similarly to the study conducted in yeast *Saccharomyces cerevisiae*, we exploited mutated forms of SPCA1 with defective transport function for either  $\text{Ca}^{2+}$  (SPCA1-Q747A),  $\text{Mn}^{2+}$  (SPCA1-G309C) or both  $\text{Ca}^{2+}$  and  $\text{Mn}^{2+}$  (SPCA1-D742Y) (Figure 65) and looked for TMEM165 protein expression recovery.

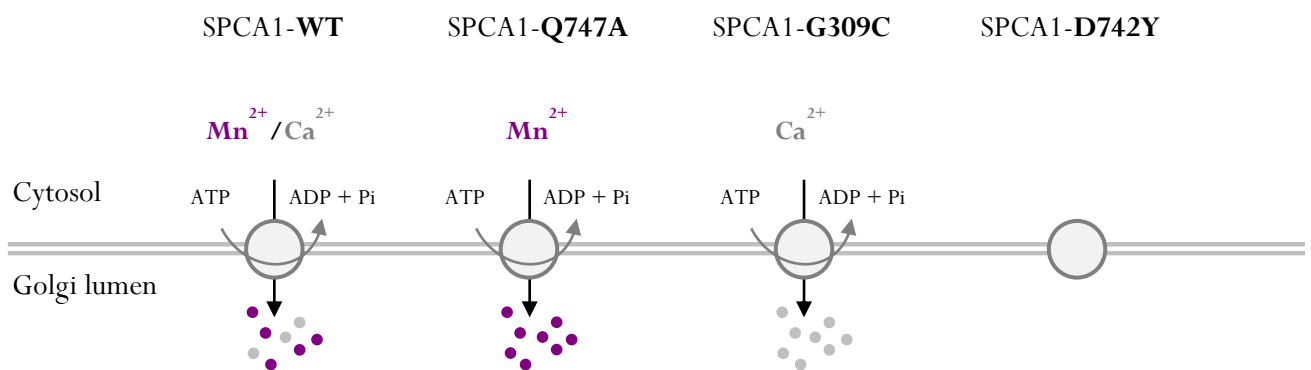


**Figure 65: SPCA1 defective mutants and associated ion pumping capacity used in the study.**

This last publication has been signed as co-author with Elodie Lebretonchel, a former PhD student in the team at the time.

## 4.2. Publication

# Investigating the functional link between TMEM165 and SPCA1

Elodie Lebretonchel<sup>1,2,\*</sup>, Marine Houdou<sup>1,\*</sup>, Hans-Heinrich Hoffmann<sup>3</sup>, Kateryna Kondratska<sup>4,5</sup>, Marie-Ange Krzewinski<sup>1</sup>, Dorothee Vicogne<sup>1</sup>, Charles M. Rice<sup>3</sup>, André Klein<sup>1,2</sup> and  François Foulquier<sup>1</sup>

<sup>1</sup>Univ. Lille, CNRS, UMR 8576 – UGSF - Unité de Glycobiologie Structurale et Fonctionnelle, F-59000 Lille, France; <sup>2</sup>Univ. Lille, CHU Lille, Centre de Biologie et Pathologie, UAM de glycopathologies, Centre de Biologie et Pathologie, F-59000 Lille, France; <sup>3</sup>Laboratory of Virology and Infectious Disease, The Rockefeller University, New York, NY 10065, U.S.A; <sup>4</sup>Univ. Lille, INSERM U1003 - PHYCEL - Physiologie Cellulaire, F-59000 Lille, France; <sup>5</sup>Laboratory of Excellence, Ion Channels Science and Therapeutics, Université de Lille, Villeneuve d'Ascq, France

**Correspondence:** François Foulquier (francois.foulquier@univ-lille.fr)

TMEM165 was highlighted in 2012 as the first member of the Uncharacterized Protein Family 0016 (UPF0016) related to human glycosylation diseases. Defects in TMEM165 are associated with strong Golgi glycosylation abnormalities. Our previous work has shown that TMEM165 rapidly degrades with supraphysiological manganese supplementation. In this paper, we establish a functional link between TMEM165 and SPCA1, the Golgi Ca<sup>2+</sup>/Mn<sup>2+</sup> P-type ATPase pump. A nearly complete loss of TMEM165 was observed in SPCA1-deficient Hap1 cells. We demonstrate that TMEM165 was constitutively degraded in lysosomes in the absence of SPCA1. Complementation studies showed that TMEM165 abundance was directly dependent on SPCA1's function and more specifically its capacity to pump Mn<sup>2+</sup> from the cytosol into the Golgi lumen. Among SPCA1 mutants that differentially impair Mn<sup>2+</sup> and Ca<sup>2+</sup> transport, only the Q747A mutant that favors Mn<sup>2+</sup> pumping rescues the abundance and Golgi subcellular localization of TMEM165. Interestingly, the overexpression of SERCA2b also rescues the expression of TMEM165. Finally, this paper highlights that TMEM165 expression is linked to the function of SPCA1.

## Introduction

Organelle ionic homeostasis within the secretory pathway is regulated by Ca<sup>2+</sup> and Mn<sup>2+</sup> ion concentrations through the action of transporters and pumps. Cation homeostasis is known to be crucial for many cellular processes including vesicular fusion events, the secretion of proteins as well as for the activity of Golgi glycosyltransferases and glycosidases [1]. This cation homeostasis stems from a balance between Ca<sup>2+</sup> influx and efflux but its molecular mechanisms have not been completely defined nor have the different actors been identified [2,3]. A major regulator of Ca<sup>2+</sup>/Mn<sup>2+</sup> homeostasis in the Golgi compartment is the P-type ATPase SPCA1 encoded by *ATP2C1* [4,5]. While the function of SPCA1 in regulating Golgi Ca<sup>2+</sup> homeostasis has been well documented, less is known about its role in Mn<sup>2+</sup> homeostasis. It has been hypothesized that SPCA1 might play a role in Mn<sup>2+</sup> detoxification given that cytosolic Mn<sup>2+</sup> accumulation [6] is detrimental for many cellular processes, resulting in neurological disorders similar to Parkinson's disease [7]. In 2012, we described TMEM165 as the first member of the Uncharacterized Protein Family 0016 (UPF0016) related to human diseases [8]. TMEM165 is believed to be a Ca<sup>2+</sup>/H<sup>+</sup> transporter located in the Golgi and in lysosomes, where it participates in the homeostasis of pH and Ca<sup>2+</sup> ion concentration. This protein is highly conserved through evolution and defects in TMEM165 lead to strong Golgi glycosylation abnormalities responsible for a congenital disorder of glycosylation (TMEM165-CDG or CDG-IIk) [9,10]. Interestingly, these defects are completely rescued by Mn<sup>2+</sup> supplementation in the culture medium, suggesting the involvement of TMEM165 in Golgi Mn<sup>2+</sup> homeostasis [11,12]. Similar functions have been observed

\*These authors equally contributed to this work.

Received: 26 June 2019  
Revised: 7 October 2019  
Accepted: 17 October 2019

Accepted Manuscript online:  
17 October 2019  
Version of Record published:  
11 November 2019

for TMEM165 orthologs of plants, bacteria and yeast. In *Arabidopsis thaliana*, PAM71 (photosynthesis affected mutant 71) has been shown to be required for efficient  $Mn^{2+}$  uptake at the thylakoid membrane [13]. In the cyanobacterial model strain *Synechocystis sp.* PCC 6803, the Mnx protein was also determined to be a  $Mn^{2+}$  ion exporter [14]. When expressed in the bacterial model *Lactococcus lactis*, the yeast ortholog of TMEM165 (Gdt1p) was shown to be involved in  $Mn^{2+}$  transport [15]. Interestingly, we also found that TMEM165 is specifically degraded in lysosomes in response to high extracellular  $Mn^{2+}$  concentration, reinforcing the link between this protein and cellular  $Mn^{2+}$  homeostasis [16]. The cellular function of other UPF0016 members is certainly more complex as it has been previously reported that Gdt1p is also involved in  $Ca^{2+}$  transport [16]. Gdt1p might act as  $Ca^{2+}/Mn^{2+}$  antiporter in the Golgi apparatus. However, this model has been challenged by recent results showing that Gdt1p was necessary to retrieve  $H^+$  and Pi products generated during glycosylation in the Golgi lumen [2,17].

Our recent work in yeast suggested a link between Gdt1p and Pmr1p (ortholog of SPCA1 in yeast), the P-type ATPase ortholog of SPCA1 and one of the main  $Ca^{2+}/Mn^{2+}$  pump in the Golgi. We indeed demonstrated that the activity of Gdt1p in Golgi glycosylation maintenance depends on the ion transported by Pmr1p [18].

In this paper, we investigated the functional link between TMEM165 and SPCA1. We show that TMEM165 expression depends on SPCA1 as a lack of SPCA1 led to the complete loss of TMEM165. Complementation studies showed that TMEM165 abundance was directly dependent on the nature of the ion transported by SPCA1.

## Experimental Antibodies

Anti-TMEM165 and anti- $\beta$ -actin antibodies were purchased from Millipore Sigma (Burlington, MA, U.S.A.), anti-LAMP2 antibody from Santa Cruz Biotechnology (Dallas, TX, U.S.A.), anti-GM130 antibody from BD Biosciences (Franklin Lakes, NJ, U.S.A.), anti-SPCA1 from Abnova (Taipei City, Taiwan), anti-TGN46 from Bio-Rad (U.S.A.), anti-SERCA2 antibody was purchased from Millipore (Darmstadt, Germany) and anti-GPP130 (GOLPH4) antibody from Abcam (Cambridge, U.K.). Polyclonal goat anti-rabbit IgG and goat anti-mouse IgG horseradish peroxidase-conjugated were from Dako (Denmark) and donkey anti-sheep IgG horseradish peroxidase-conjugated was purchased from R&D Systems (Minneapolis, U.S.A.). Alexa 488- or Alexa 568-conjugated secondary antibodies were from Molecular Probes (Thermo Fisher Scientific, Waltham, MA, U.S.A.).

## Cell culture, transfection and other reagents

Hap1 cells were kindly provided by Pr C.M. Rice (Laboratory of Virology and Infectious Disease, The Rockefeller University, New York, NY, U.S.A.) [19] and maintained at 37°C in humidity-saturated 5%  $CO_2$  atmosphere in Iscove's modified Dulbecco's medium (IMDM) supplemented with 10% fetal bovine serum. For the complementation studies, SPCA1 isoform 1D was chosen for all experiments, as it has no truncated N- or C-terminus compared with the 1A-F isoforms. When used, MG132 (Sigma) was added for 8 h at the final concentration of 10  $\mu M$  and chloroquine (ICN Biomedicals) for 8 /24 h at 100  $\mu M$ . MG132 efficacy was assessed by Western blot using an anti-ubiquitin mouse antibody. All other chemicals were from Sigma-Aldrich unless otherwise specified.

HeLa cells were maintained in Dulbecco's modified eagle's medium (DMEM) supplemented with 10% FBS, at 37°C in humidity-saturated 5%  $CO_2$  atmosphere. The HeLa SPCA1 KO cells were provided by Dr. Charles Rice (The Rockefeller University) and generated as described in Hoffmann et al., (<https://www.ncbi.nlm.nih.gov/pubmed/29024641>). Transfections were performed using Lipofectamine 2000<sup>®</sup> (Thermo Scientific) according to the manufacturer's guidelines. Human SERCA2b plasmid (pcDNA3.1+) was purchased from Addgene.

## Vector construction and generation of stable cell line

Q747A-SPCA1 plasmid vector was generated by E-Zyvec<sup>®</sup> (Lille, France). Hap1 SPCA1 KO cells were transfected in a six-well plate at 70% confluence with SPCA1 (Q747A) plasmid using TurboFectin<sup>™</sup> 8.0 (Origene) at a ratio of 4 : 1 ( $\mu l$  TurboFectin: $\mu g$  plasmid) in IMDM supplemented with 10% FBS A. Cells were incubated with the lipid-DNA complexes for 24 h and then ten times diluted in culture medium containing 0.5  $\mu g/ml$  puromycin (Gibco Life Technologies) as the selective agent. The medium was changed every 3 days for

12 days, maintaining puromycin pressure at 0.5 µg/ml. Cells were then screened for Q747A-SPCA1 expression via Western blot and immunofluorescence.

### **Western blotting**

Cells were pelleted and lysed in RIPA Buffer (50 mM Tris-HCl pH 7.9, 120 mM NaCl, 1% NP-40, 1 mM EDTA, 1 mM Na<sub>3</sub>VO<sub>4</sub>, 5 mM NaF) supplemented with a cocktail of protease inhibitors (Roche, Meylan, France) and lysed by ultrasonic treatment for 2 min. The concentration of extracted proteins was determined with the Micro BCA™ Protein Assay Reagent kit (Thermo Fisher Scientific, Waltham, MA U.S.A.). Ten or twenty microgram of total proteins of each sample were dissolved in reducing NuPage® Sample buffer and resolved by MOPS 4–12% Bis-Tris gel (Thermo Fisher Scientific, Waltham, MA, U.S.A.). After transfer with iBlot 2 Dry Blotting System (Thermo Fisher Scientific, Waltham, MA, U.S.A.), nitrocellulose membranes were blocked using TBS (tris buffer saline) containing 0.05% Tween 20 and either 5% (w/v) bovine serum albumin (BSA) or 5% (w/v) non-fat dried milk for at least 1 h. Primary antibodies rabbit anti-TMEM165, mouse anti-SPCA1, mouse anti-LAMP2 and sheep anti-TGN46 were incubated at least 1 h at room temperature (RT) or overnight at 4°C in TBS, 0.05% Tween 20 (TBS-T) and 5% (w/v) BSA or 5% (w/v) non-fat dried milk at respectively, 1 : 3 000, 1 : 4 000 and 1 : 2 000 dilution. Anti-β-actin mouse antibody was used for quantification at 1 : 20 000 in TBS-T and 5% (w/v) non-fat dried milk. All the membranes were washed three times 5 min in TBS-T after the addition of the primary and the secondary antibodies. Either goat anti-rabbit IgG, goat anti-mouse IgG (Dako, Agilent technologies, Santa Clara, U.S.A.) or donkey anti-sheep HRP-conjugated were used as secondary antibodies at a dilution of 1 : 10 000 or 1 : 20 000. Signal was detected using chemiluminescence reagent (Pierce™ Pico Plus Western Blotting Substrate (Thermo Fisher Scientific, Waltham, MA, U.S.A.) on imaging film (GE Healthcare, Buckinghamshire, U.K.) or Camera Fusion® (Vilber Lourmat) and its software.

### **Immunofluorescence imaging**

Twenty-four hours after transfection, cells were seeded on coverslips, washed once with DPBS+/+ (Dulbecco's phosphate saline buffer with calcium and manganese) fixed with methanol for 10 min or 4% paraformaldehyde (PFA) in 0.1 M sodium phosphate buffer (PBS, pH 7.2) for 30 min at RT, and then washed twice with PBS. Cells fixed with PFA were permeabilized in 0.5% Triton X100 for 15 min. Fixed cells were saturated 1 h in blocking buffer (0.2% gelatin, 2% BSA and 2% fetal bovine serum (Lonza) in PBS) and then incubated with primary antibody diluted at 1 : 100 in blocking buffer for 1 h.

After three washes with PBS, cells were incubated with Alexa 488- or Alexa 568-conjugated secondary antibodies diluted at 1 : 600 in blocking buffer for 1 h. Fifteen minutes of DAPI 1 : 200 in PBS were used to stain cells nuclei. Coverslips were mounted on glass slides with 6 µl of Mowiol. Immunostaining and fluorescent proteins were detected through an inverted Zeiss LSM700 confocal microscope. Data acquisition was done using ZEN pro 2.3 SP1 software (Carl Zeiss GmbH, Jena, Germany) and quantifications were done using ImageJ (Fiji) plugin (National Institutes of Health, Bethesda, MD, U.S.A.; <http://imagej.nih.gov/ij>) developed by the local TisBio (<http://tisbio.wixsite.com/tisbio>) facility.

### **qRT-PCR analysis**

Total RNA was extracted using NucleoSpin® RNA Plus Kit (Macherey-Nagel) following manufacturer protocol. cDNA was synthesized by reverse transcription. Two microgram of total RNA was reverse transcribed into cDNA at 42°C using random hexamer primers (PerkinElmer) and MuLV reverse transcriptase (PerkinElmer) in a 20 µl final volume. qRT-PCR was performed in triplicate in 96-well plates in a real-time thermal cycler Cfx C1000 (Bio-Rad) using EvaGreen Supermix (Bio-Rad). Primers used for hTMEM165 (forward GGGATTGGCAGTAATTGGAGGA; reverse AGCCGGCCCGGGTCGAGGACCCC); hGAPDH (forward TTCGTCATGGCTGTGAACCA, reverse CAGTGATGCGCATGGACTGT); hHPRT (forward GGCGTCGTGATTAGTGATGAT, reverse CGAGCAAGACGTTTCAGTCCT).

### **Proximity ligation assay (PLA) and microscopy analysis**

Duolink® PLA Kit (Sigma-Aldrich) was used with red (DUO92008) detection reagents, anti-mouse MINUS probe (DUO92004) and anti-rabbit PLUS probe (DUO92002). Cells were fixed, blocked and incubated with primary antibodies as for standard immunofluorescence except that the mouse anti-SPCA1 antibody was from Abcam (Cambridge, U.K.) dilution 1 : 50. The protocol was followed according to the manufacturer recommendations. Coverslips were mounted on glass slides with Mounting Medium including DAPI (DUO82040). The

acquisition was made with Zeiss LSM700 confocal microscope. PLA was quantified as the total number of spots was normalized on the number of cells. All the analyses were performed by TisGolgi.

## Results

### TMEM165 expression is altered in SPCA1 KO cells

Our previous work on yeast strongly indicated a potential link between Gdt1p and Pmr1p, the yeast orthologs of the mammalian proteins TMEM165 and SPCA1 [18]. To test this hypothesis in mammalian cells, the expression of TMEM165 was first evaluated in Hap1 cells deficient for SPCA1 by Western blot and immunofluorescence. As shown in [Figure 1A](#), a nearly complete loss of TMEM165 is observed in SPCA1 KO cells compared with control cells. Quantification indicated that the decrease of TMEM165 exceeded 90% ([Figure 1B](#)). The lack of TMEM165 was also seen by immunofluorescence where a decrease in Golgi-associated TMEM165 was observed ([Figure 1C](#)). As defects in TMEM165 lead to strong Golgi glycosylation abnormalities, we assessed the glycosylation status of LAMP2 and TGN46 by Western blot in WT and SPCA1 KO cells. Surprisingly, there was no change in LAMP2 or TGN46 gel mobility suggesting that the lack of SPCA1 and subsequently TMEM165 did not lead to major glycosylation alterations ([Figure 1D](#)).

Interestingly, despite the decrease of TMEM165 in the Golgi, weak peripheral punctate structures were apparent, suggesting that TMEM165 was re-located and potentially targeted for lysosomal degradation in the absence of SPCA1 (data not shown). To address whether TMEM165 is subjected to lysosomal degradation in SPCA1 KO cells, we tested the impact of the lysosomotropic agent chloroquine (CQ) on its cellular abundance by Western blot at different times. As shown in [Figure 1E](#) and Supplementary Figure S1A,B, the abundance of TMEM165 was recovered in CQ treated SPCA1 KO cells. Quantification indicated an 80% rescue of TMEM165 levels in SPCA1 KO cells treated with CQ for 24 h ([Figure 1F](#)). The lysosomal degradation of TMEM165 was also confirmed by immunofluorescence where co-localization of TMEM165 ( $63 \pm 1\%$ ) with LAMP2 is observed in CQ treated SPCA1 KO cells ([Figure 1G](#)). The degradation of TMEM165 in SPCA1 KO cells occurs specifically in lysosomes as we demonstrated the absence of proteasomal degradation by using MG132, a proteasomal inhibitor (Supplementary Figure S1C,D). Altogether these results suggest that lack of SPCA1 leads to lysosomal degradation of TMEM165.

### TMEM165 stability depends on the function of SPCA1

To determine whether the observed instability of TMEM165 was dependent on specific functions of SPCA1, we reconstituted SPCA1 KO Hap1 cells with either SPCA1 WT (isoform 1D) or SPCA1 harboring point mutations that impair its ion transport activities. While G309C blocks primarily  $Mn^{2+}$  pumping, D742Y impairs both  $Ca^{2+}$  and  $Mn^{2+}$  pumping [19]. First, to test the inability of the mutated SPCA1 to import  $Mn^{2+}$  inside the Golgi lumen, the stability of GPP130 was followed under  $Mn^{2+}$  pressure by Western blot. In accordance with the literature [20], we showed that the quantity of GPP130 was reduced when SPCA1 KO Hap1 cells reconstituted with wild-type SPCA1 isoform 1D were cultured in the presence of  $500 \mu M Mn^{2+}$ . A 60% decrease is observed after 2 h  $Mn^{2+}$  treatment in control cells ([Figure 2A](#), quantification not shown). Interestingly, in SPCA1 KO cells and SPCA1 KO HAP1 cells reconstituted with either G309C or D742Y, the  $Mn^{2+}$  induced degradation of GPP130 is either blocked or strongly delayed ([Figure 2A](#), quantification not shown). We can indeed see a slight effect of the  $Mn^{2+}$  induced degradation of GPP130 in G309C-SPCA1 cells where a 40% decrease is observed. Altogether these results demonstrate a severe impairment of the  $Mn^{2+}$  import inside the Golgi lumen when cells are subjected to high  $Mn^{2+}$  exposure. The stability of TMEM165 was then investigated in these cells. While the abundance of TMEM165 was fully recovered in SPCA1 KO cells reconstituted with WT-SPCA1 isoform 1D ([Figure 2A,C](#)), the expression of the two mutant constructs (G309C and D742Y) had no effect on TMEM165 abundance ([Figure 2A,C](#)). The real-time PCR analysis was also performed and no difference in TMEM165 mRNA expression could be observed (Supplementary Figure S1E). We then analyzed the subcellular localization of TMEM165 in SPCA1 KO cells complemented with the different SPCA1 constructs ([Figure 2C](#)). Only the expression of WT-SPCA1 isoform 1D rescued the Golgi subcellular localization of TMEM165, while expression of the mutated forms of SPCA1 had no effect ([Figure 2C](#)). The glycosylation status of LAMP2 and TGN46 was assessed by Western blot in reconstituted SPCA1 KO cells and no defects were observed in their gel mobility (Supplementary Figure S1F).

We then wondered whether CQ might rescue TMEM165 levels in SPCA1 KO cells. As shown in [Figure 3](#), levels of TMEM165 were restored in CQ treated cells. As in SPCA1 KO cells treated with CQ ([Figure 1F](#)),

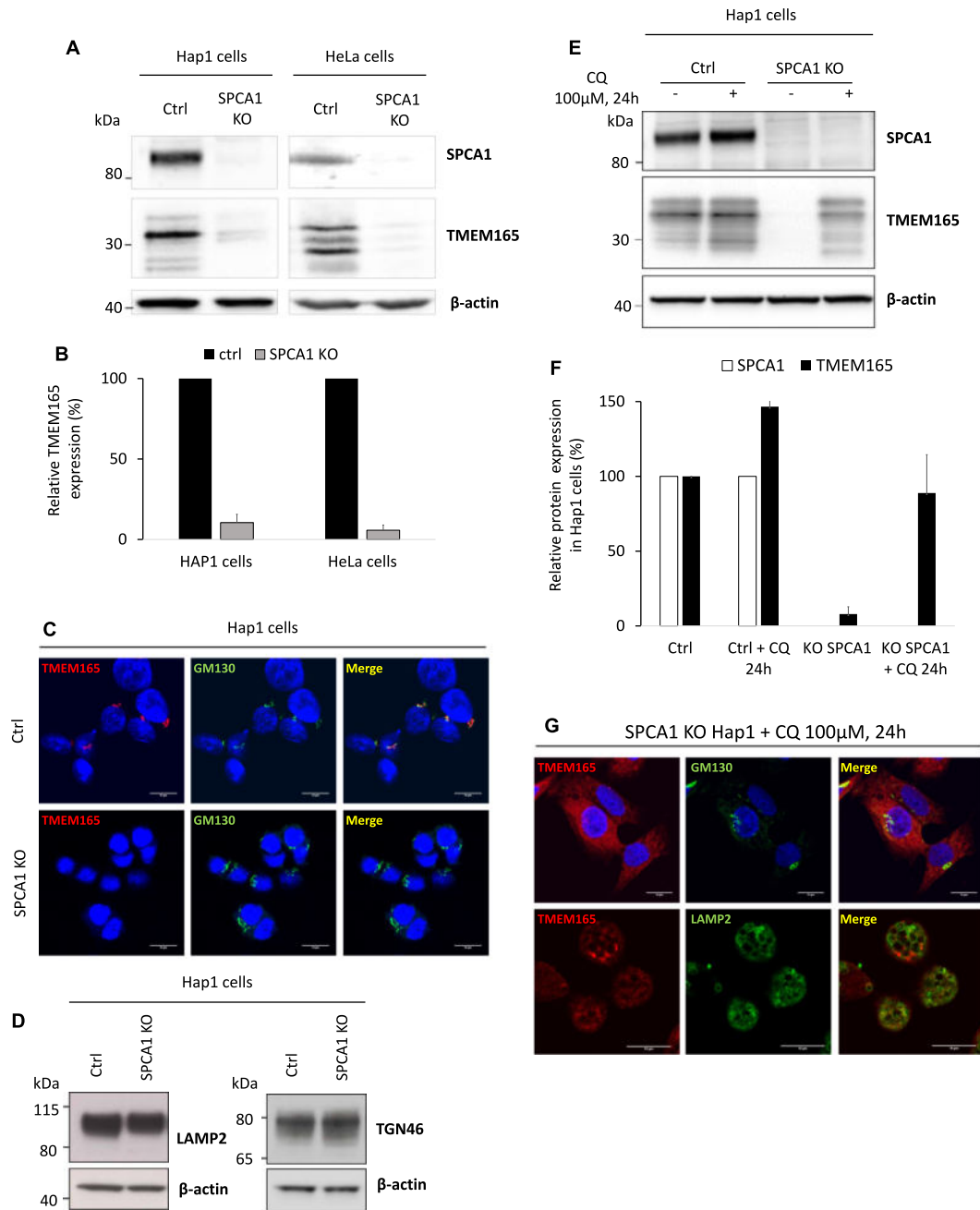


**Figure 1. TMEM165 expression in SPCA1 KO cells.**

(A) Expression of TMEM165 and SPCA1 in Hap1 and HeLa control cells versus SPCA1 KO cells. Total cell lysates were prepared, subjected to SDS-PAGE and Western blot with the indicated antibodies. (B) Quantification of TMEM165 protein expression ( $N = 3$ ) in Hap1 and HeLa control cells versus SPCA1 KO cells. (C) Subcellular localization and abundance of TMEM165 in Hap1 control and SPCA1 KO cells. (D) Expression of LAMP2 and TGN46 in Hap1 control cells versus SPCA1 KO cells. (E) Expression of TMEM165 and SPCA1 in Hap1 control cells versus SPCA1 KO cells with or without chloroquine (CQ) treatment (100  $\mu$ M, 24 h). (F) Quantification of TMEM165 and SPCA1 proteins expression ( $N = 3$ ) in Hap1 control and SPCA1 KO cells. (G) Subcellular localization and abundance of TMEM165 in Hap1 control and SPCA1 KO cells with CQ treatment (100  $\mu$ M, 24 h). LAMP2 is used as a lysosomal marker and nuclei are stained with DAPI staining (blue). Scale bars, 10  $\mu$ m.

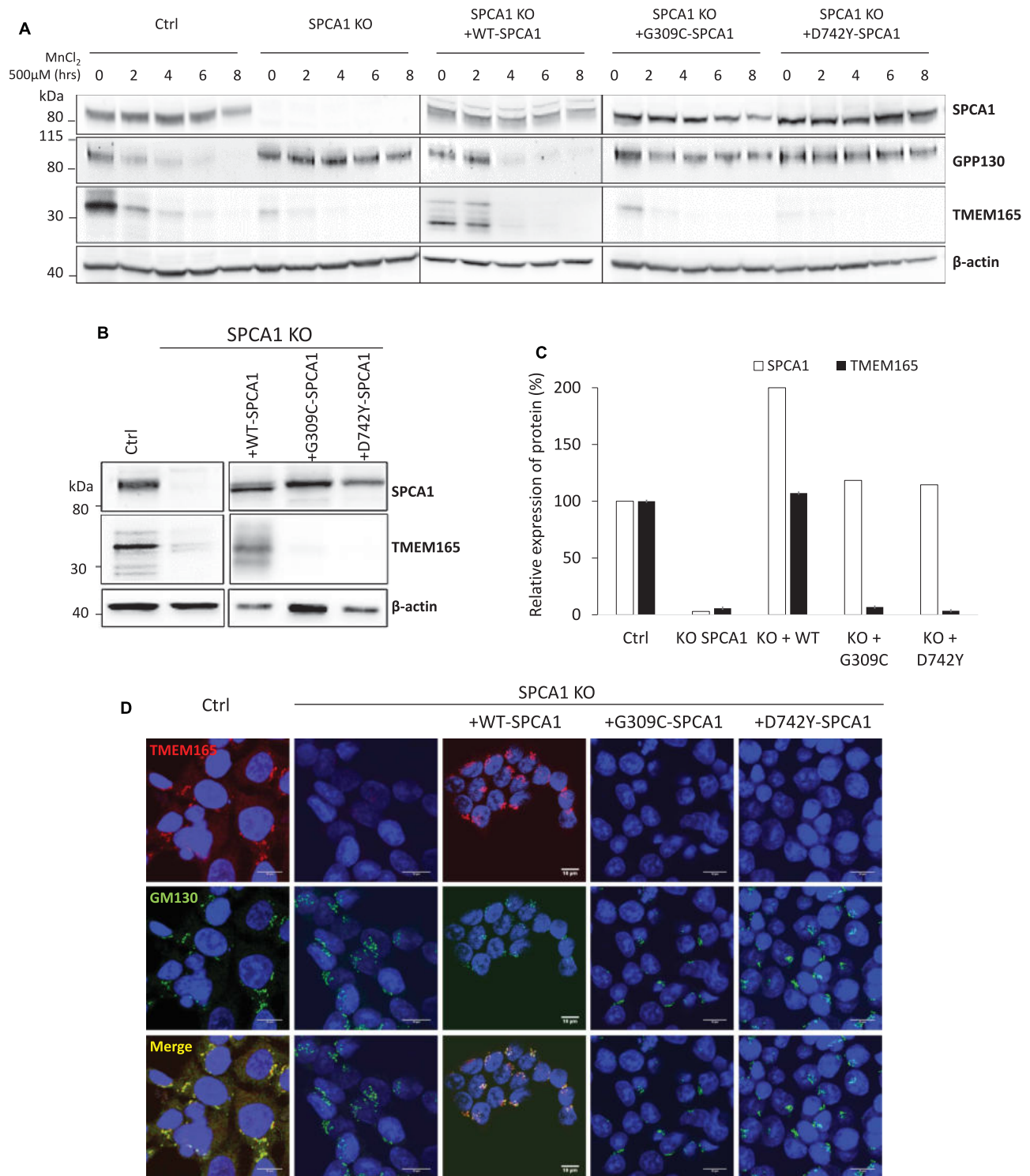


**Figure 2. TMEM165 expression in complemented Hap1 SPCA1 KO cells.**

(A) Expression of TMEM165, GPP130 and SPCA1 in Hap1 SPCA1 KO cells complemented with WT-SPCA1 and mutated SPCA1 constructs: G309C-SPCA1 and D742Y-SPCA1. Total cell lysates were prepared, subjected to SDS-PAGE and Western blot with the indicated antibodies. (B) Expression of TMEM165 and SPCA1 in Hap1 SPCA1 KO cells complemented with WT-SPCA1 and mutated SPCA1 constructs: G309C-SPCA1 and D742Y-SPCA1. Total cell lysates were prepared, subjected to SDS-PAGE and Western blot with the indicated antibodies. (C) Quantification of TMEM165 and SPCA1 proteins expression ( $N = 3$ ). (D) Subcellular localization and abundance of TMEM165 in Hap1 SPCA1 KO cells complemented with WT-SPCA1, G309C-SPCA1 and D742Y-SPCA1. GM130 is used as Golgi marker and nuclei are stained with DAPI staining (blue).



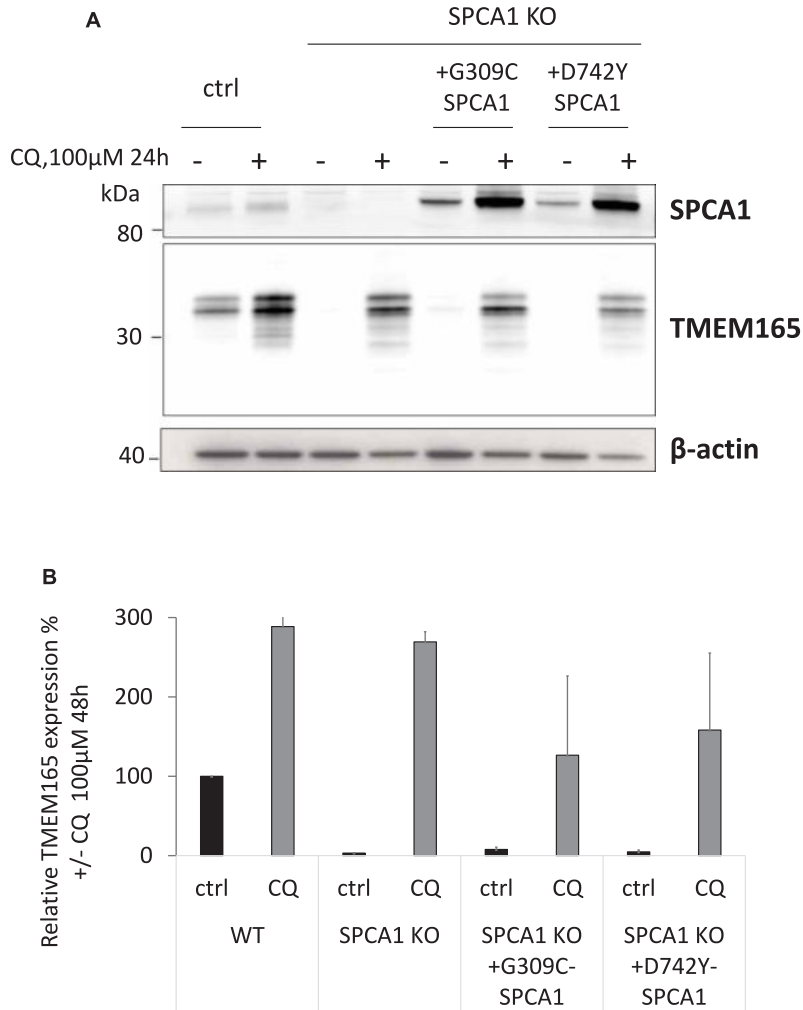


**Figure 3. Effect of chloroquine (CQ) on TMEM165 expression in complemented Hap1 SPCA1 KO cells.** (A) Expression of TMEM165 and SPCA1 in Hap1 control and SPCA1 KO cells and KO cells complemented with G309C-SPCA1 and D742Y-SPCA1, with or without chloroquine (CQ) treatment (100 μM, 24 h). (B) Quantification of TMEM165 protein expression in Hap1 control and SPCA1 KO cells and KO cells complemented with G309C-SPCA1 and D742Y-SPCA1, with or without chloroquine (CQ) treatment (100 μM, 24 h).

lysosomal subcellular localization of TMEM165 was observed after CQ treatment in all complemented SPCA1 KO Hap1 cells (data not shown). These results demonstrate that the level and subcellular Golgi localization of TMEM165 is not dependent on the Ca<sup>2+</sup> transport function of SPCA1 or its presence.

### TMEM165 stability depends on the Mn<sup>2+</sup> pumping function of SPCA1

Our previous results suggest that the stability of TMEM165 is dependent on SPCA1's ion transport function. It has been observed that TMEM165 and Gdt1p are degraded in response to high manganese concentration. We reason that SPCA1 mutants unable to transport Mn<sup>2+</sup> cause a Mn<sup>2+</sup> build-up and therefore TMEM165 degradation. This result converges with the observation that TMEM165 and Gdt1p are degraded in response to high Mn<sup>2+</sup> concentrations [20,21]. When cells were cultured in the presence of high Mn<sup>2+</sup>, a Mn-induced lysosomal degradation of TMEM165 was observed. To confirm this point, we took advantage of the Q747A-SPCA1 mutant identified to favor Mn<sup>2+</sup> transport [22]. Transient expression experiments were first performed in Hap1 SPCA1 KO cells (Figure 4A). As shown in Figure 4A, the transient expression of Q747A-SPCA1 fully rescues the abundance and the Golgi subcellular localization of TMEM165. We also observed co-localization between

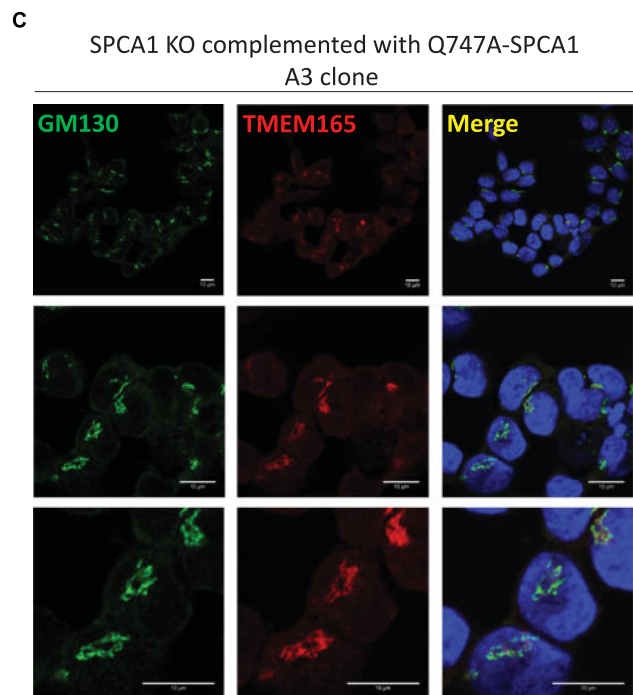
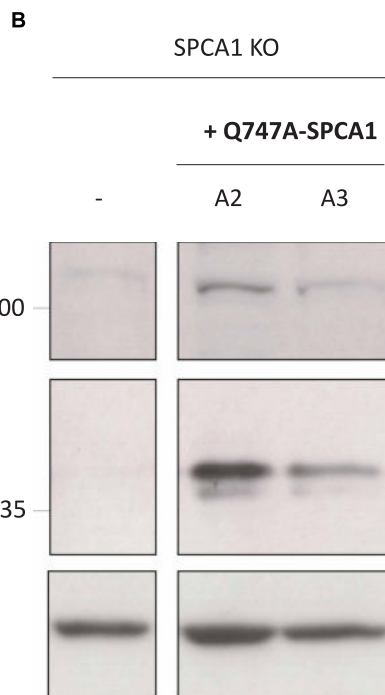
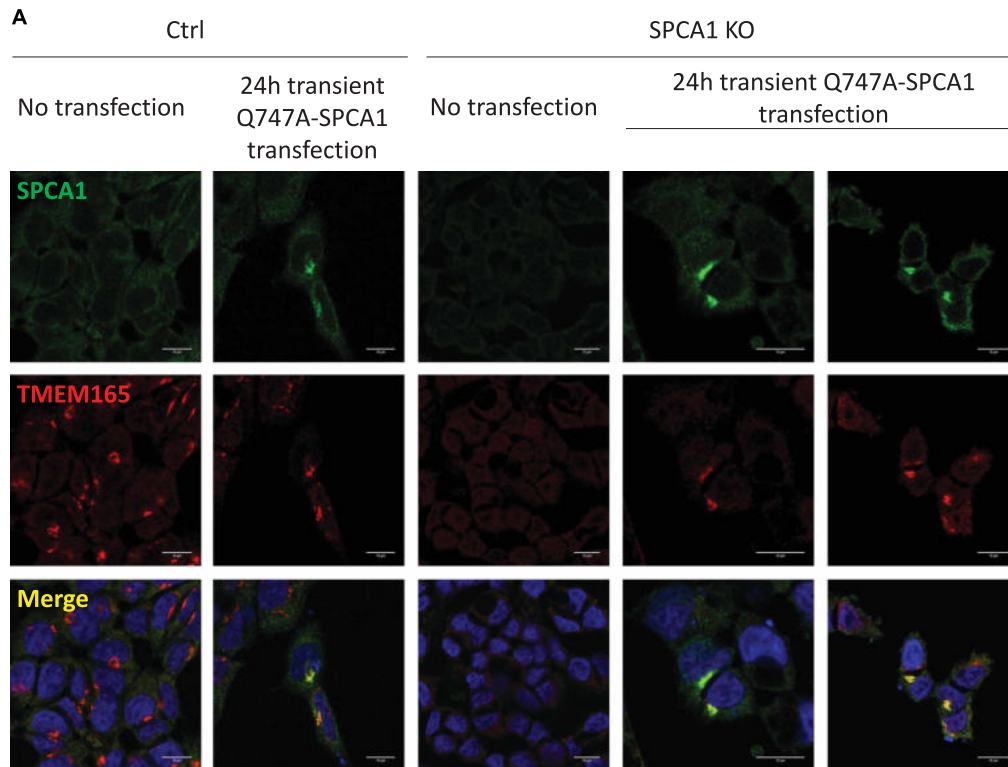


**Figure 4. Q747A-SPCA1 expression stabilizes TMEM165 expression.**

Part 1 of 2

(A) Hap1 control and SPCA1 KO cells were transiently transfected with Q747A-SPCA1 for 24 h in IMDM supplemented with 10% FBS. Cells were then fixed, permeabilized and labeled with antibodies against TMEM165 and SPCA1 before confocal microscopy visualization. DAPI staining (blue) was performed, showing nuclei. Scale bars, 10  $\mu$ m. (B) Hap1 SPCA1 KO cells were transfected with Q747A-SPCA1 for 24 h in IMDM supplemented with 10% FBS. Cells were diluted ten times in culture medium containing 0.5  $\mu$ g/ml puromycin as the selective agent and cultured for several days. Four polyclonal populations were then screened by Western blot. Total cell lysates were prepared, subjected to SDS-PAGE and Western blot

with the indicated antibodies. (C) Immunofluorescence analysis of A3 clone. Cells were fixed, permeabilized and labeled with antibodies against TMEM165 and GM130 before confocal microscopy visualization. DAPI staining (blue) was performed, showing nuclei. Scale bars, 10  $\mu\text{m}$ .

---

TMEM165 and SPCA1 in both control and SPCA1 KO cells reconstituted with Q747A-SPCA1. In non-transfected cells, the Golgi subcellular localization of SPCA1 was not observed possibly due to low antibody sensitivity. These results were then confirmed in Hap1 cells stably expressing Q747A-SPCA1 mutant. Western blot experiments showed rescued protein levels of TMEM165 in two different tested clones (A2, A3) compared with SPCA1 KO cells (Figure 4B). Additionally, immunofluorescence experiments of the A3 clone confirmed TMEM165's subcellular Golgi localization (Figure 4C). These results link the stability of TMEM165 to SPCA1's function in pumping  $\text{Mn}^{2+}$  from the cytosol into the Golgi lumen and highlight TMEM165's sensitivity to high cytosolic manganese concentrations.

We then exploited our recent results demonstrating the involvement of the sarco/endoplasmic reticulum  $\text{Ca}^{2+}$ -ATPase (SERCA) pumps in the rescue of the Golgi N-glycosylation defects in TMEM165 KO cells by extracellular  $\text{Mn}^{2+}$  [23]. The hypothesis underlying this result strongly suggested that SERCA pumps were capable to pump  $\text{Mn}^{2+}$  from the cytosol to the ER lumen. In line with this, we then wondered whether an over-expression of SERCA in KO SPCA1 cells could rescue the abundance and Golgi subcellular localization of TMEM165 by decreasing the cytosolic Mn accumulation. To address this point, HeLa SPCA1 KO cells were used to transiently overexpressed SERCA2b. As shown in Figure 5A, the transient expression of SERCA2b in HeLa SPCA1 KO cells rescues the abundance of TMEM165. Immunofluorescence experiments were then performed in order to confirm the Western blot results. We showed that TMEM165 Golgi subcellular localization is specifically rescued in cells overexpressing SERCA2b (Figure 5B).

## Proximity between TMEM165 and SPCA1

To evaluate a potential interaction between SPCA1 and TMEM165, proximity ligation assays (PLA) using Hap1 control cells and SPCA1 KO cells as negative controls were performed. Endogenous interactions of TMEM165 with SPCA1 were clearly visible in control cells with an average of 35 dots per cell; however, the interaction was strongly reduced in SPCA1 KO cells (Figure 6). This result suggests a potential interaction between TMEM165 and SPCA1 or at least their close localization since both proteins reside in the Golgi compartment.

## Discussion

The regulation of  $\text{Mn}^{2+}$  homeostasis in the secretory pathway is fundamental as many ER/Golgi glycosyltransferases are  $\text{Mn}^{2+}$  dependent [24]. The underlying molecular mechanisms involved in such regulation are not completely understood. Our previous work uncovered a role for TMEM165, a member of the Uncharacterized Protein Family 0016 (UPF0016), in Golgi  $\text{Mn}^{2+}$  homeostasis [12]. Defects in TMEM165 and its yeast ortholog Gdt1p have been shown to be associated with strong Golgi glycosylation abnormalities [20]. Furthermore, the stability of both proteins is dependent on  $\text{Mn}^{2+}$  ion levels as high  $\text{Mn}^{2+}$  concentration targets them for degradation in lysosomes (TMEM165) or vacuoles (Gdt1p) [21,25]. Another Golgi protein is known to be involved in  $\text{Ca}^{2+}/\text{Mn}^{2+}$  pumping named SPCA1 (Secretory pathway  $\text{Ca}^{2+}$ -ATPase pump type 1). In this paper, we investigated the functional link between TMEM165 and SPCA1. We demonstrate that TMEM165 expression was dependent on SPCA1 as a lack of SPCA1 led to a nearly complete loss of TMEM165. TMEM165 was localized to and specifically degraded in lysosomes of SPCA1-deficient cells, which could be stabilized by the lysosomotropic agent CQ. Complementation studies showed that TMEM165 abundance was dependent on the ion pumped by SPCA1, specifically  $\text{Mn}^{2+}$ . Among SPCA1 mutants, only the Q747A mutant, which exhibits an enhanced  $\text{Mn}^{2+}$  pumping activity, fully rescued TMEM165 stability and Golgi subcellular localization. Two other SPCA1 mutants, G309C which blocks  $\text{Mn}^{2+}$  but not  $\text{Ca}^{2+}$  pump activity and D742Y that alters both  $\text{Ca}^{2+}$  and  $\text{Mn}^{2+}$  binding [19] did not rescue the stability of TMEM165. These results are in strong concordance with the observed  $\text{Mn}^{2+}$  sensitivity of TMEM165 and its lysosomal targeting at high  $\text{Mn}^{2+}$  culture conditions [21]. It is possible that the lack of SPCA1 results in cytosolic manganese accumulation, which then mimicks conditions where cells are exposed to high extracellular manganese concentrations. These results suggest that the stability

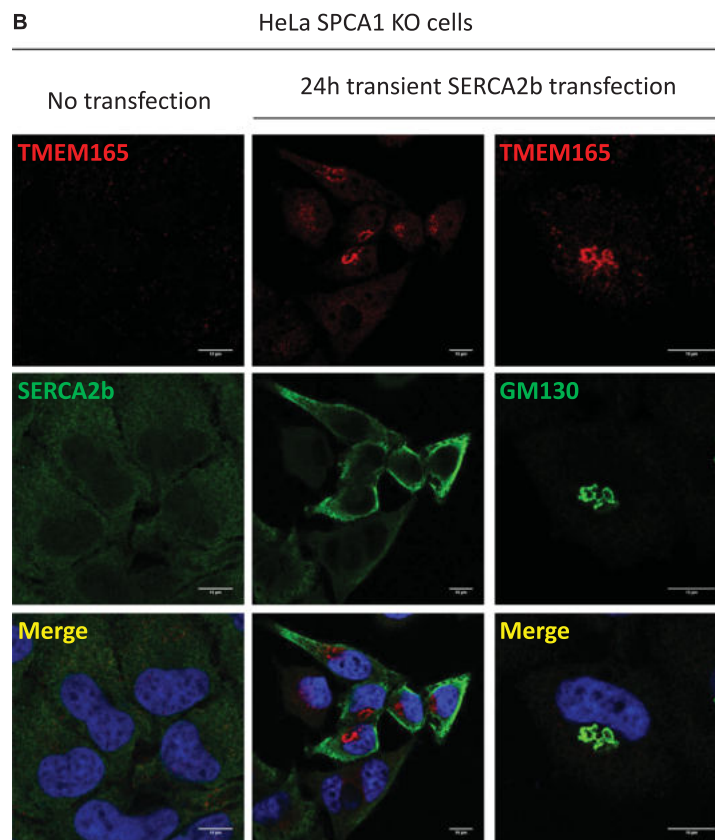
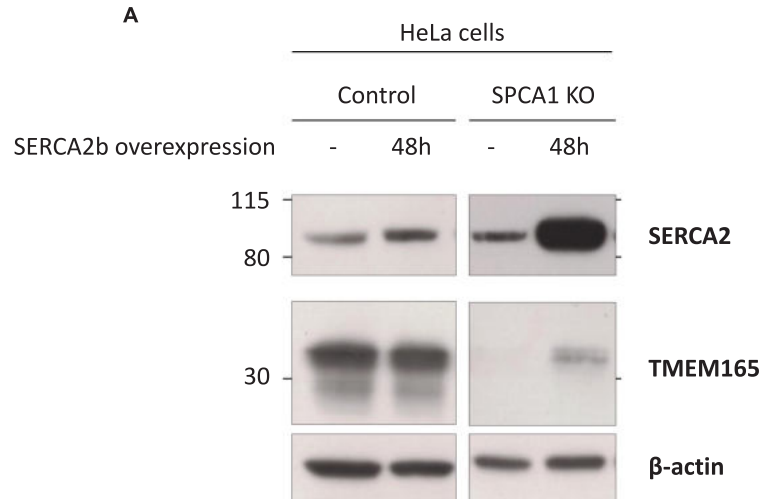


**Figure 5. TMEM165 expression is rescued in the Golgi apparatus when overexpressing SERCA2b in HeLa SPCA1 KO cells.**

(A) HeLa control and SPCA1 KO cells were transiently transfected with SERCA2b for 48 h. Total cell lysates were prepared, subjected to SDS-PAGE and Western blot with the indicated antibodies. (B) Subcellular localization of TMEM165 in HeLa SPCA1 KO cells overexpressing SERCA2b. Cells were fixed, permeabilized and labeled with antibodies against TMEM165, SERCA2 and GM130 before confocal microscopy visualization. DAPI staining (blue) was performed, showing nuclei. Scale bars, 10  $\mu$ m.

A

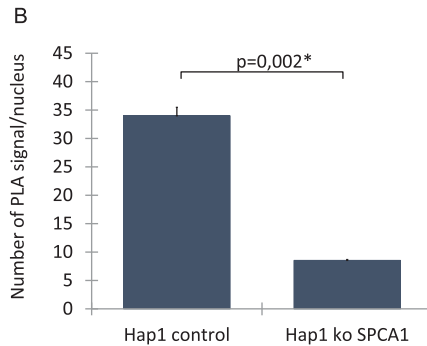
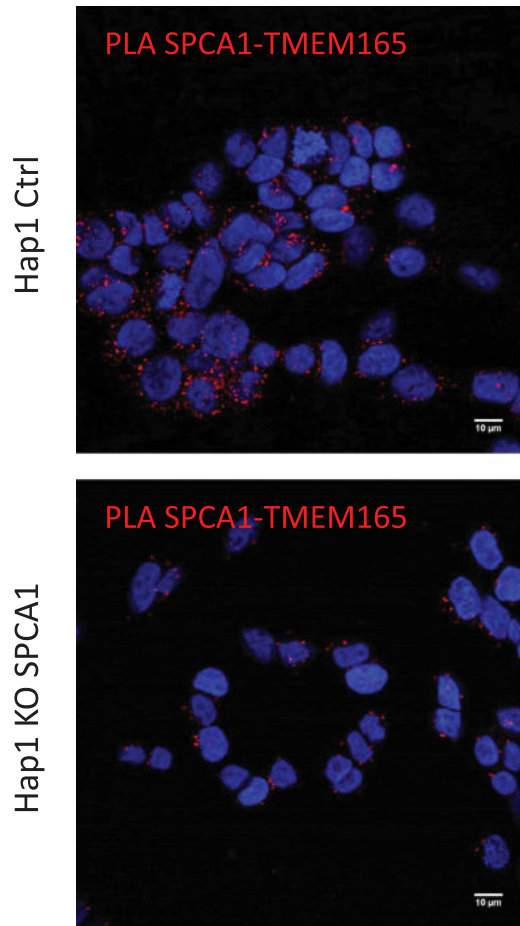


**Figure 6. A. Representative image of Proximity Ligation Assay of protein–protein proximity between TMEM165 and SPCA1.**

(A) Hap1 control and SPCA1 KO cells were stained with anti-TMEM165 rabbit polyclonal antibody 1 : 100 and anti-SPCA1 mouse polyclonal antibody 1 : 100. Each red dot represents a positive signal of protein–protein interaction and nuclei were counterstained with DAPI (blue). (B) Quantification of the red dots per nucleus in Hap1 control versus SPCA1 KO cells ( $N = 2$ , 100 cells analyzed).

of TMEM165 may depend on cytosolic  $Mn^{2+}$  ion changes rather than luminal changes in the Golgi. The manganese sensitive region(s) of TMEM165 have not been identified. TMEM165 possesses two highly conserved consensus motifs; an E-x-G-D-K-T motifs facing the cytosol and an E-x-G-D-R-S-Q motif exposed in the Golgi lumen, both predicted to be implicated in the transport function of UPF0016 members [12,16]. While the exact functions of these two motifs in Golgi glycosylation and  $Mn^{2+}$  ion sensitivity are not yet clear, previous work indicated that the E108G TMEM165-CDG mutant [16,25] was resistant to manganese supplementation. As this acidic amino acid is present in the first conserved motif, it seems likely that the E-x-G-D-K-T motif facing the cytosol plays a role in the  $Mn^{2+}$  ion sensitivity of TMEM165.

The importance of TMEM165 in Golgi glycosylation has been established in humans, yeast and mammalian cells. Strong Golgi glycosylation defects are observed when TMEM165 is absent [8]. Interestingly, this is not the case for SPCA1 KO cells. The molecular mechanisms by which SPCA1 KO cells maintain their apparent glycosylation is not understood. This could be linked to recent observations that in absence of TMEM165, glycosylation defects are rescued by exogenous  $Mn^{2+}$  and involve SERCA pump activity [23]. In SPCA1-deficient cells, it is likely that cytosolic  $Mn^{2+}$  accesses the Golgi via the activity of SERCA pumps. Given SERCA pumps do not transport  $Mn^{2+}$  as efficiently as SPCA1, we can't exclude the fact that other mechanisms may compensate for a lack of  $Mn^{2+}$  transport via SPCA1.

Additionally, it is well known that SPCA1 is involved in manganese detoxification when cells are exposed to high manganese concentrations [6]. This process is considered to be essential by decreasing cytosolic manganese concentrations, which would otherwise impair many cytosolic processes by competing with other divalent ions. Our results reinforce a model in which both SPCA1 and TMEM165 participate in manganese detoxification. According to recent studies, the direction of  $Mn^{2+}$  transport is the same for these two proteins [15]. As such, TMEM165 could act in concert with SPCA1 to conduct detoxification. The question of why TMEM165 is degraded during cytosolic manganese accumulation remains open. It is likely that the transport function of TMEM165 is yet to be fully elucidated. Some results suggest that TMEM165 might function as an antiporter using a Golgi luminal ion gradient (where the counter ion can be  $Ca^{2+}$ ,  $H^+$  or Pi) to either import  $Mn^{2+}$  and/or  $Ca^{2+}$  to the Golgi lumen [2,18]. The degradation of TMEM165 could be required to prevent the collapse of a Golgi luminal gradient essential for maintaining other critical Golgi functions. As secondary transporters exhibit a high capacity for transport with low ion affinity, it is likely that TMEM165 could also work in reverse. In this scenario, the degradation of TMEM165 would prevent the accumulation of  $Mn^{2+}$  in the Golgi lumen due to the activity of SPCA1. The observed proximity of TMEM165 and SPCA1 might be important for regulating their activities. This unambiguously demonstrates the role of these two proteins in the regulation of Ca and Mn cellular homeostasis.

In conclusion, our results reveal a functional link between TMEM165 and SPCA1 thereby opening new concepts in  $Ca^{2+}/Mn^{2+}$  Golgi homeostasis regulation, crucial for many fundamental cellular processes such as protein secretion as well as glycosylation. There are indeed growing evidences pointing to dysfunctions of  $Ca^{2+}$  ATPase in colon, lung and breast cancers [26] and future directions in tumor progression and/or metabolic disease mechanisms must take into account the existence of this close link between TMEM165 and SPCA1.

### Abbreviations

ATP2C1, calcium-transporting ATPase type 2C member 1; BSA, bovine serum albumin; CDG, congenital disorders of glycosylation; CQ, chloroquine; DMEM, Dulbecco's modified eagle's medium; GPP130, Golgi phosphoprotein 4; IMDM, Iscove's modified Dulbecco's medium; LAMP2, lysosomal-associated membrane protein 2; Mn, manganese;  $Mn^{2+}$ , manganese, ion (2+);  $MnCl_2$ , manganese (II) chloride tetrahydrate; PAM71, photosynthesis affected mutant 71; PFA, paraformaldehyde; PLA, proximity ligation assay; RT, room temperature; SERCA, sarco/endoplasmic reticulum  $Ca^{2+}$ -ATPase; SPCA1, secretory pathway  $Ca^{2+}$ -ATPase 1; TBS, tris buffer saline; TGN46, *Trans*-Golgi network integral membrane protein 2; TMEM165, transmembrane protein 165; UPF, uncharacterized protein family.

### Author Contribution

Designed the experiments: E.L., M.H., A.K., F.F.; Performed the experiments: E.L., M.H., M.-A.K., D.V., K.K.; Analyzed the data: E.L., M.H., M.-A.K., H.-H.H., A.K. and F.F.; Wrote the paper: C.M.R., A.K. and F.F.

### Funding

This work was supported by grants from Agence Nationale de la Recherche (SOLV-CDG project to FF), EURO-CDG-2 that has received a funding from the European Union's Horizon 2020 research and innovation program under the ERA-NET Cofund action N° 643578 and within the scope of the International Associated Laboratory 'Laboratory for the Research on Congenital Disorders of Glycosylation – from cellular mechanisms to cure – GLYCOLAB4CDG'.

### Acknowledgements

We are indebted to Dr. Dominique Legrand for the Research Federation FRABio (Univ. Lille, CNRS, FR 3688, FRABio, Biochimie Structurale et Fonctionnelle des Assemblages Biomoléculaires) for providing the scientific and technical environment conducive to achieving this work. We thank the Bioluminescence Center of Lille, especially Christian Slomianny and Elodie Richard, for the use of the Leica LSM700 and the Leica LSM780.

### Competing Interests

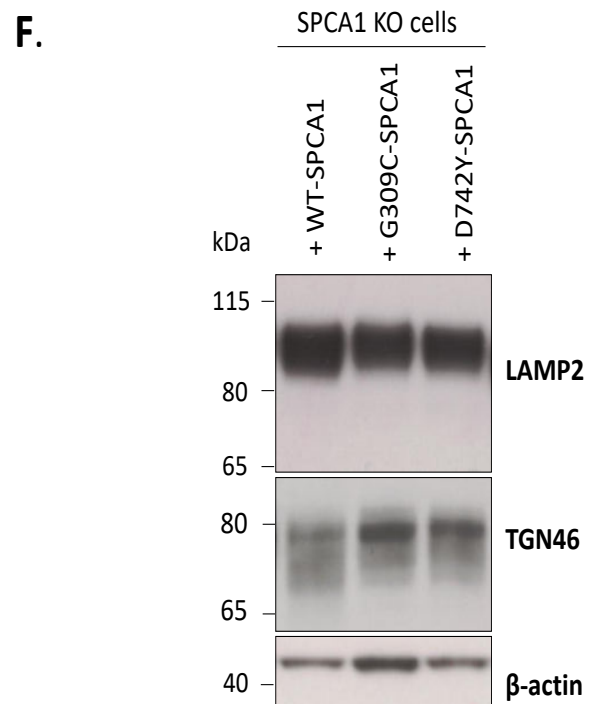
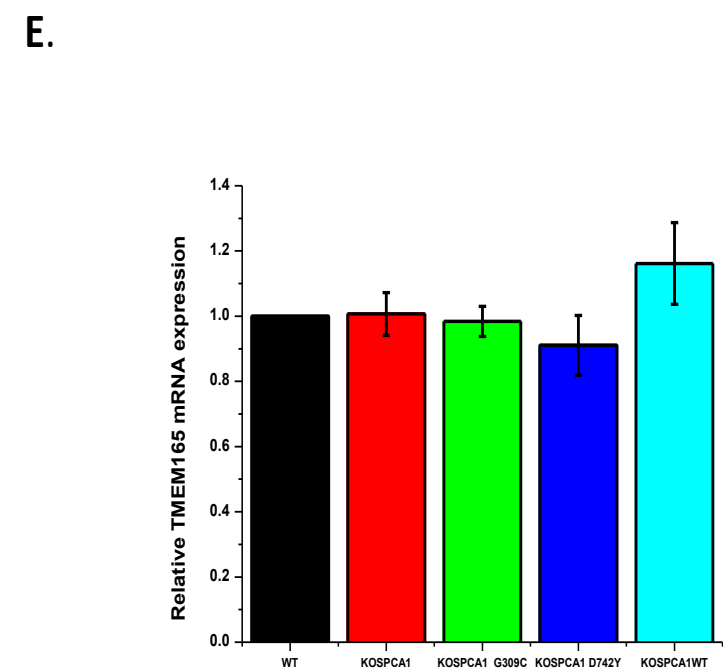
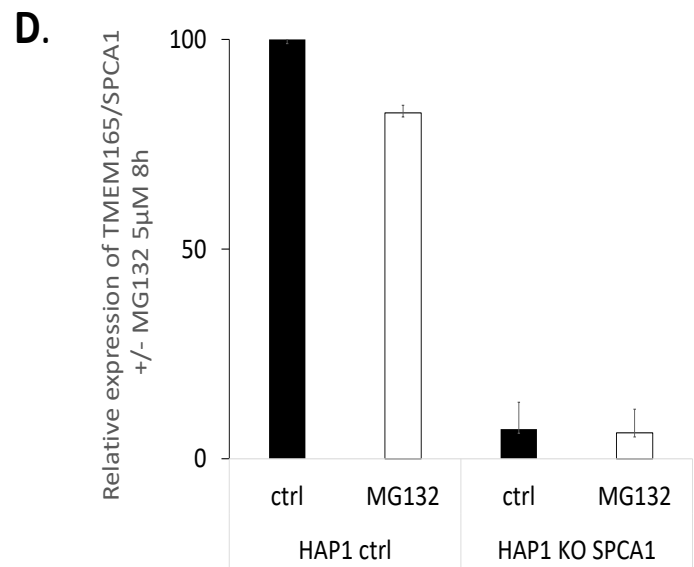
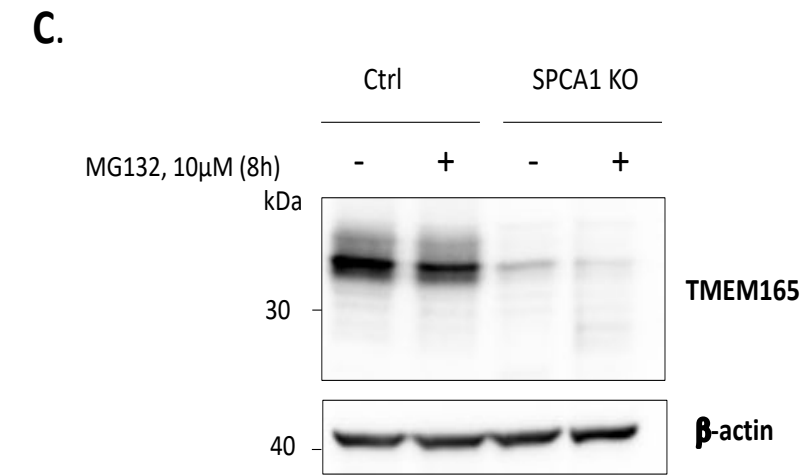
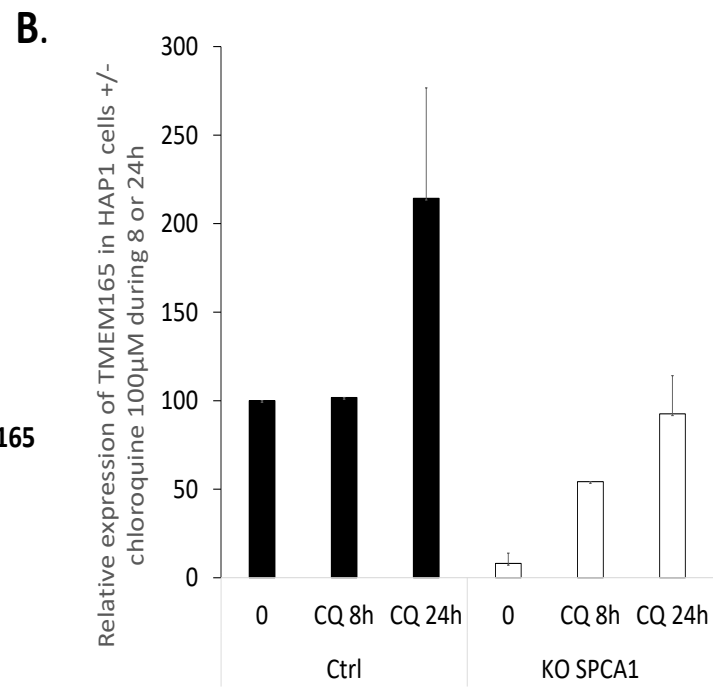
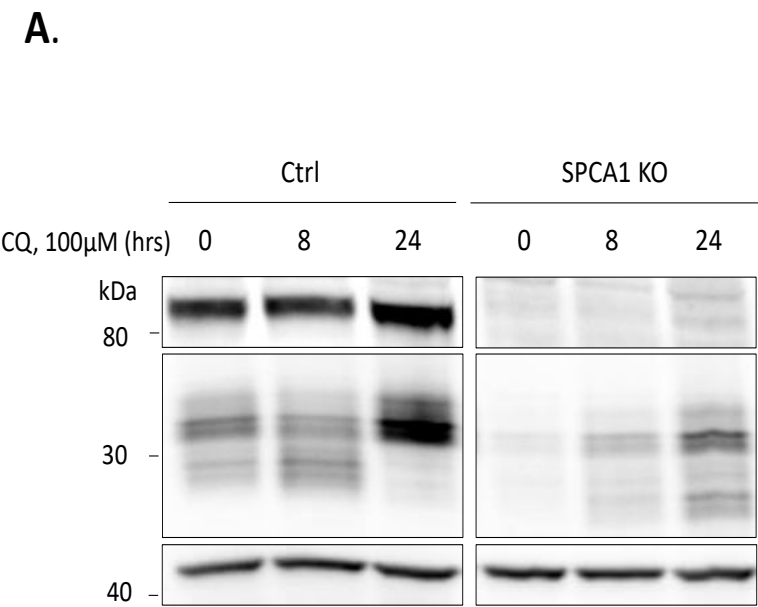
The Authors declare that there are no competing interests associated with the manuscript.

### References

- 1 Powell, J.T. and Brew, K. (1976) Metal ion activation of galactosyltransferase. *J. Biol. Chem.* **251**, 3645–3652 PMID:932001

- 2 Demaegd, D., Foulquier, F., Colinet, A.-S., Gremillon, L., Legrand, D., Mariot, P. et al. (2013) Newly characterized Golgi-localized family of proteins is involved in calcium and pH homeostasis in yeast and human cells. *Proc. Natl Acad. Sci. U.S.A.* **110**, 6859–6864 <https://doi.org/10.1073/pnas.1219871110>
- 3 Reinhardt, T.A., Lippolis, J.D. and Sacco, R.E. (2014) The Ca(2+)/H(+) antiporter TMEM165 expression, localization in the developing, lactating and involuting mammary gland parallels the secretory pathway Ca(2+) ATPase (SPCA1). *Biochem. Biophys. Res. Commun.* **445**, 417–421 <https://doi.org/10.1016/j.bbrc.2014.02.020>
- 4 Hu, Z., Bonifas, J.M., Beech, J., Bench, G., Shigihara, T., Ogawa, H. et al. (2000) Mutations in ATP2C1, encoding a calcium pump, cause Hailey–Hailey disease. *Nat. Genet.* **24**, 61–65 <https://doi.org/10.1038/71701>
- 5 Ton, V.-K., Mandal, D., Vahadji, C. and Rao, R. (2002) Functional expression in yeast of the human secretory pathway Ca<sup>2+</sup>, Mn<sup>2+</sup>-ATPase defective in Hailey–Hailey disease. *J. Biol. Chem.* **277**, 6422–6427 <https://doi.org/10.1074/jbc.M110612200>
- 6 Leitch, S., Feng, M., Muend, S., Braiterman, L.T., Hubbard, A.L. and Rao, R. (2011) Vesicular distribution of Secretory Pathway Ca<sup>2+</sup>-ATPase isoform 1 and a role in manganese detoxification in liver-derived polarized cells. *BioMetals* **24**, 159–170 <https://doi.org/10.1007/s10534-010-9384-3>
- 7 Guilarte, T.R. (2010) Manganese and Parkinson's disease: a critical review and new findings. *Environ. Health Perspect.* **118**, 1071–1080 <https://doi.org/10.1289/ehp.0901748>
- 8 Foulquier, F., Amyere, M., Jaeken, J., Zeevaert, R., Schollen, E., Race, V. et al. (2012) TMEM165 deficiency causes a congenital disorder of glycosylation. *Am. J. Hum. Genet.* **91**, 15–26 <https://doi.org/10.1016/j.ajhg.2012.05.002>
- 9 Jaeken, J. and Péanne, R. (2017) What is new in CDG? *J. Inher. Metab. Dis.* **40**, 569–586 <https://doi.org/10.1007/s10045-017-0050-6>
- 10 Zeevaert, R., de Zegher, F., Sturiale, L., Garozzo, D., Smet, M., Moens, M. et al. (2013) Bone dysplasia as a key feature in three patients with a novel congenital disorder of glycosylation (CDG) type II due to a deep intronic splice mutation in TMEM165. *JIMD Rep.* **8**, 145–152 [https://doi.org/10.1007/8904\\_2012\\_172](https://doi.org/10.1007/8904_2012_172)
- 11 Morelle, W., Potelle, S., Witters, P., Wong, S., Climer, L., Lupashin, V. et al. (2017) Galactose supplementation in patients with TMEM165-CDG rescues the glycosylation defects. *J. Clin. Endocrinol. Metab.* **102**, 1375–1386 <https://doi.org/10.1210/je.2016-3443>
- 12 Dulary, E., Potelle, S., Legrand, D. and Foulquier, F. (2017) TMEM165 deficiencies in congenital disorders of glycosylation type II (CDG-II): clues and evidences for roles of the protein in Golgi functions and ion homeostasis. *Tissue Cell* **49**, 150–156 <https://doi.org/10.1016/j.tice.2016.06.006>
- 13 Schneider, A., Steinberger, I., Herdean, A., Gandini, C., Eisenhut, M., Kurz, S. et al. (2016) The evolutionarily conserved protein PHOTOSYNTHESIS AFFECTED MUTANT71 is required for efficient manganese uptake at the thylakoid membrane in Arabidopsis. *Plant Cell* **28**, 892–910 <https://doi.org/10.1105/tpc.15.00812>
- 14 Brandenburg, F., Schoffman, H., Kurz, S., Krämer, U., Keren, N., Weber, A.P.M. et al. (2017) The *Synechocystis* manganese exporter Mnx is essential for manganese homeostasis in cyanobacteria. *Plant Physiol.* **173**, 1798–1810 <https://doi.org/10.1104/pp.16.01895>
- 15 Thines, L., Deschamps, A., Sengottaiyan, P., Savel, O., Stribny, J. and Morsomme, P.) The yeast protein Gdt1p transports Mn<sup>2+</sup> ions and thereby regulates manganese homeostasis in the Golgi. *J. Biol. Chem.* **293**, 8048–8055 <https://doi.org/10.1074/jbc.RA118.002324>
- 16 Colinet, A.-S., Sengottaiyan, P., Deschamps, A., Colsoul, M.-L., Thines, L., Demaegd, D. et al. (2016) Yeast Gdt1 is a Golgi-localized calcium transporter required for stress-induced calcium signaling and protein glycosylation. *Sci. Rep.* **6**, 24282 <https://doi.org/10.1038/srep24282>
- 17 Snyder, N.A., Stefan, C.P., Soroudi, C.T., Kim, A., Evangelista, C. and Cunningham, K.W. (2017) H<sup>+</sup> and Pi byproducts of glycosylation affect Ca<sup>2+</sup> homeostasis and are retrieved from the Golgi complex by homologs of TMEM165 and XPR1. *G3 (Bethesda)* **7**, 3913–3924 <https://doi.org/10.1534/g3.117.300339>
- 18 Dulary, E., Yu, S.-Y., Houdou, M., de Bettignies, G., Decool, V., Potelle, S. et al. (2018) Investigating the function of Gdt1p in yeast Golgi glycosylation. *Biochim. Biophys. Acta* **1862**, 394–402 <https://doi.org/10.1016/j.bbagen.2017.11.006>
- 19 Hoffmann, H.-H., Schneider, W.M., Blomen, V.A., Scull, M.A., Hovnanian, A., Brummelkamp, T.R. et al. (2017) Diverse viruses require the calcium transporter SPCA1 for maturation and spread. *Cell Host Microbe* **22**, 460–470.e5 <https://doi.org/10.1016/j.chom.2017.09.002>
- 20 Potelle, S., Morelle, W., Dulary, E., Duvet, S., Vicogne, D., Spriet, C. et al. (2016) Glycosylation abnormalities in Gdt1p/TMEM165 deficient cells result from a defect in Golgi manganese homeostasis. *Hum. Mol. Genet.* **25**, 1489–1500 <https://doi.org/10.1093/hmg/ddw026>
- 21 Potelle, S., Dulary, E., Climer, L., Duvet, S., Morelle, W., Vicogne, D. et al. (2017) Manganese-induced turnover of TMEM165. *Biochem. J.* **474**, 1481–1493 <https://doi.org/10.1042/BCJ20160910>
- 22 Mukhopadhyay, S. and Linstedt, A.D. (2011) Identification of a gain-of-function mutation in a Golgi P-type ATPase that enhances Mn<sup>2+</sup> efflux and protects against toxicity. *Proc. Natl Acad. Sci. U.S.A.* **108**, 858–863 <https://doi.org/10.1073/pnas.1013642108>
- 23 Houdou, M., Lebretonchel, E., Garat, A., Duvet, S., Legrand, D., Decool, V. et al. (2019) Involvement of thapsigargin- and cyclopiazonic acid-sensitive pumps in the rescue of TMEM165-associated glycosylation defects by Mn<sup>2+</sup>. *FASEB J.* **33**, 2669–2679 <https://doi.org/10.1096/fj.201800387R>
- 24 Audry, M., Jeanneau, C., Imbert, A., Harduin-Lepers, A., Delannoy, P. and Breton, C. (2011) Current trends in the structure-activity relationships of sialyltransferases. *Glycobiology* **21**, 716–726 <https://doi.org/10.1093/glycob/cwq189>
- 25 He, W. and Hu, Z. (2012) The role of the Golgi-resident SPCA Ca<sup>2+</sup>/Mn<sup>2+</sup> pump in ionic homeostasis and neural function. *Neurochem. Res.* **37**, 455–468 <https://doi.org/10.1007/s11064-011-0644-6>
- 26 Dang, D. and Rao, R. (2016) Calcium-ATPases: gene disorders and dysregulation in cancer. *Biochim. Biophys. Acta* **1863**, 1344–1350 <https://doi.org/10.1016/j.bbamcr.2015.11.016>

# Supp Fig. 1





### 4.3. Complementary results

In this study we strongly emphasized that the lack of SPCA1 leads to cytosolic Mn<sup>2+</sup> build-up responsible for the constitutive lysosomal degradation of TMEM165. To strengthen this hypothesis, we took advantage of the results obtained in TMEM165 KO HEK cells linking the severity of the glycosylation defects to Mn levels in the FBS used in cell culture (Paper 2, [509]) and then wondered whether an extremely low Mn FBS level was sufficient to spontaneously rescue the abundance of TMEM165 in absence of SPCA1. To tackle this point, control and SPCA1 KO cells were cultured for several weeks using two different FBS with either high (FBS2, 1.08μM Mn) or low (FBS4, 0.61μM Mn) Mn levels, as quantified in Paper 2 [509]. Every week, cells were harvested and immunofluorescence was performed at different passages (P2, P5 and P8) (Figure 66).

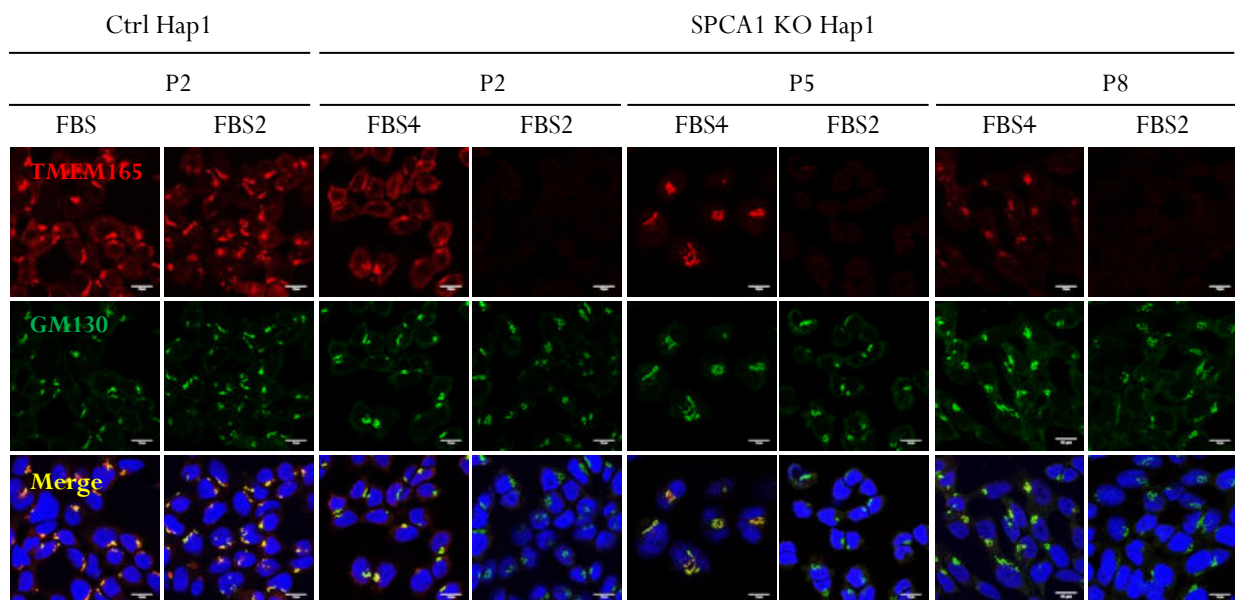


**Figure 66: In SPCA1 KO cells, TMEM165 expression depends on the FBS used for cell culture.** Control (Ctrl) and SPCA1 KO Hap1 cells were cultured in IMDM supplemented with either 10% FBS2 or 10% FBS4 for several passages. Cells were then fixed, permeabilized and labeled with antibodies against TMEM165 and GM130 before confocal microscopy visualization. DAPI staining (blue) was performed, showing nuclei. Scale bars, 10μm.

While no expression of TMEM165 was detected with FBS2, a clear recovery of TMEM165 in the Golgi apparatus was observed with FBS4. This result demonstrates that Mn level in the FBS stabilizes TMEM165 in SPCA1 deficient cells and reinforce the functional link between SPCA1, TMEM165 and Mn pressure. Culturing cells with a low Mn content FBS implies that cytosolic Mn<sup>2+</sup> may be more diluted through cell divisions and passages whereas a higher extracellular Mn level would rather promote Mn<sup>2+</sup> entry and accumulation which is detrimental for the stability of TMEM165.

## 4.4. Conclusion

This study shed light on very interesting concepts linking the functions of three proteins involved in  $\text{Ca}^{2+}/\text{Mn}^{2+}$  intracellular homeostasis: TMEM165, SPCA1 and SERCA2.

### 4.5.1. Link between TMEM165, SPCA1, SERCA2 and cytosolic $\text{Mn}^{2+}$ pressure

In this paper, we highlighted that TMEM165 protein expression level and Golgi subcellular localization were dependent on SPCA1 ability to import cytosolic  $\text{Mn}^{2+}$  into the Golgi lumen. In the model presented in Figure 67, we assumed that the lack of SPCA1 results in a rather high cytosolic  $[\text{Mn}^{2+}]$  accumulation responsible for the constitutive  $\text{Mn}^{2+}$ -induced lysosomal degradation of TMEM165.

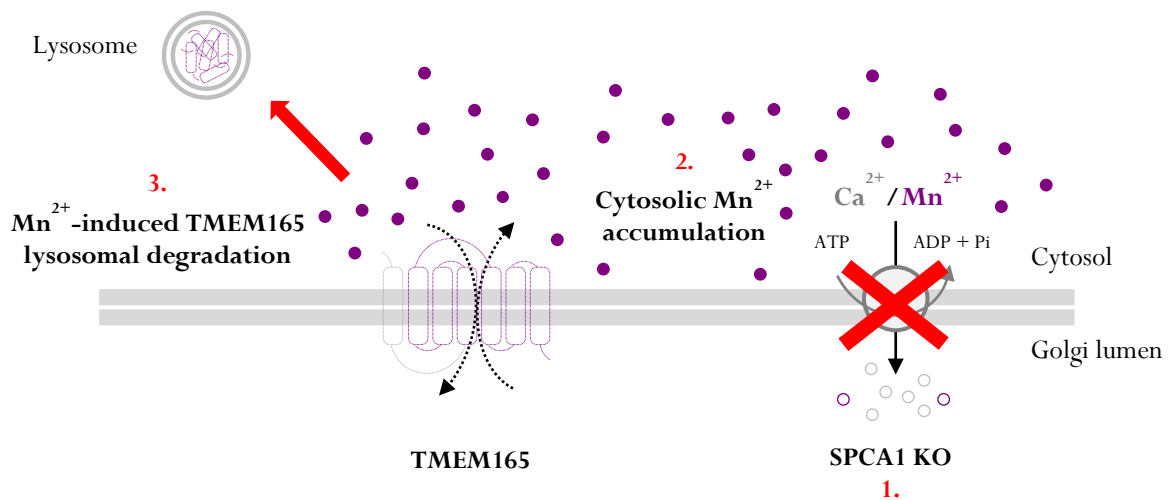


**Figure 67: Model of  $\text{Mn}^{2+}$ -induced TMEM165 lysosomal degradation due to a lack of SPCA1.** We reasoned that SPCA1 KO (1.) leads to higher cytosolic  $\text{Mn}^{2+}$  accumulation (2.) which is detrimental to TMEM165 by promoting its lysosomal degradation induced by elevated cytosolic  $[\text{Mn}^{2+}]$  (3.).

As already described in Chapter 3, previous works of the team have characterized TMEM165 as a new Golgi  $\text{Mn}^{2+}$  sensor being rapidly degraded *via* a still unclear lysosomal degradation pathway [307]. Here, we demonstrated that TMEM165 is specifically addressed into the lysosomes in case of SPCA1 deficiency which could be stabilized by the lysosomotropic agent chloroquine. In addition, several lines of evidence strengthen this statement. First, TMEM165 abundance and subcellular localization are only recovered in SPCA1 deficient cells complemented with a form of SPCA1 able to import  $\text{Mn}^{2+}$  into the Golgi lumen (*i.e.* SPCA1-WT and SPCA1-Q747A). Hence, cytosolic  $\text{Mn}^{2+}$  transport into the Golgi would lower cytosolic  $[\text{Mn}^{2+}]$  until a “TMEM165 sensitive threshold” preventing its lysosomal degradation. Second, by overexpressing SERCA2b in SPCA1 KO cells, we demonstrated that TMEM165 abundance was also recovered. In this case, we assumed that SERCA2 would decrease the overall cytosolic  $[\text{Mn}^{2+}]$  accumulation by pumping  $\text{Mn}^{2+}$  into the ER and further redistribution within the detoxification pathway. This finding is directly related to our first publication (Paper 1, [231]) in which we highlighted that likely SERCA2 pumps could transport cytosolic  $\text{Mn}^{2+}$  ions into the ER to

sustain Golgi glycosylation reactions. Third, as mentioned in Complementary results (4.3), Mn levels in the FBS stabilize TMEM165 in SPCA1 KO Hap1 cells suggesting that a higher Mn pressure applied to the cells would induce TMEM165 degradation. All in all, these three pathways leading to TMEM165 recovery in SPCA1 KO cells are summarized in Figure 68.

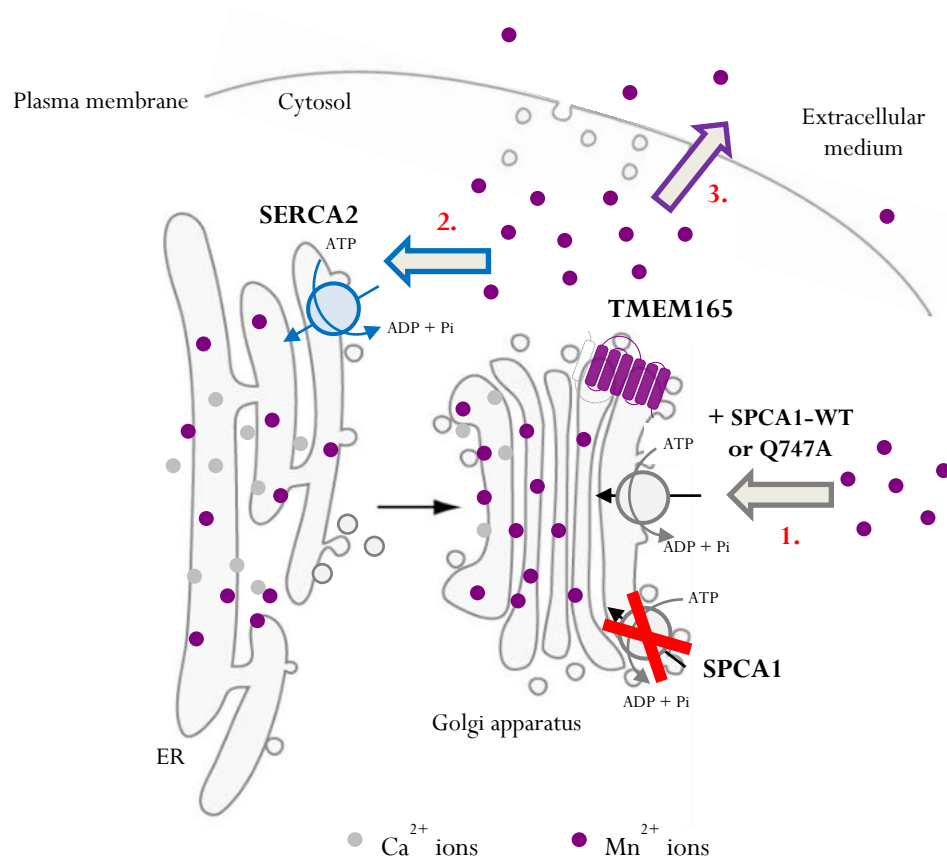


**Figure 68: How to rescue TMEM165 abundance and Golgi subcellular localization in SPCA1 KO cells?** This scheme represents three pathways (1., 2. and 3.) identified in our study enabling TMEM165 stabilization/recovery. **1.** Complementation of SPCA1 deficient cells with a form of SPCA1 able to transport Mn<sup>2+</sup> (-WT or - Q747A), **2.** Overexpression of SERCA2b in SPCA1 deficient cells and **3.** Culturing SPCA1 deficient cells with a low Mn content FBS.

#### 4.5.2. TMEM165 as a new Golgi localized cytosolic Mn<sup>2+</sup> sensor

The hypothesis according to which TMEM165 would be a Golgi localized cytosolic Mn<sup>2+</sup> sensor originates from the antagonist results we obtained on TMEM165 and GPP130 stabilities upon MnCl<sub>2</sub> treatment (500μM, up to 8h) in SPCA1 KO and complemented Hap1 cells. As a reminder, GPP130 is a *cis*-Golgi protein well characterized by Linstedt's group over the past twenty years [257,499,500,518] as an intraluminal Golgi Mn sensor. Upon extracellular Mn exposure, GPP130 exits the Golgi apparatus through the TGN and traffics to multivesicular bodies (MVBs) where the protein is internalized into intraluminal vesicles for subsequent degradation by lysosomal hydrolases [499]. It has been shown that Mn<sup>2+</sup> responsiveness of GPP130 occurs through its luminal stem domain that needs to be specifically targeted to the *cis*-Golgi [257,499]. Here, we corroborated GPP130 luminal sensitivity to Mn<sup>2+</sup> and further highlighted cytosolic Mn<sup>2+</sup> sensitivity for TMEM165. Indeed, while TMEM165 is constitutively degraded in SPCA1 KO Hap1 cells and undergoes similar Mn<sup>2+</sup>-induced degradation kinetics upon MnCl<sub>2</sub> exposure in control and SPCA1 KO Hap1 cells complemented with SPCA1-WT, the lack of SPCA1 or the reconstitution of SPCA1 deficient cells with either SPCA1-G309C or -D742Y prevents GPP130 degradation which protein levels remain quite stable. Mn<sup>2+</sup> effect on GPP130 stability was only observed in control and SPCA1 KO Hap1 cells complemented with SPCA1-WT.

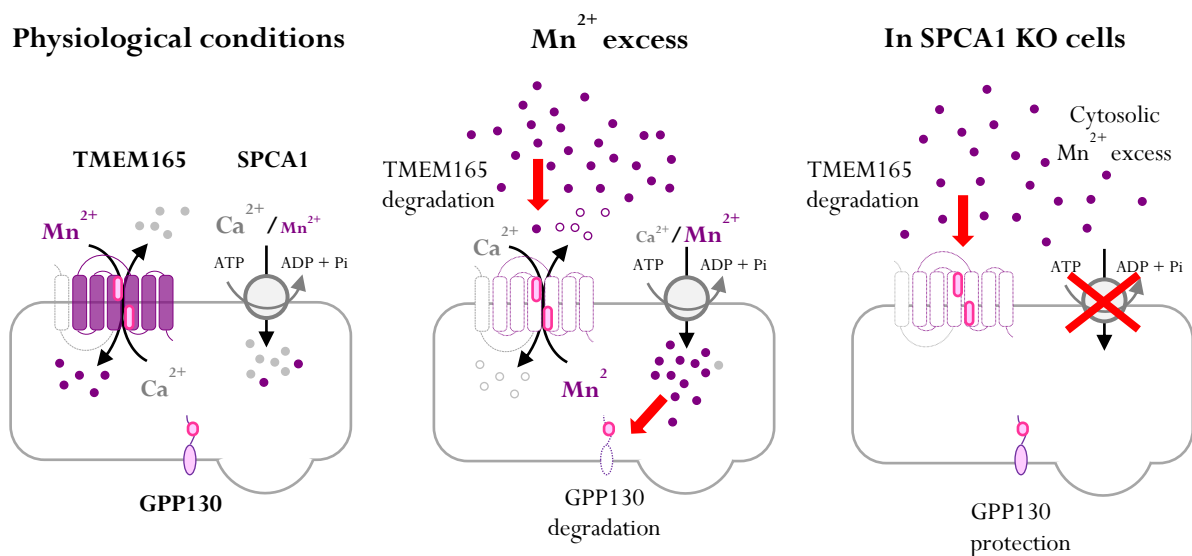


**Figure 69: TMEM165 and GPP130 stabilities towards cytosolic or intraluminal Mn<sup>2+</sup> excess.** Pink shapes on TMEM165 and GPP130 symbolize the Mn<sup>2+</sup> sensitive domains of each protein.

In other words, when SPCA1 can pump cytosolic Mn<sup>2+</sup>, degradation of GPP130 is induced whereas TMEM165 protein expression is recovered. The other way around, when SPCA1 is lacking or unable to import Mn<sup>2+</sup> into the Golgi lumen, GPP130 is protected from Mn<sup>2+</sup>-induced degradation whereas TMEM165 is subjected to constitutive lysosomal degradation. All in all, TMEM165 and GPP130 are two Golgi localized Mn<sup>2+</sup> responsive proteins with TMEM165 being sensitive to cytosolic accumulation

of  $Mn^{2+}$  while GPP130 senses intraluminal  $Mn^{2+}$  accumulation. This concept is summarized in Figure 69. Given the specificity of each protein to sense cytosolic or luminal accumulation of  $Mn^{2+}$  and the previous identification of GPP130 luminal stem region as its Mn sensitive domain, we then wondered whether  $Mn^{2+}$  sensitive domain(s) of TMEM165 would face the cytosol. To answer this question, a whole study has been conducted in the team in which I contributed leading to a publication [477] (Appendix II) that will not be further described here.

#### 4.5.3. No glycosylation defects associated to SPCA1 and subsequent TMEM165 deficiencies

The main achievement from this study conducted in SPCA1 KO cells was to reveal the constitutive lysosomal degradation of TMEM165 in absence of SPCA1. We then wondered whether a glycosylation defect could be observed in those cells since TMEM165 deficiency leads to strong Golgi glycosylation abnormalities ([64,65,506,509] and Paper 1, [231]). Remarkably and as presented in Figure 1D and supplementary Figure 1F of Paper 4, no change in the electrophoretic migrations of LAMP2 and TGN46 were observed in SPCA1 KO cells complemented or not, reflecting no glycosylation defects for these two proteins. Thus, the lack of SPCA1 and subsequently those of TMEM165 did not lead to major glycosylation alterations suggesting that Golgi  $Mn^{2+}$  levels are sufficient to sustain glycosylation reactions in case of both SPCA1 and TMEM165 deficiencies. Nonetheless, how can we explain that severe glycosylation defects are observed in TMEM165 KO cells whereas it is not the case in SPCA1 KO cells lacking TMEM165 expression? This question will be further addressed in the following section in which unpublished data will be provided to strengthen our suggested hypothesis.



---

## **General discussion and perspectives on Part II**

---





Given the two studies in either yeast *Saccharomyces cerevisiae* or mammalian cells, our work shed light on a conserved functional link between Gdt1p/TMEM165 and Pmr1p/SPCA1 in Golgi glycosylation and/or in the regulation of Golgi  $\text{Ca}^{2+}$  and  $\text{Mn}^{2+}$  homeostasis. In case of TMEM165/Gdt1p deficiency, we demonstrated that Golgi  $\text{Mn}^{2+}$  homeostasis was likely controlled by the activity of SERCA pumps in mammals and those of Pmr1p in yeasts. These fundamental differences in the regulation of Golgi ion homeostasis pinpoint intrinsic differences between yeast and humans, especially because yeasts do not express any SERCA orthologs. Therefore, it is conceivable that during evolution, Pmr1p acquired a specialized function in  $\text{Mn}^{2+}$  import into the Golgi lumen to prevent Golgi glycosylation abnormalities. Conversely, in mammals, SPCA1 may have evolved as the main Golgi  $\text{Ca}^{2+}$  importer and TMEM165, as the main Golgi  $\text{Mn}^{2+}$  importer. Hence, in case of TMEM165 deficiency, SPCA1 fails to rescue Golgi glycosylation defects caused by a disrupted Golgi  $\text{Mn}^{2+}$  homeostasis but SERCA2 pumps become essential in the uptake and further redistribution of cytoplasmic  $\text{Mn}^{2+}$  to the Golgi apparatus. If this SERCA2-dependent mechanism occurs in TMEM165 KO cells, it should also happen in SPCA1 KO cells since the absence of SPCA1 causes TMEM165 deficiency.

### **1. Involvement of likely SERCA pumps in Golgi glycosylation maintenance in SPCA1 deficient cells lacking TMEM165 expression**

To test whether SERCA pumps play a role in Golgi glycosylation maintenance in SPCA1 deficient cells, control and SPCA1 KO HeLa and Hap1 cells were treated with 50nM thapsigargin for 24h. Interestingly, as shown in Figure 70, thapsigargin treatment induces a huge glycosylation defect on LAMP2 in both SPCA1 KO cell lines. This result highly suggests the involvement of SERCA2-like proteins in Golgi glycosylation maintenance in SPCA1 KO Hap1 cells lacking TMEM165 protein expression. Assuming that thapsigargin does not impact LAMP2 electrophoretic migration profile in control cells, we then wondered whether SPCA1 or TMEM165 could overcome SERCA2 inhibition. Previous thapsigargin treatment was re-performed in all Hap1 cells including control, SPCA1 KO and complemented cells with -WT, -G309C and -D742Y. This time, both LAMP2 and TGN46 migration profiles were assessed (Figure 71). In Figure 71, very similar results are obtained between control, SPCA1 KO and SPCA1 KO Hap1 cells complemented with the inactive form of SPCA1 (-D742Y) or its predominantly  $\text{Ca}^{2+}$  pumping form (-G309C). However, in SPCA1 KO cells complemented with SPCA1-WT, thapsigargin treatment does not induce any glycosylation defect on both LAMP2 and TGN46. It is to note that the only difference between the functionality of SPCA1-WT and -G309C lies in the ability for the WT form to import  $\text{Mn}^{2+}$  into the Golgi lumen.

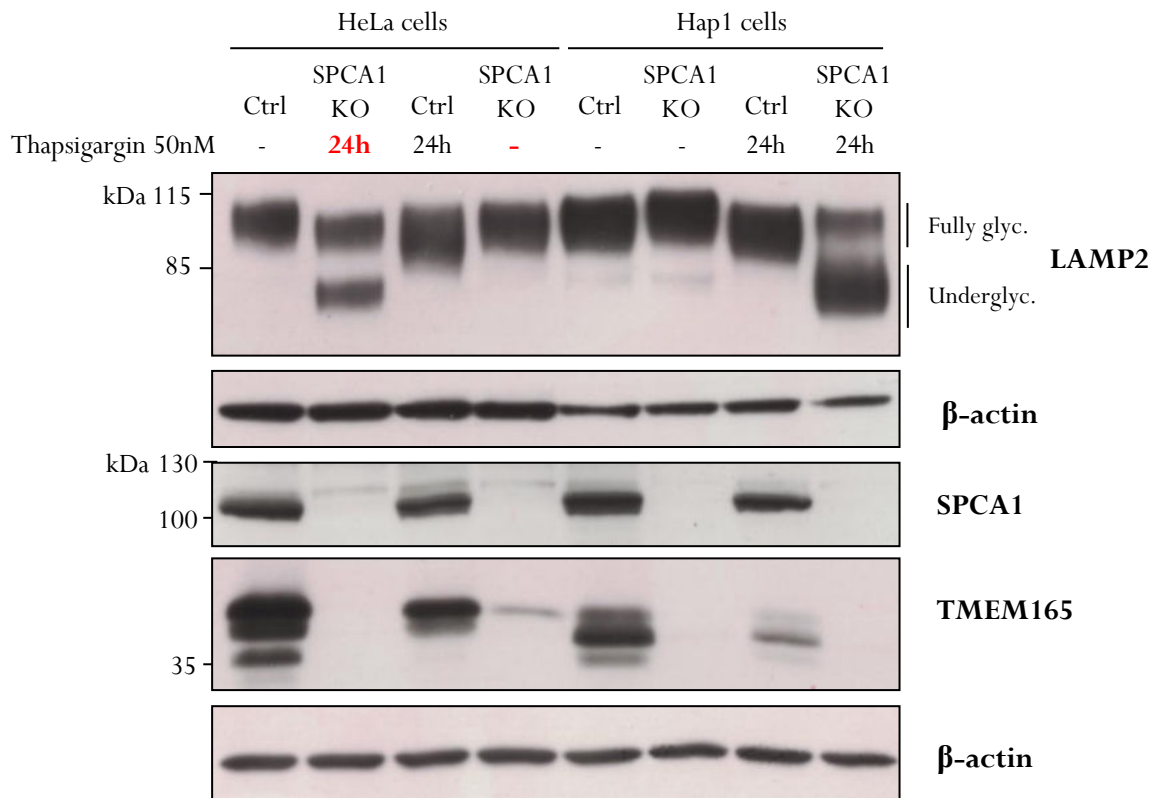


**Figure 70: Involvement of thapsigargin sensitive pumps in regulating Golgi glycosylation in SPCA1 KO HeLa and Hap1 cells.** Control (Ctrl) and SPCA1 KO Hap1 cells were treated with 50nM thapsigargin for 24h. Total cell lysates were prepared, subjected to SDS-PAGE and western blot with the indicated antibodies. Red information results from a mistake during sample loading.

This  $Mn^{2+}$  pumping activity of SPCA1-WT is also required for TMEM165 recovery and thapsigargin has no effect in cell lines expressing TMEM165 (control and SPCA1 KO Hap1 cells complemented with SPCA1-WT). Hence, this result emphasizes that the  $Mn^{2+}$  pumping activity of SPCA1 seems to be required to protect the cells from the thapsigargin-induced glycosylation defect in SPCA1 deficient cells by rescuing TMEM165 expression and function in glycosylation. In the coming weeks, this hypothesis will be challenged by the analysis of such thapsigargin treatment in SPCA1 KO Hap1 cells complemented with SPCA1-Q747A *i.e.* the hyperactive SPCA1  $Mn^{2+}$  transporter. If our reasoning is correct, since  $Mn^{2+}$  pumping by SPCA1-Q747A stabilizes TMEM165 (Figure 4, Paper 4), we should not get any Golgi glycosylation defect after thapsigargin treatment in those cells thanks to TMEM165 recovery. In addition, such inhibition of SERCA2 will be double checked by the use of cyclopiazonic acid, exactly what we have done in Paper 1. At last, mass spectrometry of total N-glycans will also be analyzed in all control, SPCA1 KO and complemented cell lines including Q747A to extend our observations on LAMP2 and TGN46 at the structural level on all N-linked glycoproteins.

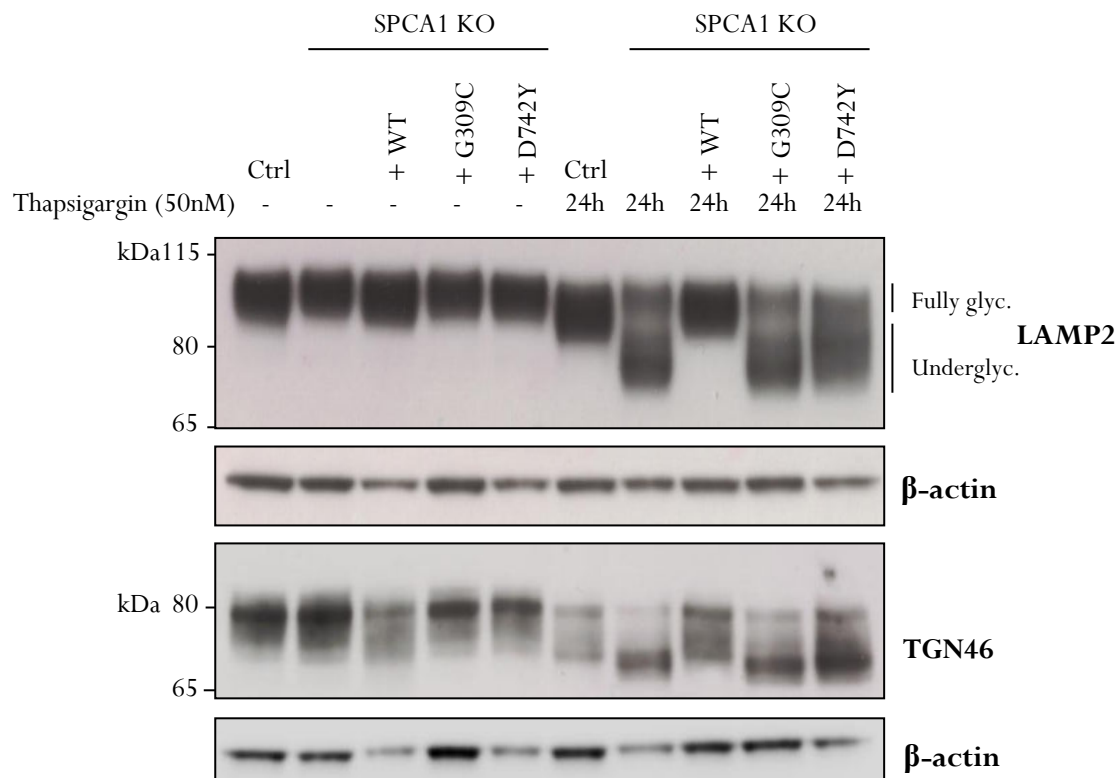


**Figure 71: Thapsigargin induces Golgi glycosylation defect only in SPCA1 deficient Hap1 cells lacking functional SPCA1 and TMEM165.** Control (Ctrl), SPCA1 KO and complemented Hap1 cells were treated with 50nM thapsigargin for 24h. Total cell lysates were prepared, subjected to SDS-PAGE and western blot with the indicated antibodies.

## 2. SPCA1-mediated $Mn^{2+}$ import is not required to sustain Golgi glycosylation in TMEM165 deficient cells

Here, we strongly believe that the lack of glycosylation defect in thapsigargin-treated SPCA1 KO cells complemented with SPCA1-WT could be explained by TMEM165 rescue. However, another possibility would be that only the  $Mn^{2+}$  pumping activity of WT-SPCA1 could be sufficient to feed the Golgi apparatus and sustain the glycosylation process. To address this point, TMEM165 KO HEK cells were transfected with the hyperactive  $Mn^{2+}$  transporter SPCA1-Q747A for 24h and LAMP2 glycosylation profile was assessed by western blot. As shown in Figure 72, while correctly overexpressed, there is no effect of SPCA1-Q747A on LAMP2 gel mobility. This result suggests that the presumed higher SPCA1-mediated  $Mn^{2+}$  import into the Golgi lumen is not sufficient to suppress Golgi glycosylation defects associated to TMEM165 deficiency. From this experiment, we were unfortunately unable to confirm the functionality of SPCA1-Q747A that is to say, a higher  $Mn^{2+}$  entry into the Golgi lumen.

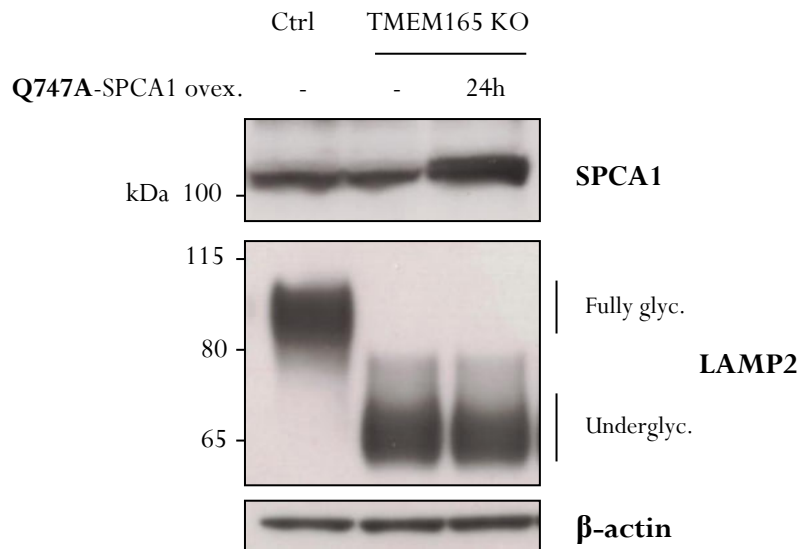


**Figure 72: SPCA1  $Mn^{2+}$  pumping activity is not required to sustain glycosylation in TMEM165 KO HEK cells.** TMEM165 KO HEK cells were transiently transfected with Q747A-SPCA1 for 24h. Total cell lysates were prepared, subjected to SDS-PAGE and western blot with the indicated antibodies.

Assuming its functionality, this result raised intriguing questions: How to explain that  $Mn^{2+}$  imported by SPCA1-WT/-Q747A in Hap1 cells could decrease cytosolic  $Mn^{2+}$  levels resulting in TMEM165 recovery while not allowing Golgi glycosylation rescue in TMEM165 deficient cells? Why do not SPCA1-mediated  $Mn^{2+}$  entry into the Golgi lumen overcome Golgi glycosylation defect while providing the missing ions? Would  $Mn^{2+}$  pumped by SPCA1 not be available for Golgi GTs in the right compartment, preventing glycosylation reactions to occur? Would SPCA1-mediated  $Mn^{2+}$  entry in the Golgi be exclusively redirected into the detoxifying pathway without biological relevance for Golgi glycosylation? Why do TMEM165 deficient cells need SERCA pumps instead of SPCA1 to sustain Golgi glycosylation reactions? Why does TMEM165/SERCA-mediated  $Mn^{2+}$  import into the Golgi lumen seem to be more biologically relevant than those of SPCA1? Another three years of PhD would be necessary to properly answer all of these questions. However, from what I understood of the system linking TMEM165, SPCA1 and SERCA2, one explanation could be acceptable. According to the subcellular localization of TMEM165, SERCA and SPCA1, one can imagine that intracellular  $Mn^{2+}$  may be sequestered according to different pools along the secretory pathway. Indeed, (i) SERCA pumps are predominantly localized in the ER and more rarely in the *cis*-Golgi, (ii) the Golgi localized proportion of TMEM165 is mainly expressed in the medial/*trans*-Golgi and (iii) SPCA1 is found exclusively localized in the late Golgi (*trans*-/TGN) and secretory vesicles. Hence, while importing cytosolic  $Mn^{2+}$ , SERCA will mainly fulfill the early cistern of the Golgi apparatus, TMEM165 the medial one and SPCA1 the very late ones. Therefore, depending on the ion requirements of each GT in each Golgi compartment, a deficiency in  $Mn^{2+}$  transport in either *cis*-Golgi, *medial*-Golgi or TGN may have none to critical impact on Golgi glycosylation reactions. With regards to the N-linked glycosylation,  $Mn^{2+}$ -dependent GTs are

found in either *cis*-, *medial*- and *trans*-Golgi explaining why in TMEM165 deficient cells (i) the solely  $Mn^{2+}$  pumping activity of SPCA1 is not sufficient to suppress N-linked glycosylation defect (SPCA1 is expressed to far from the *cis*- and *medial*-Golgi  $Mn^{2+}$ -dependent GTs) and also why (ii) SERCA2 overexpression induces a N-linked glycosylation rescue (SERCA2 can provide  $Mn^{2+}$  in the *cis*-Golgi during initiating steps of N-glycans maturation). The other way around, in SPCA1 deficient cells, cytosolic  $Mn^{2+}$  accumulation promotes SERCA2-mediated  $Mn^{2+}$  entry into the ER and supplies the *cis*-Golgi to initiated N-glycan maturation. Then, either residual TMEM165 supplies medial/*trans*-Golgi with  $Mn^{2+}$  or  $Mn^{2+}$  reaches these compartments by vesicular trafficking which may be facilitated by the higher cytosolic Mn levels in SPCA1 deficient cells.



---

## **General conclusion**

---





# 1. Role of TMEM165/Gdt1p in Golgi glycosylation

## 1.1. TMEM165 in Golgi glycosylation

### 1.1.1. TMEM165 deficiency leads to strong and multiple glycosylation defects due to disrupted Golgi Mn<sup>2+</sup> homeostasis

In 2012, pathogenic mutations in *TMEM165* have been identified to cause a type II CDG especially characterized by severe skeletal abnormalities as the main clinical feature [64,505]. *TMEM165* encodes TMEM165, a transmembrane protein belonging to the UPF0016 family with unclear physiological functions related to Mn<sup>2+</sup> and Ca<sup>2+</sup> homeostasis [304,497]. At the beginning of my PhD, TMEM165 deficiency was associated to severe N-linked and glycosphingolipid glycosylation defects [64,65,506]. In particular, mass spectrometry analyses of the total N-glycans from TMEM165 KO HEK cells revealed a strong galactosylation defect, a moderate GlcNAcylation defect and a very slight sialylation defect, all assumed to be due to a disrupted Golgi Mn<sup>2+</sup> homeostasis [65].

With regards to glycosphingolipids, the gangliosides series were also analyzed *via* mass spectrometry in control and TMEM165 KO HEK cells. Remarkably, only traces level of two specific gangliosides (GM3 and GM2) were found in TMEM165 deficient cells while control cells expressed a broader range of species (GM3, GM2, GM1, GD2 and GD1). Gangliosides biosynthesis occurs in the Golgi apparatus and is initiated by several Mn<sup>2+</sup>-dependent GTs amongst the galactosyltransferases, B4GALT5/6 and the GalNAc transferase, B3GALTN1. Given that TMEM165 deficiency alters Golgi Mn<sup>2+</sup> homeostasis; a defect in these specific steps was not surprising, leading to abort ganglioside structures reflecting galactosylation and/or GalNAcylation defects. Following this idea, additional Golgi glycosylation pathways involving Mn<sup>2+</sup>-dependent GTs were analyzed during my PhD.

At first, resulting from a collaboration with Dr. Mohamed Ouzzine, a GAG defect on both heparan sulfate (HS) and chondroitin sulfate (CS) chains was observed in TMEM165-CDG patients' fibroblasts and TMEM165 KO ATDC5 cells, a chondrogenic mouse-derived cell lines. Here again, Mn<sup>2+</sup>-dependent GTs such as the xylosyltransferases XYLT1/2 and the galactosyltransferases B4GALT7/6 are involved in the biosynthesis of the common tetrasaccharide core GAG linker GlcA-Gal-Gal-Xyl-Ser/Thr. In addition, other GTs yielding HS and CS chains such as EXTL3 and CHSY1 are also Mn<sup>2+</sup>-dependent and their improper activity could result in the synthesis of shorter HS and CS chains. Thus, the GAG glycosylation defect in TMEM165 KO cells could result either from undergalactosylation, underGlcNAcylation and/or underGalNAcylation. In a recent collaborative study with Dr. Arnaud Bruneel, another GAG defect was observed on circulating proteoglycans bikunin from TMEM165 patients' sera [511]. Briefly, three major serum bikunin isoforms can be found each bearing different

PTMs amongst a unique CS chain (urinary trypsin inhibitor, UTI) or a unique CS chain esterified by one glycoprotein (pro- $\alpha$ -trypsin inhibitor, P $\alpha$ I) or two glycoproteins (inter- $\alpha$ -trypsin inhibitor, ITI) names “heavy chains”. TMEM165 deficiency results in a huge glycosylation defect on UTI bikunin associated with lower levels of ITI and P $\alpha$ I, both suggesting altered CS initiation and/or elongation. Given that CS chains are initiated downstream the synthesis of the core tetrasaccharide GlcA-Gal-Gal-Xyl-Ser/Thr, we highly suspect that TMEM165 deficiency does not affect it although its synthesis also requires Mn<sup>2+</sup>-dependent GTs. The underlying hypothesis would be that TMEM165 deficiency would mainly impact the Golgi Mn<sup>2+</sup> homeostasis of the Golgi cisternae it belongs to. Therefore, according to the subcellular localization of the Golgi GTs and their proper Mn<sup>2+</sup> requirements, a lack of TMEM165 will only affect specific Mn<sup>2+</sup>-dependent reaction of the *medial-/trans*-Golgi.

Finally, we provided some insights into the potential O-GalNAcylation defect associated to TMEM165 deficiency. This was first reported by Xia *et al.* in 2013 suggesting an undersialylation of O-linked mucin type in TMEM165-CDG patients fibroblasts expressing higher T antigens (Gal-GalNAc-Ser/Thr) than sialylT ones (Sia-Gal-GalNAc-Ser/Thr) [507]. Using an indirect lectin approach, we observed a higher abundance of Tn antigens (GalNAc-Ser/Thr) with unsubstituted GalNAc residues in TMEM165 KO HEK cells, confirming an O-GalNAc glycosylation defects in these cells (see Figure 56). In addition, we also observed a shift in the electrophoretic migration of TGN46 that we assigned to a major O-linked glycosylation defect, as explained in the General discussion and perspectives on Part I.

Altogether, TMEM165 deficiency leads to severe N-linked, O-linked, GAGs and ganglioside defects, all related to Golgi Mn<sup>2+</sup> deficiency. As summarized in Table 24, many GTs belonging to multiple glycosylation pathways are Mn<sup>2+</sup>-dependent. In the future, it could be of interest to deeper characterized TMEM165 glycosylation defects in all the glycosylation pathways by looking specifically to any accumulation of truncated glycan structures before each Mn<sup>2+</sup>-dependent reaction, especially for Golgi glycosylation reactions occurring in the *medial-/trans*-Golgi.

**Table 204: List of putative and known Mn<sup>2+</sup>-dependent GTs.** Genes/enzymes written in purple share a Mn<sup>2+</sup>-dependency by similarity or can act with others cation than Mn<sup>2+</sup>. GalT: galactosyltransferase, GalNAcT: N-acetyl-galactosaminyltransferase, GlcT: glucosyltransferase, GlcNAcT: N-acetyl-glucosaminyltransferase, SiaT: sialyltransferase and XylT: xylosyltransferase.

| Glycosylation pathway | Genes and corresponding Mn <sup>2+</sup> -dependent enzymes |  |
|-----------------------|---|--|
|                       | Genes   | Enzymes  |
| <i>N-linked</i>       |   |  |
|                       | <i>B4GALT1</i>  | β-1,4-GalT 1   |
|                       | <i>UGGT1/2</i>  | UDP-glucose glycoprotein GlcT 1 and 2                  |
|                       | <i>B4GALT2-5</i>  | β-1,4-GalT 2, 3, 4 and 5                               |
|                       | <i>MGAT1</i>  | Mannosyl (α-1,3-)-glycoprotein β-1,2-GlcNAcT 1         |
|                       | <i>MGAT4A/4B</i>  | Mannosyl (α-1,3-)-glycoprotein β-1,4-GlcNAcT 4a and 4b |
|                       | <i>MGAT5B</i>   | Mannosyl (α-1,3-)-glycoprotein β-1,6-GlcNAcT 5c        |
| <i>O-linked</i>       |   |  |
| O-GalNAcylation       | <i>B4GALNT2</i>   | β-1,4-GalNAcT 2  |
|                       | <i>GALNT1-3 /10</i>   | Polypeptide GalNAcT 1, 2, 3 and 10                     |
|                       | <i>FUT3/5/7</i>   | FucT 3, 5 and 7  |
|                       | <i>GALNTX</i>   | Polypeptide GalNAcT X                                  |
| O-mannosylation       | <i>B4GAT1</i>   | β-1,4-glucuronyltransferase 1                          |
|                       | <i>LARGE1/2</i>   | LARGE xyloxy- and glucuronyltransferase 1 and 2        |
|                       | <i>POMGNT1</i>  | Protein O-linked mannose GlcNAcT 1                     |
| O-fucosylation        | <i>LFNG</i>   | β-1,3-GlcNAcT lunatic fringe                           |
|                       | <i>MNFG</i>   | β-1,3-GlcNAcT manic fringe                             |
|                       | <i>RFNG</i>   | β-1,3-GlcNAcT radical fringe                           |
| O-glucosylation       | <i>XXYL1</i>  | Xyloside XylT1   |
| GAGs                  | <i>B3GAT1/3</i>   | β-1,3-glucuronyltransferase 1 and 3                    |
|                       | <i>B4GALT7</i>  | β-1,4-GalT 7   |
|                       | <i>CHPF</i>   | Chondroitin polymerizing factor                        |
|                       | <i>CHSY1/3</i>  | Chondroitin sulfate synthase 1 and 3                   |
|                       | <i>XYLT1</i>  | XylT 1   |
|                       | <i>EXT1/2</i>   | Exostosin-1 and -2                                     |
|                       | <i>EXTL1-3</i>  | Exostosin-like GTs 1, 2 and 3                          |
|                       | <i>XYLT2</i>  | XylT 2   |
| <i>Glycolipids</i>    |   |  |
|                       | <i>B3GALNT1</i>   | β-1,3-GalNAcT 1  |
|                       | <i>B4GALNT1</i>   | β-1,4-GalNAcT 1  |
|                       | <i>B4GALT1/3/5/6</i>  | β-1,4-GalT 1, 3, 5 and 6                               |
|                       | <i>ST3GAL5</i>  | α-1,3-SiaT 5   |
|                       | <i>UGT8</i>   | UDP-Gal ceramide GalT 8                                |
|                       | <i>A3GALT2</i>  | α-1,3-GalT 2   |
|                       | <i>B3GALT4/5</i>  | β-1,3-GalT 4 and 5                                     |
|                       | <i>B3GNT5</i>   | LacCer β-1,3-GlcNAcT 5                                 |
|                       | <i>GBGT1</i>  | Globoside α-1,3-GalNAcT 1                              |

### 1.1.2. Exogenous Mn<sup>2+</sup> and Gal to suppress glycosylation defects in TMEM165 deficient cells

We remarkably found that all glycosylation defects associated to TMEM165 deficiency could be suppressed by a MnCl<sub>2</sub> addition. Conversely, Gal supplementation only fully restored N-linked glycosylation since partial recovery of glycosphingolipids and mucin types were observed in TMEM165 KO HEK cells and no effect of Gal addition was observed on GAG HS and CS chain defects (Table 22). Altogether, MnCl<sub>2</sub> has a broader and more efficient effect on Golgi glycosylation reactions than Gal. One explanation could be that more glycosylation reactions are Mn<sup>2+</sup>-dependent than Gal-dependent. Therefore, according to the glycosylation pathway as well as the nature of each glycosylation reaction in a given subcompartment of the secretory pathway, Mn<sup>2+</sup> and Gal requirements may differ. In TMEM165 KO cells, Golgi Mn<sup>2+</sup> deficiency is assumed to be restricted to the medial/*trans*-Golgi, where the protein is predominantly found. Consequently, only Mn<sup>2+</sup> dependent GTs of the *medial/trans*-Golgi should be altered in case of TMEM165 deficiency. As already mentioned, this hypothesis has recently been strengthened by the interesting result of a GAG defect on bikunin suggesting an alteration during CS chain elongation without any impairment in the biosynthesis of the core tetrasaccharide GAG linker: GlcA-Gal-Gal-Xyl-Ser/Thr [511]. Given that (i) the core structure is synthesized in the *cis*-Golgi and (ii) CS chains elongation likely occurs in the *medial*-Golgi, this result emphasizes that the lack of efficient Mn<sup>2+</sup> transport in a specific compartment only affect the Mn<sup>2+</sup>-dependent limiting reactions of this particular compartment. Therefore, all the reactions upstream from the defective Golgi cisternae will not be affected by the local Mn<sup>2+</sup> deficiency whereas all the reactions downstream will be.

### 1.1.3. SERCA2 to sustain Golgi glycosylation in TMEM165 and SPCA1-deficient cells

As one of the main achievement of my PhD, we demonstrated that Mn<sup>2+</sup>-induced N-glycosylation rescue in TMEM165 KO HEK cells was achieved *via* the ER and likely thanks to the Mn<sup>2+</sup> pumping activity of SERCA2 pumps. In addition, we also provided evidence that SERCA2 overexpression initiated the suppression of LAMP2 glycosylation defect in TMEM165 deficient cells. This brandy new concept (Figure 49) would link for the first time the function of reticular P-type ATPases in Golgi glycosylation maintenance. Moreover, using SPCA1 KO Hap1/HeLa cells subsequently deficient for TMEM165, we assumed that the lack of Golgi glycosylation defects in those cells result from SERCA2 activity in Mn<sup>2+</sup> pumping since SERCA2 inhibition by pharmacological agents disrupted Golgi glycosylation reactions.

Taking as a whole, our work unveils unexpected function of reticular P-type ATPases in the maintenance of Golgi ion homeostasis *via* their Mn<sup>2+</sup> pumping activity allowing proper Golgi functions in glycosylation in case of TMEM165 deficiency.

## 1.2. Gdt1p in Golgi glycosylation

### 1.2.1. Gdt1p deficiency leads to Golgi glycosylation defects upon high external CaCl<sub>2</sub> pressure

Differing from TMEM165, in yeast, Gdt1p deficiency does not induce any Golgi glycosylation defects until *gdt1Δ* mutants are grown under high external [CaCl<sub>2</sub>] ranging between 400 to 700 mM. In this case, we and others have identified both N- and O-linked glycosylation abnormalities thanks to western blot analyses of different glycosylation markers (secreted invertase, carboxypeptidase Y and Gas1p) and NMR experiments on total mannans. We finally demonstrated that Gdt1p was required to sustain both N- and O-linked glycosylation reactions only under high external CaCl<sub>2</sub> concentrations whereas in normal cell culture conditions, Gdt1p function in glycosylation is dispensable [65,239,240]. Since it has been well established in literature that Pmr1p deficiency led to strong Golgi glycosylation abnormalities [236,238], we further investigated the link between Gdt1p and Pmr1p towards their function in Golgi glycosylation (Paper 3, [240]). Our results highlighted a functional link between these two proteins pinpointing a crucial role for Gdt1p in Golgi glycosylation only when Pmr1p is unable to transport Mn<sup>2+</sup> into the Golgi apparatus.

### 1.2.2. Exogenous Mn<sup>2+</sup> to suppress Golgi glycosylation defects in *gdt1Δ* yeasts cultured in Ca<sup>2+</sup>-enriched medium, *pmr1Δ* and double mutant *gdt1Δ/pm1Δ*

Exactly as for TMEM165 deficient cells, we found that MnCl<sub>2</sub> supplementation to the Ca<sup>2+</sup>-enriched medium of *gdt1Δ* suppressed the glycosylation defects associated to both Gdt1p deficiency and high CaCl<sub>2</sub> pressure. However, since (i) no SERCA orthologs are found expressed in yeast and (ii) Pmr1p deficiency led to severe Golgi glycosylation defects, we further investigated the proper functions of Pmr1p and Gdt1p in Golgi glycosylation. We suggested that MnCl<sub>2</sub> supplementation to the Ca<sup>2+</sup>-enriched medium of *gdt1Δ* yeasts could enhance the Mn<sup>2+</sup> pumping activity of Pmr1p resulting in the suppression of the glycosylation abnormalities. Then, it is likely that Mn<sup>2+</sup>-induced glycosylation rescue in *gdt1Δ* grown in a high CaCl<sub>2</sub> environment results from the Mn<sup>2+</sup> pumping activity of Pmr1p into the Golgi lumen. However, while looking to the double mutant *gdt1Δ/pm1Δ*, Golgi glycosylation abnormalities were also suppressed by MnCl<sub>2</sub> supplementation (Table 23). Thus, how to explain that in absence of Gdt1p and Pmr1p, extracellular MnCl<sub>2</sub> enters the cells and the Golgi lumen to suppress the glycosylation defect? One can imagine a similar mechanism that the one explained in human TMEM165 deficient cells (Paper 1, [231]). However, given that no SERCA orthologs are found expressed in yeast, we presumed that cytosolic Mn<sup>2+</sup> could reach the Golgi lumen *via* the activity of an unknown ER- or Golgi-localized transporter. As mentioned in Chapter 2, section 2.4, one candidate could be the P-type

ATPase Cod1p/Spf1p since its role in ER Mn<sup>2+</sup> homeostasis [220] was first suggested before its function in cellular sterol homeostasis [219]. To test whether Spf1p is involved, it could be worth to study Golgi glycosylation capacities in the triple mutant *spf1Δ/gdt1Δ/pmr1Δ* grown with MnCl<sub>2</sub> supplementation.

### 1.3. Differences between TMEM165 and Gdt1p in Golgi glycosylation

Different functions for Gdt1p and TMEM165 in Golgi glycosylation are observed. First, TMEM165 deficiency alters Golgi Mn<sup>2+</sup> homeostasis whereas Gdt1p did not, suggesting distinct function for both protein in the regulation of Golgi Mn<sup>2+</sup> homeostasis. Second, strong glycosylation abnormalities characterize the yeast null mutant *pmr1Δ* while in human, no direct link between glycosylation and SPCA1 deficiency has been established yet. Moreover, our results emphasized that Gdt1p function in glycosylation was Pmr1p-dependent. In physiological conditions, we suggested that Pmr1p had a critical role in Golgi glycosylation *via* its Mn<sup>2+</sup> transport activity whereas Gdt1p function was dispensable. On the other hand, when Pmr1p was only able to pump Ca<sup>2+</sup> into the Golgi lumen, we found that Gdt1p became essential to feed the Golgi apparatus with Mn<sup>2+</sup> and ensure proper Golgi glycosylation reactions. In mammalian cells, although a functional link between TMEM165 and SPCA1 has been established, the ion pumping activity of SPCA1 did not influence Golgi glycosylation capacities that we assumed to be sustained thanks to the activity of SERCA pumps. Therefore, our comparative studies between yeasts and humans revealed a crucial role for TMEM165 and Pmr1p in Golgi glycosylation while Gdt1p and SPCA1 are secondary players in this process. We then strongly believe that in human cells, (i) TMEM165 mainly imports cytosolic Mn<sup>2+</sup> to feed the Golgi apparatus and sustain the glycosylation process while (ii) in yeast, Gdt1p Mn<sup>2+</sup> activity is only required when the one sustained *via* Pmr1p is lacking, defining Gdt1p as the leak channel of Pmr1p and Pmr1p the main Mn<sup>2+</sup> importer of the Golgi apparatus. Nonetheless, why TMEM165/Gdt1p and SPCA1/Pmr1p have evolved differently during evolution is still an opened question.

## 2. TMEM165/Gdt1p as Golgi Mn<sup>2+</sup> sensitive proteins

At the very beginning of my PhD, our lab had demonstrated that both TMEM165 and Gdt1p were two Golgi-localized proteins sensitive to Mn<sup>2+</sup> and specifically degraded following high extracellular MnCl<sub>2</sub> exposure [307]. While we provided evidence that TMEM165 was a cytosolic Mn<sup>2+</sup> sensor (Paper 4, [461]), we did not further investigate whether cytosolic or intraluminal Mn<sup>2+</sup> accumulation was responsible for Gdt1p degradation. Moreover, the molecular mechanisms of such Mn<sup>2+</sup>-induced degradation of TMEM165 and Gdt1p are still not elucidated and might involve degradation partners that we need to identify in the future. Beyond these mechanistic aspects, we found that Mn<sup>2+</sup>-induced degradation was conserved between yeasts and humans. Then, we wondered: what would be the selective advantage conferred by such mechanism during evolution? In other words, what would be the biological relevance to get rid of TMEM165 and Gdt1p in case of Mn<sup>2+</sup> overload? One spontaneous answer would be: to prevent cells from Mn<sup>2+</sup> toxicity. Indeed, upon MnCl<sub>2</sub> exposure, cells need to prevent the cytosol from Mn<sup>2+</sup> accumulation to toxic levels. In human cells, one way to cope with cytosolic Mn<sup>2+</sup> excess implies SPCA1 in a so-called detoxification pathway. Actually, SPCA1 switches from Ca<sup>2+</sup> to Mn<sup>2+</sup> and massively imports Mn<sup>2+</sup> into the Golgi lumen, which is further removed from the cell *via* secretory vesicles. In this case, as a secondary active transporter, TMEM165 would transport Mn<sup>2+</sup> back to the cytosol, annihilating the function of SPCA1. Since TMEM165 is degraded by high cytosolic Mn<sup>2+</sup> accumulation, we believe that TMEM165 Mn<sup>2+</sup>-induced degradation is necessary to protect the cell from Mn<sup>2+</sup> cytotoxicity by allowing SPCA1 to ensure its detoxifying function (Figure 73). The other possibility would be that TMEM165 physically interacts with SPCA1 and that interaction would govern SPCA1 ion specificity. In presence of TMEM165, SPCA1 would mainly pump Ca<sup>2+</sup> even in case of cytosolic Mn<sup>2+</sup> accumulation. Therefore, one can imagine that the degradation of TMEM165 would be essential to turn on SPCA1 in a Mn<sup>2+</sup> detoxification mode. Finally, a third possibility would be a direct function of TMEM165 in Mn<sup>2+</sup> import at the plasma membrane, given that a small fraction of the protein is localized at the cell surface [307,488]. We indeed recently demonstrated by using the Mn<sup>2+</sup>-quenching technique that Mn<sup>2+</sup> influx at the plasma membrane was dependent on TMEM165 expression levels. As such, the observed Mn<sup>2+</sup>-induced degradation would prevent a massive TMEM165-dependent entry of Mn<sup>2+</sup> inside the cell. This mechanism has already been observed in yeast *Saccharomyces cerevisiae* with the constitutive degradation of Smf1p and Smf2p in case of Mn<sup>2+</sup> excess (see Chapter 2, section 3.3.).

## Physiological conditions

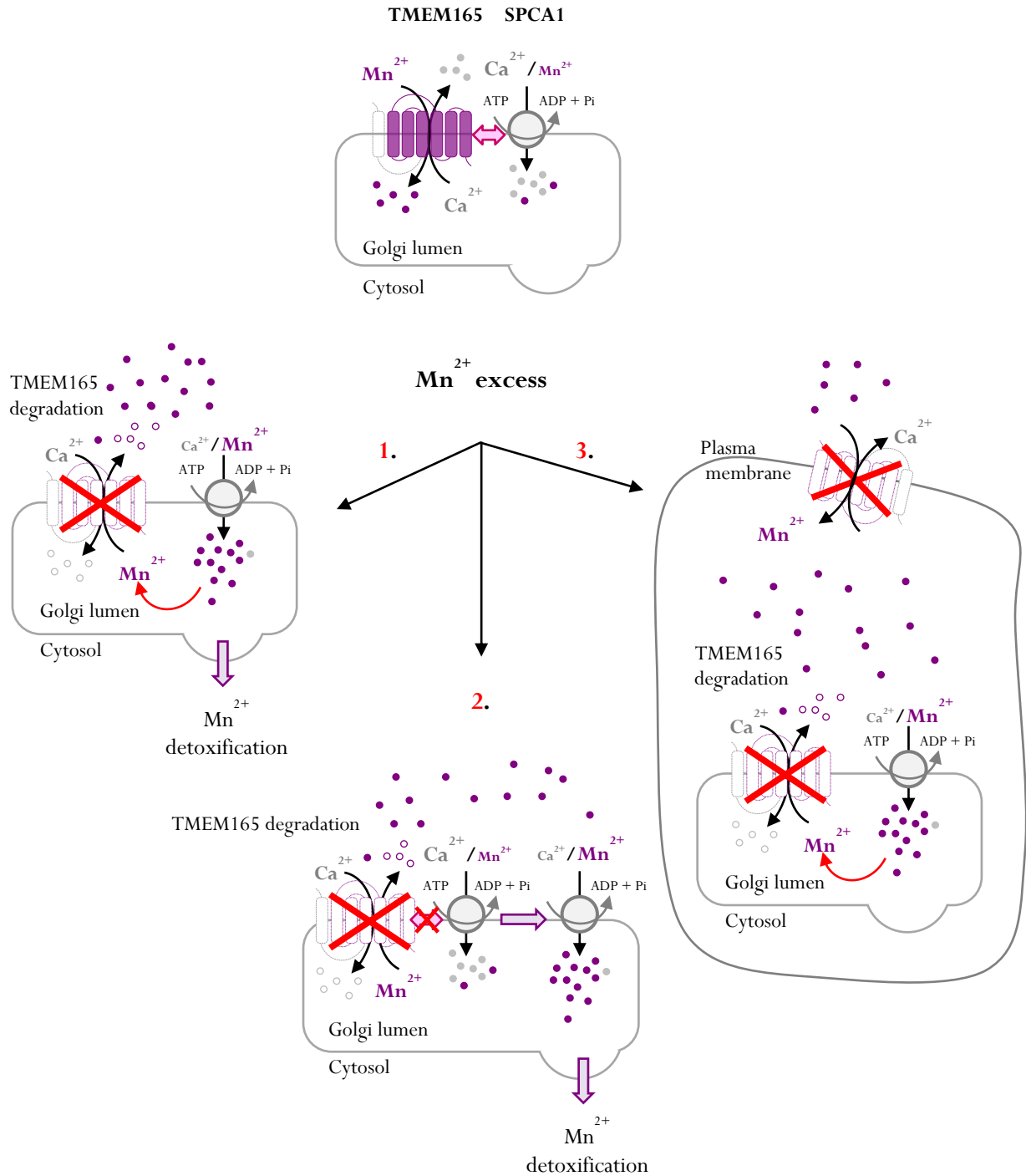


**Figure 73: Putative models for the Mn<sup>2+</sup>-induced degradation of TMEM165.** In physiological conditions, this scheme is similar to the one presented in Figure 46. In case of Mn<sup>2+</sup> excess, the three models described in the text are represented. **1.** Mn<sup>2+</sup>-induced TMEM165 degradation to avoid the annihilation of SPCA1's function. **2.** TMEM165 degradation is necessary to turn on SPCA1 in a Mn<sup>2+</sup> detoxification pathway. **3.** TMEM165 degradation at the plasma membrane to prevent higher Mn<sup>2+</sup> entry and accumulation into the cytosol.

With regards to the yeast *Saccharomyces cerevisiae*, in case of Mn<sup>2+</sup> excess, the detoxification pathway not only implies Pmr1p but two additional vacuolar Mn<sup>2+</sup> importers: Ccc1p and Ypk9p (Chapter 2, section 3.3.). In this case, Pmr1p, Ccc1p and Ypk9p would act in concert to lower cytosolic Mn<sup>2+</sup> levels by



sequestering  $Mn^{2+}$  into secretory vesicles and the vacuole. Therefore, the  $Mn^{2+}$  gradient established in the Golgi lumen would remain similar to that in physiological conditions. Given that Gdt1p is thought to be the leak channel of Pmr1p, Gdt1p would continuously transport  $Mn^{2+}$  back into the cytosol, annihilating the functions of Pmr1p, Ccc1p and Ypk9p. Hence, Gdt1p would be degraded to prevent too much  $Mn^{2+}$  leakage that becomes toxic for the cell in case of  $Mn^{2+}$  overload (Figure 74).

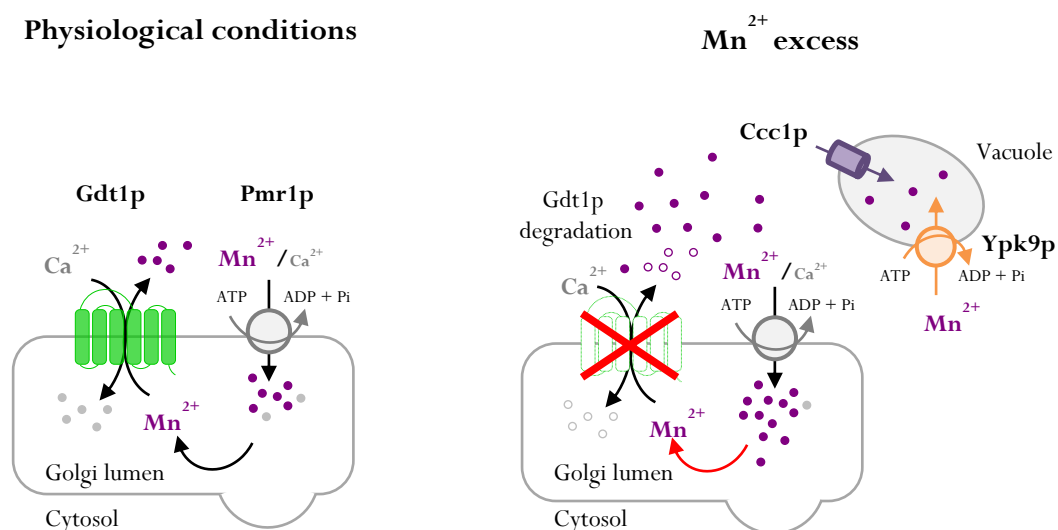


**Figure 74: Putative model for the  $Mn^{2+}$ -induced degradation of Gdt1p in yeast *Saccharomyces cerevisiae*.** In physiological conditions, this scheme is similar to the one presented in Figure 46. However, in case of  $Mn^{2+}$  excess, Pmr1p, Ccc1p and Ypk9p will engage themselves in a detoxification pathway, aiming at sequestering  $Mn^{2+}$  into the Golgi lumen and the vacuole. Given that Gdt1p is thought to be the leak channel of Pmr1p, in case of  $Mn^{2+}$  excess, this  $Mn^{2+}$  sent back to the cytosol is deleterious for cell survival leading to the degradation of Gdt1p.

Nonetheless, these hypothetical models are based on current knowledge and might be challenged in the next few years according to additional work in the field.

### 3. TMEM165 and Golgi ion homeostasis: $Mn^{2+}$ , $Ca^{2+}$ and... $H^+$ !

The ultimate achievement of this PhD yields to an interplay between TMEM165, SERCA2 and SPCA1, three key players in the regulation of cellular and intracellular  $Ca^{2+}/Mn^{2+}$  homeostasis. Using isogenic cell lines either deficient for TMEM165 or SPCA1; we clearly established a functional link between these two proteins that seems to be conserved throughout evolution from lower to higher eukaryotes. In addition, our work also shed light on the potential involvement of SERCA pumps in Golgi glycosylation in both TMEM165 and SPCA1 deficient cells. A strong argument supporting this model is the huge glycosylation defect observed on LAMP2 and TGN46 in SPCA1 KO cells treated with thapsigargin. In this case, all three key players are functionally missing and the subsequent Golgi glycosylation defect can result from either  $Ca^{2+}$  or  $Mn^{2+}$  deficiency given that thapsigargin inhibit both SERCA2  $Ca^{2+}$  and  $Mn^{2+}$  pumping activities. Intriguingly, the induction of such Golgi glycosylation defect in SPCA1 deficient

cells treated with thapsigargin was completely suppressed only when SPCA1 transports  $Mn^{2+}$  allowing the recovery of TMEM165. Since a similar result was obtained using cyclopiazonic acid, we highly suggested that TMEM165 could protect the cells from SERCA inhibition by counteracted its effect on Golgi glycosylation. Nonetheless, what is not clear is whether  $Ca^{2+}$  or  $Mn^{2+}$  deficiency induced by thapsigargin has a higher impact on the glycosylation process. Indeed, the use of thapsigargin and cyclopiazonic acid to inhibit SERCA pumps activity results in drastically low  $[Ca^{2+}]$  in the ER. This disrupted  $Ca^{2+}$  homeostasis in itself may alter some crucial  $Ca^{2+}$ -dependent processes occurring in the ER such as quality control for N-glycoproteins, transport of N-glycoproteins from the ER to the ERGIC and targeting of misfolded N-glycoproteins to the ERAD pathway, all requiring the activity of  $Ca^{2+}$ -dependent lectins. Moreover,  $Ca^{2+}$  homeostasis along the secretory pathway also contributes to proteolytic cleavages, secretory cargo concentration and secretion, protein trafficking and sorting. Therefore, in our cell models defective for TMEM165, we need to keep in mind that beside Golgi  $Mn^{2+}$ , Golgi  $Ca^{2+}$  homeostasis might also be impaired. Hence, as an on-going project in the team, we intend to look closely to potential variations in  $Ca^{2+}$  homeostasis in both TMEM165 and SPCA1 KO. Finally, as TMEM165 deficiency led to lysosomal overacidification, pH within the secretory pathway of TMEM165 deficient cells might also be impaired. Given that pH as well as  $Ca^{2+}$  regulates the intravesicular trafficking of secretory cargoes, one can imagine that in addition to a disrupted  $Mn^{2+}$  homeostasis in the *medial-/trans*-Golgi, TMEM165 deficiency also impacts protein trafficking within the Golgi apparatus. Since glycosylation reactions require a close proximity of all the glycosylation machinery members (glycosylation enzyme, donor substrate (*i.e.* nucleotide sugars) and acceptor substrate (*i.e.* the protein to be glycosylated)), a de-synchronization between (i) speed of trafficking, (ii) time of residence of the glycosylation machinery in each cisterna and (iii) efficiency of the glycosylation reaction may lead in improper Golgi glycosylation functions. Overall, Golgi  $Mn^{2+}$ ,  $Ca^{2+}$  and  $H^+$  homeostasis are intimately related and disturbance in one of them may reverberate to the other(s). As depicted in Figure 75, in case of TMEM165 deficiency, Golgi glycosylation defects may result from alterations in one or all of them.

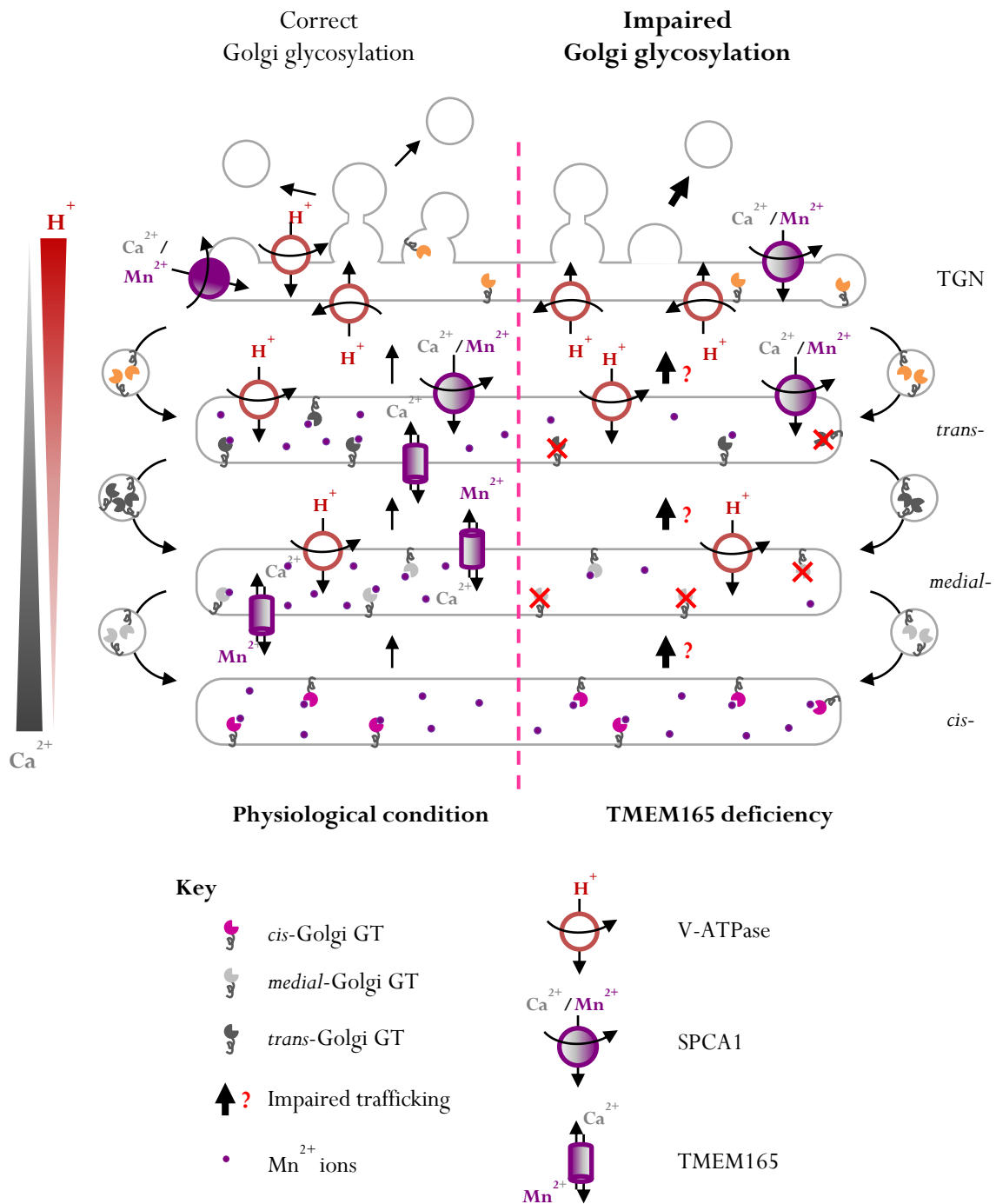


**Figure 75: Importance of Golgi ion homeostasis to sustain glycosylation reactions.** The scheme depicts the key players in the regulation of pH and  $Mn^{2+}/Ca^{2+}$  Golgi homeostasis. In case of TMEM165 deficiency,  $Mn^{2+}$  homeostasis is altered, mainly in the *medial*-/*trans*-Golgi impairing the activities of specific GTs. One can imagine that  $Ca^{2+}$  homeostasis is also affected by a lack of TMEM165 since it is supposed to act as a  $Mn^{2+}/Ca^{2+}$  antiporter. An accumulation of  $Ca^{2+}$  in the Golgi would favor faster trafficking events resulting in shorter retention time of the glycoprotein in each Golgi compartment.

## 4. TMEM165 and SPCA1 in human related diseases

### 4.1. TMEM165 and SPCA1 deficiencies

Based on our work and literature, TMEM165 and SPCA1 are two proteins highly involved in intracellular  $\text{Ca}^{2+}$  and  $\text{Mn}^{2+}$  homeostasis. While pathogenic mutations in *TMEM165* cause a type II CDG [64], *ATP2C1* haploinsufficiency results in a skin disorder named Hailey-Hailey Disease (HHD) [249,250]. TMEM165-CDG, together with SLC39A8-CDG [67], are the two first CDGs in which Golgi glycosylation defects result from a primary disorder in cellular  $\text{Mn}^{2+}$  metabolism. With regards to HHD, this skin disorder characterized by the loss of cell-to-cell adhesion between keratinocytes apparently results from insufficient  $\text{Ca}^{2+}$  levels within the epidermis. In particular, cultured HHD keratinocytes have elevated  $[\text{Ca}^{2+}]_{\text{cytosol}}$  and are less responsive to increasing extracellular  $[\text{Ca}^{2+}]$  than healthy cells suggesting that mutations in *ATP2C1* alter intracellular  $\text{Ca}^{2+}$  regulation in both resting and stimulated conditions. From our fundamental study on isogenic SPCA1 KO Hap1 cells, we demonstrated a functional link between TMEM165 and SPCA1. In this pathophysiological context of HHD, one can imagine that mutations in *ATP2C1* may alter the functional interaction between SPCA1 and TMEM165. Indeed, since keratinocytes differentiation is a  $\text{Ca}^{2+}$ -dependent process, increasing cytosolic  $\text{Ca}^{2+}$  levels might promote the  $\text{Ca}^{2+}$  import into the Golgi lumen through TMEM165 instead of  $\text{Mn}^{2+}$  due to both competition effect and altered SPCA1 function in  $\text{Ca}^{2+}$  pumping. As a consequence,  $\text{Ca}^{2+}$  entry in the Golgi apparatus may dilute intraluminal concentration of  $\text{Mn}^{2+}$  and subsequently alter Golgi glycosylation functions. So far, no glycosylation abnormalities have been observed in patients suffering from HHD. However, since cell-to-cell adhesion between keratinocytes involved glycoproteins such as desmosomal cadherines, it could be worth to further explore this idea. As a first step, we wanted to confirm and extend our fundamental findings of a functional link between TMEM165 and SPCA1 in the pathophysiological condition of HHD. Therefore, we conducted a study in HHD patients' keratinocytes and fibroblasts to investigate whether the partial loss of SPCA1 had an impact on TMEM165 expression, subcellular localization and  $\text{Mn}^{2+}$ -induced degradation [462]. Actually, no change in TMEM165 stability was observed between patients and healthy individuals' fibroblasts. However, while applying a  $\text{MnCl}_2$  pressure, TMEM165 became highly sensitive to lower  $\text{MnCl}_2$  concentrations in both patients' fibroblasts and keratinocytes compared to healthy individuals. This undoubtedly links the functionality of SPCA1 to the stability of TMEM165 in both HHD fibroblasts and keratinocytes upon  $\text{MnCl}_2$  exposure. This result suggests the use of the  $\text{Mn}^{2+}$ -induced degradation of TMEM165 to monitor the functionality of SPCA1 in HHD patients' cells.

So far, both TMEM165 and SPCA1 deficiencies resulted in altered  $Mn^{2+}$  and/or  $Ca^{2+}$  homeostasis at the cellular levels, culminating in very different clinical phenotypes between a multi-systemic disorder (TMEM165-CDG) and a much localized skin disorder (HHD) at the body level. Conversely, TMEM165 and SPCA1 have also been identified in other pathophysiological contexts such as cancers, where both proteins are found overexpressed.

#### 4.2. TMEM165 and SPCA1 overexpression in cancers

Apart from being involved in a CDG, *TMEM165* was recently reported overexpressed in several human cancers including breast and hepatocellular carcinomas [519,520]. With regards to different breast cancer subtypes, TMEM165 becomes highly expressed according to the invasiveness of the cancer and this higher expression is correlated with poor prognosis in breast cancer patients. In healthy conditions, it is known from literature that TMEM165 is up-regulated by 25 times in lactating mammary glands where it acts in Golgi  $Ca^{2+}$  and  $Mn^{2+}$  homeostasis maintenance to sustain and support proper lactose synthase functions during milk production [260,504]. However, in case of breast cancer, TMEM165 up-regulation was shown to promote cell migration, invasiveness and tumor growth presumably by inducing an overall N-glycosylation change in breast cancer cells. These changes in glycosylation are thought to promote the expression of key glycoproteins involved in the regulation of epithelial-mesenchymal transition, a cellular process critical to initiate cancer metastasis [519]. Apart from TMEM165, SPCA1 is also implicated in breast cancers being highly expressed in basal-like breast cancers compared to its rather low expression in luminal subtypes [521–523]. In two separate studies led in the breast cancer cell line MDA-MB-231, authors highlighted that SPCA1 overexpression led to higher  $Ca^{2+}$  levels within the secretory pathway. This  $Ca^{2+}$  increase was assumed to (i) contribute to the proteolytic processing of the pro-insulin-like growth factor 1 receptor (IGF1R) protein whose higher expression in breast cancers has been associated to cancer initiation, evasion of apoptosis and cell proliferation [521] and (ii) might initiate a mineralization process in the secretory pathway, culminating in the formation of microcalcifications, which are a typical radiographic signature of breast cancers [523]. Given that *TMEM165* knockout in the breast cancer cell line MDA-MB-231 results in significant reduction of cell migration and tumor growth, TMEM165 up-regulation is thought to be a good marker of breast cancer invasiveness, placing it at a potential therapeutic target [519]. Similarly, *ATP2C1* silencing in MDA-MB-231 cell line (i) reduces the levels of functional IGF1R concomitantly to the higher accumulation of its inactive form in the TGN and also (ii) significantly reduces the formation of microcalcifications [523]. Altogether, SPCA1 up-regulation is assumed to be a potential marker for basal-like breast cancers also making it a potential target in the treatment of this specific breast cancer.



## References

1. Schwarz DS, Blower MD. The endoplasmic reticulum: structure, function and response to cellular signaling. *Cell. Mol. Life Sci.* 2016 ; 73 : 79–94.
2. Kurokawa K, Nakano A. The ER exit sites are specialized ER zones for the transport of cargo proteins from the ER to the Golgi apparatus. *The Journal of Biochemistry* 2019 ; 165 : 109–114.
3. Linders, Horst, Beest, *et al.* Stx5-Mediated ER-Golgi Transport in Mammals and Yeast. *Cells* 2019 ; 8 : 780.
4. Papanikou E, Glick BS. The yeast Golgi apparatus: Insights and mysteries. *FEBS Letters* 2009 ; 6.
5. Suda Y, Nakano A. The Yeast Golgi Apparatus: The Yeast Golgi Apparatus. *Traffic* 2012 ; 13 : 505–510.
6. Potelle S, Klein A, Foulquier F. Golgi post-translational modifications and associated diseases. *J. Inherit. Metab. Dis.* 2015 ; 38 : 741–751.
7. Glick BS, Nakano A. Membrane Traffic Within the Golgi Apparatus. *Annu. Rev. Cell Dev. Biol.* 2009 ; 25 : 113–132.
8. Raote I, Malhotra V. Protein transport by vesicles and tunnels. *Journal of Cell Biology* 2019 ; 218 : 737–739.
9. Maeda Y. pH Control in Golgi Apparatus and Congenital Disorders of Glycosylation. In : Taniguchi N, Endo T, Hart GW, *et al.*, editors. *Glycoscience: Biology and Medicine*. Tokyo : Springer Japan, 2015 : 921–925.
10. Li J, Ahat E, Wang Y. Golgi Structure and Function in Health, Stress, and Diseases. In : Kloc M, editor. *The Golgi Apparatus and Centriole*. Cham : Springer International Publishing, 2019 : 441–485.
11. Khosrowabadi E, Kellokumpu S. Golgi pH and Ion Homeostasis in Health and Disease. Berlin, Heidelberg : Springer Berlin Heidelberg, 2020 :
12. Blackburn JB, D'Souza Z, Lupashin VV. Maintaining order: COG complex controls Golgi trafficking, processing, and sorting. *FEBS Lett* 2019 ; 593 : 2466–2487.
13. Pokrovskaya ID, Willett R, Smith RD, *et al.* Conserved oligomeric Golgi complex specifically regulates the maintenance of Golgi glycosylation machinery. *Glycobiology* 2011 ; 21 : 1554–1569.
14. Willett R, Ungar D, Lupashin V. The Golgi puppet master: COG complex at center stage of membrane trafficking interactions. *Histochem Cell Biol* 2013 ; 140 : 271–283.
15. Smith RD, Lupashin VV. Role of the conserved oligomeric Golgi (COG) complex in protein glycosylation. *Carbohydrate Research* 2008 ; 343 : 2024–2031.
16. Foulquier F. COG defects, birth and rise! *Biochimica et Biophysica Acta (BBA) - Molecular Basis of Disease* 2009 ; 1792 : 896–902.
17. Schapiro FB, Grinstein S. Determinants of the pH of the Golgi Complex. *J. Biol. Chem.* 2000 ; 275 : 21025–21032.
18. Pizzo P, Lissandron V, Capitanio P, *et al.* Ca(2+) signalling in the Golgi apparatus. *Cell Calcium* 2011 ; 50 : 184–192.
19. Kellokumpu S. Golgi pH, Ion and Redox Homeostasis: How Much Do They Really Matter? *Front. Cell Dev. Biol.* 2019 ; 7 : 93.
20. Jefferies KC, Cipriano DJ, Forgac M. Function, structure and regulation of the vacuolar (H<sup>+</sup>)-ATPases. *Archives of Biochemistry and Biophysics* 2008 ; 476 : 33–42.
21. Maeda Y, Ide T, Koike M, *et al.* GPHR is a novel anion channel critical for acidification and functions of the Golgi apparatus. *Nat Cell Biol* 2008 ; 10 : 1135–1145.
22. Nakamura N, Tanaka S, Teko Y, *et al.* Four Na<sup>+</sup>/H<sup>+</sup> Exchanger Isoforms Are Distributed to Golgi and Post-Golgi Compartments and Are Involved in Organelle pH Regulation. *J. Biol. Chem.* 2005 ; 280 : 1561–1572.
23. Lawrence SP, Bright NA, Luzio JP, *et al.* The Sodium/Proton Exchanger NHE8 Regulates Late Endosomal Morphology and Function. *MBoC* 2010 ; 21 : 3540–3551.

24. Milosavljevic N, Monet M, Léna I, *et al.* The Intracellular Na<sup>+</sup>/H<sup>+</sup> Exchanger NHE7 Effects a Na<sup>+</sup>-Coupled, but Not K<sup>+</sup>-Coupled Proton-Loading Mechanism in Endocytosis. *Cell Reports* 2014 ; 7 : 689–696.
25. Rivinoja A, Pujol FM, Hassinen A, *et al.* Golgi pH, its regulation and roles in human disease. *Annals of Medicine* 2012 ; 44 : 542–554.
26. Van Baelen K, Dode L, Vanoevelen J, *et al.* The Ca<sup>2+</sup>/Mn<sup>2+</sup> pumps in the Golgi apparatus. *Biochimica et Biophysica Acta (BBA) - Molecular Cell Research* 2004 ; 1742 : 103–112.
27. Vanoevelen J, Dode L, Van Baelen K, *et al.* The Secretory Pathway Ca<sup>2+</sup> /Mn<sup>2+</sup> -ATPase 2 Is a Golgi-localized Pump with High Affinity for Ca<sup>2+</sup> Ions. *J. Biol. Chem.* 2005 ; 280 : 22800–22808.
28. Stribny J, Thines L, Deschamps A, *et al.* The human Golgi protein TMEM165 transports calcium and manganese in yeast and bacterial cells. *J. Biol. Chem.* 2020 ; 295 : 3865–3874.
29. Vangheluwe P, Sepúlveda MR, Missiaen L, *et al.* Intracellular Ca<sup>2+</sup> - and Mn<sup>2+</sup> -Transport ATPases. *Chem. Rev.* 2009 ; 109 : 4733–4759.
30. Chen J, Sitsel A, Benoy V, *et al.* Primary Active Ca<sup>2+</sup> Transport Systems in Health and Disease. *Cold Spring Harb Perspect Biol* 2020 ; 12 : a035113.
31. Wolf FI, Trapani V. MagT1: a highly specific magnesium channel with important roles beyond cellular magnesium homeostasis. *Magnesium Research* 2011 ; 24 : 86–91.
32. Zhou H, Clapham DE. Mammalian *MagT1* and *TUSC3* are required for cellular magnesium uptake and vertebrate embryonic development. *PNAS* 2009 ; 106 : 15750–15755.
33. Goytain A, Quamme GA. Identification and characterization of a novel family of membrane magnesium transporters, MMgT1 and MMgT2. *American Journal of Physiology-Cell Physiology* 2008 ; 294 : C495–C502.
34. Liuzzi JP, Cousins RJ. MAMMALIAN ZINC TRANSPORTERS. *Annu. Rev. Nutr.* 2004 ; 24 : 151–172.
35. Huang L, Tapaamorndech S. The SLC30 family of zinc transporters – A review of current understanding of their biological and pathophysiological roles. *Molecular Aspects of Medicine* 2013 ; 34 : 548–560.
36. Jeong J, Eide DJ. The SLC39 family of zinc transporters. *Molecular Aspects of Medicine* 2013 ; 34 : 612–619.
37. Polishchuk R, Lutsenko S. Golgi in copper homeostasis: a view from the membrane trafficking field. *Histochem Cell Biol* 2013 ; 140 : 285–295.
38. Foulquier F, Legrand D. Biometals and glycosylation in humans: Congenital disorders of glycosylation shed lights into the crucial role of Golgi manganese homeostasis. *Biochimica et Biophysica Acta (BBA) - General Subjects* 2020 ; 1864 : 129674.
39. Linders PTA, Peters E, Beest M ter, *et al.* Sugary Logistics Gone Wrong: Membrane Trafficking and Congenital Disorders of Glycosylation. *IJMS* 2020 ; 21 : 4654.
40. Oka T, Ungar D, Hughson FM, *et al.* The COG and COPI Complexes Interact to Control the Abundance of GEARs, a Subset of Golgi Integral Membrane Proteins. *Molecular Biology of the Cell* 2004 ; 15 : 13.
41. Smith RD, Willett R, Kudlyk T, *et al.* The COG Complex, Rab6 and COPI Define a Novel Golgi Retrograde Trafficking Pathway that is Exploited by SubAB Toxin. *Traffic* 2009 ; 10 : 1502–1517.
42. Shestakova A, Suvorova E, Pavliv O, *et al.* Interaction of the conserved oligomeric Golgi complex with t-SNARE Syntaxin5a/Sed5 enhances intra-Golgi SNARE complex stability. *Journal of Cell Biology* 2007 ; 179 : 1179–1192.
43. Willett R, Kudlyk T, Pokrovskaya I, *et al.* COG complexes form spatial landmarks for distinct SNARE complexes. *Nat Commun* 2013 ; 4 : 1553.
44. Kudlyk T, Willett R, Pokrovskaya ID, *et al.* COG6 Interacts with a Subset of the Golgi SNAREs and Is Important for the Golgi Complex Integrity: COG6 and Golgi SNAREs. *Traffic* 2013 ; 14 : 194–204.



45. Willett R, Blackburn JB, Climer L, *et al.* COG lobe B sub-complex engages v-SNARE GS15 and functions via regulated interaction with lobe A sub-complex. *Sci Rep* 2016 ; 6 : 29139.
46. Wu X, Steet RA, Bohorov O, *et al.* Mutation of the COG complex subunit gene COG7 causes a lethal congenital disorder. *Nature Medicine* 2004 ; 10 : 518–523.
47. Foulquier F, Vasile E, Schollen E, *et al.* Conserved oligomeric Golgi complex subunit 1 deficiency reveals a previously uncharacterized congenital disorder of glycosylation type II. *Proceedings of the National Academy of Sciences* 2006 ; 103 : 3764–3769.
48. Foulquier F, Ungar D, Reynders E, *et al.* A new inborn error of glycosylation due to a Cog8 deficiency reveals a critical role for the Cog1–Cog8 interaction in COG complex formation. *Human Molecular Genetics* 2007 ; 16 : 717–730.
49. Kranz C, Ng BG, Sun L, *et al.* COG8 deficiency causes new congenital disorder of glycosylation type IIIh. *Human Molecular Genetics* 2007 ; 16 : 731–741.
50. Reynders E, Foulquier F, Leão Teles E, *et al.* Golgi function and dysfunction in the first COG4-deficient CDG type II patient. *Human Molecular Genetics* 2009 ; 18 : 3244–3256.
51. Paesold-Burda P, Maag C, Troxler H, *et al.* Deficiency in COG5 causes a moderate form of congenital disorders of glycosylation. *Human Molecular Genetics* 2009 ; 18 : 4350–4356.
52. Lubbehusen J, Thiel C, Rind N, *et al.* Fatal outcome due to deficiency of subunit 6 of the conserved oligomeric Golgi complex leading to a new type of congenital disorders of glycosylation. *Human Molecular Genetics* 2010 ; 19 : 3623–3633.
53. Kodera H, Ando N, Yuasa I, *et al.* Mutations in COG2 encoding a subunit of the conserved oligomeric golgi complex cause a congenital disorder of glycosylation: COG2 mutations cause congenital disorder of glycosylation. *Clin Genet* 2015 ; 87 : 455–460.
54. D'Souza Z, Taher FS, Lupashin VV. Golgi inCOGnito: From vesicle tethering to human disease. *Biochimica et Biophysica Acta (BBA) - General Subjects* 2020 ; 1864 : 129694.
55. Shestakova A, Zolov S, Lupashin V. COG Complex-Mediated Recycling of Golgi Glycosyltransferases is Essential for Normal Protein Glycosylation: COG Complex and Golgi Glycosylation. *Traffic* 2006 ; 7 : 191–204.
56. Reynders E, Foulquier F, Annaert W, *et al.* How Golgi glycosylation meets and needs trafficking: the case of the COG complex. *Glycobiology* 2011 ; 21 : 853–863.
57. Rivinoja A, Hassinen A, Kokkonen N, *et al.* Elevated Golgi pH impairs terminal N-glycosylation by inducing mislocalization of Golgi glycosyltransferases. *J. Cell. Physiol.* 2009 ; 220 : 144–154.
58. Maeda Y, Kinoshita T. The Acidic Environment of the Golgi Is Critical for Glycosylation and Transport. *Methods in Enzymology*. Elsevier, 2010 : 495–510.
59. Kornak U, Reynders E, Dimopoulou A, *et al.* Impaired glycosylation and cutis laxa caused by mutations in the vesicular H<sup>+</sup>-ATPase subunit ATP6V0A2. *Nat. Genet.* 2008 ; 40 : 32–34.
60. Guillard M, Dimopoulou A, Fischer B, *et al.* Vacuolar H<sup>+</sup>-ATPase meets glycosylation in patients with cutis laxa. *Biochimica et Biophysica Acta (BBA) - Molecular Basis of Disease* 2009 ; 1792 : 903–914.
61. Van Damme T, Gardeitchik T, Mohamed M, *et al.* Mutations in ATP6V1E1 or ATP6V1A Cause Autosomal-Recessive Cutis Laxa. *Am J Hum Genet* 2017 ; 100 : 216–227.
62. Jansen EJ, Timal S, Ryan M, *et al.* ATP6AP1 deficiency causes an immunodeficiency with hepatopathy, cognitive impairment and abnormal protein glycosylation. *Nat Commun* 2016 ; 7 .
63. Rujano MA, Cannata Serio M, Panasyuk G, *et al.* Mutations in the X-linked ATP6AP2 cause a glycosylation disorder with autophagic defects. *The Journal of Experimental Medicine* 2017 ; 214 : 3707–3729.
64. Foulquier F, Amyere M, Jaeken J, *et al.* TMEM165 Deficiency Causes a Congenital Disorder of Glycosylation. *The American Journal of Human Genetics* 2012 ; 91 : 15–26.
65. Potelle S, Morelle W, Dulary E, *et al.* Glycosylation abnormalities in Gdt1p/TMEM165 deficient cells result from a defect in Golgi manganese homeostasis. *Hum. Mol. Genet.* 2016 ; 25 : 1489–1500.

66. Dulary E, Potelle S, Legrand D, *et al.* TMEM165 deficiencies in Congenital Disorders of Glycosylation type II (CDG-II): Clues and evidences for roles of the protein in Golgi functions and ion homeostasis. *Tissue Cell* 2017 ; 49 : 150–156.
67. Park JH, Hogrebe M, Grüneberg M, *et al.* SLC39A8 Deficiency: A Disorder of Manganese Transport and Glycosylation. *Am. J. Hum. Genet.* 2015 ; 97 : 894–903.
68. Park JH, Hogrebe M, Fobker M, *et al.* SLC39A8 deficiency: biochemical correction and major clinical improvement by manganese therapy. *Genet Med* 2018 ; 20 : 259–268.
69. Lombard V, Golaconda Ramulu H, Drula E, *et al.* The carbohydrate-active enzymes database (CAZy) in 2013. *Nucl. Acids Res.* 2014 ; 42 : D490–D495.
70. Hansen L, Lind-Thomsen A, Joshi HJ, *et al.* A glycoGene mutation map for discovery of diseases of glycosylation. *Glycobiology* 2015 ; 25 : 211–224.
71. Joshi HJ, Hansen L, Narimatsu Y, *et al.* Glycosyltransferase genes that cause monogenic congenital disorders of glycosylation are distinct from glycosyltransferase genes associated with complex diseases. *Glycobiology* 2018 ; 28 : 284–294.
72. Oriol R, Martinez-Duncker I, Chantret I, *et al.* Common Origin and Evolution of Glycosyltransferases Using Dol-P-monosaccharides as Donor Substrate. *Molecular Biology and Evolution* 2002 ; 19 : 1451–1463.
73. Lairson LL, Henrissat B, Davies GJ, *et al.* Glycosyltransferases: Structures, Functions, and Mechanisms. *Annu. Rev. Biochem.* 2008 ; 77 : 521–555.
74. Breton C, Fournel-Gigleux S, Palcic MM. Recent structures, evolution and mechanisms of glycosyltransferases. *Current Opinion in Structural Biology* 2012 ; 22 : 540–549.
75. Gloster TM. Advances in understanding glycosyltransferases from a structural perspective. *Current Opinion in Structural Biology* 2014 ; 28 : 131–141.
76. Albuquerque-Wendt A, Hütte HJ, Buettner FFR, *et al.* Membrane Topological Model of Glycosyltransferases of the GT-C Superfamily. *IJMS* 2019 ; 20 : 4842.
77. Paulson JC, Colley KJ. Glycosyltransferases. Structure, localization, and control of cell type-specific glycosylation. *The Journal of Biological Chemistry* 1989 ; 264 : 17615–17618.
78. Ronak Y. Patel, Petety V. Balaji. Length and Composition Analysis of the Cytoplasmic, Transmembrane and Stem Regions of Human Golgi Glycosyltransferases. *PPL* 2007 ; 14 : 601–609.
79. Lommel M, Schott A, Jank T, *et al.* A Conserved Acidic Motif Is Crucial for Enzymatic Activity of Protein O -Mannosyltransferases. *J. Biol. Chem.* 2011 ; 286 : 39768–39775.
80. Joost H-G, Bell GI, Best JD, *et al.* Nomenclature of the GLUT/SLC2A family of sugar/polyol transport facilitators. *American Journal of Physiology-Endocrinology and Metabolism* 2002 ; 282 : E974–E976.
81. Mueckler M, Thorens B. The SLC2 (GLUT) family of membrane transporters. *Molecular Aspects of Medicine* 2013 ; 34 : 121–138.
82. Sosicka P, Ng BG, Freeze HH. Therapeutic Monosaccharides: Looking Back, Moving Forward. *Biochemistry* 2019 ; acs.biochem.9b00565.
83. Varki A, Cummings RD, Esko JD, *et al.* eds. *Essentials of Glycobiology*. 3rd ed. Cold Spring Harbor (NY) : Cold Spring Harbor Laboratory Press, 2015 : p.
84. Jaeken J, Vanderschueren-Lodeweyckx M, Casaer P. Familial psychomotor retardation with markedly fluctuating serum prolactin, FSH and GH levels, partial TGB-deficiency, increased serum arylsulphatase A and increased CSF protein: a new syndrome? *Pediatr Res* n.d. ; 179.
85. Jaeken J, Eijk HG van, Heul C van der, *et al.* Sialic acid-deficient serum and cerebrospinal fluid transferrin in a newly recognized genetic syndrome. *Clinica Chimica Acta* 1984 ; 144 : 245–247.
86. Van Schaftingen E, Jaeken J. Phosphomannomutase deficiency is a cause of carbohydrate-deficient glycoprotein syndrome type I. *FEBS Letters* 1995 ; 377 : 318–320.
87. Matthijs G, Schollen E, Pardon E, *et al.* Mutations in PMM2, a phosphomannomutase gene on chromosome 16p13, in carbohydrate-deficient glycoprotein type I syndrome (Jaeken syndrome). *Nat. Genet.* 1997 ; 16 : 88–92.

88. Gerardy-Schahn R, Oelmann S, Bakker H. Nucleotide sugar transporters: Biological and functional aspects. *Biochimie* 2001 ; 83 : 775–782.
89. Ishida N, Kawakita M. Molecular physiology and pathology of the nucleotide sugar transporter family (SLC35). *Pflügers Archiv European Journal of Physiology* 2004 ; 447 : 768–775.
90. Song Z. Roles of the nucleotide sugar transporters (SLC35 family) in health and disease. *Molecular Aspects of Medicine* 2013 ; 34 : 590–600.
91. Hadley B, Maggioni A, Ashikov A, *et al.* Structure and function of nucleotide sugar transporters: Current progress. *Computational and Structural Biotechnology Journal* 2014 ; 10 : 23–32.
92. Parker JL, Newstead S. Structural basis of nucleotide sugar transport across the Golgi membrane. *Nature* 2017 ; 551 : 521–524.
93. Hadley B, Litfin T, Day CJ, *et al.* Nucleotide Sugar Transporter SLC35 Family Structure and Function. *Computational and Structural Biotechnology Journal* 2019 ; 17 : 1123–1134.
94. Parker JL, Newstead S. Gateway to the Golgi: molecular mechanisms of nucleotide sugar transporters. *Current Opinion in Structural Biology* 2019 ; 57 : 127–134.
95. Dean N, Zhang YB, Poster JB. The VRG4 Gene Is Required for GDP-mannose Transport into the Lumen of the Golgi in the Yeast, *Saccharomyces cerevisiae*. *J. Biol. Chem.* 1997 ; 272 : 31908–31914.
96. Roy SK, Chiba Y, Takeuchi M, *et al.* Characterization of Yeast Yea4p, a Uridine Diphosphate- N -acetylglucosamine Transporter Localized in the Endoplasmic Reticulum and Required for Chitin Synthesis. *J. Biol. Chem.* 2000 ; 275 : 13580–13587.
97. Kainuma M, Chiba Y, Takeuchi M, *et al.* Overexpression ofHUT1 gene stimulatesin vivo galactosylation by enhancing UDP-galactose transport activity in*Saccharomyces cerevisiae*. *Yeast* 2001 ; 18 : 533–541.
98. Lowenthal MS, Davis KS, Formolo T, *et al.* Identification of Novel N-Glycosylation Sites at Noncanonical Protein Consensus Motifs. *J. Proteome Res.* 2016 ; 15 : 2087–2101.
99. Dutta D, Mandal C, Mandal C. Unusual glycosylation of proteins: Beyond the universal sequon and other amino acids. *Biochimica et Biophysica Acta (BBA) - General Subjects* 2017 ; 1861 : 3096–3108.
100. Kukuruzinska MA, Lennon K. Protein N-Glycosylation: Molecular Genetics and Functional Significance. *Critical Reviews in Oral Biology & Medicine* 1998 ; 9 : 415–448.
101. Helenius J, Ng DTW, Marolda CL, *et al.* Translocation of lipid-linked oligosaccharides across the ER membrane requires Rft1 protein. *Nature* 2002 ; 415 : 447–450.
102. Haeuptle MA, Hennet T. Congenital disorders of glycosylation: an update on defects affecting the biosynthesis of dolichol-linked oligosaccharides. *Hum. Mutat.* 2009 ; 30 : 1628–1641.
103. Denecke J, Kranz C. Hypoglycosylation due to dolichol metabolism defects. *Biochimica et Biophysica Acta (BBA) - Molecular Basis of Disease* 2009 ; 1792 : 888–895.
104. Wolfe LA, Morava E, He M, *et al.* Heritable disorders in the metabolism of the dolichols: A bridge from sterol biosynthesis to molecular glycosylation. *Am. J. Med. Genet.* 2012 ; 160C : 322–328.
105. Buczkowska A, Swiezewska E, Lefeber DJ. Genetic defects in dolichol metabolism. *J Inherit Metab Dis* 2015 ; 38 : 157–169.
106. Mohanty S, P Chaudhary B, Zoetewey D. Structural Insight into the Mechanism of N-Linked Glycosylation by Oligosaccharyltransferase. *Biomolecules* 2020 ; 10 : 624.
107. Helenius A, Aebi M. Roles of N-Linked Glycans in the Endoplasmic Reticulum. *Annu. Rev. Biochem.* 2004 ; 73 : 1019–1049.
108. Galli C, Bernasconi R, Soldà T, *et al.* Malectin Participates in a Backup Glycoprotein Quality Control Pathway in the Mammalian ER. *PLoS ONE* 2011 ; 6 : e16304.
109. Ferris SP, Kodali VK, Kaufman RJ. Glycoprotein folding and quality-control mechanisms in protein-folding diseases. *Disease Models & Mechanisms* 2014 ; 7 : 331–341.
110. Kozlov G, Gehring K. Calnexin cycle – structural features of the ER chaperone system. *FEBS J* 2020 ; febs.15330.

111. Dejgaard S, Nicolay J, Taheri M, *et al.* The ER Glycoprotein Quality Control System. n.d. ; 15.
112. Määttänen P, Gehring K, Bergeron JJM, *et al.* Protein quality control in the ER: The recognition of misfolded proteins. *Seminars in Cell & Developmental Biology* 2010 ; 21 : 500–511.
113. Totani K, Ihara Y, Tsujimoto T, *et al.* The Recognition Motif of the Glycoprotein-Folding Sensor Enzyme UDP-Glc:Glycoprotein Glucosyltransferase <sup>†</sup>. *Biochemistry* 2009 ; 48 : 2933–2940.
114. Hosokawa N, Wada I, Hasegawa K, *et al.* A novel ER  $\alpha$ -mannosidase-like protein accelerates ER-associated degradation. *EMBO Rep* 2001 ; 2 : 415–422.
115. Molinari M. Role of EDEM in the Release of Misfolded Glycoproteins from the Calnexin Cycle. *Science* 2003 ; 299 : 1397–1400.
116. Hirao K, Natsuka Y, Tamura T, *et al.* EDEM3, a Soluble EDEM Homolog, Enhances Glycoprotein Endoplasmic Reticulum-associated Degradation and Mannose Trimming. *J. Biol. Chem.* 2006 ; 281 : 9650–9658.
117. Ninagawa S, Okada T, Sumitomo Y, *et al.* EDEM2 initiates mammalian glycoprotein ERAD by catalyzing the first mannose trimming step. *Journal of Cell Biology* 2014 ; 206 : 347–356.
118. Kanehara K, Kawaguchi S, Ng DTW. The EDEM and Yos9p families of lectin-like ERAD factors. *Seminars in Cell & Developmental Biology* 2007 ; 18 : 743–750.
119. Hosomi A, Tanabe K, Hirayama H, *et al.* Identification of an Htm1 (EDEM)-dependent, Mns1-independent Endoplasmic Reticulum-associated Degradation (ERAD) Pathway in *Saccharomyces cerevisiae*: APPLICATION OF A NOVEL ASSAY FOR GLYCOPROTEIN ERAD. *J. Biol. Chem.* 2010 ; 285 : 24324–24334.
120. Nagae M, Yamaguchi Y, Taniguchi N, *et al.* 3D Structure and Function of Glycosyltransferases Involved in N-glycan Maturation. *IJMS* 2020 ; 21 : 437.
121. Orlean P. Architecture and Biosynthesis of the *Saccharomyces cerevisiae* Cell Wall. *Genetics* 2012 ; 192 : 775–818.
122. Nakayama K, Nagasu T, Shimma Y, *et al.* OCH1 encodes a novel membrane bound mannosyltransferase: outer chain elongation of asparagine-linked oligosaccharides. *The EMBO Journal* 1992 ; 11 : 2511–2519.
123. Nagasu T, Shimma Y-I, Nakanishi Y, *et al.* Isolation of new temperature-sensitive mutants of *Saccharomyces cerevisiae* deficient in mannose outer chain elongation. *Yeast* 1992 ; 8 : 535–547.
124. Nakayama K, Nakanishi-Shindo Y, Tanaka A, *et al.* Substrate specificity of  $\alpha$ -1,6-mannosyltransferase that initiates N-linked mannose outer chain elongation in *Saccharomyces cerevisiae*. *FEBS Letters* 1997 ; 412 : 547–550.
125. Yip CL, Welch SK, Klebl F, *et al.* Cloning and analysis of the *Saccharomyces cerevisiae* MNN9 and MNN1 genes required for complex glycosylation of secreted proteins. *Proceedings of the National Academy of Sciences* n.d. ; 91 : 2723–2727.
126. Wiggins CAR, Munro S. Activity of the yeast MNN1 -1,3-mannosyltransferase requires a motif conserved in many other families of glycosyltransferases. *Proceedings of the National Academy of Sciences* 1998 ; 95 : 7945–7950.
127. Jungmann J, Munro S. Multi-protein complexes in the cis Golgi of *Saccharomyces cerevisiae* with. n.d. ; 12.
128. Stolz J, Munro S. The Components of the *Saccharomyces cerevisiae* Mannosyltransferase Complex M-Pol I Have Distinct Functions in Mannan Synthesis. *J. Biol. Chem.* 2002 ; 277 : 44801–44808.
129. Striebeck A, Robinson DA, Schüttelkopf AW, *et al.* Yeast Mnn9 is both a priming glycosyltransferase and an allosteric activator of mannan biosynthesis. *Open Biol.* 2013 ; 3 : 130022.
130. Jungmann J, Rayner JC, Munro S. The *Saccharomyces cerevisiae* Protein Mnn10p/Bed1p Is a Subunit of a Golgi Mannosyltransferase Complex. *J. Biol. Chem.* 1999 ; 274 : 6579–6585.
131. Neiman M, Manus V, Galibert F, *et al.* *Saccharomyces cerevisiae* HOC1, a Suppressor of pkcl, Encodes a Putative Glycosyltransferase. n.d. ; 9.

132. Rayner JC, Munro S. Identification of the *MNN2* and *MNN5* Mannosyltransferases Required for Forming and Extending the Mannose Branches of the Outer Chain Mannans of *Saccharomyces cerevisiae*. *J. Biol. Chem.* 1998 ; 273 : 26836–26843.
133. Lussier M, Sdicu A-M, Bussey H. The KTR and MNN1 mannosyltransferase families of *Saccharomyces cerevisiae*. *Biochimica et Biophysica Acta (BBA) - General Subjects* 1999 ; 1426 : 323–334.
134. Lussier M, Sdicu A-M, Camirand A, *et al.* Functional Characterization of the YUR1, KTR1, and KTR2 Genes as Members of the Yeast KRE2/MNT1 Mannosyltransferase Gene Family. *J. Biol. Chem.* 1996 ; 271 : 11001–11008.
135. Lussier M, Sdicu A-M, Bussereau F, *et al.* The Ktr1p, Ktr3p, and Kre2p/Mnt1p Mannosyltransferases Participate in the Elaboration of Yeast O - and N -linked Carbohydrate Chains. *J. Biol. Chem.* 1997 ; 272 : 15527–15531.
136. Wang X-H, Nakayama K, Shimma Y, *et al.* *MNN6* , a Member of the *KRE2/MNT1* Family, Is the Gene for Mannosylphosphate Transfer in *Saccharomyces cerevisiae*. *J. Biol. Chem.* 1997 ; 272 : 18117–18124.
137. Odani T, Shimma Y, Tanaka A, *et al.* Cloning and analysis of the *MNN4* gene required for phosphorylation of N-linked oligosaccharides in *Saccharomyces cerevisiae*. *Glycobiology* 1996 ; 6 : 805–810.
138. Jigami Y, Odani T. Mannosylphosphate transfer to yeast mannan. *Biochimica et Biophysica Acta (BBA) - General Subjects* 1999 ; 1426 : 335–345.
139. Fuhrmann U, Bause E, Legler G, *et al.* Novel mannosidase inhibitor blocking conversion of high mannose to complex oligosaccharides. *Nature* 1984 ; 307 : 755–758.
140. Schachter H. The “yellow brick road” to branched complex N-glycans. *Glycobiology* 1991 ; 1 : 454–461.
141. Schachter H. Complex N-glycans: the story of the “yellow brick road.” *Glycoconj J* 2014 ; 31 : 1–5.
142. Roth J, Zuber C. Quality control of glycoprotein folding and ERAD: the role of N-glycan handling, EDEM1 and OS-9. *Histochem Cell Biol* 2017 ; 147 : 269–284.
143. Suzuki T, Seko A, Kitajima K, *et al.* Identification of peptide:N-glycanase activity in mammalian-derived cultures cells. *Biochemical and Biophysical Research Communications* 1993 ; 194 : 1124–1130.
144. Suzuki T. Cytoplasmic peptide:N-glycanase and catabolic pathway for free N-glycans in the cytosol. *Seminars in Cell & Developmental Biology* 2007 ; 18 : 762–769.
145. Suzuki T, Yano K, Sugimoto S, *et al.* Endo- -N-acetylglucosaminidase, an enzyme involved in processing of free oligosaccharides in the cytosol. *Proceedings of the National Academy of Sciences* 2002 ; 99 : 9691–9696.
146. Suzuki T, Hara I, Nakano M, *et al.* Man2C1, an  $\alpha$ -mannosidase, is involved in the trimming of free oligosaccharides in the cytosol. *Biochemical Journal* 2006 ; 400 : 33–41.
147. Suzuki T. Catabolism of N-glycoproteins in mammalian cells: Molecular mechanisms and genetic disorders related to the processes. *Molecular Aspects of Medicine* 2016 ; 51 : 89–103.
148. Enns GM, , FORGE Canada Consortium, Shashi V, *et al.* Mutations in *NGLY1* cause an inherited disorder of the endoplasmic reticulum–associated degradation pathway. *Genet Med* 2014 ; 16 : 751–758.
149. Lam C, Ferreira C, Krasnewich D, *et al.* Prospective phenotyping of *NGLY1-CDDG*, the first congenital disorder of deglycosylation. *Genet Med* 2017 ; 19 : 160–168.
150. Cashman KD. Calcium intake, calcium bioavailability and bone health. *Br J Nutr* 2002 ; 87 : S169–S177.
151. Li K, Wang X-F, Li D-Y, *et al.* The good, the bad, and the ugly of calcium supplementation: a review of calcium intake on human health. *CIA* 2018 ; Volume 13 : 2443–2452.
152. Beto JA. The Role of Calcium in Human Aging. *Clin Nutr Res* 2015 ; 4 : 1.

153. Song L. Calcium and Bone Metabolism Indices. *Advances in Clinical Chemistry*. Elsevier, 2017 : 1–46.
154. O’Neal SL, Zheng W. Manganese Toxicity Upon Overexposure: a Decade in Review. *Curr Environ Health Rep* 2015 ; 2 : 315–328.
155. Chen P. Manganese metabolism in humans. *Front Biosci* 2018 ; 23 : 1655–1679.
156. Scientific Opinion on Dietary Reference Values for calcium *EFSA Journal* n.d. ; 82.
157. Erikson KM, Aschner M. 10. MANGANESE: ITS ROLE IN DISEASE AND HEALTH. In : Carver PL, editor. *Essential Metals in Medicine: Therapeutic Use and Toxicity of Metal Ions in the Clinic*. Berlin, Boston : De Gruyter, 2019 : 253–266.
158. Aschner JL, Aschner M. Nutritional aspects of manganese homeostasis. *Molecular Aspects of Medicine* 2005 ; 26 : 353–362.
159. Au C, Benedetto A, Aschner M. MANGANESE IN EUKARYOTES: THE ROLE OF DMT. 2009 ; 17.
160. Fitsanakis VA, Zhang N, Garcia S, *et al*. Manganese (Mn) and Iron (Fe): Interdependency of Transport and Regulation. *Neurotox Res* 2010 ; 18 : 124–131.
161. Finley JW, Johnson PE, Johnson LK. Sex affects manganese absorption and retention by humans from a diet adequate in manganese. *The American Journal of Clinical Nutrition* 1994 ; 60 : 949–955.
162. Finley JW. Manganese absorption and retention by young women is associated with serum ferritin concentration. *The American Journal of Clinical Nutrition* 1999 ; 70 : 37–43.
163. Scientific Opinion on Dietary Reference Values for manganese *EFSA Journal* n.d. ; 44.
164. Thomas JW. Metabolism of Iron and Manganese. *Journal of Dairy Science* 1970 ; 53 : 1107–1123.
165. Martins AC, Krum BN, Queirós L, *et al*. Manganese in the Diet: Bioaccessibility, Adequate Intake, and Neurotoxicological Effects. *J. Agric. Food Chem.* 2020 ; acs.jafc.0c00641.
166. Fitsanakis VA, Piccola G, Marreilha dos Santos AP, *et al*. Putative proteins involved in manganese transport across the blood-brain barrier. *Hum Exp Toxicol* 2007 ; 26 : 295–302.
167. Peres TV, Schettinger MRC, Chen P, *et al*. “Manganese-induced neurotoxicity: a review of its behavioral consequences and neuroprotective strategies.” *BMC Pharmacol Toxicol* 2016 ; 17 : 57.
168. Horning KJ, Caito SW, Tipps KG, *et al*. Manganese Is Essential for Neuronal Health. *Annu. Rev. Nutr.* 2015 ; 35 : 71–108.
169. Clarke B. Normal Bone Anatomy and Physiology. *CJASN* 2008 ; 3 : S131–S139.
170. Rizzuto R, Pozzan T. When calcium goes wrong: genetic alterations of a ubiquitous signaling route. *Nat Genet* 2003 ; 34 : 135–141.
171. Tuschl K, Mills PB, Clayton PT. Manganese and the Brain. *International Review of Neurobiology*. Elsevier, 2013 : 277–312.
172. Tagliabracci VS, Engel JL, Wen J, *et al*. Secreted Kinase Phosphorylates Extracellular Proteins That Regulate Biomineralization. *Science* 2012 ; 336 : 1150–1153.
173. Ishikawa HO, Xu A, Ogura E, *et al*. The Raine Syndrome Protein FAM20C Is a Golgi Kinase That Phosphorylates Bio-Mineralization Proteins. *PLoS ONE* 2012 ; 7 : e42988.
174. Thines, Deschamps, Stribny, *et al*. Yeast as a Tool for Deeper Understanding of Human Manganese-Related Diseases. *Genes* 2019 ; 10 : 545.
175. Whittaker JW. Manganese superoxide dismutase. *Metal ions in biological systems* 2000 ; 37 : 587–611.
176. Whittaker MM, Whittaker JW. Metallation state of human manganese superoxide dismutase expressed in *Saccharomyces cerevisiae*. *Archives of Biochemistry and Biophysics* 2012 ; 523 : 191–197.
177. Kiningham KK. Chapter 3. Manganese Superoxide Dismutase. In : Costa L, Aschner M, editors. *Issues in Toxicology*. Cambridge : Royal Society of Chemistry, 2014 : 77–118.
178. Barnese K, Gralla EB, Cabelli DE, *et al*. Manganous Phosphate Acts as a Superoxide Dismutase. *J. Am. Chem. Soc.* 2008 ; 130 : 4604–4606.
179. Archibald FS, Fridovich I. The scavenging of superoxide radical by manganous complexes: In vitro. *Archives of Biochemistry and Biophysics* 1982 ; 214 : 452–463.

180. Lapinskas PJ, Cunningham KW, Liu XF, *et al.* Mutations in PMR1 suppress oxidative damage in yeast cells lacking superoxide dismutase. *Mol. Cell. Biol.* 1995 ; 15 : 1382–1388.
181. Lapinskas PJ, Lin S-J, Culotta VC. The role of the *Saccharomyces cerevisiae* CCC1 gene in the homeostasis of manganese ions. *Mol Microbiol* 1996 ; 21 : 519–528.
182. Culotta VC, Daly MJ. Manganese Complexes: Diverse Metabolic Routes to Oxidative Stress Resistance in Prokaryotes and Yeast. *Antioxidants & Redox Signaling* 2013 ; 19 : 933–944.
183. Reddi AR, Culotta VC. Regulation of Manganese Antioxidants by Nutrient Sensing Pathways in *Saccharomyces cerevisiae*. *Genetics* 2011 ; 189 : 1261–1270.
184. McNaughton RL, Reddi AR, Clement MHS, *et al.* Probing in vivo Mn<sup>2+</sup> speciation and oxidative stress resistance in yeast cells with electron-nuclear double resonance spectroscopy. *Proceedings of the National Academy of Sciences* 2010 ; 107 : 15335–15339.
185. Roels H, Lauwerys R, Buchet J-P, *et al.* Epidemiological survey among workers exposed to manganese: Effects on lung, central nervous system, and some biological indices. *Am. J. Ind. Med.* 1987 ; 11 : 307–327.
186. Sikk K, Haldre S, Aquilonius S-M, *et al.* Manganese-Induced Parkinsonism due to Ephedrone Abuse. *Parkinson's Disease* 2011 ; 2011 : 1–8.
187. Ainārs S, Ināra L, Viesturs L, *et al.* A Parkinsonian Syndrome in Methcathinone Users and the Role of Manganese. *The New England Journal of Medicine* 2008 ; 9.
188. Boycott KM, Beaulieu CL, Kernohan KD, *et al.* Autosomal-Recessive Intellectual Disability with Cerebellar Atrophy Syndrome Caused by Mutation of the Manganese and Zinc Transporter Gene SLC39A8. *The American Journal of Human Genetics* 2015 ; 97 : 886–893.
189. Tuschl K, Meyer E, Valdivia LE, *et al.* Mutations in SLC39A14 disrupt manganese homeostasis and cause childhood-onset parkinsonism–dystonia. *Nat Commun* 2016 ; 7 : 11601.
190. Quadri M, Federico A, Zhao T, *et al.* Mutations in SLC30A10 Cause Parkinsonism and Dystonia with Hypermanganesemia, Polycythemia, and Chronic Liver Disease. *The American Journal of Human Genetics* 2012 ; 90 : 467–477.
191. Tuschl K, Clayton PT, Gospe SM, *et al.* Syndrome of Hepatic Cirrhosis, Dystonia, Polycythemia, and Hypermanganesemia Caused by Mutations in SLC30A10 , a Manganese Transporter in Man. *The American Journal of Human Genetics* 2012 ; 90 : 457–466.
192. Anagianni S, Tuschl K. Genetic Disorders of Manganese Metabolism. *Curr Neurol Neurosci Rep* 2019 ; 19 : 33.
193. Zogzas CE, Mukhopadhyay S. Inherited Disorders of Manganese Metabolism. In : Aschner M, Costa LG, editors. *Neurotoxicity of Metals*. Cham : Springer International Publishing, 2017 : 35–49.
194. Winslow JWW, Limesand KH, Zhao N. The Functions of ZIP8, ZIP14, and ZnT10 in the Regulation of Systemic Manganese Homeostasis. *IJMS* 2020 ; 21 : 3304.
195. Mukhopadhyay S. Familial manganese-induced neurotoxicity due to mutations in SLC30A10 or SLC39A14. *NeuroToxicology* 2018 ; 64 : 278–283.
196. Harischandra DS, Ghaisas S, Zenitsky G, *et al.* Manganese-Induced Neurotoxicity: New Insights Into the Triad of Protein Misfolding, Mitochondrial Impairment, and Neuroinflammation. *Front. Neurosci.* 2019 ; 13 : 654.
197. Peres TV, Parmalee NL, Martinez-Finley EJ, *et al.* Untangling the Manganese- $\alpha$ -Synuclein Web. *Front. Neurosci.* 2016 ; 10 .
198. Aschner M, Guilarte TR, Schneider JS, *et al.* Manganese: Recent advances in understanding its transport and neurotoxicity. *Toxicology and Applied Pharmacology* 2007 ; 221 : 131–147.
199. Aschner M, Erikson KM, Hernández EH, *et al.* Manganese and its Role in Parkinson's Disease: From Transport to Neuropathology. *Neuromol Med* 2009 ; 11 : 252–266.
200. Balachandran RC, Mukhopadhyay S, McBride D, *et al.* Brain manganese and the balance between essential roles and neurotoxicity. *J. Biol. Chem.* 2020 ; 295 : 6312–6329.
201. Keen CL, Ensunsa JL, Watson MH, *et al.* Nutritional aspects of manganese from experimental studies. *Neurotoxicology* 1999 ; 20 : 213–223.

202. Carl GF, Blackwell LK, Barnett FC, *et al.* Manganese and Epilepsy: Brain Glutamine Synthetase and Liver Arginase Activities in Genetically Epilepsy Prone and Chronically Seizured Rats. *Epilepsia* 1993 ; 34 : 441–446.
203. Riley LG, Cowley MJ, Gayevskiy V, *et al.* A SLC39A8 variant causes manganese deficiency, and glycosylation and mitochondrial disorders. *J Inherit Metab Dis* 2017 ; 40 : 261–269.
204. Chan H, Babayan V, Blyumin E, *et al.* The P-Type ATPase Superfamily. *J Mol Microbiol Biotechnol* 2010 ; 19 : 5–104.
205. Axelsen KB, Palmgren MG. Evolution of Substrate Specificities in the P-Type ATPase Superfamily. *J Mol Evol* 1998 ; 46 : 84–101.
206. Palmgren MG, Axelsen KB. Evolution of P-type ATPases. *Biochimica et Biophysica Acta (BBA) - Bioenergetics* 1998 ; 1365 : 37–45.
207. Palmgren MG, Nissen P. P-Type ATPases. *Annu. Rev. Biophys.* 2011 ; 40 : 243–266.
208. Sørensen DM, Møller AB, Jakobsen MK, *et al.* Ca<sup>2+</sup> Induces Spontaneous Dephosphorylation of a Novel P5A-type ATPase. *J. Biol. Chem.* 2012 ; 287 : 28336–28348.
209. Sørensen DM, Buch-Pedersen MJ, Palmgren MG. Structural divergence between the two subgroups of P5 ATPases. *Biochimica et Biophysica Acta (BBA) - Bioenergetics* 2010 ; 1797 : 846–855.
210. Sørensen DM, Hølemans T, Veen S van, *et al.* Parkinson disease related ATP13A2 evolved early in animal evolution. *PLoS ONE* 2018 ; 13 : e0193228.
211. Albers RW. Biochemical Aspects of Active Transport. *Annu. Rev. Biochem.* 1967 ; 36 : 727–756.
212. Post RL, Hegyváry C, Kume S. Activation by Adenosine Triphosphate in the Phosphorylation Kinetics of the Sodium and Potassium Ion Transport Adenosine Triphosphatase. *The Journal of Biological Chemistry* 1972 ; 247 : 6530–6540.
213. Palmgren M, Østerberg JT, Nintemann SJ, *et al.* Evolution and a revised nomenclature of P4 ATPases, a eukaryotic family of lipid flippases. *Biochimica et Biophysica Acta (BBA) - Biomembranes* 2019 ; 1861 : 1135–1151.
214. Cronin SR, Rao R, Hampton RY. Cod1p/Spf1p is a P-type ATPase involved in ER function and Ca<sup>2+</sup> homeostasis. *Journal of Cell Biology* 2002 ; 157 : 1017–1028.
215. Andersen JP, Vestergaard AL, Mikkelsen SA, *et al.* P4-ATPases as Phospholipid Flippases—Structure, Function, and Enigmas. *Front. Physiol.* 2016 ; 7 .
216. Veen S van, Sørensen DM, Hølemans T, *et al.* Cellular function and pathological role of ATP13A2 and related P-type transport ATPases in Parkinson's disease and other neurological disorders. *Front. Mol. Neurosci.* 2014 ; 7 .
217. Catty P, Kerchove d'Exaerde A de, Goffeau A. The complete inventory of the yeast *Saccharomyces cerevisiae* P-type transport ATPases. *FEBS Letters* 1997 ; 409 : 325–332.
218. Veen S van, Martin S, Van den Haute C, *et al.* ATP13A2 deficiency disrupts lysosomal polyamine export. *Nature* 2020 ; 578 : 419–424.
219. Sørensen DM, Hølen HW, Pedersen JT, *et al.* The P5A ATPase Spf1p is stimulated by phosphatidylinositol 4-phosphate and influences cellular sterol homeostasis. *MBoC* 2019 ; 30 : 1069–1084.
220. Cohen Y, Megyeri M, Chen OCW, *et al.* The Yeast P5 Type ATPase, Spf1, Regulates Manganese Transport into the Endoplasmic Reticulum. *PLoS ONE* 2013 ; 8 : e85519.
221. Primeau JO, Armanious GP, Fisher ME, *et al.* The SarcoEndoplasmic Reticulum Calcium ATPase. In : Harris JR, Boekema EJ, editors. *Membrane Protein Complexes: Structure and Function.* Singapore : Springer Singapore, 2018 : 229–258.
222. Cali T, Brini M, Carafoli E. Regulation of Cell Calcium and Role of Plasma Membrane Calcium ATPases. *International Review of Cell and Molecular Biology.* Elsevier, 2017 : 259–296.
223. Møller JV, Olesen C, Winther A-ML, *et al.* The sarcoplasmic Ca<sup>2+</sup>-ATPase: design of a perfect chemi-osmotic pump. *Quart. Rev. Biophys.* 2010 ; 43 : 501–566.
224. Gong D, Chi X, Ren K, *et al.* Structure of the human plasma membrane Ca<sup>2+</sup>-ATPase 1 in complex with its obligatory subunit neuroplastin. *Nat Commun* 2018 ; 9 : 3623.



225. Inoue M, Sakuta N, Watanabe S, *et al.* Structural Basis of Sarco/Endoplasmic Reticulum Ca<sup>2+</sup>-ATPase 2b Regulation via Transmembrane Helix Interplay. *Cell Reports* 2019 ; 27 : 1221-1230.e3.
226. Sitsel A, De Raeymaecker J, Drachmann ND, *et al.* Structures of the heart specific SERCA 2a Ca<sup>2+</sup> - ATPase. *EMBO J* 2019 ; 38 .
227. Cunningham KW, Fink GR. Ca<sup>2+</sup> TRANSPORT IN SACCHAROMYCES CEREVISIAE. n.d. ; 10.
228. Periasamy M, Kalyanasundaram A. SERCA pump isoforms: Their role in calcium transport and disease. *Muscle Nerve* 2007 ; 35 : 430–442.
229. Altshuler I, Vaillant JJ, Xu S, *et al.* The Evolutionary History of Sarco(endo)plasmic Calcium ATPase (SERCA). *PLoS ONE* 2012 ; 7 : e52617.
230. Vandecaetsbeek I, Trekels M, De Maeyer M, *et al.* Structural basis for the high Ca<sup>2+</sup> affinity of the ubiquitous SERCA2b Ca<sup>2+</sup> pump. *Proceedings of the National Academy of Sciences* 2009 ; 106 : 18533–18538.
231. Houdou M, Lebredonchel E, Garat A, *et al.* Involvement of thapsigargin– and cyclopiazonic acid–sensitive pumps in the rescue of TMEM165-associated glycosylation defects by Mn<sup>2+</sup>. *The FASEB Journal* 2019 ; 33 : 2669–2679.
232. Chiesi M, Inesi G. Adenosine 5'-Triphosphate Dependent Fluxes of Manganese and Hydrogen Ions in Sarcoplasmic Reticulum Vesicle. n.d. ; 7.
233. Yonekura S-I, Toyoshima C. Mn<sup>2+</sup> transport by Ca<sup>2+</sup>-ATPase of sarcoplasmic reticulum. *FEBS Lett* 2016 ; 590 : 2086–2095.
234. Smith RA, Duncan MJ, Moir DT. Heterologous Protein Secretion from Yeast. *Science* 1985 ; 229 : 1219–1224.
235. Rudolph HK, Antebi A, Fink GR, *et al.* The Yeast Secretory Pathway Is Perturbed by Mutations in PMR1, a Member of a Ca<sup>2+</sup> ATPase Family. *Cell*. 1989 ; 58 : 133–145.
236. Antebi A, Fink GR. The yeast Ca(2+)-ATPase homologue, PMR1, is required for normal Golgi function and localizes in a novel Golgi-like distribution. *MBoC* 1992 ; 3 : 633–654.
237. Wuytack F, Raeymaekers L, Missiaen L. PMR1/SPCA Ca<sup>2+</sup> pumps and the role of the Golgi apparatus as a Ca<sup>2+</sup> store. *Pflügers Arch - Eur J Physiol* 2003 ; 446 : 148–153.
238. Dürr G, Strayle J, Plemper R, *et al.* The medial -Golgi Ion Pump Pmr1 Supplies the Yeast Secretory Pathway with Ca<sup>2+</sup> and Mn<sup>2+</sup> Required for Glycosylation, Sorting, and Endoplasmic Reticulum-Associated Protein Degradation. *MBoC* 1998 ; 9 : 1149–1162.
239. Colinet A-S, Sengottaiyan P, Deschamps A, *et al.* Yeast Gdt1 is a Golgi-localized calcium transporter required for stress-induced calcium signaling and protein glycosylation. *Sci Rep* 2016 ; 6 : 24282.
240. Dulary E, Yu S-Y, Houdou M, *et al.* Investigating the function of Gdt1p in yeast Golgi glycosylation. *Biochim. Biophys. Acta* 2017 ; 1862 : 394–402.
241. Xiang M, Mohamalawari D, Rao R. A Novel Isoform of the Secretory Pathway Ca<sup>2+</sup>,Mn<sup>2+</sup>-ATPase, hSPCA2, Has Unusual Properties and Is Expressed in the Brain. *Journal of Biological Chemistry* 2005 ; 280 : 11608–11614.
242. Dode L, Andersen JP, Vanoevelen J, *et al.* Dissection of the Functional Differences between Human Secretory Pathway Ca<sup>2+</sup>/Mn<sup>2+</sup>-ATPase (SPCA) 1 and 2 Isoenzymes by Steady-state and Transient Kinetic Analyses. *J. Biol. Chem.* 2006 ; 281 : 3182–3189.
243. Pestov NB, Dmitriev RI, Kostina MB, *et al.* Structural evolution and tissue-specific expression of tetrapod-specific second isoform of secretory pathway Ca<sup>2+</sup>-ATPase. *Biochemical and Biophysical Research Communications* 2012 ; 417 : 1298–1303.
244. Cross BM, Hack A, Reinhardt TA, *et al.* SPCA2 Regulates Orai1 Trafficking and Store Independent Ca<sup>2+</sup> Entry in a Model of Lactation. *PLoS ONE* 2013 ; 8 : e67348.
245. Smaardijk S, Chen J, Wuytack F, *et al.* SPCA2 couples Ca<sup>2+</sup> influx via Orai1 to Ca<sup>2+</sup> uptake into the Golgi/secretory pathway. *Tissue and Cell* 2017 ; 49 : 141–149.

246. Fairclough RJ, Dode L, Vanoevelen J, *et al.* Effect of Hailey-Hailey Disease Mutations on the Function of a New Variant of Human Secretory Pathway Ca<sup>2+</sup>/Mn<sup>2+</sup>-ATPase (hSPCA1). *J. Biol. Chem.* 2003 ; 278 : 24721–24730.
247. Micaroni M, Giacchetti G, Plebani R, *et al.* ATP2C1 gene mutations in Hailey–Hailey disease and possible roles of SPCA1 isoforms in membrane trafficking. *Cell Death Dis* 2016 ; 7 : e2259–e2259.
248. Missiaen L, Raeymaekers L, Dode L, *et al.* SPCA1 pumps and Hailey–Hailey disease. *Biochemical and Biophysical Research Communications* 2004 ; 322 : 1204–1213.
249. Sudbrak R. Hailey-Hailey disease is caused by mutations in ATP2C1 encoding a novel Ca<sup>2+</sup> pump. *Human Molecular Genetics* 2000 ; 9 : 1131–1140.
250. Hu Z, Bonifas JM, Beech J, *et al.* Mutations in ATP2C1, encoding a calcium pump, cause Hailey-Hailey disease. *Nat Genet* 2000 ; 24 : 61–65.
251. Hailey H, Hailey H. Familial benign chronic pemphigus. *Arch Dermatol Syphilol* 1939 ; 679–685.
252. Kellermayer R. Hailey-Hailey disease as an orthodisease of PMR1 deficiency in *Saccharomyces cerevisiae*. *FEBS Letters* 2005 ; 579 : 2021–2025.
253. Behne MJ, Tu C-L, Aronchik I, *et al.* Human Keratinocyte ATP2C1 Localizes to the Golgi and Controls Golgi Ca<sup>2+</sup> Stores. *Journal of Investigative Dermatology* 2003 ; 121 : 688–694.
254. Van Baelen K, Vanoevelen J, Callewaert G, *et al.* The contribution of the SPCA1 Ca<sup>2+</sup> pump to the Ca<sup>2+</sup> accumulation in the Golgi apparatus of HeLa cells assessed via RNA-mediated interference. *Biochemical and Biophysical Research Communications* 2003 ; 306 : 430–436.
255. Ton V-K, Mandal D, Vahadji C, *et al.* Functional Expression in Yeast of the Human Secretory Pathway Ca<sup>2+</sup>, Mn<sup>2+</sup>-ATPase Defective in Hailey-Hailey Disease. *J. Biol. Chem.* 2002 ; 277 : 6422–6427.
256. Leitch S, Feng M, Muend S, *et al.* Vesicular distribution of Secretory Pathway Ca<sup>2+</sup>-ATPase isoform 1 and a role in manganese detoxification in liver-derived polarized cells. *Biometals* 2011 ; 24 : 159–170.
257. Mukhopadhyay S, Linstedt AD. Identification of a gain-of-function mutation in a Golgi P-type ATPase that enhances Mn<sup>2+</sup> efflux and protects against toxicity. *Proceedings of the National Academy of Sciences* 2011 ; 108 : 858–863.
258. Cunningham K, Fink G. Calcineurin-dependent growth control in *Saccharomyces cerevisiae* mutants lacking PMC1, a homolog of plasma membrane Ca<sup>2+</sup> ATPases. *The Journal of Cell Biology* 1994 ; 124 : 351–363.
259. Carafoli E. Biogenesis: Plasma membrane calcium ATPase: 15 years of work on the purified enzyme<sup>1</sup>. *FASEB j.* 1994 ; 8 : 993–1002.
260. Reinhardt TA, Lippolis JD, Shull GE, *et al.* Null Mutation in the Gene Encoding Plasma Membrane Ca<sup>2+</sup>-ATPase Isoform 2 Impairs Calcium Transport into Milk. *J. Biol. Chem.* 2004 ; 279 : 42369–42373.
261. Brini M. Plasma membrane Ca<sup>2+</sup>-ATPase: from a housekeeping function to a versatile signaling role. *Pflugers Arch - Eur J Physiol* 2009 ; 457 : 657–664.
262. Brini M, Cali T, Ottolini D, *et al.* The plasma membrane calcium pump in health and disease. *FEBS J* 2013 ; 280 : 5385–5397.
263. Stafford N, Wilson C, Oceandy D, *et al.* The Plasma Membrane Calcium ATPases and Their Role as Major New Players in Human Disease. *Physiological Reviews* 2017 ; 97 : 1089–1125.
264. Strehler EE. Plasma membrane calcium ATPases: From generic Ca<sup>2+</sup> sump pumps to versatile systems for fine-tuning cellular Ca<sup>2+</sup>. *Biochemical and Biophysical Research Communications* 2015 ; 460 : 26–33.
265. Krebs J. The Plasma Membrane Calcium Pump (PMCA): Regulation of Cytosolic Ca<sup>2+</sup>, Genetic Diversities and Its Role in Sub-plasma Membrane Microdomains. In : Krebs J, editor. *Membrane Dynamics and Calcium Signaling*. Cham : Springer International Publishing, 2017 : 3–21.
266. Islam MdS ed. *Calcium Signaling*. Cham : Springer International Publishing, 2020 : p.

267. Schatzmann H. ATP-dependant  $\text{Ca}^{++}$ -extrusion from human red cells. *Experientia* 1966 ; 22 : 364–365.
268. Zylińska L, Soszyński M. Plasma membrane  $\text{Ca}^{2+}$ -ATPase in excitable and nonexcitable cells. *Acta Biochim Pol* 2000 ; 47 : 529–539.
269. Brini M, Carafoli E. The Plasma Membrane  $\text{Ca}^{2+}$  ATPase and the Plasma Membrane Sodium Calcium Exchanger Cooperate in the Regulation of Cell Calcium. *Cold Spring Harbor Perspectives in Biology* 2011 ; 3 : a004168–a004168.
270. Suzuki C. Immunochemical and Mutational Analyses of P-type ATPase Spf1p Involved in the Yeast Secretory Pathway. *Bioscience, Biotechnology, and Biochemistry* 2001 ; 65 : 2405–2411.
271. Suzuki C, Shimma Y. P-type ATPase spf1 mutants show a novel resistance mechanism for the killer toxin SMKT. *Mol Microbiol* 1999 ; 32 : 813–823.
272. Ando A, Suzuki C. Cooperative function of the CHD5-like protein Mdm39p with a P-type ATPase Spf1p in the maintenance of ER homeostasis in *Saccharomyces cerevisiae*. *Mol Genet Genomics* 2005 ; 273 : 497–506.
273. Cronin SR, Khoury A, Ferry DK, *et al.* Regulation of Hmg-Coa Reductase Degradation Requires the P-Type Atpase Cod1p/Spf1p. *The Journal of Cell Biology* 2000 ; 148 : 915–924.
274. Vashist S, Frank CG, Jakob CA, *et al.* Two Distinctly Localized P-Type ATPases Collaborate to Maintain Organelle Homeostasis Required for Glycoprotein Processing and Quality Control. *MBoC* 2002 ; 13 : 3955–3966.
275. Schmidt K, Wolfe DM, Stiller B, *et al.*  $\text{Cd}^{2+}$ ,  $\text{Mn}^{2+}$ ,  $\text{Ni}^{2+}$  and  $\text{Se}^{2+}$  toxicity to *Saccharomyces cerevisiae* lacking YPK9p the orthologue of human ATP13A2. *Biochemical and Biophysical Research Communications* 2009 ; 383 : 198–202.
276. Gitler AD, Chesi A, Geddie ML, *et al.*  $\alpha$ -Synuclein is part of a diverse and highly conserved interaction network that includes PARK9 and manganese toxicity. *Nat Genet* 2009 ; 41 : 308–315.
277. Chesi A, Kilaru A, Fang X, *et al.* The Role of the Parkinson's Disease Gene PARK9 in Essential Cellular Pathways and the Manganese Homeostasis Network in Yeast. *PLoS ONE* 2012 ; 7 : e34178.
278. Covy JP, Waxman EA, Giasson BI. Characterization of cellular protective effects of ATP13A2/PARK9 expression and alterations resulting from pathogenic mutants. *J. Neurosci. Res.* 2012 ; 90 : 2306–2316.
279. Tan J, Zhang T, Jiang L, *et al.* Regulation of Intracellular Manganese Homeostasis by Kufor-Rakeb Syndrome-associated ATP13A2 Protein. *J. Biol. Chem.* 2011 ; 286 : 29654–29662.
280. Ramirez A, Heimbach A, Gründemann J, *et al.* Hereditary parkinsonism with dementia is caused by mutations in ATP13A2, encoding a lysosomal type 5 P-type ATPase. *Nat Genet* 2006 ; 38 : 1184–1191.
281. Di Fonzo A, Chien HF, Socal M, *et al.* ATP13A2 missense mutations in juvenile parkinsonism and young onset Parkinson disease. *Neurology* 2007 ; 68 : 1557–1562.
282. Yang X, Xu Y. Mutations in the *ATP13A2* Gene and Parkinsonism: A Preliminary Review. *BioMed Research International* 2014 ; 2014 : 1–9.
283. Park J-S, Blair NF, Sue CM. The role of ATP13A2 in Parkinson's disease: Clinical phenotypes and molecular mechanisms: ATP13A2 in Parkinson's Disease. *Mov Disord.* 2015 ; 30 : 770–779.
284. Park J-S, Koentjoro B, Veivers D, *et al.* Parkinson's disease-associated human ATP13A2 (PARK9) deficiency causes zinc dyshomeostasis and mitochondrial dysfunction. *Human Molecular Genetics* 2014 ; 23 : 2802–2815.
285. Rinaldi DE, Corradi GR, Cuesta LM, *et al.* The Parkinson-associated human P5B-ATPase ATP13A2 protects against the iron-induced cytotoxicity. *Biochimica et Biophysica Acta (BBA) - Biomembranes* 2015 ; 1848 : 1646–1655.
286. De La Hera DP, Corradi GR, Adamo HP, *et al.* Parkinson's disease-associated human P5B-ATPase ATP13A2 increases spermidine uptake. *Biochem. J.* 2013 ; 450 : 47–53.
287. Holemans T, Sorensen DM, Veen S van, *et al.* A lipid switch unlocks Parkinson's disease-associated ATP13A2. *PNAS* 2015 ; 112 : 9040–9045.

288. Martin S, Veen S van, Holemans T, *et al.* Protection against Mitochondrial and Metal Toxicity Depends on Functional Lipid Binding Sites in ATP13A2. *Parkinson's Disease* 2016 ; 2016 : 1–11.
289. Vallipuram J, Grenville J, Crawford DA. The E646D-ATP13A4 Mutation Associated with Autism Reveals a Defect in Calcium Regulation. *Cell Mol Neurobiol* 2010 ; 30 : 233–246.
290. Kwasnickacrawford D, Carson A, Roberts W, *et al.* Characterization of a novel cation transporter ATPase gene (ATP13A4) interrupted by 3q25–q29 inversion in an individual with language delay. *Genomics* 2005 ; 86 : 182–194.
291. Cai X, Lytton J. The Cation/Ca<sup>2+</sup> Exchanger Superfamily: Phylogenetic Analysis and Structural Implications. *Molecular Biology and Evolution* 2004 ; 21 : 1692–1703.
292. Lytton J. Na<sup>+</sup>/Ca<sup>2+</sup> exchangers: three mammalian gene families control Ca<sup>2+</sup> transport. *Biochemical Journal* 2007 ; 406 : 365–382.
293. Khananshvili D. The SLC8 gene family of sodium–calcium exchangers (NCX) – Structure, function, and regulation in health and disease. *Molecular Aspects of Medicine* 2013 ; 34 : 220–235.
294. Sharma V, O'Halloran DM. Recent structural and functional insights into the family of sodium calcium exchangers: Sodium Calcium Transporters. *genesis* 2014 ; 52 : 93–109.
295. Jalloul AH, Szerencsei RT, Rogasevskaia TP, *et al.* Structure–function relationships of K<sup>+</sup>-dependent Na<sup>+</sup>/Ca<sup>2+</sup> exchangers (NCKX). *Cell Calcium* 2020 ; 86 : 102153.
296. Hassan MT, Lytton J. Potassium-dependent sodium-calcium exchanger (NCKX) isoforms and neuronal function. *Cell Calcium* 2020 ; 86 : 102135.
297. Schnetkamp PPM, Jalloul AH, Liu G, *et al.* The SLC24 Family of K<sup>+</sup>-Dependent Na<sup>+</sup>–Ca<sup>2+</sup> Exchangers. *Current Topics in Membranes*. Elsevier, 2014 : 263–287.
298. Miseta A, Kellermayer R, Aiello DP, *et al.* The vacuolar Ca<sup>2+</sup> /H<sup>+</sup> exchanger Vcx1p/Hum1p tightly controls cytosolic Ca<sup>2+</sup> levels in *S. cerevisiae*. *FEBS Letters* 1999 ; 451 : 132–136.
299. Pozos T, Sekler I, Cyert MS. The product of HUM1, a novel yeast gene, is required for vacuolar Ca<sup>2+</sup>/H<sup>+</sup> exchange and is related to mammalian Na<sup>+</sup>/Ca<sup>2+</sup> exchangers. *Molecular and Cellular Biology* 1996 ; 16 : 3730–3741.
300. Cunningham KW, Fink GR. Calcineurin Inhibits VCX1-Dependent H<sup>+</sup>/Ca<sup>2+</sup> Exchange and Induces Ca<sup>2+</sup> ATPases in *Saccharomyces cerevisiae*. *MOL. CELL. BIOL.* 1996 ; 16 : 12.
301. Pittman JK, Cheng N-H, Shigaki T, *et al.* Functional dependence on calcineurin by variants of the *Saccharomyces cerevisiae* vacuolar Ca<sup>2+</sup>/H<sup>+</sup> exchanger Vcx1p: Yeast vacuolar cation/H<sup>+</sup> transport. *Molecular Microbiology* 2004 ; 54 : 1104–1116.
302. Zhao DY, Xu MH, Zhang MY, *et al.* Vcx1-D1 (M383I), the Vcx1 mutant with a calcineurin-independent vacuolar H<sup>+</sup>/Ca<sup>2+</sup> exchanger activity, confers calcineurin-independent Mn<sup>2+</sup> tolerance in *Saccharomyces cerevisiae*. n.d. ; 30.
303. Demaegd D, Colinet A-S, Deschamps A, *et al.* Molecular Evolution of a Novel Family of Putative Calcium Transporters. *PLoS ONE* 2014 ; 9 : e100851.
304. Demaegd D, Foulquier F, Colinet A-S, *et al.* Newly characterized Golgi-localized family of proteins is involved in calcium and pH homeostasis in yeast and human cells. *Proceedings of the National Academy of Sciences* 2013 ; 110 : 6859–6864.
305. Colinet A-S, Thines L, Deschamps A, *et al.* Acidic and uncharged polar residues in the consensus motifs of the yeast Ca<sup>2+</sup> transporter Gdt1p are required for calcium transport. *Cellular Microbiology* 2017 ; 19 : e12729.
306. Thines L, Deschamps A, Sengottaiyan P, *et al.* The yeast protein Gdt1p transports Mn<sup>2+</sup> ions and thereby regulates manganese homeostasis in the Golgi. *J. Biol. Chem.* 2018 ; 293 : 8048–8055.
307. Potelle S, Dulary E, Climer L, *et al.* Manganese-induced turnover of TMEM165. *Biochemical Journal* 2017 ; 474 : 1481–1493.
308. WestSg AH, Neupert W. Two Related Genes Encoding ExtremelyHydrophobic Proteins Suppress a Lethal Mutation inthe Yeast Mitochondrial Processing Enhancing Protein. n.d. ; 9.
309. Vidal SM, Malo D, Skamene E. Natural Resistance to Infection with Intracellular Parasites: Isolation of a Candidate for Beg. n.d. ; 17.

310. Cellier M, Prive G, Belouchi A, *et al.* Nramp defines a family of membrane proteins. *Proceedings of the National Academy of Sciences* 1995 ; 92 : 10089–10093.
311. Nevo Y, Nelson N. The NRAMP family of metal-ion transporters. *Biochimica et Biophysica Acta (BBA) - Molecular Cell Research* 2006 ; 1763 : 609–620.
312. Czachorowski M, Lam-Yuk-Tseung S, Cellier M, *et al.* Transmembrane Topology of the Mammalian Slc11a2 Iron Transporter. *Biochemistry* 2009 ; 48 : 8422–8434.
313. Forbes JR, Gros P. Iron, manganese, and cobalt transport by Nramp1 (Slc11a1) and Nramp2 (Slc11a2) expressed at the plasma membrane. *Blood* 2003 ; 102 : 1884–1892.
314. Andrews NC. The iron transporter DMT1. *The International Journal of Biochemistry & Cell Biology* 1999 ; 31 : 991–994.
315. Gunshin H, Mackenzie B, Berger UV, *et al.* Cloning and characterization of a mammalian proton-coupled metal-ion transporter. *Nature* 1997 ; 388 : 482–488.
316. Tandy S, Williams M, Leggett A, *et al.* Nramp2 Expression Is Associated with pH-dependent Iron Uptake across the Apical Membrane of Human Intestinal Caco-2 Cells. *Journal of Biological Chemistry* 2000 ; 275 : 1023–1029.
317. Picard V, Govoni G, Jabado N, *et al.* Nramp 2 (DCT1/DMT1) Expressed at the Plasma Membrane Transports Iron and Other Divalent Cations into a Calcein-accessible Cytoplasmic Pool. *J. Biol. Chem.* 2000 ; 275 : 35738–35745.
318. Garrick MD, Dolan KG, Horbinski C, *et al.* DMT1: A mammalian transporter for multiple metals. n.d. ; 14.
319. Garrick MD, Singleton ST, Vargas F, *et al.* DMT1: Which metals does it transport? *Biol. Res.* 2006 ; 39 .
320. Lee PL, Gelbart T, West C, *et al.* The Human Nramp2 Gene: Characterization of the Gene Structure, Alternative Splicing, Promoter Region and Polymorphisms. *Blood Cells, Molecules, and Diseases* 1998 ; 24 : 199–215.
321. Yanatori I, Kishi F. DMT1 and iron transport. *Free Radical Biology and Medicine* 2019 ; 133 : 55–63.
322. Hubert N, Hentze MW. Previously uncharacterized isoforms of divalent metal transporter (DMT)-1: Implications for regulation and cellular function. *Proceedings of the National Academy of Sciences* 2002 ; 99 : 12345–12350.
323. Yanatori I, Tabuchi M, Kawai Y, *et al.* Heme and non-heme iron transporters in non-polarized and polarized cells. *BMC Cell Biol* 2010 ; 11 : 39.
324. Gruenheid S, Canonne-Hergaux F, Gauthier S, *et al.* The Iron Transport Protein NRAMP2 Is an Integral Membrane Glycoprotein That Colocalizes with Transferrin in Recycling Endosomes. *Journal of Experimental Medicine* 1999 ; 189 : 831–841.
325. Tabuchi M, Tanaka N, Nishida-Kitayama J, *et al.* Alternative Splicing Regulates the Subcellular Localization of Divalent Metal Transporter 1 Isoforms. *MBoC* 2002 ; 13 : 4371–4387.
326. Tabuchi M, Yoshimori T, Yamaguchi K, *et al.* Human NRAMP2/DMT1, Which Mediates Iron Transport across Endosomal Membranes, Is Localized to Late Endosomes and Lysosomes in HEP-2 Cells. *J. Biol. Chem.* 2000 ; 275 : 22220–22228.
327. Chua ACG, Morgan EH. Manganese metabolism is impaired in the Belgrade laboratory rat. *Journal of Comparative Physiology B: Biochemical, Systemic, and Environmental Physiology* 1997 ; 167 : 361–369.
328. Fleming MD, Romano MA, Su MA, *et al.* Nramp2 is mutated in the anemic Belgrade (b) rat: Evidence of a role for Nramp2 in endosomal iron transport. *Proceedings of the National Academy of Sciences* 1998 ; 95 : 1148–1153.
329. Fleming MD, Trenor CC, Su MA, *et al.* Microcytic anemia mice have a mutation in NRAMP2, a candidate iron transporter gene. *Nat Genet* 1997 ; 16 : 383–386.
330. Su MA, Iii CCT, Fleming JC, *et al.* The G185R Mutation Disrupts Function of the Iron Transporter Nramp2. n.d. ; 7.

331. Knopfel M, Zhao L, Garrick MD. Transport of Divalent Transition-Metal Ions Is Lost in Small-Intestinal Tissue of b/b Belgrade Rats. n.d. ; 12.
332. Portnoy ME, Liu XF, Culotta VC. *Saccharomyces cerevisiae* Expresses Three Functionally Distinct Homologues of the Nramp Family of Metal Transporters. *MOL. CELL. BIOL.* 2000 ; 20 : 10.
333. Cohen A, Nelson H, Nelson N. The Family of SMF Metal Ion Transporters in Yeast Cells. *J. Biol. Chem.* 2000 ; 275 : 33388–33394.
334. Supek F, Supekova L, Nelson H, *et al.* A yeast manganese transporter related to the macrophage protein involved in conferring resistance to mycobacteria. *Proceedings of the National Academy of Sciences* 1996 ; 93 : 5105–5110.
335. Luk EE-C, Culotta VC. Manganese Superoxide Dismutase in *Saccharomyces cerevisiae* Acquires Its Metal Co-factor through a Pathway Involving the Nramp Metal Transporter, Smf2p. *J. Biol. Chem.* 2001 ; 276 : 47556–47562.
336. Culotta VC, Yang M, Hall MD. Manganese Transport and Trafficking: Lessons Learned from *Saccharomyces cerevisiae*. *Eukaryotic Cell* 2005 ; 4 : 1159–1165.
337. Baltaci AK, Yuce K. Zinc Transporter Proteins. *Neurochem Res* 2018 ; 43 : 517–530.
338. Kambe T, Tsuji T, Hashimoto A, *et al.* The Physiological, Biochemical, and Molecular Roles of Zinc Transporters in Zinc Homeostasis and Metabolism. *Physiological Reviews* 2015 ; 95 : 749–784.
339. Kimura T, Kambe T. The Functions of Metallothionein and ZIP and ZnT Transporters: An Overview and Perspective. *IJMS* 2016 ; 17 : 336.
340. Tuschl K, Mills PB, Parsons H, *et al.* Hepatic cirrhosis, dystonia, polycythaemia and hypermanganesaemia—A new metabolic disorder. *J Inherit Metab Dis* 2008 ; 31 : 151–163.
341. Bosomworth HJ, Thornton JK, Coneyworth LJ, *et al.* Efflux function, tissue-specific expression and intracellular trafficking of the Zn transporter ZnT10 indicate roles in adult Zn homeostasis. *Metallomics* 2012 ; 4 : 771.
342. Leyva-Illades D, Chen P, Zogzas CE, *et al.* SLC30A10 Is a Cell Surface-Localized Manganese Efflux Transporter, and Parkinsonism-Causing Mutations Block Its Intracellular Trafficking and Efflux Activity. *Journal of Neuroscience* 2014 ; 34 : 14079–14095.
343. Chen P, Bowman AB, Mukhopadhyay S, *et al.* SLC30A10: A novel manganese transporter. *Worm* 2015 ; 4 : e1042648.
344. Zogzas CE, Aschner M, Mukhopadhyay S. Structural Elements in the Transmembrane and Cytoplasmic Domains of the Metal Transporter SLC30A10 Are Required for Its Manganese Efflux Activity. *J. Biol. Chem.* 2016 ; 291 : 15940–15957.
345. Zogzas CE, Mukhopadhyay S. Putative metal binding site in the transmembrane domain of the manganese transporter SLC30A10 is different from that of related zinc transporters. *Metallomics* 2018 ; 10 : 1053–1064.
346. Carmona A, Zogzas CE, Roudeau S, *et al.* SLC30A10 Mutation Involved in Parkinsonism Results in Manganese Accumulation within Nanovesicles of the Golgi Apparatus. *ACS Chem. Neurosci.* 2019 ; 10 : 599–609.
347. Lechpammer M, Clegg MS, Muzar Z, *et al.* Pathology of inherited manganese transporter deficiency: Postmortem Analysis of Inherited Manganism. *Ann Neurol.* 2014 ; 75 : 608–612.
348. Taylor CA, Hutchens S, Liu C, *et al.* SLC30A10 transporter in the digestive system regulates brain manganese under basal conditions while brain SLC30A10 protects against neurotoxicity. *J. Biol. Chem.* 2019 ; 294 : 1860–1876.
349. Taylor KM, Morgan HE, Johnson A, *et al.* Structure-function analysis of a novel member of the LIV-1 subfamily of zinc transporters, ZIP14. *FEBS Letters* 2005 ; 579 : 427–432.
350. Fujishiro H, Yano Y, Takada Y, *et al.* Roles of ZIP8, ZIP14, and DMT1 in transport of cadmium and manganese in mouse kidney proximal tubule cells. *Metallomics* 2012 ; 4 : 700.
351. Nebert DW, Gálvez-Peralta M, Hay EB, *et al.* ZIP14 and ZIP8 zinc/bicarbonate symporters in *Xenopus oocytes*: characterization of metal uptake and inhibition. *Metallomics* 2012 ; 4 : 1218.

352. Zhao N, Gao J, Enns CA, *et al.* ZRT/IRT-like Protein 14 (ZIP14) Promotes the Cellular Assimilation of Iron from Transferrin. *J. Biol. Chem.* 2010 ; 285 : 32141–32150.
353. Scheiber IF, Wu Y, Morgan SE, *et al.* The intestinal metal transporter ZIP14 maintains systemic manganese homeostasis. *J. Biol. Chem.* 2019 ; 294 : 9147–9160.
354. Aydemir TB, Thorn TL, Ruggiero CH, *et al.* Intestine-specific deletion of metal transporter Zip14 (Slc39a14) causes brain manganese overload and locomotor defects of manganism. *n.d.* ; 26.
355. Nebert DW, Liu Z. SLC39A8 gene encoding a metal ion transporter: discovery and bench to bedside. *Hum Genomics* 2019 ; 13 : 51.
356. Girijashanker K, He L, Soleimani M, *et al.* Slc39a14 Gene Encodes ZIP14, A Metal/Bicarbonate Symporter: Similarities to the ZIP8 Transporter. *Mol Pharmacol* 2008 ; 73 : 1413–1423.
357. He L, Girijashanker K, Dalton TP, *et al.* ZIP8, Member of the Solute-Carrier-39 (SLC39) Metal-Transporter Family: Characterization of Transporter Properties. *Mol Pharmacol* 2006 ; 70 : 171–180.
358. Liu Z, Li H, Soleimani M, *et al.* Cd<sup>2+</sup> versus Zn<sup>2+</sup> uptake by the ZIP8 HCO<sub>3</sub><sup>-</sup>-dependent symporter: Kinetics, electrogenicity and trafficking. *Biochemical and Biophysical Research Communications* 2008 ; 365 : 814–820.
359. Choi E-K, Nguyen T-T, Gupta N, *et al.* Functional analysis of SLC39A8 mutations and their implications for manganese deficiency and mitochondrial disorders. *Sci Rep* 2018 ; 8 : 3163.
360. Eide DJ. The molecular biology of metal ion transport in *Saccharomyces cerevisiae*. *Annu. Rev. Nutr.* 1998 ; 18 : 441–469.
361. Lin SJ, Culotta VC. Suppression of oxidative damage by *Saccharomyces cerevisiae* ATX2, which encodes a manganese-trafficking protein that localizes to Golgi-like vesicles. *Mol. Cell. Biol.* 1996 ; 16 : 6303–6312.
362. Abboud S, Haile DJ. A Novel Mammalian Iron-regulated Protein Involved in Intracellular Iron Metabolism. *J. Biol. Chem.* 2000 ; 275 : 19906–19912.
363. Donovan A, Brownlie A, Zhou Y, *et al.* Positional cloning of zebrafish ferroportin1 identifies a conserved vertebrate iron exporter. *Nature* 2000 ; 403 : 776–781.
364. McKie AT, Marciani P, Rolfs A, *et al.* A Novel Duodenal Iron-Regulated Transporter, IREG1, Implicated in the Basolateral Transfer of Iron to the Circulation. *Molecular Cell* 2000 ; 5 : 299–309.
365. McKie AT, Barlow DJ. The SLC40 basolateral iron transporter family (IREG1/ferroportin/MTP1). *Pflügers Archiv European Journal of Physiology* 2004 ; 447 : 801–806.
366. Donovan A, Lima CA, Pinkus JL, *et al.* The iron exporter ferroportin/Slc40a1 is essential for iron homeostasis. *Cell Metabolism* 2005 ; 1 : 191–200.
367. Madejczyk MS, Ballatori N. The iron transporter ferroportin can also function as a manganese exporter. *Biochimica et Biophysica Acta (BBA) - Biomembranes* 2012 ; 1818 : 651–657.
368. Yin Z, Jiang H, Lee E-SY, *et al.* Ferroportin is a manganese-responsive protein that decreases manganese cytotoxicity and accumulation. *Journal of Neurochemistry* 2010 ; 112 : 1190–1198.
369. Choi E-K, Nguyen T-T, Iwase S, *et al.* Ferroportin disease mutations influence manganese accumulation and cytotoxicity. *FASEB j.* 2019 ; 33 : 2228–2240.
370. Jin L, Frazer DM, Lu Y, *et al.* Mice overexpressing hepcidin suggest ferroportin does not play a major role in Mn homeostasis. *Metallomics* 2019 ; 11 : 959–967.
371. Karakus E, Wannowius M, Müller SF, *et al.* The orphan solute carrier SLC10A7 is a novel negative regulator of intracellular calcium signaling. *Sci Rep* 2020 ; 10 : 7248.
372. Zhao Y, Yan H, Happeck R, *et al.* The plasma membrane protein Rch1 is a negative regulator of cytosolic calcium homeostasis and positively regulated by the calcium/calcineurin signaling pathway in budding yeast. *European Journal of Cell Biology* 2016 ; 95 : 164–174.
373. Ashikov A, Abu Bakar N, Wen X-Y, *et al.* Integrating glycomics and genomics uncovers SLC10A7 as essential factor for bone mineralization by regulating post-Golgi protein transport and glycosylation. *Human Molecular Genetics* 2018 ; 27 : 3029–3045.

374. Godoy JR, Fernandes C, Döring B, *et al.* Molecular and phylogenetic characterization of a novel putative membrane transporter (SLC10A7), conserved in vertebrates and bacteria. *European Journal of Cell Biology* 2007 ; 86 : 445–460.
375. Jiang L, Alber J, Wang J, *et al.* The *Candida albicans* plasma membrane protein Rch1p, a member of the vertebrate SLC10 carrier family, is a novel regulator of cytosolic Ca<sup>2+</sup> homeostasis. *Biochemical Journal* 2012 ; 444 : 497–502.
376. Dubail J, Huber C, Chantepie S, *et al.* SLC10A7 mutations cause a skeletal dysplasia with amelogenesis imperfecta mediated by GAG biosynthesis defects. *Nature Communications* 2018 ; 9 : 3087.
377. Jensen LT, Ajua-Alemanji M, Culotta VC. The *Saccharomyces cerevisiae* High Affinity Phosphate Transporter Encoded by PHO84 Also Functions in Manganese Homeostasis. *J. Biol. Chem.* 2003 ; 278 : 42036–42040.
378. Fu D, Beeler T, Dunn T. XII. Yeast sequencing reports. Sequence, mapping and disruption of CCC1, a gene that cross-complements the Ca<sup>2+</sup>-sensitive phenotype of csg1 mutants. *Yeast* 1994 ; 10 : 515–521.
379. Li L, Chen OS, Ward DM, *et al.* CCC1 Is a Transporter That Mediates Vacuolar Iron Storage in Yeast. *J. Biol. Chem.* 2001 ; 276 : 29515–29519.
380. Chen OS, Kaplan J. CCC1 Suppresses Mitochondrial Damage in the Yeast Model of Friedreich's Ataxia by Limiting Mitochondrial Iron Accumulation. *J. Biol. Chem.* 2000 ; 275 : 7626–7632.
381. Putney Jr JW. A model for receptor-regulated calcium entry. *Cell Calcium* 1986 ; 1–12.
382. Prakriya M, Lewis RS. Store-Operated Calcium Channels. *Physiol Rev* 2015 ; 95 : 54.
383. Liou J, Kim ML, Do Heo W, *et al.* STIM Is a Ca<sup>2+</sup> Sensor Essential for Ca<sup>2+</sup>-Store-Depletion-Triggered Ca<sup>2+</sup> Influx. *Current Biology* 2005 ; 15 : 1235–1241.
384. Roos J, DiGregorio PJ, Yeromin AV, *et al.* STIM1, an essential and conserved component of store-operated Ca<sup>2+</sup> channel function. *Journal of Cell Biology* 2005 ; 169 : 435–445.
385. Feske S. CRAC channels and disease – From human CRAC channelopathies and animal models to novel drugs. *Cell Calcium* 2019 ; 80 : 112–116.
386. Vig M. CRACM1 Is a Plasma Membrane Protein Essential for Store-Operated Ca<sup>2+</sup> Entry. *Science* 2006 ; 312 : 1220–1223.
387. Prakriya M, Feske S, Gwack Y, *et al.* Orai1 is an essential pore subunit of the CRAC channel. *Nature* 2006 ; 443 : 230–233.
388. Zhang SL, Yeromin AV, Zhang XH-F, *et al.* Genome-wide RNAi screen of Ca<sup>2+</sup> influx identifies genes that regulate Ca<sup>2+</sup> release-activated Ca<sup>2+</sup> channel activity. *Proceedings of the National Academy of Sciences* 2006 ; 103 : 9357–9362.
389. Lewis RS. Store-Operated Calcium Channels: From Function to Structure and Back Again. *Cold Spring Harb Perspect Biol* 2020 ; 12 : a035055.
390. Frischauf I, Fahrner M, Jardín I, *et al.* The STIM1: Orai Interaction. In : Rosado JA, editor. *Calcium Entry Pathways in Non-excitabile Cells*. Cham : Springer International Publishing, 2016 : 25–46.
391. Lunz V, Romanin C, Frischauf I. STIM1 activation of Orai1. *Cell Calcium* 2019 ; 77 : 29–38.
392. Nguyen NT, Han W, Cao W-M, *et al.* Store-Operated Calcium Entry Mediated by ORAI and STIM. In : Pollock DM, editor. *Comprehensive Physiology*. Hoboken, NJ, USA : John Wiley & Sons, Inc., 2018 : 981–1002.
393. Yen M, Lewis RS. Numbers count: How STIM and Orai stoichiometry affect store-operated calcium entry. *Cell Calcium* 2019 ; 79 : 35–43.
394. Yeung PS-W, Yamashita M, Prakriya M. Pore opening mechanism of CRAC channels. *Cell Calcium* 2017 ; 63 : 14–19.
395. Yeung PS, Yamashita M, Prakriya M. Molecular basis of allosteric Orai1 channel activation by STIM1. *J Physiol* 2020 ; 598 : 1707–1723.



396. Cheng KT, Liu X, Ong HL, *et al.* Functional Requirement for Orai1 in Store-operated TRPC1-STIM1 Channels. *J. Biol. Chem.* 2008 ; 283 : 12935–12940.
397. Cheng KT, Liu X, Ong HL, *et al.* Local Ca<sup>2+</sup> Entry Via Orai1 Regulates Plasma Membrane Recruitment of TRPC1 and Controls Cytosolic Ca<sup>2+</sup> Signals Required for Specific Cell Functions. *PLoS Biol* 2011 ; 9 : e1001025.
398. Ong HL, Souza LB de, Ambudkar IS. Role of TRPC Channels in Store-Operated Calcium Entry. In : Rosado JA, editor. *Calcium Entry Pathways in Non-excitabile Cells*. Cham : Springer International Publishing, 2016 : 87–109.
399. Williams RT, Senior PV, Stekelenburg LV, *et al.* Stromal interaction molecule 1 (STIM1), a transmembrane protein with growth suppressor activity, contains an extracellular SAM domain modified by N-linked glycosylation. *Biochimica et Biophysica Acta* n.d. ; 7.
400. Niemeyer BA. Changing calcium: CRAC channel (STIM and Orai) expression, splicing, and posttranslational modifiers. *American Journal of Physiology-Cell Physiology* 2016 ; 310 : C701–C709.
401. Smyth JT, Petranka JG, Boyles RR, *et al.* Phosphorylation of STIM1 underlies suppression of store-operated calcium entry during mitosis. *Nat Cell Biol* 2009 ; 11 : 1465–1472.
402. Kilch T, Alansary D, Peglow M, *et al.* Mutations of the Ca<sup>2+</sup> -sensing Stromal Interaction Molecule STIM1 Regulate Ca<sup>2+</sup> Influx by Altered Oligomerization of STIM1 and by Destabilization of the Ca<sup>2+</sup> Channel Orai1. *J. Biol. Chem.* 2013 ; 288 : 1653–1664.
403. Smyth JT, Beg AM, Wu S, *et al.* Phosphoregulation of STIM1 Leads to Exclusion of the Endoplasmic Reticulum from the Mitotic Spindle. *Current Biology* 2012 ; 22 : 1487–1493.
404. Feske S, Prakriya M, Rao A, *et al.* A severe defect in CRAC Ca<sup>2+</sup> channel activation and altered K<sup>+</sup> channel gating in T cells from immunodeficient patients. *Journal of Experimental Medicine* 2005 ; 202 : 651–662.
405. Feske S, Gwack Y, Prakriya M, *et al.* A mutation in Orai1 causes immune deficiency by abrogating CRAC channel function. *Nature* 2006 ; 441 : 179–185.
406. Hoover PJ, Lewis RS. Stoichiometric requirements for trapping and gating of Ca<sup>2+</sup> release-activated Ca<sup>2+</sup> (CRAC) channels by stromal interaction molecule 1 (STIM1). *Proc Natl Acad Sci USA* 2011 ; 108 : 13299–13304.
407. Hou X, Pedi L, Diver MM, *et al.* Crystal Structure of the Calcium Release-Activated Calcium Channel Orai. *Science* 2012 ; 338 : 1308–1313.
408. Putney JW. Forms and functions of store-operated calcium entry mediators, STIM and Orai. *Advances in Biological Regulation* 2018 ; 68 : 88–96.
409. Feng M, Grice DM, Faddy HM, *et al.* Store-Independent Activation of Orai1 by SPCA2 in Mammary Tumors. *Cell* 2010 ; 143 : 84–98.
410. Smaardijk S, Chen J, Kerselaers S, *et al.* Store-independent coupling between the Secretory Pathway Ca<sup>2+</sup> transport ATPase SPCA1 and Orai1 in Golgi stress and Hailey-Hailey disease. *Biochimica et Biophysica Acta (BBA) - Molecular Cell Research* 2018 ; 1865 : 855–862.
411. Dörr K, Kilch T, Kappel S, *et al.* Cell type-specific glycosylation of Orai1 modulates store-operated Ca<sup>2+</sup> entry. *Sci. Signal.* 2016 ; 9 : ra25–ra25.
412. Bonilla M, Cunningham KW. Calcium Release and Influx in Yeast: TRPC and VGCC Rule Another Kingdom. *Science Signaling* 2002 ; 2002 : pe17–pe17.
413. Locke EG, Bonilla M, Liang L, *et al.* A Homolog of Voltage-Gated Ca<sup>2+</sup> Channels Stimulated by Depletion of Secretory Ca<sup>2+</sup> in Yeast. *MOL. CELL. BIOL.* 2000 ; 18 : 9.
414. Venkatachalam K, Montell C. TRP Channels. *Annu. Rev. Biochem.* 2007 ; 76 : 387–417.
415. Samanta A, Hughes TET, Moiseenkova-Bell VY. Transient Receptor Potential (TRP) Channels. In : Harris JR, Boekema EJ, editors. *Membrane Protein Complexes: Structure and Function*. Singapore : Springer Singapore, 2018 : 141–165.
416. Palmer CP, Zhou X-L, Lin J, *et al.* A TRP homolog in *Saccharomyces cerevisiae* forms an intracellular Ca<sup>2+</sup>-permeable channel in the yeast vacuolar membrane. *Proceedings of the National Academy of Sciences* 2001 ; 98 : 7801–7805.

417. Denis V, Cyert MS. Internal Ca<sup>2+</sup> release in yeast is triggered by hypertonic shock and mediated by a TRP channel homologue. *Journal of Cell Biology* 2002 ; 156 : 29–34.
418. Chang Y, Schlenstedt G, Flockerzi V, *et al.* Properties of the intracellular transient receptor potential (TRP) channel in yeast, Yvc1. *FEBS Letters* 2010 ; 584 : 2028–2032.
419. Hamamoto S, Mori Y, Yabe I, *et al.* In vitro and in vivo characterization of modulation of the vacuolar cation channel TRPY 1 from *Saccharomyces cerevisiae*. *FEBS J* 2018 ; 285 : 1146–1161.
420. Zhou X-L, Batiza AF, Loukin SH, *et al.* The transient receptor potential channel on the yeast vacuole is mechanosensitive. *Proceedings of the National Academy of Sciences* 2003 ; 100 : 7105–7110.
421. Ruta L, Nicolau I, Popa C, *et al.* Manganese Suppresses the Haploinsufficiency of Heterozygous trpy1 $\Delta$ /TRPY1 *Saccharomyces cerevisiae* Cells and Stimulates the TRPY1-Dependent Release of Vacuolar Ca<sup>2+</sup> under H<sub>2</sub>O<sub>2</sub> Stress. *Cells* 2019 ; 8 : 79.
422. Fatt P, Katz B. The electrical properties of crustacean muscle fibres. *J. Phys* 1953 ; 171–204.
423. Zamponi GW, Striessnig J, Koschak A, *et al.* The Physiology, Pathology, and Pharmacology of Voltage-Gated Calcium Channels and Their Future Therapeutic Potential. *Pharmacol Rev* 2015 ; 67 : 821–870.
424. Catterall WA, Lenaeus MJ, Gamal El-Din TM. Structure and Pharmacology of Voltage-Gated Sodium and Calcium Channels. *Annu. Rev. Pharmacol. Toxicol.* 2020 ; 60 : 133–154.
425. Dolphin AC. A short history of voltage-gated calcium channels: Voltage-gated calcium channels. *British Journal of Pharmacology* 2009 ; 147 : S56–S62.
426. Dolphin AC. Voltage-gated calcium channels: Their discovery, function and importance as drug targets. *Brain and Neuroscience Advances* 2018 ; 2 : 239821281879480.
427. Takahashi M, Seagar MJ, Jones JF, *et al.* Subunit structure of dihydropyridine-sensitive calcium channels from skeletal muscle. *Proceedings of the National Academy of Sciences* 1987 ; 84 : 5478–5482.
428. Tanabe T, Takeshima H, Mikami A, *et al.* Primary structure of the receptor for calcium channel blockers from skeletal muscle. *Nature* 1987 ; 328 .
429. Dolphin AC. Voltage-gated calcium channels and their auxiliary subunits: physiology and pathophysiology and pharmacology: Voltage-gated calcium channels. *J Physiol* 2016 ; 594 : 5369–5390.
430. Fischer M, Schnell N, Chattaway J, *et al.* The *Saccharomyces cerevisiae* CCH1 gene is involved in calcium influx and mating. *FEBS Letters* 1997 ; 419 : 259–262.
431. Iida H, Nakamura H, Ono T, *et al.* MID1, a novel *Saccharomyces cerevisiae* gene encoding a plasma membrane protein, is required for Ca<sup>2+</sup> influx and mating. *Mol. Cell. Biol.* 1994 ; 14 : 8259–8271.
432. Martin DC, Kim H, Mackin NA, *et al.* New Regulators of a High Affinity Ca<sup>2+</sup> Influx System Revealed through a Genome-wide Screen in Yeast. *J. Biol. Chem.* 2011 ; 286 : 10744–10754.
433. Kato T, Kubo A, Nagayama T, *et al.* Genetic analysis of the regulation of the voltage-gated calcium channel homolog Cch1 by the  $\gamma$  subunit homolog Ecm7 and cortical ER protein Scs2 in yeast. *PLoS ONE* 2017 ; 12 : e0181436.
434. Muller EM, Mackin NA, Erdman SE, *et al.* Fig1p Facilitates Ca<sup>2+</sup> Influx and Cell Fusion during Mating of *Saccharomyces cerevisiae*. *J. Biol. Chem.* 2003 ; 278 : 38461–38469.
435. Erdman S, Lin L, Malczynski M, *et al.* Pheromone-regulated Genes Required for Yeast Mating Differentiation. *Journal of Cell Biology* 1998 ; 140 : 461–483.
436. Florence Reddish, Cassandra Miller, Rakshya Gorkhali, *et al.* Calcium Dynamics Mediated by the Endoplasmic/Sarcoplasmic Reticulum and Related Diseases. *IJMS* 2017 ; 18 : 1024.
437. Laver DR. Regulation of the RyR channel gating by Ca<sup>2+</sup> and Mg<sup>2+</sup>. *Biophys Rev* 2018 ; 10 : 1087–1095.
438. Beeler T, Gable K, Zhao C, *et al.* A novel protein, CSG2p, is required for Ca<sup>2+</sup> regulation in *Saccharomyces cerevisiae*. *The Journal of Biological Chemistry* 1994 ; 269 : 7279–7284.

439. Takita Y, Ohya Y, Anraku Y. The CLS2 gene encodes a protein with multiple membrane-spanning domains that is important Ca<sup>2+</sup> tolerance in yeast. *Molec. Gen. Genet.* 1995 ; 246 : 269–281.
440. Tanida I, Takita Y, Hasegawa A, *et al.* Yeast Cls2p/Csg2p localized on the endoplasmic reticulum membrane regulates a non-exchangeable intracellular Ca<sup>2+</sup> pool cooperatively with calcineurin. *FEBS Letters* 1996 ; 379 : 38–42.
441. Uemura S, Kihara A, Iwaki S, *et al.* Regulation of the Transport and Protein Levels of the Inositol Phosphorylceramide Mannosyltransferases Csg1 and Csh1 by the Ca<sup>2+</sup>-binding Protein Csg2. *J. Biol. Chem.* 2007 ; 282 : 8613–8621.
442. Espeso EA. The CRaZy Calcium Cycle. In : Ramos J, Sychrová H, Kschischo M, editors. *Yeast Membrane Transport*. Cham : Springer International Publishing, 2016 : 169–186.
443. Kim J-B. Channelopathies. *Korean J Pediatr* 2014 ; 57 : 1.
444. Honoré B, Vorum H. The CREC family, a novel family of multiple EF-hand, low-affinity Ca<sup>2+</sup>-binding proteins localised to the secretory pathway of mammalian cells. *FEBS Letters* 2000 ; 466 : 11–18.
445. Honoré B. The rapidly expanding CREC protein family: members, localization, function, and role in disease. *Bioessays* 2009 ; 31 : 262–277.
446. Yáñez M, Gil-Longo J, Campos-Toimil M. Calcium Binding Proteins. In : Islam MdS, editor. *Calcium Signaling*. Dordrecht : Springer Netherlands, 2012 : 461–482.
447. Brini M, Cali T, Ottolini D, *et al.* Calcium Pumps: Why So Many? In : Terjung R, editor. *Comprehensive Physiology*. Hoboken, NJ, USA : John Wiley & Sons, Inc., 2012 : c110034.
448. Chen J, Smaardijk S, Vandecaetsbeek I, *et al.* Regulation of Ca<sup>2+</sup> Transport ATPases by Amino- and Carboxy-Terminal Extensions: Mechanisms and (Patho)Physiological Implications. In : Chakraborti S, Dhalla NS, editors. *Regulation of Ca<sup>2+</sup>-ATPases, V-ATPases and F-ATPases*. Cham : Springer International Publishing, 2016 : 243–279.
449. Amacher JF, Brooks L, Hampton TH, *et al.* Specificity in PDZ-peptide interaction networks: Computational analysis and review. *Journal of Structural Biology: X* 2020 ; 4 : 100022.
450. Niggli V, Adunyah ES. Acidic Phospholipids, Unsaturated Fatty Acids, and Limited Proteolysis Mimic the Effect of Calmodulin on the Purified Erythrocyte Ca<sup>2+</sup>-ATPase. n.d. ; 5.
451. Ghosh B, Green MV, Krogh KA, *et al.* Interleukin-1 $\beta$  activates an Src family kinase to stimulate the plasma membrane Ca<sup>2+</sup> pump in hippocampal neurons. *Journal of Neurophysiology* 2016 ; 115 : 1875–1885.
452. Michelangeli F, East JM. A diversity of SERCA Ca<sup>2+</sup> pump inhibitors. *Biochemical Society Transactions* 2011 ; 39 : 789–797.
453. Tadini-Buoninsegni F, Smeazzetto S, Gualdani R, *et al.* Drug Interactions With the Ca<sup>2+</sup>-ATPase From Sarco(Endo)Plasmic Reticulum (SERCA). *Front. Mol. Biosci.* 2018 ; 5 : 36.
454. Verboomen H, Wuytack F, De Smedt H, *et al.* Functional difference between SERCA2a and SERCA2b Ca<sup>2+</sup> pumps and their modulation by phospholamban. *Biochemical Journal* 1992 ; 286 : 591–595.
455. Verboomen H, Wuytack F, Van den Bosch L, *et al.* The functional importance of the extreme C-terminal tail in the gene 2 organellar Ca<sup>2+</sup>-transport ATPase (SERCA2a/b). *Biochemical Journal* 1994 ; 303 : 979–984.
456. von Blume J, Alleaume A-M, Cantero-Recasens G, *et al.* ADF/Cofilin Regulates Secretory Cargo Sorting at the TGN via the Ca<sup>2+</sup> ATPase SPCA1. *Developmental Cell* 2011 ; 20 : 652–662.
457. Kienzle C, Blume J von. Secretory cargo sorting at the trans-Golgi network. *Trends in Cell Biology* 2014 ; 24 : 584–593.
458. Crevenna AH, Blank B, Maiser A, *et al.* Secretory cargo sorting by Ca<sup>2+</sup>-dependent Cab45 oligomerization at the trans-Golgi network. *Journal of Cell Biology* 2016 ; 213 : 305–314.
459. Blank B, Blume J von. Cab45—Unraveling key features of a novel secretory cargo sorter at the trans-Golgi network. *European Journal of Cell Biology* 2017 ; 96 : 383–390.

460. Deng Y, Pakdel M, Blank B, *et al.* Activity of the SPCA1 Calcium Pump Couples Sphingomyelin Synthesis to Sorting of Secretory Proteins in the Trans-Golgi Network. *Developmental Cell* 2018 ; 47 : 464-478.e8.
461. Lebretonchel E, Houdou M, Hoffmann H-H, *et al.* Investigating the functional link between TMEM165 and SPCA1. *Biochemical Journal* 2019 ; 476 : 3281–3293.
462. Roy A-S, Miskinyte S, Garat A, *et al.* SPCA1 governs the stability of TMEM165 in Hailey-Hailey disease. *Biochimie* 2020 ; 174 : 159–170.
463. Wei Y, Marchi V, Wang R, *et al.* An N-Terminal EF Hand-like Motif Modulates Ion Transport by Pmr1, the Yeast Golgi  $\text{Ca}^{2+}/\text{Mn}^{2+}$ -ATPase †. *Biochemistry* 1999 ; 38 : 14534–14541.
464. Chen J, Smaardijk S, Mattelaer C-A, *et al.* An N-terminal  $\text{Ca}^{2+}$ -binding motif regulates the secretory pathway  $\text{Ca}^{2+}/\text{Mn}^{2+}$ -transport ATPase SPCA1. *J. Biol. Chem.* 2019 ; 294 : 7878–7891.
465. Liu XF, Culotta VC. Mutational Analysis of *Saccharomyces cerevisiae* Smf1p, a Member of the Nramp Family of Metal Transporters. *Journal of Molecular Biology* 1999 ; 289 : 885–891.
466. Liu XF, Culotta VC. Post-translation Control of Nramp Metal Transport in Yeast: ROLE OF METAL IONS AND THE BSD2 GENE. *J. Biol. Chem.* 1999 ; 274 : 4863–4868.
467. Portnoy ME, Jensen LT, Culotta VC. The distinct methods by which manganese and iron regulate the Nramp transporters in yeast. 2002 ; 6.
468. Reddi AR, Jensen LT, Culotta VC. Manganese Homeostasis in *Saccharomyces cerevisiae*. *Chem. Rev.* 2009 ; 109 : 4722–4732.
469. Liu XF, Culotta VC. The requirement for yeast superoxide dismutase is bypassed through mutations in BSD2, a novel metal homeostasis gene. *Mol. Cell. Biol.* 1994 ; 14 : 7037–7045.
470. Garrick MD, Zhao L, Roth JA, *et al.* Isoform specific regulation of divalent metal (ion) transporter (DMT1) by proteasomal degradation. *Biometals* 2012 ; 25 : 787–793.
471. Foot NJ, Dalton HE, Shearwin-Whyatt LM, *et al.* Regulation of the divalent metal ion transporter DMT1 and iron homeostasis by a ubiquitin-dependent mechanism involving Ndfip2 and WWP2. *Blood* 2008 ; 112 : 4268–4275.
472. Foot NJ, Gembus KM, Mackenzie K, *et al.* Ndfip2 is a potential regulator of the iron transporter DMT1 in the liver. *Sci Rep* 2016 ; 6 : 24045.
473. Mackenzie K, Foot NJ, Anand S, *et al.* Regulation of the divalent metal ion transporter via membrane budding. *Cell Discov* 2016 ; 2 : 16011.
474. Wang X, Li GJ, Zheng W. Upregulation of DMT1 expression in choroidal epithelia of the blood–CSF barrier following manganese exposure in vitro. *Brain Research* 2006 ; 1097 : 1–10.
475. Li X, Xie J, Lu L, *et al.* Kinetics of manganese transport and gene expressions of manganese transport carriers in Caco-2 cell monolayers. *Biometals* 2013 ; 26 : 941–953.
476. Cui J, Kaandorp JA, Ositele OO, *et al.* Simulating calcium influx and free calcium concentrations in yeast. *Cell Calcium* 2009 ; 45 : 123–132.
477. Lebretonchel E, Houdou M, Potelle S, *et al.* Dissection of TMEM165 function in Golgi glycosylation and its  $\text{Mn}^{2+}$  sensitivity. *Biochimie* 2019 ; 165 : 123–130.
478. Thompson KJ, Wessling-Resnick M. ZIP14 is degraded in response to manganese exposure. *Biometals* 2019 ; 32 : 829–843.
479. Zhao N, Zhang A-S, Worthen C, *et al.* An iron-regulated and glycosylation-dependent proteasomal degradation pathway for the plasma membrane metal transporter ZIP14. *Proceedings of the National Academy of Sciences* 2014 ; 111 : 9175–9180.
480. Srikanth S, Jew M, Kim K-D, *et al.* Junctate is a  $\text{Ca}^{2+}$ -sensing structural component of Orai1 and stromal interaction molecule 1 (STIM1). *Proceedings of the National Academy of Sciences* 2012 ; 109 : 8682–8687.
481. Palty R, Raveh A, Kaminsky I, *et al.* SARAF Inactivates the Store Operated Calcium Entry Machinery to Prevent Excess Calcium Refilling. *Cell* 2012 ; 149 : 425–438.
482. Saitoh N, Oritani K, Saito K, *et al.* Identification of functional domains and novel binding partners of STIM proteins. *J. Cell. Biochem.* 2011 ; 112 : 147–156.

483. Krapivinsky G, Krapivinsky L, Stotz SC, *et al.* POST, partner of stromal interaction molecule 1 (STIM1), targets STIM1 to multiple transporters. *Proceedings of the National Academy of Sciences* 2011 ; 108 : 19234–19239.
484. Bauer MC, O’Connell D, Cahill DJ, *et al.* Calmodulin Binding to the Polybasic C-Termini of STIM Proteins Involved in Store-Operated Calcium Entry. *Biochemistry* 2008 ; 47 : 6089–6091.
485. Srikanth S, Jung H-J, Kim K-D, *et al.* A novel EF-hand protein, CRACR2A, is a cytosolic Ca<sup>2+</sup> sensor that stabilizes CRAC channels in T cells. *Nat Cell Biol* 2010 ; 12 : 436–446.
486. Krzewinski-Recchi M-A, Potelle S, Mir A-M, *et al.* Evidence for splice transcript variants of TMEM165, a gene involved in CDG. *Biochimica et Biophysica Acta (BBA) - General Subjects* 2017 ; 1861 : 737–748.
487. Schulte Althoff S, Grüneberg M, Reunert J, *et al.* TMEM165 Deficiency: Postnatal Changes in Glycosylation. In : Morava E, Baumgartner M, Patterson M, *et al.*, editors. *JIMD Reports, Volume 26*. Berlin, Heidelberg : Springer Berlin Heidelberg, 2015 : 21–29.
488. Rosnoble C, Legrand D, Demaegd D. Impact of disease-causing mutations on TMEM165 subcellular localization, a recently identified protein involved in CDG-II. *Hum. Mol. Genet.* 2013 ; 22 : 2914–2928.
489. Schneider A, Steinberger I, Herdean A, *et al.* The Evolutionarily Conserved Protein PHOTOSYNTHESIS AFFECTED MUTANT71 is Required for Efficient Manganese Uptake at the Thylakoid Membrane in Arabidopsis. *Plant Cell* 2016 ; tpc.00812.2015.
490. Eisenhut M, Hoecker N, Schmidt SB, *et al.* The Plastid Envelope CHLOROPLAST MANGANESE TRANSPORTER1 Is Essential for Manganese Homeostasis in Arabidopsis. *Molecular Plant* 2018 ; 11 : 955–969.
491. Hoecker N, Leister D, Schneider A. Plants contain small families of UPF0016 proteins including the PHOTOSYNTHESIS AFFECTED MUTANT71 transporter. *Plant Signaling & Behavior* 2017 ; 12 : e1278101.
492. Hoecker N, Honke A, Frey K, *et al.* Homologous Proteins of the Manganese Transporter PAM71 Are Localized in the Golgi Apparatus and Endoplasmic Reticulum. *Plants* 2020 ; 9 : 239.
493. Gandini C, Schmidt SB, Husted S, *et al.* The transporter SynPAM71 is located in the plasma membrane and thylakoids, and mediates manganese tolerance in *Synechocystis* PCC6803. *New Phytol* 2017 ; 215 : 256–268.
494. Brandenburg F, Schoffman H, Kurz S, *et al.* The *Synechocystis* Manganese Exporter Mnx Is Essential for Manganese Homeostasis in Cyanobacteria. *Plant Physiol.* 2017 ; 173 : 1798–1810.
495. Fisher CR, Wyckoff EE, Peng ED, *et al.* Identification and Characterization of a Putative Manganese Export Protein in *Vibrio cholerae*. *J. Bacteriol.* 2016 ; 198 : 2810–2817.
496. Zeinert R, Martinez E, Schmitz J, *et al.* Structure–function analysis of manganese exporter proteins across bacteria. *J. Biol. Chem.* 2018 ; 293 : 5715–5730.
497. Thines L, Stribny J, Morsomme P. From the Uncharacterized Protein Family 0016 to the GDT1 family: Molecular insights into a newly-characterized family of cation secondary transporters. *Microb Cell* 2020 ; 7 : 202–214.
498. Frank J, Happeck R, Meier B, *et al.* Chloroplast-localized BICAT proteins shape stromal calcium signals and are required for efficient photosynthesis. *New Phytol* 2019 ; 221 : 866–880.
499. Mukhopadhyay S, Bachert C, Smith DR, *et al.* Manganese-induced Trafficking and Turnover of the *cis*-Golgi Glycoprotein GPP130. *MBoC* 2010 ; 21 : 1282–1292.
500. Venkat S, Linstedt AD. Manganese-induced trafficking and turnover of GPP130 is mediated by sortilin. *Molecular Biology of the Cell* 2017 ; 28 : 10.
501. Snyder NA, Stefan CP, Soroudi CT, *et al.* H<sup>+</sup> and Pi Byproducts of Glycosylation Affect Ca<sup>2+</sup> Homeostasis and Are Retrieved from the Golgi Complex by Homologs of TMEM165 and XPR1. *G3* 2017 ; 7 : 3913–3924.
502. Wang H, Yang Y, Huang F, *et al.* In Situ Fluorescent and Photoacoustic Imaging of Golgi pH to Elucidate the Function of Transmembrane Protein 165. *Anal. Chem.* 2020 ; 92 : 3103–3110.

503. Reinhardt TA, Lippolis JD, Sacco RE. The Ca<sup>2+</sup>/H<sup>+</sup> antiporter TMEM165 expression, localization in the developing, lactating and involuting mammary gland parallels the secretory pathway Ca<sup>2+</sup> ATPase (SPCA1). *Biochemical and Biophysical Research Communications* 2014 ; 445 : 417–421.
504. Snyder NA, Palmer MV, Reinhardt TA, *et al.* Milk biosynthesis requires the Golgi cation exchanger TMEM165. *J. Biol. Chem.* 2019 ; 294 : 3181–3191.
505. Zeevaert R, Zegher F de, Sturiale L, *et al.* Bone Dysplasia as a Key Feature in Three Patients with a Novel Congenital Disorder of Glycosylation (CDG) Type II Due to a Deep Intronic Splice Mutation in TMEM165. In : Zschocke J, Gibson KM, Brown G, *et al.*, editors. *JIMD Reports - Case and Research Reports, 2012/5*. Berlin, Heidelberg : Springer Berlin Heidelberg, 2012 : 145–152.
506. Morelle W, Potelle S, Witters P, *et al.* Galactose Supplementation in Patients With TMEM165-CDG Rescues the Glycosylation Defects. *J. Clin. Endocrinol. Metab.* 2017 ; 102 : 1375–1386.
507. Xia B, Zhang W, Li X, *et al.* Serum N-glycan and O-glycan analysis by mass spectrometry for diagnosis of congenital disorders of glycosylation. *Analytical Biochemistry* 2013 ; 442 : 178–185.
508. Bammens R, Mehta N, Race V, *et al.* Abnormal cartilage development and altered N-glycosylation in Tmem165-deficient zebrafish mirrors the phenotypes associated with TMEM165-CDG. *Glycobiology* 2015 ; 25 : 669–682.
509. Vicogne D, Houdou M, Garat A, *et al.* Fetal Bovine Serum impacts the observed N-glycosylation defects in TMEM165 KO HEK cells. *Jrnl of Inher Metab Disea* 2019 ; jimd.12161.
510. Yamamoto K, Kawai H, Moriguchi M, *et al.* Purification and characterization of yeast UDP-N-acetylglucosamine pyrophosphorylase. *Agric. Biol. Chem.* 1976 ; 40 : 2275–2281.
511. Haouari W, Dubail J, Lounis-Ouaras S, *et al.* Serum bikunin isoforms in congenital disorders of glycosylation and linkeropathies. *n.d.* ; 35.
512. Verheijen J, Tahata S, Kozicz T, *et al.* Therapeutic approaches in Congenital Disorders of Glycosylation (CDG) involving N-linked glycosylation: an update. *Genet Med* 2019 ; .
513. Brasil S, Pascoal C, Francisco R, *et al.* CDG Therapies: From Bench to Bedside. *IJMS* 2018 ; 19 : 1304.
514. Carlsson S, Fukuda M. The polylactosaminoglycans of human lysosomal membrane glycoproteins Lamp-1 and Lamp-2. *The Journal of Biological Chemistry* 1990 ; 265 : 20488–20495.
515. Carlsson S, Lycksell P-O, Fukuda M. Assignment of O-Glycan attachment sites to the hinge-linker regions of human lysosomal membrane glycoproteins Lamp-1 and Lamp-2. *Archives of Biochemistry and Biophysics* 1993 ; 304 : 65–73.
516. Tan K-P, Ho M-Y, Cho H-C, *et al.* Fucosylation of LAMP-1 and LAMP-2 by FUT1 correlates with lysosomal positioning and autophagic flux of breast cancer cells. *Cell Death Dis* 2016 ; 7 : e2347–e2347.
517. Gonzalez A, Valeiras M, Sidransky E, *et al.* Lysosomal integral membrane protein-2: A new player in lysosome-related pathology. *Molecular Genetics and Metabolism* 2014 ; 111 : 84–91.
518. Linstedt AD, Hauri H-P. Sequence and Overexpression of GPP130/GIMPc: Evidence for Saturable pH-sensitive Targeting of a Type II Early Golgi Membrane Protein. *Molecular Biology of the Cell* 1997 ; 8 : 15.
519. Murali P, Johnson B, Lu Z, *et al.* Novel role for the Golgi membrane protein TMEM165 in control of migration and invasion for breast carcinoma. *Oncotarget* 2020 ; 11 : 2747–2762.
520. Lee J, Kim M, Park E, *et al.* TMEM165, a Golgi transmembrane protein, is a novel marker for hepatocellular carcinoma and its depletion impairs invasion activity. *Oncol Rep* 2018 ; .
521. Grice DM, Vetter I, Faddy HM, *et al.* Golgi Calcium Pump Secretory Pathway Calcium ATPase 1 (SPCA1) Is a Key Regulator of Insulin-like Growth Factor Receptor (IGF1R) Processing in the Basal-like Breast Cancer Cell Line MDA-MB-231. *JBC* 2010 ; 285 : 37458–37466.
522. Dang D, Rao R. Calcium-ATPases: Gene Disorders and Dyregulation in Cancer. *Biochimica Et Biophysica Acta* June 2016 ; 1863 : 1344–1350.

523. Dang D, Prasad H, Rao R. Secretory pathway  $\text{Ca}^{2+}$ -ATPases promote in vitro microcalcifications in breast cancer cells. *Mol Carcinog* 2017 ; 56 : 2474–2485.





## Appendix

**Appendix I :** Anomalies congénitales de la glycosylation (CDG) : 1980-2020, 40 ans pour comprendre.

**Appendix II :** Dissection of TMEM165 function in Golgi glycosylation and its Mn<sup>2+</sup> sensitivity



---

## **Appendix I :**

Anomalies congénitales de la glycosylation (CDG) :

1980-2020, 40 ans pour comprendre.

---



► La glycosylation est un processus cellulaire complexe conduisant à des transferts successifs de monosaccharides sur une molécule acceptrice, le plus souvent une protéine ou un lipide. Ce processus est universel chez tous les organismes vivants et est très conservé au cours de l'évolution. Chez l'homme, des perturbations survenant au cours d'une ou plusieurs réactions de glycosylation sont à l'origine de glycopathologies génétiques rares, appelées anomalies congénitales de la glycosylation ou *congenital disorders of glycosylation* (CDG). Cette revue propose de revisiter ces CDG, de 1980 à aujourd'hui, en présentant leurs découvertes, leurs diagnostics, leurs causes biochimiques et les traitements actuellement disponibles. ◀

## Le processus de glycosylation : entre acteurs et régulateurs

### Les acteurs au cœur de la réaction de glycosylation

La glycosylation est une modification post-traductionnelle à laquelle différents acteurs participent : (1) des enzymes de glycosylation (glycosyltransférases [GT] et glycosylhydrolases [GH]), (2) différents nucléotides sucres mono/diphosphate (NM/DP-sucres), (3) des transporteurs de nucléotides sucres (TNS), et (4) des molécules acceptrices, le plus souvent une protéine, un lipide ou un monosaccharide. Ces réactions se déroulent principalement dans le réticulum endoplasmique granuleux (REG) et/ou l'appareil de Golgi, possédant un environnement ionique spécifique, en termes de pH et d'ions divalents, nécessaire à l'activité des différentes GT pour la formation d'une liaison covalente entre un monosaccharide et la molécule acceptrice (Figure 1).

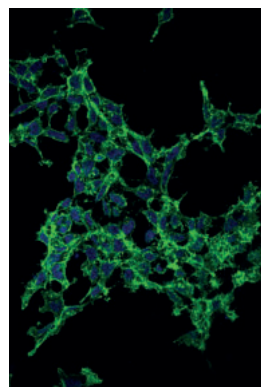
### Rôle des glycosyltransférases golgiennes dans le transfert des nucléotides sucres mono/diphosphate

Les glycosyltransférases (GT) sont les enzymes au cœur de la glycosylation. Selon leur structure, elles peuvent

# Anomalies congénitales de la glycosylation (CDG)

1980-2020, 40 ans pour comprendre

Marine Houdou, François Foulquier



Univ. Lille, CNRS, UMR 8576 - UGSF - Unité de glycobiologie structurale et fonctionnelle, Avenue Mendeleiev, 59655 Villeneuve d'Ascq, France. francois.foulquier@univ-lille.fr

être classées en deux grandes familles : les GT de type A (GT-A) et les GT de type B (GT-B). Les GT-A ont une conformation telle que les acides aminés constituant leur site catalytique forment un motif structural de type « pli Rossmann »<sup>1</sup> qui se retrouve communément dans la structure des protéines liant les nucléotides. Outre ce pli, les GT-A possèdent également dans leur structure un motif DXD (D étant un acide aspartique et X n'importe quel acide aminé) permettant la liaison d'un ion divalent impliqué dans la stabilisation du nucléotide sucre diphosphate (NDP-sucres) au niveau du site catalytique de l'enzyme. La plupart de ces enzymes requièrent comme cofacteur le manganèse (sous forme ionique Mn<sup>2+</sup>) qui est essentiel pour leurs activités [1]. Les GT-B ne possèdent, quant à elles, pas de motif DXD et sont donc considérées comme des enzymes métal/ion-indépendantes. Les GT sont toutes des protéines transmembranaires de type II, dont le domaine catalytique, porté par la partie en C-terminal de la protéine, est exposé dans la lumière de l'appareil de Golgi. Ces enzymes possèdent différents degrés de spécificité selon que l'on considère le substrat « donneur », la molécule « acceptrice » et l'anométrie (-α ou -β) de la liaison glycosidique qu'elles catalysent. Chez l'homme, les GT ont pour substrats donneurs les principaux NM/DP-sucres que sont : l'uridine diphosphate-glucose (UDP-Glc), l'UDP-galactose (UDP-Gal), l'UDP-N-acétylglucosamine (UDP-GlcNAc), l'UDP-N-acétylgalactosamine (UDP-GalNAc), l'UDP-acide glucuronique (UDP-GlcA), l'UDP-xylose (UDP-Xyl), le guanosine diphosphate-mannose (GDP-Man), le GDP-fucose (GDP-Fuc) et le

Vignette (Marquage de la lectine VVL dans les cellules HEK déficientes pour TMEM 165, © Marine Houdou).

<sup>1</sup> Structure composée d'un feuillet β fait de 6 brins en parallèle, liés à deux paires d'hélice α.

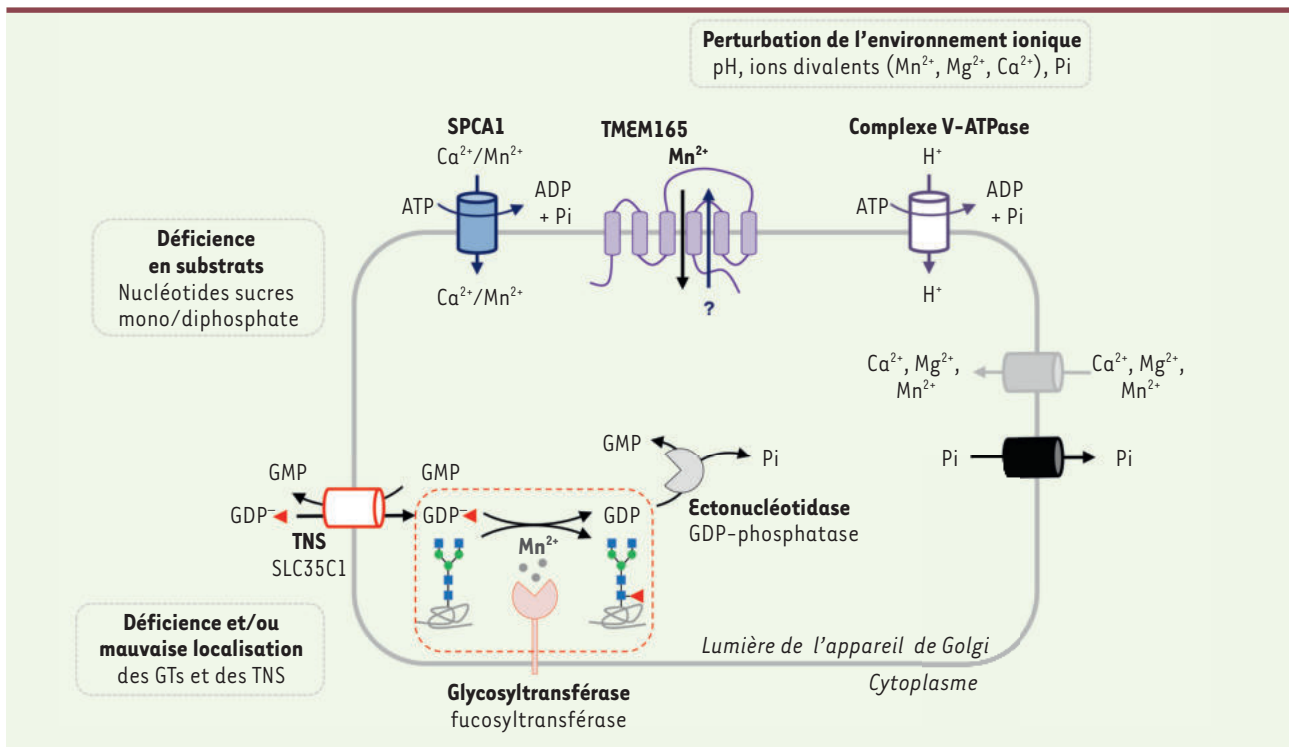


**Figure 1. Acteurs principaux requis au cours d'une réaction de glycosylation dans la lumière de l'appareil de Golgi.** La réaction de glycosylation met en jeu des acteurs primaires : une glycosyltransférase (GT), ici une fucosyltransférase ; un substrat donneur, le GDP-fucose et une molécule acceptrice, une N-glycoprotéine (cadre en pointillé rouge). Cette figure illustre également les acteurs secondaires nécessaires à cette réaction, en particulier des éctonucléotidases, différents transporteurs de cations ( $Mn^{2+}$ ,  $Mg^{2+}$ ,  $Ca^{2+}$ ), de protons ( $H^+$ ) et de phosphate inorganique ( $Pi$ ). Les encadrés en pointillé gris indiquent les causes principales de dérégulation du processus de glycosylation, pouvant aboutir à des *Congenital Disorders of Glycosylation* (CDG). Le point d'interrogation représente un ion dont la nature reste à spécifier. SPCA1 : *secretory pathway  $Ca^{2+}/Mn^{2+}$  ATPase* ; SLC35C1 : *solute carrier transporter 35C1* ; TMEM165 : *transmembrane protein 165* ; TNS : transporteur de nucléotides sucres mono/diphosphate.

cytosine monophosphate-acide sialique (CMP-Sia). Tous ces monosaccharides dits « activés » sont préalablement synthétisés dans le cytoplasme à l'exception du CMP-Sia dont la dernière étape de synthèse se déroule dans le noyau. Une fois générés, ces NM/DP-sucres sont transportés par des transporteurs de nucléotides sucres qui leurs sont spécifiques.

### Import des nucléotides sucres par les transporteurs golgiens de NM/DP-sucres

Les transporteurs de NM/DP-sucres (TNS) sont des protéines transmembranaires appartenant à la famille très conservée des SLC35 (*solute carrier transporter 35*) [2]. Les TNS golgiens importent du cytoplasme dans la lumière de l'appareil de Golgi un NM/DP-sucre (NDP) et, simultanément, exportent la forme monophosphate du nucléotide (NMP) correspondant vers le cytoplasme. Ceci est permis grâce à l'action d'éctonucléotidases qui hydrolysent les NDP générés par la réaction de glycosylation en produisant le NMP et du phosphate inorganique ( $Pi$ ) (Figure 1). La localisation subcellulaire de chaque transporteur est encore mal connue, mais elle est supposée calquer celle des GT afin que l'apport en nucléotides-sucres soit suffisant pour leurs activités.

### Rôle des glycosylhydrolases dans la maturation et la dégradation des structures glycaniques

À côté des glycosyltransférases, les glycosylhydrolases (GH), ou glycosidases, sont également des enzymes clefs du processus de glycosylation, étant responsables de l'hydrolyse des liaisons glycaniques libérant un ou plusieurs monosaccharides. Leurs actions sont essentielles dans la maturation des structures glycaniques générées au cours de la N-glycosylation. Ces enzymes ont également un rôle très important dans le recyclage de certains monosaccharides *via* la dégradation des structures glycaniques.

### La régulation de la glycosylation

La glycosylation est un processus très conservé au cours de l'évolution. Il est universel chez tous les organismes vivants, procaryotes et eucaryotes, unicellulaires et pluricellulaires. Néanmoins, au sein d'un même organisme, différentes voies de glycosylation coexistent, générant une grande diversité et complexité de structures glycaniques (Figure 2).

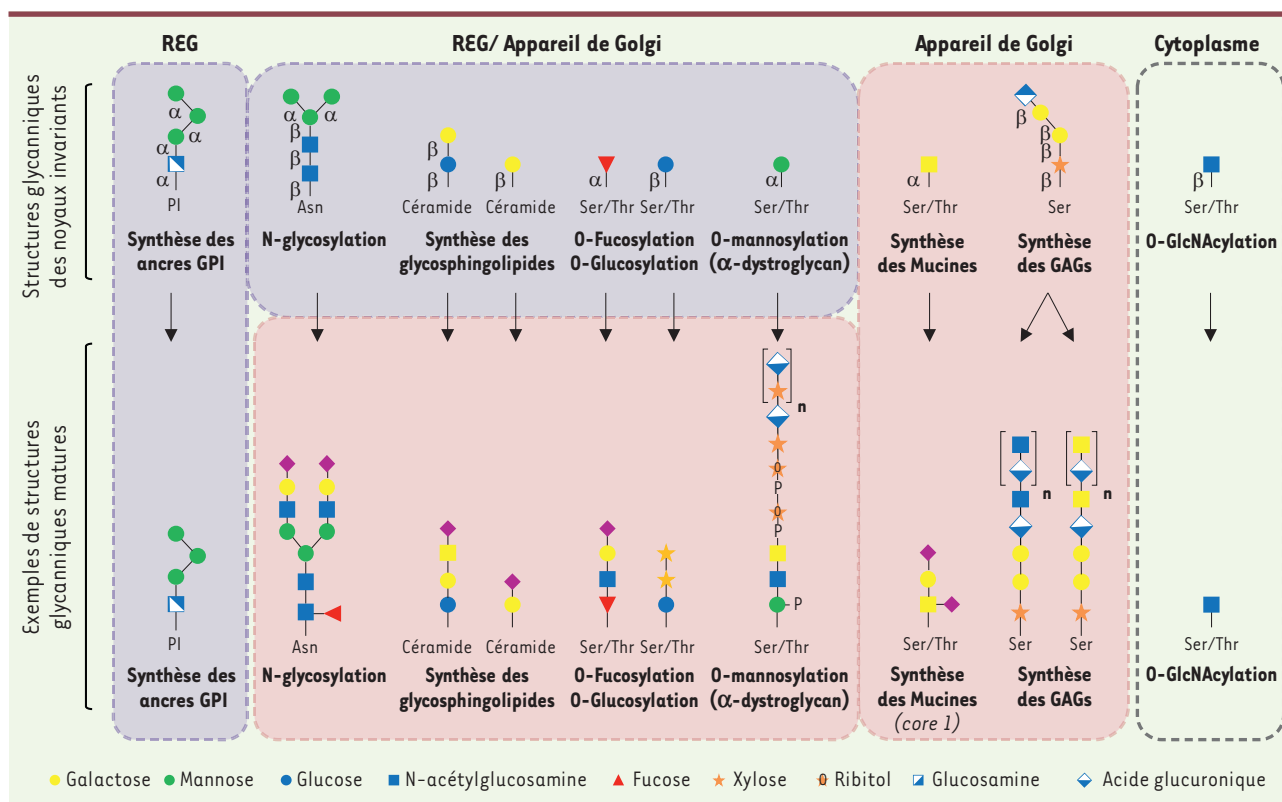


**Figure 2. Représentation schématique du lieu d'initiation (noyaux invariants) et de maturation des structures glycaniques associées aux différentes voies de glycosylation.** Le réticulum endoplasmique granuleux (REG) et l'appareil de Golgi sont schématiquement représentés par les encadrés en pointillé violet et rose, respectivement. À droite dans le cadre en pointillé gris, la voie de glycosylation cytoplasmique est également illustrée. La nature des différentes liaisons a été omise dans la schématisation des structures glycaniques matures par souci de lisibilité.  $\alpha$  et  $\beta$  représentent l'anomérisation de la liaison, Asn : asparagine, GAGs: glycosaminoglycannes, GPI : glycosylphosphatidyl inositol, n : nombre de répétitions du motif, P: phosphate, PI : phosphate inositol, Ser : sérine, Thr : thréonine.

Ce processus se doit donc d'être finement régulé afin d'assurer la fidélité des structures glycaniques qui seront retrouvées sur les protéines et/ou les lipides. Cette régulation est fondamentale et son altération est dramatiquement illustrée par l'existence des maladies génétiques rares et multi-systémiques, que l'on appelle anomalies congénitales de glycosylation (*congenital disorders of glycosylation*, CDG).

De nombreux travaux ont été entrepris afin de comprendre les mécanismes de régulation de la glycosylation, dont un dysfonctionnement a également été associé à de nombreuses autres maladies acquises, telles que certains cancers, le diabète et la mucoviscidose [3,4]. Plusieurs facteurs impliqués dans cette dérégulation ont d'ores et déjà été identifiés. Certains intéressent les protéines qui sont au cœur des réactions enzymatiques : les GT, les GH, les TNS, ou l'activation et la présentation des précurseurs oligosaccharidiques principalement. D'autres sont indirectement liés à ce processus, notamment des protéines impliquées dans la localisation subcellulaire (organisation, distribution des acteurs de la glycosylation) ou le maintien de l'homéostasie de l'appareil de Golgi.

## Les anomalies congénitales de glycosylation

Les CDG sont qualifiées de maladies rares. La déficience d'une des étapes du processus peut s'avérer létale pour l'embryon et les patients atteints de CDG, dits « hypomorphes »<sup>2</sup>, conservent une activité résiduelle malgré les déficiences génétiques altérant différentes voies de la glycosylation.

### Jaak Jaeken, père des CDG

Les premiers cas de CDG furent identifiés en 1980 par le Professeur Jaak Jaeken à l'université de Louvain en Belgique [5]. Deux sœurs jumelles monozygotes présentaient un retard psychomoteur associé à un ralentissement de la propagation de l'influx nerveux et à des anomalies de glycosylation retrouvées sur de nombreuses protéines sériques, principalement un défaut de sialylation [6]. Quinze ans plus tard, les travaux de

<sup>2</sup> Se dit d'un allèle qui réduit la fonction d'un produit génétique sans l'éliminer.

van Schaftingen, Matthijs et Jaeken mirent en évidence chez ces deux sœurs des mutations dans le gène *PMM2*, codant la phosphomannomutase 2 (*PMM2*), associées à un déficit de l'activité de l'enzyme et responsables des anomalies de glycosylation observées [7, 8]. *PMM2* est l'enzyme qui permet la conversion du mannose-6-phosphate en mannose-1-phosphate lors de la synthèse du GDP-mannose, un nucléotide sucre fondamental pour la synthèse du précurseur oligosaccharidique dans le REG, initiant la N-glycosylation. Le déficit en *PMM2* est à l'origine d'une hypoglycosylation des protéines qui est caractéristique d'un profil CDG dit « de type I ». Aujourd'hui, ce déficit reste celui dont la fréquence est la plus importante, avec plus de mille cas rapportés dans le monde.

### CDG et voies de glycosylation

La majorité des cas de CDG identifiés au cours des quarante dernières années se traduit par des défauts touchant la N-glycosylation. En 2004, Dupré *et al.* avaient publié une revue dans *médecine/sciences* qui était dédiée aux anomalies congénitales des N-glycosylprotéines [9] (→).

(→) Voir la Synthèse de T. Dupré *et al.*, *m/s* n° 3, mars 2004, page 331

Ils y décrivaient, entre autres, les bases de la compréhension des mécanismes de la N-glycosylation des protéines. Ce processus original s'initie dans le REG et se poursuit dans l'appareil de Golgi. Dans le REG, les principales étapes de la synthèse des N-glycoprotéines font intervenir d'une part la synthèse d'un précurseur oligosaccharidique lipidique, de structure  $\text{Glc}_3\text{Man}_9\text{GlcNAc}_2\text{-P-P-dolichol}$  (P, phosphate), et d'autre part, son transfert « en bloc » sur l'asparagine (Asn) de la séquence consensus Asn-X-Ser/Thr (X représentant tout acide aminé excepté Pro) portée par la protéine acceptrice. S'en suivent l'action de différentes GH impliquées dans l'acquisition du repliement correct des N-glycoprotéines et, enfin, leurs adressages, *via* le trafic vésiculaire, vers l'appareil de Golgi. Les structures N-glycanniques subissent ensuite une maturation lors du cheminement de la N-glycoprotéine dans les différents saccules de l'appareil de Golgi. L'activité de mannosidases golgiennes est nécessaire à l'action séquentielle des GT qui conduit à la formation de structures glycanniques complexes ou hybrides (Figure 2). Outre la N-glycosylation, bon nombre de glycopathologies génétiques rares impactent d'autres - voire plusieurs - voies de glycosylation au sein d'une même cellule : la O-glycosylation (O-fucosylation, O-GlcNAcylation, O-GalNAcylation, O-glycosylation), la synthèse des glycosaminoglycane (GAG), la synthèse des ancres glycosylphosphatidylinositol (GPI) (ou glypiation), la O-mannosylation de l' $\alpha$ -dystroglycan et la synthèse des glycolipides [10]. Chacune de ces voies s'initie dans un compartiment cellulaire particulier, généralement le REG et/ou l'appareil de Golgi, et génère pléthore de structures glycanniques (Figure 2).

Cent-trente-trois gènes ont été associés à différents CDG [10, 11]. La Figure 3 présente un panorama du nombre de gènes mutés, de la voie de glycosylation que ces mutations affectent, et de la localisation subcellulaire des protéines codées par ces gènes et qui sont impliquées dans ces CDG. Bien que ces dernières se localisent majoritairement dans le REG et l'appareil de Golgi, certaines

sont retrouvées dans le compartiment intermédiaire (ERGIC), le cytoplasme et à la membrane plasmique. Cette multiplicité des voies de glycosylation affectées participe très certainement à l'extrême diversité des phénotypes cliniques rencontrés.

### Quel(s) diagnostic(s) pour les CDG ?

La plupart des CDG sont des maladies multi-systémiques et 177 phénotypes cliniques différents ont été identifiés. Ils ont été classés par organes/systèmes et chacun associé à un CDG [11]. Le diagnostic de ces pathologies est ainsi difficile et l'isoélectrofocalisation (IEF) de la transferrine sérique reste, avec la chromatographie d'échange d'ions et la spectrométrie de masse, la technique de référence pour leur dépistage. Cette méthode de séparation des protéines selon leur point isoélectrique a été à l'origine du diagnostic biochimique des premiers cas de CDG ayant pour origine des mutations du gène *PMM2* en 1984 [6]. Fondée sur l'état de sialylation des deux chaînes de N-glycannes portées par la transferrine, elle permet d'identifier et de distinguer les patients (Figure 4A). Une dérégulation de la N-glycosylation au niveau de la synthèse et/ou du transfert du précurseur oligosaccharidique  $\text{Glc}_3\text{Man}_9\text{GlcNAc}_2$  produit en effet une sous-occupation des sites de N-glycosylation de la protéine et caractérise un CDG de type I (CDG-I). Les profils de type I présentent ainsi une diminution des formes tétra-sialylées de la transferrine et une augmentation des formes di et/ou asialylées (Figure 4A). Une perturbation de la N-glycosylation en aval du transfert du précurseur oligosaccharidique génère en revanche l'apparition de structures N-glycanniques dites « tronquées » caractéristiques des CDG de type II (CDG-II). Dans ce cas, les deux sites de N-glycosylation sont occupés mais le nombre d'acides sialiques terminaux varie. Une augmentation globale des formes tri-, di-, mono- et/ou asialylées de la transferrine est alors évocatrice d'un profil CDG de type II (Figure 4A). La détection des glycoformes de la transferrine sérique présente néanmoins certaines limites. Elle ne permet l'identification que de patients dont le déficit touche la N-glycosylation des protéines hépatiques. Il est donc souvent important d'examiner l'intégrité d'autres voies de glycosylation, en particulier la O-glycosylation. Le dépistage des anomalies de O-glycosylation est fondé, comme pour la transferrine, sur des méthodes de séparation de protéines comme l'IEF et/ou l'électrophorèse bidimensionnelle appliquées à l'apolipoprotéine C-III (ApoC-III) [12]. À la différence de la transferrine, l'ApoC-III n'est pas N-glycosylée mais O-glycosylée. Elle comporte une unique chaîne O-glycannique de type mucine *core 1* constituée d'une N-acétylgalactosamine,



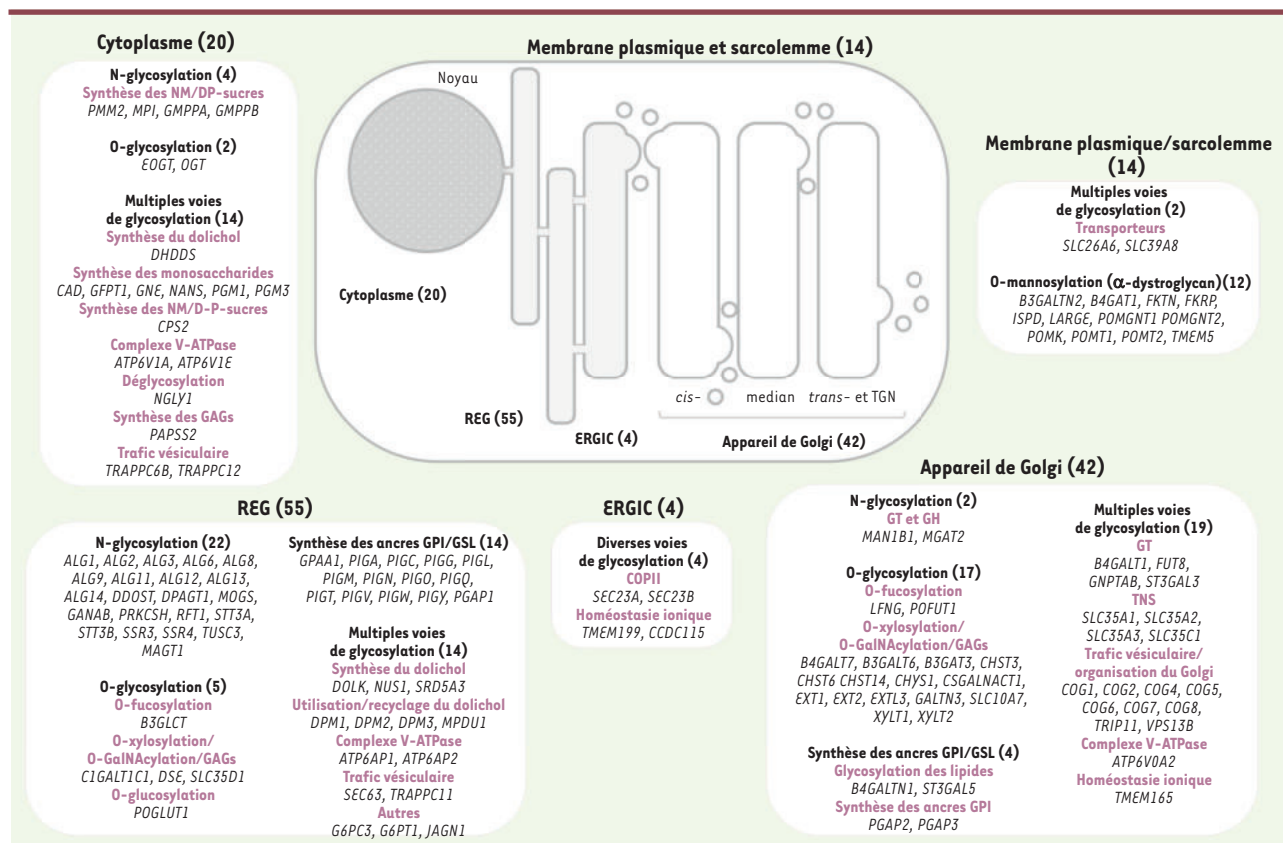


**Figure 3. Panorama de la localisation subcellulaire différentielle des protéines mutées impliquées dans les anomalies congénitales de la glycosylation (congenital disorders of glycosylation [CDG]).** Les différentes voies de glycosylation affectées y sont répertoriées ainsi que le gène déficient identifié. Le nombre de gènes impliqués dans chaque voie de glycosylation et associés à chaque compartiment subcellulaire, est indiqué entre parenthèses. ERGIC : endoplasmic reticulum to Golgi intermediate compartment ; NM/DP-sucre : nucléotides sucres mono/diphosphate ; REG : réticulum endoplasmique granuleux ; GAG : glycosaminoglycannes ; GH : glycosylhydrolases ; GPI : glycosylphosphatidyl inositol ; GT : glycosyltransférases ; TGN : trans-Golgi Network ; TNS : transporteur de nucléotides sucres.

d'un galactose et de deux acides sialiques (Figure 4B). Les profils de migration de la protéine résultant du nombre d'acides sialiques qu'elle porte témoignent ou non d'une anomalie de O-glycosylation. Le diagnostic biochimique nécessite d'être complété par un diagnostic moléculaire afin d'identifier précisément la mutation génétique causale. Des avancées majeures ont été permises grâce à l'avènement de techniques de pointe en génomique, comme illustré par la revue de Ng et Freeze [10] qui montre l'intérêt du séquençage de l'exome entier (*whole exome sequencing* ou WES) dans le diagnostic génétique des CDG avec, entre 2010 et 2017, 51 cas identifiés (sur les 177 nouveaux cas de CDG) par cette méthode. Un arbre décisionnel pour le diagnostic a également été proposé par Francisco et al. [11].

### Évolution de la nomenclature des CDG

La première tentative de classification des CDG en deux grandes familles (I et II) repose sur les résultats de profilage obtenu par IEF de la transferrine sérique (Figure 4A). Les différents CDG se distinguaient ensuite les uns des autres par une lettre, écrite en minuscule et par ordre alphabétique selon l'ordre chronologique de leur découverte.

Le CDG causé par une déficience en PMM2 fut ainsi nommé CDG-Ia. Suite au nombre croissant de nouveaux gènes identifiés, ce système de classification atteignit rapidement ses limites. Cette nomenclature ne permettait, aussi, que de classer les CDG déficients pour la N-glycosylation et occultait la nature des gènes mutés [13]. Depuis 2009, un nouveau système de nomenclature a été développé prenant en compte ces deux aspects. Chaque CDG est désormais nommé par le gène déficient, écrit en capitale sans italique, accolé du suffixe « -CDG » [14, 15] : le CDG-Ia est ainsi identifié par PMM2-CDG.

### Une ère nouvelle pour les CDG

Malgré le nombre important d'enzymes et de protéines impliquées dans les différentes voies de glycosylation, force est de constater qu'une grande majorité des CDG est causée par des mutations de gènes qui codent

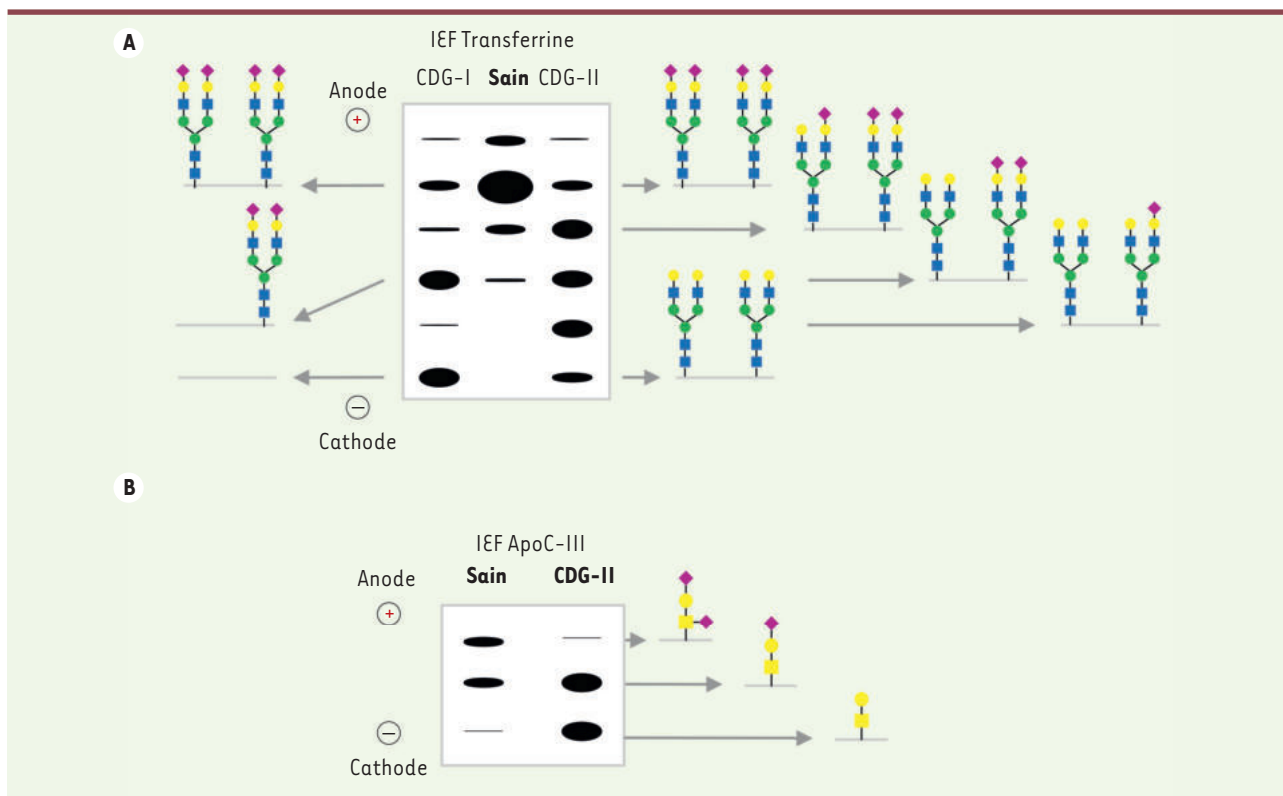


**Figure 4. Illustration du diagnostic biochimique des Congenital Disorders of Glycosylation (CDG).** Résultats schématiquement représentés issus de l'isoélectrofocalisation (IEF) de la transferrine (A.) et de l'apolipoprotéine-C III (ApoC-III) (B.), deux protéines sériques d'origine hépatique. Ces IEF permettent d'orienter le diagnostic biochimique des CDG. A. L'IEF de la transferrine permet l'identification d'anomalies de N-glycosylation par le port de 2 chaînes N-glycanniques. Selon le nombre d'acides sialiques présents et les proportions de chaque glycoforme, deux profils se distinguent reflétant un CDG-I ou un CDG-II. B. L'IEF de l'ApoC-III permet quant à elle l'identification d'anomalies de O-glycosylation reflétées par le nombre de molécules d'acide sialique présentes sur le motif O-glycannique de type mucine core 1.

des protéines participant directement aux réactions de glycosylation (GT, GH et TNS, principalement). Néanmoins, l'apparition d'un nouveau sous-groupe de patients présentant des altérations perturbant la dynamique du trafic intravésiculaire ou l'homéostasie ionique de l'appareil de Golgi, notamment celles du pH et du manganèse ( $Mn^{2+}$ ) a rendu plus complexe la définition de la maladie (Figure 5). Outre l'extrême hétérogénéité des déficiences désormais identifiées, ces nouveaux phénotypes permettent de caractériser de nouveaux acteurs de la régulation du processus de glycosylation qui sont encore méconnus.

### CDG et trafic intravésiculaire

#### Importance du trafic intravésiculaire golgien

La compartimentation cellulaire, qui permet la réalisation concomitante de nombreuses réactions biologiques, est une caractéristique fondamentale des cellules eucaryotes. Chaque organite étant délimité par une ou plusieurs bicouches lipidiques, la communication entre les compartiments ainsi que la composition et le recyclage de ces membranes, sont essentielles au maintien d'un environnement optimal (en termes de pH, homéostasie ionique, concentration en protéines et lipides).

Cette communication repose sur un ensemble de vésicules transitant depuis le REG vers la membrane plasmique via l'appareil de Golgi (trafic antérograde) et, à l'inverse, à partir de la membrane plasmique vers le réticulum en passant par l'appareil de Golgi (trafic rétrograde).

Siège de nombreuses modifications post-traductionnelles, dont les réactions de glycosylation, l'appareil de Golgi est l'un des organites les plus dynamiques de la cellule [16]. Son organisation particulière en sous-compartiments, appelés citernes (ou saccules), requiert une distribution et une localisation correctes de tous les acteurs moléculaires nécessaires à sa fonction, en particulier aux processus de glycosylation (Figure 5). L'appareil de Golgi peut compter une douzaine de saccules polarisés (définissant 4 zones : le cis-Golgi, le médian-Golgi, le trans-Golgi et le réseau trans-Golgi [TGN]) suffisamment proches les uns des autres pour former un organite compact. Il est entouré de nombreuses vésicules qui ont pour principale

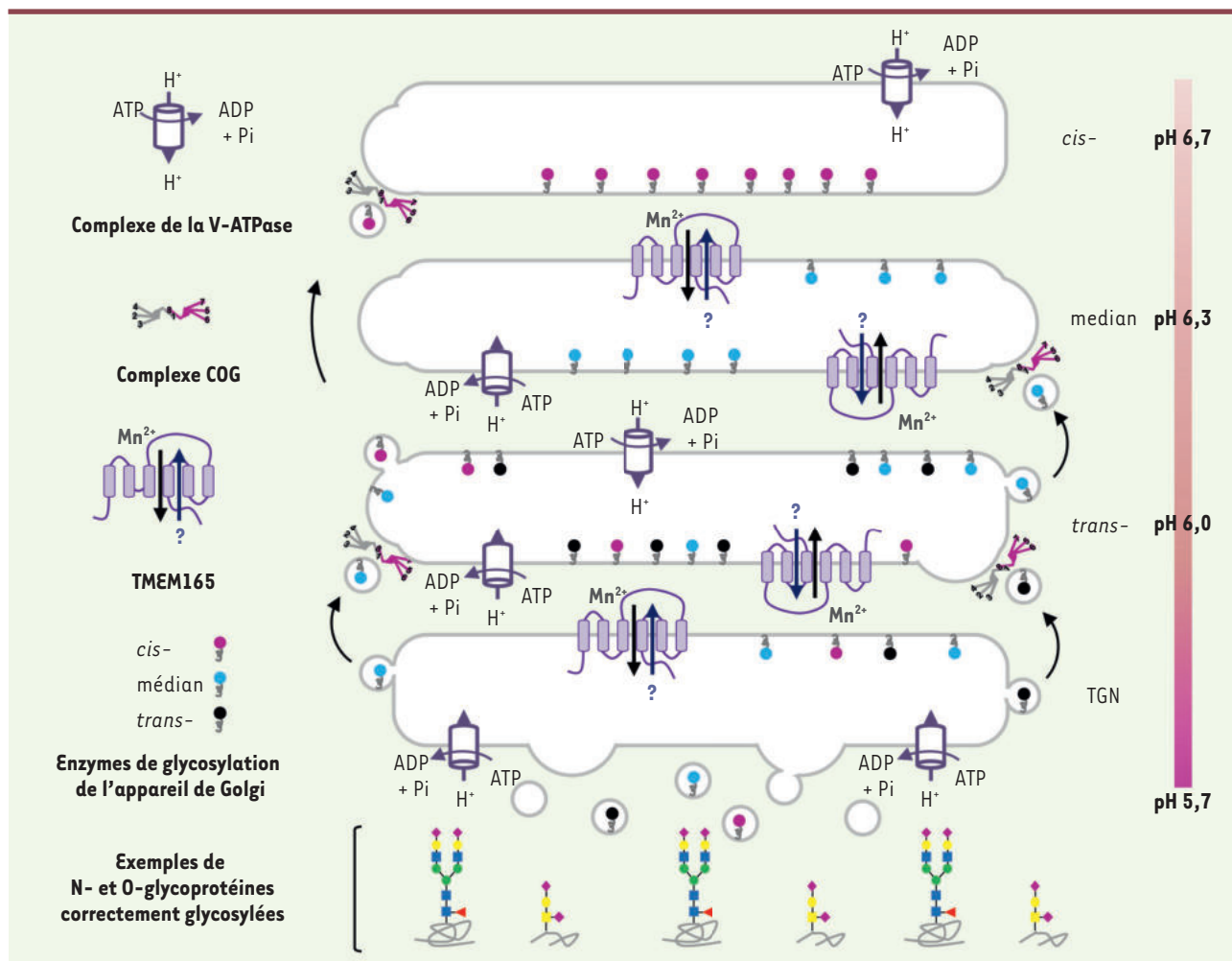


**Figure 5. Représentation schématique des mécanismes cellulaires impliqués dans la régulation de la localisation subcellulaire des GT et de leurs activités.** D'une part, le complexe COG assure la localisation correcte des GT via le trafic rétrograde. D'autre part, la V-ATPase et TMEM165 régulent les homéostasies du pH et du  $Mn^{2+}$  de l'appareil de Golgi, requises pour l'activité de ces GT. L'ensemble de ces mécanismes est essentiel à la génération de structures glycaniques matures correctes. Tout dysfonctionnement de ces mécanismes engendre un CDG. Le point d'interrogation représente un ion dont la nature reste à spécifier. COG : *Conserved Oligomeric Golgi*, TMEM165 : *Transmembrane protein 165*, TGN : *Trans-Golgi Network*.

fonction d'acheminer et de recycler des enzymes dans des citernes spécifiques. La dynamique de ce compartiment est telle que la moindre faille dans la formation, l'adressage et la fusion des vésicules a des conséquences désastreuses.

Au cours de la dernière décennie, les travaux portant sur les protéines du complexe COG (*conserved oligomeric golgi*) ont révélé son rôle essentiel dans le trafic rétrograde intravésiculaire golgien, et son implication dans la glycosylation golgienne. Le complexe COG est constitué de huit sous-unités, COG1 à COG8, réparties en deux lobes distincts : le lobe A formé des sous-unités COG1 à 4, et le lobe B qui comprend les sous-unités COG5 à 8. Ces deux lobes sont associés par une interaction établie entre les sous-unités COG1 du lobe A et COG8 du lobe B. Chaque sous-unité du complexe peut interagir avec différentes protéines qui participent au trafic intravésiculaire, telles que les SNARE (*soluble*

*N-ethylmaleimide-sensitive-factor attachment protein receptor*) et les GTPase Rab, les protéines de fusion et d'adressage des vésicules [17].

#### **Perturbation du trafic intravésiculaire golgien et CDG**

L'importance du complexe COG dans l'adressage et le recyclage des enzymes de glycosylation golgiennes a été révélée par la mise en évidence de déficits de l'une des sous-unités du complexe chez des patients souffrant de CDG-II. Les premiers cas, découverts en 2004, impliquaient COG7 [18]. Il s'agissait d'un frère et d'une sœur, présentant les symptômes cliniques d'un CDG (une hypotonie, une asphyxie périnatale et une dysmorphie - oreilles basses, peau lâche et ridée). Ils sont

décédés respectivement après cinq et dix semaines de vie des suites d'infections répétées et d'insuffisance cardiaque. Les profils d'IEF de la transferrine et d'Apoc-III étaient anormaux et une diminution de l'activité de deux GT, impliquées dans l'élongation des structures N- et O-glycanniques, a été observée. Un lien entre intégrité du trafic intravésiculaire golgien (révélé par le déficit en COG7) et le processus de glycosylation fut dès lors établi. De nombreuses mutations affectant sept des huit sous-unités constitutives du complexe COG (COG3 étant l'exception) ont par la suite été identifiées [19-25]. Environ un tiers des patients atteints de CDG-II présentent de telles mutations. Les mécanismes par lesquels sont générés les défauts de glycosylation ont fait l'objet de nombreuses études et ont partiellement été élucidés. Certaines déficiences perturbent notamment la structure même de l'appareil de Golgi et le trafic rétrograde intra-golgien de vésicules contenant des protéines importantes pour les réactions de glycosylation, telles que les GT et/ou les transporteurs de nucléotides sucres (TNS). Plus qu'une localisation golgienne anormale, les derniers travaux montrent une instabilité de certaines GT, résultant d'un adressage lysosomal inadéquat, en particulier MGAT (GLcNAc transférase 1 et 2), MAN2A1 (*α-mannosidase class 2A member 1*), B4GALT1 (*β-1,4-galactosyltransferase 1*) et ST6GAL1 (*β-galactoside alpha-2,6-sialyltransferase 1*) [26, 27]. L'altération du complexe COG est donc à l'origine de la déplétion d'acteurs clefs de la glycosylation golgienne provoquant les défauts de N- et O-glycosylation observés chez tous les patients COG-CDG.

## CDG et pH de l'appareil de Golgi

### Régulation du pH de l'appareil de Golgi

La régulation du pH de l'appareil de Golgi repose principalement sur l'activité de trois familles de protéines : les ATPases vacuolaires, encore appelées ATPases de type V (V-ATPase), qui importent des protons du cytoplasme vers la lumière de l'appareil de Golgi ; les canaux de fuite à protons, permettant d'ajuster finement le pH ; et les canaux ioniques qui assurent l'influx d'anions ou l'efflux de cations pour maintenir le potentiel membranaire [28,29]. Nous ne présenterons que les V-ATPase dont les altérations ont été révélées chez des patients CDG.

Les V-ATPase se composent d'un domaine cytoplasmique  $V_1$  et d'un domaine transmembranaire  $V_0$ , chacun de ces domaines étant lui-même constitué de plusieurs sous-unités. Leur rôle dans l'acidification des organites de la voie de sécrétion a été démontré par l'utilisation d'inhibiteurs spécifiques, tels que la bafilomycine A1 et la concanamycine A, qui conduit à une alcalinisation des compartiments acides de la cellule et de l'appareil de Golgi [30].

### Perturbation du pH de l'appareil de Golgi et CDG

Plusieurs mutations touchant différentes sous-unités de la V-ATPase sont responsables de CDG-II [31], révélant ainsi l'importance de la régulation du pH de l'appareil de Golgi dans le processus de glycosylation (Figure 5). Ainsi, des mutations du gène *ATP6VOA2* codant la sous-unité  $\alpha 2$  du domaine  $V_0$  de la V-ATPase, découvertes en 2008 par Kornak *et al.* [32] affectent la fonctionnalité de la protéine avec une alcalinisa-

tion de l'appareil de Golgi qui conduit à l'apparition de structures N- et O-glycanniques anormales, principalement asialylées et agalactosylées. Le mécanisme par lequel cette alcalinisation perturbe la glycosylation n'est pas complètement élucidé. Deux hypothèses peuvent toutefois être proposées. Cette augmentation de pH affecterait soit directement l'activité des enzymes de la glycosylation, en particulier les sialyltransférases, soit le trafic intracellulaire golgien, générant une mauvaise localisation subcellulaire de ces enzymes [29, 33, 34].

D'autres mutations responsables de CDG-II ont récemment été identifiées dans les gènes *ATP6V1A* et *ATP6V1E1* qui codent respectivement les sous-unités A et E1 du domaine  $V_1$  de la V-ATPase [35] mais également des mutations de gènes codant des protéines accessoires de la V-ATPase, comme *ATP6AP1* et *ATP6AP2*, ou encore *TMEM199* (*transmembrane protein 199*) et *CCDC115* (*coiled-coil domain containing 115*). *TMEM199* et *CCDC115* sont les orthologues humains de deux protéines de levure, *Vma12p* et *Vma22p*, qui, avec *Vma21p*, constitue un complexe qui « chaperonne » l'assemblage du domaine  $V_0$  de la V-ATPase au niveau du REG [36, 37]. Le phénotype clinique des patients est assez particulier, avec notamment des niveaux de transaminases sériques chroniquement élevés et un taux de céruloplasmine sérique faible. Curieusement, le métabolisme du cuivre est également altéré chez ces patients. Le lien entre pH du Golgi, anomalies de la glycosylation et perturbation du métabolisme du cuivre reste à explorer.

## CDG et homéostasie golgienne de l'ion manganèse ( $Mn^{2+}$ )

### Régulation de l'homéostasie golgienne du $Mn^{2+}$

Le manganèse (Mn) est un élément trace, essentiel à la réalisation de nombreux processus cellulaires physiologiques. Chez l'homme, la quantité totale de Mn, dont les formes biologiquement actives sont les ions  $Mn^{2+}$  et  $Mn^{3+}$ , est comprise entre 10 et 20 mg. Son homéostasie est principalement régulée par la balance absorption/excrétion. Les effets néfastes de l'accumulation du Mn dans l'organisme sont bien documentés. Inhalé à forte dose *via* des expositions répétées, il est neurotoxique, conduisant à un trouble neurologique appelé « manganisme » similaire à la maladie de Parkinson [38]. Cependant, aucun cas de carence en Mn n'avait été rapporté.

### Perturbation de l'homéostasie du $Mn^{2+}$ et CDG

En 2012, notre équipe a montré qu'une carence en Mn au niveau de l'appareil de Golgi, reposant sur un déficit en *TMEM165*, provoquait un CDG-II [39-41]. Par l'étude de la fonction de *TMEM165* et de son orthologue chez la

levure *Saccharomyces cerevisiae*, Gdt1p [42-44], ces travaux ont permis d'établir un lien entre homéostasie golgienne du  $Mn^{2+}$  et processus de glycosylation. TMEM165 est en effet un acteur majeur de la régulation de l'homéostasie du  $Mn^{2+}$  en permettant son import dans l'appareil de Golgi (Figure 5). À ce niveau, le  $Mn^{2+}$  est un cofacteur de nombreuses glycosyltransférases, qui, en s'associant au site catalytique, les rend actives. La déficience en TMEM165 induirait une diminution de la concentration de  $Mn^{2+}$  au niveau de la lumière de l'appareil de Golgi et affecterait principalement le transfert sur les glycoconjugués, des NDP-sucres, en particulier l'UDP-galactose et l'UDP-GalNAc. Chez les patients déficients en TMEM165, toutes les voies de glycosylation sont donc affectées, ce qui participe très certainement aux anomalies osseuses sévères observées. *In vitro*, le déficit de  $Mn^{2+}$  dans les cellules déficientes en TMEM165 peut être comblé par un apport exogène en  $Mn^{2+}$  qui permet la correction des défauts de glycosylation observés dans ces cellules [45-47]. Le mécanisme de cette restauration reste cependant encore incompris mais l'importance du REG, en particulier des pompes SERCA (*sarco endoplasmic reticulum Ca<sup>2+</sup>-ATPase*) a été suggéré : en l'absence de TMEM165, ce mécanisme permettrait de fournir en ions  $Mn^{2+}$  via le REG, l'appareil de Golgi [47].

Récemment, un autre CDG-II affectant l'homéostasie cellulaire du Mn a été rapporté. Il s'agit du SLC39A8-CDG, identifié en 2015 par Park *et al.* [48]. Contrairement à TMEM165 qui est localisé au niveau de l'appareil de Golgi, SLC39A8 est un transporteur de cations divalents situé à la membrane plasmique. Il permet l'import des ions  $Mn^{2+}$  et zinc ( $Zn^{2+}$ ) dans le cytoplasme. Comme chez les patients TMEM165-CDG, une hypogalactosylation massive des structures glycaniques associée à un phénotype clinique osseux sévère sont observés chez les patients SLC39A8-CDG.

### Quels traitements pour les CDG ?

Les résultats issus de la recherche combinés aux données cliniques permettent une meilleure compréhension des mécanismes à l'origine des défauts de glycosylation et permettent d'envisager, pour certains patients CDG, de possibles traitements. Néanmoins, aucun traitement ne permet aujourd'hui de corriger les atteintes sévères, en particulier neurologiques et osseuses, qui apparaissent chez ces patients au cours de leur développement. Nous examinerons les principales avancées et stratégies thérapeutiques actuelles ciblant les CDG [49].

#### Administration orale de monosaccharides et ions

Certains CDG résultent d'un déficit de protéines directement impliquées dans la synthèse ou le transport des nucléotides sucres. Dans certains cas, des traitements relativement simples à mettre en œuvre sont envisageables. Ils consistent en l'apport exogène du monosaccharide/ion par l'alimentation. Cette stratégie présente l'avantage d'être relativement inoffensive pour les patients et peu onéreuse. Selon le CDG considéré, une administration orale de monosaccharide peut-être combinée à celle d'éléments traces, tels que les ions  $Mn^{2+}$ . À l'heure actuelle, cette approche thérapeutique cible une dizaine de CDG et de nombreuses revues rendent compte des différents traitements établis [49-53], dont certains sont présentés ici.

#### Le D-mannose

Le D-mannose est un monosaccharide qui participe à plusieurs voies de glycosylation, dont la N-glycosylation, la O-glycosylation, la C-mannosylation et la synthèse des ancras GPI. Le premier cas de CDG ayant bénéficié de ce traitement fut un patient atteint de MPI (mannose phosphate isomérase)-CDG. L'apport exogène de D-mannose compense dans ce cas le déficit en mannose phosphate isomérase, l'enzyme responsable de la conversion du fructose-6-phosphate en mannose-6-phosphate. Ce mannose exogène est converti en mannose-6-phosphate par l'hexokinase. Il est ensuite activé en GDP-mannose afin d'être utilisé par les GT. L'administration par voie orale de D-mannose (1 g/kg par jour en trois à quatre prises), tend à normaliser le profil des glycoformes de la transferrine sérique. Elle améliore considérablement les fonctions endocriniennes et les facteurs de coagulation chez les patients traités [51]. La posologie du D-mannose doit cependant être finement ajustée en raison d'effets secondaires gastro-intestinaux et hématologiques. Ce traitement ne s'applique que pour le MPI-CDG, et non pour le PMM2 (phosphomannomutase 2)-CDG, dont la déficience affecte la conversion du mannose-6-phosphate en mannose-1-phosphate. Le traitement chez les patients souffrant de PMM2-CDG ne conduirait qu'à une augmentation de mannose-6-phosphate et non à celle de mannose-1-phosphate, produit par la PMM2. Une stratégie pharmacologique d'encapsulation du mannose-1-phosphate dans des liposomes, élaborée par la société *Glycomine*, a été entreprise pour ces patients. Cette approche prometteuse permettrait de délivrer directement le nucléotide sucre manquant aux cellules. Les premiers essais cliniques devraient débuter prochainement.

#### Le L-fucose

Le L-fucose est un monosaccharide retrouvé dans différentes structures N- et O-glycaniques ainsi que dans les glycolipides. L'import de GDP-fucose dans l'appareil de Golgi se réalise principalement grâce au transporteur SLC35C1 (*solute carrier family 35 member C1*). Chez les patients présentant un SLC35C1-CDG, l'apport exogène de L-fucose tend à normaliser le défaut de glycosylation. Le mécanisme de cette normalisation n'est pas complètement élucidé, mais il reposerait sur une augmentation de la concentration cellulaire de GDP-fucose, permettant ainsi son import dans l'appareil de Golgi malgré l'altération de son transporteur SLC35C1. Chez ces patients, principalement immunodéficients, ce traitement diminue les infections et normalise le nombre de leucocytes circulants [51].

## Le D-galactose

L'import d'UDP-galactose dans l'appareil de Golgi repose sur l'activité du transporteur SLC35A2 (*solute carrier family 35 member A2*). Un défaut de galactosylation des structures N- et O-glycanniques, ainsi que de certains glycolipides, est observé chez certains patients CDG. Ces défauts ont des origines multiples et résultent soit d'une moindre quantité d'UDP-galactose (pour les PGM1[phosphoglucomutase 1]-CDG), soit d'un défaut d'import d'UDP-galactose dans l'appareil de Golgi (pour les SLC35A2-CDG), soit, enfin, d'une altération enzymatique de son transfert sur les structures glycanniques (pour les SLC39A8-CDG et les TMEM165-CDG). Le défaut de galactosylation chez ces patients est corrigé par l'administration orale de D-galactose (entre 0,5 et 1,5 g/kg par jour) [45, 49, 51]. Les mécanismes de la restauration sont néanmoins complexes et différent selon le déficit. Une conséquence constante faisant suite à l'apport exogène de D-galactose est néanmoins l'augmentation du *pool* cytoplasmique d'UDP-galactose. Dans le cas du SLC35A2-CDG, le mécanisme reste incompris mais impliquerait vraisemblablement l'activité d'un autre transporteur golgien dans l'import d'UDP-galactose. Pour le PGM1-CDG où la conversion du glucose-6-phosphate en glucose-1-phosphate est altérée, l'apport exogène de D-galactose favoriserait à la fois la production d'UDP-galactose et d'UDP-glucose par l'action de l'UDP-galactose 4-épipimérase (GALE).

## Le D-galactose et l'ion Mn<sup>2+</sup>

Dans les cas particuliers de SLC39A8-CDG et TMEM165-CDG, un apport exogène combiné de D-galactose et d'ion Mn<sup>2+</sup> (sous la forme de MnCl<sub>2</sub> ou de MnSO<sub>4</sub>) semble être un traitement de choix. L'UDP-galactose et les ions Mn<sup>2+</sup> étant les substrats et cofacteurs de la β-1,4-galactosyltransférase (B4GALT1), leur apport exogène permettrait de stimuler son activité afin d'accroître le transfert de galactose sur les structures glycanniques. Dans le cas du SLC39A8-CDG, cette combinaison a donné des résultats prometteurs avec une normalisation des défauts de glycosylation, associée à l'amélioration de nombreux paramètres biochimiques [48, 54]. Le principal inconvénient dans la mise en place d'un tel traitement repose sur la toxicité du Mn. Il doit donc s'accompagner du contrôle de nombreux paramètres afin de prévenir ces effets toxiques sur l'organisme. Pour la déficience en TMEM165, des études *in vitro* menées sur des lignées de cellules HEK293 dans lesquelles le gène *TMEM165* a été invalidé, ont d'ores et déjà prouvé l'effet bénéfique d'une supplémentation en D-galactose et en ions Mn<sup>2+</sup> sur la restauration des profils de glycosylation des structures N-glycanniques et des glycolipides produits par les cellules [45, 47]. Des essais cliniques utilisant cette combinaison sont actuellement en cours de validation sur deux patients TMEM165-CDG.

## Transplantations

Les CDG se caractérisent par une atteinte multi-systémique [11] et dans 22 % des cas, le foie des patients est atteint, ce qui se traduit par une cirrhose, une insuffisance hépatique ou, dans les cas les plus sévères, une fibrose hépatique. C'est le cas, avec différents degrés de gravité, des patients TMEM199-CDG, CCDC115-CDG, ATPAP1-CDG, MPI-CDG, PMM2-CDG et PGM1-CDG [49]. Dans les cas de PMM2- et

PGM1-CDG, les taux élevés de transaminases associés à une stéatose confirment le dysfonctionnement du foie. Néanmoins, la question d'une transplantation de foie est délicate, puisque les taux de transaminases peuvent se normaliser au cours du temps (pour les PMM2-CDG) ou après un traitement au D-galactose (pour les PGM1-CDG). En revanche, dans le cas d'une fibrose hépatique avancée, que l'on observe principalement chez les patients MPI-CDG, la transplantation est le seul moyen de rétablir une fonction hépatique. Ces transplantations ont été réalisées avec succès chez plusieurs patients MPI-, ATP6AP1- et CCDC115-CDG. Le foie n'est malheureusement pas le seul organe sévèrement atteint chez certains patients. Pour les patients DOLK (*dolichol kinase*)-CDG, des atteintes cardiaques ont été rapportées et deux transplantations de cœur ont été réalisées avec succès. Dans les cas d'immunodéficiences sévères telles qu'on les observe chez les patients PGM3 (phosphoglucomutase 3)-CDG, une transplantation de cellules souches hématopoïétiques s'est avérée être bénéfique en diminuant les troubles immunitaires [49].

## Utilisation des chaperonnes pharmacologiques et de l'acétazolamide

Les chaperonnes pharmacologiques (CP) sont de petites molécules pouvant lier les protéines mutées mal conformées et les stabiliser et, ainsi, empêcher leur dégradation prématurée. Dans le cas du PMM2-CDG, près de 80 % des patients portent la mutation faux-sens p.R141H responsable du déficit enzymatique de la PMM2. Après le criblage haut débit de 10 000 molécules pharmacologiques, Yuste-Checa *et al.* [55] ont sélectionné quatre composés susceptibles de jouer le rôle de CP pour la PMM2. Ces composés, en stabilisant la protéine mutée, empêchent sa dégradation et favorisent le maintien de sa fonctionnalité, bien qu'elle soit altérée. Chez les patients PMM2-CDG, des accidents vasculaires cérébraux (ou *stroke like episodes*, SLE) apparaissent. Ces SLE sont également observés dans d'autres types de maladies neurologiques, dont les migraines hémiplegiques familiales (MHF). L'acétazolamide (ou AZATAX) est un traitement de choix pour ces MHF. Il réduit considérablement la fréquence de ces épisodes cérébraux. Dans le cadre du déficit de PMM2, l'AZATAX a été testé sur une cohorte de patients. Bien toléré, son administration a produit des résultats spectaculaires chez certains d'entre eux avec, notamment, une amélioration des syndromes cérébelleux moteurs. Là encore, le mécanisme d'action de l'acétazolamide reste incompris même si l'on suppose qu'il est impliqué dans la régulation d'un transporteur de calcium [56].

## Conclusion

Il y a 60 ans, face aux découvertes majeures qui concernaient l'ADN et l'ARN, la glycobiologie représentait un domaine d'étude anecdotique. Mais, depuis la détection de glycopathologies génétiques rares chez l'homme, une prise de conscience de l'importance des réactions de glycosylation et de leur régulation dans la communauté scientifique a propulsé ce domaine de recherche au tout premier plan. L'identification et la caractérisation de nouveaux CDG ont révélé des partenaires insoupçonnés de la régulation du processus de glycosylation et ont dévoilé leur importance dans d'autres voies métaboliques. Au-delà d'offrir un panorama des CDG sur les 40 dernières années, nous avons tenté de présenter les bases de cette science, la glycobiologie. Nous souhaitons que ces quelques lignes aient attisé la curiosité du lecteur en l'invitant à en découvrir davantage sur le vaste domaine des glycosciences. ♦

## SUMMARY

### Panorama on congenital disorders of glycosylation (CDG): from 1980 to 2020

Glycosylation is an essential and complex cellular process where mono-saccharides are added one by one onto an acceptor molecule, most of the time a protein or a lipid, so called glycoprotein or glycolipid. This cellular process is found in every living organism and is tightly conserved during evolution. In human, if one of the glycosylation reactions is genetically impaired, Congenital Disorders of Glycosylation (CDG) appear. CDG are a growing family of more than a hundred genetic diseases. This review offers a panorama of CDGs from 1980 to the present, their discoveries, diagnoses and treatments. ♦

Marine Houdou a été lauréate du prix des Journées André Verbert 2019, École doctorale Biologie-Santé de l'université de Lille.

## LIENS D'INTÉRÊT

Les auteurs déclarent n'avoir aucun lien d'intérêt concernant les données publiées dans cet article.

## RÉFÉRENCES

- Ramakrishnan B, Ramasamy V, Qasba PK. Structural snapshots of  $\beta$ -1,4-galactosyltransferase-I along the kinetic pathway. *J Mol Biol* 2006; 357 : 1619-33.
- Hadley B, Litfin T, Day CJ, et al. Nucleotide sugar transporter SLC35 family structure and function. *Comput Struct Biotechnol J* 2019; 17 : 1123-34.
- Brockhausen I, Schutzbach J, Kuhns W. Glycoproteins and their relationship to human disease. *Cells Tissues Organs* 1998; 161 : 36-78.
- Schachter H, Freeze HH. Glycosylation diseases: Quo vadis? *Biochim Biophys Acta* 2009; 1792 : 925-50.
- Jaeken J, Vanderschueren-Lodewyckx M, Casaer P. Familial psychomotor retardation with markedly fluctuating serum prolactin, FSH and GH levels, partial TGB-deficiency, increased serum arylsulphatase A and increased CSF protein: a new syndrome? *Pediatr Res* 1980; 14, 179.
- Jaeken J, Eijk HG van, Heul C van der, et al. Sialic acid-deficient serum and cerebrospinal fluid transferrin in a newly recognized genetic syndrome. *Clin Chim Acta* 1984; 144 : 245-47.
- Van Schaftingen E, Jaeken J. Phosphomannomutase deficiency is a cause of carbohydrate-deficient glycoprotein syndrome type I. *FEBS Lett* 1995; 377 : 318-20.
- Matthijs G, Schollen E, Pardon E, et al. Mutations in PMM2, a phosphomannomutase gene on chromosome 16p13, in carbohydrate-deficient glycoprotein type I syndrome (Jaeken syndrome). *Nat Genet* 1997; 16 : 88-92.
- Dupré T, Lavie G, Moore S, et al. Les anomalies congénitales de glycosylation des N-glycosylprotéines. *Med/Sci (Paris)* 2004; 20 : 331-8.
- Ng BG, Freeze HH. Perspectives on glycosylation and its congenital disorders. *Trends Genet* 2018; 34 : 466-76.
- Francisco R, Marques-da-Silva D, Brasil S, et al. The challenge of CDG diagnosis. *Mol Genet Metab* 2019; 126 : 1-5.
- Wopereis S. Apolipoprotein C-III isofocusing in the diagnosis of genetic defects in O-glycan biosynthesis. *Clin Chem* 2003; 49 : 1839-45.
- Jaeken J, Hennet T, Freeze HH, et al. On the nomenclature of congenital disorders of glycosylation (CDG). *J Inherit Metab Dis*. 2008; 31 : 669-72.
- Jaeken J, Hennet T, Matthijs G, et al. CDG nomenclature: time for a change! *Biochim Biophys Acta* 2009; 1792 : 825-6.
- Jaeken J. Congenital disorders of glycosylation (CDG): it's (nearly) all in it! *J Inherit Metab Dis* 2011; 34 : 853-58.
- Potelle S, Klein A, Foulquier F. Golgi post-translational modifications and associated diseases. *J Inherit Metab Dis* 2015; 38 : 741-51.
- Willett R, Ungar D, Lupashin V. The Golgi puppet master: COG complex at center stage of membrane trafficking interactions. *Histochem Cell Biol* 2013; 140 : 271-83.
- Wu X, Steet RA, Bohorov O, et al. Mutation of the COG complex subunit gene COG7 causes a lethal congenital disorder. *Nat Med* 2004; 10 : 518-23.
- Foulquier F, Vasile E, Schollen E, et al. Conserved oligomeric Golgi complex subunit 1 deficiency reveals a previously uncharacterized congenital disorder of glycosylation type II. *Proc Natl Acad Sci USA* 2006; 03 : 3764-69.
- Foulquier F, Ungar D, Reynders E, et al. A new inborn error of glycosylation due to a Cog8 deficiency reveals a critical role for the Cog1-Cog8 interaction in COG complex formation. *Hum Mol Genet* 2007; 16 : 717-30.
- Kranz C, Ng BG, Sun L, et al. COG8 deficiency causes new congenital disorder of glycosylation type IIh. *Hum Mol Genet* 2007; 16 : 731-41.
- Reynders E, Foulquier F, Leão Teles E, et al. Golgi function and dysfunction in the first COG4-deficient CDG type II patient. *Hum Mol Genet* 2009; 18 : 3244-56.
- Paesold-Burda P, Maag C, Troxler H, et al. Deficiency in COG5 causes a moderate form of congenital disorders of glycosylation. *Hum Mol Genet* 2009; 18 : 4350-6.
- Lubbehusen J, Thiel C, Rind N, et al. Fatal outcome due to deficiency of subunit 6 of the conserved oligomeric Golgi complex leading to a new type of congenital disorders of glycosylation. *Hum Mol Genet* 2010; 19 : 3623-33.
- Kodera H, Ando N, Yuasa I, et al. Mutations in COG2 encoding a subunit of the conserved oligomeric golgi complex cause a congenital disorder of glycosylation: COG2 mutations cause congenital disorder of glycosylation. *Clin Genet* 2015; 87 : 455-60.
- Pokrovskaya ID, Willett R, Smith RD, et al. Conserved oligomeric Golgi complex specifically regulates the maintenance of Golgi glycosylation machinery. *Glycobiology* 2011; 21 : 1554-69.
- Shetakova A, Zolov S, Lupashin V. COG complex-mediated recycling of Golgi glycosyltransferases is essential for normal protein glycosylation: COG complex and Golgi glycosylation. *Traffic* 2006; 7 : 191-204.
- Kellokumpu S. Golgi pH, ion and redox homeostasis: how much do they really matter? *Front Cell Dev Biol* 2019; 7 : 93.
- Rivinoja A, Hassinen A, Kokkonen N, et al. Elevated Golgi pH impairs terminal N-glycosylation by inducing mislocalization of Golgi glycosyltransferases. *J Cell Physiol* 2009; 220 : 144-54.
- Rivinoja A, Pujol FM, Hassinen A, et al. Golgi pH, its regulation and roles in human disease. *Ann Med* 2012; 44 : 542-54.
- Guillard M, Dimopoulou A, Fischer B, et al. Vacuolar H<sup>+</sup>-ATPase meets glycosylation in patients with cutis laxa. *Biochim Biophys Acta* 2009; 1792 : 903-14.
- Kornak U, Reynders E, Dimopoulou A, et al. Impaired glycosylation and cutis laxa caused by mutations in the vesicular H<sup>+</sup>-ATPase subunit ATP6V0A2. *Nat Genet* 2008; 40 : 32-4.
- Maeda Y. pH control in Golgi apparatus and congenital disorders of glycosylation. In : Taniguchi N, Endo T, Hart GW, et al., eds. *Glycoscience: biology and medicine*. Tokyo : Springer Japan, 2015 : 921-25.
- Maeda Y, Kinoshita T. The acidic environment of the Golgi is critical for glycosylation and transport. *Methods enzymology*. Amsterdam : Elsevier, 2010 : 495-510.
- Van Damme T, Gardeitchik T, Mohamed M, et al. Mutations in ATP6V1E1 or ATP6V1A cause autosomal-recessive cutis laxa. *Am J Hum Genet* 2017; 100 : 216-27.
- Jansen JC, Timal S, van Scherpenzeel M, et al. TMEM199 deficiency is a disorder of Golgi homeostasis characterized by elevated aminotransferases, alkaline phosphatase, and cholesterol and abnormal glycosylation. *Am J Hum Genet* 2016; 98 : 322-30.
- Jansen JC, Cirak S, van Scherpenzeel M, et al. CCDC115 deficiency causes a disorder of Golgi homeostasis with abnormal protein glycosylation. *Am J Hum Genet* 2016; 98 : 310-21.

## RÉFÉRENCES

38. O'Neal SL, Zheng W. Manganese toxicity upon overexposure: a decade in review. *Curr Environ Health Rep* 2015 ; 2 : 315-28.
39. Amyere M, Jaeken J, Zeevaert R, et al. TMEM165 deficiency causes a congenital disorder of glycosylation. *Am J Hum Genet* 2012 ; 91 : 15-26.
40. Zeevaert R, Zegher F de, Sturiale L, et al. Bone dysplasia as a key feature in three patients with a novel congenital disorder of glycosylation (CDG) type II due to a deep intronic splice mutation in TMEM165. In : Zschocke J, Gibson KM, Brown G, et al., eds. *JIMD reports – Case and research reports, 2012/5*. Berlin, Heidelberg : Springer Berlin Heidelberg, 2012 : 145-52.
41. Potelle S, Morelle W, Dulary E, et al. Glycosylation abnormalities in Gdt1p/TMEM165 deficient cells result from a defect in Golgi manganese homeostasis. *Hum Mol Genet* 2016 ; 25 : 1489-500.
42. Dulary E, Potelle S, Legrand D, et al. TMEM165 deficiencies in congenital disorders of glycosylation type II (CDG-II): clues and evidences for roles of the protein in Golgi functions and ion homeostasis. *Tissue Cell* 2017 ; 49 : 150-6.
43. Dulary E, Yu SY, Houdou M, et al. Investigating the function of Gdt1p in yeast Golgi glycosylation. *Biochim Biophys Acta* 2017 ; 1862 : 394-402.
44. Thines L, Deschamps A, Sengottaiyan P, et al. The yeast protein Gdt1p transports Mn<sup>2+</sup> ions and thereby regulates manganese homeostasis in the Golgi. *J Biol Chem* 2018 ; 293 : 8048-55.
45. Morelle W, Potelle S, Witters P, et al. Galactose supplementation in patients with TMEM165-CDG rescues the glycosylation defects. *J Clin Endocrinol Metab* 2017 ; 102 : 1375-86.
46. Potelle S, Dulary E, Climer L, et al. Manganese-induced turnover of TMEM165. *Biochem J* 2017 ; 474 : 1481-93.
47. Houdou M, Lebretonchel E, Garat A, et al. Involvement of thapsigargin- and cyclopiazonic acid-sensitive pumps in the rescue of TMEM165-associated glycosylation defects by Mn<sup>2+</sup>. *FASEB J* 2019 ; 33 : 2669-79.
48. Park JH, Hogrebe M, Grüneberg M, et al. SLC39A8 deficiency: a disorder of manganese transport and glycosylation. *Am J Hum Genet* 2015 ; 97 : 894-903.
49. Verheijen J, Tahata S, Kozicz T, et al. Therapeutic approaches in congenital disorders of glycosylation (CDG) involving N-linked glycosylation: an update. *Genet Med* 2019 ; 22 : 268-79.
50. Péanne R, Lonlay P de, Foulquier F, et al. Congenital disorders of glycosylation (CDG): quo vadis? *Eur J Med Genet* 2017 ; 61 : 643-63.
51. Sosicka P, Ng BG, Freeze HH. Therapeutic monosaccharides: looking back, moving forward. *Biochemistry* 2019 ; acs.biochem.9b00565.
52. Jaeken J, Péanne R. What is new in CDG? *J Inherit Metab Dis* 2017 ; 40 : 569-86.
53. Brasil S, Pascoal C, Francisco R, et al. CDG therapies: from bench to bedside. *Int J Mol Sci* 2018 ; 19 : 1304.
54. Park JH, Hogrebe M, Fobker M, et al. SLC39A8 deficiency: biochemical correction and major clinical improvement by manganese therapy. *Genet Med* 2018 ; 20 : 259-68.
55. Yuste-Checa P, Brasil S, Gámez A, et al. Pharmacological chaperoning: a potential treatment for PMM2-CDG: human mutation. *Hum Mutat* 2017 ; 38 : 160-8.
56. Martínez-Monseny AF, Bolasell M, Callejón Póo L, et al. AZATAX: acetazolamide safety and efficacy in cerebellar syndrome in PMM2 congenital disorder of glycosylation (PMM2 CDG). *Ann Neurol* 2019 ; 85 : 740-51.

**TIRÉS À PART**

M. Houdou



### Global Registry for COL6-related dystrophies

### Registre global des dystrophies liées au collagène de type VI

S'inscrire sur : [www.collagen6.org](http://www.collagen6.org)

Ou contactez-nous par e-mail à l'adresse : [collagen6registry@ncl.ac.uk](mailto:collagen6registry@ncl.ac.uk)


La traduction française sera bientôt disponible sur le site web.









**Tarifs d'abonnement m/s - 2020**

**Abonnez-vous**


**à médecine/sciences**

**> Grâce à m/s, vivez en direct les progrès des sciences biologiques et médicales**

---

**Bulletin d'abonnement**

**page 822 dans ce numéro de m/s**





---

## **Appendix II :**

Dissection of TMEM165 function in Golgi glycosylation  
and its Mn<sup>2+</sup> sensitivity

---





## Research paper

# Dissection of TMEM165 function in Golgi glycosylation and its Mn<sup>2+</sup> sensitivity

Elodie Lebretonchel <sup>a,b</sup>, Marine Houdou <sup>a</sup>, Sven Potelle <sup>a</sup>, Geoffroy de Bettignies <sup>a</sup>, Céline Schulz <sup>a</sup>, Marie-Ange Krzewinski Recchi <sup>a</sup>, Vladimir Lupashin <sup>c</sup>, Dominique Legrand <sup>a</sup>, André Klein <sup>a,b</sup>, François Foulquier <sup>a,\*</sup>

<sup>a</sup> Univ. Lille, CNRS, UMR 8576 – UGSF - Unité de Glycobiologie Structurale et Fonctionnelle, F- 59000, Lille, France

<sup>b</sup> Centre de Biologie et Pathologie, UAM de Glycopathologies, Lille Medical Center, University of Lille, 59000, Lille, France

<sup>c</sup> Department of Physiology and Biophysics, College of Medicine, University of Arkansas for Medical Sciences, Biomed 261-2, Slot 505, 200 South Cedar St., Little Rock, AR, 72205, USA



## ARTICLE INFO

## Article history:

Received 29 May 2019

Accepted 18 July 2019

Available online 24 July 2019

## Keywords:

TMEM165

CDG

UPF0016

Golgi glycosylation

Mn<sup>2+</sup>

## ABSTRACT

Since 2012, the interest for TMEM165 increased due to its implication in a rare genetic human disease named TMEM165-CDG (Congenital Disorder(s) of Glycosylation). TMEM165 is a Golgi localized protein, highly conserved through evolution and belonging to the uncharacterized protein family 0016 (UPF0016). Although the precise function of TMEM165 in glycosylation is still controversial, our results highly suggest that TMEM165 would act as a Golgi Ca<sup>2+</sup>/Mn<sup>2+</sup> transporter regulating both Ca<sup>2+</sup> and Mn<sup>2+</sup> Golgi homeostasis, the latter is required as a major cofactor of many Golgi glycosylation enzymes. Strikingly, we recently demonstrated that besides its role in regulating Golgi Mn<sup>2+</sup> homeostasis and consequently Golgi glycosylation, TMEM165 is sensitive to high manganese exposure. Members of the UPF0016 family contain two particularly highly conserved consensus motifs E-φ-G-D-[KR]-[TS] predicted to be involved in the ion transport function of UPF0016 members. We investigate the contribution of these two specific motifs in the function of TMEM165 in Golgi glycosylation and in its Mn<sup>2+</sup> sensitivity.

Our results show the crucial importance of these two conserved motifs and underline the contribution of some specific amino acids in both Golgi glycosylation and Mn<sup>2+</sup> sensitivity.

© 2019 Published by Elsevier B.V.

## 1. Introduction

Congenital Disorders of Glycosylation (CDG) are a rapidly expanding family of genetic diseases. The first patient cases were reported 38 years ago ; today more than hundred different CDG have been reported [1]. The frequency of most CDG is unknown but they are probably underestimated. The genetic transmission is mostly autosomal recessive [1]. Congenital disorders of protein glycosylation are classified in two groups. CDG-I are assembly defects in the cytosol and the endoplasmic reticulum (ER), while CDG-II are defects in glycan remodeling in the Golgi [2]. They are multisystem disorders with a broad spectrum of severity and mostly comprising neurological involvement.

In 2012, a new CDG called TMEM165-CDG or CDG-IIk (OMIM #614727) has been described [3]. To date, a dozen of TMEM165-

CDG patients have been worldwide diagnosed with a common semiology. The most severe phenotypes present a growth retardation resistant to human growth hormone, associated with a psychomotor disability, microcephaly, facial hypoplasia, hypotonia, seizures and hepatosplenomegaly with increased serum transaminases [4]. Some patients also harbor cardiac defects [5] but the pathognomonic signs remain bone and cartilage dysplasia with early and severe osteoporosis. All TMEM165-CDG present a strong defect in the Golgi glycosylation characterized by hypogalactosylation of total serum N-glycoproteins [3].

This CDG is due to a deficiency in TMEM165 protein, also named TPARL [3], a 324 amino-acids transmembrane protein member of the UPF family 0016 (Uncharacterized Protein Family 0016; Pfam PF01169). This protein is mainly localized in Golgi membranes [3,6], predominantly in the *trans*-Golgi subcompartment. Similarly to other UPF0016 family members, TMEM165 is highly conserved throughout evolution (919 different species in prokaryotes and 405 species in eukaryotes) [7].

\* Corresponding author.

E-mail address: [francois.foulquier@univ-lille.fr](mailto:francois.foulquier@univ-lille.fr) (F. Foulquier).

### Abbreviations

|                   |  |
|-------------------|--|
| CQ                | Chloroquine                                  |
| CDG               | Congenital Disorder(s) of Glycosylation      |
| GPP130            | Golgi Phosphoprotein 4                       |
| ER                | Endoplasmic Reticulum                        |
| LAMP2             | Lysosomal-associated membrane protein 2      |
| Mn                | Manganese                                    |
| Mn <sup>2+</sup>  | Manganese, ion (2+)                          |
| MnCl <sub>2</sub> | Manganese (II) chloride tetrahydratex        |
| TMEM165           | Transmembrane Protein 165                    |
| SPCA1             | Secretory-Pathway Ca <sup>2+</sup> -ATPase 1 |
| PAM71             | Photosynthesis Affected Mutant 71            |
| UPF               | Uncharacterized Protein Family               |

The cellular and molecular functions of UPF0016 family members remain controversial. Gdt1p (Grc1 dependent translation factor 1), the yeast ortholog of TMEM165 in *Saccharomyces cerevisiae* was initially postulated to be a Ca<sup>2+</sup>/H<sup>+</sup> exchanger [8]. Recent results however question the nature of the exchanged ions. Unexpectedly, PAM71 (Photosynthesis Affected Mutant 71), the *Arabidopsis thaliana* plant ortholog of TMEM165 has been shown to function as a Ca<sup>2+</sup>/Mn<sup>2+</sup> cation antiport transporter localized in the thylakoid membranes system and crucial for the regulation of chloroplastic Mn<sup>2+</sup> homeostasis [9]. In addition, we recently demonstrated that the Golgi glycosylation defect due to TMEM165 deficiency also results from a defect in Golgi Mn<sup>2+</sup> homeostasis [10]. Very importantly, a slight Mn<sup>2+</sup> supplementation is sufficient to suppress the observed Golgi glycosylation defect in both deficient yeasts and human cells [11]. Furthermore, our recent studies suggested the function of Gdt1p as a Ca<sup>2+</sup>/Mn<sup>2+</sup> cation antiport transporter [12]. In agreement with these results, Thines and collaborators have recently demonstrated that the yeast protein Gdt1p transports Mn<sup>2+</sup> ions and thereby regulates manganese homeostasis in the Golgi [13].

Protein sequence alignments between PAM71, TMEM165 and Gdt1p underline highly conserved amino acids (Fig. 1) [12]. Two patterns of highly conserved successive amino acid sequences emerge from this alignment: E-x-G-D-K-[TF] and E-x-G-D-R-[SQ]. These motifs are enshrined in the first and fourth transmembrane protein domains (TM1 and TM4) (Fig. 1).

In this paper, we particularly explored the contribution of these two highly conserved motifs in the function of TMEM165 in Golgi glycosylation and also in its Mn<sup>2+</sup> sensitivity.

## 2. MATERIAL and METHODS

### 2.1. Sequence alignment

Uniprot accession codes are: *Homo sapiens* TMEM165\_HUMAN, *Arabidopsis thaliana* PAM71\_ARATH and *Saccharomyces cerevisiae* GDT1\_YEAST.

### 2.2. Cell culture, transfection and treatment

Control and KO TMEM165 HEK293T cells were maintained in Dulbecco's Modified Eagle's Medium (DMEM) supplemented with 10% fetal bovine serum (FBS) (Lonza, Basel, Switzerland), at 37 °C in humidity-saturated 5% CO<sub>2</sub> atmosphere. Transfections were performed using 4 µl of Lipofectamine 2000<sup>®</sup> (Thermo Scientific) for 0.5 µg of plasmid for each well of 6 wells-plate at 70% confluence in 1 ml DMEM medium. Transfections were stopped after 5 h. Wells

were split 24 h after transfection and treated 48 h post-transfection. Manganese (II) chloride tetrahydrate, from Riedel-de-Haën (Seelze, Germany) treatment 500 µM was pursued for 4 and 8 h. Chloroquine (ICN Biomedicals) 100 µM was added 1 h before manganese as a pretreatment.

### 2.3. Constructs, vector engineering and mutagenesis

Mutated TMEM165 plasmids were generated and supplied by e-Zyvec (Lille, France).

### 2.4. Antibodies and other reagents

Anti-TMEM165 and anti-β-actin antibodies were purchased from MilliporeSigma (Burlington, MA, USA), anti-LAMP2 antibody from Santa Cruz Biotechnology (Dallas, TX, USA) and anti-GM130 antibody from BD Biosciences. Polyclonal goat anti-rabbit IgG and goat anti-mouse IgG Horse Radish Peroxidase-conjugated were from Dako (Denmark).

### 2.5. Immunofluorescence staining

Cells were seeded on coverslips for 12–24 h, washed once in Dulbecco's Phosphate Buffer Saline (DPBS, Lonza) containing Calcium and Manganese and fixed with 4% paraformaldehyde (PAF) in PBS (Phosphate Buffer Saline) pH 7.3, for 30 min at room temperature. Coverslips were subsequently washed three times with PBS. Cells were permeabilized with 0.5% Triton X-100 in PBS for 15 min then washed three times with PBS. Coverslips were then saturated for 1 h in blocking buffer [0.2% gelatin, 2% Bovine Serum Albumin (BSA), 2% FBS (Lonza) in PBS], followed by the incubation for 1 h with primary antibody diluted at 1:100 in blocking buffer, except for GPP130 that was diluted at 1:300. After washing with PBS, cells were incubated for 1 h with Alexa 488- or Alexa 568- secondary antibody (Life Technologies) diluted at 1:600 in blocking buffer. After three washes with PBS, nuclei were labeled with DAPI 1:300 for 15 min and then coverslips were mounted on glass slides with Mowiol. Fluorescence was detected through an inverted Zeiss LSM700 confocal microscope. Acquisitions were done with ZEN pro 2.1 software (Zeiss, Oberkochen, Germany).

### 2.6. Image analyses

Immunofluorescent images were edited using imageJ software (<http://imagej.nih.gov/ij>) developed by Fiji<sup>®</sup>.

### 2.7. Western blotting

Cells were collected in PBS after 2 washes and centrifuged at 6000 rpm for 10 min. Cells were lysed in RIPA buffer [Tris/HCl 50 mM pH 7.9, NaCl 120 mM, NP40 0.5%, EDTA 1 mM, Na<sub>3</sub>VO<sub>4</sub> 1 mM, NaF 5 mM] supplemented with a protease inhibitors mix (Roche Diagnostics, Penzberg, Germany) by a 30 min centrifugation at 14 000 rpm. Concentration of extracted proteins was determined with the Micro BCA<sup>™</sup> Protein Assay Reagent kit (Thermo Fisher Scientific, Waltham, MA USA). For LAMP2 study only samples were preheated 10 min at 95 °C. 10 or 20 µg of total proteins of each sample were dissolved in reducing NuPage<sup>®</sup> Sample buffer and resolved by MOPS 4–12% Bis-Tris gel (Thermo Fisher Scientific, Waltham, MA USA) and then transferred with iBlot 2 Dry Blotting System (Thermo Fisher Scientific, Waltham, MA USA). Nitrocellulose membranes were blocked 1 h in TBS (Tris Buffer Saline) containing 0.05% Tween 20 5% (w/v) non-fat dried milk for at least 1 h at room temperature, then incubated 1 h with primary antibodies (used at a dilution of 1:2000 for TMEM165, 1: 20 000 for β Actin)

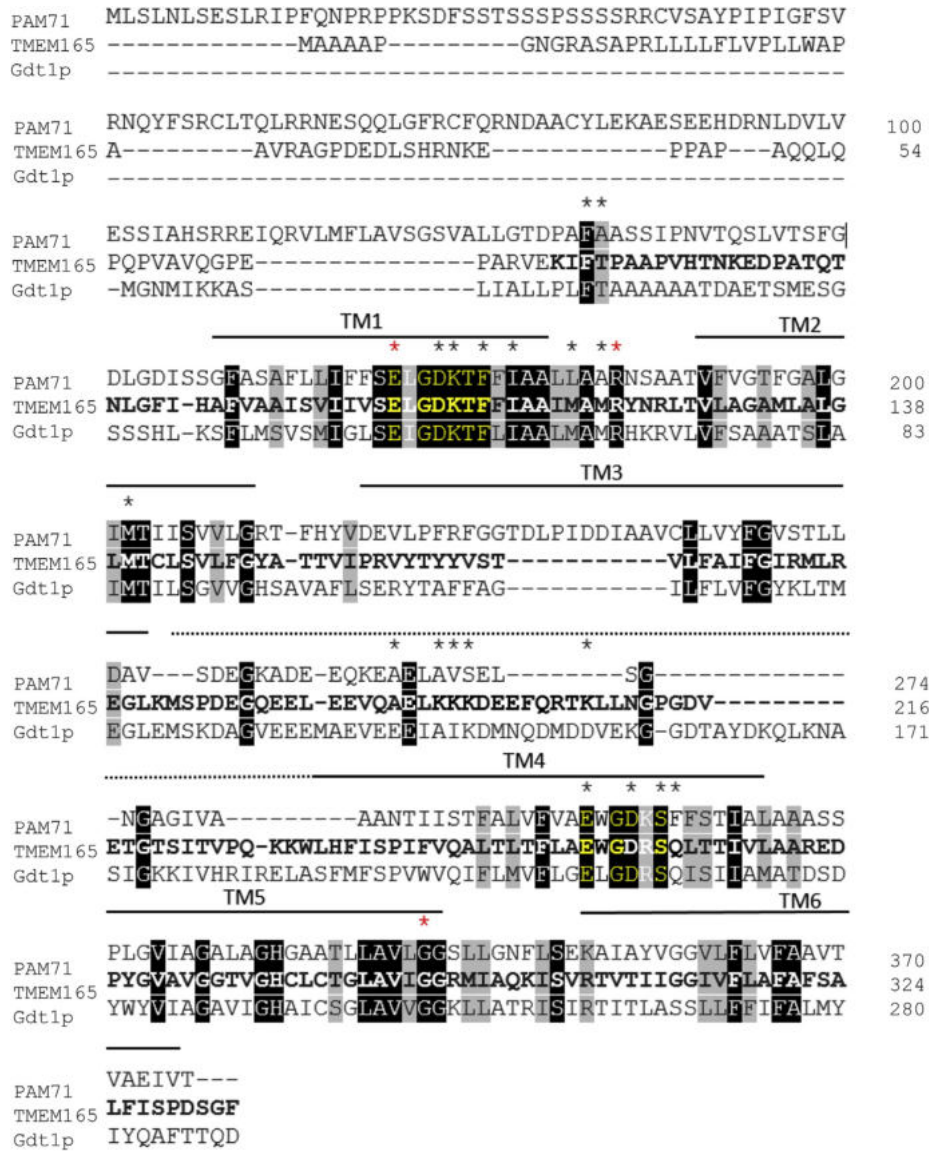


**Fig. 1. Protein sequence alignment of TMEM165 and its orthologs PAM71 from *Arabidopsis thaliana* and Gdt1p from *Saccharomyces cerevisiae*.** The sequences were found in Uniprot database ([www.uniprot.org](http://www.uniprot.org)) and the protein sequence alignment was generated using Clustal Omega (<https://www.ebi.ac.uk/Tools/msa/clustalo>). Black boxes indicate the amino acid residues that are identical whereas gray boxes show the homologous amino acid residues. The black asterisks indicate the position of the generated mutated amino acids. The red asterisks indicate the mutated amino acids found in TMEM165-CDG patients' proteins. The bold characters correspond to the amino acid residues that are found conserved in the mammalian TMEM165 sequence (SwissProt Database) using the Cobalt-NCBI multiple alignment tool (NCBI). Conserved domains (motif 1 and 2) are highlighted in yellow. Black horizontal bars on the top of the sequences indicate the amino acids within the predictive transmembrane domains (TMHMM v2.0 server tool). The dotted line indicates the cytosolic central loop.

and overnight for LAMP2 primary antibody 1:20 000. After three 5 min-TBS-T washes, membranes were incubated with respective secondary antibodies for 1 h (1:10 000 dilution for polyclonal goat anti-rabbit IgG and 1:20 000 for goat anti-mouse IgG Horse Radish Peroxidase-conjugated).

Signal was detected using chemiluminescence reagent Pierce™ Pico Plus Western Blotting Substrate (Thermo Fisher Scientific, Waltham, MA USA) on imaging film (GE Healthcare, Buckinghamshire, UK) or Camera Fusion® (Vilber Lourmat) and its software.

**3. Results**

**3.1. Functionality of TMEM165 mutants in Golgi glycosylation**

The ability for TMEM165 to rescue LAMP2 glycosylation defect

in TMEM165 KO HEK293T cells was used to investigate the involvement each amino acid of the two highly conserved sequences. To explore this, 10 different mutations in the most conserved amino acids that lay in the two signature-motifs were generated (Fig. 1). The wild type (wt-) and mutated forms of TMEM165 were then transiently expressed in TMEM165 KO HEK293T cells and the Golgi glycosylation of LAMP2 was followed by Western blot experiments as previously described [14] (Fig. 2A). Compared to untransfected cells (KO), the expression of the wt-TMEM165 rescued fully glycosylated forms of LAMP2 similar to control cells. Even though the mutated forms of TMEM165 transfection gave heterogeneous results (Fig. 2A), only 3 mutants showed a partial restoration of LAMP2 glycosylation: E108G-, K112G-, R252G-TMEM165, E108G and R252G giving the mildest restorations. Interestingly among all our mutants, 6 of the conserved E-x-GDKT/E-x-GDRSQ motifs are unable to restore

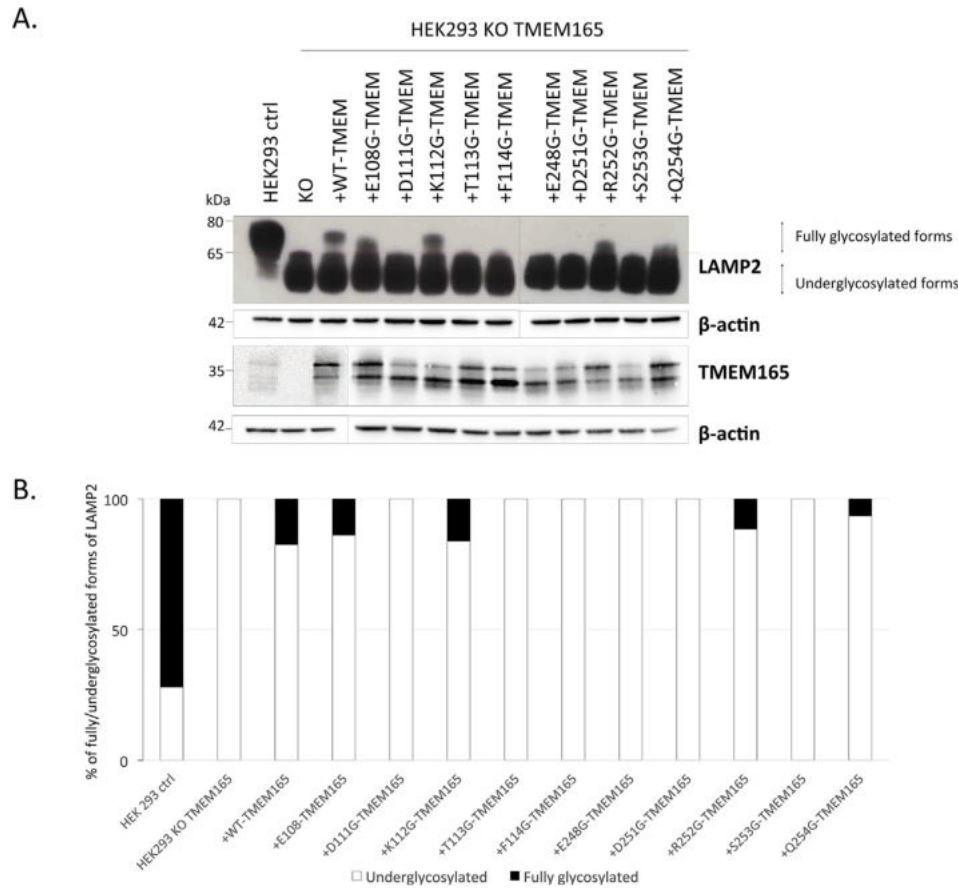


**Fig. 2. LAMP2 glycosylation profile after TMEM165 mutants transfection.** HEK293T KO TMEM165 cells were transfected with empty-vector, wild-type or TMEM165 constructs. Total cells lysates were obtained, subjected to SDS-PAGE, Western blot was performed with the respective antibodies. **A.** LAMP2 and TMEM165 profiles obtained 24 h after transfection. **B.** Ratio of fully glycosylated forms of LAMP2 (percentage of fully glycosylated forms versus the total LAMP2). **C.** Immunofluorescence analysis of the expression and localization of TMEM165 in transfected cells with mutated forms of TMEM165 in conserved amino-acids. (GM130 = Golgi marker) **D.** Illustration of red and green fluorescence merge with RGB Profiler (ImageJ Fiji®).

LAMP2 glycosylation (Fig. 2B). The mutants (D111G-, T113G-, F114G-, E248G-, D251G-, S253G-, Q254G) were found unable to restore LAMP2 glycosylation (Fig. 2B). This result is characteristic from these two motifs as most of the TMEM165 mutated forms, except G304R (patient mutation), were able to rescue LAMP2 glycosylation (Supp. Fig. 1).

To assess these results, the expression level among the mutated forms of TMEM165 was then investigated by Western blot experiments. Although the TMEM165 profile is found heterogeneous with two major bands, there was no major difference in TMEM165 expression level (Fig. 2A). Altogether these results emphasize the importance of some specific amino acids of the two conserved motifs in TMEM165 function in Golgi glycosylation.

### 3.2. Subcellular localization of TMEM165 mutants

The functionality of TMEM165 mutants in Golgi glycosylation depends of the TMEM165 mutants' expression but also on their subcellular Golgi localization. To reinforce the above results, the Golgi localization of the mutated forms of TMEM165 was then investigated by immunofluorescence and confocal microscopy experiments.

Most of the mutated forms of TMEM165 displayed a Golgi localization as observed by colocalization experiments using the GM130 Golgi marker (Fig. 2C and D). Very interestingly, the D251G-

and S253G-TMEM165 mutants, did not entirely colocalize with GM130 as vesicular structures localized throughout the cytoplasm could be detected. To further assess the subcellular localization of these mutants, immunofluorescence staining using the lysosomal/endosomal intracellular marker LAMP2 was performed. A partial colocalization was observed with LAMP2 demonstrating the differential subcellular localization for these mutated forms (Supplementary Figs. 2A and B). For these mutants, it is likely that the observed lack of Golgi glycosylation restoration results from a subcellular mislocalization.

### 3.3. Sensitivity of TMEM165 mutants to manganese exposure

We recently highlighted that, when exposed to high manganese concentration, TMEM165 was efficiently targeted to lysosomes for degradation [15]. As for the glycosylation study, we investigated the  $Mn^{2+}$  sensitivity of these different mutants. To assess this point, the wild-type and mutated forms of TMEM165 were transiently transfected in KO cells. The impact of high  $Mn^{2+}$  concentration supplementation on the stability and subcellular localization was investigated during a 4 and 8 h time course by Western blot (Fig. 3) and immunofluorescence experiments (data not shown). Diagrams under each mutant's Western blot describe the quantification of the remaining TMEM165 after 4 and 8 h of  $Mn^{2+}$  treatment. As previously published [15] we observed that TMEM165 in normal

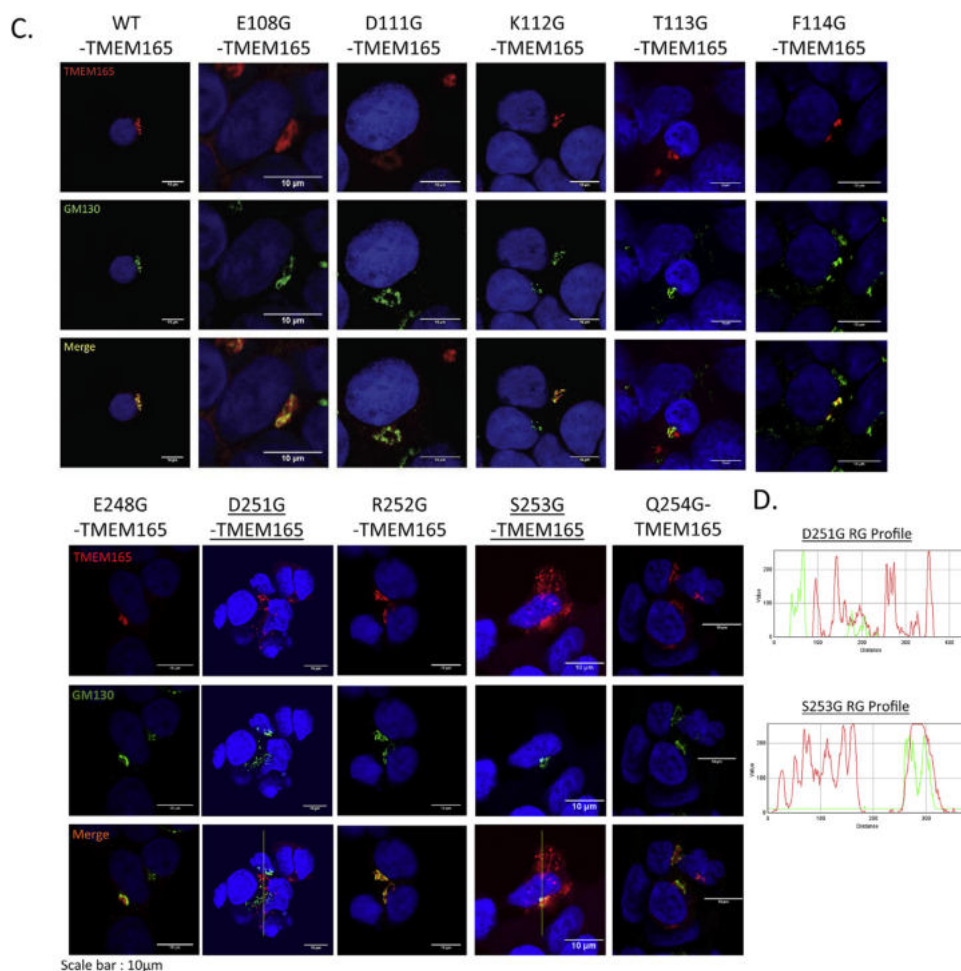


Fig. 2. (continued).

HEK293T cells is highly sensitive to manganese, with a complete loss of this protein after 8 h treatment (Fig. 3A). Same observation is made after transfection of the wild-type form of TMEM165 in HEK293T KO TMEM165 cells with a loss over 75% of TMEM165 expression after 4 h manganese treatment (Fig. 3A).

Concerning the mutated forms of TMEM165, 5 are found partially resistant, E108G, D111G, T113G, D251G and S253G. At the opposite, K112G, F114G, E248G, R252G and Q254G are sensitive to manganese treatment. These results were confirmed by immunofluorescence confocal microscopy (data not shown) and demonstrate the crucial importance of specific amino acids in the differential Mn induced sensitivity of TMEM165.

#### 3.4. The functional mutants are targeted and degraded into lysosomes

We recently established that the  $Mn^{2+}$  induced degradation of TMEM165 was inhibited by chloroquine treatment [15]. To assess whether the mutated forms of TMEM165 fall under the same regulation, the stability of wt- and mutated forms of TMEM165 were analyzed by Western blot and immunofluorescence after  $Mn^{2+}$  exposure, in the presence or the absence of chloroquine. The degradation of every mutated forms of TMEM165 was completely blocked by chloroquine (data not shown). The molecular mechanism by which TMEM165 is sent to lysosomes following  $Mn^{2+}$  exposure is currently unknown. Monoubiquitination is known to be a very efficient mechanism to target proteins for lysosomal

degradation. It appears that the cytosolic loop of TMEM165 contains 4 lysine residues K198, K199, K200 and K208 that could be involved in the  $Mn^{2+}$  induced lysosomal targeting. In order to investigate the role of these lysines, TMEM165 mutants (K198R, K199R, K200R, K208R and K198–K200R) were generated and analyzed by Western blot and immunofluorescence after  $Mn^{2+}$  exposure, in the presence or in the absence of chloroquine (Supp. Figure 3). We observed that after  $Mn^{2+}$  exposure, the lysine mutants of TMEM165 were localized in the Golgi and were degraded similarly to what is observed for wt-TMEM165. Altogether, these results indicate that the lysine residues of the cytosolic loop are not involved in the expression, neither in the Golgi localization nor in its  $Mn^{2+}$ -induced degradation of TMEM165.

#### 4. Discussion

Although the precise molecular and cellular functions of TMEM165 are still under debate, its functional role in Golgi glycosylation is now clearly established. The link between TMEM165 and cellular/Golgi  $Mn^{2+}$  homeostasis maintenance is shown by (i) the alteration of GPP130  $Mn^{2+}$  induced degradation in TMEM165 depleted cells, (ii) the restoration of Golgi glycosylation by  $Mn^{2+}$  supplementation [11], and (iii) the TMEM165  $Mn^{2+}$  sensitivity [15]. It is now highly suspected that TMEM165 functions as a Golgi  $Ca^{2+}/Mn^{2+}$  transporter regulating both  $Ca^{2+}/Mn^{2+}$  Golgi homeostasis. As observed in yeasts, the Golgi glycosylation defect due to a lack of TMEM165 would result in an alteration of the Golgi  $Mn^{2+}$

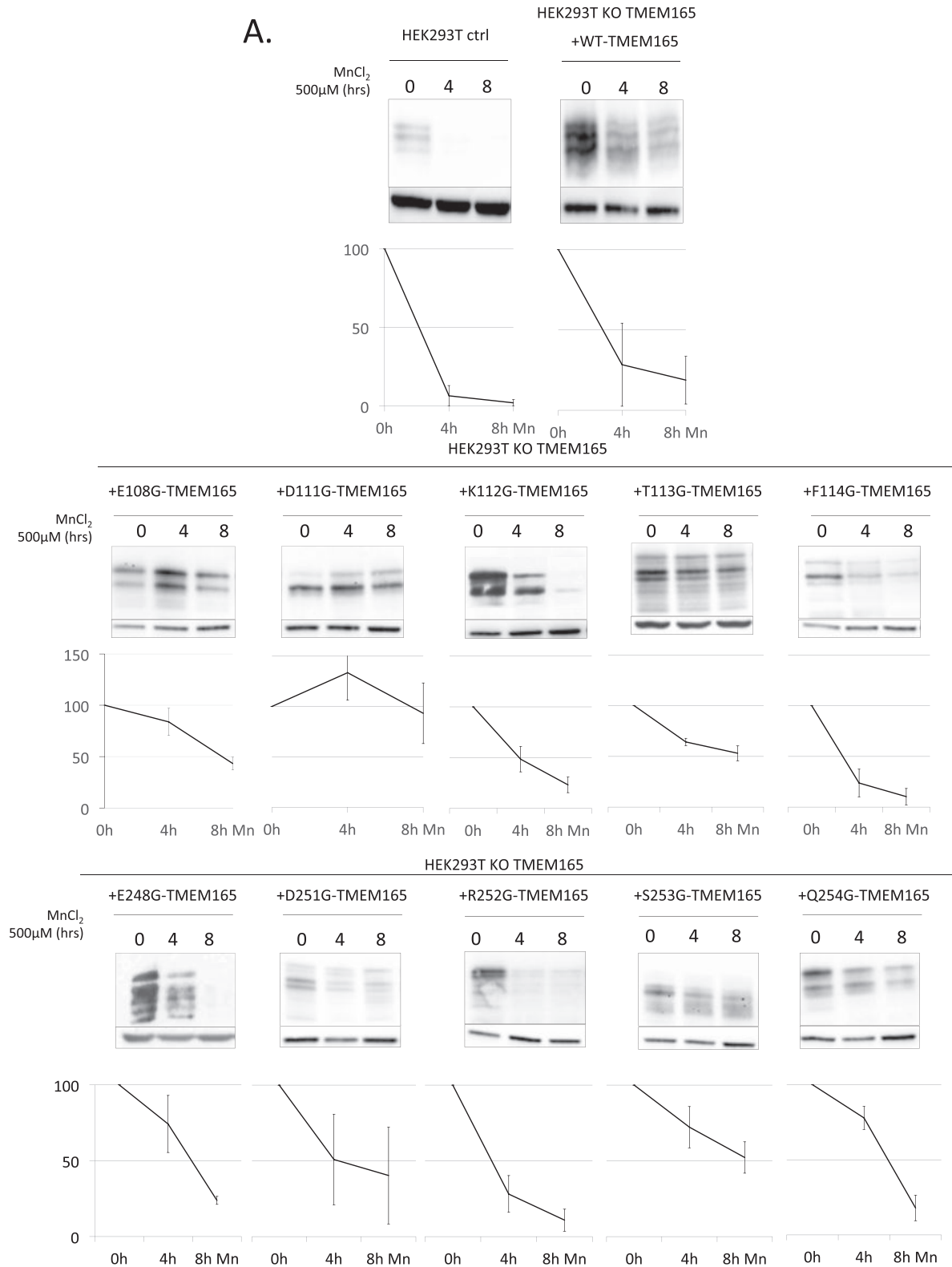


**Fig. 3. Sensitivity of TMEM165 mutants to manganese exposure.** TMEM165 expression in cells transfected with transfected cells forms of TMEM165 in the conserved sequences with or without manganese ( $N \geq 3$ ) **A.** In control cells and transfected cells with WT-TMEM165. **B.** In the cytosolic E-x-G-D-K-[TF] motif. **C.** In the luminal E-x-G-D-R-[SQ] motif. Relative quantification of TMEM165 degradation at 4 and 8 h manganese treatment below each respective Western blot.



homeostasis crucial for the activities of Golgi glycosyltransferases using UDP-sugars as donors [11]. TMEM165 is a member of the UPF0016 family characterized by two highly conserved consensus motifs E- $\phi$ -G-D-[KR]-[TS]. Our previous results showed that the E- $\phi$ -G-D-K-T motif (motif 1) was facing the cytosol while the E- $\phi$ -G-D-R-S (motif 2) was exposed to the Golgi luminal side and hence are predicted to be involved in the transport function of UPF0016 members [15]. In this paper we wanted to further understand the contribution of these two highly conserved motifs in the role of TMEM165 in Golgi glycosylation and also in its sensitivity to high  $Mn^{2+}$  concentration.

Our results first emphasized that some of the mutated forms of TMEM165 are unable to rescue Golgi glycosylation. The mutation of the amino acid E108G does not seem to strongly affect the function of TMEM165 in Golgi glycosylation as a slight restoration of LAMP2 glycosylation is observed. At the opposite, the E248G mutation (second motif) cannot rescue Golgi glycosylation. Interestingly, the polar amino acids (T113 and S253) are found crucial for the function of TMEM165 in Golgi glycosylation while basic amino acids (K112 and R252) are dispensable. We hypothesize that these polar amino acids, via post-translational modifications, play a crucial role in the regulation of TMEM165 functionality.

As proposed for yeasts, it is most likely that amino acids of the two conserved motifs constitute the cation binding sites of TMEM165. In such hypothesis, mutations in specific amino acids of the two conserved motifs alter the transport function of TMEM165 by impairing cation affinity or pocket conformation changes.

The other particularity of TMEM165 is its sensitivity to high  $Mn^{2+}$  concentrations. We recently demonstrated that following high  $Mn^{2+}$  exposure, TMEM165 was targeted to lysosomes for its degradation [15]. The targeting molecular mechanism is unclear but recent investigations propose the requirement of Sortilin in the  $Mn^{2+}$  induced degradation of TMEM165 [16]. The  $Mn^{2+}$  sensitivity of the mutated forms of TMEM165 was evaluated. As pointed out for the glycosylation, most of the generated mutated forms of TMEM165 are resistant to  $Mn^{2+}$  exposure and only few are sensitive. Our results demonstrate that the acidic amino acids (E and D) of the first conserved motif are crucial in conferring the  $Mn^{2+}$  sensitivity to TMEM165. The two resistant mutants D251G and S253G of the second motif are insensitive to manganese presumably due to their mislocalization. Another interesting observation deals with the T113G that is also clearly found resistant to Mn exposure while correctly Golgi localized. The roles of these amino acids in the  $Mn^{2+}$  induced degradation mechanism/Golgi subcellular localization are not clear but one can imagine that they are part of a regulatory mechanism that delicately governs the Golgi ion homeostasis.

In conclusion, this paper highlights the importance of the two very conserved regions for the functionality of TMEM165 in Golgi glycosylation, its subcellular Golgi localization and  $Mn^{2+}$  sensitivity.

### Authors contribution

Conceived and designed experiments: F.F., A.K., and D.L. Performed experiments: E.L., M.H. and S.P. Contributed reagents/materials: V.L., C.S. Analyzed data: E.L., M.H., G.D.B., and M.K.R. Wrote the paper: F.F., A.K., and D.L.

### Competing interests

The author(s) declare no competing interests.

### Declaration of interests

The authors declare that they have no known competing financial interests or personal relationships that could have appeared to influence the work reported in this paper.

### Acknowledgements

This work was supported by grants from Agence Nationale de la Recherche (SOLV-CDG project to F.F.), and EURO-CDG-2 that has received a funding from the European Union's Horizon 2020 research and innovation program under the ERA-NET Cofund action N° 643578. We are also indebted to Dr Dominique Legrand for the Research Federation FRABio (Univ. Lille, CNRS, FR 3688, FRABio, Biochimie Structurale et Fonctionnelle des Assemblages Biomoléculaires) for providing the scientific and technical environment conducive to achieving this work. We thank the Bioluminescence Center of Lille, especially Christian Slomianny and Elodie Richard, for the use of the Leica LSM700.

### Appendix A. Supplementary data

Supplementary data to this article can be found online at <https://doi.org/10.1016/j.biochi.2019.07.016>.

### References

- [1] J. Jaeken, R. Péanne, What is new in CDG? *J. Inher. Metab. Dis.* 40 (2017) 569–586, <https://doi.org/10.1007/s10545-017-0050-6>.
- [2] M. Aebi, A. Helenius, B. Schenk, R. Barone, A. Fiumara, E.G. Berger, T. Hennet, T. Imbach, A. Stutz, C. Bjursell, A. Uller, J.G. Wahlström, P. Briones, E. Cardo, P. Clayton, B. Winchester, V. Cormier-Dalre, P. de Lonlay, M. Cuer, T. Dupré, N. Seta, T. de Koning, L. Dorland, F. de Loos, L. Kupers, Carbohydrate-deficient glycoprotein syndromes become congenital disorders of glycosylation: an updated nomenclature for CDG. *First International Workshop on CDGs, Glycoconj. J.* 16 (1999) 669–671.
- [3] F. Foulquier, M. Amyere, J. Jaeken, R. Zeevaert, E. Schollen, V. Race, R. Bammens, W. Morelle, C. Rosnoblet, D. Legrand, D. Demaegd, N. Buiet, D. Cheillan, N. Guffon, P. Morsomme, W. Annaert, H.H. Freeze, E. Van Schaftingen, M. Vikkula, G. Matthijs, TMEM165 deficiency causes a congenital disorder of glycosylation, *Am. J. Hum. Genet.* 91 (2012) 15–26, <https://doi.org/10.1016/j.ajhg.2012.05.002>.
- [4] D. Marques-da-Silva, R. Francisco, D. Webster, V. dos Reis Ferreira, J. Jaeken, T. Puliniikunnil, Cardiac complications of congenital disorders of glycosylation (CDG): a systematic review of the literature, *J. Inher. Metab. Dis.* 40 (2017) 657–672, <https://doi.org/10.1007/s10545-017-0066-y>.
- [5] D. Marques-da-Silva, V. dos Reis Ferreira, M. Monticelli, P. Janeiro, P.A. Videira, P. Witters, J. Jaeken, D. Cassiman, Liver involvement in congenital disorders of glycosylation (CDG). A systematic review of the literature, *J. Inher. Metab. Dis.* 40 (2017) 195–207, <https://doi.org/10.1007/s10545-016-0012-4>.
- [6] C. Rosnoblet, D. Legrand, D. Demaegd, H. Hacine-Gherbi, G. de Bettignies, R. Bammens, C. Borrego, S. Duvert, P. Morsomme, G. Matthijs, F. Foulquier, Impact of disease-causing mutations on TMEM165 subcellular localization, a recently identified protein involved in CDG-II, *Hum. Mol. Genet.* 22 (2013) 2914–2928, <https://doi.org/10.1093/hmg/ddt146>.
- [7] D. Demaegd, A.-S. Colinet, A. Deschamps, P. Morsomme, Molecular evolution of a novel family of putative calcium transporters, *PLoS One* 9 (2014) e100851, <https://doi.org/10.1371/journal.pone.0100851>.
- [8] D. Demaegd, F. Foulquier, A.-S. Colinet, L. Gremillon, D. Legrand, P. Mariot, E. Peiter, E. Van Schaftingen, G. Matthijs, P. Morsomme, Newly characterized Golgi-localized family of proteins is involved in calcium and pH homeostasis in yeast and human cells, *Proc. Natl. Acad. Sci.* 110 (2013) 6859–6864.
- [9] A. Schneider, I. Steinberger, A. Herdean, C. Gandini, M. Eisenhut, S. Kurz, A. Morper, N. Hoecker, T. Rühle, M. Labs, U.I. Flüggé, S. Geimer, S.B. Schmidt, S. Husted, A.P.M. Weber, C. Spetea, D. Leister, The evolutionarily conserved protein PHOTOSYNTHESIS AFFECTED MUTANT71 is required for efficient manganese uptake at the thylakoid membrane in Arabidopsis, *Plant Cell* 2015 (2016) 00812, <https://doi.org/10.1105/tpc.15.00812>.
- [10] S. Potelle, W. Morelle, E. Dulary, S. Duvert, D. Vicogne, C. Spriet, M.-A. Krzewinski-Recchi, P. Morsomme, J. Jaeken, G. Matthijs, G. De Bettignies, F. Foulquier, Glycosylation abnormalities in Gdt1p/TMEM165 deficient cells result from a defect in Golgi manganese homeostasis, *Hum. Mol. Genet.* 25 (2016) 1489–1500, <https://doi.org/10.1093/hmg/ddw026>.
- [11] W. Morelle, S. Potelle, P. Witters, S. Wong, L. Climer, V. Lupashin, G. Matthijs, T. Gadomski, J. Jaeken, D. Cassiman, E. Morava, F. Foulquier, Galactose supplementation in patients with TMEM165-CDG rescues the glycosylation

- defects, *J. Clin. Endocrinol. Metab.* 102 (2017) 1375–1386, <https://doi.org/10.1210/jc.2016-3443>.
- [12] E. Dulary, S. Potelle, D. Legrand, F. Foulquier, TMEM165 deficiencies in Congenital Disorders of Glycosylation type II (CDG-II): clues and evidences for roles of the protein in Golgi functions and ion homeostasis, *Tissue Cell* 49 (2017) 150–156, <https://doi.org/10.1016/j.tice.2016.06.006>.
- [13] L. Thines, A. Deschamps, P. Sengottaiyan, O. Savel, J. Stribny, P. Morsomme, The yeast protein Gdt1p transports Mn<sup>2+</sup> ions and thereby regulates manganese homeostasis in the Golgi, *J. Biol. Chem.* 293 (2018) 8048–8055, <https://doi.org/10.1074/jbc.RA118.002324>.
- [14] M. Houdou, E. Lebretonchel, A. Garat, S. Duvet, D. Legrand, V. Decool, A. Klein, M. Ouzzine, B. Gasnier, S. Potelle, F. Foulquier, Involvement of thapsigargin– and cyclopiazonic acid–sensitive pumps in the rescue of TMEM165-associated glycosylation defects by Mn<sup>2+</sup>, *FASEB J.* 33 (2019) 2669–2679, <https://doi.org/10.1096/fj.201800387R>.
- [15] S. Potelle, E. Dulary, L. Climer, S. Duvet, W. Morelle, D. Vicogne, E. Lebretonchel, M. Houdou, C. Spriet, M.-A. Krzewinski-Recchi, R. Peanne, A. Klein, G. de Bettignies, P. Morsomme, G. Matthijs, T. Marquardt, V. Lupashin, F. Foulquier, Manganese-induced turnover of TMEM165, *Biochem. J.* 474 (2017) 1481–1493, <https://doi.org/10.1042/BCJ20160910>.
- [16] S. Venkat, A.D. Linstedt, Manganese-induced trafficking and turnover of GPP130 is mediated by sortilin, *Mol. Biol. Cell* (2017), <https://doi.org/10.1091/mbc.E17-05-0326> mbc.E17-05-0326.

## Résumé

La glycosylation est un processus cellulaire universel chez tous les organismes vivants visant aux transferts successifs de monosaccharides sur une molécule acceptrice, le plus souvent une protéine, un lipide ou un autre monosaccharide. Chez les eucaryotes, différentes voies de glycosylation coexistent, aboutissant à la biosynthèse d'une grande diversité de structures glycaniques aux fonctions diverses. Chez l'homme, des perturbations au cours d'une ou plusieurs réactions de glycosylation sont à l'origine de glycopathologies génétiques rares appelées *Congenital Disorders of Glycosylation* (CDG). L'une d'entre elles, TMEM165-CDG, a été identifiée en 2012 par notre équipe et est au cœur de ces travaux. Des mutations pathogéniques dans le gène *TMEM165* sont en effet responsables de l'apparition de sévères défauts de glycosylation caractérisés par la présence de structures N-glycaniques principalement sous-galactosylées. Lors de la caractérisation de ces anomalies de glycosylation, les travaux de l'équipe ont rapidement établi un lien entre déficience en *TMEM165* et dérégulation de l'homéostasie du manganèse ( $Mn^{2+}$ ) de l'appareil de Golgi. Dès lors, et au regard de précédents résultats de l'équipe, une fonction d'antiport  $Ca^{2+}/Mn^{2+}$  fut assignée à *TMEM165*, permettant l'import d'ions  $Mn^{2+}$  dans l'appareil de Golgi afin d'assurer un environnement ionique adéquat et nécessaire au bon déroulement des réactions de glycosylation. De façon extrêmement intéressante, il s'avère qu'un apport exogène de  $Mn^{2+}$  dans le milieu de culture de cellules déficientes en *TMEM165* corrige complètement les défauts de N-glycosylation observés dans ces cellules. Par ailleurs, *TMEM165*, tout comme *Gdt1p*, son orthologue chez la levure *Saccharomyces cerevisiae*, est une protéine extrêmement sensible aux ions  $Mn^{2+}$  étant rapidement dégradée *via* la voie lysosomale en présence de fortes concentrations de  $Mn^{2+}$ . Un lien étroit s'établit donc entre fonctions de *TMEM165/Gdt1p*, homéostasie du  $Mn^{2+}$  de l'appareil de Golgi et glycosylation golgienne ; trois aspects qui furent au centre de mes travaux. Plus particulièrement, ma thèse porte sur (i) la compréhension des mécanismes de correction des défauts de glycosylation observés dans les cellules déficientes en *TMEM165* et induits par le  $Mn^{2+}$  et (ii) les liens potentiels entre différents acteurs essentiels au maintien de l'homéostasie ionique de la voie de sécrétion que sont les pompes calciques ( $Ca^{2+}$ ) réticulaires *SERCA2*, *TMEM165* et *SPCA1*, seule pompe ATPasique de l'appareil de Golgi connue à ce jour pour importer à la fois des ions  $Ca^{2+}$  et  $Mn^{2+}$ . A travers l'utilisation de lignées cellulaires humaines génétiquement invalidées pour *TMEM165* ou *ATP2C1* et de levures déficientes en *Gdt1p* et/ou *Pmr1p*, notre étude a conduit à l'élaboration de différents concepts reliant intimement ces protéines. D'une part, nous avons démontré que l'activité des pompes *SERCA* était cruciale au maintien des réactions de glycosylation golgiennes en absence de *TMEM165* par leur contribution dans le pompage et la redistribution des ions  $Mn^{2+}$  depuis le cytosol vers l'appareil de Golgi. D'autre part, *TMEM165* est indispensable au maintien des réactions de glycosylation golgiennes en absence de *SPCA1* et lorsque *SERCA2* est inhibée par des agents pharmacologiques. Parallèlement, nos travaux ont mis en évidence que l'expression et la stabilité des protéines *TMEM165*, chez l'homme et *Gdt1p*, chez la levure étaient directement liées aux capacités de *SPCA1* et *Pmr1p* à importer des ions  $Mn^{2+}$  dans l'appareil de Golgi. Bien que des différences s'observent entre l'homme et la levure *Saccharomyces cerevisiae*, l'ensemble de mes travaux illustre l'importance de l'homéostasie ionique de l'appareil de Golgi dans le maintien du processus de glycosylation golgien.

## Abstract

Glycosylation is a universal cellular process in all living organisms where monosaccharides are added one by one onto an acceptor molecule, most of the time a protein, a lipid or another monosaccharide. In eukaryotes, many glycosylation pathways occur simultaneously, resulting in the biosynthesis of a broad variety of glycan structures with different functions. In humans, if one -or more- glycosylation reactions are genetically impaired, Congenital Disorders of Glycosylation (CDG) appear. One of them, TMEM165-CDG, was identified in 2012 by our group and is at the heart of this work. Pathogenic mutations in *TMEM165* gene cause severe glycosylation defects mainly characterized by hypo-galactosylated N-glycan structures. While characterizing these glycosylation abnormalities, a link has rapidly been established by the team between TMEM165 deficiency and Golgi manganese ( $Mn^{2+}$ ) homeostasis disruption. Therefore, and based on previous work, TMEM165 was assumed to act as a  $Ca^{2+}/Mn^{2+}$  antiporter, allowing the import of  $Mn^{2+}$  into the Golgi lumen in order to sustain an adequate ionic environment, required for all glycosylation reactions. Interestingly, we also found that exogenous addition of  $Mn^{2+}$  in the culture medium of TMEM165 deficient cells completely rescues the N-glycosylation defects observed in these cells. Moreover, TMEM165, like Gdt1p its yeast ortholog, is a protein highly sensitive to  $Mn^{2+}$ , being rapidly degraded *via* the lysosomal pathway in the presence of high  $Mn^{2+}$  concentrations. All in all, a close link exists between TMEM165/Gdt1p, Golgi  $Mn^{2+}$  homeostasis and Golgi glycosylation; the three major aspects focused in the PhD research. More precisely, my thesis focuses on (i) understanding the mechanisms of  $Mn^{2+}$ -induced glycosylation rescue in TMEM165 deficient cells and (ii) the potential links between different key players acting in the regulation of the secretory pathway ionic homeostasis which are the Sarco/Endoplasmic Reticulum calcium ( $Ca^{2+}$ )-ATPase SERCA2, TMEM165 and SPCA1 (Secretory Pathway  $Ca^{2+}/Mn^{2+}$ -ATPase), the only pump of the Golgi apparatus known to import both  $Ca^{2+}$  and  $Mn^{2+}$  in the Golgi lumen. Through the use of isogenic human cell lines knockout for either *TMEM165* or *SPCA1* and yeasts lacking Gdt1p and Pmr1p, we highlighted three main concepts that closely link these proteins: TMEM165 (Gdt1p), SPCA1 (Pmr1p) and SERCA2. On the one hand, we demonstrated that the activity of SERCA pumps is crucial to sustain Golgi glycosylation reactions in absence of TMEM165 by their contribution in  $Mn^{2+}$  pumping and redistribution into the Golgi lumen. On the other hand, TMEM165 was found essential for maintaining Golgi glycosylation reactions in absence of SPCA1 and when SERCA2 are inhibited by pharmacological agents. Moreover, we also shed light on the fact that expression and stability of TMEM165 (in humans) and Gdt1p (in yeast) were directly linked to the capacities of SPCA1 and Pmr1p to import  $Mn^{2+}$  into the Golgi lumen. Although differences exist between humans and yeast *Saccharomyces cerevisiae*, all of our work illustrates the crucial importance of the ionic homeostasis of the Golgi apparatus to sustain Golgi glycosylation reactions.